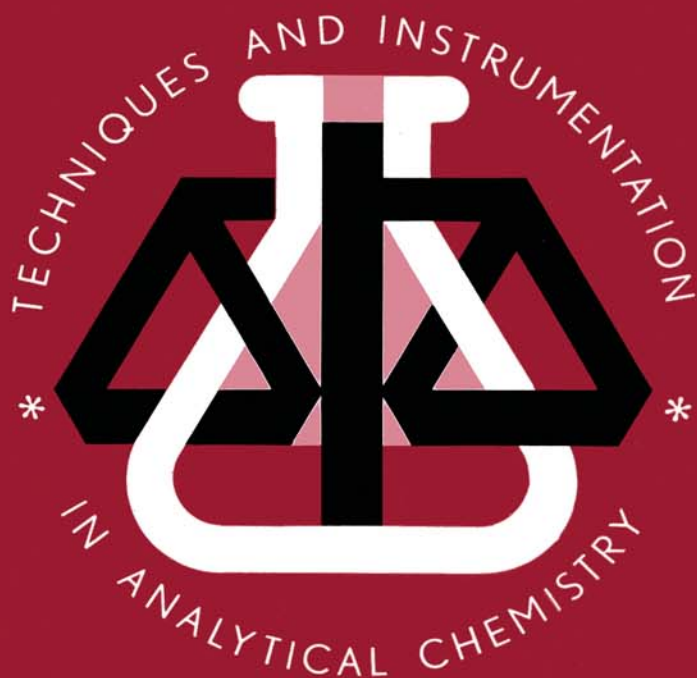


20



**ANALYTICAL PYROLYSIS
OF NATURAL ORGANIC
POLYMERS**

S.C. Moldoveanu

ELSEVIER

TECHNIQUES AND INSTRUMENTATION IN ANALYTICAL CHEMISTRY — VOLUME 20

**ANALYTICAL PYROLYSIS
OF NATURAL ORGANIC POLYMERS**

TECHNIQUES AND INSTRUMENTATION IN ANALYTICAL CHEMISTRY

- Volume 1 **Evaluation and Optimization of Laboratory Methods and Analytical Procedures. A Survey of Statistical and Mathematical Techniques**
by D.L. Massart, A. Dijkstra and L. Kaufman
- Volume 2 **Handbook of Laboratory Distillation**
by E. Krell
- Volume 3 **Pyrolysis Mass Spectrometry of Recent and Fossil Biomaterials. Compendium and Atlas**
by H.L.C. Meuzelaar, J. Haverkamp and F.D. Hileman
- Volume 4 **Evaluation of Analytical Methods in Biological Systems**
Part A. Analysis of Biogenic Amines
edited by G.B. Baker and R.T. Coutts
Part B. Hazardous Metals in Human Toxicology
edited by A. Vercauysse
Part C. Determination of Beta-Blockers in Biological Material
edited by V. Marko
- Volume 5 **Atomic Absorption Spectrometry**
edited by J.E. Cantle
- Volume 6 **Analysis of Neuropeptides by Liquid Chromatography and Mass Spectrometry**
by D.M. Desiderio
- Volume 7 **Electroanalysis. Theory and Applications in Aqueous and Non-Aqueous Media and in Automated Chemical Control**
by E.A.M.F. Dahmen
- Volume 8 **Nuclear Analytical Techniques in Medicine**
edited by R. Cesareo
- Volume 9 **Automatic Methods of Analysis**
by M. Valcárcel and M.D. Luque de Castro
- Volume 10 **Flow Injection Analysis – A Practical Guide**
by B. Karlberg and G.E. Pacey
- Volume 11 **Biosensors**
by F. Scheller and F. Schubert
- Volume 12 **Hazardous Metals in the Environment**
edited by M. Stoeppler
- Volume 13 **Environmental Analysis. Techniques, Applications and Quality Assurance**
edited by D. Barceló
- Volume 14 **Analytical Applications of Circular Dichroism**
edited by N. Purdie and H.G. Brittain
- Volume 15 **Trace Element Analysis in Biological Specimens**
edited by R.F.M. Herber and M. Stoeppler
- Volume 16 **Flow-through (Bio)Chemical Sensors**
by M. Valcárcel and M.D. Luque de Castro
- Volume 17 **Quality Assurance for Environmental Analysis**
Method Evaluation within the Measurements and Testing Programme (BCR)
edited by Ph. Quevauviller, E.A. Maier and B. Griepink
- Volume 18 **Instrumental Methods in Food Analysis**
edited by J.R.J. Paré and J.M.R. Bélanger
- Volume 19 **Trace Determination of Pesticides and their Degradation Products in Water**
by D. Barceló and M.-C. Hennion
- Volume 20 **Analytical Pyrolysis of Natural Organic Polymers**
by S.C. Moldoveanu

TECHNIQUES AND INSTRUMENTATION IN ANALYTICAL CHEMISTRY — VOLUME 20

ANALYTICAL PYROLYSIS OF NATURAL ORGANIC POLYMERS

Serban C. Moldoveanu

*Brown & Williamson Tobacco Corporation,
Research and Development,
2600 Weaver Road, Macon GA 31217,
USA*



1998

ELSEVIER

Amsterdám — Lausanne — New York — Oxford — Shannon — Singapore — Tokyo

ELSEVIER SCIENCE B.V.
Sara Burgerhartstraat 25
P.O. Box 211, 1000 AE Amsterdam, The Netherlands

© 1998 Elsevier Science B.V. All rights reserved.

This work and the individual contributions contained in it are protected under copyright by Elsevier Science B.V., and the following terms and conditions apply to its use:

Photocopying

Single photocopies of single chapters may be made for personal use as allowed by national copyright laws. Permission of the publisher and payment of a fee is required for all other photocopying, including multiple or systematic copying, copying for advertising or promotional purposes, resale, and all forms of document delivery. Special rates are available for educational institutions that wish to make photocopies for non-profit educational classroom use.

Permissions may be sought directly from Elsevier Science Rights & Permissions Department, PO Box 800, Oxford OX5 1DX, UK; phone: (+44) 1865 843830, fax: (+44) 1865 853333, e-mail: permissions@elsevier.co.uk. You may also contact Rights & Permissions directly through Elsevier's home page (<http://www.elsevier.nl>), selecting first 'Customer Support', then 'General Information', then 'Permissions Query Form'.

In the USA, users may clear permissions and make payments through the Copyright Clearance Center, Inc., 222 Rosewood Drive, Danvers, MA 01923, USA; phone: (978) 7508400, fax: (978) 7504744, and in the UK through the Copyright Licensing Agency Rapid Clearance Service (CLARCS), 90 Tottenham Court Road, London W1P 0LP, UK; phone: (+44) 171 436 5931; fax: (+44) 171 436 3986. Other countries may have a local reprographic rights agency for payments.

Derivative Works

Subscribers may reproduce tables of contents for internal circulation within their institutions. Permission of the publisher is required for resale or distribution of such material outside the institution. Permission of the publisher is required for all other derivative works, including compilations and translations.

Electronic Storage or Usage

Permission of the publisher is required to store or use electronically any material contained in this work, including any chapter or part of a chapter. Contact the publisher at the address indicated.

Except as outlined above, no part of this work may be reproduced, stored in a retrieval system or transmitted in any form or by any means, electronic, mechanical, photocopying, recording or otherwise, without prior written permission of the publisher.

Address permissions requests to: Elsevier Science Rights & Permissions Department, at the mail, fax and e-mail addresses noted above.

Notice

No responsibility is assumed by the Publisher for any injury and/or damage to persons or property as a matter of products liability, negligence or otherwise, or from any use or operation of any methods, products, instructions or ideas contained in the material herein. Because of rapid advances in the medical sciences, in particular, independent verification of diagnoses and drug dosages should be made.

First edition 1998

Library of Congress Cataloging in Publication Data

A catalog record from the Library of Congress has been applied for.

ISBN: 0-444-82203-8

♾ The paper used in this publication meets the requirements of ANSI/NISO Z39.48-1992 (Permanence of Paper).
Printed in The Netherlands.

Preface

The study of natural organic polymers is an extremely complex and difficult task. Among many other tools utilized for this study, one is analytical pyrolysis. Analytical pyrolysis viewed as an analytical technique is described in the first part of this book. The second part presents the results of pyrolysis for individual natural organic polymers and some chemically modified natural organic polymers. It describes the main pyrolysis products of these compounds as well as the proposed pyrolysis mechanisms. This part is intended to be the core of the book, and it is an attempt to capture as much as possible from the chemistry of the pyrolytic process of natural organic polymers. The third part of the book is more concise and describes some of the practical applications of analytical pyrolysis on natural organic polymers and their composite materials. These applications are related to analysis, characterization, or comparison of complex samples. However, it includes only examples on different subjects, and it is not a comprehensive presentation. A variety of details on specific applications are described in the original papers published in dedicated journals such as the "Journal of Analytical and Applied Pyrolysis."

The book includes a number of topics ranging from those related to biochemistry to some from physics and covering problems such as mechanisms in organic chemistry or instrumentation in analytical chemistry. For this reason, additional information from related fields is needed sometimes for a better understanding of the subject. However, the intention of the author was to present the book, as much as possible, as a uniform subject and not as a conglomerate of scientific papers. Some previously written materials, such as Irwin's excellent book on analytical pyrolysis, were a guide for this purpose.

The three parts of the book are covered in 18 chapters, each divided into sections. Some sections are further divided by particular subjects. References are given for each chapter. Although representative information was carefully included, the references were not exhaustive. With the modern capability of literature search, an effort to include in the book all possible reports would be unnecessary. Most of the information in the book came from published literature. This includes original papers and also different books. As an example, the book of H. L. C. Meuzelaar, J. Haverkamp, and F. D. Hileman on pyrolysis-mass spectrometry of biomaterials was a valuable source of information for this subject. A few unpublished personal results were also included.

Help for improvements in the presentation of the material for this book was provided by the editor, Mr. D. Coleman, by Mr. B. F. Price, Director of Analytical Research at Brown & Williamson, and by Ms. Carol Benton who also made numerous corrections to the material and prepared the index. The cooperation of two of the author's coworkers, Mr. J. B. Forehand and Dr. N. P. Kulshreshtha, was very useful for including most of the original data.

This Page Intentionally Left Blank

Table of Contents

Part 1. An Introduction to Analytical Pyrolysis	1
1. Introduction and Nomenclature	3
1.1. Pyrolysis as a Chemical Process	3
1.2. The Scope of Analytical Pyrolysis	3
1.3. Analytical Pyrolysis Applied to Natural Organic Polymers	5
References	6
2. The Chemistry of the Pyrolytic Process	9
2.1. General Remarks	9
2.2. Elimination Reactions in Pyrolysis	9
<i>Pyrolytic elimination with E_i mechanism</i>	9
<i>Fragmentations</i>	12
<i>Extrusion reactions</i>	13
<i>Elimination involving free radicals</i>	13
<i>1,4 Conjugate eliminations</i>	14
2.3. Rearrangements Taking Place in Pyrolysis	14
<i>Migration of a group</i>	15
<i>Electrocyclic rearrangements</i>	15
<i>Sigmatropic rearrangements</i>	15
2.4. Oxidations and Reductions Taking Place in Pyrolysis	16
2.5. Substitutions and Additions Taking Place in Pyrolysis	16
<i>Substitutions</i>	16
<i>Additions</i>	18
2.6. Typical Polymer Degradations during Pyrolysis	20
<i>Polymeric chain scission</i>	20
<i>Side group reactions</i>	25
<i>Combined reactions</i>	25
2.7. Pyrolysis in the Presence of Additional Reactants or with Catalysts	28
<i>Pyrolysis in the presence of oxygen</i>	28
<i>Pyrolysis in the presence of hydrogen</i>	29
<i>Pyrolysis in the presence of water</i>	29
<i>Pyrolysis in the presence of quaternary N alkyl (or alkyl, aryl) ammonium hydroxides</i>	30
References	31
3. Physico-Chemical Aspects of the Pyrolytic Process	33
3.1. Thermodynamic Factors in Pyrolytic Chemical Reactions	33
3.2. Kinetic Factors in Pyrolytic Chemical Reactions	36
3.3. Models Attempting to Describe the Kinetics of the Pyrolytic Processes of Solid Samples	41
3.4. Pyrolysis Kinetics for Uniform Repetitive Polymers	47
3.5. Pyrolytic Processes Compared with Combustion	53
3.6. Pyrolysis Process Compared to Ion Fragmentation in Mass Spectrometry	55
<i>Pyrolysis of polyisoprene and ion fragments formation from oligomers of isoprene</i>	58

<i>Pyrolysis of saccharides compared to ion fragments formation</i>	59
<i>Pyrolysis of lignin models compared to ion fragments formation</i>	61
<i>Pyrolysis of amino acids compared to ion fragments formation</i>	63
<i>Pyrolysis of nucleic acids compared to ion fragments formation from adenosine-5'-phosphate and 2-deoxyadenosine-5'-phosphate</i>	66
3.7. Theoretical Approaches for Chemical Pyrolytic Reactions	66
References	68
4. Instrumentation Used for Pyrolysis	71
4.1. The Temperature Control of the Pyrolytic Process	71
4.2. Curie Point Pyrolysers	80
4.3. Resistively Heated Filament Pyrolysers	84
4.4. Furnace Pyrolysers	86
4.5. Radiative Heating (Laser) Pyrolysers	87
4.6. Other Pyrolyser Types	91
4.7. Comparison of Analytical Performances of Different Pyrolyser Types	91
References	94
5. Analytical Techniques Used with Pyrolysis	97
5.1. The Selection of the Analytical Technique and the Transfer of the Pyrolysate to the Analytical Instrument	97
<i>Transfer of the pyrolysate to the analytical instrument</i>	97
5.2. Pyrolysis-Gas Chromatography (Py-GC)	100
<i>Transfer of the pyrolysate to the gas chromatograph</i>	101
<i>The partition process in a chromatographic separation</i>	102
<i>Chromatographic column efficiency</i>	104
<i>Peak separation in gas chromatography</i>	109
<i>Sample capacity</i>	110
<i>Isothermal and programmed temperature gas chromatography</i>	111
<i>Basic description of the gas chromatograph</i>	113
<i>The chromatographic column</i>	115
<i>Bidimensional Py-GC</i>	119
<i>Concentration techniques used in Py-GC</i>	124
<i>Data processing in Py-GC</i>	126
5.3. Mass Spectrometers as Detectors in Pyrolysis-Gas Chromatography	132
<i>Ion generation</i>	132
<i>Separation of ions by their m/z ratio</i>	134
<i>Ion detection</i>	137
<i>MS/MS systems</i>	138
<i>Data processing in Py-GC/MS</i>	138
5.4. Pyrolysis-Mass Spectrometric (Py-MS) Techniques	144
<i>Sample preparation in Py-MS</i>	148
<i>Direct probe and filament Py-MS techniques</i>	149
<i>Curie point Py-MS technique</i>	150
<i>Laser Py-MS techniques</i>	151
<i>Field ionization and field desorption techniques used in Py-MS</i>	154
<i>Photoionization used in Py-MS</i>	157
<i>Other techniques used in MS and their relation to pyrolysis</i>	159
5.5. Data Interpretation in Pyrolysis - Mass Spectrometry (Py-MS)	161
<i>Data pretreatment in Py-MS</i>	162

<i>Py-MS data analysis with univariate statistical techniques</i>	163
<i>Multivariate data sets</i>	170
<i>Measures for comparing multivariate Py-MS data</i>	171
<i>Cluster analysis of Py-MS data</i>	177
<i>Discriminant analysis applied to Py-MS data</i>	179
<i>Factor analysis applied to Py-MS data</i>	180
<i>Other techniques utilized in the analysis of Py-MS data</i>	185
5.6. Infrared Spectroscopy (IR) Used as a Detecting Technique for Pyrolysis	186
5.7. Other Analytical Techniques in Pyrolysis	188
References	194

Part 2. Analytical Pyrolysis of Organic Biopolymers 201

6. Analytical Pyrolysis of Polyterpenes	203
6.1. Natural Rubber	203
6.2. Vulcanized Rubber	210
6.3. Other Polyterpenes	214
References	215
7. Analytical Pyrolysis of Polymeric Carbohydrates	217
7.1. Monosaccharides, Polysaccharides and General Aspects of their Pyrolysis	217
<i>Pyrolysis of monosaccharides</i>	220
<i>Classification of polymeric carbohydrates</i>	230
<i>Summary of the features of pyrolysis of polysaccharides</i>	233
7.2. Cellulose	237
<i>Initial pyrolytic reactions during cellulose pyrolysis</i>	239
<i>Further pyrolytic reactions during cellulose pyrolysis</i>	241
<i>Compounds identified in cellulose pyrolysates</i>	245
<i>Cellulose pyrolysis at higher temperatures</i>	249
<i>Mechanisms in the formation of small molecules during cellulose pyrolysis</i> ...	251
<i>Cellulose pyrolysis in acidic or basic conditions or in the presence of salts</i> ...	255
<i>Pyrolysis of cellulose in air</i>	256
<i>Kinetics of cellulose pyrolysis</i>	256
7.3. Chemically Modified Celluloses	257
<i>Pyrolysis of cellulose nitrate, sulfate, and phosphate</i>	257
<i>Cellulose acetate</i>	258
<i>Paper sizing study using pyrolysis</i>	262
<i>Alkali cellulose</i>	262
<i>Cellulose xanthate</i>	263
<i>Cellulose ethers</i>	263
<i>Mechanisms in the pyrolysis of cellulose derivatives</i>	271
7.4. Amylose and Amylopectin	273
<i>Pyrolysis of starch</i>	274
<i>Modified starches</i>	279
7.5. Pectins	282
<i>Mechanisms in the formation of small molecules in pectin pyrolysates</i>	288
7.6. Gums and Mucilages	289
7.7. Hemicelluloses and Other Plant Polysaccharides	291

7.8. Algal Polysaccharides	297
7.9. Microbial Polysaccharides	300
7.10. Lipopolysaccharides from the Cell Surface of Bacteria	304
7.11. Fungal Polysaccharides	304
7.12. Glycogen	305
7.13. Chitin	306
7.14. Proteoglycans	308
References	311
8. Analytical Pyrolysis of Polymeric Materials with Lipid Moieties	317
8.1. Classification of Complex Lipids and Analytical Pyrolysis of Simple Lipids	317
<i>Classification of lipids</i>	317
<i>Analytical pyrolysis of simple lipids</i>	321
8.2. Complex Lipids	323
References	324
9. Analytical Pyrolysis of Lignins	327
9.1. Lignin	327
<i>Mechanisms in the formation of small molecules in lignin pyrolysis</i>	337
<i>Pyrolysis of lignin in the presence of acids, bases or salts</i>	340
<i>Kinetics of lignin pyrolysis</i>	340
9.2. Lignocellulosic Materials	342
9.3. Chemically Modified Lignins	345
References	350
10. Analytical Pyrolysis of Polymeric Tannins	351
10.1. Polymeric tannins	352
References	354
11. Analytical Pyrolysis of Caramel Colors and of Maillard Browning Polymers ..	355
11.1. Pyrolysis of Caramel Colors	355
11.2. Sugar-Ammonia and Sugar-Amines Browning Polymers	355
11.3. Sugar-Amino Acid Browning Polymers	364
References	370
12. Analytical Pyrolysis of Proteins	373
12.1. Protein Structure and Pyrolysis of Amino Acids	373
<i>Pyrolysis of amino acids</i>	376
12.2. Peptides	380
12.3. Simple Proteins	386
12.4. Conjugated Proteins	394
References	396
13. Nucleic Acids	399
13.1. Classification of Nucleic Acids and Pyrolysis of Oligonucleotides	399
13.2. Pyrolysis of Nucleic Acids	403
13.3. Pyrolysis of Pt-DNA complexes	406
References	406

14. Analytical Pyrolysis of Several Organic Geopolymers	409
14.1. Humin, Humic Acids, and Fulvic Acids	409
14.2. Coal	416
14.3. Peat	423
14.4. Kerogens	426
References	430
15. Analytical Pyrolysis of Other Natural Organic Polymers	435
15.1. Uncommon Organic Polymers	435
15.2. Diversity of Organic Polymers	436
References	437
 Part 3. Applications of Analytical Pyrolysis on Composite Natural Organic Materials	 439
16. Analytical Pyrolysis of Plant Materials	441
16.1. Wood	441
16.2. Leaves and Other Plant Parts	442
<i>Pyrolysis of pine needles</i>	443
<i>Pyrolysis products and smoke from the leaf of <i>Nicotiana tabacum</i></i>	444
<i>Pyrolysis of other plant tissues</i>	461
16.3. Decomposing and Subfossil Plant Materials	462
16.4. Pulp and Paper	464
References	466
17. Analytical Pyrolysis of Microorganisms	471
17.1. Characterization of Microorganisms by Pyrolytic Techniques	471
17.2. Utilization of Pyrolytic Techniques to Detect Biomass	477
References	479
18. Other Applications of Analytical Pyrolysis	485
18.1. Pyrolytic Techniques Used in Pathology	485
18.2. Pyrolytic Techniques Used in Food Characterization	486
18.3. Pyrolytic Techniques Used in Forensic Science, Archeology, and Art	486
18.4. Pyrolysis Used for Waste Characterization	487
References	489
 Index	 491

This Page Intentionally Left Blank

PART 1

An Introduction to Analytical Pyrolysis

This Page Intentionally Left Blank

CHAPTER 1. Introduction and Nomenclature

1.1 Pyrolysis as a Chemical Process.

Pyrolysis is defined as a chemical degradation reaction that is caused by thermal energy alone [1,2,3]. The term *chemical degradation* refers to the decompositions and eliminations that occur in pyrolysis with formation of molecules smaller than the starting material. The requirement that thermal energy is the only cause of these chemical degradations refers to the absence of an added reagent to promote pyrolysis. However, instead of heat itself, temperature (which is the intensive parameter of heat) is more appropriate to use in the definition of pyrolysis. The term *pyrolysis* should be used to indicate the chemical transformation of a sample when heated at a temperature significantly higher than ambient. Otherwise, a chemical decomposition caused by thermal energy but taking place at a very low temperature or in a very long period of time would be considered pyrolysis. Pyrolysis is indeed a special type of reaction, because at elevated temperatures certain reactions have much higher rates, and many compounds undergo reactions that do not occur at ambient or slightly elevated temperatures.

The pyrolytic reactions usually take place at temperatures higher than 250–300° C, commonly between 500° C and 800° C. The chemical transformations taking place under the influence of heat at a temperature between 100° C and 300° C are commonly called *thermal degradations* [4] and not pyrolysis. Mild pyrolysis is considered to take place between 300° C and 500° C and vigorous pyrolysis above 800° C.

The term pyrolysis is not restricted to the decomposition of pure compounds. The same term is frequently used in the literature in connection with the thermal decomposition of many complex materials such as coal, oil shales, etc. or even of composite materials such as wood or whole microorganisms.

There are a few problems associated with the definition of the term pyrolysis as being related to heat alone. For example, it is not possible to be sure that no catalytic effects are associated with some thermal decompositions [1] or that no chemical reactions take place between the pyrolysis products (one or more such products acting as reagents). The chemical interactions between the reaction products in pyrolysis and the catalytic effects are decreased by performing the pyrolysis in an atmosphere of inert gas or at reduced pressure. A pyrolysis that is influenced by the intentional addition of a catalyst is named *catalytic pyrolysis*. Also, pyrolysis in the presence of a reagent added on purpose has been reported. In this type of pyrolysis, the decomposition of the sample is still caused by heat alone, but a reagent is present and may react with the pyrolysis products to generate new compounds. Sometimes, from the organic polymers, molecules larger than a starting constituent can also be generated during pyrolysis [5].

1.2 The Scope of Analytical Pyrolysis.

Analytical pyrolysis is by definition the characterization of a material (or a chemical process) by chemical degradation reactions induced by thermal energy. It consists of a collection of techniques involving pyrolysis performed with the purpose of obtaining analytical information on a given sample. The type of analytical information can be

qualitative, quantitative, or structural. Pyrolysis itself, being a chemical reaction, does not provide analytical data unless it is associated with some kind of measurement process. The measurement is commonly part of a typical analytical technique such as a chromatographic or spectroscopic one. The purpose of the analytical technique is the analysis of the pyrolysis product [*pyrolysate (pyrolyzate)*].

If a physical property of a sample is measured during heating as a function of temperature, the technique is commonly named a *thermoanalytical* technique. Analytical pyrolysis is considered somehow apart from the other thermoanalytical techniques such as thermometry, calorimetry, thermogravimetry, differential thermal analysis, etc. In contrast to analytical pyrolysis, thermoanalytical techniques are not usually concerned with the chemical nature of the reaction products during heating. Certainly, some overlap exists between analytical pyrolysis and other thermoanalytical techniques. The study of the kinetics of the pyrolysis process, for example, was found to provide useful information about the samples and it is part of a series of pyrolytic studies (e.g. [6-8]). Also, during thermoanalytical measurements, analysis of the decomposition products can be done. This does not transform that particular thermoanalysis into analytical pyrolysis (e.g. [9]). A typical example is the analysis of the gases evolved during a chemical reaction as a function of temperature, known as EGA (evolved gas analysis).

There are many applications of analytical pyrolysis and a large number of them are geared toward polymer analysis or composite material analysis. The analysis of intact polymers, for example, is a rather difficult task. Polymers are not volatile; some of them have low solubility in most solvents and some decompose easily during heating. Therefore the direct application of powerful analytical tools such as gas chromatography/mass spectroscopy (GC/MS) cannot be done directly on most polymers. The same is true for many composite materials. Pyrolysis of these kinds of samples (polymers, composite organic materials) generates, in most cases, smaller molecules. These can easily be analyzed using GC/MS or other sensitive analytical procedures. From the "fingerprint" of the pyrolysis products, valuable information can be obtained about the initial sample. In analytical pyrolysis, instead of adjusting the analytical method for a particular sample, the sample is "adjusted" for a particularly good analytical technique. Analytical pyrolysis is therefore a special methodology which allows the use of available proven analytical methods for the analysis of samples that are not originally amiable to a particular analytical method. These characteristics of analytical pyrolysis indicate that there will be two separate subjects of interest when discussing analytical pyrolysis:

- the pyrolytic process, and
- the analytical method that is applied for the analysis of the pyrolysis products.

The purpose of analytical pyrolysis is to provide analytical information on the initial sample. The pyrolysis itself is just a process that allows the transformation of the sample into other compounds. The fact that no catalytic effects take place in addition to the pure thermal decomposition is not important. Also the breaking or the formation of chemical bonds makes no difference for the purpose of analytical pyrolysis. On the other hand, a set of conditions such as good reproducibility, formation of stable reaction products, etc. is very important for the chemical process generated by heat to make it adequate for providing correct analytical information. The experimental conditions used

for performing pyrolytic reactions play an important role for the end result of the process. For this reason, the pyrolytic process in analytical pyrolysis must be strictly controlled regarding the temperature, pyrolysis time, atmosphere, etc.

Commonly, analytical pyrolysis is performed as *flash pyrolysis*. This is defined as a pyrolysis that is carried out with a fast rate of temperature increase, of the order of $10,000^{\circ}$ K/s. After the final pyrolysis temperature is attained, the temperature is maintained essentially constant (*isothermal pyrolysis*). Special types of analytical pyrolysis are also known. One example is *fractionated pyrolysis* in which the same sample is pyrolysed at different temperatures for different times in order to study special fractions of the sample. Another special type is *stepwise pyrolysis* in which the sample temperature is raised stepwise and the pyrolysis products are analyzed between each step. *Temperature-programmed pyrolysis* in which the sample is heated at a controlled rate within a temperature range is another special type.

Pyrolysis is commonly carried out in an inert atmosphere. However, *oxidative pyrolysis* (a pyrolysis that occurs in the presence of an oxidative atmosphere) or *reductive pyrolysis* (a pyrolysis that occurs in the presence of a reducing atmosphere) is sometimes utilized.

There are numerous analytical techniques associated (hyphenated) with pyrolysis and many literature sources describing these analytical techniques. One of the most common such techniques is *pyrolysis-gas chromatography* (Py-GC). In this technique the volatile pyrolysates are directly conducted into a gas chromatograph for separation and detection (a *volatile pyrolysate* is that portion of the pyrolysate that has adequate vapor pressure to reach the detector). Another common technique is *pyrolysis-gas chromatography/mass spectrometry* (Py-GC/MS). In this technique the volatile pyrolysates are separated and analyzed by on-line gas chromatography/mass spectrometry. Infrared analysis can be used in the same way as mass spectrometry in another hyphenated technique, *pyrolysis-gas chromatography/infrared spectroscopy* (Py-GC/IR). The chromatographic separation can sometimes be excluded from the analytical process following the pyrolysis. This is, for example, the case of *pyrolysis-mass spectrometry* (Py-MS), in which the volatile pyrolysates are detected and analyzed by on-line mass spectrometry, and *pyrolysis-infrared spectroscopy* (Py-IR). A variety of other techniques are also utilized for the analysis of pyrolysates.

1.3 Analytical Pyrolysis Applied to Natural Organic Polymers.

The usefulness of analytical pyrolysis in polymer characterization, identification, or quantitation has long been demonstrated. The first application of analytical pyrolysis can be considered the discovery in 1860 of the structure of natural rubber as being polyisoprene [10]. This was done by the identification of isoprene as the main pyrolysis product of rubber. Natural organic polymers and their composite materials such as wood, peat, soils, bacteria, animal cells, etc. are good candidates for analysis using a pyrolytic step.

In principle, there is no difference between the analytical pyrolysis of natural organic polymers and that of other samples. Although the basics are the same, there are

numerous specific aspects regarding the application of analytical pyrolysis in the analysis of natural organic polymers.

The most important information obtained in the analytical pyrolysis of polymers is the description of the resulting chemical compounds during or after pyrolysis. The nature and quantity of the compounds generated during pyrolysis provide the pertinent information about the sample either as a "fingerprint" of the sample or by the correlation of the degradation products of the polymer or material with its structure. For the polymers made from connected identical units (repetitive polymers), this correlation is simpler. However, for non-repetitive polymers, such as lignin or Maillard browning polymers, it is more difficult to understand the polymeric structure from their pyrolysis products.

The applications of pyrolysis to both natural or synthetic polymers range from the polymer detection used for example in forensic science to the microstructure elucidation of specific polymers or to the identification of other compounds present in the polymers (anti-oxidants, plasticizers, etc.). Applications to complex polymeric materials are in the field of classification of microorganisms, fossil materials, etc. Also, the degradation of polymers during heating is a subject of major interest in many practical applications regarding the properties of polymers. Analytical pyrolysis can also be used for obtaining information on the resulting chemicals during the burning of different materials. It should be noted that burning in itself is the chemical reaction with oxygen, which leads most organic compounds to form CO_2 , CO , H_2O , N_2 , etc. However, incomplete burning (smoldering) and the pyrolysis around the burning area generate pyrolysates that can have complex compositions. Their analysis can be important in connection with health issues, environmental problems, or taste of food or of cigarettes.

The first part of this book, dedicated to the description of the analytical pyrolysis methodology, will not be specific to natural organic polymers. The second and the third part, however, will cover only applications specific to natural organic polymers, chemically modified natural organic polymers, and their composite materials.

References 1.

1. C. D. Hurd, *The Pyrolysis of Carbon Compounds*, A.C.S. monograph series, The Chemical Catalog Co., New York, 1929.
2. W. J. Irwin, *J. Anal. Appl. Pyrol.*, 1 (1979) 3.
3. I. Ericsson, R. P. Lattimer, *J. Anal. Appl. Pyrol.*, 14 (1989) 219.
- 3a. P. C. Uden, Nomenclature and Terminology for Analytical Pyrolysis (IUPAC recommendations 1993), *J. Anal. Appl. Pyrol.*, 31 (1995) 251.
4. L. S. Ettre, A. Zlatkis, *The Practice of Gas Chromatography*, Interscience, New York, 1967.
5. T. P. Wampler (ed.), *Applied Pyrolysis Handbook*, M. Dekker Inc., New York, Basel, Hong Kong, 1995.

6. S. A. Liebman, E. J. Levy, (ed.) *Pyrolysis and GC in Polymer Analysis*, M. Dekker, New York, 1985, p. 149.
7. M. Blazso, G. Varhegyi, E. Jakab, *J. Anal. Appl. Pyrol.*, 2 (1980) 177.
8. J. Piskorz, D. Radlein, D. S. Scott, *J. Anal. Appl. Pyrol.*, 9 (1986) 121.
9. W. W. Wendland, *Thermal Analysis*, J. Wiley, New York, 1986.
10. G. C. Williams, *J. Chem. Soc.*, 15 (1862) 110.

This Page Intentionally Left Blank

Chapter 2. The Chemistry of the Pyrolytic Process

2.1 General Remarks.

The pyrolysis of one molecular species may consist of one or more pyrolytic reactions occurring simultaneously or sequentially. The path of a pyrolytic process depends on the experimental conditions. Mainly for polymers, after a first decomposition reaction step, it is common to have subsequent steps. In this case, the polymeric chain scission, for example, is followed by other pyrolytic reactions of the small molecules generated from the polymer. Therefore, pyrolysis of both small and large molecules occurs in the pyrolysis of a polymer. The result is a complex sequence of chemical reactions with a variety of compounds generated.

When composite materials are pyrolysed, more than one molecular species is subject to thermal degradation. However, for composite materials each component can be considered as starting the pyrolytic process independently, which reduces somewhat the complexity of the problem.

The pyrolytic process is commonly performed in an inert atmosphere or even at low pressure. However, it is not always possible to perform the process in gas phase (such as for polymers). Even in gas phase, but mainly in condensed phase, a series of chemical interactions may occur between different pyrolysis products. This, in addition to the multi-step characteristics, makes the result of the pyrolytic process extremely complex. The individual reaction types taking place during pyrolysis can, however, be studied independently.

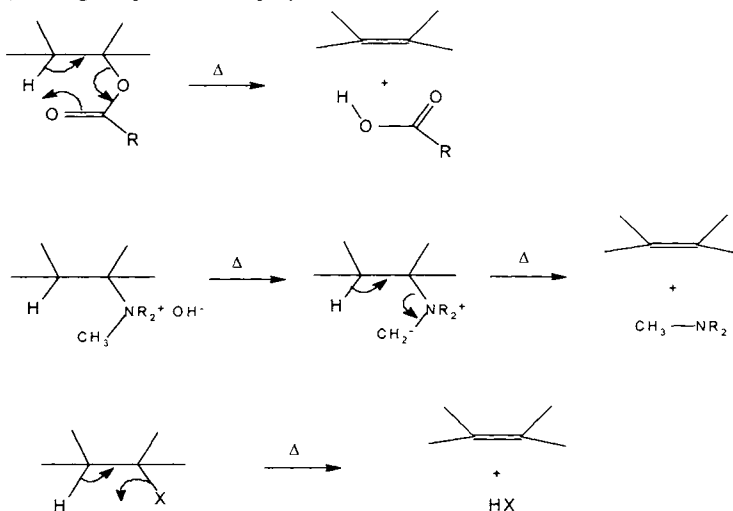
2.2 Elimination Reactions in Pyrolysis.

The pyrolytic elimination is a model reaction, which probably dominates many pyrolytic processes. The β elimination with two groups lost from adjacent atoms is common in pyrolysis. A model pyrolytic elimination takes place with no other reagent present and often requires gas phase. For this reason, the typical E_2 mechanism where a proton and another group from a molecule depart simultaneously, the proton being pulled by a base, is not common in pyrolysis in gas phase. The same is true for the E_1 mechanism. More common for the gas phase pyrolysis is an E_i mechanism. However, for polymers where the pyrolysis takes place in condensed phase, E_2 and E_1 mechanisms are not excluded. There are also several other mechanisms that have been found to operate in pyrolytic eliminations.

- *Pyrolytic elimination with E_i mechanism.*

A first type of mechanism involves a cyclic transition state, which may be four-, five- or six-membered [1]. No discrete intermediate is known in this mechanism

(concerted mechanism). Some examples of different sizes of cyclic transition state (heating is symbolized by Δ) are



The two groups (one being the H in the above examples) leave at about the same time and bond to each other. The designation of this mechanism is E_1 (in Ingold terminology). There are typical characteristics for the E_1 mechanism:

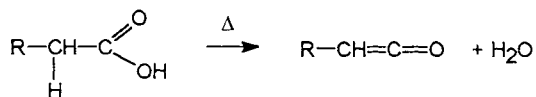
- The kinetics is of the first order.
- It does not take place with a free radical mechanism (free radical inhibitors do not slow the reaction).
- The elimination takes place in a "syn" position.

During pyrolytic reactions of E_1 type, if a double bond is present, the formation of a conjugate system is preferred if sterically possible. Otherwise, the orientation in the pyrolytic elimination is statistical and is determined by the number of β hydrogens. The newly formed double bond goes mainly toward the least highly substituted carbon (Hofmann's rule). In the bridged systems, the double bond is formed away from the bridgehead. Also, for the E_1 mechanism, a cis β hydrogen is required. Therefore, in cyclic systems, if there is a cis hydrogen on only one side, the double bond will go that way. However, when there is a six-membered transition state, this does not necessarily mean that the leaving groups must be cis to each other, since such transition states do not need to be completely coplanar. If the leaving group is axial, then the hydrogen must be equatorial and cis to the leaving group, since the transition state cannot be realized when the groups are both axial. But if the leaving group is equatorial, it can form a transition state with a β hydrogen that is either axial (cis) or equatorial (trans).

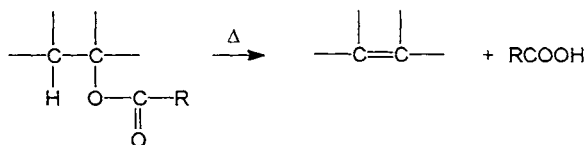
In some cases, an E_1 mechanism appears to be followed and the more stable olefin is formed. Instead of Hofmann's rule, Zaitsev's rule is followed (the double bond goes mainly toward the most highly substituted carbon). Also, in some reactions the direction of elimination is determined by the need to minimize steric interactions, sometimes even when the steric hindrance appears only during the transition state.

Cases of E_i eliminations are common in pyrolysis. Most of these reactions occur with double or triple bond formation. Several examples are given below.

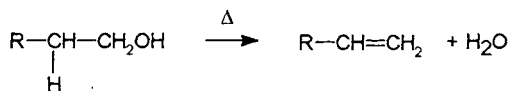
- Dehydration of some carboxylic acids with the formation of ketenes:



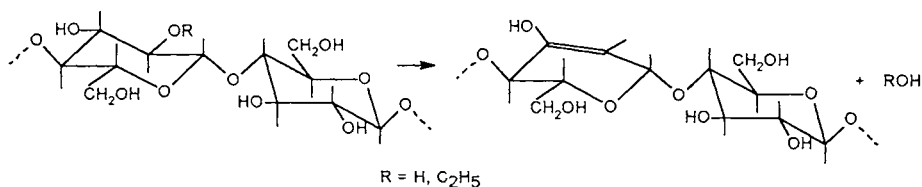
- Elimination of an acid from some esters:



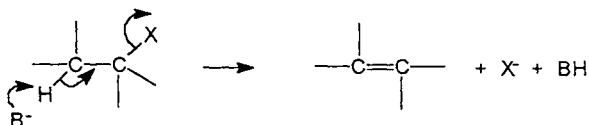
- Elimination of water from alcohols:



When occurring for large molecules, it is not always possible to assign to the elimination an E_i mechanism. An example is the elimination of water or ethanol during the pyrolysis of cellulose or ethyl cellulose, respectively:

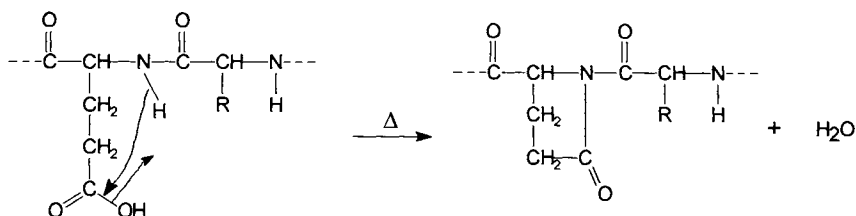


This reaction may have either an E_i mechanism or an E_2 mechanism because it takes place in condensed phase. It should be remembered that an E_2 reaction occurs as follows:



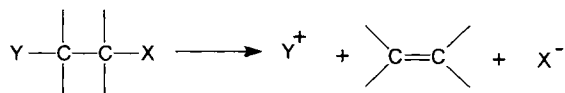
The impurities in the polymer may act as a proton acceptor. The formation of a dehydrated cellulose is, for example, favored by the presence of traces of a strong base (NaOH) in the polymer. This base pulls off the protons during dehydration. The polymer in itself may act as a base, for example in the elimination of H_2SO_4 from cellulose sulfate (see Section 7.3).

Besides β eliminations, 1,3 or 1,n eliminations may also take place during pyrolysis with the formation of cycles. An example of this type of reaction occurs during the pyrolysis of certain peptides (and proteins). A glutamic acid unit, for example, can eliminate water by the following reaction:

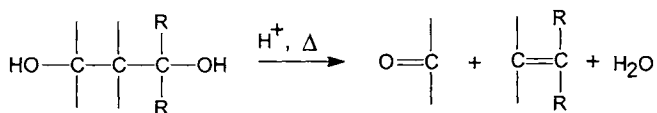


- *Fragmentations.*

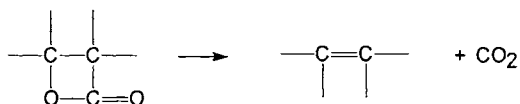
In an elimination, one carbocation can be a leaving group. In this situation, the reaction is called a fragmentation. The reaction commonly takes place in substances of the form Y-C-C-X, where X could be halogen, OH_2^+ , OTs, NR_3^+ , etc. (Ts is p-toluenesulfonate or tosylate). The fragmentation can be written schematically:



An example of this type of reaction is the following dehydration of 1,3-diols:

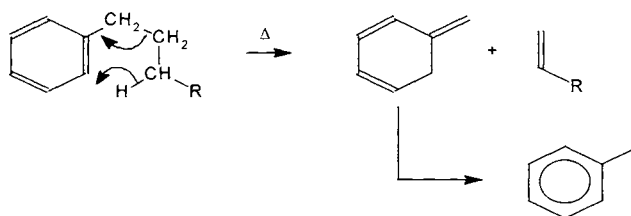


Another example is the decomposition of β -lactones (applies also to ketene dimers):

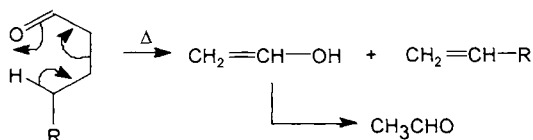


Some examples of fragmentation reactions are given below.

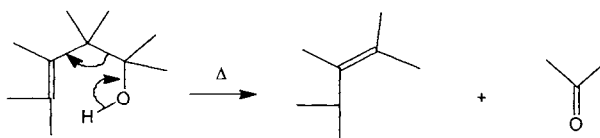
Fragmentation of alkyl-aromatic hydrocarbons:



Fragmentation of certain ketones:



The double (or triple) bond formation does not take place exclusively between carbon atoms. It may occur between carbon and nitrogen or carbon and oxygen. An example is the pyrolysis of β -hydroxy olefins:



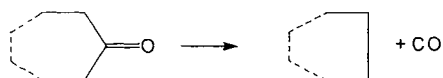
During pyrolysis, numerous other fragmentation reactions may occur, although the mechanism is not always E_i , E_1 or E_2 type (see eliminations involving radicals).

- *Extrusion reactions.*

An extrusion reaction is a reaction of the type:

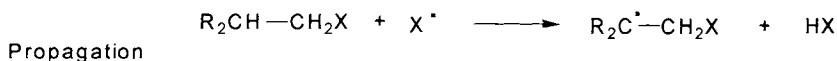
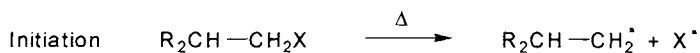


Decarboxylation of β -lactones described above may be considered a degenerate reaction of this type. Another example is the loss of CO from certain ketones:

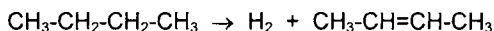
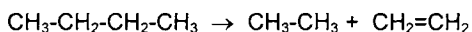
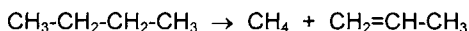


- *Elimination involving free radicals.*

Another common type of mechanism found to operate in pyrolytic eliminations involves free radicals. Initiation occurs by pyrolytic cleavage. A schematic example of this type of reaction is



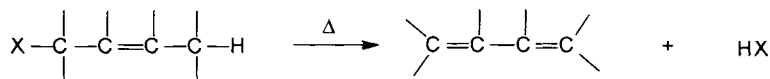
Free radical eliminations are frequent during pyrolytic reactions, and they are common for linear chain polymers. At higher temperatures (600° C–900° C) this type of reaction is also common for small molecules and explains the formation of unsaturated or aromatic hydrocarbons from aliphatic ones. As an example, butane decomposition may take place as follows:



More examples of this type of reaction will be given in Section 2.6.

- 1,4 Conjugate eliminations.

In addition to the main mechanisms, another possible type of elimination is the 1,4 conjugate elimination. This type of mechanism is not very common [1]. The elimination takes place as follows:

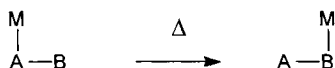


2.3 Rearrangements Taking Place in Pyrolysis.

A rearrangement is a reaction in which a group moves (migrates) from one atom to another in the same molecule. A variety of rearrangements can take place during pyrolysis. Several known types are the following:

- *Migration of a group.*

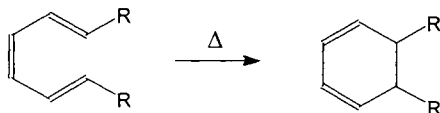
Most migrations take place from one atom to an adjacent one (1,2 shift). However, migrations over higher distances are also known. A typical 1,2 shift takes place as follows:



The migration group M may move with its electron pair, without its electron pair, or with only one electron. In this last case, a free radical rearrangement takes place. The free radical rearrangement involves a first step of free radical formation, and then the actual migration takes place. During pyrolysis, under the influence of heat, the formation of free radicals is rather common. A typical characteristic for 1,2 free radical migrations is that this type of migration is not known for hydrogens, is uncommon for methyl groups, and is not too frequent for alkyl groups in general. More complicated mechanisms may occur for diradicals [1]. The 1,2 shifts are more common for aryl, vinyl, acetoxy, and halogen migrating groups. Longer free-radical migrations are known even for hydrogen. These types of reactions are common during the pyrolytic process, and several examples will be discussed in the second part of this book.

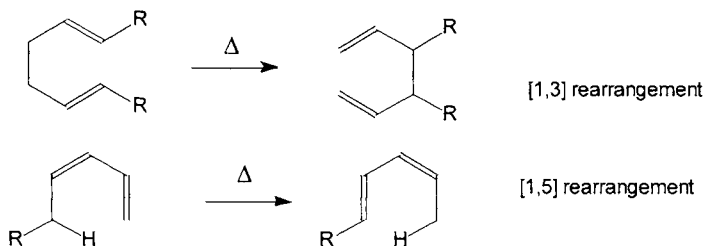
- *Electrocyclic rearrangements.*

A different type of known rearrangement is the electrocyclic rearrangement. This takes place for example for 1,3,5 trienes, which are converted to 1,3 cyclohexadienes when heated, as follows:



- *Sigmatropic rearrangements.*

Sigmatropic rearrangements are also non-1,2 shifts. This rearrangement consists of a migration of a σ bond adjacent to one or more π systems to a new position in the molecule, with a new reorganized π system. Examples are



The order [i,j] of the sigmatropic reaction is determined by counting the atoms over which each end of the σ bond has moved. For a more detailed discussion about rearrangement reactions see e.g. [3].

2.4 Oxidations and Reductions Taking Place in Pyrolysis.

The oxidation/reduction defined as an increase/decrease, respectively, in the oxidation number, cannot be applied directly in organic chemistry. This is due to the difficulty of defining the oxidation number for organic compounds. For example, the carbon in pentane has the formal oxidation number -2.4, while in methane it is -4. For this reason, an "approximate" oxidation number must be assigned to each compound more or less arbitrarily. Saturated hydrocarbons have the assigned oxidation number -4; alkenes, alcohols, mono-chlorinated aliphatic hydrocarbons, and amines have the assigned oxidation number -2; compounds with triple bonds, aldehydes, ketones, diols, etc. have the assigned oxidation number 0; acids, amides, and trichlorinated aliphatic hydrocarbons have the assigned oxidation number +2; and CO_2 and CCl_4 have the assigned oxidation number +4. Using this arbitrary assignment, the common definition for oxidation/reduction can be applied.

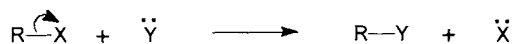
The hydrogen elimination is a typical oxidation reaction that is not uncommon in pyrolysis. Some other oxidations or reductions may take place during pyrolysis as a subsequent reaction to the initial process. Certain free-radical substitutions that involve the transfer of a hydrogen atom can also be considered oxidation/reduction reactions. It should be noted that oxidation due to the presence of oxygen (intended or accidental) may also take place during pyrolysis (below ignition temperature). As an example, substituted ethyl celluloses degrade oxidatively [3a]. The reaction probably starts with the initiation step at free aldehyde groups and has a free radical mechanism (see Section 7.3). This explains the formation of formic acid, acetaldehyde, ethanol, ethyl formate, ethane, CO_2 , CO, etc. from this material.

2.5 Substitutions and Additions Taking Place in Pyrolysis.

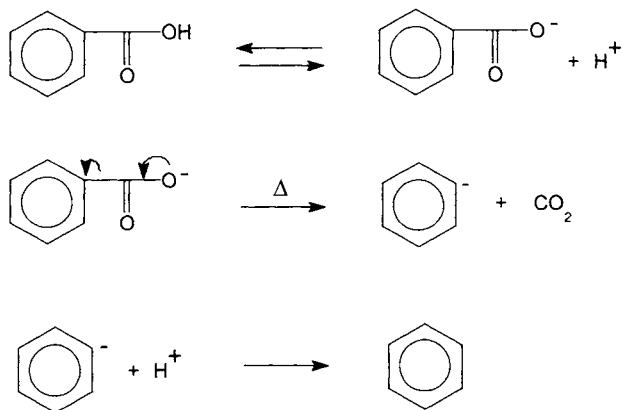
Either as a first step of pyrolysis, or as a result of the interaction of molecules resulting from previous pyrolysis steps, substitutions and additions are common reactions during the pyrolytic process.

- *Substitutions.*

Substitutions are very common chemical reactions. The increased reaction rate due to the high temperature in pyrolysis makes reactions of this type possible. The nucleophilic substitution takes place with the attack of a reagent that brings an electron pair to the substrate. This pair is used to form a new bond. The leaving group retains its electron pair. The general scheme of this type of reaction can be written as follows:



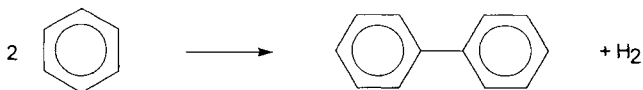
It is interesting to note that the decarboxylation mechanism of aromatic acids is probably an electrophilic substitution. This reaction is not uncommon during pyrolysis. For example, the decarboxylation of benzoic acid takes place as an aromatic electrophilic substitution:



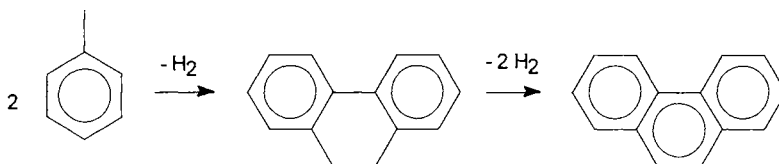
In the electrophilic aromatic substitution, in the first step the electrophile attacks the substrate with the formation of an arenium ion. This is followed by a second step in which one of the leaving groups departs.

The decarboxylation of aliphatic acids may take place as an aliphatic electrophilic substitution but also in some cases can be regarded as an elimination reaction using a cyclic mechanism as described in Section 2.1.

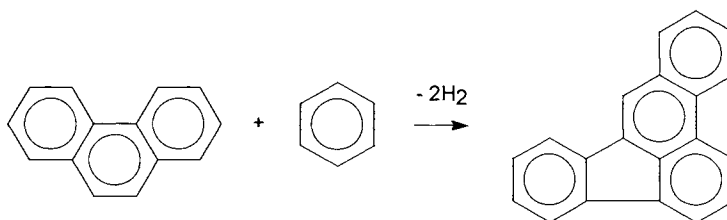
Free radical substitutions are also known to occur in pyrolytic reactions. An example of this type is the formation of biphenyl from benzene at $700^\circ C$ (this reaction can be viewed as an oxidation because of the hydrogen elimination). It is likely that similar reactions take place in the pyrolysis of coal and kerogen.



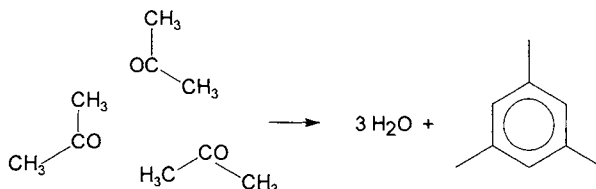
This type of reaction may also take place for substituted benzene:



and can further generate higher polynuclear aromatic hydrocarbons. An example is given for the formation of benzo[b]fluoranthene:

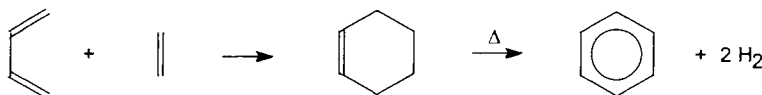


An interesting example of a substitution reaction is the condensation of acetone with the formation of a molecule that is more stable at higher temperatures.

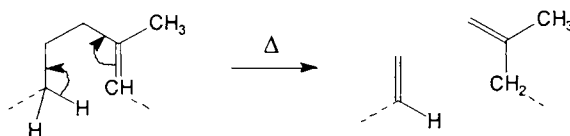


- Additions.

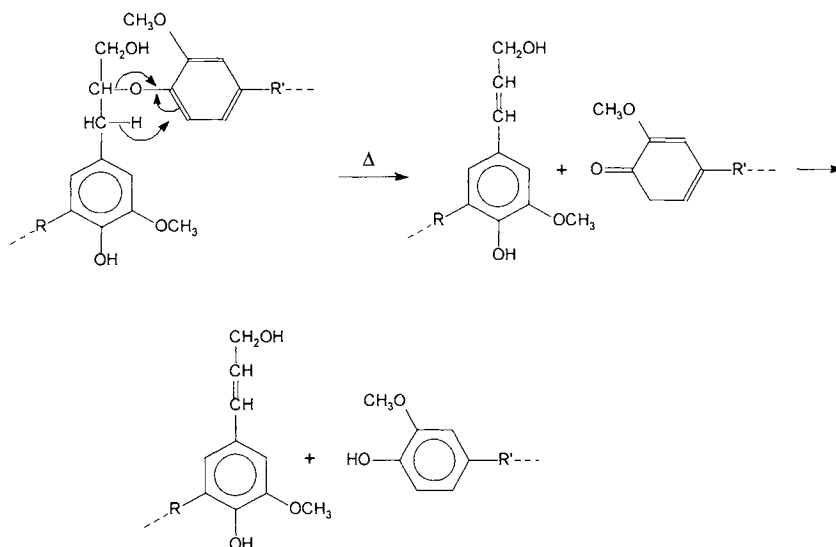
The addition reactions take place at a carbon-carbon multiple bond, or carbon-hetero atom multiple bond. Because of this peculiarity, the addition reactions are not common as the first step in pyrolysis. The generation of double bonds during pyrolysis can, however, continue with addition reactions. The additions can be electrophilic, nucleophilic, involving free radicals, with a cyclic mechanism, or additions to conjugated systems such as Diels-Alder reaction. This type of reaction may explain, for example, the formation of benzene (or other aromatic hydrocarbons) following the radicalic elimination during the pyrolysis of alkanes. In these reactions, after the first step with the formation of unsaturated hydrocarbons, a Diels-Alder reaction may occur, followed by further hydrogen elimination:



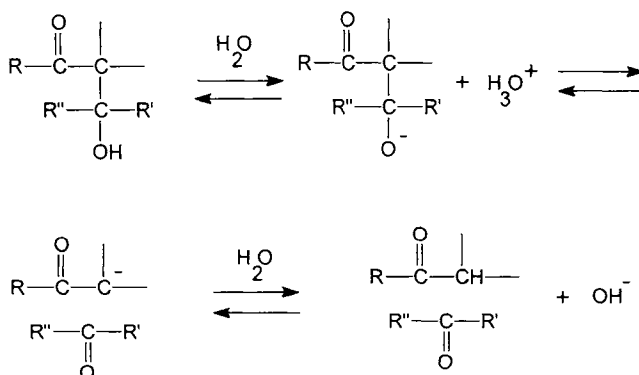
Some pyrolytic reactions can be seen as a reverse (retrograde) addition. Diels-Alder reaction for example is known to be reversible and retro Diels-Alder reactions are rather common. The retro-ene reaction (retro hydro-allyl addition), for example, takes place by the following mechanism:



A possible retro-ene reaction may take place during the lignin degradation, as follows:



Retro-aldol condensations are also known to take place during pyrolysis. The mechanism of these reactions can be written as follows:



An example of a retrograde aldol reaction (retroaldolization) is probably the pyrolytic decomposition of cellulose with formation of hydroxyacetaldehyde (see Section 7.2). Other mechanisms for pyrolysis of cellulose are also possible [3]. More paths for the same process is a common occurrence in pyrolysis, and more than one mechanism is frequently needed to explain the variety of reaction products.

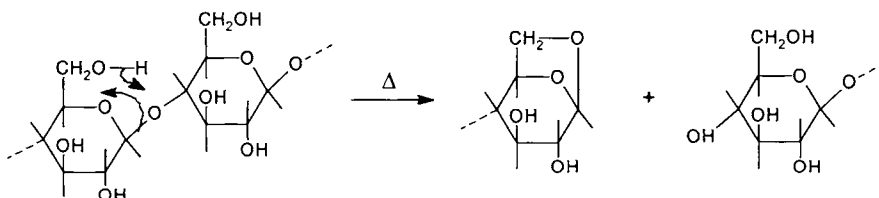
2.6 Typical Polymer Degradations during Pyrolysis.

Any polymer degradation during pyrolysis consists of chemical reactions of the types described in Section 2.1 to Section 2.5. However, for a better understanding of the expected pyrolysis products of a polymer, a specific classification can be made allowing the correlation of the nature of the reaction products with the structure of the polymer. It is possible to categorize polymer degradation reactions as follows:

- Polymeric chain scission.

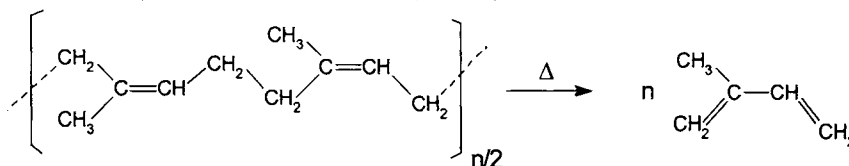
The polymeric chain scission is an elimination reaction that takes place by breaking the bonds that form the polymeric chain. When the reaction takes place as a successive removal of the monomer units from the polymeric chain, it is called a *depolymerization*. It also may occur as a *random cleavage* of the polymer chain, and this happens mainly when the bonding energies are similar along the chain. If no intramolecular rearrangement takes place, the result of random cleavage is the formation of oligomers. If the chain scission is followed by secondary reactions, this leads to a variety of compounds such as cyclic oligomers.

The chain scission can be seen as a pyrolytic elimination reaction. All mechanisms described in Section 2.2 may take place during chain scission. A reaction of chain scission with a cyclic transition state may take place, for example, during cellulose pyrolysis:



This reaction is considered a transglycosidation reaction.

Some other chain scissions have a free radical mechanism [4,5]. As an example, the formation of isoprene from natural rubber probably falls in this class:

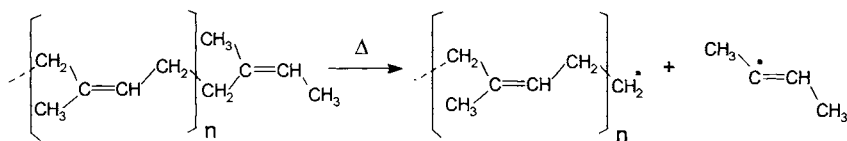
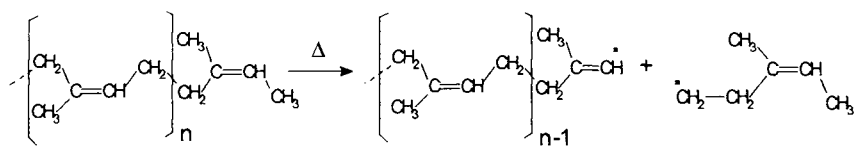


Only up to 58% of natural rubber can be practically depolymerized to isoprene during pyrolysis. A random chain scission may also take place along the polymeric chain. The result is the formation of molecules of lower molecular weight. However, in order to be volatile enough to be analyzed by typical analytical techniques associated with analytical pyrolysis, these fragments have to be relatively small. The formation of monomers as a final step in the random chain scission is not uncommon, and sometimes it is difficult to decide if a depolymerization or a random chain scission was the first step in pyrolysis.

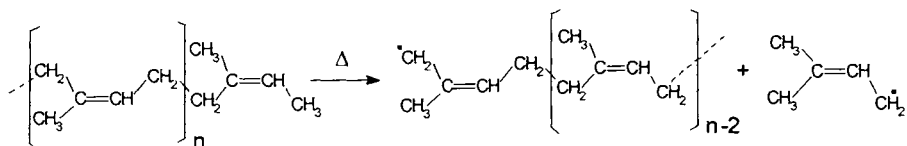
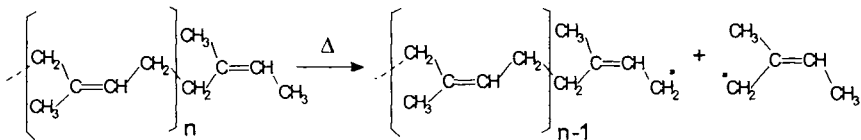
The free radical mechanism responsible for the polymeric chain scission is basically not different from elimination involving free radicals described in Section 2.2. However, the process can be more complicated and some particularities are described below.

For the initiation step, the free radicals formed may consist of one free radical chain plus one monomeric free radical, one free radical chain plus one low molecular weight free radical different from the monomer, or may consist of two free radical chains. The random chain scission could take place truly randomly or at the weaker link. Some possibilities are exemplified below with poly-isoprene taken as the model:

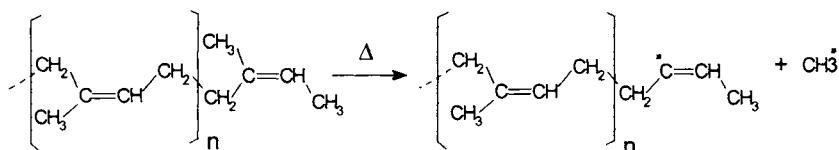
A. α -chain scission (for this particular reaction it is estimated that the bond dissociation energy is about 83–94 kcal mol⁻¹):



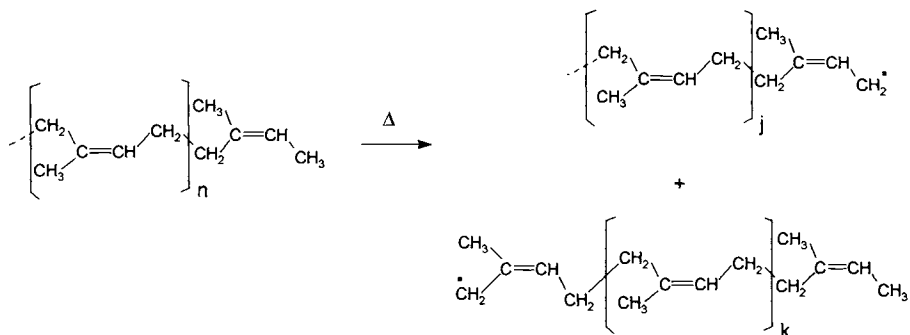
B. β -chain scission (for this particular reaction it is estimated that the bond dissociation energy is about 61.5–63 kcal mol⁻¹):



C. methyl scission:

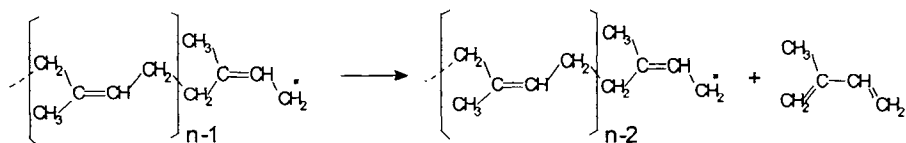


The scission may take place at the end of the chain or in the middle of it:

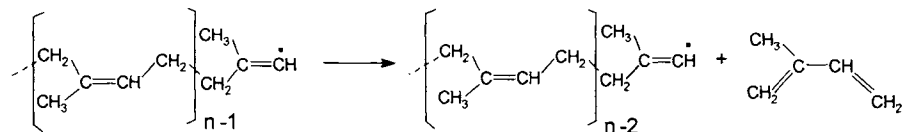


These types of mechanisms can be applied to most linear polymers. During the initiation reaction, the weaker bonds usually tend to dissociate first. It was noticed, for example, that the bonds (not including the bond to an sp^2 carbon) of a carbon atom in α position to the double bond (the allyl carbon) are weaker than other C-C or C-H bonds. Therefore, the polymer containing an allyl carbon will be more likely to be involved in an initiation reaction. However, other reactions are not excluded in the free radical formation.

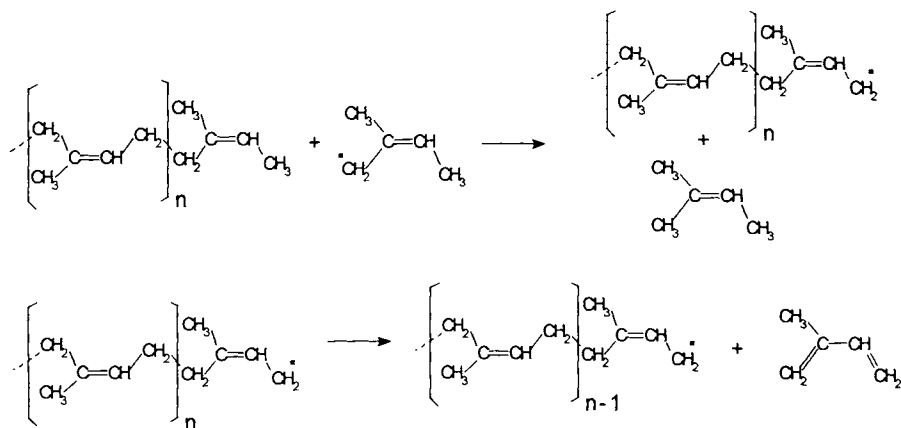
Propagation is the second step in the free radical chain reaction. The free radicals generated by β -chain scission can eliminate the monomer by scission of another β -link and shorten the macromolecular radical chain by the reaction:



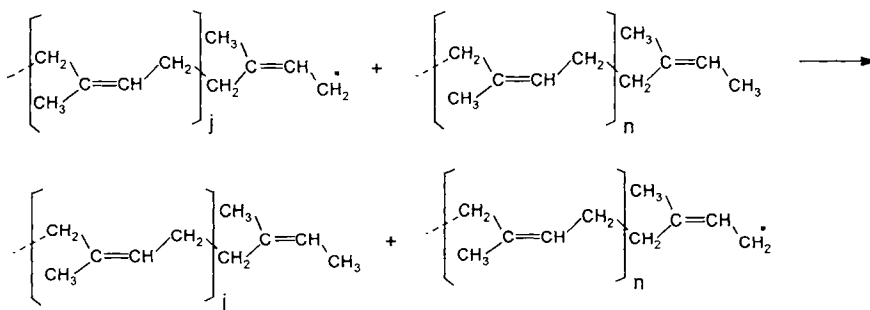
The free radicals formed by α -scission can also eliminate the monomer by the reaction:



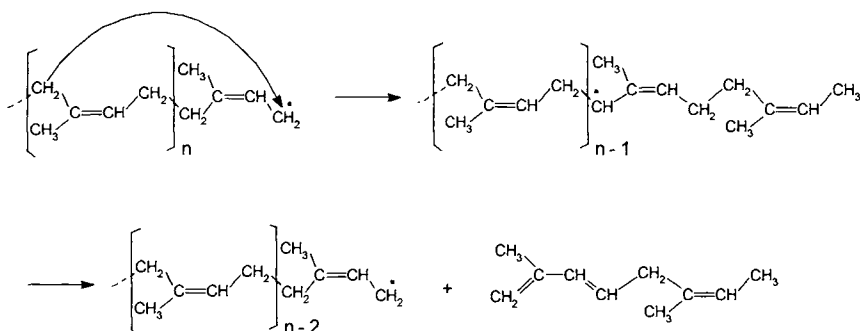
As a rule, the stability of the free radical chains is higher than that of a small free radical. As a result, a simple propagation reaction may take place with the formation of monomers by the following scheme:



The disproportionation reaction of the free radical chain can generate the monomer as a successive process. There are, however, some other issues regarding the propagation for free radical chain reactions. In addition to the "regular" propagation step, different reactions may occur in a so-called transfer step. In this step, the free radical chain reacts with another molecule and generates a different radical chain and a new polymeric molecule. There are two possible types of transfer reactions. The transfer step can be an intermolecular chain transfer or an intramolecular chain transfer. An example of an intermolecular chain transfer is

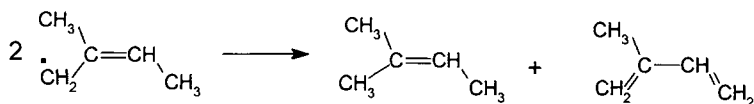


An intramolecular (free radical) chain transfer takes place as an intramolecular rearrangement, and an example of this kind of transfer is shown below:

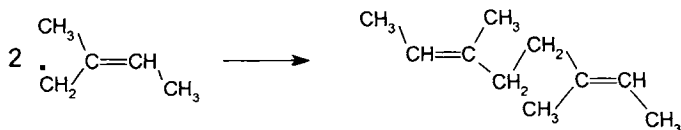


This type of reaction explains (in part) the formation of the isoprene dimer during rubber pyrolysis. The same compound may also be formed from other reactions such as isoprene dimerization.

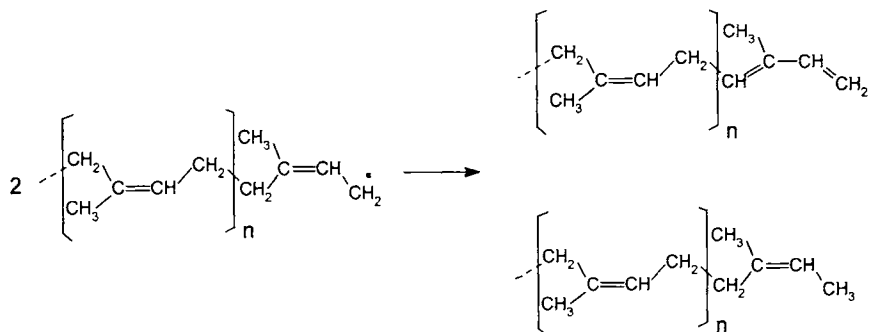
The radical reactions can be terminated by the usual disproportionation:



The recombination of the two free radicals is also possible:



The same types of reactions may take place for the free radical chains. Either a disproportionation or a recombination may take place. The disproportionation for the polymer used here as an example will be



In the discussion of the example chosen above, not all the possibilities were considered. For example, during the propagation process the formation of smaller molecules from the free radical chains were shown to take place with the dissociation of the weaker bonds, which are expected to dissociate first. This was also shown for the free radical formation. The strength of the bond being broken is commonly unknown, but it can be derived from tabulated heats of formation as shown in Section 3.1. Besides the weaker bonds, other bonds can also be dissociated, most commonly when there are small differences between the bond dissociation energies.

Another source of generating a variety of compounds during pyrolysis is the diversity of intramolecular transfer steps. This explains for example the formation of 1-methyl-4-isopropenylcyclohexene (limonene) during the pyrolysis of polyisoprene (see Section 6.1).

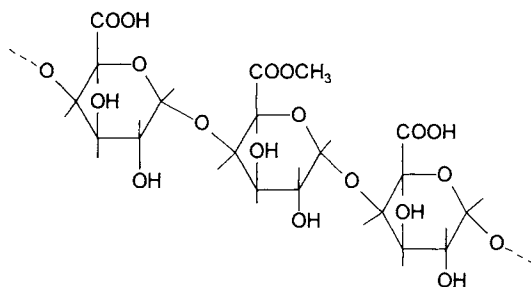
Only some of the possible alternatives are considered above. The complexity of the result of a polymer pyrolysis is, therefore, considerable, even considering only the chain scission.

- Side group reactions.

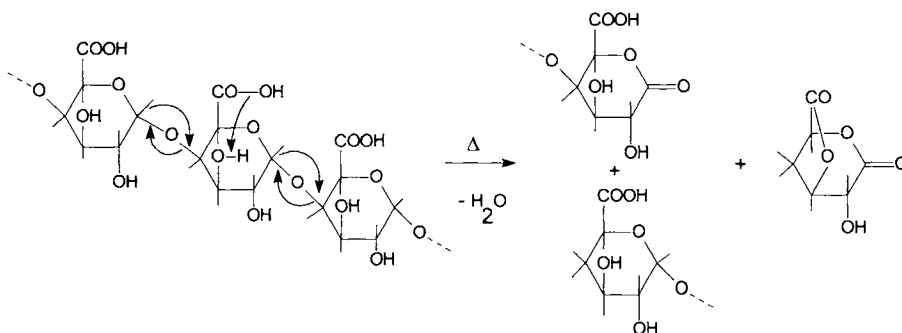
Side group reactions are common during pyrolysis and they may take place before chain scission. The presence of water and carbon dioxide as main pyrolysis products in numerous pyrolytic processes can be explained by this type of reaction. The reaction can have either an elimination mechanism or, as indicated in Section 2.5 for the decarboxylation of aromatic acids, it can have a substitution mechanism. Two other examples of side group reactions were given previously in Section 2.2, namely the water elimination during the pyrolysis of cellulose and ethanol elimination during the pyrolysis of ethyl cellulose. The elimination of water from the side chain of a peptide (as shown in Section 2.5) also falls in this type of reaction. Side eliminations are common for many linear polymers. However, because these reactions generate smaller molecules but do not affect the chain of the polymeric materials, they are usually continued with chain scission reactions.

- Combined reactions.

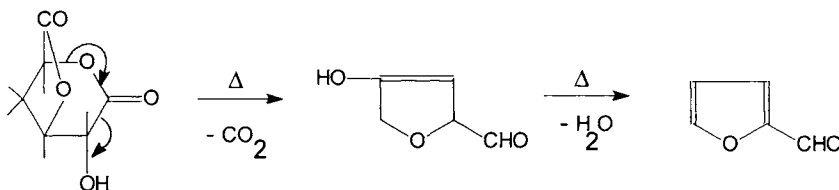
Eliminations and other reactions do not necessarily take place only on the polymeric chain or only on the side groups. Combined reactions may take place, either with a cyclic transition state or with free radical formation. The free radicals formed during polymeric chain scission or during the side chain reactions can certainly interact with any other part of the molecule. Particularly in the case of natural organic polymers, the products of pyrolysis and the reactions that occur can be of extreme diversity. A common result in the pyrolysis of polymers is, for example, the carbonization. The carbonization is the result of a sequence of reactions of different types. This type of process occurs frequently, mainly for natural polymers. An example of combined reactions is shown below for an idealized structure of pectin. Only three units of monosaccharide are shown for idealized pectin, two of galacturonic acid and one of methylated galacturonic acid:



Two pyrolysis products that are formed during pectin pyrolysis are furfural (2-furancarboxaldehyde, 2-furaldehyde) and 4-(hydroxymethyl)-1,4-butyrolactone. The proportion of the butyrolactone compared to that of furaldehyde in the pyrolysis products of pectin was found to correlate with the methylation degree of pectin [6]. The formation of 2-furaldehyde from the galacturonic unit probably takes place with the following mechanism (hydrogens are shown with shorter bonds):



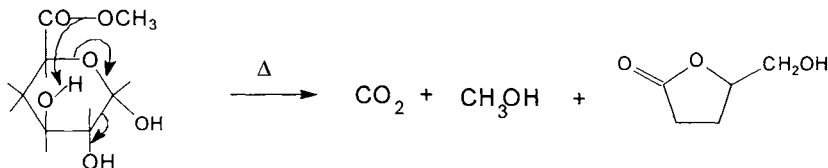
The intermediate compound assumed to be 2-hydroxy-4,8-dioxabicyclo[3.2.1]octane-2,6-dione is not a stable molecule and continues to decompose, without being possible to be isolated, with the formation of another unstable molecule that eliminates water:



The reaction may take place preferentially at the end of the chain. This reaction explains the elevated levels of 2-furaldehyde in the pyrolysis products of pectin.

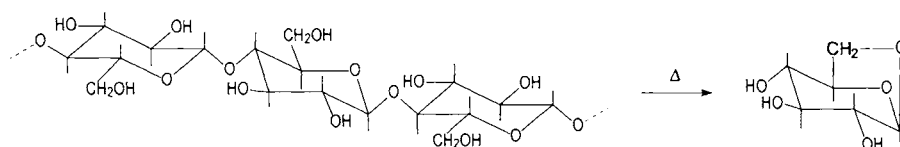
For the formation of 4-(hydroxymethyl)-1,4-butyrolactone, a more complicated process must be assumed. A contribution with H atoms is needed from two neighboring monosaccharide units toward the methylated middle unit, forming the monomeric unit shown below. Therefore, a slightly different cleavage of the polysaccharide chain is

postulated as compared to the previous pathway. After this, more eliminations take place for the monomeric unit which probably undergoes the following reactions:

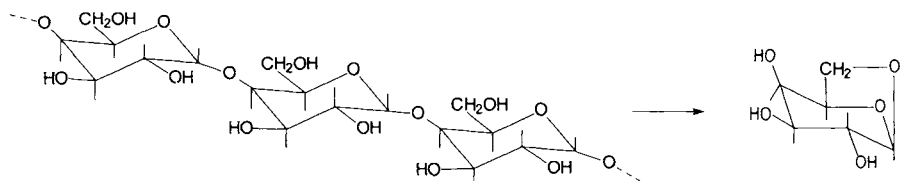


The H atom in the OH group connected to carbon 3 of the monosaccharide unit will generate methanol with the OCH₃ group, and the O will connect with the carbon from the carboxylic group to form the 1,4-butyrolactone cycle.

One important feature that should be noticed for pyrolytic reactions is that the preexistent isomerism is commonly not affected during pyrolysis (if the particular bonds remain in the pyrolysate). As an example, during the pyrolysis of polysaccharides common pyrolysis products are the anhydrosugars of the specific monosaccharide units that form the polysaccharide. The anhydrosugar maintains the stereoisomerism of the monosaccharide unit. For example, the pyrogram of a (1 → 4)-linked glucose-containing polysaccharide (cellulose) gives as a main pyrolysis product 1,6-anhydroglucopyranose:



At the same time, the pyrolysis of a (1 → 4)-linked galactose-containing polysaccharide gives as a main product 1,6-anhydrogalactopyranose:



A variety of pyrolytic reactions are presented further, in the second part of this book, where the pyrolysis products of different polymeric materials are described. These pyrolytic reactions are not, however, different in principle from the basic kinds of reactions discussed in Section 2.2 to Section 2.5.

Pyrolytic reactions can appear much more complicated compared to any of the previous models. However, this is mainly due to subsequent reactions taking place after the initial elimination step. A common cause of this problem is related to the fact that the reactions do not actually take place in ideal gas phase. Some pyrolytic processes may

take place in true condensed phase. Multiple reaction paths and the interaction of the resulting molecules are, therefore, inevitable. Also, additional issues may affect the practical results of a pyrolysis. Some are related to the fact that the true pyrolysis can be associated with reactions caused by the presence (intentional or not) of non-inert gases such as oxygen or hydrogen that may be present during the heating. Also, the pyrolysed materials may be in contact with non-inert surfaces that can have catalytic effects. In order to diminish these effects in the pyrolysis done for analytical purposes, an inert gas frequently is present during the pyrolytic reaction.

The subsequent reactions after the initial pyrolytic process can be utilized with practical results. Besides the pyrolysis of a pure sample, the intentional pyrolysis of a mixture in which one of the components generates reactive products (such as tetramethyl ammonium hydroxide) can be applied to influence the chemical structure of the products generated at the end of the pyrolysis. This subject will be discussed in Section 2.7.

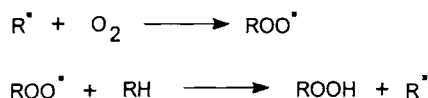
2.7 Pyrolysis in the Presence of Additional Reactants or with Catalysts.

Pyrolytic reactions, mainly for analytical purposes, are commonly done in a helium atmosphere. Sometimes these reactions are done, intentionally or not, in the presence of additional reactants or in the presence of catalysts. The most common additional reactants are probably oxygen, hydrogen, water, and quaternary N-alkyl (or aryl) ammonium hydroxides. Oxygen from the air and water are sometimes unintentionally present during pyrolysis. The presence of an additional reactant can modify the result of the pyrolytic reaction.

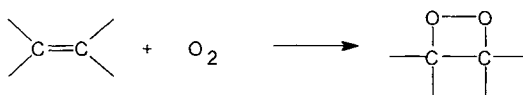
- Pyrolysis in the presence of oxygen.

Oxygen can be a participant in the pyrolysis in two different ways: it can be present as atmospheric oxygen, or it may be already reacted with part of the sample in an autoxidation process by exposure of the sample to air and light over a period of time.

In the presence of excess air, above the flaming temperature of the utilized material burning and not pyrolysis will take place. Although burning is commonly associated with secondary pyrolytic processes, this is not the subject of interest here. The results of the pyrolytic process in the presence of air (below the flaming temperature) can be seen more like a vacuum pyrolysis catalyzed by oxygen [7]. In this type of situation, the pyrolysis products are not significantly different from those obtained without oxygen, but the rate of the reaction is different. However, oxidations may also take place. Free oxygen has an unusual molecule. In its ground state each of the two highest occupied molecular orbitals, which are degenerated, contain unpaired electrons (a triplet state of the molecule). This means that ordinary oxygen has the properties of a diradical. Although not extremely reactive, this diradical will react rapidly with many radicals in a chain oxidation as follows:



In an excited electronic state (singlet oxygen) oxygen is much more reactive. The oxygen in a singlet state can be generated by a photochemical reaction and may react with a wide variety of materials by a so-called autoxidation process. The singlet oxygen can react with the double bond forming a dioxetane intermediate:



Polymers exposed to air and light may contain oxidized groups such as peroxides (~OOR). The O-O bond is weak (30–50 kcal/mol) and, upon heating, dissociates to form free RO· radicals and radical chains. These radicals may influence the composition of the pyrolysis products. Autoxidation may take place in food, paint, rubber, etc. It is important, therefore, to consider this possibility when evaluating the composition of the pyrolysis products of a material that was exposed to air and light although the pyrolysis is performed in an inert gas.

- Pyrolysis in the presence of hydrogen.

In principle hydrogen can react with numerous chemical compounds. However, molecular hydrogen as such is not very reactive. In most chemical reactions, only the hydrogen generated directly in the reaction medium is active (i.e. from Zn and HCl). Pyrolysis in molecular hydrogen proceeds in most cases in a manner similar to the pyrolysis in an inert gas (helium or nitrogen). In order to make use of the hydrogen reactivity, a catalyst must be used. Common catalysts are metals such as platinum or nickel. In analytical pyrolysis, hydrogen and a catalyst can be used [8] with the purpose of diminishing the number of species resulting in pyrolysis. When the pyrolytic process is followed by a chromatographic separation, the chromatogram of the pyrolysate (the pyrogram) can appear to be too complicated. If this pyrogram consists, for example, of groups of compounds with the same carbon chain but containing single and multiple bonds, this can be simplified by hydrogenation. For each group of compounds, only the saturated one will appear after a catalytic hydrogenation. The procedure can be useful only in some particular cases and it is not commonly used.

- Pyrolysis in the presence of water.

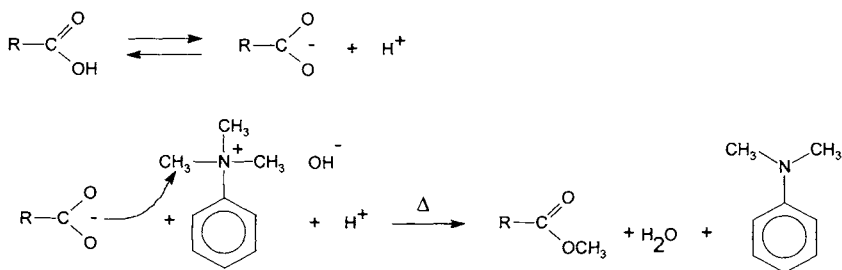
The presence of water as a reaction product from the pyrolytic processes or as adsorbed water on the material to be pyrolysed is not unusual. However, in analytical pyrolysis, water is not commonly added to the sample. During some pyrolytic processes with industrial applications such as wood pyrolysis, water is sometimes added intentionally. The main effect of water during pyrolysis is hydrolysis. This takes place as the temperature elevates. For polymers like cellulose or starch, the chain scission by hydrolysis (instead of transglycosidation) is the main effect of water addition. This can be seen in the modification of the yields of different final pyrolysis products. Therefore, the reproducibility in analytical pyrolysis may be influenced by the variability of water content of the initial sample [9].

- *Pyrolysis in the presence of quaternary N alkyl (or alkyl, aryl) ammonium hydroxides.*

Tetramethyl ammonium hydroxide was initially introduced as a methylating reagent for pyrolytic methylation of compounds containing acidic NH or OH groups in the hot injection port of a gas chromatograph [10]. The procedure was further applied with different pyrolytic techniques by directly adding tetramethyl ammonium hydroxide together with the material to be pyrolysed [11,12]. The derivatization reagents are applied on the sample either as an aqueous solution (for tetramethyl ammonium hydroxide) or as methanolic solutions. Not only tetramethyl ammonium hydroxide was used as an "in situ" derivatization reagent. Other quaternary N alkyl (or alkyl, aryl) ammonium hydroxides were successfully used as derivatization reagents. Such reagents are tetrabutyl ammonium hydroxide [13], phenyltrimethyl ammonium hydroxide (or trimethyl anilinium hydroxide or TMAH), and (m-trifluoromethylphenyl)trimethyl ammonium hydroxide (or trimethyl-trifluoro-m-tolyl ammonium hydroxide or TMTFTH) [14]. Also, other pyrolytic derivatizations with the formation of ethyl, propyl, hexyl, etc. derivatives are known [10].

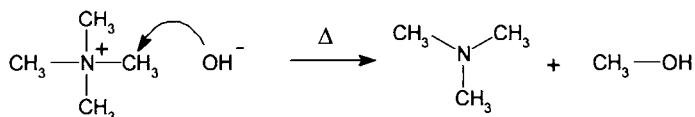
The alkylation was found to take place with a high yield for organic acids and phenols that have a pKa < 12. The aliphatic alcohols with a pKa = 16–19, the aliphatic amines, and the amides either do not undergo alkylation or give poor results under normal pyrolytic derivatization conditions. One interesting finding is that in the presence of an alkylammonium hydroxide aldehydes can undergo Cannizzaro disproportionation and generate acids that will form their esters [15]. Conventional pyrolysis on several aldehydes did not show the formation of acids, while pyrolysis in the presence of TMAH showed acid formation.

The typical derivatization of an organic acid using TMAH takes place as follows:

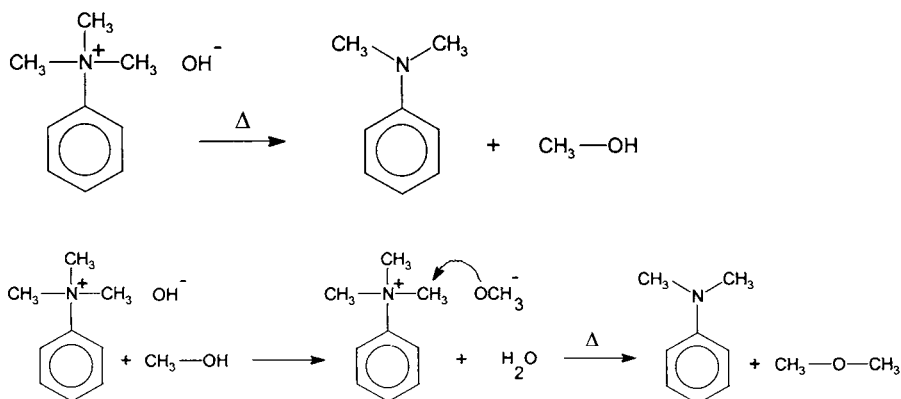


The temperatures required for this type of reaction differ from compound to compound, but in general it should be higher than 250–300° C. These temperatures are easily attained with common pyrolysis instrumentation.

During pyrolysis, quaternary ammonium hydroxide is also decomposed. The decomposition of tetramethyl ammonium hydroxide takes place by the following reaction:



Methanol is not the only result in this reaction. Dimethyl ether is also formed in different proportions. This reaction product may be formed from water elimination between two alcohol molecules or, more likely, from the reaction of methanol with tetramethyl ammonium hydroxide. This reaction is exemplified for TMAH:



Anisole can also be formed during the decomposition of TMAH. This can be explained by the nucleophilic displacement of the trimethyl ammonium group following the attack of the methoxide ion.

References 2.

1. J. March, *Advanced Organic Chemistry*, J. Wiley, New York, 1992.
2. A. D. Pouwels, G. B. Eijkel, J. J. Boon, *J. Anal. Appl. Pyrol.*, 14 (1989) 237.
3. C. D. Nenitzescu, *Chimie Organica*, vol. 1, Ed. Technica, Bucuresti, 1960.
- 3a. R. T. Conley, *Thermal Stability of Polymers*, M. Dekker Inc., New York 1970, chap. 12.
4. P. W. Arisz, J. J. Boon, *J. Anal. Appl. Pyrol.*, 25 (1993) 371.
5. H. H. Jellinek, *Aspects of Degradation and Stabilization of Polymers*, Elsevier, Amsterdam, 1980.
6. R. E. Aries, C. S. Gutteridge, W. A. Laurie, *Anal. Chem.*, 60 (1988) 1498.

7. A. Basch, M. Lewin, J. Polymer Sci., 11 (1973) 3095.
8. S. Tsuge, Y. Sugimura, T. Nagaya, J. Anal. Appl. Pyrol., 1 (1980) 221.
9. G. Verhegyi, P. Szabo, W. S. M. Mok, M. J. Antal, J. Anal. Appl. Pyrol., 26 (1993) 159.
10. W. C. Kossa, J. MacGee, S. Ramachandran, A. J. Weber, J. Chromatog. Sci., 17 (1979) 177.
11. H. Hardell, J. Anal. Appl. Pyrol., 27 (1993) 73.
12. H. Ohtani, S. Ueda, Y. Tsukahara, C. Watanabe, S. Tsuge, J. Anal. Appl. Pyrol., 25 (1993) 1.
13. J. Pecci, T. J. Giovannello, J. Chromatog., 109 (1975) 163.
14. K. O. Gerhardt, C. W. Gehrke, J. Chromatog., 143 (1977) 335.
15. I. Tanczos, M. Schoflinger, H. Schmidt, J. Balla, J. Anal. Appl. Pyrol., 42 (1997) 21.

Chapter 3. Physico-Chemical Aspects of the Pyrolytic Process

3.1 Thermodynamic Factors in Pyrolytic Chemical Reactions.

Pyrolytic reactions are not different in principle from any other chemical reactions. A few general considerations about the thermodynamic factors in chemical reactions are, therefore, useful for the understanding of the parameters affecting the pyrolytic process.

In thermodynamics (see e.g. [1]) it is shown that for any isolated (closed) system (which does not exchange energy with its surroundings), spontaneous transformations take place with an increase in the entropy ΔS of the system. For a non-isolated system in isothermal conditions, spontaneous processes take place with a negative variation of free enthalpy ΔG where

$$\Delta G = \Delta H - T \Delta S \quad (1)$$

and where ΔH is the variation in enthalpy of the system and T is the absolute temperature (measured in Kelvin degrees $^{\circ}K$, where $0^{\circ}K = -273.15^{\circ}C$). From formula (1) for ΔG and from the fact that a spontaneous process takes place with a negative variation of free enthalpy, it can be seen that a system will have the spontaneous tendency to lower its enthalpy (or energy $\Delta E = \Delta H - P \Delta V$ at constant volume) and to increase its entropy. For a transformation at constant pressure and temperature, equilibrium will correspond to a minimum of the free enthalpy. Otherwise, the process would spontaneously continue. Therefore we will have

$$\delta G = 0 \quad \text{or} \quad \Delta G = 0 \quad (2)$$

For a chemical reaction, the variation of enthalpy, entropy, and free enthalpy can be calculated from the particular values of reactants and products. If the values are considered at constant pressure of 1 atm., the standard values for the thermodynamic functions (noted $^{\circ}$) will be obtained as follows:

$$\Delta H^{\circ} = \sum \Delta H^{\circ}_{\text{products}} - \sum \Delta H^{\circ}_{\text{reactants}} \quad (3)$$

$$\Delta S^{\circ} = \sum \Delta S^{\circ}_{\text{products}} - \sum \Delta S^{\circ}_{\text{reactants}} \quad (4)$$

$$\Delta G^{\circ} = \sum \Delta G^{\circ}_{\text{products}} - \sum \Delta G^{\circ}_{\text{reactants}} \quad (5)$$

Because ΔG , ΔH , and ΔS are temperature dependent, they must be calculated at a certain temperature. Values of thermodynamic functions at 298.15 $^{\circ}K$ (or 25 $^{\circ}C$) for many chemical compounds are tabulated. For a large number of organic compounds, the decomposition reactions at standard temperature of 25 $^{\circ}C$ have negative values for the standard free enthalpy ΔG° . These reactions should, therefore, occur spontaneously. However, their reaction rates are in most cases slow enough (see Section 3.2) such that this assures the chemical stability of numerous organic

compounds. This also points out the importance of the kinetic factors over the thermodynamic ones in pyrolytic reactions.

As mentioned before, each term in the expression of the equation for free enthalpy depends on temperature. At lower temperatures, enthalpy will play a more important role. At higher temperatures, the entropy term $T \Delta S$ will be more important. For most chemical reactions, an equilibrium is attained at a certain temperature when $\Delta G = 0$ due to the opposite contribution of products and reactants to the total value of ΔG . From the expression for ΔG we can write the following equation for equilibrium:

$$\Delta H = T \Delta S \quad (6)$$

or for the standard values at constant pressure of 1 atm. we can write:

$$\Delta H^{\circ} = T \Delta S^{\circ} \quad (7)$$

For a pyrolytic process, the temperature T satisfying relation (7) is defined as the *ceiling temperature* T_C :

$$T_C = \Delta H^{\circ} / \Delta S^{\circ} \quad (8)$$

The ceiling temperature T_C can be considered the upper temperature at which a pyrolytic process will reach equilibrium. It may be seen, therefore, as a recommended temperature for pyrolysis. However, in practice, the application for macromolecules of the above relations is not straightforward. The theory was developed for ideal systems (sometimes in gas phase), and although in principle this theory should hold true for any system, its application to condensed phases or polymeric materials may be accompanied by effects difficult to account for (phase change, melting, cage effect [2], etc.). The reaction rate could also be low at calculated T_C values. For this reason, temperatures 50°C or 100°C higher than T_C must frequently be used as practical values of the temperature used in pyrolysis.

The free enthalpy of a chemical process is related to the equilibrium constant K of that process. This constant allows (in principle) the calculation of the concentrations of the products giving the concentration of the reactants. Considering a reaction of the type:



the equilibrium constant K will have the expression:

$$K = \frac{[B][C][D] \dots}{[A]} \quad (10)$$

It was shown in thermodynamics (i. e. [3]) that K is related to the variation of the standard free enthalpy ΔG° by the relation:

$$\Delta G^{\circ} = -R T \ln K \quad (11)$$

Both ΔG° and K will be temperature dependent (R is the gas constant and in IS units $R = 8.31451 \text{ J deg}^{-1} \text{ mol}^{-1} = 1.987 \text{ cal deg}^{-1} \text{ mol}^{-1}$). Because the value for ΔG° is not

always known at pyrolysis temperature, the practical utility of this relation for pyrolytic processes is limited. However, the dependence of the equilibrium constant on temperature indicates that in analytical pyrolysis a good reproducibility can be obtained only if the temperature is accurately controlled.

The use of thermochemical data in pyrolysis is commonly limited to some predictions regarding the possible mechanism of a pyrolytic process. One such prediction refers to the impossibility of generating ions by a pyrolytic process at temperatures within the common range of use (up to 1000°–1200° C). A classical calculation for a mono-atomic gas (with the molecules having three degrees of freedom) indicates that the average energy per molecule is $3/2 k T$ where k is the Boltzmann constant ($k = 13.805 \cdot 10^{-24} \text{ J deg}^{-1}$). For an ionization potential of 10 eV, this would correspond to a temperature of 77,372.4° K. Although the ionization potentials of some molecules is lower than 10 eV and their number of degrees of freedom in gas phase is higher than three, temperatures higher than 5,000 to 10,000° K would be required for their ionization.

At the same time, the radical formation through thermolytic reactions is rather common. For example, the thermodynamic factors may allow prediction of the structure of the most likely radical to be formed in a pyrolytic process. This calculation can be based on the strength of a bond that breaks. The enthalpy (energy) for the dissociation of a bond A-B is not always available. However, for a homolytic dissociation with formation of free radicals, the enthalpy can be derived [4] from tabulated heats of formations ΔH_f^0 , using the relation:

$$\Delta H_f^0 (\text{A-B}) = \Delta H_f^0 (\text{A}\cdot) + \Delta H_f^0 (\text{B}\cdot) - \Delta H_f^0 (\text{AB}) \quad (12)$$

The $\Delta H_f^0 (\text{AB})$ values are easily available. Tables with heats of formation for radicals are less common but still available in literature (e.g. [2,5,6]), sometimes together with homolytic bond dissociations calculated based on equation (12).

The use of thermodynamic data for predicting the reaction path can, for example, be applied for the thermal decomposition of aliphatic hydrocarbons. This example is more related to practical applications for petroleum products, but can explain the yield of certain compounds in secondary steps for the pyrolysis of polymers such as rubber.

For the alkane pyrolysis, two main reaction paths are possible (see also Section 2.2), one with dehydrogenation and the other with fragmentation. The free enthalpies for these reactions are as follows:



It is interesting that the ΔG expressions are practically independent of the number of carbons in the molecule. At low temperatures, both reactions have positive ΔG values, and therefore do not take place. However, thermodynamically the fragmentation is favored because for this reaction $\Delta G = 0$ at about 270° C, while for dehydrogenation $\Delta G = 0$ only at 622° C. Therefore, during pyrolysis at 450° C–550° C it is unlikely that hydrogen will be formed from hydrocarbons.

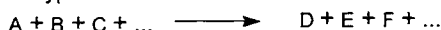
3.2 Kinetic Factors in Pyrolytic Chemical Reactions.

Kinetic factors play an important role in the pyrolytic process. Both theoretical and practical aspects require information on reaction kinetics. Among the practical applications requiring information on pyrolysis kinetics are the formation of hydrocarbons from kerogens, the generation of gases from coal during coke fabrication, and cellulose pyrolysis related to fire problems. The implications of kinetic factors for analytical pyrolysis are mainly related to the proper choice of certain experimental conditions such as pyrolysis temperature or time. Also, because the rate of reactions during pyrolysis is significantly affected by temperature, it is much easier to control reproducibility in isothermal conditions than in a temperature gradient. This explains why the analytical pyrolysis is commonly conducted in isothermal conditions.

In order to understand better the problems related to kinetic factors in pyrolytic reactions, a few basic concepts will be reviewed. The *reaction rate* of a chemical process where R is a reactant and P is a product is defined as the variation of the concentration of R or of P versus time. The reaction rate can be expressed by the relation:

$$-\frac{d[R]}{dt} = \frac{d[P]}{dt} \quad (1)$$

where [R] or [P] are the (molar) concentrations at any time during the reaction. If in a chemical reaction of the type:



the rate of reaction depends linearly of the concentration of one reactant A, then

$$-\frac{d[A]}{dt} = k[A] \quad (2)$$

This type of reaction is of the first order. The constant k is the *rate constant*. Concentrations are commonly expressed in mol / L, and k is expressed in s^{-1} . The rate constant k is temperature dependent and it is a constant only in isothermal conditions.

It is possible that the rate of reaction depends on the concentrations of the A and B species simultaneously. In this case the dependence is given by

$$-\frac{d[A]}{dt} = -\frac{d[B]}{dt} = k[A][B] \quad (3)$$

and the reaction is of the second order. The reaction rate constant k for second order kinetics are expressed in $mol^{-1} s^{-1}$. These are different from the units used for the constant for first order kinetics.

Some chemical reactions have a reaction rate of the form:

$$-\frac{d[A]}{dt} = k[A]^n \quad (4)$$

where n is the reaction order. The value of n can be an integer, or for certain chemical reactions it can be a fractional number.

In order to understand how the constant k depends on temperature, it was assumed that the chemical reactions may take place only when the molecules collide. Following this collision, an intermediate state called an activated complex is formed. The reaction rate will depend on the difference between the energy of the reactants and the energy of the activated complex. This energy E^\ddagger is called activation energy (other notation E^a). The reaction rate will also depend on the frequency of collisions. Based on these assumptions it was shown (e.g. [3]) that k has the following expression (Arrhenius reaction rate equation):

$$k = A \exp\left(-\frac{E^\ddagger}{RT}\right) \quad (5)$$

where A is a parameter related to the collision number and it is called *frequency factor* and R is the *gas constant* ($R = 8.31451 \text{ J deg}^{-1} \text{ mol}^{-1}$). Relation (5) indicates the explicit dependence of the rate constant k on temperature (expressed in $^\circ \text{K}$).

For pyrolytic reactions, the variation of the molar concentration $[A]$ of a substance during the pyrolysis is not always the most appropriate parameter to be monitored. The calculation of $[A]$ can be a problem for many types of samples, and very frequently during pyrolysis, not only one decomposition process takes place. In this case, the overall reaction kinetics must be considered. A more convenient parameter for monitoring pyrolytic reactions is, for example, the sample weight. For a reaction of the first order, by multiplying equation (2) with the volume V and the molecular weight M of the substance A , ($W = [A] V M$) we will have

$$-\frac{dW}{dt} = kW \quad (6)$$

where W is the weight (mass) of the sample at any time during the reaction. This type of equation can approximate (with good results) the kinetics for many pyrolytic processes. Equation (6) can be easily integrated to give:

$$\ln W \Big|_{t=0}^t = -k t \quad \text{or} \quad \ln \frac{W}{W_0} = -k t \quad \text{or} \quad \frac{W}{W_0} = \exp(-k t) \quad (7)$$

where W_0 is the initial sample weight (at $t = 0$).

In some cases, the pyrolysis leaves a residue of undecomposed sample of the weight W_f (final weight). In this case relation (6) will be

$$-\frac{dW}{dt} = k(W - W_f) \quad (8)$$

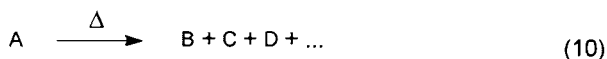
This type of relation can be applied to pyrolytic processes even if the reaction is not of the first order. In this case the reaction rate is described by the relation:

$$-\frac{dW}{dt} = k(W - W_f)^n \quad (9)$$

and the reaction order n is not necessarily an integer. Relations of the type (6), (8) or (9) that were used for weight can be applied for other parameters. Examples of such parameters are the residual mass fraction (W/W_0) where W_0 is the initial sample weight, the volatilized mass fraction ($1 - W/W_0$), or for uniform polymers the number of polymer molecules.

Equations of the type indicated above can be used to describe the kinetics of a single chemical process or overall reaction kinetics. Measurements of the variation of W in time in isothermal conditions allows the calculation of the constant k and order n for which a best fit of the experimental data can be obtained. For different reaction orders, Arrhenius formula for k given by relation (5) is usually still applicable. Once the values for k and n are known for a given reaction, the reaction kinetics can be described in a wider range of conditions.

The theory described so far is commonly applied for small molecules and usually takes place in gas phase. Many of these reactions are of the first order. Therefore, it can be expected that these are unimolecular reactions. However, chemical reactions are supposed to take place only when the molecules collide. It is necessary, therefore, to understand how the molecular collision concept is applicable to a unimolecular reaction of the type:



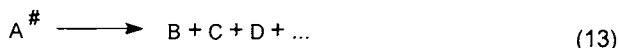
when it takes place in gas phase and possibly at low pressure. For this type of reaction, the reacting molecule still acquires energy by collision with another molecule:



The energized molecule does not, however, react immediately and it is still able to lose its energy by collision with another molecule. A redistribution of the energy takes place afterwards, and this process is expressed schematically as



In this process the acquired energy is passed to one or more bonds that are weak enough to break. The process can continue with the chemical decomposition:



Based on the assumptions indicated above, the kinetics of many unimolecular reactions can be described with relatively good approximation by relation (2) or (6). The activation energy $E^\#$ in the Arrhenius equation will be, in this case, the difference between the energy of the molecule A and the energy of the activated complex $A^\#$.

The unimolecular reaction theory was successfully applied to the rate of dissociation of ions created in mass spectrometry. In this situation, the rate constant k for the dissociation is dependent on the internal energy of the ion. A simplified form (an approximation) for the expression of the rate constant is, in this case,

$$k = A [(E-E_0)^{(s-1)}] / E \quad (14)$$

where A is the frequency factor, E is the internal energy of the ion, E_0 is the activation energy for a reaction to take place, s is a parameter related to the number of vibrational states of the ion (effective number of oscillators). For a pyrolytic process, the same theory can be used for compounds generated after the volatilization of the sample (e.g. [7]) when further pyrolysis takes place in gas phase. The pyrolysis of small molecules may take place as a second step in the pyrolysis of a polymer when small molecules are generated in the first step of the pyrolysis. A plot of k given by relation (14) for two hypothetical reactions is shown in Figure 3.2.1. Curve A corresponds to a reaction with a higher activation energy (0.03 eV) and higher frequency factor (10^6) while curve B corresponds to a reaction with lower activation energy (0.003 eV) and lower frequency factor (10^5). At lower temperature (lower energy for the molecule) reaction B will be predominant, while at higher temperature reaction A will prevail.

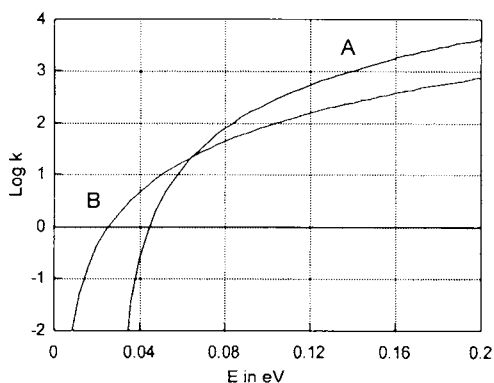


FIGURE 3.2.1. $\text{Log } k$ given by relation (14) for two hypothetical unimolecular reactions.

When the pyrolytic process does not occur in gas phase, different problems appear. Although equations of the type (6) with k expressed by rel. (5) or (14) can be used in certain cases, these may lead to incorrect results in many cases. Various empirical models were developed for describing the reaction kinetics during the pyrolysis of solid samples. Most of these models attempt to establish equations that will globally describe the kinetics of the process and fit the pyrolysis data. Several models of this type will be described in Section 3.3. A different approach can be chosen, mainly for uniform repetitive polymers. In such cases, a correct equation can be developed for the description of the reaction kinetics. This is based on the study of the steps occurring during pyrolysis involving a free radical chain mechanism. The subject will be discussed in some detail in Section 3.4.

The temperature dependence of the rate of reactions is particularly important for the pyrolytic processes. Relation (5) can be used for the understanding of the common choices for the pyrolysis parameters. As an example, we can take the pyrolysis of cellulose [8]. Assuming a kinetics of the first order (pseudo first order), the activation energy in Arrhenius equation was estimated $E^\# = 100.7 \text{ kJ / mol}$. The frequency factor was estimated $9.60 \cdot 10^5 \text{ s}^{-1}$. These values will lead to the following expression for the weight variation of a cellulose sample during pyrolysis:

$$-\frac{dW}{dt} = 9.6 \cdot 10^5 \exp\left(-\frac{100700}{8.3146 \cdot T}\right) \cdot W \quad (15)$$

The variation of the reaction rate constant k with temperature for this pyrolytic process is shown in Figure 3.2.2.

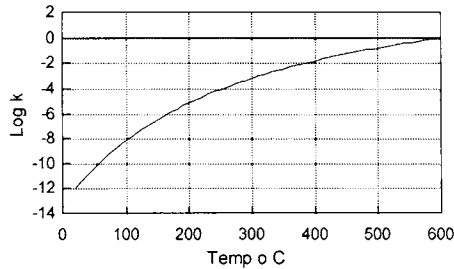


FIGURE 3.2.2. The variation of the reaction rate constant k (log scale) with temperature for a reaction described by rel. (15).

Using the integrated form of this equation (see rel. (7)), the values for W/W_0 for cellulose can be obtained for different temperatures and pyrolysis times. Assuming a pyrolysis time of 10 s in isotherm conditions at different temperatures [in rel. (15), T should be expressed in $^\circ \text{K}$], several values for W/W_0 expressed in % are given in Table 3.2.1. These calculated values for W/W_0 used $E^\#$ and A extrapolated for a wider range of temperatures than those reported in literature [8] for cellulose. The only purpose of these calculations is to illustrate the effect of temperature on the rate of pyrolysis. From Table 3.2.1 it can be seen that around 200°C cellulose is not significantly decomposed. Around 400°C the decomposition starts, and around 600°C the decomposition is practically complete. In analytical pyrolysis, 600°C and 10 s pyrolysis time (total heating time THT) could, therefore, be recommended for the experimental conditions of cellulose pyrolysis.

TABLE 3.2.1. Calculated values for W/W_0 for pyrolysis of cellulose expressed in %, assuming a first order kinetics and 10 s pyrolysis time (THT).

$T^\circ \text{C}$	$k \text{ (s}^{-1}\text{)}$	$W/W_0 \text{ \%}$
200	$7.34 \cdot 10^{-6}$	99.99
400	0.0147	86.01
500	0.1511	22.07
600	0.9084	0.01

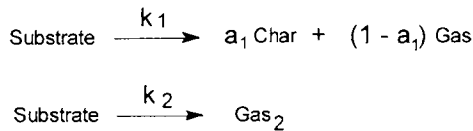
3.3 Models Attempting to Describe the Kinetics of the Pyrolytic Processes of Solid Samples.

The kinetics equation of the type

$$-\frac{dW}{dt} = k W \quad (1)$$

as shown in Section 3.2 is commonly applied for describing the overall reaction kinetics during pyrolysis. However, this equation provides only an approximation when the process is not composed of a single reaction. The pyrolysis of solid samples is usually a complicated process and rel. (1) may lead to erroneous results. The simpler relations valid for the kinetics in homogeneous systems do not fit well the experimental data for solid samples. Factors related to heterogeneous reactions must be taken into account in this case. A series of more elaborate models have been developed [8, 8a].

One such model [8] is still based on the overall equation of type (1), but involves two reaction paths that are considered important during pyrolysis. One path takes place with the formation of both volatile compounds (gas) and char, and the other with the exclusive formation of a gas. The theory attempts to account for the description of both the gas formation and solid residue formation. The chemical reactions can be described in this case by the following two processes:



If W is the weight of the substrate at a certain time t during the reaction and W_0 is the initial mass, then $F = W/W_0$ is the mass (weight) fraction of the unreacted substrate at the given time t . We can note with C the mass fraction of char relative to W_0 and with G the mass fraction of gas relative to W_0 . With these notations the kinetics of the reaction will be described by the equations:

$$\frac{dF}{dt} = -(k_1 + k_2) F \quad (2a)$$

$$\frac{dC}{dt} = a_1 k_1 F \quad (2b)$$

$$\frac{dG}{dt} = [(1 - a_1) k_1 + k_2] F \quad (2c)$$

As seen from rel. (2a), the overall kinetics for F is considered of the first order. Between F , C and G there is the equation:

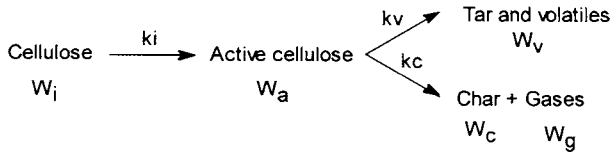
$$F + C + G = 1 \quad (3)$$

and from equations (2b) and (2c) it can be shown that we have in isothermal conditions:

$$\frac{C}{G} = \frac{a_1 k_1}{(1-a_1) k_1 + k_2} \quad (4)$$

Using equations (3) and (4), equations (2a–2c) can be written as depending on only one variable. This variable should be easily monitored experimentally. Such a variable is the mass fraction of the gas G or the mass fraction of the solid residue $(1 - G)$. The three equations (2a–2c) can be initially used to calculate the values for k_1 , k_2 and a_1 . This can be done using a best-fit technique for experimental data that are assumed to be described by equations (2) in isothermal conditions. Once the values for k_1 , k_2 and a_1 are known, the kinetics equations can be integrated and solved for any time t . This model has been successfully applied, for example, to describe the pyrolysis of cellulose and of pine needles [8]. In analytical pyrolysis this model can be used to determine the amount of gas generated during pyrolysis. Also, analytical pyrolysis data can be used to fit the kinetics model for use in other practical applications.

Another model for the kinetics of cellulose pyrolysis assumes the formation of an active cellulose intermediate. Using this assumption, the kinetics of the pyrolysis process can be described similarly to the previous model as follows [9]:



$$\frac{d W_i}{dt} = k_i W_i \quad (2a')$$

$$\frac{d W_a}{dt} = k_i W_i - (k_v + k_c) W_a \quad (2b')$$

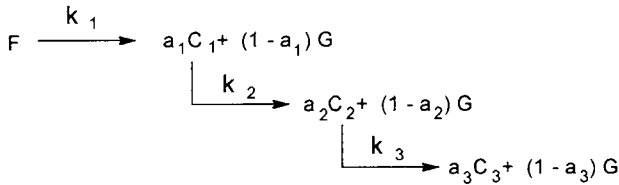
$$\frac{d W_c}{dt} = 0.35 k_c W_a \quad (2c')$$

$$k_i = 1.7 \cdot 10^{21} \exp(-58000/RT) \text{ min}^{-1}$$

$$k_v = 1.9 \cdot 10^{16} \exp(-47300/RT) \text{ min}^{-1}$$

$$k_c = 3.4 \cdot 10^{11} \exp(-25000/RT) \text{ min}^{-1}$$

A more elaborate model similar to the previous one is based on the assumption that more than one chemical reaction takes place during pyrolysis. This model has been successfully applied for the description of cellulose pyrolysis [10]. In this model, it is proposed that pyrolysis follows a chemical reaction of the type:



In this scheme, F is the unreacted substrate, C_1 , C_2 , C_3 are intermediate pyrolysis solid products, and G is gaseous reaction product. Assuming first order kinetics for each reaction step, and using the same symbols for the molecules as well as for the mass fraction of involved substances, the corresponding rate equations for this process can be written as follows:

$$\frac{dF}{dt} = -k_1 F \quad (5a)$$

$$\frac{dC_1}{dt} = a_1 k_1 F - k_2 C_1 \quad (5b)$$

$$\frac{dC_2}{dt} = a_2 k_2 C_1 - k_3 C_2 \quad (5c)$$

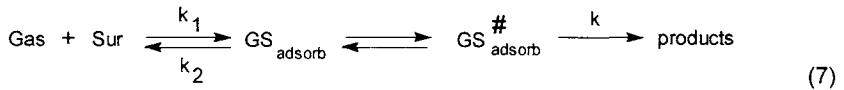
$$\frac{dC_3}{dt} = a_3 k_3 C_2 \quad (5d)$$

In equations (5), F is the mass fraction of the unreacted starting substance (mass of unreacted starting substance divided by the initial mass W_0), C_1 is the symbol for the mass fraction of substance C_1 , etc. Using the symbol \mathcal{W} for the mass fraction of the remaining solid material, we can write:

$$F + C_1 + C_2 + C_3 = \mathcal{W} \quad (6)$$

The equations (5) with equation (6) can be solved analytically, when a_1 , a_2 , and a_3 , as well as k_1 , k_2 , and k_3 are known. This will provide the values for \mathcal{W} at any time during pyrolysis. The values for the reaction constants k_1 , k_2 , and k_3 can be calculated for different temperatures based on the Arrhenius equation (rel. (5) Section 3.2) if the values for the activation energy $E^\#$ and for the frequency factor A are known for each step reaction. The values for a_1 , a_2 , and a_3 can be adjusted at a chosen temperature to fit the experimental data. The application of the above model for cellulose pyrolysis (up to 350° C) used the following values: $a_1 = 0.75$, $a_2 = 0.99$, $a_3 = 0.22$, $E^\#_1 = 174$ (kJ / mol), $E^\#_2 = 178$ (kJ / mol), $E^\#_3 = 179$ (kJ / mol), and $A_1 = 7.3 \cdot 10^{13}$ (min^{-1}), $A_2 = 1.9 \cdot 10^{14}$ (min^{-1}), $A_3 = 1.2 \cdot 10^{14}$ (min^{-1}). Excellent agreement with experimental data was obtained [10]. However, the large number of optimized parameters raise the question of a good agreement of the theory with the experiment based only on the "flexibility" of the model.

A different model [11] that can be used to obtain the kinetics equation for a pyrolytic reaction is adapted from the theory developed for the kinetics of heterogeneous catalytic reactions. This theory is described in literature for various cases regarding the determining step of the reaction rate. The case that can be adapted for a pyrolytic process in solid state is that of a heterogeneous catalytic reaction with the rate-determining step consisting of a first-order unimolecular surface reaction. For the catalytic reaction of a gas, this case can be written as follows:



where Gas denotes the gas, Sur denotes the surface, and $\text{GS}^{\#}$ the activated complex of the gas adsorbed on the active center of the catalyst surface. The determining step of this type of reaction can be considered the decomposition of the activated complex. Its reaction rate α can be described by the equation:

$$\alpha = - \frac{d[\text{product}]}{dt} = k[\text{GS}] \quad (8)$$

When the surface is saturated with gas molecules, we have $[\text{GS}] = C_A$ where C_A is the concentration of active sites on the surface of the catalyst. The reaction rate becomes

$$\alpha = k C_A \quad (9)$$

Rel. (9) indicates that the kinetics of a catalytic reaction described by equation (7) does not depend on the concentration of the reacting gas (is of zero order as a function of gas concentration). For rel. (9) the evaluation of k is based on statistical thermodynamics applied to transition state theory for chemical reactions [12]. This theory shows that k has the following expression:

$$k = (k T / h) \exp [(- \Delta H^{\#} + T \Delta S^{\#}) / RT] \quad (10)$$

where k is Boltzmann's constant, h is Planck's constant ($h = 0.66252 \cdot 10^{-33} \text{ J s}$) and $\Delta H^{\#} - T \Delta S^{\#}$ is the activation free enthalpy. This activation free enthalpy is equal to the difference between the free enthalpy of the reactant and the free enthalpy of the activated complex $\text{GS}^{\#}$. The activation free enthalpy is related to the activation energy $E^{\#}$ by the relation:

$$\Delta H^{\#} = E^{\#} - nRT \quad (11)$$

where n is the reaction molecularity and $E^{\#}$ is the activation energy defined in Section 3.2.

The above considerations can be applied for describing the kinetics of a pyrolytic process using a few modifications. The reaction rate α as defined above (rel. (8)) can be replaced by a proportional parameter v where $v = - dW / dt$. This can be done by multiplying α with $(M S_a W)$ and division with \backslash . This gives the following relation:

$$v = \alpha M S_a W / N \quad (12)$$

where M is the molecular weight of the substance to be pyrolysed, W is its amount, S_a is the specific active surface area (unit of active surface per unit of mass), and $N = 6.023 \cdot 10^{23}$ is Avogadro's number. The rate v is a more appropriate parameter to be monitored, being the rate for the pyrolysis of the substance in the amount W . Also, C_A in rel. (9) should be replaced by C_M , where C_M is the superficial density of molecules that can be decomposed. In this case, rel. (9) will become:

$$v = k M S_a W C_M / N \quad (13)$$

Considering that a solid is made from different layers which decompose from the superficial layer toward the center, and each layer is considered a reaction front, we can write

$$M C_M / N = L \rho \quad (14)$$

where L is the average distance between two reaction fronts (L can be taken from the molecular crystalline structure as the distance between two layers of molecules), and ρ is the density of the material. In this case, rel. (13) becomes

$$v = -dW / dt = k L \rho S_a W \quad (15)$$

Because of the changes in the composition of the reactive part of a material during pyrolysis, the active surface area S_a is not a constant during the pyrolytic process. In general $S_a = f(W)$, and several functional dependencies were chosen between S_a and W . A common choice is

$$S_a = a (W / W_0)^b \quad (16)$$

where a and b are constants and not necessarily integers. In these conditions, we will have for the expression of the reaction rate

$$-dW / dt = k L \rho a (W / W_0)^b W \quad (17)$$

or in the typical form of a rate equation

$$-dW / dt = k' (W / W_0)^b W \quad (18)$$

This relation explains why the kinetics order of pyrolytic reactions in solid state can have a non-integer value. The formula for k' can be obtained by combining equation (17) with the value for k given by equation (10) and with equation (11) where $n = 1$. We will have

$$k' = L \rho (k T / h) a \exp [(-E^\# + T \Delta S^\#) / RT + 1] \quad (19)$$

Writing this relation in the form of an Arrhenius rate constant we have

$$k' = A \exp (-E^\# / RT) \quad (20)$$

where

$$A = L \rho (k T / h) a \exp (\Delta S^\# / R + 1) \quad (21)$$

The above theory has been applied to different practical systems such as cellulose and tars [9]. The values used for cellulose, for example, were the activation energy E^\ddagger between 100 kJ mol^{-1} and 250 kJ mol^{-1} , the frequency factor A between 10^6 s^{-1} and $5 \cdot 10^{17} \text{ s}^{-1}$, and the values for b (related to the order) between 0 to 1. The large variation in the choice of these values indicates the lack of precise information about the parameters used in equations (18) to (21).

A more empirical approach [13] for describing the kinetics of the pyrolytic reactions in solid state is to use a parametric equation that includes formulas for all possible categories of kinetics mechanisms known to occur for the chemical reactions of solid samples. Considering F the mass fraction of the unreacted substance at the time t , the empirical kinetics equation for heterogeneous systems can be expressed in the general form:

$$\frac{dF}{dt} = -k f(F) \quad (22)$$

where k is a constant and $f(F)$ is a function that can be chosen of the form:

$$f(F) = F^m (1 - F)^n [-\ln(1 - F)]^p \quad (23)$$

The terms in equation (23) attempt to describe the reaction rate controlled by the movement of the phase boundary, diffusion, nucleation in solid state, etc., and different values (including zero values) for m , n and p were proposed in literature (see e.g. [14]). Different combinations of m , n , and p values were found suitable for describing different dominating processes. Table 3.3.1 indicates some common values for m , n and p used in equation (23).

TABLE 3.3.1. *Common values from literature [13] for m , n and p in equation (23).*

m	n	p	Type of process
0	0	0	Phase boundary reaction
0	1/2, 2/3	0	Phase boundary reaction
0	1	0	Unimolecular decay
$m < 1, 3/4$	0	0	Nucleation
1	0	0	Linear growth of nuclei
-1	0	0	Diffusion
0	0	-1	Diffusion
$0.5 < m < 1$	$0.5 < n < 1$	0	Nucleation
$m > 1$	$n < 1$	0	Linear growth of nuclei
0	1	1/2, 2/3, 3/4	Growth of nuclei
0	0	-1	Diffusion
m	n	p	Any complicated case

It has already been shown that (see e.g. rel. (21)) the temperature dependence of the reaction rate is not always as simple as described by the Arrhenius equation with A constant. Even for gases, besides the explicit dependence of T shown in equation (5) Section 3.2, k also depends on temperature through the parameter A . Theoretically, for gases it can be shown that this parameter is dependent on the square root of temperature (e.g. [15]), although for practical purposes and within a narrow temperature interval A is sometimes considered to be a constant. The calculated values for A are not

always in good agreement with the experiment [3]. One particular cause of this disagreement is that not all the molecular collisions in a chemical reaction are "effective," and some steric considerations should be included in the calculations. Also, for unimolecular reactions, the description resulting from collisions of molecules of the same type did not provide complete explanations for the calculation of k in a series of instances. For unimolecular reactions, a more elaborate theory (RRKM) was developed (see e.g. [16]), which obtains a better agreement with the experimental data for k .

For the reactions in solid state, several empirical equations were proposed to better simulate the dependence on temperature of the reaction rate. This dependence can be described for example by equations of more complicated forms such as:

$$\frac{dF}{dt} = -k(T) f(F) g(F, T) \quad (24)$$

where $k(T)$ is given by the Arrhenius formula (rel. (5) Section 3.2), $f(F)$ is an empirical function of the form given by rel. (23), and the implicit function $g(F, T)$ is also empirically adjusted for a better fit of the experimental data. The factor $g(F, T)$ attempts to account for conversion-temperature cross terms. The integration of the differential equation of the type given in rel. (24) was done for a series of particular expressions for $f(F)$ commonly taking $g(F, T) = 1$. Even more complicated expressions than rel. (24) were proposed (see e.g. [2]) for the description of the temperature dependence of solid state reaction kinetics.

3.4 Pyrolysis Kinetics for Uniform Repetitive Polymers.

Thermal decomposition of uniform repetitive polymers was extensively studied in literature [17–19] in relation to the thermal stability of synthetic polymers. A kinetics equation has been developed based on the study of the steps occurring during pyrolysis involving a free radical chain mechanism [17]. For some natural polymers such as rubber, this theory is directly applicable. However, for non-repetitive polymers, or for polymers with more complex decomposition pathways, the theory does not provide appropriate kinetics equations.

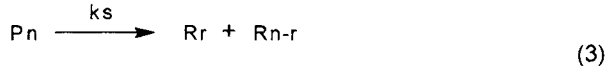
The pyrolytic process of a repetitive polymer frequently takes place with the formation of small volatile molecules and has a polymeric chain scission mechanism, as described in Section 2.6. Considering a polymer with a degree of polymerization (DP) n , the end scission reaction can be described by the chemical equation:



where P_n is the molecule of the polymer, R_1 is the radical with one monomeric unit, and R_{n-1} is the radical with $n-1$ monomeric units. Using the notation P_n not only for the molecule itself but also for the number of polymeric molecules with the DP = n , the kinetics of the reaction can be described by the equation:

$$\frac{dP_n}{dt} = k_e P_n \quad (2)$$

where a first order reaction kinetics is assumed. This relation is similar to equation (2) from Section 3.2, where the concentration is replaced by the number of molecules. For most polymers the end scission reaction plays a more important role compared to any individual random scission (see Section 2.6). However, random scission reactions with formation of radicals should also be considered. These are described by reactions of the type:

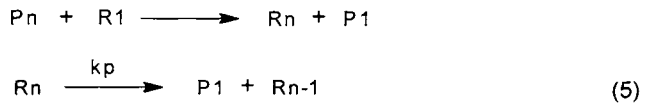


The kinetics equation obtained by considering all reactions (3), with $r = 2, 3, \dots$ will be

$$\frac{dP_n}{dt} = -k_s (n-1) P_n \quad (4)$$

It should also be noted that in the chemical reactions (1) and (3) only the macromolecules with the $DP = n$ were considered, but the polymer does not consist of molecules with only one degree of polymerization. This fact will be considered later.

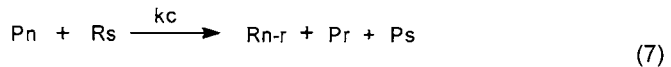
After the radical formation, intermolecular chain transfer reactions take place. A special case of chain transfer is the propagation reaction (see Section 2.1) of the type:



The kinetics of radical R_n disappearance will be expressed by the equation:

$$\frac{dR_n}{dt} = -k_p R_n \quad (6)$$

More general types of chain transfer reactions can be written as a sum of the two previous reactions, as follows:



The kinetics equation for all propagation and chain transfer reactions can be written as follows:

$$\frac{dP_n}{dt} = k_c (R/V)(n-1) P_n + k_c (R/V) \sum_{j=n+1}^N P_j + k_c (R_n/V) \sum_{i=L}^N P_i \quad (8)$$

where the first term accounts for the rate of disappearance of P_n by transfer type initiation, the middle term accounts for the formation of P_r , and the last term accounts for the formation of P_s by termination of a radical by transfer. In equation (8), R is the total number of radicals, V is the sample volume, and R_n is the number of radicals with $DP = n$. Also, in equation (8) L is the degree of polymerization of the smallest non-volatile molecule, and N is the maximum degree of polymerization in the sample.

The polymeric chain scission mechanism is terminated as shown in Section 2.6 by one or more of the following types of termination reaction:

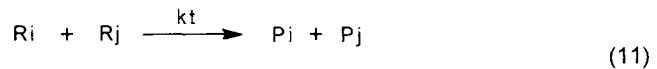
- First order termination (due to disproportionation, etc.)



with the kinetics described by the equation

$$\frac{dP_n}{dt} = k_t R_n \quad (10)$$

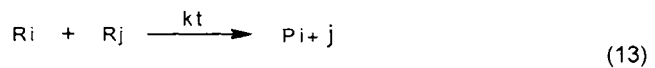
- Second order disproportionation



with the kinetics described by the equation

$$\frac{dP_n}{dt} = k_t (R/V) R_n \quad (12)$$

- Second order recombination



with the kinetics described by the equation

$$\frac{dP_n}{dt} = k_t \frac{1}{2} \sum_{i+j=n}^N (R_i R_j / V) \quad (14)$$

The total rate of change in the number of macromolecules with the $DP = n$ can be expressed by adding equation (2), (4), and (8) and one of the equations (10), (12), or (14). The result can be simplified by using the formula

$$k_c (R_n / V) \sum_{n=i}^N n P_n = k_c R_n (do / M) \quad (15)$$

where ρ_0 is the density of the sample and M is the molecular weight of a monomeric unit. The final formula, which gives the kinetics of the decomposition of molecules P_n , will be

$$\frac{dP_n}{dt} = k_e P_n - (n-1)[k_s + k_c (R/V)] P_n + k_c \left[\left(\frac{\rho_0}{M} \right) R_n + \left(\frac{R}{V} \right) \sum_{j=n+1}^N P_j \right] + k_t \beta R_n \quad (16)$$

In equation (16), β is the term accounting for the termination step, and it can be

$$\beta = 1 \quad \text{for first order} \quad (17a)$$

$$\beta = R/V \quad \text{for second order disproportionation} \quad (17b)$$

$$\beta = \frac{1}{2 R_n} \sum_{i+j=n}^N (R_i R_j / V) \quad \text{for second order recombinations} \quad (17c)$$

Similar considerations with those described for P_n can be made for the calculation of the rate of reactions of R_n species. The rate of change of the number of radicals R_n can be described by the equation:

$$\frac{dR_n}{dt} = k_e P_{n+1} + [2k_s + k_c (R/V)] \sum_{j=n+1}^N P_j - [k_c \left(\frac{\rho_0}{M} \right) + k_p + k_t \beta] R_n + k_p R_{n+1} \quad (18)$$

The kinetics equations (16) and (18) will allow the calculation of the weight loss rate for the polymer during pyrolysis. However, as previously indicated, the polymer does not consist of molecules with only one degree of polymerization. Therefore, a global kinetics equation for all the polymerization degrees $n = 2, 3, 4, \dots, N$ should be obtained. For this purpose it is convenient to use the symbol M_0 for the total number of polymeric molecules, where

$$M_0 = \sum_{n=2}^N P_n \quad (19)$$

and the symbol M_1 for the total number of monomeric units in the polymer sample, where

$$M_1 = \sum_{n=2}^N n P_n \quad (20)$$

The ratio M_1/M_0 is the average degree of polymerization and we can use the notation

$$x = M_1/M_0 \quad (21)$$

The average degree of polymerization x depends on time (as M_0 and M_1 depend on time) during the pyrolytic process. The initial value of x^0 (for $t=0$) is a constant for a certain material. Using rel. (20), we can also write the formula for the weight W (in g) of the polymer,

$$W = M \sum_{n=2}^N n P_n = M M_1 \quad (22)$$

The rate loss of the weight W during pyrolysis can be easily calculated from the loss of M_1 (number of monomeric units).

With the above notations we can take now the sum over n in equation (16) for the whole range of polymeric species ($n = 2, 3, \dots, N$). The sum will give

$$\frac{dM_0}{dt} = \frac{d \sum_{n=2}^N P_n}{dt} = k_e M_0 - k_s M_1 + [k_c (d_0 / M) + k_t \beta] (R - R_1) \quad (23)$$

Taking the sum over n in equation (18) and assuming that the concentration of radicals in a steady state is constant ($dR_n/dt = 0$), we can write

$$0 = [2k_s + k_c (R / V)] M_1 - 2k_e M_1/x - [k_c (d_0 / M) + k_t \beta] R \quad (24)$$

Adding equation (23) and (24) we will obtain

$$\frac{dM_0}{dt} = (k_s + k_c R/V) M_1 + k_e M_1 - [k_c (d_0 / M) + k_t \beta] R_1 \quad (25)$$

where the first two terms account for the gain in molecules by initiation and transfer, and the third term accounts for the loss by termination of R_1 followed by evaporation of P_1 .

In order to find the corresponding kinetics equation for M_1 , equation (16) and (18) are multiplied by n , then the sum over all values of polymerization degrees $n = 2, 3, \dots, N$, is taken, and the two expressions are added. This gives the formula:

$$\frac{dM_1}{dt} = - [k_c (d_0 / M) + k_t \beta] R_1 - k_p (R - R_1) \quad (26)$$

The first term in equation (26) accounts for the weight loss due to termination of R_1 and the second for the weight loss due to unzipping.

The solution of rate equation (25) or (26) is not always simple. A series of particular cases were, however, easier to solve. For this purpose, several parameters describing the polymer should be introduced. One parameter defined originally for the polymerization reaction is the kinetics chain length $\bar{\epsilon}$. The kinetics chain length is defined as the average number of monomers that react with an active center from its formation until it is terminated during the polymerization process. In the same manner, for the depolymerization process, the zip length $1/\gamma$ is defined. This is the average number of monomer molecules eliminated per kinetics chain during depolymerization. Low values of $1/\gamma$ mean that little monomer is eliminated during depolymerization but not

necessarily that there is little degradation. It can be shown [20] that the zip length can be defined using the relation:

$$1/\gamma = \frac{\text{probability of propagation}}{\text{probability of termination} + \text{probability of transfer}} = \frac{k_p R}{k_t \beta R + k_c (d_o / M) R} \quad (27)$$

Eliminating R - R1 and R1 in rel. (25) and (26) with the aid of rel. (24) and (27), we will obtain

$$\frac{dM_1}{dt} = (1 - 1/\gamma) \frac{dM_0}{dt} [(1 + 1/\gamma) k_s + k_c R/V] M_1 - (1 + 1/\gamma) k_e M_0 \quad (28)$$

The behavior of a polymer during depolymerization depends very much on the initial average degree of polymerization x^0 and the ratio between x^0 and the zip length $1/\gamma$. If the degree of polymerization is high ($1/\gamma < x^0$), then only a part of the polymer chain will be degraded by depolymerization. The remaining part will be still considered polymer together with the chains that have remained intact. The value of x of the polymer thus decreases. On the other hand if the DP is low compared to the zip length ($1/\gamma > x^0$), then some chains will be completely converted to monomer, the other chains retaining the original degree of polymerization.

The initial molecular weight distribution of the polymer is another factor determining the possibility to solve the kinetics equations. Solutions are possible when the polymer is close to a monodisperse system or when the molecular weight distribution of the polymer is known and can be described by a specific formula. A case like this is that of the "most probable" type polymer, where the distribution P_n is related to x by the formula:

$$P_n = \frac{M_1}{x^2} (1 - 1/x)^{n-1} \quad (29)$$

The average sample weight MM_1 and the average degree of polymerization P_n vary with time during depolymerization; however, due to the random nature of the process, equation (29) is preserved.

Certainly, the type of termination as indicated above (see rel. (10), (12), or (14)), may also influence the type of solution for the kinetics equations.

Based on these considerations, several particular equations for the number of monomer units lost (weight loss when using rel. (22)) during pyrolysis can be established such that a solution can be simple to obtain. A summary of these equations is given in Table 3.4.1 (see. e.g. [21]).

TABLE 3.4.1. A summary of equations with readily obtained solutions allowing the calculation of the weight loss during pyrolysis of repetitive polymers.

Zip length $1/\gamma$ vs. polym. deg. x^0	Initiation	Termination	MW distribution	Weight loss rate equations ($M1 = W/M$)
$1/\gamma < x^0$ short	random	first order	any	$\frac{dM1}{dt} - 2ks(1/\gamma) M1$
$1/\gamma < x^0$ short	random	disprop.	any	$\frac{dM1}{dt} - 2ks(1/\gamma) M1$
$1/\gamma < x^0$ short	random	recombin.	most probable	$\frac{dM1}{dt} - 4ks(1/\gamma) M1$
$1/\gamma > x^0$ long	random	any	monodisp.	$\frac{dM1}{dt} - ks x^0 M1$
$1/\gamma > x^0$ long	random	any	most probable	$\frac{dM1}{dt} - 2 ks x M1$
$1/\gamma < x^0$ short	end	first order	monodisp.	$\frac{dM1}{dt} - \frac{ke}{x \gamma} M1$
$1/\gamma < x^0$ short	end	first order	most probable	$\frac{dM1}{dt} - \frac{ke}{x^0 \gamma} M1$
$1/\gamma < x^0$ short	end	disprop.	monodisp.	$\frac{dM1}{dt} - \frac{ke}{x \gamma} M1$
$1/\gamma < x^0$ short	end	disprop.	most probable	$\frac{dM1}{dt} - \frac{ke}{x^0 \gamma} M1$
$1/\gamma < x^0$ short	end	recombin.	most probable	$\frac{dM1}{dt} - (ke/2) M1$
$1/\gamma > x^0$ long	end	any	any	$\frac{dM1}{dt} - ke M1$

3.5 Pyrolytic Processes Compared with Combustion.

Combustion is an oxidation process (commonly using oxygen) that generates heat and may induce pyrolysis. Especially for solid samples, the zones close to the burning area are heated by conduction, convection, or radiation and materials suffer pyrolytic processes. Pyrolysates as well as undecomposed small molecules frequently evolve from these heated areas by volatilization, steam distillation, aerosol formation, etc. Numerous studies are reported regarding the burning of solid materials [16a], but the subject of combustion is outside the scope of this book. Several studies of the pyrolysates generated during burning have been done using flash pyrolysis. Although the two processes have some differences, valuable information can be obtained on pyrolysates generated during burning either by the use of gradient pyrolysis or by repeated flash pyrolysis at different final pyrolysis temperatures (see Section 4.1).

Significant effort has been made for example to understand the generation of cigarette smoke. Smoke is more complex than a tobacco pyrolysate, because during smoking several simultaneous processes take place. One process is indeed pyrolysis, and this takes place in a range of temperatures as the burning zone of the cigarette progresses. An additional process is the volatilization (distillation) of certain fractions of tobacco leaf.

Steam distillation and aerosol formation are also present during smoking. Certain chemical reactions also occur, the main reaction being the combustion [16b]. Some compounds formed during smoking are filtered or condensed and remain in the unsmoked portion of the cigarette, while the transfer of a model pyrolysate to an analytical instrument may be more complete. An additional factor that should be considered when comparing cigarette smoke with tobacco leaf pyrolysates is that cigarettes may contain a tobacco blend, reconstituted tobaccos, and certain additives such as glycerin, sugars, and flavors. Also, the cigarette paper may have its own contribution to the smoke composition. A schematic diagram of a burning cigarette [16b] is shown in Figure 3.5.1.

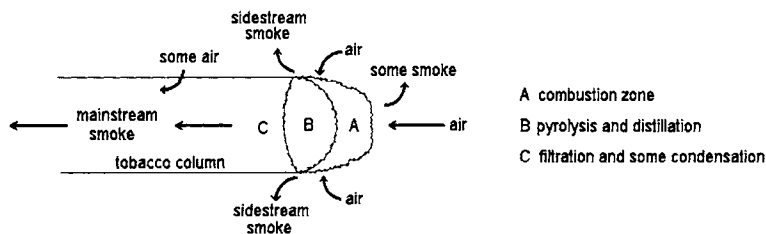


FIGURE 3.5.1. Schematic diagram of a burning cigarette [16b].

The temperatures in a burning cigarette vary depending on the place in the cigarette and also on the time during puffing. It reaches temperatures around 900° C or even higher, but a temperature gradient from room temperature up to the maximum exists across section B (Figure 3.5.1) where the pyrolysis takes place.

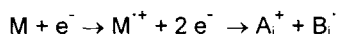
The cigarette generates sidestream smoke, mainstream smoke, and also some gases that may evolve through the cigarette paper. The chemical composition of the two types of smoke (mainstream and sidestream) is quite different and depends on the temperature distribution and the amount of oxygen reaching the pyrolysis zone. Sidestream smoke, compared to mainstream, contains a significantly higher proportion of compounds pyrolysed at higher temperatures and of combustion products, while mainstream smoke is richer in distilled compounds. Several processes during smoke formation depend on temperature distribution. Evaporation of volatiles takes place mainly between 70° C to 200° C. Sugars, lignin, pectin, proteins and hemicelluloses pyrolyse between 200° C and 400° C; cellulose, amino acids, and esters pyrolyse between 400° C and 600° C; inorganics decompose at higher temperatures. In addition to pyrolysis, combustion reactions contribute mainly to the formation of CO₂, CO and H₂O [16c]. The role of these components of smoke is important in experimental pyrolysis because they provide in the pyrolysis zone a non-oxidative atmosphere similar to flash pyrolysis in an inert gas. Secondary heterogeneous reactions may also take place during burning, where the pyrolysis or combustion products further react under the influence of heat, and possibly under some catalytic effects of the solid surfaces.

The study of smoke composition for other materials can also be related to pyrolysis. Smoking of certain foods is commonly practiced and the subject is very important for evaluating the taste/ flavor of food or for health issues associated with smoke constituents. Again, analytical pyrolysis can be used as a tool for investigating pyrolysis products in smoke.

3.6 Pyrolysis Process Compared to Ion Fragmentation in Mass Spectrometry.

Molecular fragmentation is a usual process during pyrolysis. In mass spectrometry, molecules are also fragmented following an ionization step. This ionization is commonly done using an electron bombardment (electron ionization or EI) with electrons having energy of 70 eV and at a very low pressure (in vacuum 10^{-2} to 10^{-3} Pa). During pyrolysis ions are not formed (as shown in Section 3.1), because the energies involved in the pyrolytic process are much lower than the required level for ion formation (ionization potential of many molecules are around 10 eV) and commonly the pressure is around 100 kPa. These essential differences make the two processes not equivalent. In addition to that, mass spectrometry in its typical form is applied to small molecules (expansion of mass spectrometry to large molecules can be done only using special techniques). Pyrolysis of polymers seems therefore a separate subject. However, a comparison of the results of fragmentations in pyrolysis and in mass spectrometry of certain molecules shows significant similarities [21]. Because during polymer pyrolysis two steps can be distinguished, the first being the fragmentation of the polymer and the second being further pyrolysis of the small molecules generated in the first step, the parallel can be also meaningful for polymer pyrolysis. A short description of mass spectra fragments generation is needed to better understand the analogy.

In mass spectrometry, the electrons interact with the molecules M to eject an additional electron leaving a positively charged species (with an odd number of electrons) of the type $M^{+\cdot}$. The ions also receive energy during the electron impact, and the excess of energy induces fragmentation (with fragment ions A_i^+ commonly but not always with an even number of electrons):

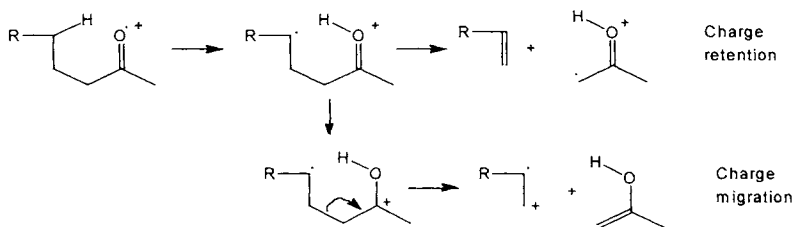


The formation of molecular ions takes place with a range of internal energies, and more than one fragmentation path is possible for a given molecule. The mass spectrum is given as a chart showing the ion abundance (normalized to the most abundant ion) versus m/z of the fragments. For the interpretation of the mass spectra, two main questions should be answered, namely:

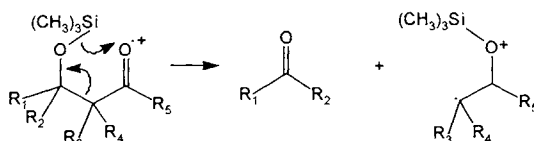
- which bond breaks in the molecule, and
- where the charge will go between the two fragments (the neutral fragments are not seen in mass spectroscopy).

The ionization process takes place in a "vertical" or Frank-Condon process, which means that the geometry of the molecule does not change during the ionization (the movement of the atoms is too slow to be affected by the ionization). Indeed, the energy of 70 eV for an electron corresponds to a (formal) velocity equal to $4.96 \cdot 10^9$ cm/s. At this speed, the time required for the electron to traverse a molecule of 1 μm in diameter is about $2 \cdot 10^{-16}$ s. The time of interaction is, therefore, at least 50 times shorter than the period of the most rapid molecular vibration (which is C-H stretching). However, the redistribution of electronic charge between the bonds takes place very rapidly such that all bonds are affected simultaneously in the ionization process. However, complete energy randomization and neglect of the electronic state functions is not true for molecules with many π electrons or heteroatoms with non-bonding valence electrons. In a molecular ion, the charge can be localized or delocalized, depending on the molecule.

Rearrangements accompanying fragmentation are common during fragment ion formation. Especially common are the rearrangements involving migration of hydrogen atoms. One such mechanism involves a γ -H rearrangement to an unsaturated group (such as =O, etc.) and a β -cleavage (McLafferty rearrangement).



The same type of reaction may take place for the migration of other groups besides hydrogen, such as $\text{Si}(\text{CH}_3)_3$ group.



In general, the most abundant fragment-ion corresponds to reactions that form the most stable products (ion and neutral radical). Steric effects can also be of key importance. The abundance of a product ion is affected by its stability. Ion stabilization may be achieved through electron sharing involving a nonbonding orbital of a heteroatom, such as in the acetyl ion $\text{CH}_3\text{-C}^+=\text{O} \leftrightarrow \text{CH}_3\text{-C}\equiv\text{O}^+$ (which is isoelectronic with $\text{CH}_3\text{-C}\equiv\text{N}$), or through resonance stabilization, such as in the case of allyl cation $\text{CH}_2=\text{CH-CH}_2^+ \leftrightarrow \text{CH}_2^+ \text{-CH}=\text{CH}_2$. Also, the fragment with the higher tendency to retain the unpaired electron should have the higher ionization energy (potential) I . Therefore, there is a higher probability for forming the fragment ion of lower I value (Stevenson's rule). Because this ion is usually the more stable ion, it is the more abundant ion resulting from the bond cleavage. The preference of a reaction pathway can also be increased by radical stabilization. This radical stabilization is enhanced on carbon by delocalization (e.g., allyl radical), increased branching (e.g., tert-butyl radical), or the presence of electronegative sites such as an oxygen (e.g., alkoxy radical). The neutral product can also be a molecule. Small molecules such as H_2 , CH_4 , H_2O , C_2H_4 , CO , NO , CH_3OH , H_2S , HCl , $\text{CH}_2=\text{C}=\text{O}$, and CO_2 are favored.

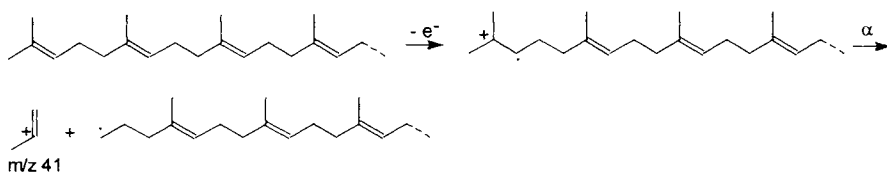
The rules indicated above seem to not have much connection to the fragmentation results obtained in pyrolysis. For example, Stevenson's rule, the charge site ionization mechanism, and the sigma electron ionization mechanism are not applicable to pyrolysis products, as the molecules in pyrolysis are not ionized. On the other hand, the α cleavage and certain rearrangements may be similar for the two processes. Also the fact that small molecule elimination is favored in mass spectrometry makes possible that, with a certain frequency, pyrolysis products are similar to mass fragments obtained in mass spectrometry.

A different perspective on mass spectral fragmentation can be obtained considering the energy of the molecular ion formed during the EI process. The ions with low energy states can be related to thermal processes [21,22], and this may provide information on the thermal decompositions. In addition to standard ionization procedures, special techniques that provide milder ionization conditions such as field ionization (see Section 5.4) offer an even closer similarity to the pyrolytic process.

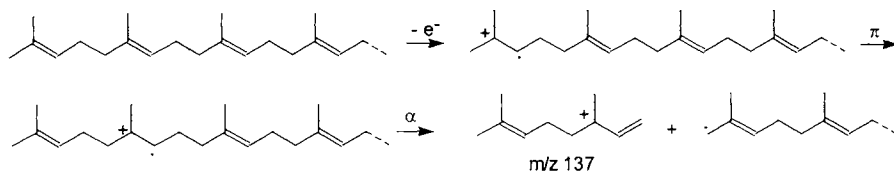
Similarities between mass spectral and thermal fragmentations are particularly common in certain reaction types. Electrocyclic reactions, for example, are frequently similar in the two processes. The thermal process has in general a higher stereoselectivity (because of the higher aromaticity in even-electron systems). Retro-Diels-Alder reactions are typical examples for the similarity of the two processes. Internal displacement reactions may also be similar in the two processes, mainly in the case of internal radical displacements. The relationship between mass spectra and thermal fragmentation is complex, and it is useful to discuss it for separate classes of compounds.

- Pyrolysis of polyisoprene and ion fragments formation from oligomers of isoprene.

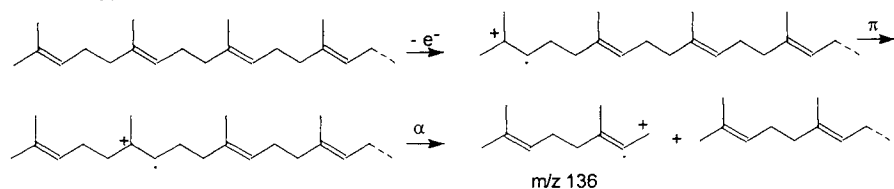
Pyrolysis of polyisoprene takes place by a free radical mechanism and generates mainly isoprene (MW=68), a dimer of isoprene (DL-limonene, MW=138), and several other unsaturated hydrocarbons (see Sections 2.6 and 6.1). The mass spectra fragmentation (generating fragments with specific mass/charge (m/z) ratios) of a model molecule simulating polyisoprene (isoprene oligomer) occurs by the mechanisms as indicated below:



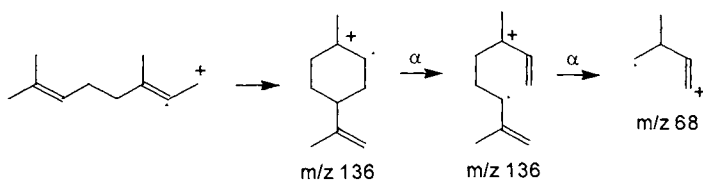
When a migration of the π electrons (π) takes place, the mechanism can be of the type;



or of the type:



Also possible, are reactions of the type:



The fragments from the pyrolysis and the mass spectra generated from a model isoprene oligomer are therefore very similar. This result is expected, due to the high number of π electrons in the polyisoprene molecule [22].

- Pyrolysis of saccharides compared to ion fragments formation.

Polysaccharides pyrolyse by different mechanisms (see Section 7.1 and 7.2), the first step being in most cases a chain scission (by transglycosidation or retroaldolization). Mass spectral fragments from polysaccharides cannot be obtained by standard EI techniques; however, mass spectra are reported for di or trisaccharides. As examples, two mass spectra are given below, for 4-O- β -D-galactopyranosyl- β -D-glucopyranose in Figure 3.6.1 and for O- α -D-glucopyranosyl-(1 \rightarrow 3)- β -D-fructofuranosyl-(2 \rightarrow 1)- α -D-glucopyranoside in Figure 3.6.2.

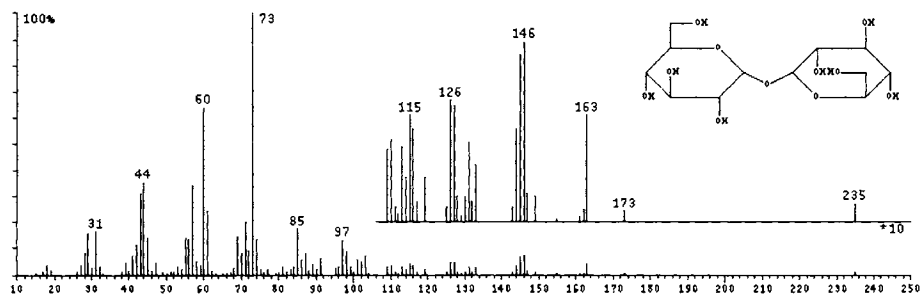


FIGURE 3.6.1. Mass spectrum (EI at 70 eV) for 4-O- β -D-galactopyranosyl- β -D-glucopyranose.

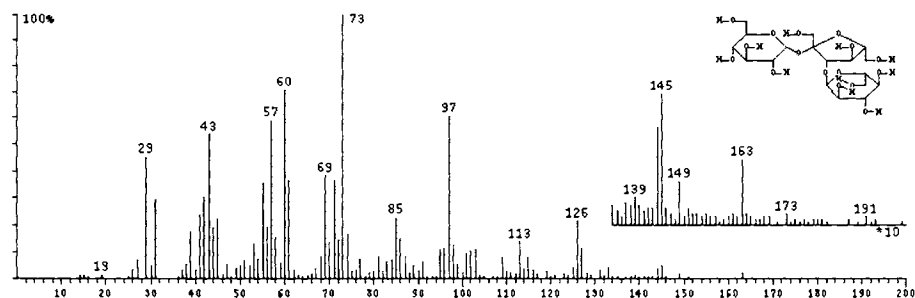
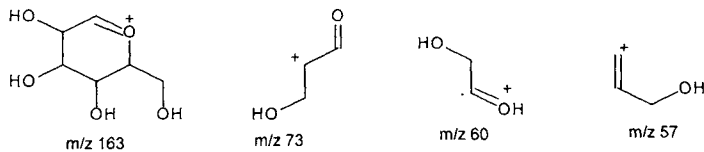
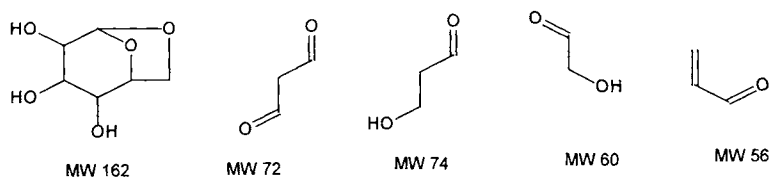


FIGURE 3.6.2. Mass spectrum (EI at 70 eV) for O- α -D-glucopyranosyl-(1 \rightarrow 3)- β -D-fructofuranosyl-(2 \rightarrow 1)- α -D-glucopyranoside.

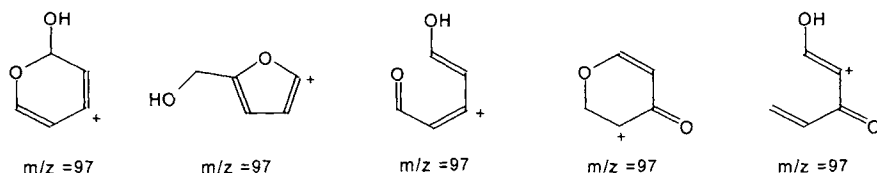
Typical mass spectra fragments from saccharides are likely to have the following structures:



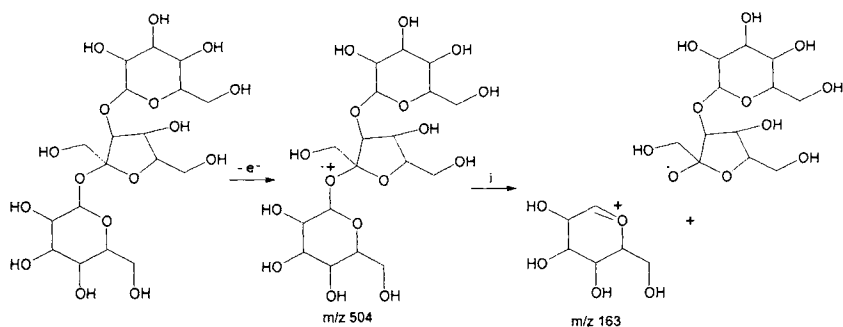
These fragments have good resemblance with compounds detected in pyrolysis of sugars (see Sections 7.1 and 7.2) such as:



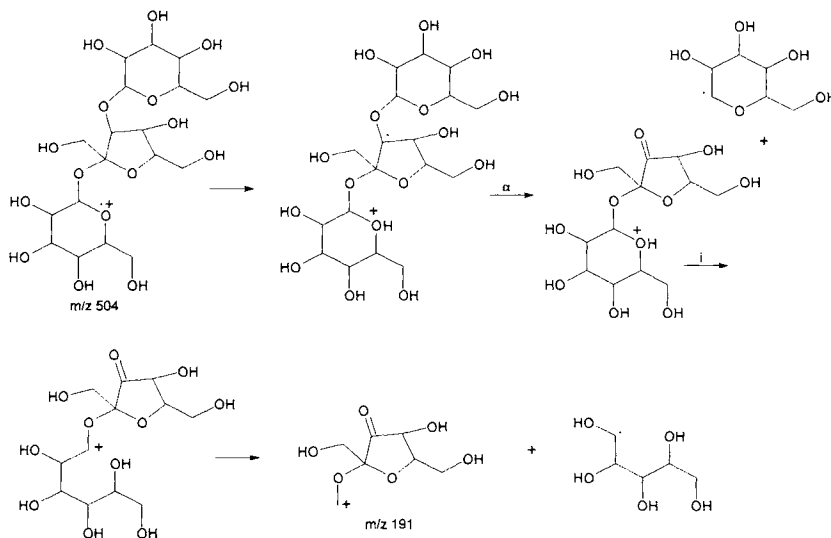
Numerous structures can be proposed for the ion with $m/z = 97$, which also have correspondents in the pyrolysates:



The formation of the mass spectra fragments can be explained by a variety of mechanisms. For example, the formation of the ion m/z 163 for the trisaccharide with the spectrum shown in Figure 3.6.2 can be explained as follows:



(α indicates radical site initiation with α cleavage, i indicates charge site initiation mechanism). The formation of the ion with m/z 191 can be explained by the following mechanism:



Larger ions are not abundant in the mass spectrum of *O*- α -D-glucopyranosyl-(1 \rightarrow 3)- β -D-fructofuranosyl-(2 \rightarrow 1)- α -D-glucopyranoside. Similarly to the formation of the fragments in pyrolysis, the pyranose or furanose type cycles have the tendency to maintain their integrity compared to the ether bonds. This contributes to the similarity between mass spectra fragments and pyrolysis fragments for this class of compounds. However, the pyrolysis products show in general a wider variety of compounds as compared to mass spectra fragmentation. The lack of secondary reactions involving the mass spectra fragments is probably due to the low pressure in which the fragmentation takes place in a mass spectrometer.

- Pyrolysis of lignin models compared to ion fragments formation.

Lignin is another example where pyrolysis and mass spectra fragments show similarities. This can easily be explained by the presence of aromatic rings and heteroatoms in its structure [22]. A study on two trimeric lignin models by pyrolysis and by mass spectrometry [23] showed a good similarity between the fragments generated by the two techniques. Figure 3.6.3 shows the mass spectrum (obtained using EI with 70 eV) of ω -guaiacoxy-acetoguaiacone-benzylether (trimer A), and Figure 3.6.4 shows the spectrum of ω -syringoxy-acetoguaiacone-benzylether (trimer B).

The fragments seen in these spectra correspond well with compounds detected in the pyrolysis products of the two compounds, as well as with compounds seen in the pyrolysis products of several lignins (see Section 9.1). The compounds found in the pyrolysis products (generated at 600 $^{\circ}$ C) of the two lignin models that are similar to the fragments seen in the mass spectra are shown in Table 3.6.1.

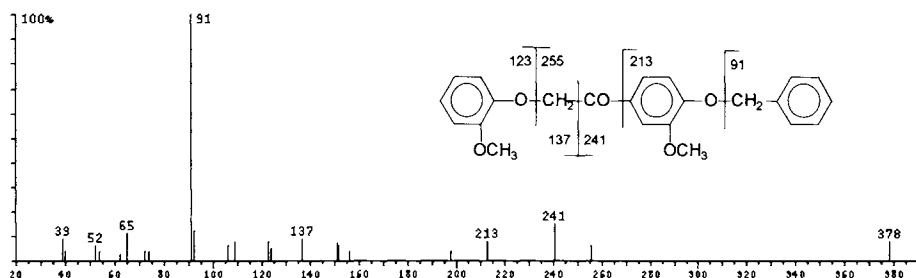


FIGURE 3.6.3. Mass spectrum (EI at 70 eV) of ω -guaiacoxy-acetoguaiacone-benzylether (trimer A).

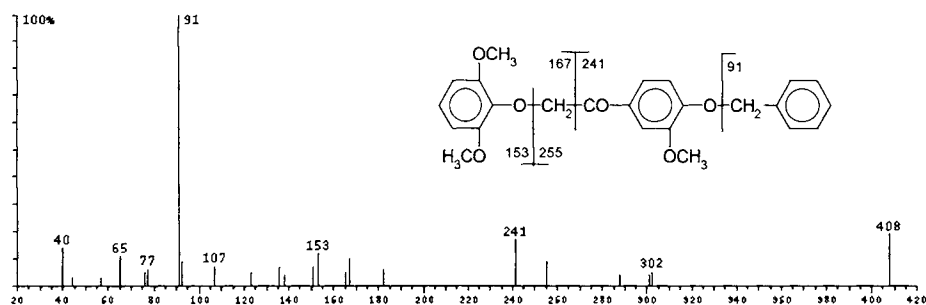


FIGURE 3.6.4. Mass spectrum (EI at 70 eV) of ω -syringoxy-acetoguaiacone-benzylether (trimer B).

TABLE 3.6.1. Compounds found in the pyrolysis products and their relative intensities for two lignin models. The similar fragments seen in their mass spectra are also shown.

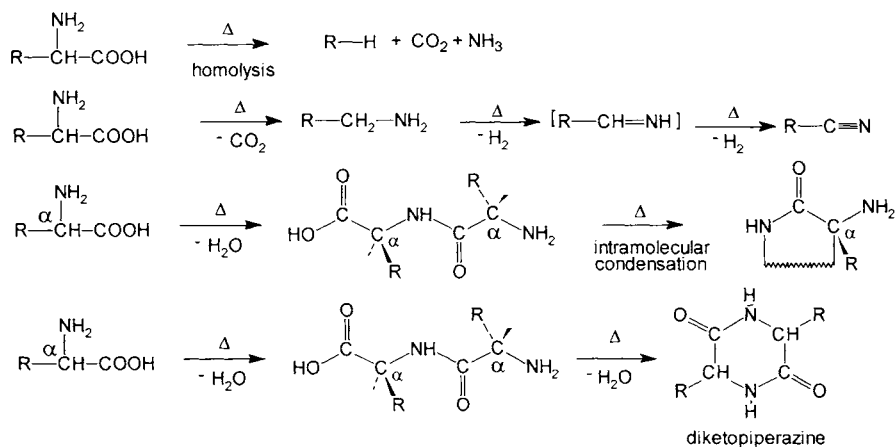
Compound	MW	Rel. intensity for trimer A	Rel. intensity for trimer B	Fragment in MS
methylbenzene	92	73	100	91
dimethylbenzene	106	28	19	?
phenol	94	42	26	?
vinylbenzene	104	23	15	?
2-hydroxybenzaldehyde	122	72	9	123
guaiacol	124	59	21	123
3-methoxybenzaldehyde	136	0	22	137
2-methoxybenzaldehyde	136	65	0	137
1,3-dimethoxybenzene	138	0	14	137
vanillin	152	5	9	153
syringol	154	0	29	153
acetoguaiacone	166	18	20	167
1,2-diphenylethane	182	100	42	?
vanillin-benzyl ether	242	19	0	241
2,6-dimethoxybenzophenone	242	0	5	241
acetoguaiacone-benzyl ether	256	27	6	255

Table 3.6.1 also shows a few compounds with relative high intensity that are not present in the fragments for the mass spectra but are present in the pyrolysis products. These compounds are commonly a result of further secondary reactions, which seems to be more common in pyrolysis as also seen in the case of saccharides.

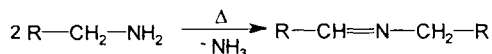
The presence of free radicals in pyrolytic reactions seems to be a common event, as seen by the increase in certain more stable species as the pyrolysis temperature increases. At elevated temperatures, higher levels of aromatic compounds, polynuclear aromatic compounds, or small molecules tend to be formed. These compounds were not seen in the mass spectra fragments, where only intramolecular rearrangements are more common.

- Pyrolysis of amino acids compared to ion fragments formation.

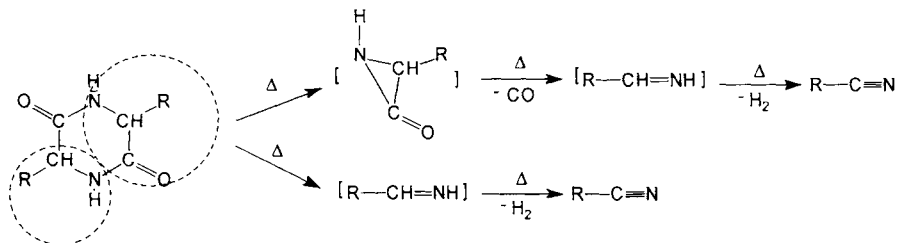
Pyrolysis of α -amino acids has significant implications in the interpretation of the results of peptide and protein pyrolysis. Amino acid thermal decomposition takes place through four main fragmentation pathways as shown below:



The amines may react further with the elimination of ammonia:

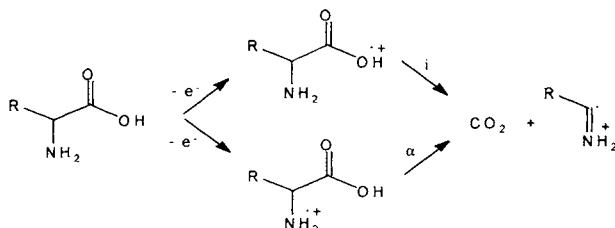


Also, diketopiperazines may undergo further pyrolysis decomposing as follows:



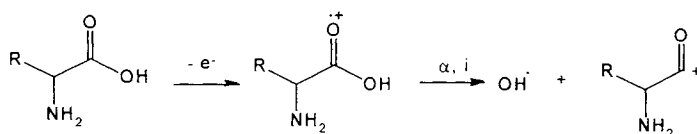
In a mass spectrometer, the ions are generated by EI from amino acids through one of the following schemes:

-Elimination of CO_2 generating ions of the form $\text{R-C}=\text{NH}_2^+$ that takes place as follows:

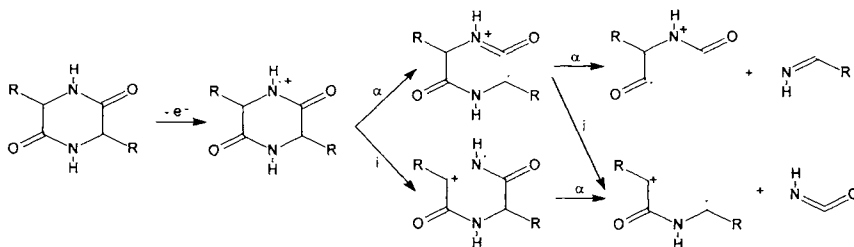


The result of this path of ion formation is equivalent to the amine formation by amino acid decarboxylation.

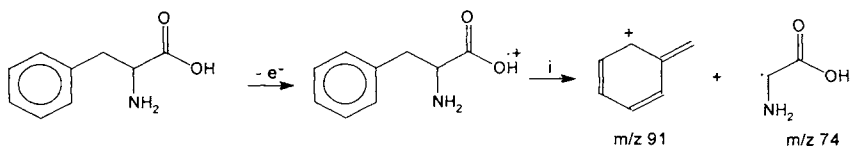
- Elimination of an OH group that is similar to the first step in water elimination by pyrolysis.



- The formation of diketopiperazines (DKP) is also possible when heating occurs before the ion formation in the mass spectrometric analysis of amino acids. These compounds will further form characteristic ions by the scheme:



- Reactions equivalent with homolysis (from the previous scheme) generating hydrocarbons are also possible in the mass spectrometer. As an example, for phenylalanine it is characteristic to have an ion formation process of the type:



The mass spectrum of phenylalanine is shown in Figure 3.6.5, and the fragment formation by reactions equivalent to those from pyrolysis is obvious.

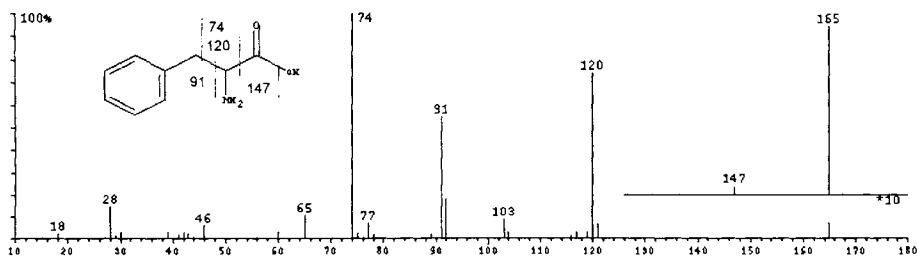


FIGURE 3.6.5. Mass spectrum (EI at 70 eV) of phenylalanine.

The results for amino acids show that the main pyrolysis products are similar to the ion fragmentation that takes place upon electron impact. For the case of peptides and proteins, most of the effort has been done in obtaining ions of large fragments in order to account as much as possible for the protein structure [24]. Several mass spectra of substituted diketopiperazines obtained from peptide pyrolysis are shown in Figures 3.6.6 a to 3.6.6 f. The fragments generated in their mass spectra are similar to some small molecules obtained in amino acid pyrolysis.

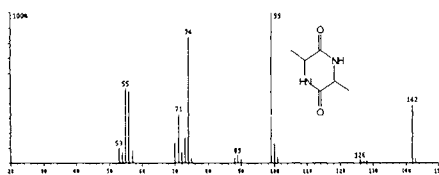


FIGURE 3.6.6 a. MS of 2,5-dimethyl DKP

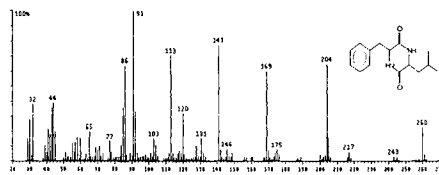


FIGURE 3.6.6 b. MS of 2-benzyl-5-(methylpropyl) DKP

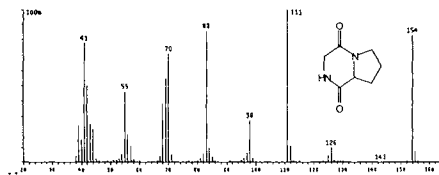


FIGURE 3.6.6 c. MS of 1,4-diazabicyclo[4,3,0]nonane-2,5-dione

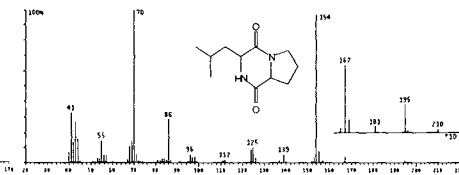


FIGURE 3.6.6 d. MS of 1,4-diazabicyclo[4,3,0]nonane-3-methylpropyl-2,5-dione

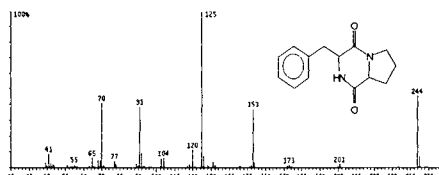


FIGURE 3.6.6 e. MS of 1,4-diazabicyclo[4,3,0]nonane-3-benzyl-2,5-dione

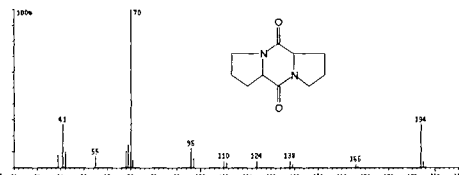


FIGURE 3.6.6 f. MS of octahydro-5H,10H-dipyrrolo[1,2-a:1',2'-d]pyrazine-5,10-dione

For example, in alanine pyrolysis 1,4-dimethylpiperazin-2,5-dione itself is formed (see Figure 3.6.6 a). Pyrolysis of phenylalanine generates toluene analogous to ion 91 in Figures 3.6.6 b and 3.6.6 e, pyrolysis of leucine generates 3-methylbutylamine

analogous to ion 86 in Figures 3.6.6 b and 3.6.6 d, and pyrolysis of proline generates pyrroline analogous to the ion with m/z 70 in Figures 3.6.6 c, 3.6.6 d, 3.6.6 e and 3.6.6 f.

- Pyrolysis of nucleic acids compared to ion fragments formation from adenosine-5'-phosphate and 2-deoxyadenosine-5'-phosphate.

Direct MS with EI ionization is not applicable to nucleic acids. However, a parallel that can be easily made is between the Py-MS results on nucleic acids and EI mass spectra of adenosine phosphate and deoxyadenosine phosphate. The mass spectra of adenosine phosphate and deoxyadenosine phosphate are known only for the silylated corresponding compounds and are shown in Figures 13.1.4 and 13.1.5. The spectra indicate the formation of fragments such as the phosphate group, the purine base, and fragments resulting from the breaking of the ribose/deoxyribose ring. These fragments, although obtained from a silylated material, can be compared to those seen in the Py-MS of nucleic acids (see Section 13.1).

For all the classes of compounds discussed above, it is possible to trace similarities between pyrolysis fragmentations and mass spectral fragmentations. However, it is not always simple to predict the result of each of the two processes. This adds supplementary complications for the interpretation of the data in the Py-MS analytical technique where the two processes are combined (see Sections 5.4 and 5.5).

3.7. Theoretical Approaches for Chemical Pyrolytic Reactions.

There have been numerous attempts to approach chemical reactivity using theoretical tools such as those provided by quantum chemistry [21,22,25,26]. This has been done using "reactivity indices," attempting to calculate the energies along the reaction path using semiempirical molecular orbital (MO) techniques with program packages such as MOPAC [27,28 29], or using bond dissociation energies calculated from the heats of formation [29]. This type of approach is not directly applicable to the reactions involving polymers. However, pyrolysis of polymers frequently involves secondary processes of pyrolysis of small molecules generated by depolymerization in the first step of the reaction. Also, some bond energies are influenced only by the nature of the bonding atoms and by the immediate neighboring atoms in the molecule. This allows a transferability of certain parameters from small molecules to the polymer [25].

As indicated in Chapter 2, a variety of reaction types occur in pyrolysis. Among these are eliminations with E_i mechanism, fragmentations, eliminations involving free radicals, electrocyclic rearrangements, radicalic substitutions, retro-ene reactions, etc. Theoretical calculations for the eliminations with E_i mechanism and retro-ene reactions require in general that the calculations be done for each particular case. However, the reactions involving radicals allow the transferability of some general results. As an example, the use of rel. 12 Section 3.1 gives the dissociation energy for an A-B bond that suffers homolytic dissociation when the heats of formation of the radicals $\Delta H_f^0(A\cdot)$ and $\Delta H_f^0(B\cdot)$ and of the molecule $\Delta H_f^0(AB)$ are known.

One theoretical approach for the calculation of certain thermodynamic properties of molecules is the use of semiempirical (MO) calculations. As an example, the heat of

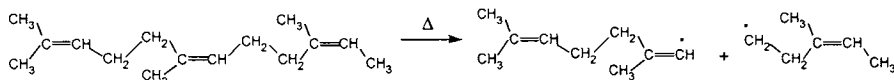
formation can be calculated with satisfactory precision using for example the MOPAC package. Also, *ab initio* MO techniques such as Gaussian 94 [30,31] can be utilized for the same purpose. In MOPAC, the calculated self-consistent field energy E_{SCF} is parameterized to reproduce as closely as possible the heat of formation at 25° C for most molecules.

One advantage of these theoretical calculations is that the values can be calculated at different temperatures. This allows a better utilization of the data for the estimation of the values to be utilized in pyrolytic processes. Table 3.7.1 gives some data regarding experimental and calculated heats of formation for several organic radicals using three semiempirical MO parameterizations in MOPAC [27], namely PM3, MNDO and AM1. As seen from Table 3.6.1, vinyl and allyl radicals show the best match. Calculations for molecules containing π electrons and especially those with aromatic character show a better agreement with experimental data.

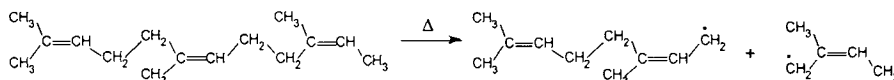
TABLE 3.7.1. *Experimental and calculated (using MOPAC) heats of formation for several organic radicals [27].*

Radical	Exp. ΔH_f° (A \cdot) kcal	Calc. ΔH_f° (A \cdot) kcal	Difference PM3 kcal	Difference MNDO kcal	Difference AM1 kcal
methyl	34.8	29.8	-5.0	-9.0	-3.6
vinyl	59.6	63.3	3.7	4.2	5.2
ethyl	25.0	17.3	-7.7	-12.2	-6.9
allyl	40.0	39.6	-0.4	-4.6	-1.4
i-propyl	16.8	5.5	-11.3	-15.4	-10.0
i-butyl	4.5	-5.9	-10.4	-11.7	-7.4
methoxy	-0.5	-6.8	-6.3	0.3	-3.2
cyanide	104.0	128	24.0	25.3	10.4

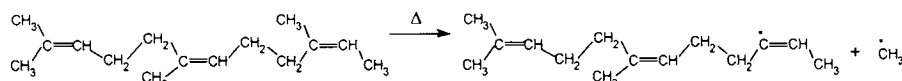
An example of a theoretical calculation is shown below for an isoprene trimer. The three main possible paths for the formation of radicals, as shown in Section 2.6, are α scission:



β -scission:



and methyl scission:



The calculated heats of formation and the bond dissociation energies are given in Table 3.7.2. The calculations were done using MOPAC 7 with AM1 Hamiltonian for two different temperatures [32].

TABLE 3.7.2. *Bond dissociation energies for an isoprene trimer.*

Reaction	ΔH A-B kcal	Temperature 25° C			Temperature 500° C			
		ΔH A*	ΔH B*	ΔH dissoc.	ΔH A-B kcal	ΔH A*	ΔH B*	ΔH dissoc.
α scission	-18.75	46.35	20.69	85.79	35.33	78.4	43.02	86.09
β scission	-18.75	14.96	21.57	55.28	35.33	50.79	39.9	55.36
CH ₃ elim.	-18.75	33.71	31.25	83.71	35.33	83.16	36.39	84.22

The data from Table 3.7.2 show that during polymer chain scission the initiation reaction is more likely to take place by β scission (lower dissociation energy). Methyl elimination and α scission probably play a less important role in the initiation reaction. The values calculated for 25° C and 500° C did not show differences between them.

A larger oligomer such as a nonamer gave using the MOPAC calculation the following results for the α scission: ΔH A-B = - 43.08 kcal, ΔH A* = 20.80 kcal, ΔH B* = 20.69 kcal, with a resulting $\Delta H_{\text{dissoc.}}$ = 84.57 kcal. This result confirms that the larger radicals have lower heats of formation (compare ΔH A* = 20.80 kcal for the nonamer with ΔH A* = 46.35 kcal for the trimer), and the bond dissociation energies are practically not influenced by the length of the polymer (number of carbon atoms).

References 3.

1. I. M. Klotz, R. M. Rosenberg, *Chemical Thermodynamics*, Wiley, New York, 1994.
2. S. A. Liebman, E. J. Levy, ed., *Pyrolysis and GC in Polymer Analysis*, M. Dekker Inc., New York, 1985.
3. E. G. Tibor, S. Geza, *Chimie Fizica Teoretica*, vol. 2, Ed. Technica, Bucuresti, 1958.
4. S. W. Benson, *J. Chem. Ed.*, 42 (1965) 502.
5. J. A. Settula, J. J. Russell, D. J. Gutman, *J. Am. Chem. Soc.*, 112 (1990) 1347.
6. J. March, *Advanced Organic Chemistry*, J. Wiley, New York, 1992, p. 191.
7. Y. S. Stein, M. J. Antal, M. Jones, *J. Anal. Appl. Pyrol.*, 4 (1983) 283.
8. C. A. Zaror, D. L. Pyle, *J. Anal. Appl. Pyrol.*, 10 (1983) 1.
- 8a. J. R. MacCallum, *J. Anal. Appl. Pyrol.*, 11 (1987) 65.
9. F. Shafizadeh, *J. Anal. Appl. Pyrol.*, 3 (1982) 283.
10. R. Font, A. N. Garcia, *J. Anal. Appl. Pyrol.*, 35 (1995) 249.
11. S. S. Alves, J. L. Figueiredo, *J. Anal. Appl. Pyrol.*, 17 (1989) 37.
12. W. F. K. Wyenne-Jones, H. Eyring, *J. Chem. Phys.*, 3 (1935) 492.
13. V. Swaminathan, N. S. Madhavan, *J. Anal. Appl. Pyrol.*, 3 (1981) 131.

14. J. Sestak, G. Berggren, *Thermochimica Acta*, 3 (1971) 1.
15. S. Glasstone, K. J. Laidler, H. Eyring, *The Theory of Rate Processes*, McGraw Hill, New York, 1941.
16. P. J. Robinson, K. A. Holbrook, *Unimolecular Reactions*, J. Wiley, New York, 1972.
- 16a. I. Glassman, *Combustion*, Academic Press, Orlando, 1987.
- 16b. R. R. Baker, *J. Anal. Appl. Pyrol.*, 11 (1987) 555.
- 16c. R. R. Baker, *J. Anal. Appl. Pyrol.*, 4 (1983) 297.
17. R. T. Conley, ed., *Thermal Stability of Polymers*, M. Dekker Inc., New York, 1970.
18. H. H. G. Jellinek, ed. *Aspects of Degradation and Stabilization of Polymers*, Elsevier, Amsterdam, 1980.
19. C. H. Bamford, C. F. H. Tipper, ed., *Comprehensive Chemical Kinetics*, vol. 14 Elsevier, Amsterdam, 1975.
20. H.-G. Elias, *Macromolecules*, vol. 2, Plenum, New York, 1978.
21. R. C. Dougherty, *J. Am. Chem. Soc.*, 90 (1968) 5780.
22. R. C. Dougherty, *J. Am. Chem. Soc.*, 90 (1968) 5788.
23. O. Faix, D. Meyer, I. Fortmann, *J. Anal. Appl. Pyrol.*, 14 (1988) 135.
24. C. Fenselau, *Mass Spectrometry for the Characterization of Microorganisms*, ACS Symposium 541, Washington D.C., 1994.
25. S. C. Moldoveanu, A. Savin, *Aplicatii in Chimie ale Metodelor Semiempirice de Orbitali Moleculari*, Ed. Academiei RSR, Bucuresti, 1980.
26. A. Streitwieser Jr., *Molecular Orbital Theory for Organic Chemists*, John Wiley, New York, 1961.
27. J. J. P. Stewart, *J. Comp.-Aided Mol. Design*, 4 (1990) Special Issue.
28. M. J. S. Dewar, E. F. Healy, J. J. P. Stewart, *J. Chem. Soc. Faraday Trans. II*, 3 (1984) 227.
29. J. J. P. Stewart, MOPAC-7, QCPE 113, Indiana Univ., Bloomington 1994.
30. D. W. Rogers, *Computational Chemistry Using the PC*, VCH, New York, 1994.
31. M. J. Frisch, A. Frish, J. B. Foresman, *Gaussian 94*, Gaussian Inc., Pittsburgh, 1995.
32. S. C. Moldoveanu, unpublished results.

This Page Intentionally Left Blank

Chapter 4. Instrumentation Used for Pyrolysis

4.1 The Temperature Control of the Pyrolytic Process.

Analytical pyrolysis requires heating of the sample at a temperature significantly higher than ambient, commonly between 500° C and 800° C. For special purposes this temperature can be higher. The pyrolytic process is done in a pyrolysis unit (pyrolyser) which commonly interfaces with an analytical instrument (see Section 1.2). The analytical instrument is used for the measurement of the pyrolysis products. It is also possible to perform "off line" pyrolysis (no direct interface to an analytical instrument), followed by the analytical measurement. The pyrolysers have a source of heat where the sample is pyrolysed. The pyrolysis products are usually swept by a flow of gas from the pyrolyser into the analytical instrument.

There are several procedures to perform pyrolysis: flash pyrolysis (pulse mode), slow gradient heating pyrolysis (continuous mode), step pyrolysis, etc. Commonly, the pyrolysis for analytical purposes is done in pulse mode. This consists of a very rapid heating of the sample from ambient temperature, targeting isothermal conditions at a temperature where the sample is completely pyrolysed. Controlled slow temperature gradients are also possible in pyrolysis, but their use in analytical pyrolysis is limited. Step pyrolysis heats the sample rapidly but in steps, each step following a plateau of constant temperature kept for a limited time period.

There are several construction principles for pyrolysers, such as inductively heated, resistively heated filament, furnace type, and radiative heated. The principles of construction for the main types of pyrolysers will be discussed in Section 4.2 to Section 4.6.

A pyrolysis unit usually consists of a controller and the pyrolyser itself. The controller provides the appropriate electrical energy needed for heating. A simplified scheme of a pyrolyser (based on the design of a flash heated filament system made by CDS Inc.) is shown in Figure 4.1.1.

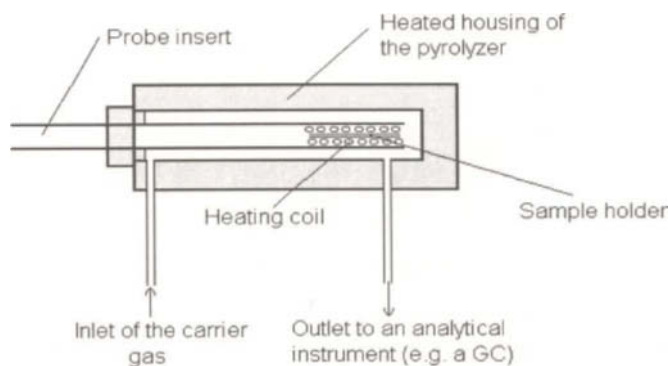


FIGURE 4.1.1. The simplified scheme of a pyrolyser (based on the design of a heated filament system made by CDS Inc.).

The main heating element where pyrolysis occurs is represented in Figure 4.1.1 as a coil, that can be heated at high temperatures. This heating element can differ depending on the pyrolyser principle and instrument type. The pyrolyser body (sometimes called interface) is a housing for the main heating element connected to an analytical instrument. Inside the interface, a probe insert can be introduced which contains the sample as is or in a sample holder. In Figure 4.1.1, the main heating coil is also attached to the probe insert, but this can differ again depending on the instrument type. A stream of inert gas flows through the interface. The interface (pyrolyser body) is also heated but at lower temperatures to avoid the condensation of pyrolysis products.

An essential requirement of the pyrolysis unit used for analytical purposes is that of reproducibility. The primary condition for achieving reproducibility is to use a precisely controlled temperature (other parameters such as the amount of sample or the pyrolyser type will be discussed later in the book). The isothermal condition targeted for performing flash pyrolysis is referred to as *equilibrium temperature* (T_{eq}). The T_{eq} is also named *final pyrolysis temperature* because in practice it is not possible to heat a sample instantly, although very short times for reaching T_{eq} can be achieved. The choice of T_{eq} temperature depends on the material to be pyrolysed and on the scope of the analysis. Generally, as the pyrolysis temperature T_{eq} increases, smaller and less characteristic fragments begin to dominate the pyrogram. Dehydration processes, even for non-polymeric substances, and formation of small molecules more stable at higher temperatures are common above 600° C.

The dependence of the composition of the pyrolysis products on temperature can be exemplified by the study of the monomer and dimer formation during the flash pyrolysis of natural rubber at different temperatures [1]. Figure 4.1.2 shows the plot of monomer/dimer ratio for flash pyrolysis of rubber at discrete temperatures between 300° C and 500° C. The figure indicates the increase in monomer formation at higher temperatures. More examples will be given when pyrolysis for particular biopolymers is discussed.

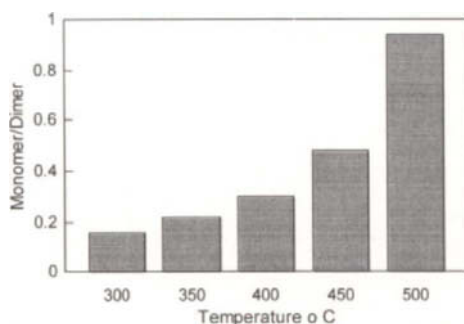


FIGURE 4.1.2. *The ratio monomer/dimer in the pyrolysis of natural rubber.*

Because pyrolysis is frequently a complex process, there is no precise rule to indicate which T_{eq} temperature should be chosen for a given sample. The ceiling temperature T_c (see Section 3.1), which may be seen as a recommended temperature for pyrolysis, was not proven in practice as a reliable guidance for the choice of T_{eq} . For this reason, in the specialized literature the description of the pyrolysis products of a certain material

is almost always associated with the description of experimental conditions for the pyrolysis.

The *total pyrolysis time* (or *total heating time* THT) is another parameter used to control the pyrolytic process. This parameter should be chosen long enough for the total amount of sample to be pyrolysed during THT. Because longer THTs than those exactly needed for the pyrolysis of the sample are commonly used, this parameter is not critical as long as the whole sample is pyrolysed within THT.

The cooling of the sample from the T_{eq} value may play a certain role in reproducibility, and the cooling may be related to THT. Some variability can be introduced if the pyrolysate is swept from the main heating source at different temperatures. At lower temperatures some condensation may take place in the pyrolyser, affecting the analytical results. This problem is commonly avoided using appropriate heating of the pyrolyser body (housing heating). The temperature of the housing is commonly maintained above the temperature of condensation of the components in the pyrolysate, which should be further analyzed. The heating of the pyrolyser body, however, needs to be done such that the sample does not get heated before pyrolysis. When the sample is introduced in the pyrolyser, there is commonly a waiting time before the sample gets pyrolysed. For pyrolysers with autosamplers, this waiting time can be quite significant. It is very important for the reproducibility in analytical pyrolysis that the sample does not suffer modifications during this waiting time.

Once a T_{eq} is chosen, a second problem must be solved. A given elevated temperature cannot be reached instantly even for a small mass of material. It always requires a short interval of time. This interval is referred to as *temperature rise time* (TRT). Pyrolysis units capable of generating isothermal conditions in a very short TRT (flash pyrolysis) are commonly available.

The control of sample temperature in slowly varying non-isothermal conditions is not necessarily harder to achieve than that in isothermal conditions. However, it has been shown [2] that the heating rate during thermal decomposition is a sensitive parameter for reproducibility, and it must be precisely controlled. In flash pyrolysis the heating rate still needs to be reproducible, but the related problems are less critical than the gradient control. Secondary reactions are much more likely to occur in slow gradient pyrolysis. Also, when the pyrolysis unit is interfaced with an analytical instrument such as a gas chromatograph, pyrolysis in a short time interval is preferred because this will allow the chromatographic separation of the pyrolysate without the supplementary need of a "focusing" step. When the pyrolysate is generated in a relatively long period of time, a cryo-focusing step is commonly used before the chromatographic separation starts. To avoid this type of problem, most models of pyrolysers are designed to provide a well-controlled constant temperature in a very short TRT.

As indicated above, to achieve control of the pyrolysis course in flash pyrolysis, it is necessary for the sample to be reproducibly heated. Ideally, the total decomposition of the sample should occur over the same temperature range. The reason for a precise temperature control is illustrated in an example shown in Figure 4.1.3. This figure gives the weight variation of a sample where the pyrolytic processes may occur following two independent reaction kinetics, both of the first order: process (1) with $E^\ddagger = 100.7$ kJ/mol and $A = 9.6 \cdot 10^5$ sec⁻¹ and process (2) with $E^\ddagger = 65$ kJ/mol and $A = 5.5 \cdot 10^3$ sec⁻¹ (the kinetics parameters were selected from data indicated for cellulose pyrolysis).

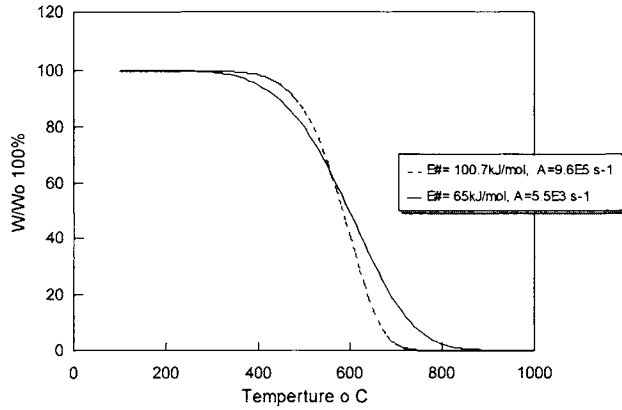


FIGURE 4.1.3. The ratio W/W_o for a pyrolytic process controlled by two kinetics.

The pyrolysis time (THT) in this example is 1.0 s. At temperatures up to 560°C , process (2) will dominate the pyrolysis, while at temperatures higher than 560°C , the pyrolysis will be dominated by process (1). If the pyrolysis products for process (1) are different from those for process (2), it can be seen that a small variation in the temperature profile may significantly modify the analytical results producing more of the products from process (1) or more from process (2). Therefore, the importance of TRT is more significant when rapid degradation reactions occur during pyrolysis. Equal TRT values are essential for the reproducibility of analytical pyrolysis mainly for fast processes.

During the temperature rise time (TRT), the kinetic constant k will vary. Assuming a linear temperature increase with the rate q and starting at T_o , the temperature is given at a certain moment t by the formula:

$$T = T_o + q t \tag{1}$$

Based on equation (1), assuming a first order reaction and using rel. (5) Section 3.2 for k , we have

$$\frac{dW}{dt} = A \exp \left[\frac{-E^{\#}}{R (T_o + q t)} \right] W \tag{2}$$

or separating the variables we have

$$\frac{dW}{W} = A \exp \left[\frac{-E^{\#}}{R (T_o + q t)} \right] dt \tag{3}$$

Equation (3) can be, in principle, integrated for the interval of time between $t = 0$ and the time $t = \text{TRT}$ when temperature ramping discontinues and T_{eq} is attained. However, the integration result of the right term of equation (3) can be expressed only as a slowly convergent series, which is difficult to calculate numerically. A numerical integration can

easily be done to get the variation of W/W_0 for specific values of A , and E^\ddagger , T_0 , q , and THT. The values for A and E^\ddagger depend on the compound to be pyrolysed, while T_0 , q , and total pyrolysis time THT are chosen values for each experiment.

As an example, Figure 4.1.4 a shows the variation of k for cellulose pyrolysis (parameters used in [8], Section 3.2), with $T_0 = 200^\circ\text{C}$, $q = 10^\circ\text{C/ms}$, a ramping time of 40 ms, and the THT = 500 ms. This will give $T_{eq} = 600^\circ\text{C}$. Figure 4.1.4 b shows the variation of W/W_0 % as calculated by numerical integration of equation (3) when k remains constant after 40 ms. As seen in Figure 4.1.4 b, only a small part of the sample is decomposed during TRT. This shows that for this particular case, the heating rate is not (within limits) such a critical parameter. Most of the sample is pyrolysed in isothermal conditions at T_{eq} for this case.

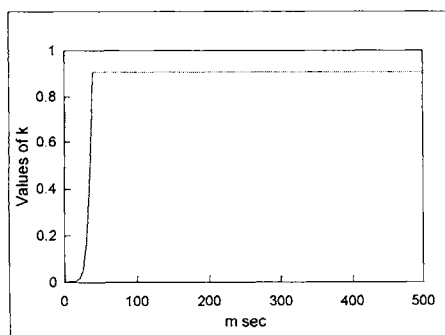


FIGURE 4.1.4 a. Variation of k with time during cellulose pyrolysis. Temp. ramp 10°C/msec , starting temp. 200°C , TRT 40 msec, THT 500 msec.

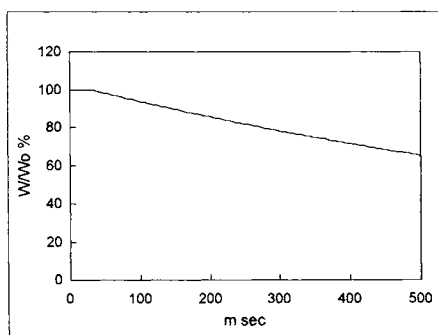


FIGURE 4.1.4 b. Variation of W/W_0 with time during cellulose pyrolysis. Temp. ramp 10°C/msec , starting temp. 200°C , TRT 40 msec, THT 500 msec.

However, it has been calculated for a series of materials that pyrolysis may be effectively complete before equilibrium temperature is attained [3]. This is determined by the nature of each compound reflected in the values of the frequency factor A and activation energy E^\ddagger . Figure 4.1.5 shows the variation of W/W_0 for three ideal compounds having the same frequency factor $A = 10^6\text{ sec}^{-1}$ and different activation energies E^\ddagger (100 kJ/mol, 80 kJ/mol, and 60 kJ/mol). In these examples, $T_0 = 200^\circ\text{C}$, $q = 10^\circ\text{C/ms}$, TRT = 40 ms, and THT = 500 ms.

It can be seen that for compounds with lower activation energies E^\ddagger , the values for TRT and q and the reproducibility of the heating can become very important factors. This is due to the fact that most of the sample is pyrolysed during the TRT, in non-isothermal conditions. Concern has been raised [3] about the frequency of this situation in practice. Based on the calculations shown above for the example of cellulose, sample decomposition is not always so rapid, and commonly, THT values much larger than TRT are needed for the decomposition of the whole sample. It should also be noted that the conclusions regarding this problem are dependent on the values used in equation (3) for the frequency factor A and for activation energy E^\ddagger of a given compound.

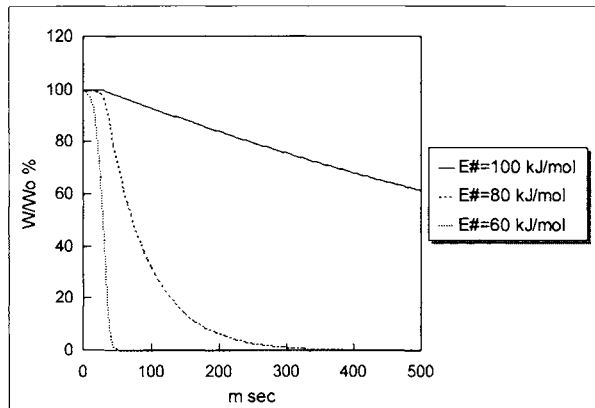


FIGURE 4.1.5. Variation of W/W_o with time for several $E^\#$ values in a hypothetical reaction. Temp. ramp 10°C/msec , starting temp. 200°C , TRT 40 msec, THT 500 msec.

Besides the reaction rate k previously defined in Section 3.2, which provides an instantaneous description of how fast a certain process is at a given temperature, some "integral" parameters (within a time range) were defined for the same purpose. One such parameter is the half decomposition time $t_{1/2}$, which is the time required to get $W/W_o = 1/2$. Making the approximation that k does not vary with the heating time (extremely short TRT or very high values for $E^\#$), the formula for $t_{1/2}$ calculated from rel. (7) Section 3.2 is the following:

$$t_{1/2} = (\log 2) / k \quad (4)$$

However, the required approximations for the validity of equation (4) are rather difficult to meet in practice. Another integral parameter used for the characterization of the speed of a reaction is the characteristic temperature T_s [3]. When a sample is heated and reaches T_s (starting from a low value T_o where no decomposition occurs), only 36.8% ($100/e$ %) of the initial sample is supposed to remain un-pyrolised. This parameter is particularly useful when the sample decomposes rapidly during TRT. T_s depends on the nature of the compound to be pyrolised (through k), on the heating rate q , and on the starting temperature T_o . T_s has a meaning only if $T_s < T_{eq}$.

The attaining of T_{eq} temperature by the sample is not controlled solely by the heat source of the pyrolyser but also by the sample properties and the pyrolyser construction. This is caused by the variations in the process of heat transfer to the sample from the heat source. For example, the sample characteristics such as the mass m and the specific heat c will influence the increase of the sample temperature by the formula $\Delta T = Q/(m c)$. In addition, phase changes and exothermic and endothermic chemical reactions in the sample may play an important role in temperature rise. To diminish the variations determined by these processes, a very small sample size is recommended. A study done on the temperature variation of a filament pyrolyser [4] showed a decrease of the nominal temperature of the filament for the first part of the THT, when the sample load increased, due to heat absorption by the sample.

Also, the pyrolyser construction plays an important role in the rate of attaining the T_{eq} temperature. This construction may determine the way in which heat is transferred to the sample. This transfer process can be understood by evaluating the heat transfer mechanisms, which are conduction, convection, and radiation. The heat transfer rate q in $J/s = W$ (watts) by unidirectional conduction for a small element of a material having the area A and thickness dx is given by Fourier's law:

$$q = -k A \frac{dT}{dx} \quad (5)$$

where k is a conductivity constant expressed in $J/(s \text{ cm } K^\circ)$ and dT is the infinitesimal temperature difference between the two faces of the material (the minus sign indicates the decrease of the temperature of the heat source). Equation (5) can be integrated for different body shapes (slab, cylinder, hollow cylinder, etc.). In all cases the heat flow depends linearly on the temperature difference across the material.

Convection will be responsible for a heat transfer between a retaining wall and a fluid. The rate of heat transfer will be given in this case by the formula:

$$q = h A \Delta T \quad (6)$$

where h is the convective (film) coefficient expressed in $J/(s \text{ cm}^2 \text{ K}^\circ)$, A is the area of the retaining wall, and ΔT is the temperature difference between the surface and the main body of the fluid. Heat transfer through convection takes more complicated expressions when phase changes occur on the surface.

The heat transfer through radiation between two surfaces at temperatures T_1 and respectively T_2 , both of area A , is given by the formula:

$$q = A \varepsilon \sigma (T_1^4 - T_2^4) \quad (7)$$

where ε is the emissivity of the two surfaces ($\varepsilon = 1$ for a black body), and where σ is the Stefan-Boltzmann constant $\sigma = 5.67 \cdot 10^{-12} \text{ J/[s cm}^2 \text{ (K}^\circ)^4]$.

Several aspects of sample heating can be rationalized using the above formulas. For example, equations (5)–(7) indicate that the heat transfer is dependent on the area A through which the heat flows. For conduction, A is the contact area between the sample and the heat source. Therefore, a good contact is useful for this type of heating. When the sample vaporizes, this contact can be easily diminished. The sample conductivity will also play an important role in this type of heating. Heating through convection depends on fluid flow on the hot surface, and this may be low for many polymeric materials. Heating through radiation is very dependent on temperature (fourth power), but it is not the main heat transfer mechanism at lower temperatures.

One way to produce a rapid heat transfer to the sample is to diminish the sample size [5]. This implies that the amount of heat required by the sample to reach a certain temperature is small and that the heat can be transferred rapidly. Typical sample sizes in analytical pyrolysis vary from a few μg to a few mg . A small sample size is, however, related to other effects, some advantageous and some not. Secondary reactions during pyrolysis are diminished for a small sample, but the contact with metal surfaces may

increase (relative to the amount of sample), which is not desirable because of possible catalytic effects. One determining factor that does not allow a significant decrease in the sample size is the limited sensitivity of the analytical procedure following pyrolysis. A sample that is too small may not be appropriate because the pyrolysis products cannot be properly detected. Also, the weight of a sample that is too small is difficult to measure with enough accuracy and precision. For materials that are not homogeneous, the smaller the sample, the more difficult it is to obtain a representative sample. Restrictions to the choice of the sample size are also related to the losses due to the possibly incomplete transfer of the pyrolysate to the analytical instrument. This subject will be mentioned further as it relates to the analytical instrumentation attached to the pyrolyser.

Assuming a perfect contact between the sample and the heating element of the pyrolyser, calculations were done to find the transmission of heat into the sample as a function of time and sample layer thickness [5a]. Several simplifying assumptions were made for this calculation, such as that the sample is homogenous, the starting temperature of the sample is uniform, and no loss of heat occurs at the sample outside surface. Also, it was assumed that the heating element has a linear temperature increase with the rate q and starting at a temperature T_0 (see rel. 1). For the time $t > TRT$, the temperature of the heating element was assumed constant at T_{eq} . Using a one-dimensional heat equation, the temperature T at the time " t " and at the depth " x " in the sample can be calculated using the relation:

$$T(x, t) = \Phi(x, t) \quad \text{for } 0 < t < TRT \quad (8a)$$

$$T(x, t) = T_0 + \Phi(x, t) - \Phi(x, t - TRT) \quad \text{for } t > TRT \quad (8b)$$

where:

$$\Phi(x, t) = T_0 + q t - q (l^2 - x^2) / (2 a) + [(16 q l^2) / (\pi^3 a)] S \quad (9a)$$

$$S = \sum \{(-1)^n \cos[(n+1/2) \pi x / l]\} / (2 n + 1)^3 \exp \{ -(n+1/2) \pi / l]^2 a t \} \quad (9b)$$

and where the sum \sum is taken over $n = 0, 1, 2, \dots, \infty$, where l is the sample layer thickness, and " a " is the thermal diffusivity of the material to be pyrolysed. These relations are obtained based on the formula for a fundamental solution of the heat equation for one dimension: $a \, d^2T/dx^2 = dT/dt$.

For a sample with thermal diffusivity $a = 2 \cdot 10^{-7} \text{ m}^2 / \text{s}$, initial temperature $T_0 = 20^\circ \text{C}$, heating rate $q = 5000^\circ \text{C} / \text{s}$ and $TRT = 0.1 \text{ s}$, for three layer thicknesses l of 0.1 mm, 0.25 mm and 0.5 mm, the values for $T(x, t)^\circ \text{C}$ at $x = 0$ (surface of the sample) are shown in Figure 4.1.6.

It can be seen from Figure 4.1.6 that considering only the thermal conductivity, the sample temperature increases very slowly compared to that of the heating element when the sample thickness is not extremely small. Fortunately, other types of heat transfer take place simultaneously, and part of this effect is diminished. However, to avoid a temperature gradient in the sample bulk, the sample should cover the heating surface in a thin and uniform film.

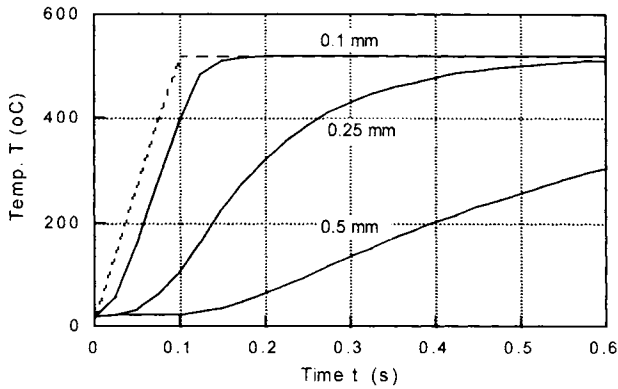


FIGURE 4.1.6. The variation of $T(x, t)$ °C at $x = 0$ as a function of t , for three layer thicknesses l of 0.1 mm, 0.25 mm, and 0.5 mm. The dotted line shows the temperature of the heating element.

The actual temperature acquired by the sample during pyrolysis can be standardized between different pyrolysers using a model compound. The procedure is based on the dependence of the composition of the pyrolysis products on temperature. One such compound chosen as a standard is an isoprene/styrene copolymer, trade name Kraton 1107 [6]. This copolymer decomposes generating isoprene, dipentene, styrene, dimethylvinylcyclohexene, and other small molecules. The ratio of isoprene to dipentene was found to be proportional with the pyrolysis temperature between 500° C and 850° C, with a good correlation coefficient (0.964). Several restrictions were imposed on the pyrolysis, such as a heating rate q higher than 2° C/msec and THT longer than 500 msec. The calibration with Kraton 1107 was done by performing the pyrolysis in an inductively heated or a resistively heated filament pyrolyser and the analysis using a gas chromatographic technique. The isoprene/dipentene ratio was obtained from the ratio of the chromatographic peak areas of isoprene and dipentene. A collective study [6] generated the data shown in Table 4.1.1.

TABLE 4.1.1. The isoprene/dipentene ratio as a function of temperature for the pyrolysis of Kraton 1107 in an inductively heated or a resistively heated filament pyrolyser.

Temp. ° C	isoprene/ dipentene
650	1.76
700	2.52
750	3.21

The dependence of T °C as a function of $R = \text{isoprene/dipentene}$ can be given by the expression:

$$T = 527.9 + 68.9 \cdot R \quad (10)$$

In principle, equation (10) allows the calibration of any pyrolyser for a series of given temperatures with corresponding temperatures acquired by the sample. It is interesting, however, that a study regarding the pyrolysis of Kraton 1107 in a furnace pyrolyser [7] found linearity between T and R only at temperatures between 450° C and 625° C.

4.2 Curie Point Pyrolysers.

Ferromagnetic conductors can be rapidly heated by interaction with a high frequency (radio frequency, RF) electromagnetic field. The sample to be pyrolysed can be placed in close contact with the conductor that can be shaped into different forms such as a wire, ribbon, or cylinder to properly hold the sample. The heating of the conductor and subsequently of the sample can be realized in a short time interval (TRT), commonly between 10 to 100 ms. Eddy currents in the conductor surface (skin) and hysteresis losses due to changes in the magnetic polarity cause the temperature to increase rapidly when the conductor is placed in the high frequency electromagnetic field. The increase in temperature is, however, limited for these ferromagnetic conductors to the Curie point temperature [8]. This is a temperature specific for each material where the transition from ferromagnetic to paramagnetic properties occurs. In this way, besides a rapid heating, a well-defined end temperature is attained. This end temperature (Curie point) depends on the composition of the ferromagnetic metal or alloy. Table 4.2.1 gives the Curie point temperatures for several Fe/Ni/Co alloys.

TABLE 4.2.1. Curie points of several ferromagnetic alloys.

Fe %	Ni %	Co %	Curie point temp. °C
0.0	100	0.0	358
61.7	0.0	38.3	400
55.0	45.0	0.0	400
50.6	49.4	0.0	510
40.0	60.0	0.0	590
42.0	41.0	16.0	600
29.2	70.8	0.0	610
33.3	33.3	33.4	700
100.0	0.0	0.0	770
0.0	55.0	45.0	800
0.0	40.0	60.0	900
0.0	0.0	100.0	1128

As seen in Table 4.2.1, temperatures in a wide range can be obtained using different compositions for the ferromagnetic alloy. However, the temperatures obtained with Curie point instruments cannot be varied continuously.

The commonly used RF frequencies in Curie point pyrolysers are 400 to 1000 kHz, and the power outputs range from 100 to 1500 watts. The rate of temperature rise depends on the conductor mass and specific heat, as well as on the power consumption of the ferromagnetic conductor. This power consumption per unit surface is related to the amount of heat generated by the conductor and implicitly to the temperature. The power consumption per unit surface N ($\text{cal cm}^{-2} \text{sec}^{-1}$) of a ferromagnetic conductor located along the axis inside a high frequency induction coil is given by the formula:

$$N = 2 \pi \sqrt{2} H^2 \rho (1/s) F(d,s) \quad (1)$$

where

$$s = \left(\frac{\rho}{\pi \nu \mu_0 \mu_r} \right)^{1/2} \quad (2)$$

and

- H is the magnetic field inside the coil (in Oe),
- d is the diameter of the conductor,
- ρ is the specific resistance of the conductor,
- s is the skin depth of the eddy current,
- F is a function of d/s and as $d/s \rightarrow \infty$ the function $F \rightarrow 1/\sqrt{2}$,
- $\mu_0 = 4 \pi \cdot 10^{-9}$ V sec / A cm (vacuum permeability),
- μ_r is the relative permeability of the material and $\mu_r \approx 1$ for non-ferromagnetic materials and $\mu_r > 1$ for ferromagnetic conductors, and
- ν is the frequency of the field (RF).

This formula does not explicitly contain the temperature as a variable, but it can explain the limiting of the temperature increase at the Curie point. When the ferromagnetic conductor reaches the Curie point, the relative permeability μ_r of the ferromagnetic conductor suddenly drops. This generates a sudden increase in the skin depth s and therefore a decrease in $1/s$ and $F(d,s)$ such that the power consumption of the conductor decreases. A further increase in temperature is therefore inhibited. Detailed graphs describing the variation of N as a function of temperature when different parameters are modified in rel. (1) are available in literature [8].

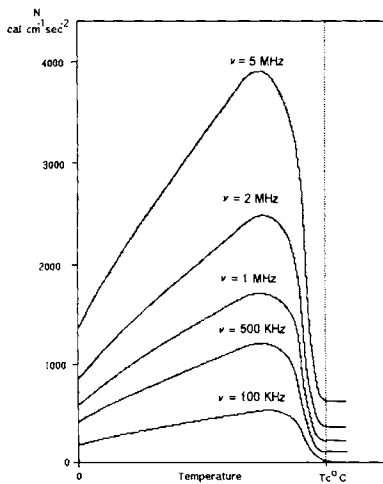


FIGURE 4.2.1a. The power consumption N as a function of temperature for an iron wire with $d = 2$ mm at different frequencies in a field of 1170 Oe.

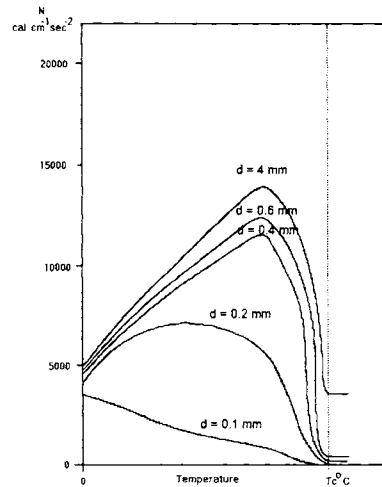


FIGURE 4.2.1b. The power consumption N as a function of temperature for different diameters of an iron wire in a high frequency field of 1170 Oe at 2 MHz.

As an example, Figure 4.2.1a shows the power consumption N as a function of temperature for an iron conductor with $d = 2$ mm at different frequencies in a field of 1170 Oe, and Figure 4.2.1b shows the power consumption N as a function of temperature for different diameters of an iron wire in a high frequency field of 2 MHz and 1170 Oe.

The temperature increase in time is fairly abrupt, as shown in Figure 4.2.2a for an iron wire in a high frequency induction field of 382 Oe and 1.2 MHz and in Figure 4.2.2b for an iron wire in a high frequency induction field of 1170 Oe and 480 kHz [8].

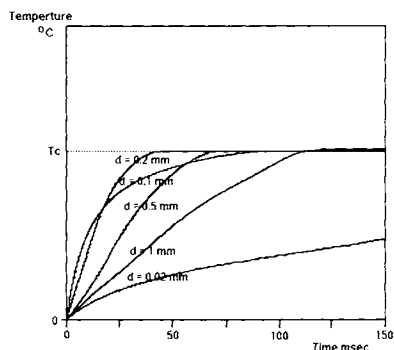


FIGURE 4.2.2a. Temperature variation versus time for an iron wire in a high frequency induction field of 382 Oe and 1.2 MHz.

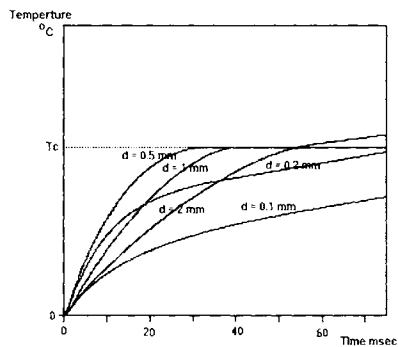


FIGURE 4.2.2b. Temperature variation versus time for an iron wire in a high frequency induction field of 1170 Oe and 480 kHz.

As seen in Figures 4.2.2a and 4.2.2b, the TRT time can be as low as 30 ms or even lower when higher frequencies are utilized.

Different practical constructions of a Curie point pyrolyser are commercially available. In these systems, the sample is put in direct contact with the ferromagnetic alloy, which is usually in the shape of a ribbon that can be folded over the sample forming a sample holder. The sample and its holder are maintained in a stream of inert gas in a similar way as for resistively heated filaments. The housing where the sample and its ferromagnetic holder are introduced is also heated to avoid the condensation of the pyrolysate but without decomposing the sample before pyrolysis. These types of requirements are achieved, for example, in a pyrolyser with autosampling capability [8a] shown in Figure 4.2.3. In this system, the sample is put on a ferromagnetic foil, which is folded to form a sample container. The folded foil is introduced in a foil magazine, which is kept at room temperature. The foil magazine is provided with a foil injector that can push the foil into the middle of an RF coil. At the time of injection the RF is activated and the sample is heated at the pyrolysis temperature T_{eq} . The foil is then removed with a retractable magnet and disposed in a trap for used foil. The region where the pyrolysis takes place is made from an inert material and is heated by a secondary source (at about 250° C) to prevent condensation of the pyrolysis products.

The Curie point pyrolysers have several advantages when compared to other systems. The TRT is usually short and the heating rate is reproducible. The T_{eq} temperature is accurately reproducible for the same alloy. The contact between the sample and the heated alloy is good, which assures that the heat transfer to the sample is rapid and uniform. On the other hand, the set temperatures can only be discrete and are limited to the values offered by different alloys. Even though the direct contact of the sample with the ferromagnetic alloy offers the advantage of a good heat transfer, it can be a

source of catalytic interferences. For this reason some suppliers offer gold plated ferromagnetic sample holders.

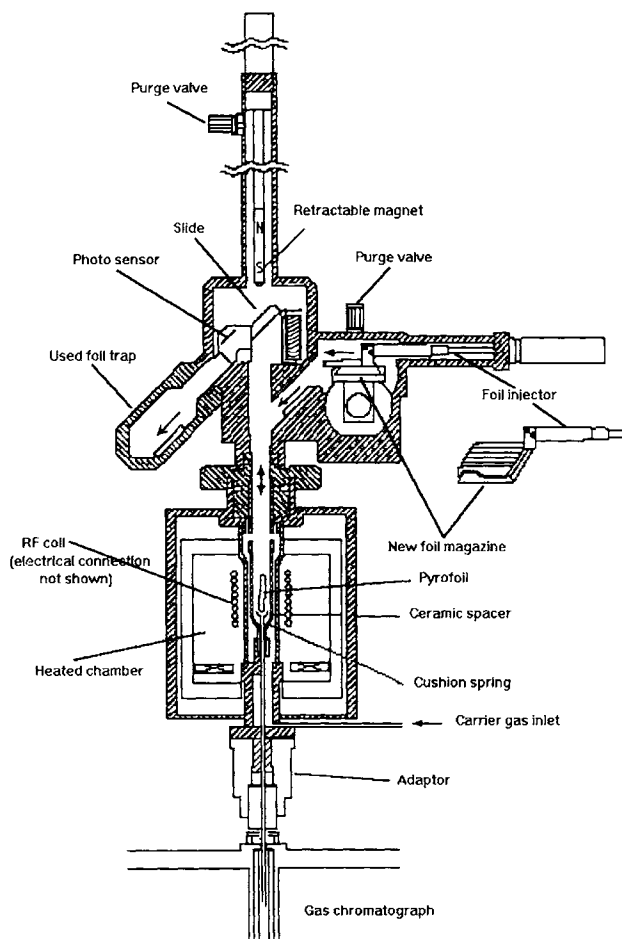


FIGURE 4.2.3. Curie point pyrolyser with autosampling capability (DyChrom model JPS-330).

An important capability of Curie point pyrolysers should be that the sample does not suffer any modifications before the pyrolysis step itself. As previously indicated, the housing of the pyrolyser must be heated (commonly with electrical resistances) to avoid condensation or other modifications of the pyrolysate. However, because a waiting time is inherent between the moment of sample introduction in the pyrolyser and the start of the pyrolysis itself, the sample may be heated by radiation from the sample housing. Several Curie point pyrolysers [8b] have the capability to drop the ferromagnetic foil containing the sample from a cool zone into the induction area, which is pre-heated to avoid condensation. The pyrolysis takes place immediately after the sample is transferred into this induction area such that no uncontrolled preliminary sample decomposition takes place.

4.3 Resistively Heated Filament Pyrolysers.

Resistively heated filament pyrolysers were used for a long time in polymer pyrolysis [9]. A schematic drawing of a common filament pyrolyser is shown in Figure 4.1.1. The principle of this type of pyrolyser is that an electric current passing through a resistive conductor generates heat in accordance with Joule's law:

$$Q = I^2 R t = (V^2 t) / R \quad (1)$$

where Q is the amount of heat (in J), I is the current intensity (in A), R is the electrical resistance of the conductor (in Ohms), t is the time in sec and V is the voltage (in V). A simple flash pyrolysis unit that operates at a fixed voltage could easily be constructed. However, such a unit operating within common values for the current intensity and voltage will have a TRT that is too long to be appropriate for flash pyrolysis. Systems with boosted current or boosted voltage were used to achieve a more rapid heating [10]. These systems apply a superimposed constant current with an initial boost pulse to assure a rapid temperature increase at the beginning of the heating period.

Modern equipment uses a feedback controlled temperature filament. The electrical circuit of such a system is given in Figure 4.3.1.

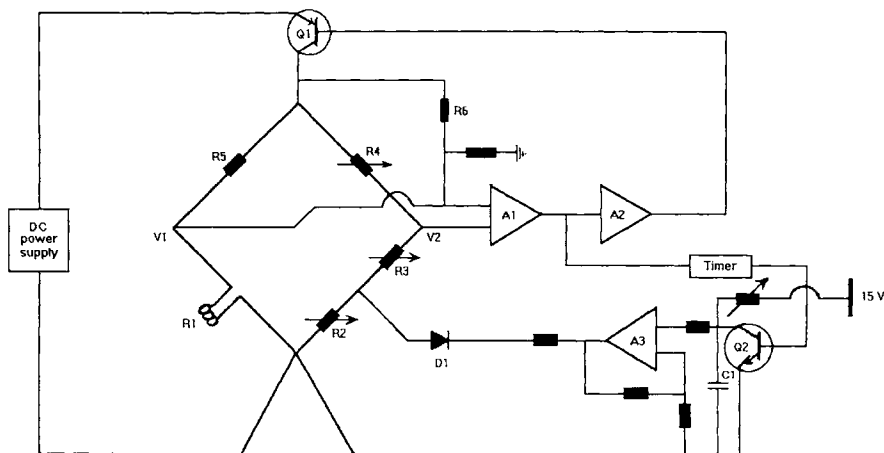


FIGURE 4.3.1. Circuit diagram of a pyrolyser with boosted heated filament and with feedback controlled temperature.

This type of pyrolyser commonly uses a platinum filament that has a precisely determined electrical resistance $R1$. This filament is incorporated in a Wheatstone electrical bridge. This bridge is balanced ($V1 = V2$) when the values of the electrical resistances in the bridge fulfill the relation:

$$R1/(R2 + R3) = R5/R4 \quad (2)$$

To start the pyrolysis, the operational amplifier A1 through the power amplifier A2 switches on the power transistor Q1, and the power supply provides full current to the

bridge. This causes the filament R1 to be rapidly heated. The other resistors in the bridge must have low temperature coefficients. The temperature increase causes an increase in the resistance of the filament, and the bridge voltage imbalance decreases. This diminishes the base current in transistor Q1 through the operational amplifier A1 and consequently diminishes the power across the bridge and the filament. The filament is kept at a defined temperature after the initial surge. The circuit including resistor R6 is used to linearize this control. The base current of the transistor Q1 can be switched off by the timer after a set time interval.

Besides "switch on" and "switch off" capability the circuit shown in Figure 4.3.1 has the capability to vary linearly the heating rate. This is achieved by providing a linearly increasing voltage to the bridge between R2 and R3. This voltage modifies the degree of imbalance of the bridge controlling the heating rate of the filament. This type of pyrolyser can provide heating rates as fast as $20^{\circ}\text{C}/\text{msec}$ and as slow as $0.1^{\circ}\text{C}/\text{msec}$ and a heating range from ambient up to 1200°C .

Even more sophisticated pyrolysis systems are available [11], such as those that allow programmed heated rates at different time intervals. Values for TRT as low as 7 msec from ambient to 1000°C were reported [12], as illustrated in Figure 4.3.2 showing the temperature measurement of a ribbon type filament heated at maximum rate.

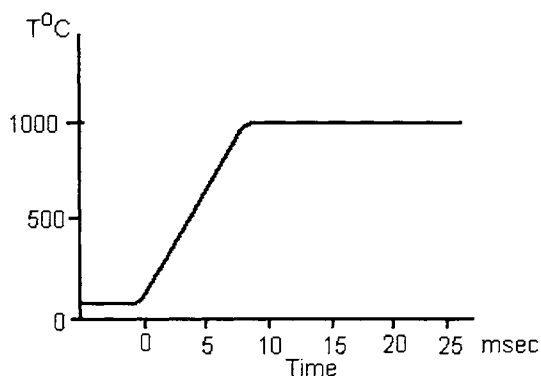


FIGURE 4.3.2. *Temperature measurement of a ribbon type filament heated at maximum rate.*

Several other procedures for a precise temperature control of the filament are also available, such as the use of optical pyrometry or thermocouples [13, 14].

The filament shape commonly used in resistively heated pyrolysers is either a ribbon or a coil. The sample can be put directly on the filament or in a silica tube that fits in the platinum coil. A silica (quartz) tube used as a sample container can be extremely useful in accommodating for pyrolysis of a wide variety of samples. However, when a silica tube is used, the TRT times are increased due to the larger mass that needs to be heated. The filament, the silica tube (if present), and the sample are maintained in a stream of inert gas and inside a heated housing as described in Section 4.1. This secondary heating is necessary as mentioned before to avoid the condensation of the pyrolysate. The stream of gas inside the heated chamber can be used further as a

carrier gas if the pyrolyser is interfaced with an analytical instrument such as a gas chromatograph. This requires that the pressure of the carrier gas should be higher than atmospheric pressure. The housing heating in itself should not produce any thermal degradation of the sample prior to pyrolysis.

There are several advantages of the resistively heated filament pyrolysers compared to other types. They can achieve very short TRT values, the temperature range is large, and T_{eq} can be set at any desired value in this range. Several commercially available instruments are capable of performing programmed pyrolysis, and autosampling capability is also available (such as the CDS AS-2500).

Some problems are inherent to this type of pyrolyser. One such problem is that the set temperature and the actual temperature of the filament must be calibrated. The filament electrical resistance is part of the temperature controlling circuit. This resistance may modify in time, mainly in the systems where the sample is put directly on the filament. Because of this, the correspondence between the set operating temperature and the actual temperature will change during the life of the filament. Even in correctly operating instruments, problems may occur in achieving the T_{eq} as precisely as the manufacturer may indicate [11a].

Another problem with the filament pyrolysers is the possibility that the filament may be non-uniformly heated over its length. This may determine different T_{eq} 's in different points of the filament. If the sample is not always placed in the same point of the filament in repeated experiments, this may introduce a rather drastic reproducibility problem. In spite of these disadvantages, the resistively heated filament pyrolysers are among the most common ones, and very good reproducibility has been reported frequently [12].

4.4 Furnace Pyrolysers.

Furnace pyrolysers are devices used in both flash pyrolysis and slow gradient pyrolysis. For flash pyrolysis, the common principle of use is to keep the furnace at the desired temperature and to suddenly introduce the sample into the furnace. The heating of the furnace is commonly done using electrical heating, which can be controlled using thermocouples and feedback systems for maintaining the correct temperature. An inert gas flow is commonly passed through the furnace to sweep the pyrolysis products into the analytical instrument. For analytical purposes it is, therefore, preferable to have small furnaces with low dead volumes, such that the gas flow can be kept at relatively low values. On the other hand, if the mass of the furnace is small, the sample introduction may modify the furnace temperature. Several designs were used for furnace pyrolysers, a successful one being a vertical furnace that allows the sample to be dropped from a cool zone into a heated zone [15].

A factor that must be considered with furnace pyrolysers as well as with the other types of pyrolysers is the achieving of short TRT values. A slow sample introduction in the hot zone of the furnace will end in a long TRT. A poor contact between the sample and the hot source may also lead to long TRT, most of the heat being transferred by radiation and convection and not by conduction. However, fairly short TRTs in furnace pyrolysers were reported in literature [16,17].

Another problem with the furnace pyrolysers can be the difference in the temperature between the furnace and the sample. Again, due to the poor contact between the sample and the hot source, the sample may reach a lower actual temperature than the temperature of the furnace wall. It is interesting that in microfurnace systems there were reported variations in the pyrolysis products as compared to the results obtained in inductively or filament heated pyrolysers [7,18]. As an example, a study done on Kraton 1107 [7] decomposition found linearity between the oven temperature and the ratio of two decomposition monomers (styrene and dipentene) only in a narrow temperature range, namely from 450° C to 625° C. Kraton 1107 was found to decompose in filament or Curie point pyrolysers such that linearity can be noticed between temperature and styrene/dipentene ratio from 500° C to 850° C. The reproducibility of pyrolysis in a furnace was also found lower than for other pyrolysers [7].

The mechanical problems related to the rapid solid sample introduction or related to the introduction of solid samples with no air leak makes this type of pyrolyser more appropriate for liquid or even gas sample pyrolysis. Also, it being possible to build large furnace pyrolysers, this type is successfully used when larger amounts of sample are necessary to be pyrolysed. This is a common case for the pyrolysis of non-homogeneous samples when a few mg of sample do not represent well the average sample composition.

Slow gradient pyrolysis (at programmed rates) can easily be performed with furnace pyrolysers, although rapid programmed heating (heating with a controlled, relatively high rate) is more difficult to achieve. A system using a PTV (Programmable Temperature Vaporization) injector has been reported [18a] as being used successfully for programmed heating in two different steps, one at 200° C and another at 450° C. The heating gradient was, however, not faster than 8° C/ s. Slow gradient temperatures are also commonly used in a series of thermal analysis instruments that are equipped with programmable furnaces. However, these thermoanalytical techniques are sometimes classified separate from pyrolysis as previously indicated (see Section 1.2).

Other different models of furnace pyrolysers were also reported in literature [18b]. As an example, a two-temperature zone furnace was made, and it was utilized to provide information about more volatile compounds trapped (adsorbed) in a sample as well as for performing true pyrolysis. In this system, the sample is heated first at 300° C where the volatile compounds are eliminated, and then the sample is pyrolysed at 550° C.

Sealed vessel pyrolysis is another pyrolysis type that is performed in furnace type pyrolysers. In this type of pyrolysis, the sample is heated for a relatively long period of time, in a sealed vessel, generally at relatively low temperature (below 350° C). The pyrolysis products are further analyzed, commonly by off-line procedures (GC, GC/MS, FTIR, etc). The technique allows the pyrolysis to be performed for as long as months and to use different atmospheres (inert or reactive) [17a]. The procedure is not used only as an analytical tool, and it can be seen as a preparative pyrolysis technique.

4.5 Radiative Heating (Laser) Pyrolysers.

Laser pyrolysers are practically the only type of radiative heating pyrolyser with certain applicability. Attempts were made in the past to use a strong light/heat source and

focus the beam with lenses [19] to achieve the desired power output. However, the laser as a radiative energy source is much more convenient. The laser beam can be focused onto a small spot of a sample to deliver the radiative energy. This provides a special way to pyrolyse only a small portion of a sample. A variety of laser types were used for pyrolysis purposes: normal pulsed, Q-switched, or continuous wave (cw) [20, 20a], at different energy levels. More common are the normal pulsed high-power lasers. Some instruments use condensing lenses to enhance the energy delivered to a small area of the sample.

A range of energies can be transferred to the sample by the laser. For a spot of about 1 mm diameter, a typical pulsed laser used for pyrolysis can generate a mean power density of 0.2–2.0 MW/(cm²). This high energy is partly absorbed by the sample and a rapid volatilization and decomposition takes place. A plume is commonly generated along the axis of the beam and more radiative energy is absorbed in this plume.

The theory of thermal aspects of laser desorption has been developed for a substrate surface subjected to pulsed laser irradiation, assuming that the laser intensity has a Gaussian distribution [21]. The given surface is covered with the organic layer, which does not absorb the laser energy. However, the heat flux in the substrate that absorbs the energy heats the sample to the same temperature as the substrate. For this case, the laser intensity flux $I(r,t)$ is given by

$$I(r,t) = I_{\max} p(t) \exp(-r^2/d^2) \quad (1)$$

where I_{\max} is the maximum laser intensity flux, $p(t)$ describes the variation in time of the pulse intensity ($p(t) = 1$ at the maximum), d is the radius of the Gaussian spot, and r is the distance from the center of the spot to the point where the intensity is considered. The flux F in the surface is

$$F(r,t) = (1 - R) I_{\max} p(t) \exp(-r^2/d^2) \quad (2)$$

where R is the reflection coefficient of the surface. The temperature increase ΔT is given by the relation:

$$\Delta T(r,t) = [(1 - R) I_{\max} d^2 / \lambda] (\kappa / \pi)^{1/2} \int_0^t [p(t-x) x^{-1/2} / (4\kappa x + d^2)] \exp[-r^2 / (4\kappa x + d^2)] dx \quad (3)$$

where λ is the thermal conductivity and κ is the thermal diffusivity of the sample. For very short time intervals δt , rel (3) can be approximated by

$$\Delta T(r,t) = [(1 - R) / \lambda] (\kappa / \pi)^{1/2} I_{\max} \exp[-r^2 / d^2] P(t) \quad (4a)$$

where

$$P(t) = \int_0^t p(t-x) x^{-1/2} dx \quad (4b)$$

The expression of $p(t)$ depends on the laser construction, and it is difficult to determine an analytical function for $p(t)$. However, it is possible to consider a model where $p(t)$ has a Gaussian expression and then the integral $P(t)$ can be calculated. Taking the pulse

maximum intensity at $0.5 \mu\text{s}$ and the peak width $2\sigma = 200 \text{ ns}$ (at 60.653% of the Gaussian height), the shape of the laser pulse is shown in Figure 4.5.1a, and the variation of the integral $P(t)$ is shown in Figure 4.5.1b.

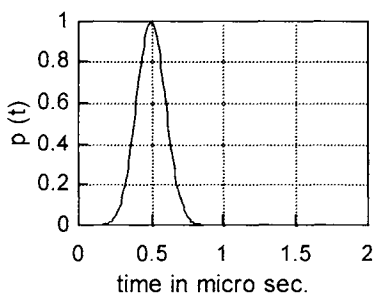


FIGURE 4.5.1a. $p(t)$ as a Gaussian peak shape with maximum at $0.5 \mu\text{s}$ and $2\sigma = 200 \text{ ns}$

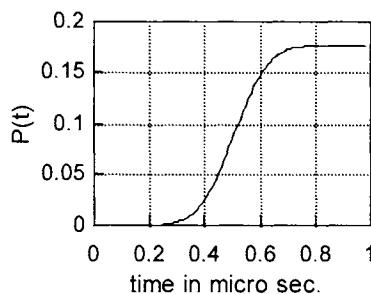


FIGURE 4.5.1b. $P(t)$ for a Gaussian $p(t)$ shown in Figure 4.5.1a

The variation in $\Delta T^\circ \text{ K}$ (or $^\circ \text{C}$) can be estimated knowing R , λ and κ , as well as r and d . For a stainless steel surface $\lambda = 17 \text{ W} / (\text{K}^\circ \text{ m})$, and $\kappa = 4 \cdot 10^{-6} \text{ m}^2 \text{ s}^{-1}$ and assuming $d = 0.12 \text{ mm}$, $r = 0.12 \text{ mm}$, $R = 0.8$ (arbitrarily), and $I_{\text{max}} = 1 \text{ MW/cm}^2$ and introducing these values in rel. (4), the value for ΔT° is 8300°C . For $r = 0.24 \text{ mm}$, ΔT° is only 413°C .

These calculations show that the temperature of the plume may rise fairly high and values as high as 10000°C were reported. However, more reasonable values range from 500°C to 2000°C . At temperatures as high as 2000°C , only some stable radicals will exist. Therefore, the part of the sample taken into the plume will generate after cooling only non-characteristic small molecules such as acetylene. The free radicals in the plume may also produce unexpected secondary reactions. However, enough heat is transmitted by the hot plasma around the focus point of the laser. This heat will produce pyrolysis products similar to those generated by other pyrolysis techniques. Some secondary reactions may take place between these pyrolysis products and the free radicals from the plume.

The maximum energy of the laser can be higher than needed for the pyrolysis purposes and needs to be attenuated. For a cw laser with a nominal energy of 100 W , the output has to be attenuated by operating the laser at about 10 W and by splitting the beam. Figure 4.5.2 shows simplified diagrams of two laser micropyrolysis set-ups. The first apparatus is used for a cw laser. It has as a part of the set-up a microscope, which allows the inspection of the area to be analyzed and the focusing of the beam on the portion of interest on the sample. The laser beam is also split (and attenuated) in the microscope by using a semitransparent mirror which allows control of the percent of the beam intensity that reaches the sample (5–15%).

For a cw laser, powers between 0.5 to 5 W with exposures varying from 1 s up to 5 min . were utilized for pyrolysis. The surface of the area exposed to the laser was also varied from $20 \mu\text{m}^2$ to $400 \mu\text{m}^2$. The second apparatus uses a pulsed laser (pulse energy of about 1 joule) and an alignment laser to focus the beam on the sample.

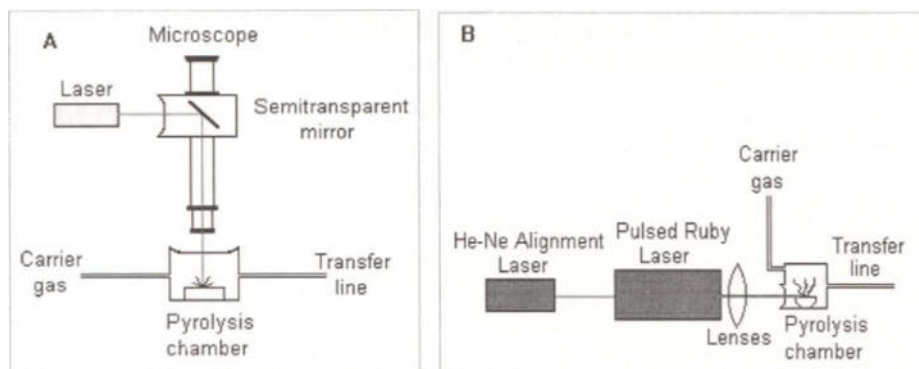


FIGURE 4.5.2. *Simplified diagrams of two laser micropyrolysis setups: A cw laser with a microscope, B pulse laser with alignment low power laser.*

Besides the formation of some unusual products due to secondary reactions, there are several other problems regarding the use of lasers as an energy source for pyrolysis. A first problem is related to the absorption of the radiative energy into the sample. Transparent samples do not absorb the radiative energy properly. For this reason, several procedures were utilized to make the sample more opaque. One such procedure consists of adding into the sample powdered graphite [21a] or a metal such as nickel [22]. This addition can, however, modify the course of the pyrolysis by catalytic effects or side reactions. A different procedure consists of depositing the sample in a very thin layer on a support that absorbs the radiation generating heat. In particular, a blue cobalt-glass rod has been used [22] as a support for the sample, with temperatures attaining 900–1200° C.

Another typical property of the laser pyrolysis is that it can achieve very short TRT times and also very short cooling times, in the range of 100 to 300 μ s. This will contribute to the uniqueness of the degradation conditions for the laser pyrolysis, which are rather different from the other types. In addition to this, the capability to pyrolyse only a very small area of the sample is characteristic for most laser pyrolysers. This directional nature can be of exceptional utility when combined with the microscopic inspection of a particular sample. In order to direct the laser beam to the right place on the sample, commercially available laser pyrolysers may also have a low energy laser, or "alignment" laser, which allows the selection of the desired spot on the sample to perform the pyrolysis. Inclusions, samples containing inhomogeneities, etc. can be successfully analyzed using this technique.

On the other hand, deliberate defocusing of the laser beam was also experimented [23] in order to cover a wider area on the sample for performing pyrolysis. Several alternative approaches were also experimented in order to provide more detailed information on polymers. For the study of the order of formation of specific molecular fragments during thermal degradation, for example, a time resolved laser induced degradation was applied [24]. Also, attempts were made to use specific wavelengths corresponding to a given vibration of the molecule in order to break specific bonds, using lasers as a source of energy.

A problem with lasers is the difficulty of knowing precisely the equivalent temperature of pyrolysis. Also, due to some inherent characteristics of laser pyrolysis, its reproducibility is not always good. Several studies [e.g. 25] showed variability in the total mass of material pyrolysed and difficulties in the control of the pyrolysis temperature. The secondary reactions with the radicals from the plume (although catalytic reactions are probably absent) also make this technique less reproducible.

Besides conventional laser pyrolysis, several other techniques evolved around the concept of evaporating the sample using a laser beam. However, most of these techniques were developed with the purpose of preserving the structure of the analyte while transferring it into an ionized gas form. Techniques such as MALDI (matrix assisted laser desorption/ionization) [26–29] are commonly used for the analysis of biopolymers. In this type of technique, the matrix will protect the biopolymer from thermal degradation while allowing its transfer into an ionized gas form. MALDI has been developed in association with a mass spectrometric (MS) detection system that is able to see large ions. Some other techniques involving lasers as a source of ions for mass spectrometry will be discussed in Section 5.3.

4.6 Other Pyrolyser Types.

Besides the previously described pyrolyser types, some other pyrolysers have been constructed and reported in literature [16,30,32]. Some are based on variations of typical pyrolyser systems. One such system uses a microfurnace pyrolyser with the capability to hydrogenate the pyrolysis products. For this purpose, the system uses hydrogen carrier, and, in line with the microfurnace, it has a catalyst column containing a solid support with Pt-catalyst (and a precolumn portion to trap non-volatile pyrolysis products) [31].

A different system utilizes as a source of heat an electric arc [30], but limited applications were reported for it, and also an infrared pyrolyser is manufactured [32]. Other techniques such as photolysis [33] were utilized for breaking down polymers for further analysis. However, these cannot be considered pyrolytic procedures. A theoretical approach has been developed [33] to compare mass spectrometric, thermolytic and photolytic fragmentation reactions.

4.7 Comparison of Analytical Performances of Different Pyrolyser Types.

Comparisons between the results obtained using different pyrolysers are not uncommon in literature [16,34-36]. These comparisons have two objectives: to assess the quality of the analytical results (reproducibility, sensitivity, etc.) of a certain type of pyrolyser and to indicate how the results of one pyrolyser can be compared to those of another type.

The comparison is not always straightforward because the analytical instrument at the end of the pyrolyser may play an important role regarding the quality of the data. A global view of different characteristics of the main pyrolyser types is given in Table 4.7.1.

TABLE 4.7.1. Comparison of the main characteristics of several pyrolysers.

Property	Curie point	Heated filament	Micro furnace	Laser
Temperature limit °C	1128	1100	1500	high
Temperature control	discrete	continuous	continuous	uncontrolled
Use of temp. gradients	not possible	possible	common	possible
Minimum TRT	70 ms	10 ms	0.2s - 1 min	10 µs
Sample size µg	10 - 1000	10 - 1000	50 -5,000	20 -500
Reproducibility	very good	very good	good	poor
Catalytic reactions	some	low	low	very low
Use with analytical instruments	on-line/off line	on-line/off line	on-line/off line	on-line/off line

The reproducibility of the results for heated filament pyrolysers (CDS Pyroprobe 1000) and Curie point pyrolysers (Horizon Instruments) was reported for several samples [34]. This included several synthetic polymers, dammar resin, chitin, an insect cuticle, a hardwood (cherry), a seed coat (water lily), lycopod cuticle (fossil *Eskdalia*), as well as several organic geological samples. All samples were pyrolysed at 610° C for 5 s in a flow of helium. The residence time in the pyrolyser before pyrolysis was kept constant and the temperature of the sample housing was 250° C. Other parameters such as the temperature of the transfer line to the analytical instrument were also the same. Both systems were connected to a GC/MS system for the pyrolysates analysis.

The reproducibility of the analysis was evaluated both qualitatively and quantitatively. It was found that for most samples the results are obtained with good reproducibility for the same instrument and with relatively minor differences between the two types of instruments. For example, the results for a cherry wood pyrolysate [34] were compared by measuring the variability in the peak areas in the total ion chromatogram (TIC) of a selected number of compounds. These peak areas are shown in Table 4.7.2.

TABLE 4.7.2. The area counts for the chromatographic peaks corresponding to several syringyl derivatives from cherry hardwood pyrolysate [34] for a filament pyrolyser (samples F1, F2, F3) and a Curie point pyrolyser (samples C1, C2, C3).

2,6-dimethoxy-R-phenol where -R- is	F1	F2	F3	Mean	S.D.	C1	C2	C3	Mean	S.D.
2,6-dimethoxyphenol	8	7.8	8.6	8.13	0.42	6.6	6.7	6.4	6.57	0.15
-4-methyl-	9.3	9.4	9.9	9.53	0.32	8.5	7.9	8.2	8.20	0.30
-4-ethyl-	4.1	3.9	4.1	4.03	0.12	2.5	2.5	2.1	2.37	0.23
-4-ethenyl-	21.1	20	20.8	20.63	0.57	18.4	18.8	18.9	18.70	0.26
-4-(1-propenyl)-	4	3.8	3.6	3.80	0.20	4.4	4.4	5	4.60	0.35
-4-propyl-	1	0.9	1	0.97	0.06	0.8	0.7	0.6	0.70	0.10
-4-formyl-	11.1	10.1	9.3	10.17	0.90	17.4	19.9	21.5	19.60	2.07
-4-(2-(Z)-propenyl)-	2.8	2.5	2.2	2.50	0.30	3.1	3	2.6	2.90	0.26
-4-(2-(E)-propenyl)-	3.7	7.3	6.3	5.77	1.86	4.6	2.7	0.6	2.63	2.00
-4-ethanal-	12.3	12.4	11.9	12.20	0.26	12.9	12.7	13.8	13.13	0.59
-4-aceto-	10.3	9.7	9.3	9.77	0.50	10.1	10.6	10.8	10.50	0.36
-4-(2-propanone)-	7	7.5	7.9	7.47	0.45	6	5.7	4.8	5.50	0.62
-4-(3-propanone)-	1.7	1.1	1.5	1.43	0.31	1.5	1.4	1.4	1.43	0.06
-4-(1-hydroxypropyl)-	0.7	0.6	0.5	0.60	0.10	1.3	1	1	1.10	0.17
-4-(2-propenal)-	2.9	3	3	2.97	0.06	2	2.1	2.5	2.20	0.26

As seen in Table 4.7.2, the reproducibility is rather good for each pyrolyser, and also the two types of instruments generated comparable results. However, for a few samples,

the similarity between the results on the two instruments was not very good. This is explained by other characteristics of the two pyrolysers such as the dead volume of the pyrolysing chamber or the amount of pyrolysate that reaches the analytical instrument.

In a different study [35] using a geopolymer (torbanite) as a sample, a comparison between four different types of pyrolysing techniques was performed. The four techniques were A - laser micropyrolysis, B - sealed vessel microscale furnace pyrolysis, C - resistively heated pyrolysis (HP 18580 A Pyroprobe), and D - microfurnace pyrolysis (SGE Pyrojector). The pyrolysate was obtained in different conditions. The laser micropyrolysis was performed with a cw Nd:YAG laser with an output at 1064 nm and the power sent to the sample of 1.5 W for a time duration of 300 s and an irradiation area obtained through a 10x objective. For the sealed vessel microscale furnace, the sample weighed about 2 mg and the pyrolysis was done at 325° C for 72 hours. The Pyroprobe pyrolysis was done at 900° C in a quartz tube, while the Pyrojector system heated the sample at 510° C. The analysis was done using a GC/MS technique (see Section 5.3) with the separation on a 5% phenyl 95% methyl silicone column. The results regarding the variation in the chromatographic peak heights for n-alkanes generated from the pyrolysed torbanite [35] are shown in Figure 4.7.1.

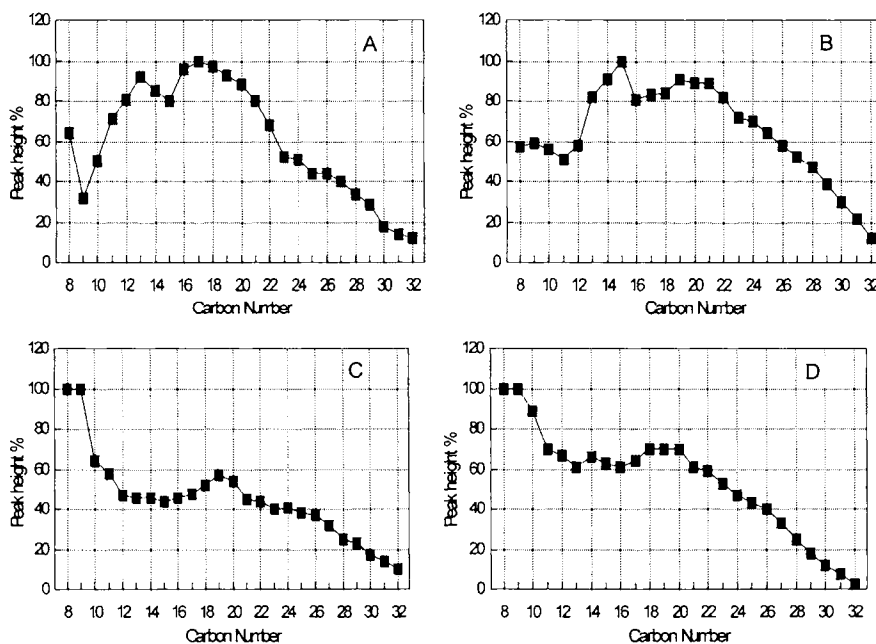


FIGURE 4.7.1. The variation in chromatographic peak heights for n-alkanes generated from torbanite pyrolysed by several techniques [35]: A - laser micropyrolysis, B - sealed vessel microscale furnace pyrolysis, C - resistively heated pyrolysis (HP 18580 A Pyroprobe), and D - microfurnace pyrolysis (SGE Pyrojector).

As seen from Figure 4.7.1, the composition of the pyrolysate varies considerably from technique to technique. The pyrolysis temperature seems to play a secondary role in generating differences, as can be seen by comparing Figures 4.7.1 C and 4.7.1 D.

From the studies done to compare different pyrolytic procedures, it was found that differences in the instrumentation play an important role regarding the dissimilarity of the results, even when they are operated at comparable parameters. Equal in importance to the temperature control characteristics are the heat transfer parameters from the heating element itself or from the probe housing, etc. The dead volumes, the gas flow through the pyrolyser, etc. may also play a role in the pyrolysis outcome.

The reproducibility of analytical pyrolysis was investigated in several other studies. The reproducibility on natural polymers and using non-standard techniques (FIMS, FDMS, MS with ionization at lower energies, etc.) were proven less reproducible than the work done on synthetic polymers and using either Curie-point or filament pyrolysis and standard GC/MS or MS analysis.

References 4.

1. S. A. Groves, R. L. Lehrle, M. Blazso, T. Szekely, *J. Anal. Appl. Pyrol.*, 19 (1991) 301.
2. E. L. Simons, A. E. Newkirk, *Talanta*, 11 (1964) 549.
3. F. Farre-Rius, G. Guiochon, *Anal. Chem.*, 40 (1968) 998.
4. R. L. Levy, D. L. Fanter, C. J. Wolf, *Anal. Chem.*, 44 (1972) 38.
5. W. Winding, P. G. Kistemaker, J. Haverkamp, *J. Anal. Appl. Pyrol.*, 1 (1979) 39.
- 5a. A. van der Kaaden, R. Hoogerbrugge, P. G. Kistemaker, *J. Anal. Appl. Pyrol.*, 9 (1986) 267.
6. E. J. Levy, J. Q. Walker, *J Chromatog. Sci.*, 22 (1984) 49.
7. P. A. Dawes, M. K. Cumbers, P. A. Hilling, *J. High Res. Chrom.*, 11 (1988) 328.
8. C. Buchler, W. Simon, *J Chromatog. Sci.*, 8 (1970) 323.
- 8a. A. Onishi, M. Endo, S. Uchino, N. Harashima, N. Oguri, *J. High Res. Chrom.*, 16 (1993) 353.
- 8b. A Onishi, N. Oguri, P. Kim, *J. Chromatog. Sci.*, 31 (1993) 380.
9. C. E. R. Jones, A. F. Moyels, *Nature*, 189 (1961) 222.
10. R. S. Lehrle, J. C. Robb, *J. Gas Chromatog.*, 5 (1967) 89.
11. S. A. Liebman, D. H. Ahlstrom, C. R. Foltz, *J. Polym. Sci.*, 16 (1978) 3139.
- 11a. G. Wells, K. J. Voorhees, J. H. Futrell, *Anal. Chem.*, 52 (1980) 1782.
12. S. A. Liebman, E. J. Levy, *Pyrolysis and GC in Polymer Analysis*, M. Dekker Inc., New York (1985) p. 29.

13. I. Tyden-Ericsson, *Chromatographya*, 6 (1973) 353.
14. I. Ericsson, *J. Anal. Appl. Pyrol.*, 2 (1980) 187.
15. S. Tsuge, T. Takeuki, *Anal. Chem.*, 49 (1977) 348.
16. W. J. Irwin, *Analytical Pyrolysis*, M. Dekker Inc. New York, 1982.
17. P. G. Simmonds, G. P. Shulman, C. H. Stenbridge, *J. Chromatog. Sci.*, 7 (1969) 36.
- 17a. W. K. Siefert, *Geochim. Cosmochim. Acta*, 42 (1978) 478.
18. J. Q. Walker, C. J. Wolf, *J. Chromatog. Sci.*, 8 (1970) 513.
- 18a. M. H. P. M. van Leishout, H-G. Janssen, C. A. Cramers, M. J. J. Hetem, H. J. P. Schalk, *J. High Res. Chrom.*, 19 (1996) 193.
- 18b. C. Watanabe, K. Teraishi, S. Tsuge, H. Ohtani, K. Hashimoto, *J. High Res. Chrom.*, 14 (1991) 269.
19. S. B. Martin, R. W. Ramstad, *Anal. Chem.*, 33 (1961) 982.
20. N. E. Vanderborgh, C. E. Roland Jones, *Anal. Chem.*, 55 (1983) 527.
- 21 G. J. Q. van der Peyl, J. Haverkamp, P. G. Kistemaker, *Intern J. Mass Spectrom. Ion Phys.*, 42 (1982) 125.
- 21a. W. T. Ristau, N. E. Vanderborg, *Anal. Chem.*, 44 (1972) 359.
22. D. L. Fanter, R. L. Levy, C. J. Wolf, *Anal. Chem.*, 44 (1972) 43.
23. B. T. Guran, R. T. O'Brien, D. H. Anderson, *Anal. Chem.*, 42 (1970) 115.
24. S. G. Coloff, N. E. Vanderborgh, *Anal. Chem.*, 45 (1973) 1507.
25. G. J. Q. van der Peyl, K. Isa, J. Haverkamp, P. G. Kistemaker, *Intern. J. Mass Spectrom. Ion Phys.*, 47 (1983) 11.
26. A. Burlingame, R. K. Boyd, S.J. Gaskell, *Anal. Chem.*, 68 (1996) 599R.
27. M. Karas, F. Hillenkamp, *Anal. Chem.*, 60 (1988) 2299.
28. B. Stahl, M. Steup, M. Karas, F. Hillenkamp, *Anal. Chem.*, 63 (1991) 1463.
29. R. S. Brown, J. J. Lennon, *Anal. Chem.*, 67 (1995) 1998.
30. J. C. Sternberg, R. L. Litle, *Anal. Chem.*, 38 (1966) 321.
31. S. Tsuge, *Trends in Anal. Chem.*, 1 (1981) 87.
32. A. D. Hendricker, F. Basile, K. J. Voorhees, *J. Anal. Appl. Pyrol.*, 46 (1998) 65.

33. R. C. Dougherty, *J. Am. Chem. Soc.*, 90 (1968) 5780.
34. B. A. Stankiewicz, P. F. Bergen, M. B. Smith, J. F. Carter, D. E. G. Briggs, R. P. Evershed, *J. Anal. Appl. Pyrol.*, 45 (1998) 133.
35. P. F. Greenwood, S. C. George, M. A. Wilson, K. J. Hall, *J. Anal. Appl. Pyrol.*, 38 (1996) 101.
36. M. J. Whitehouse, J. J. Boon, J. M. Bracewell, C. S. Guteridge, A. J. Pidduck, D. J. Puckey, *J. Anal. Appl. Pyrol.*, 8 (1985) 515.

Chapter 5. Analytical Techniques Used with Pyrolysis

5.1 The Selection of the Analytical Technique and the Transfer of the Pyrolysate to the Analytical Instrument.

Selection of the analytical instrumentation for the analysis of the pyrolysate is a very important step for obtaining the appropriate results on a certain practical problem. However, not only technical factors are involved in this selection; the availability of a certain instrumentation is most commonly the limiting factor. Gas chromatography (GC) and gas chromatography-mass spectrometry (GC/MS) are, however, the most common techniques utilized for the on-line or off-line analysis of pyrolysates. The clear advantages of these techniques such as sensitivity and capability to identify unknown compounds explain their use. However, the limitations of GC to process non-volatile samples and the fact that larger molecules in a pyrolysate commonly retain more structural information on a polymer would make HPLC or other techniques more appropriate for pyrolysate analysis. However, not many results on HPLC analysis of pyrolysates are reported (see section 5.6). This is probably explained by the limitations in the capability of compound identification of HPLC, even when it is coupled with a mass spectrometric system. Other techniques such as FTIR or NMR can also be utilized for the analysis of pyrolysates, but their lower sensitivity relative to mass spectrometry explains their limited usage.

The selection of the analytical instrument is also related to a special optimization of the pyrolytic process. For example, a series of parameters were studied regarding the optimization of pyrolysis-gas chromatographic analysis. Among these are the parameters used for the control of the pyrolytic process (see Section 4.1) such as the temperature/time profile, the temperature rise time (TRT), the housing temperature, the sample size, and, also, the carrier gas flow-rate and the material of the sample holder [1]. The results showed that in order to obtain the best results in Py-GC, it is not always necessary to perform the pyrolysis at ideal parameters, and the pyrolytic conditions should be chosen based on the practical problem to be solved. For example, lower final temperatures or slower heating rates may provide more information for structural studies. Even a complete transfer of the pyrolysate into the chromatographic column may be in particular situations detrimental, because it may overload the chromatographic column and lead to poor chromatographic separation.

- Transfer of the pyrolysate to the analytical instrument.

Numerous techniques and procedures have been reported for the transfer of the pyrolysate to the analytical instrument [see e.g. 1a]. These may depend on the pyrolysing instrument and also on the procedure utilized for the analysis of the pyrolysate. There are two main types of transfer: on-line and off-line.

On-line transfer is frequently utilized, and a variety of instruments have been designed with this capability. In these instruments, the pyrolysis products are swept by a flow of gas from the pyrolyser into the analytical instrument. For gas chromatographs (GC) used as the analytical instrument, the pyrolysate is either transferred into the injection

port of the GC, or a piece of deactivated capillary fused silica is passed through the injection port and goes directly into the pyrolyser (see Section 5.2). A complete transfer of pyrolysate is desirable. However, higher boiling point compounds are sometimes difficult to transfer. Also, for a complete analysis of the pyrolysate, the compounds associated with the char sometimes must be analyzed. This non-volatile part is not transferred by a gas flow. Also, as indicated in Section 4.1, after the pyrolysis step, some variability can be generated when the pyrolysate is transferred to the analytical instrument, because at lower temperatures some condensation may take place in the pyrolyser and in the transfer line, thus affecting the analytical results.

This problem is commonly addressed by using appropriate heating of the pyrolyser body as well as of the transfer line and by avoiding condensations or other sample modifications. However, no pyrolysis system can prevent some condensation of high-boiling components of pyrolysate in the reaction zone and on the way to the analytical instrument. Although this phenomenon is difficult to notice during the analysis, the highest-boiling products are not recorded in the pyrogram. On the other hand, when the housing of the pyrolyser is hot, the composition of a thermally sensitive sample can change before the proper pyrolysis. Effort has been made to avoid irreversible condensation of the heavy pyrolysate components and decomposition of the sample before pyrolysis. If the analytical instrument following the pyrolyser is a GC, the temperature of the housing and of the transfer lines is chosen in accordance with the highest temperature used for the gas chromatograph.

Another problem regarding the transfer is assuring appropriate gas flow between the pyrolyser and the analytical instrument. When the analytical instrument is a GC, it is common that the gas sweeping the pyrolysate is also the carrier gas for the chromatographic separation (see Section 5.2). For the separation of pyrolysis products in a capillary column, diffusion processes taking place when the carrier gas passes from pyrolyser to the column and the shape and size of joining elements affect the efficiency of separation. For Curie point and filament pyrolysers and for a GC as the analytical instrument, this task is readily achieved. However, for microfurnace pyrolysers, the gas flow may raise some problems [1]. Also, for the direct connection of the pyrolyser with a mass spectrometer, the gas flow in the system is critical for maintaining the appropriate pressure in the mass spectrometer. For this reason, an expansion chamber is commonly added between the heating element of the pyrolyser and the mass spectrometer source [2].

Some special type transfer capabilities for the pyrolysate were reported with improved results regarding the transfer, for example using a system similar to that of an "on-column" injector employed to separate high-boiling compounds [3]. In this system, the carrier gas is introduced through a tube, which is properly sealed to the entry of the capillary pre-column and can be lifted or lowered by means of a telescopic joint. A ferromagnetic wire can be introduced through a gasket in the head of an uncoated capillary pre-column. The wire tip with the sample deposited on it reaches into the induction coil, which generates the frequency necessary for the heating. When the power to the coil is turned on (electrical current with the frequency of about 1 MHz), the sample on the wire is pyrolysed. The pyrolysis products pass through the pre-column to the basic capillary column. Initially, the coil and the pre-column are not heated. When pyrolysis is completed, some part of pre-column with pyrolysate accumulated in it is lowered in the GC oven. Now, the pyrolysis products can be evaporated and separated at a constant or programmed temperature profile. It is important that the reaction zone,

which is initially cold, can be heated in the course of analysis to the maximum temperature allowable for a given stationary phase present in a column. The separation of the heavy products can be carried out at the maximum temperature for the column utilized. No loss in separation efficiency results from any factors impacting from outside the column since the whole process takes place inside the capillary column.

Also, as indicated in Section 4.6, a catalytic hydrogenation step can be added after pyrolysis. For this purpose, in line with a microfurnace the system has a column where the catalyst is put on a solid support [4]. More details regarding sample transfer will be given in Sections 5.2 and 5.3.

Off-line transfer is not as common as on-line but was applied in situations such as the following: use of a furnace pyrolyser when a relatively large amount of pyrolysate is available and only a small portion must be analyzed, a special derivatization of the pyrolysate is needed, or an analytical instrument not connected or difficult to connect to the pyrolyser is used for analysis. Derivatization is, for example, a very common practice in gas chromatography. It is done mainly with the purpose of increasing the volatility of the analytes by decreasing their polarity and the capability of hydrogen bond formation. Common derivatizations are permethylation and trimethylsilylation. However, depending on the nature of the compounds to be analyzed, numerous other derivatization types are utilized. A few examples are given in Table 5.1.1.

The derivatization is commonly done for medium and low volatility compounds. The volatile compounds are more frequently analyzed by on-line techniques without derivatization, although on-line derivatization is occasionally utilized (such procedures were discussed in Section 2.7). When the off-line derivatization is done for the pyrolysate generated in a furnace, no particular precautions are recommended. For Curie-point or filament type pyrolysers, the pyrolysate can be collected in a deactivated piece of capillary column connected to the pyrolyser and cooled either in an ice bath or at lower temperatures needed for capturing more volatile compounds.

TABLE 5.1.1. *Some common derivatizations utilized in GC analysis.*

Compounds to be derivatized	Derivative type	Reagents	Ref.
alcohols	methyl	diazomethane/fluoroboric acid	5
..	trimethylsilyl	bis(trimethylsilyl)-trifluoroacetamide (BSTFA)	6
..	..	trimethylchlorosilane (TMCS)	6
..	..	BSTFA + 1% TMCS	6
..	..	N-trimethylsilylimidazole (TMSI)	6
..	t-butyl(dimethyl)silyl	(N-methyl-N-(t-butyl(dimethyl)silyl)-trifluoroacetamide (MTBSTFA)	6
..	d ₉ -trimethylsilyl	bis(d ₉ -trimethylsilyl)-trifluoroacetamide (BSTFA)	
..	acetyl	acetic anhydride/pyridine	7
..	pentafluorobenzoyl	pentafluorobenzoyl chloride	8
..	trifluoroacetyl	N-methyl-bis(trifluoroacetamide) MBTFA	9
..	..	bis(trifluoroacetamide) BTFA	9
..	..	trifluoroacetic acid anhydride (TFAA)	6
..	..	trifluoroacetylimidazol (TFAI)	6
..	pentafluoropropionyl	pentafluoropropionic acid anhydride (PFAA)	6, 10
..	heptafluorobutyryl	heptafluorobutyric acid anhydride (HFAA)	6
thiols	pentafluorobenzoyl	pentafluorobenzoyl chloride	11
phenols	methyl	diazomethane	10

TABLE 5.1.1. *Some common derivatizations utilized in GC analysis (continued).*

Compounds to be derivatized	Derivative type	Reagents	Ref.
-"	methyl	methyl iodide/K ₂ CO ₃	12
-"	pentafluorobenzoyl	pentafluorobenzoyl bromide	13
-"	trimethylsilyl	bis(trimethylsilyl)-trifluoroacetamide (BSTFA)	6
-"	2,4-dinitrophenyl	2,4-dinitrofluorobenzene (DNFP)	14
amines (primary and secondary)	N-methyl	methyl iodide/NaH	15
-"	N-acetyl	acetic anhydride/pyridine	10
-"	N-trifluoroacetyl	TFAA, TFAI	10
-"	N-pentafluoropropionyl	PFAA	11
-"	N-heptafluorobutyryl	HFAA	16
-"	N-trichloroacetyl	trichloroacetic acid anhydride	10
-"	N-trimethylsilyl	BSTFA	6
-"	-"	TMCS	6
-"	-"	BSTFA + 1% TMCS	6
-"	-"	TMSI	6
-"	N-t-butylidimethylsilyl	MTBSTFA	6
-"	2,4-dinitrophenyl	2,4-dinitrofluorobenzene (DNFB)	17
amines (primary)	Schiff base	pentafluorobenzaldehyde (PFBA)	18
amines (tertiary)	N-trifluoroacetyl	TFAA	10
acids	methyl ester	methanol/HCl	10
-"	-"	methanol/BF ₃	19
-"	-"	methyl iodide/K ₂ CO ₃	10
-"	-"	tetramethylammonium hydroxide (TMAH)	20
-"	-"	diazomethane	10
-"	isopropyl ester	isopropanol/BF ₃	21
-"	trimethylsilyl	BSTFA	6
-"	-"	TMCS	6
-"	-"	BSTFA + 1% TMCS	6
-"	-"	TMSI	6
-"	t-butylidimethylsilyl	MTBSTFA	6
amino acids	trimethylsilyl	BSTFA	22
-"	t-butylidimethylsilyl	MTBSTFA	23
-"	pentafluoropropionyl-isopropyl	PFP-IP	24
aldehydes and ketones	phenylhydrazine	phenylhydrazine	25
-"	p-nitrobenzoyloxime	p-nitrobenzoyloxamine	10
-"	2,4-dinitrophenylhydrazine	2,4-dinitrophenylhydrazine (DNPH)	26
-"	trimethylsilyl	ethyl trimethylsilyl acetate/tetrabutylammonium fluoride	27

Off line derivatization has also been utilized for the derivatization of pyrrolsate to be analyzed by high-pressure liquid chromatography (HPLC) techniques [6, 10, 28].

5.2. Pyrolysis Gas Chromatography (Py-GC).

One of the most common analytical techniques following pyrolysis is gas chromatography (GC). Gas chromatography is in fact a separation technique, but gas chromatographs (GC) are usually equipped with detectors and the measurement of the separated analytes is common. A large amount of information is available regarding gas chromatography, e.g. [29], and some aspects are pertinent to pyrolysis. Several basic concepts in chromatography will be presented in this section.

- Transfer of the pyrolysate to the gas chromatograph.

The gas chromatographic separation takes place in a column in which the analytes are "injected" as a mixture and are ideally eluted one by one at different times by a flowing gas. In on-line Py-GC the pyrolyser is directly interfaced with the GC and the pyrolysate is sent with the flowing gas to the chromatographic column as a narrow zone loaded with the analytes. A simplified diagram of an on-line pyrolyser gas chromatograph (Py-GC) is shown in Figure 5.2.1.

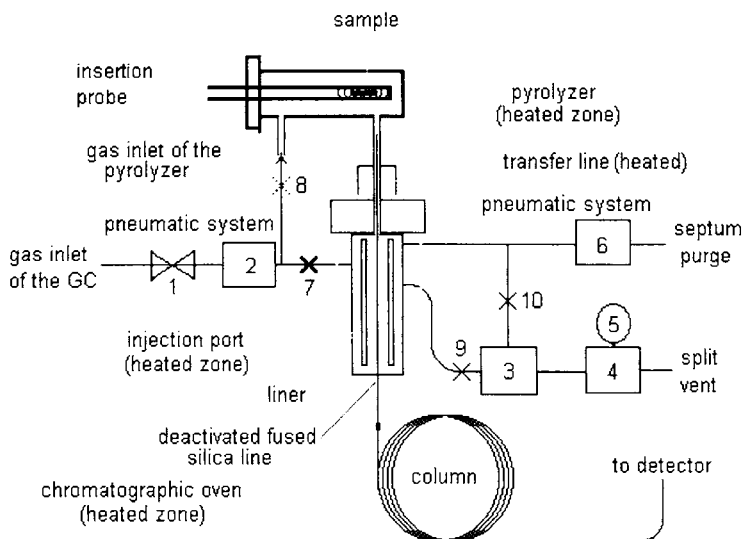


FIGURE 5.2.1. *Simplified diagram of a Py-GC system (not to scale).* The pyrolyser is schematized as a heated filament type. A piece of a deactivated fused silica line is passed through the injection port of the GC and goes directly into the pyrolyser. This piece of fused silica is connected to the column, which is put in the GC oven. The pneumatic system consists of (1) a mass flow controller, (2) an electronic flow sensor, (3) a solenoid valve, (4) a backpressure regulator, (5) a pressure gauge, and (6) septum purge controller. The connection (7) is closed when working in Py-GC mode, and connection (8) is open. (Connection (7) is open when the system works as a GC only.) Connection (9) is closed and connection (10) is open when the GC works in splitless mode (purge off). Connection (10) is closed and connection (9) is open when the GC works in split mode (purge on). No details on the GC oven or on the detector are given.

Figure 5.2.1 is not to scale and shows in more detail the connection from the pyrolyser (as a filament pyrolyser) to the GC, the injection port, and the pneumatic system of the GC. In this diagram a piece of deactivated fused silica passes through the injection port of the GC and goes directly into the pyrolyser. In other systems the injection port is not bypassed and the pyrolysate is carried into the injection port through the transfer line and further into the analytical column. Also, some systems have the capability to automatically isolate the GC when the insertion probe is removed and air can penetrate into the GC.

There are a series of problems related to the sample size in pyrolysis that were previously discussed (Section 4.1). The sample size and the flow of gas used in the pyrolyser should match to a certain extent the requirements of the sample size imposed

by the GC system. However, frequently the pyrolysers are constructed with the purpose of being connected to a GC system, and there are no significant discrepancies between the sample size of the pyrolyser and of the GC or between the gas flow in the pyrolyser and that required by the GC. Also, pyrolysis is commonly performed in a flow of an inert gas, and this can be used as the carrier gas for the chromatography. Some pyrolysers have the capability to perform pyrolysis in a different gas from the carrier gas. However, this technique has relatively limited applicability.

- *The partition process in a chromatographic separation.*

Once the sample reaches the chromatographic column, the separation process starts. The time necessary for a component injected into the chromatographic column to elute is called the *absolute retention time* t_R . The separation is based on different retention times of the components of the mixture. These retention times are different because the partition of each analyte between the two phases, the gas phase in motion and the stationary phase, are different. Hydrogen, helium, and nitrogen are common gases used as mobile phase. Two basic types of columns are known: packed columns containing solid support particles coated with the stationary phase, and open-tubular columns with the stationary phase as a film on the inner wall (capillary columns). Because the retention time $t_R(i)$ of the analyte "i" is temperature dependent, the chromatographic column of any (GC) is put in an oven with temperature control capability.

The retention of an analyte in the stationary phase can be characterized with several parameters, one of them being the *partition coefficient* (or *distribution constant*) K_i (or K_{iD}). This is defined for a component "i" by the relation:

$$K_i = C_{i,s} / C_{i,g} \quad (1a)$$

where $C_{i,s}$ is the concentration of the component "i" in the stationary phase, and $C_{i,g}$ is the concentration in the gas phase. The distribution constant K_i for a given system depends on temperature but also may vary for different concentrations $C_{i,s}$ and $C_{i,g}$. The graph representing $C_{i,s}$ as a function of $C_{i,g}$ at a given temperature is called an isotherm. Its equation is

$$C_{i,s} = K_i C_{i,g} \quad (1b)$$

The isotherm is a straight line when K_i is a true constant, but it is a (non-linear) curve when the distribution constant K_i varies with $C_{i,s}$ and $C_{i,g}$. Depending on the isotherm type, the chromatographic process can be classified as linear or nonlinear.

Besides the linearity of the isotherms, some other factors should be considered in the characterization of a chromatographic process. An ideal process would take place with (thermodynamically) reversible exchange of the analytes between the two phases and with instantaneous equilibrium. However, this case is not met in practice. Whereas the isotherms commonly encountered in gas chromatography are linear, the process is never ideal. When the sample is injected as a narrow "square" zone, and when the chromatography is linear-nonideal, diffusion effects and nonequilibrium generate broadening of the elution zones. The broadened zones of the eluting components have a Gaussian distribution of the concentrations because they are generated by a random process. For nonlinear isotherms the shape of the eluting peaks is not Gaussian. An

illustration of the process of peak broadening for an eluting analyte in a linear-nonideal chromatogram is given in Figure 5.2.2.

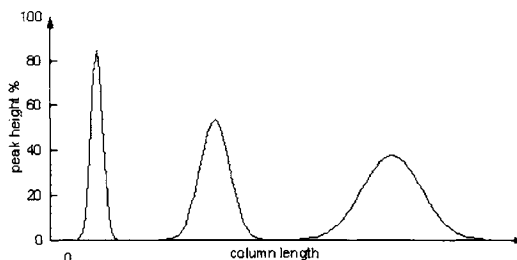


FIGURE 5.2.2. Peak broadening of an eluting analyte along the column.

Because the elution appears as a broadened zone, the retention time t_R must be measured when the analyte reaches the maximum of its Gaussian elution peak. The absolute retention time t_R is the sum of the (average) time spent by a component in the mobile phase (t_m) and the (average) time spent in the stationary phase (t_R):

$$t_R = t_m + t_R \quad (2)$$

The time spent by a component in the stationary phase t_R is compound specific (the index "i" indicating analyte "i" was omitted), but the time spent in the mobile phase is the same for any component and depends on the *linear flow rate* u of the gas, and the *column length* L , where

$$t_m = L / u \quad (3)$$

In practice, the value of t_m can be estimated from the time necessary to elute an unretained component (when $t_R = 0$).

The retention time t_R can be correlated to the distribution constant for a given analyte. For this purpose, each concentration in rel. (1) will be expressed as a ratio between the fraction of molecules in the corresponding phase and the volume of that phase. If R is the fraction of molecules (for the analyte "i") in the gas phase and $1 - R$ the fraction of molecules in the stationary phase, then

$$K_i = \left(\frac{1 - R}{V_s} \right) / \left(\frac{R}{V_g} \right) \quad (4)$$

where V_g is the volume occupied by the gas and V_s is the volume of the stationary phase. On the other hand, the ratio of the time spent by a component in the stationary phase versus the time spent in the gas phase should be equal to the molar distribution of component "i" between the two phases:

$$t_R / t_m = (1 - R) / R = k_i \quad (5)$$

where k_i (or k if the index "i" is omitted) is called the *capacity factor*. Therefore for a given analyte we can write:

$$K_i = k_i \beta = (t_R / t_m) \beta = [(t_R - t_m) / t_m] \beta \quad (6)$$

where β is called the *phase ratio* and has the expression:

$$\beta = V_g / V_s \quad (7)$$

For a capillary column with the internal radius r and the film thickness of the stationary phase d_f , the phase ratio β can be approximated by the formula:

$$\beta = r / (2 d_f) \quad (8)$$

and its typical values are between 50 and 500 (usually the columns have a diameter between 0.2 mm to 0.5 mm and the film thickness between 0.1μ to 1μ). Common values for t_m range from 20–30 s to several minutes, and k values may range from 1 to 100 or more. Analytes with high boiling points and/or high polarity have in general higher elution times and higher values for k (although the chromatographic process is different from a distillation).

- *Chromatographic column efficiency.*

Regarding the peak broadening for a linear-nonideal process, this is based on the assumption that the peak shape is Gaussian and therefore the peak intensity I can be expressed as a function of distance z (from start) by the equation:

$$I(z) = (2\pi \sigma^2)^{-1/2} \exp[-(z - \zeta)^2 / 2\sigma^2] \quad (9)$$

where ζ is the middle of the zone (and the maximum of the Gaussian curve) and σ determines the extent of peak broadening. The Gaussian curve in equation (9) was taken normalized (unit area under the curve), and it is 2σ broad at 60.653% of its height. Peak broadening expressed as a function of distance along the column can also be expressed as a function of time t the analyte spent in the column. The parameters z and t are related by the formula:

$$z = t R u \quad (10)$$

where u and R were already defined. The peak broadening is measured using the peak width W_h (in time) at the half height of the Gaussian curve or the *peak width at the baseline* W_b (in time). Figure 5.2.3 shows the measurements of t_R , W_b , and W_h on a recorded chromatographic peak.

From rel. (9) and (10) it can be calculated that between W_h , W_b and σ there are the relations:

$$\sigma = (8 \text{Ln } 2)^{-1/2} W_h R u = 0.4247 W_h R u \quad (11a)$$

$$\sigma = 0.25 W_b R u \quad (11b)$$

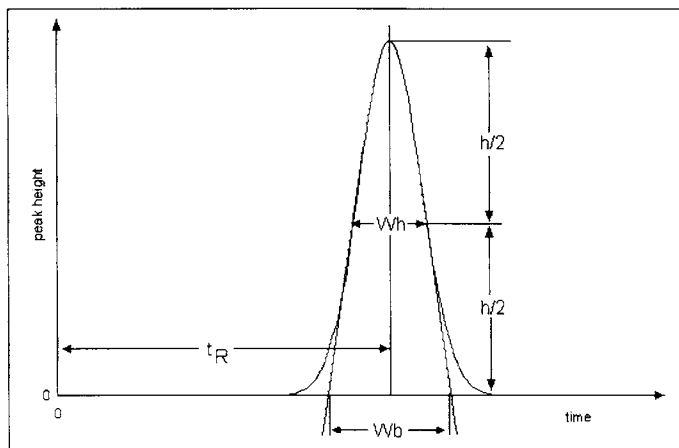


FIGURE 5.2.3. Measurements of retention time t_R and peak broadening W_b and W_h on a recorded chromatogram.

Peak broadening is a result of ordinary diffusion, eddy diffusion (due to flow along longer or shorter paths in packed columns), and local non-equilibrium. The eddy diffusion is absent in capillary columns. The zone spreading due to the ordinary diffusion σ_D can be expressed by the formula:

$$\sigma_D^2 = 2 D t_m \quad (12)$$

where D is a *diffusion coefficient*. Rel. (12) is equivalent to Einstein's formula for the mean value of square of displacements in Brownian motion.

The zone spreading due to eddy diffusion σ_E can be expressed by:

$$\sigma_E^2 = L d_p \quad (13)$$

where d_p is the average diameter of a particle (in a packed column) and where L is the column length. Rel. (13) can be obtained using a random walk model [e.g. 30] for the molecules moving in a packed chromatographic column.

The non-equilibrium effects determine the zone spreading σ_K expressed by the formula:

$$\sigma_K^2 = [2R (1-R) L u] / \varkappa \quad (14)$$

where \varkappa is the transition rate of molecules from stationary phase to mobile phase. This formula can also be obtained using the random walk model [30].

The combined effect of zone spreading will be characterized by:

$$\sigma^2 = \sigma_D^2 + \sigma_E^2 + \sigma_K^2 \quad (15)$$

The value of σ^2 is related to another parameter used to characterize zone spreading, namely the *height equivalent to a theoretical plate* H which is defined as

$$H = \sigma^2 / L \quad (16)$$

This parameter is very useful in chromatography for the characterization of peak broadening per unit length of the column. In addition to H , the peak broadening characterization in a column can be done using the *theoretical plate number* n . For a column of length L , n is defined as

$$n = L / H \quad (17a)$$

Rel. (17a) indicates that n is proportional to the column length L and inversely proportional to H . The theoretical plate number n can be expressed as a function of length using a simple substitution of rel. (16) in rel. (17a):

$$n = L^2 / \sigma^2 \quad (17b)$$

Noticing that $L = t_R R u$ and using rel. (16) and (11b), n can be expressed as a function of time:

$$n = 16 t_R^2 / W_b^2 \quad (17c)$$

In addition to the theoretical plate number, an *effective plate number* N is defined by substituting t_R in rel. (17c) with $t_{R'}$. The formula for N will be

$$N = 16 t_{R'}^2 / W_b^2 \quad (18)$$

Rel. (18) shows how N depends on chromatographic retention time $t_{R'}$, and since $t_{R'}$ is compound related (index "i" omitted), it also shows that N (as well as n) are compound dependent. Both rel. (17c) and (18) can be used to measure the theoretical plate number or effective plate number based on experimental data obtained with a given column. This measurement is useful in practice to select columns (higher n gives lower peak broadening) and also to assess the loss in performance of a column after a certain period of usage.

Since n is a function of t_R and N is function of $t_{R'}$, it is useful to note the following relation between t_R and $t_{R'}$:

$$t_R / t_{R'} = k / (k + 1) \quad (19)$$

(where the index "i" for k was omitted). Using rel. (19), the following relation can be obtained between n and N :

$$N = n [k / (1 + k)]^2 \quad (20)$$

A more detailed study for these formal parameters can be done by introducing the expressions for σ_D^2 , σ_E^2 and σ_K^2 in rel. (15) and (16). With these substitutions H will have the following formula:

$$H = 2D / u + d_p + [2R(1-R) / \alpha] u \quad (21a)$$

which can be written in the general form:

$$H = A + B / u + C u \quad (21b)$$

where A is the eddy diffusion term, B is the ordinary diffusion term, and C the non-equilibrium mass-transfer term. Rel. (21b) is known as van Deemter equation and is used to describe the dependence of peak broadening in the gas chromatographic process as a function of linear gas velocity u . A graphic representation of van Deemter equation and its terms is given in Figure 5.2.4.

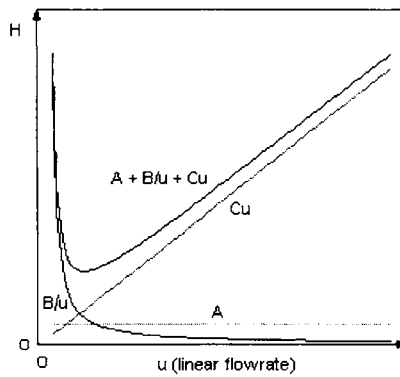


FIGURE 5.2.4. Van Deemter equation showing the dependence of H as a function of linear gas velocity u .

The minimum value for H can easily be obtained from equation (21b) by taking the derivative and the value for u where the derivative is null. This is obtained for the flow u given by

$$u = (B / C)^{1/2} \quad (22)$$

The best H_{\min} that can be obtained for a given column is

$$H_{\min} = A + 2(BC)^{1/2} \quad (23)$$

For a capillary column, equations (22) and (23) can lead to practical conclusions. The eddy diffusion in this case does not exist, and therefore $A = 0$. The value for B is obtained from rel. (12), replacing D with D_g , which is the diffusion coefficient of a component in the mobile phase. Therefore,

$$B = 2 D_g \quad (24)$$

The values for C are composed of two terms C_g and C_s , and

$$C = C_g + C_s \quad (25)$$

The first term describes the resistance to mass transfer into the gas phase and the second, into the stationary phase. These terms have the following expressions [31]:

$$C_g = (r^2 / D_g) [(1 + 6k + 11k^2) / 24 (1+k)^2] \tag{26a}$$

$$C_s = (d_r^2 / D_s) [(2k / 3 (1+k)^2)] \tag{26b}$$

where D_s is the diffusion coefficient in the stationary phase and d_r was previously defined (as the film thickness of the stationary phase). Taking $A = 0$ and introducing rel. (24), (26a), and (26b) in rel. (23), the value for H_{min} for a capillary column becomes

$$H_{min} = r (\mathcal{F}_1 + \mathcal{F}_2)^{1/2} \tag{27}$$

where

$$\mathcal{F}_1 = (1 + 6k + 11k^2) / [3 (1+k)^2] \tag{28a}$$

$$\mathcal{F}_2 = (D_g / D_s) (1 / \beta^2) \{(4 k / [3 (1+k)^2])\} \tag{28b}$$

For capillary columns with very thin coating, β is relatively large and \mathcal{F}_2 is small. Neglecting \mathcal{F}_2 the expression for H_{min} becomes

$$H_{min} = r (\mathcal{F}_1)^{1/2} \tag{29}$$

Figure 5.2.5 shows the variation of \mathcal{F}_1 as a function of k (with k between 1 and 20).

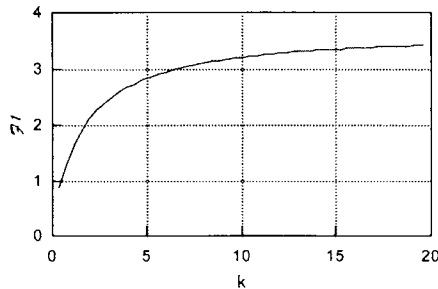


FIGURE 5.2.5. Variation of \mathcal{F}_1 as a function of k

This formula shows that for large β , the narrower is the capillary column (small r), the smaller are the values for H_{min} that can be obtained. When the values for β are relatively low (thick film capillary columns) and accepting that the ratio D_g / D_s can be large, the term \mathcal{F}_2 must be taken into consideration in rel. (27) for H_{min} . The factor depending on k is relatively small and, after reaching a maximum, decreases as k increases as shown in Figure 5.2.6.

As indicated in rel. (17a), the value for n is inversely proportional to H_{min} . Therefore the lower is the value for H_{min} , the higher is the value for n .

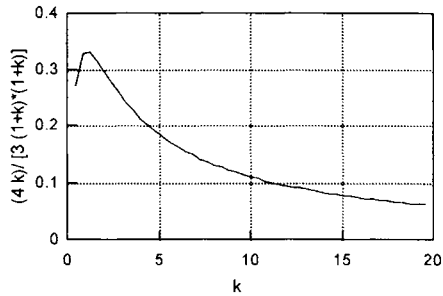


FIGURE 5.2.6. The factor depending on k in the expression of \mathcal{P}_2 .

- Peak separation in gas chromatography.

The peak separation will depend on the nature of the two components to be separated. The more different are the distribution constants K_i and K_j for the components, the more different are their retention times t_{Ri} , as seen in rel. (6). The separation factor α is commonly used to characterize the separation, where

$$\alpha = t_{Ri} / t_{Rj} = K_i / K_j = k_i / k_j \quad (30)$$

A good separation is attained for a large separation factor (by convention $\alpha > 1$) when the $k_i k_j$ product is as close as possible to unity. An evaluation of how well two peaks are separated can be obtained from the chromatogram using the formula:

$$R_s = (2 \Delta t_R) / (W_{b1} + W_{b2}) \quad (31)$$

where R_s is called *resolution* and $\Delta t_R = t_{R1} - t_{R2}$. The values Δt_R , W_{b1} and W_{b2} are measured from the chromatogram as shown in Figure 5.2.7.

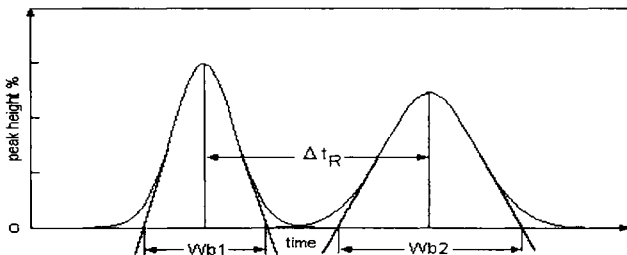


FIGURE 5.2.7. Measurement of Δt_R , W_{b1} and W_{b2} on a chromatogram, for the calculation of resolution

The two peaks are considered base to base separated when $R_s > 1$, which corresponds to $\Delta t_R = W_b$ (when W_{b1} is assumed equal to W_{b2}). Therefore, a good separation will be achieved when

$$\Delta t_R > 4 \sigma \quad (32)$$

The resolution R_s depends on the capacity factors k_i , separation factor α and the number of theoretical plates n . Assuming that $W_{b1} = W_{b2}$ and noticing that

$$\Delta t_R = (\alpha - 1) \alpha^{-1} t_R \quad (33)$$

rel. (31) can be written

$$R_s = (\alpha - 1) \alpha^{-1} (t_R / W_b) = 0.25 (n)^{1/2} (\alpha - 1) \alpha^{-1} k (k + 1)^{-1} \quad (34)$$

where the index "i" was neglected for k and for t_R (k refers to the larger of the two k_i , k_j). Rel. (34) can be used in the choice of a certain value for the number of theoretical plates n for an analytical column when α and k are known and the separation R_s is set higher than unity. This number should be

$$n > 16 (\alpha - 1)^{-2} \alpha^2 k^{-2} (k + 1)^2 \quad (35)$$

The separation of two components on a chromatographic column will be better when n is higher or H_{min} is lower.

- Sample capacity.

In addition to different column characteristics, one more factor must be taken into consideration in gas chromatography, namely the sample capacity. This is defined as the maximum permissible sample size that can be injected into a column without more than 10% loss of efficiency, and it is expressed as

$$A = a v_{eff} (n)^{1/2} \quad (36)$$

where A is the maximum permissible volume of vaporized sample (exclusive of the carrier gas), a is a constant depending on the system, n is the number of theoretical plates and v_{eff} is given by [32]

$$v_{eff} = V_g / n + K V_s / n \quad (38)$$

and it is called the effective volume of one plate. Using rel. (6) and (7) in rel (38), the value for A becomes

$$A = a (\pi r^2 L) (1 + k) (n)^{-1/2} \quad (39)$$

The reported values for a are on the order of 10^{-2} , and common values for A for capillary columns are less than 0.1 mL (gas in normal conditions).

This limitation indicated by the theory regarding the sample volume injected in a GC system imposes a serious problem when analyzing traces in a given sample. The detectors used in GC have limited sensitivity (see further), and an amount of sample below a certain limit cannot be detected. Therefore, a compromise should be chosen such that the sample should be small enough to be accommodated by the chromatographic column but sufficiently large for the detector sensitivity.

An alternative for achieving a lower column load and enough analyte in the detector is to perform an additional separation before the analytes reach the analytical column. In this separation, part of the sample that is not of interest can be eliminated, and at the same time the important analytes can be kept. This preliminary separation can be done using bidimensional chromatography (see further), but simpler techniques are also reported, such as programmed temperature vaporization (PTV) injection, etc.

- Isothermal and programmed temperature gas chromatography.

As indicated previously, the retention time of an analyte is temperature dependent. For this reason, the gas chromatographic separations are always performed at controlled temperatures. The temperature can be kept constant (isotherm separation), can be modified at a given rate (gradient separation), or may consist of a sequence of isotherm and gradient portions. The temperature program is commonly chosen to achieve two main practical purposes: an acceptable separation of the components of the sample and a reasonable time span for the whole chromatographic process. While as a rule the separation is better at lower temperatures, isothermal chromatography is not practical for complex samples. The elution times in a gas chromatographic separation depend on the boiling points of the constituents of the sample (similarly to a distillation process). Because of that, when the isothermal conditions are set significantly lower than the boiling point of a given compound, its elution can take a very long time. The light fractions of a sample may elute very fast and with poor or no separation if the temperature is set too high. When the components of a sample cover a wide range of volatilities, a good separation cannot be done using isothermal conditions.

The gas chromatographic separation in temperature gradient is affected by more than one factor [32]. Simultaneously there is variation in the gas flow, variation in the distribution constants, and variation in peak broadening.

In isothermal conditions a constant inlet gas pressure would automatically maintain a constant volumetric and linear flow rate. When the temperature of the column is programmed while the inlet gas pressure is kept constant, the flow rate will change considerably, becoming lower because of the modifications of the column geometry, expansion of the gas, and modifications of the gas viscosity, which increases with $(T)^{1/2}$. Besides isobaric operation, which is common, constant flow at programmed temperature capability is also available for certain instruments.

The distribution constant is another parameter varying with the temperature. Being an equilibrium constant, it is expected that its variation follows the formula:

$$\Delta G^0 = -RT \ln K_i \quad (40)$$

which is identical to rel. (11) Section 3.1, where ΔG^0 is the standard free enthalpy for solute to be transferred from the mobile to the stationary phase. Rel (40) can be written in the form:

$$k_i \beta = \exp(-\Delta G^0 / RT) \quad (41)$$

The phase ratio β does not vary with the temperature, the one that varies being the capacity factor k_i . For a hypothetical system with $\Delta G^0 = -20000 \text{ J mol}^{-1}$ and $\beta = 100$, the variation of k_i with the temperature is shown in Figure 5.2.8.

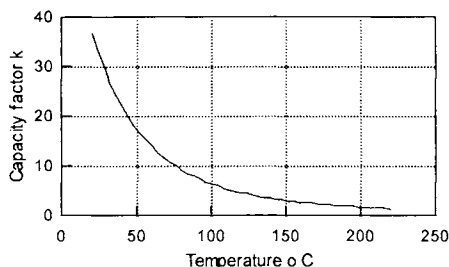


FIGURE 5.2.8. The variation of k_i with the temperature for a system with $\Delta G^0 = -20000 \text{ J mol}^{-1}$ and $\beta = 100$.

As seen in Figure 5.2.8, the value of k_i tends to 1 when the temperature increases. From rel. (5) it can be seen that in this case $t_{R'}$ tends to become equal to t_m . The resolution R_s given by rel. (34) and depending on the ratio $k / (k+1)$ will decrease as temperature increases. The variation of the ratio $k / (k+1)$ with the temperature for the same hypothetical system with $\Delta G^0 = -20000 \text{ J mol}^{-1}$ and $\beta = 100$ is shown in Figure 5.2.9.

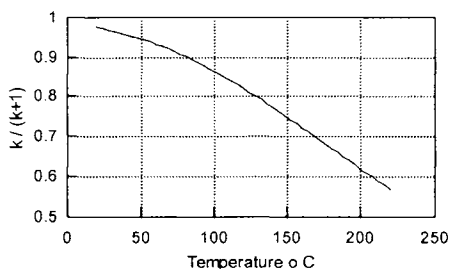


FIGURE 5.2.9. The variation of $k / (k+1)$ with $T^\circ \text{ C}$ for a system with $\Delta G^0 = -20000 \text{ J mol}^{-1}$ and $\beta = 100$.

Similar considerations can be applied to the variation of α with temperature. The general formula for its dependence is

$$\log \alpha = a (1 / T) + b \quad (42)$$

which indicates that α decreases when T increases. More elaborate studies were done to precisely calculate the variation of $t_{R'}$ or of other chromatographic parameters with temperature [33,34]. However, in practice these calculations do not have significant applicability.

Because, as a general rule, the chemical composition of pyrolysates is complicated, program temperature separations are applied in almost all Py-GC separations. Higher

temperatures are needed for the analysis of polar and/or high boiling point constituents. Usually, the main limiting factor to this temperature increase is not the excessive decrease in the values for k and α , but the decomposition (bleeding) of the stationary phase used as a column coating.

- Basic description of the gas chromatograph.

The gas chromatograph (GC) has in principle three parts: the injector (inlet system), the oven with the analytical column, and the detector. Detailed descriptions of each of these parts can be found in dedicated literature [e.g. 29, 35] and may vary for different GC models.

The injector (injection port) allows the sample to be placed at the beginning of the chromatographic column in a narrow zone loaded with the analytes. Also, the carrier gas flows into the injection port. The pressure of the carrier gas (head column pressure) may be utilized to control the gas flow in the analytical column. Depending on the length and the diameter of the column, this head pressure is chosen between 2–3 and 20–30 psi (1 psi = 6894.757 Pa, 1 barr = 10^5 Pa, 1 Torr = 133.322 Pa). In the common split/splitless inlet system, the sample is vaporized by setting a specific temperature for the injection port (higher than the boiling point of the solvent for the solution analyses), and an aliquot of it is sent into the column. This aliquot must be chosen such that the sample capacity of the column is not exceeded. The minimum amount of sample needed to reach the column is determined by the sensitivity of the detector. Once a certain volume of sample has been "injected," the amount going into the column can still be adjusted by choosing the split or splitless mode and by varying the split ratio (the ratio of the total gas flow and the flow in the analytical column). On-column injection ports where the sample (as is) is placed at the beginning of the column, large volume injection ports, programmed temperature/controlled purge injection ports, etc. are also known, as gas chromatography undergoes significant development.

Large volume injection techniques for example are designed to put more sample in the GC system, but to eliminate the highly volatile components from the sample (usually the solvent if the sample is injected as a diluted solution) maintaining a reduced sample load. For on-line Py-GC systems where there is no solvent, this system is not applicable. However, it can be practiced for off-line pyrolysis [35a]. A PTV vaporizing injection introduces a large volume of sample solution (10 μ L to 50 μ L or more) in a cold injector of small volume, which is rapidly heated and using an open split valve eliminates a considerable portion of this solvent [36]. Py-GC systems with gradient (or step) heating of the pyrolyser may achieve the same purpose, to send into the chromatographic column only a fraction (of interest) from the whole pyrolysate.

The usual injection port system adapted for Py-GC is, however, the split/splitless one. With this, the sample can be either transferred from the pyrolyser into the injection port of the GC and then to the analytical column, which is connected at the bottom of the injection port, or a piece of capillary fused silica is passed from the pyrolyser through the injection port and it is connected to the analytical column. The split/splitless pneumatic system is shown schematically in Figure 5.2.1. In this pneumatic system the connection (10) can be closed and connection (9) open, and then the GC works in split mode (purge on), allowing only a small portion of the sample to reach the beginning of the analytical column. The rest of the sample is swept out of the system. When connection

(9) is closed and connection (10) is open, the GC works in splitless mode (purge off) and more sample is sent to the analytical column. If the on-line Py-GC system does not bypass the injection port, the split or splitless modes can be chosen to adjust the amount of sample sent to the analytical column by choosing one mode or the other and by adjusting the split ratio. The system with the piece of fused silica in the pyrolyser will work more similarly to a splitless mode, and a larger portion of the sample will go into the analytical column. As described previously (Section 5.1), Py-GC inlets similar to on-column injection are also known.

The oven of the GC provides a controlled temperature for the chromatographic column. In most GC systems, the set temperature can be kept within 0.1°C , and a range between -100°C to 400°C can be achieved using either a cryogenic agent (liquid N_2 or CO_2) or electric heating. Also, the GC ovens are commonly able to provide temperature gradients such that a sequence of isotherm and gradient portions (three or four ramps) is available.

The detector of a GC is an important part of the instrument, as gas chromatography is used as an analytical technique and not only as a separation procedure. The detector senses the presence of a component different from the carrier gas and generates an electrical signal preferably proportional with the amount of the analyte. Various sensitive detectors are utilized. Also, some detectors are non-selective and do not have the capability of qualitative identification of the eluting compounds. Some detectors are element specific and can determine if the eluting compounds contain for example nitrogen or sulfur. Instruments such as a mass spectrometer or an infrared spectrophotometer can also be used as detectors for the GC, offering the capability of qualitative identification of the eluting compounds. Elaborate descriptions of different detectors can be found in literature [e.g. 36a]. Some of the detectors known in gas chromatography are indicated in Table 5.2.1.

TABLE 5.2.1. *Main types of GC detectors*

Detector type	Abbrev.	Sensitivity in g of sample	Type of selectivity
Thermal conductivity	TCD	10^{-3} to 10^{-8}	non-selective
Flame ionization	FID	10^{-3} to 10^{-11}	non-selective
Nitrogen phosphorus	NPD	10^{-5} to 10^{-12}	nitrogen, phosphorus specific
Other thermionic			
Electron capture	ECD	10^{-6} to 10^{-13}	halogen, some carbonyl
Flame photometry	FPD	10^{-6} to 10^{-10}	some specificity
Photoionization	PID	10^{-5} to 10^{-12}	non-selective (with some exceptions)
Electrolytic conductivity	Hall	10^{-6} to 10^{-11}	halogen, sulfur, nitrogen
Sulfur chemiluminescent		10^{-6} to 10^{-14}	sulfur
Nitrogen chemiluminescent		10^{-5} to 10^{-13}	nitrogen, NO
Atomic emission	AE		specific elements
Helium ionization	HID		
Mass selective	MSD	instr. dependent	qualitative and quantitative
Infrared	IRD	instr. dependent	qualitative and quantitative

There are several important characteristics of a good detector: sensitivity, dynamic range, stability, and for specific ones selectivity. Sensitivity should be in fact characterized by two parameters: the ratio of the detector response to the amount of sample (sensitivity slope) and the minimum detectable level of a given compound (commonly measured for a signal to noise ratio of 3). The dynamic range is the range

of sample amount for which the detector can be calibrated to provide accurate concentration in quantitative measurement. Stability refers to the capability to generate the same response for the same amount of sample.

Among the GC detectors the most frequently utilized is probably the FID. A wide variety of technical developments were done for improving FID performances regarding construction, the flow of the gases, and electronic detection of the signal. For example, both analog (continuous) and digital monitoring of the signal were developed, but the signal sampling with a certain frequency (such as 60 times in a sec.) is the more common procedure in modern instruments.

Another possible detector for GC is the mass spectrometer. This detector (which was in fact developed independently as a stand-alone instrument) offers the capability of compound identification. Extensive literature is available regarding gas chromatography/mass spectrometry (GC/MS) analysis of organic molecules [e.g. 37, 38]. More information about this technique is given in Section 5.3. A variety of other detectors were used in Py-GC, such as NPD, which is practically a modified FID, PID and ECD, which are very sensitive detectors for specific classes of compounds, and AED [38a]. With an AED detector, it is possible for example to monitor in parallel eluting compounds that contain carbon, hydrogen, oxygen, nitrogen, and sulfur.

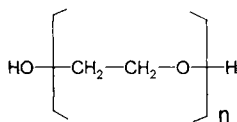
- The chromatographic column.

Two basic types of columns are known: packed columns and open-tubular columns (capillary columns). The packed columns contain solid particles of certain dimensions coated with the stationary phase, while the capillary columns contain the stationary phase as a film on the inner wall. The stationary phase is commonly a liquid on a stationary surface, a cross-linked material, or a bonded phase. Some special columns such as capillary columns containing fine solid particles coated with the stationary phase are also known. The use of regular packed columns is limited to specific applications, while the capillary columns are widely utilized. The capillary columns are commonly made from silica and have an outer coating (polyimide, aluminum, etc.) that improves their mechanical resistance. The column internal diameter (i.d.) can be chosen in a range between 50–100 μm to 0.6 mm or even wider. The columns are classified as microbore for i.d. < 0.1 mm, minibore for i.d. = 0.18 mm, narrow bore for i.d. = 0.25, regular for i.d. = 0.32 mm, and megabore for i.d. = 0.53 mm. The film thickness on the inner wall of the column is a very important parameter, determining the value for β . The film thickness may be chosen between 0.1 μm to 5 μm , a frequently utilized film thickness being 0.25 μm . The length of the capillary column is another important parameter (determining the value for n), lengths between 10 m and 100 m being common.

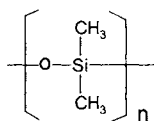
For capillary columns, numerous stationary phases are known [e.g. 39] but a few of them are very frequently utilized because of their ability to separate a variety of compounds. Such phases are

- polyethylene glycol, which is a polar material and is used for the separation of the analytes based on their differences in polarity and tendency to form hydrogen bonds,

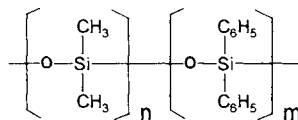
- dimethylpolysiloxane, which is non-polar and is used for separations based mainly on the boiling point of the analytes, and
- dimethylpolysiloxane copolymer with a certain amount (such as 5%) of diphenylpolysiloxane, which has some polarity.



Polyethylene glycol

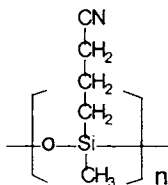


Dimethylpolysiloxane

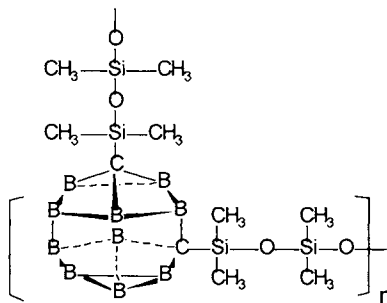


Diphenyldimethylpolysiloxane

Many other choices are available for the stationary phase of the chromatographic column. Some are modifications of stationary phases indicated above, such as polysilylphenylenemethylphenylsiloxane, which can be used as a replacement for diphenyldimethylpolysiloxane or polyethylenglycol ester replacing polyethylenglycol. Others are more special phases, such as cyanopropyl(methyl)polysiloxane, which is a polar phase with higher temperature resistance than polyethylene glycol, or carboranedimethylsiloxane, which is non-polar and very resistant to high temperatures.



Cyanopropylpolysiloxane



Carboranedimethylpolysiloxane

Several other stationary phases made from different proportions of typical phases (methyl, phenyl, cyanopropyl), or from special compounds such as polytrifluoropropylsiloxane, or different columns such as PLOT (porous layer open tubular), columns coated with a modified graphitized carbon or with a silicone based polymer with chiral groups incorporated into the polymeric chain, columns coated with derivatized cyclodextrins (for the separation of chiral compounds), etc. are also utilized.

The choice of the chemical nature of the stationary phase in a chromatographic column determines at least in part the range of compounds that can be analyzed. This chemical nature is selected based on the composition of the sample (polarity, volatility, etc.) and offers an important practical procedure for obtaining larger values for α (and therefore a better separation). An example showing the separation of the same material on two different columns can be seen in Figures 5.2.10 and 5.2.11.

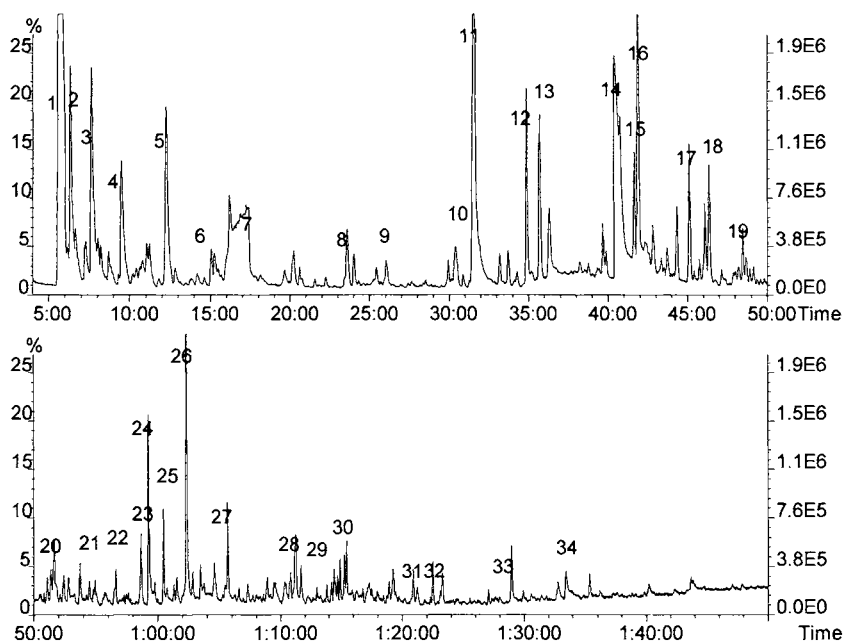


FIGURE 5.2.10. Cellulose pyrolysate obtained at 590° C by Py-GC/MS. The separation was done on a Carbowax type column. #1 CO₂, #2 acetaldehyde, #3 acetone, #4 2-butanone, #5 2,3-butandione, #6 toluene, #7 water, #8 cyclopentanone, #9 methylfuran, #10 3-hydroxy-2-butanone, #11 hydroxypropanone, #12 cyclopent-1-en-2-one, #13 2-methylcyclopentenone, #14 acetic acid, #15 acetic acid anhydride, #16 furancarboxaldehyde, #17 methylcyclopentenone, #18 dimethylcyclopentenone, #19 5-methylfuran-carboxaldehyde, #20 2,3-dihydro-2-furanone, #21 furan-2-methanol, #22 3-methylfuran-2-one, #23 2(5H)-furanone, #24 hydroxycyclopentenone, #25 3,5-dimethylcyclopentan-1,2-dione, #26 2-hydroxy-3-methyl-2-cyclopenten-1-one, #27 2-hydroxy-3-ethyl-2-cyclopenten-1-one, #28 2,3-dimethyl-2-cyclopenten-1-one, #29 phenol, #30 dimethylphenol, #31 3-ethyl-2,4(3H,5H)-furanone, #32 3-butenic acid, #33 1,4:3,6-dianhydro- α -D-glucopyranose, #34 5-(hydroxymethyl)-furfural.

These figures, which have significant differences, show the pyrograms of a cellulose pyrolysate obtained at 590° C, separated on a Carbowax column (Figure 5.2.10) or on a methyl 5% phenyl silicone column (Figure 5.2.11).

The Carbowax column was 60 m long, 0.32 mm i.d. and 0.25 μ film thickness. The methyl-phenyl silicone column was also 60 m long, 0.32 mm i.d. and 1 μ film thickness. The temperature for the GC separations started at 50° C and the rate of the temperature increase was 2° C/ min for both columns (the maximum temperature for the Carbowax column was 240° C and for the methyl-phenyl silicone column was 310° C but the same time span is shown in Figures 5.2.10 and 5.2.11).

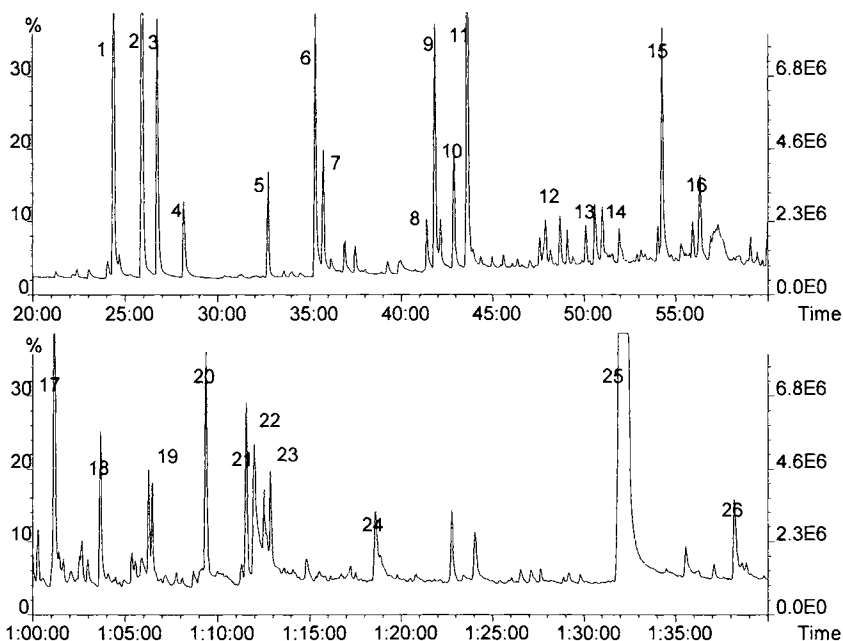


FIGURE 5.2.11. Cellulose pyrolysate obtained at 590^o C and separated on a methyl silicone with 5% phenyl silicone type column. #1 acetic anhydride, #2 pentanal, #3 2-hydroxybutanedialdehyde, #4 1,4-dioxadiene, #5 tetrahydro-2-furanmethanol, #6 2-(hydroxymethyl)-furan, #7 3-methyl-2-hexanone, #8 2-methoxy-2,3-dihydrofuran, #9 2(5H)-furanone, #10 1-acetyloxypropan-2-one, #11 hydroxycyclopentenone, #12 5-methylfurfural, #13 2,3-dihydro-5-methylfuran-2-one, #14 1-cyclopentylethanone, #15 2-hydroxy-3-methyl-2-cyclopenten-1-one, #16 3,5-dimethylcyclopentan-1,2-dione, #17 unknown, #18 3-ethyl-2,4(3H,5H)-furandione, #19 6-methyl-1,4-dioxaspiro[2.4]heptan-5-one, #20 1-hydroxy-3,6-dioxabicyclo[3.2.1]octan-2-one, #21 1,4:3,6-dianhydro- α -D-glucopyranose, #22 5-(hydroxymethyl)-furfural, #23 4-cyclopenten-1,2,3-triol, #24 5-ethyl-3-hydroxy-4-methyl-tetrahydrofuran-2-one, #25 levoglucosan, #26 1,6-anhydro- β -D-glucofuranose.

The pyrolysate of cellulose contains both volatile and less volatile compounds. In order to identify as many as possible of these compounds it is necessary to apply different chromatographic conditions, one to monitor the volatile less polar compounds and the other to see the heavier more polar molecules generated during pyrolysis. A change in the choice of the chromatographic column is one possible way to obtain different information on a pyrolysate analysis.

The detector used for the GC in the previous examples was a mass spectrometer (MS). This allowed identification of a series of compounds in the chromatograms, and some of them are indicated on the figures. The two chromatograms show complementary information, and only a limited number of compounds were common (as identified by the MS detector). For example, levoglucosan, a major cellulose pyrolysis product, is seen only in the chromatogram from Figure 5.2.11. In these chromatograms compounds such as HCHO, CH₃OH, and CO were not seen because the mass spectrometer used

for the analysis had the mass range detection with a low cut-off at $m/z = 32$. Most identifications were done by mass spectra library search (see Section 5.3).

The analysis of higher molecular weight compounds encounters difficulties using GC/MS technique. Most of these difficulties are the result of the limited volatility of polar or heavy molecules. Also, larger molecules have a lower capability to form ions in the MS (this capability can be significantly different from compound to compound), and most MS instruments have limitations regarding the maximum m/z value that can be analyzed. As indicated previously, the volatility problem can be addressed by using derivatization techniques. However, this usually requires off-line Py-MS instrumentation. Other analytical techniques are sometimes more appropriate for analysis of large molecules.

The choice of the chromatographic column must also take into consideration the maximum temperature required for the elution of the analytes from the column (which must be as complete as possible). As indicated previously, the stability of the stationary phase during heating is very important for a good chromatographic analysis. Column decomposition (column bleed) at higher temperatures must be as low as possible because it interferes with the detector response, and this is an important parameter in selecting a column. Polymer pyrolysis frequently generates in the pyrolysate oligomers or other relatively large molecules with high boiling points. If the transfer lines from the pyrolyser to the GC and the injection port of the GC are set at high temperatures, some of these oligomers may reach the beginning of the chromatographic column and remain adsorbed in the stationary phase. This may lead to a rapid deterioration of the column quality. One common procedure to alleviate this problem is the addition of a piece of deactivated fused silica (or retention gap) before the analytical column. This retention gap is sometimes named precolumn; however, this name is more properly used for the first analytical column in bidimensional systems. The retention gap can be changed more frequently than the analytical column. The function of the retention gap is in fact more complex, allowing for example some "focusing" of the zone where the sample is placed in the column and increasing the chromatography resolution [40].

- Bidimensional Py-GC.

The complex nature of pyrolysates requires in some situations a better separation of the components than commonly possible using standard chromatography. This can be easily understood by estimating the number p of visible peaks in a chromatogram compared to the real number of components m . The relation between the two parameters is [40a]

$$p = m \exp(-m/n_c) \quad (43a)$$

where n_c is the *peak capacity* defined as the maximum number of peaks that can be put side by side (with acceptable resolution) into the available separation space in a chromatographic separation (n_c in rel. 43 should be chosen as the value corresponding to a critical resolution). In isotherm conditions, n_c can be estimated with the formula:

$$n_c = 0.5 (n)^{1/2} \quad (44)$$

where n is the number of theoretical plates of the column. This shows that even for a good column ($n=300000$), n_c has values between 250 and 300. Considering a mixture

with $m = n_c$, rel. (43a) indicates that only 36.8% of expected number of peaks are observed, the rest of them being merged with the others. The number of single component peaks s is even lower, and it is estimated by the formula [40a]:

$$s = m \exp(-2m/n_c) \quad (43b)$$

which shows that only 13.5% of the total number of components appear as single component peaks. In practice, it is therefore impossible to completely separate a mixture with more than 30 to 40 components using one chromatographic column.

For a better separation, the peaks from a given interval in the first chromatogram can be subject to a second separation. Bidimensional gas chromatography has been developed with the purpose to address this problem of the separation of complex mixtures [40a]. The technique allows a small portion to be cut from a chromatographic separation and to be sent to a second chromatographic column for additional separation. This process can be accomplished in different instrumental setups. One such system, allowing bidimensional chromatographic separation with one GC oven, is shown in Figure 5.2.12.

In this system, the sample is injected as usual and sent to the first chromatographic column (Column 1) where the separation takes place. The eluted compounds and the carrier gas go into the mid-point restrictor and may take two different paths.

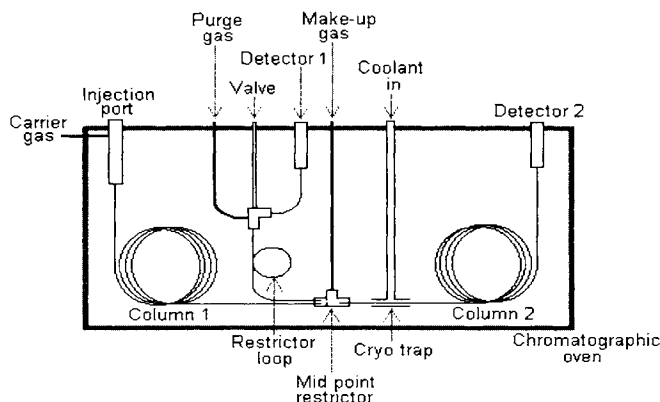


FIGURE 5.2.12. *Bidimensional chromatographic system with one GC oven.*

The first possible path does not use the second column, and the eluted compounds are diverted through the restrictor loop to the detector (Detector 1). For this case, the valve to Detector 1 is open. At the same time enough make-up gas is sent to the mid-point restrictor in order to have flow in the second column (Column 2) and through Detector 2. Gas chromatographic columns must have a flow of inert gas when heated to avoid the degradation of the stationary phase. No bidimensional separation takes place when this path is activated.

The second possible path uses the second column and leads to bidimensional separation. In this case, the valve to Detector 1 is closed, and the flow is forced to the

second column. A so-called heart-cut is taken from the first separation by sending the eluted compounds to the second column. The make-up gas is stopped or reduced in this case. Because the peak broadening will be too large if the material from the first column goes directly to the second separation, a cryo-focusing step is needed. A small portion of the beginning of the second column passes through a cryo-trap, cooled at a low temperature (-60°C to -100°C , or even lower) with liquid CO_2 or N_2 . The heart-cut materials are accumulated in a narrow zone as long as the cryo-trap is cold, and the heart-cut is taken. The cryo-trap is maintained cold as long as the system is not ready for the second separation.

In practice, a first chromatographic run is commonly done in single dimension mode, using the first path previously described (no heart-cut), with a temperature oven program that is suitable for the separation in the first column. After this run, one or more narrow regions of interest are selected from the single dimension chromatogram for taking heart-cuts. In a following run with a heart-cut, the cryo-trap is set cold a few minutes before the heart-cut is taken. Then, at the precise established run-time the valve to Detector 1 is closed and the mid-point restrictor is set for heart-cut mode. The analytes of interest are collected in the cryo-trap. After the heart-cut is taken, the oven temperature program may be continued or the oven may be reset for the new program needed for the separation in the second column. When the second separation starts, either the cryo-trap is heated or the cooling is stopped and the entire column takes the temperature of the GC oven. The separation in the second column proceeds with the second temperature program for the oven.

It is common to use different stationary phases for Column 1 and Column 2. A variety of possibilities are available, but frequently one column is polar while the other is non-polar. In this way, one separation is done mainly depending on the polarity of the analytes, while the second separation is done based mainly on boiling point differences. Both polar/non-polar and non-polar/polar pairs have been utilized depending on the specific need for the separation.

As an example, a bidimensional separation was performed for a segment in a separation of a cellulose pyrolysate. Figure 5.2.13(A) shows the chromatogram of a pyrolysate obtained at 600°C from microcrystalline cellulose. The results were obtained on a $30\text{ m} \times 0.32\text{ mm}$ Carbowax column with $0.5\text{ }\mu\text{m}$ film thickness as a first dimension separation in a bidimensional system similar to the one shown in Figure 5.2.12.

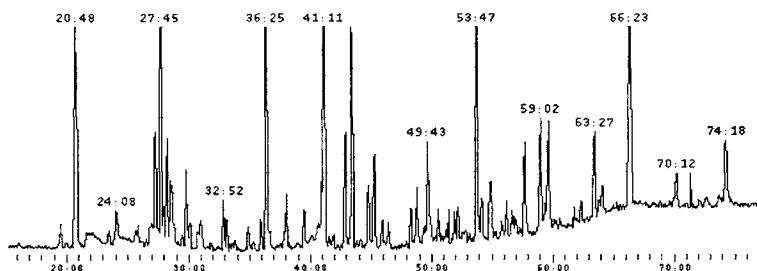


FIGURE 5.2.13(A). *The chromatogram of the pyrolysate obtained from microcrystalline cellulose at 600°C with the separation on a $30\text{ m} \times 0.32\text{ mm}$ Carbowax column, $0.5\text{ }\mu\text{m}$ film thickness.*

In this separation, a 10-mL sample (large volume) containing a solution in tert-butyl methyl ether (tBME) of the pyrolysate of 1 mg cellulose obtained at 600° C was injected (off-line pyrolysis). The PTV injector was programmed at 20° C initial temperature for 2 min. and ramped with 10° C/min at 250° C and kept at this temperature for 1 min. Then the injector was further heated at 300° C. The split vent purge time was 2.5 min. The oven temperature for the first dimension separation was kept at 35° C for 2.5 min. then heated with 30° C/min. at 55° C and further heated with 3° C/min. to 240° C. The detector used in the first dimension was an MS system, which allowed the identification of a series of compounds from this chromatogram. The peak identification is given in Table 5.2.2.

TABLE 5.2.2. *Identification of a series of peaks from cellulose pyrolysate shown in Figure 5.2.13(A).*

Ret. time	Compound name	Formula	MW
20:48	hydroxypropanone	C3H6O2	74
27:16	acetic acid	C2H4O2	60
27:45	methyl pyruvate	C4H6O3	102
28:15	furancarboxaldehyde	C5H4O2	96
30:07	1-(2-furanyl)-ethanone	C6H6O2	110
32:52	2-methyl-2-propenoic acid ethenyl ester	C6H8O2	112
33:09	5-methylfurancarboxaldehyde	C6H6O2	110
36:25	furfuryl alcohol	C5H6O2	98
38:04	a dihydroxybenzene ?	C6H6O2	110
41:11	3-hydroxycyclopent-2-en-1-one	C5H6O2	98
42:54	4-cyclopentene-1,2,3-triol	C5H8O3	116
43:28	2-hydroxy-3-methyl-2-cyclopenten-1-one	C6H8O2	112
44:48	2,5-dihydroxy-3-methyl-2-cyclopenten-1-one	C6H10O3	128
45:17	2,5-dihydroxy-2-cyclopenten-1-one	C5H6O3	114
45:56	2-hydroxy-3-ethyl-2-cyclopenten-1-one	C7H10O2	126
48:18	cyclotene	C6H8O2	112
48:50	3-hydroxy-2-methyl-4H-pyran-4-one (maltol)	C6H6O3	126
49:43	2-ethylcyclopentanone ?	C7H12O	112
49:58	phenol	C6H6O	94
50:37	2-ethyl-5-methylcyclopentan-1-one ?	C8H14O	126
51:55	isomaltol	C6H6O3	126
52:21	5-hydroxymethylfuran-2-one	C5H8O3	116
53:47	hexanal	C6H12O	100
54:12	tetrahydro-5-methyl-furfuryl alcohol	C6H12O2	116
54:58	dihydro-4-methyl-2(3H)-furanone	C5H8O2	100
55:00	tetrahydro-2H-pyran-2-one ? or isomer of dihydro-4-methyl-2(3H)-furanone	C5H8O2	100
56:16	3-buten-1,2-diol or 3-hydroxytetrahydrofuran ?	C4H8O2	88
56:43	propylcarboxaldehyde	C8H10O2	138
57:45	5-ethyl-dihydro-2-furanone	C6H10O2	114
59:02	mix		
59:43	3,5-dihydroxy-2-methyl-4H-pyran-4-one	C6H6O4	142
63:27	1,4:3,6-dianhydro- α -D-glucopyranose	C6H8O4	144
64:07	1,2,3-benzenetriol	C6H6O3	126
66:23	5-hydroxymethylfurfural	C6H6O3	126
74:13	1,3-benzenediol	C6H6O2	110

Figure 5.2.13(B) shows the run-time interval between 52.5 to 56.5 min. (magnified) of the same chromatogram. From Table 5.2.2 it is possible to recognize the compounds detected in the run-time interval 52.5 to 56.5 min. (black borders).

A heart-cut of this interval was taken in the GC bidimensional system, and the separation was performed on a 30 m x 0.32 mm DB5 column with 0.5 μm film thickness. The oven temperature for the second separation was initially kept at 45° C for 5 min. and then heated with a ramp of 3° C/min. to 240° C. The detector used for the second dimension was also an MS system. The chromatographic results are shown in Figure 5.2.13(C).

By comparison of Figure 5.2.13(B) with Figure 5.2.13(C), it is clear that a much better separation can be obtained using a bidimensional system for the heart-cut interval. This allows the identification of a series of peaks, and they are indicated in Table 5.2.3. The peaks that were previously identified in the first dimension can be recognized in Table 5.2.3 (black borders).

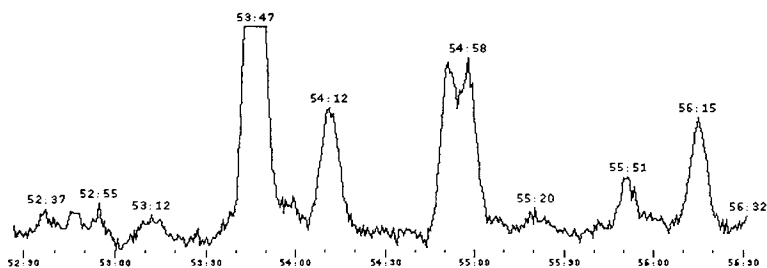


FIGURE 5.2.13(B). The segment between 52.5 min. and 56.5 min. from the chromatogram of cellulose pyrolysate shown in Figure 5.2.13(A).

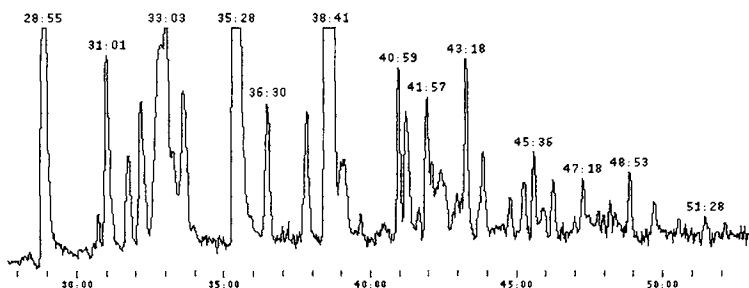


FIGURE 5.2.13(C). The chromatogram of the heart-cut taken between 52.5 min. and 56.5 min. in the second dimension separation from the chromatogram of cellulose pyrolysate shown in Figure 5.2.13(A). The second separation was done on a 30 m x 0.32 mm DB5 column, 1.0 μm film thickness. The peaks at 38:33 and 38:41 min. corresponding to the peaks at 54.12 and 54.58 in Figure 5.2.13(B) are only partially separated (not at the baseline) and appear as one peak due to magnification.

Besides the system described previously, other instrumental setups are reported or manufactured, including double-oven bidimensional systems, systems allowing the monitoring of the separation in the first dimension even when the heart-cut is taken, etc. Also, two independent GC systems have been used for the analysis of complex samples [40b], mainly associated with programmed temperature pyrolysis. When two groups of compounds of very different volatility are generated in pyrolysis, the volatiles that evolve

at lower temperature can be trapped and analyzed on-line by one GC, and the pyrolysate obtained at higher temperatures can be analyzed separately by a second on-line GC (see Section 14.4).

TABLE 5.2.3. Identification of a series of peaks shown in Figure 5.2.13(C), heart-cut of the run-time interval between 52.5 and 56.5 min. of the chromatogram for cellulose pyrolysate shown in Figure 5.2.13(A).

Ret. time	Compound name	Formula	MW
28:55	3-buten-1,2-diol or 3-hydroxytetrahydrofuran ?	C4H8O2	88
31:01	5-methyl-2(5H)-furanone	C5H6O2	98
31:40	2,3-dihydro-5,6-dimethyl-1,4-dioxin	C6H10O2	114
32:40	tetrahydro-5-methyl-furfuryl alcohol	C6H12O2	116
33:03	1,6-heptadien-ol	C7H12O	112
33:40	3-methylphenol	C7H8O	108
35:28	hexanal	C6H12O	100
36:30	1-(2-furany)-propanone	C7H8O2	124
37:50	cyclopropanecarboxylic acid ?	C4H6O2	86
38:33	dihydro-4-methyl-2(3H)-furanone	C5H8O2	100
38:41	tetrahydro-2H-pyran-2-one ? or isomer of dihydro-4-methyl-2(3H)-furanone	C5H8O2	100
39:08	2,3,5-trimethylphenol ?	C9H12O	138
39:38	2,5-dimethylphenol	C8H10O	122
40:59	4-methyl-4-penten-2-one ?	C6H10O	98
41:25	2,3,6-trimethylphenol ?	C9H12O	138
41:57	4-hydroxybenzaldehyde	C7H6O2	122
43:18	2-coumaranone	C8H6O2	134
43:50	propylcarboxaldehyde	C8H10O2	138
44:56	2,6-dimethylphenol ?	C8H10O	122
45:10	(1,1'-bicyclopentyl)-2-ol	C10H18O	154
45:36	a dihydroxytrimethylbenzene	C9H12O2	152
46:20	2-methyl-4-(1-methylethyl)-2-cyclohexen-1-one	C10H16O	152
47:18	6-methyl-3-(1-methylethyl)-2-cyclohexen-1-one	C10H16O	152
48:55	5-methyl-1(3H)-isobenzofuranone	C9H8O2	148
49:50	a methylisobenzofuranone isomer ?	C9H8O2	148
51:28	4-methyl-1-indanone	C10H10O	146

- Concentration techniques used in Py-GC.

Concentration techniques in GC are used mainly for trace analysis. Pyrolysis commonly generates enough material for a GC analysis even when a very small amount of sample is taken for analysis. For this reason, concentration techniques are not frequently associated with Py-GC. However, in some instances it is necessary to analyze both the volatile compounds that are generated at mild heating of the polymer (sometimes below 100° C) and also the typical pyrolysis products. Several two-step (or multi-step) experiments were reported [40c] that allow this type of analysis.

For the analysis of traces of volatile materials, purge-and-trap is a common procedure. It consists of purging the sample (heated at a given temperature usually below 100° C) with an inert gas and passing the purging gas over a solid-phase adsorbent, such as Tenax. The solid-phase adsorbent is kept at a low temperature (such as 20° C).

After a certain purging period, a six-way valve allows switching of the flow through the system as shown in the simplified diagram of a purge-and-trap system given in Figure

5.2.14. The solid-phase adsorbent is heated (at a temperature commonly between 200° C and 300° C) to desorb the analytes in a stream of carrier gas that is sent to a GC.

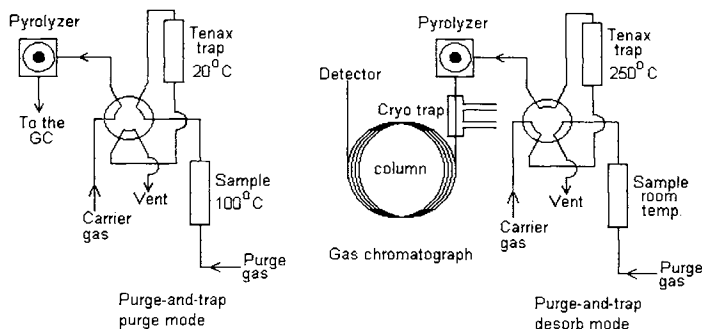


FIGURE 5.2.14. Simplified diagram of a purge-and-trap system with an on-line pyrolyser connected to a GC.

A cryo-trap is usually necessary to focus the analytes before the GC separation with a purge-and-trap. The desorption of the analytes from the trap is not instantaneous, and several minutes of heating are required to release them. This would lead to broad peaks in the GC separation. Also, it is common before the desorption of the trap at high temperature to include a short pre-desorption period when the trap is vented at room temperature for elimination of water or other materials that are not desired in the GC.

The system shown in Figure 5.2.14 also has a pyrolysing interface included between the purge-and-trap and the GC (a CDS 1000 interface has been used for this purpose [40d]). With this system it is possible to analyze a sample first for the volatiles released at low temperatures and then to pyrolyse it. The process must be done in two different steps (purge-and-trap first, and pyrolysis separately) but has the advantage of using exactly the same GC setup for all the compounds in a sample. Using the cryo-focusing trap, the relatively large volume of the pyrolyser interface does not affect the chromatography.

The principle of the purge-and trap system is based on the partition of compounds between a gas and a solid adsorbing phase. The apparent volume of the absorbing solid can be measured and is defined by

$$V_a = n R T / P \quad (45)$$

where n is the number of moles, R is the gas constant, T is temperature and P the pressure of gas adsorbed by the solid. If C_o is the initial concentration of an analyte "i" in the solid sample, the concentration C will be lower after a volume of gas is passed over it. The mass balance gives

$$V_a C_o = V_a C + V_g C_g \quad (46)$$

where V_g and C_g are the volume and the concentration of the gas. The partition constant between the gas and the solid (which is temperature dependent) is given by rel. (1a) and for this case can be written:

$$K = C / C_g \quad (1c)$$

From rel. (46) and (1c), it can be obtained:

$$V_a C_o = C_g (K V_a + V_g) \quad (47)$$

Rel. (47) gives the relation between the initial concentration of an analyte C_o in a solid phase and its concentration in the gas phase C_g , assuming equilibrium conditions. The same equation can be applied for the desorption of the analyte from the sample and for the absorption and desorption of the analytes from the trap. The equilibrium conditions are not commonly fulfilled in purge-and-trap systems, the amount of analyte in the gas phase ($C_g V_g$) being in general lower than the one given by rel. (46).

Pyrolysates can be analyzed off-line in a purge-and-trap system if only the volatiles are of interest in an analysis.

- Data processing in Py-GC.

In principle, there are no particular differences in the chromatographic data interpretation whether the sample is a pyrolysate or a different material. The signal generated by a GC detector is commonly recorded and can be displayed as a chromatographic plot or a chromatogram (a pyrogram if the sample is a pyrolysate) in which the sample components appear as peaks. These peaks ideally have a Gaussian shape. The chromatograms can be generated with a non-selective detector without the capability of qualitative identification (such as a FID) or using one with qualitative identification capability such as a mass spectrometer (MS). Data processing for a Py-GC/MS system will be further discussed in Section 5.3.

Besides generating a chromatographic plot, the signal from most GC detectors can be further processed electronically in an "integrator." From the FID signal, for example, both qualitative and quantitative information can be extracted by determining the retention time and the area of each peak. The integrator is able to detect the chromatographic peaks using the variation in the slope of the signal. If the difference in the intensity of the signal for two or three consecutive points along the chromatogram is higher than a given threshold, the integrator recognizes the beginning of a peak. Similarly, the end of a peak is detected when the difference in the intensity becomes too small. For each peak, the area can be measured, and this is done by using a numerical integration [e.g. 40] procedure. The peak is "divided" in slices, each slice with a measured height and a fixed width. The total area is the sum of the areas of those slices. In modern electronic integrators these processes are transparent for the user, who is only able to select certain parameters such as the signal threshold for peak detections, the minimum area to be recorded, or how to handle peak shoulders, etc. Integrators can tabulate the information regarding each chromatographic peak such as: retention time, peak area, relative peak area (to the total area of all detected peaks), peak height, relative peak height, type of baseline in the region of each peak, etc. The qualitative information in a chromatogram is related to the retention time of the peaks, while the peak area is used for quantitative analysis.

Although no structural information for an analyte can be obtained from a chromatogram generated with a FID (or similar type of detector), chromatograms are widely used for

qualitative analysis. This can be done in several ways. One possibility is to match the retention times of standards identical to the compounds that are analyzed. The retention time of each compound has a specific value in given chromatographic conditions (although the danger always exists that different compounds may have the same retention time). One problem with this approach is that by changing the chromatographic conditions (like carrier gas head pressure, column dimensions, etc.), these retention times vary. One procedure to avoid this variability is to replace the retention time of a compound with a *retention index* I_j [41]. The retention index is a measure of the relative retention in isotherm conditions using the normal alkanes as a standard reference. In isotherm conditions, the retention times of normal alkanes increase exponentially with the carbon number of the alkane. By measuring the adjusted retention times $t_{R'}$ (in isotherm conditions) for a series of normal alkanes, a scale is generated. The retention index for a given compound "j" showing a peak between the alkane with N carbons and the alkane with $(N + u)$ carbons is defined as

$$I_j = 100 N + 100 u \left(\frac{\log t_{R'j} - \log t_{R' N}}{\log t_{R' (N+u)} - \log t_{R' N}} \right) \quad (48)$$

where $t_{R'}$ are the corresponding adjusted retention times. The retention index for the alkanes with N carbons considering rel. (48) will be $100 N$. The retention index is dependent on temperature and on the nature of the stationary phase. The dependence of the retention index on temperature can be approximated with the formula [42]:

$$\Delta I / 10^\circ \text{C} = (I_{T_1} - I_{T_2}) / [10 (T_2 - T_1)] \quad (49)$$

where T_1 and T_2 are two different temperatures. This relation is not well obeyed by polar compounds or when the difference between T_1 and T_2 is larger than 50°C .

Extensions of the definition of a retention index were done by choosing gradient temperature conditions [42] or methyl esters as standards instead of normal hydrocarbons. Tables for retention indexes of certain substances have been published [43]. However, the retention index system has limited utility for the GC analysis of pyrolysates due to the complexity of such samples.

In addition to the standard information provided by the retention time (index) and peak area, global comparisons between chromatograms can be done based on total peak area in the chromatogram or based on the profile of the chromatogram. Total peak areas in the chromatogram can be obtained easily, and most integrators using electronic data processing provide this number. However, it is possible that the sum of all peak areas may include solvents or compounds that are not of interest. Also, this number depends on the amount of sample taken in analysis. For Py-GC this can fluctuate rather considerably, and repeated runs of the same sample may generate quite different results if the amount of sample to be pyrolysed is not carefully measured.

Global profile comparisons are also useful for comparing complex samples and were used to differentiate the pyrograms for different composite materials such as microorganisms. A simple global comparison is commonly obtained using a similarity index. There are various ways to calculate such an index. One procedure [42a], which is aimed to qualitatively compare two chromatograms A and B, uses the relation:

$$S\% = 100 N_c / (N_c + N_u^{(A)} + N_u^{(B)}) \quad (50)$$

where N_c is the number of peaks that are common in the two chromatograms, $N_u^{(A)}$ is the number of unique peaks in chromatogram A, and $N_u^{(B)}$ the number of unique peaks in chromatogram B. The peaks are commonly tabulated with electronic integrators and their number is readily obtainable. The pairing of peaks is done based on their retention times, which must be equal or within a small interval. $S\% = 100$ when the chromatograms have the same compounds and 0% when no two peaks correspond to the same retention time. This comparison does not take into account the peak areas.

Another method does take into account the areas of a series of peaks from the two chromatograms to be compared. The selected peaks are indexed 1, 2, 3... n, and the areas in the first chromatogram are $A_1, A_2, A_3...A_n$, and in the second one the areas are $B_1, B_2, B_3, ...B_n$. A fit factor F can be calculated for example using the formula:

$$F = 100 \{1 - \sum (A_i - B_i)^2 / \sum [(A_i)^2 + (B_i)^2]\} \quad (i = 1, \dots, n) \quad (51)$$

Again, the peaks must be paired based on their retention times, which must be equal or within a small interval. For a perfect fit, rel. (51) gives a factor $F = 100\%$, and no match gives $F = 0\%$. The peak areas in rel. (51) can be replaced by normalized peak areas, where the normalization is done for each chromatogram by an internal standard or by the total peak area.

The calculation of a fit factor or a similarity based on peak areas can also be done using other expressions. For example, a similarity index SI can be calculated using the ratios of the peak areas, which are taken as

$$R_i = A_i / B_i \text{ or } B_i / A_i \quad \text{such that } R_i < 1 \quad (52a)$$

and $R_i = 0$ for each missing corresponding peak in any of the chromatograms. Then the similarity can be calculated using the formula:

$$SI = (\sum R_i) / n \quad (i = 1, 2, 3...n) \quad (52b)$$

The SI value can also be expressed in percentage (by multiplying SI with 100).

The absolute peak areas in rel. (52a) may be replaced by the peak areas normalized by an internal standard, or by the sum of all peak areas, or by the concentrations of the corresponding compounds 1, 2, 3,...n, (if these concentrations are known).

As an example, the similarity using rel. (52b) was calculated between a chromatogram of a silylated cellulose pyrolysate obtained off-line at 510°C with a filament flash pyrolyser and that of a silylated starch pyrolysate obtained in the same conditions. The calculation gave a $SI \approx 0.61$. At the same time duplicates of two runs of cellulose gave a $SI \approx 0.92$ (a perfect similarity should be $SI = 1.0$, but fluctuation in the peaks areas in the duplicate chromatograms make this case unlikely). The pyrogram for cellulose is shown in Figure 5.2.15 and the one for starch is shown in Figure 5.2.16.

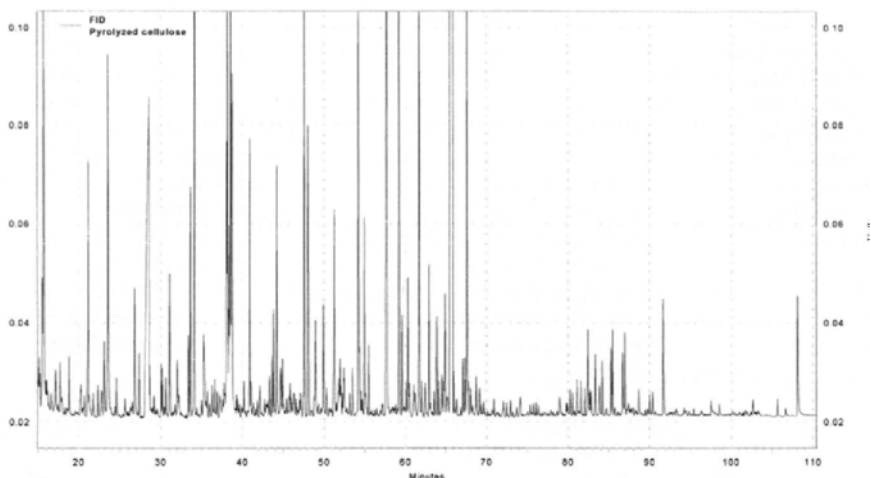


FIGURE 5.2.15. *The chromatogram of a silylated cellulose pyrolysate obtained off-line at 510° C with a filament flash pyrolyser.*

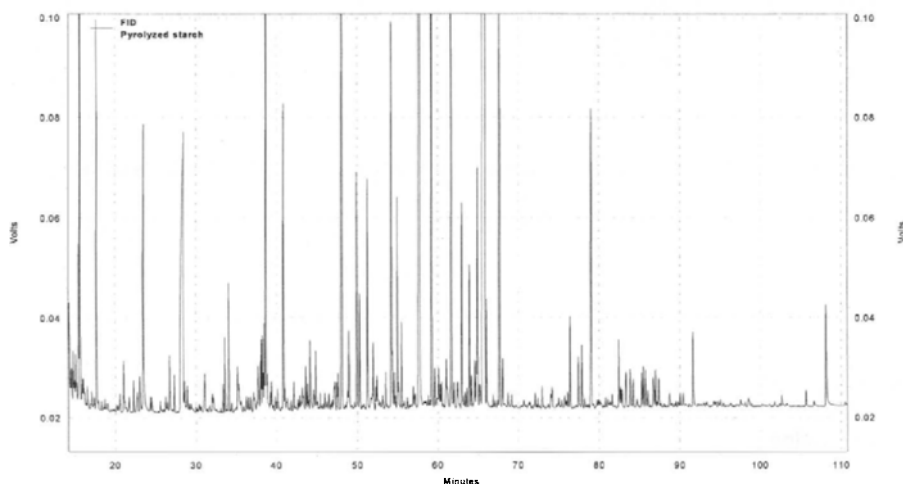


FIGURE 5.2.16. *The chromatogram of a silylated starch pyrolysate obtained off-line at 510° C in a filament flash pyrolyser.*

The derivatization of the pyrolysate was done with BSTFA in t-butyl methyl ether. The separation was obtained on a methylsilicone 5% phenylsilicone column (DB5), 60 m long, 0.32 mm i.d., with 0.25 μm film thickness. The oven temperature started at 50° C and was increased with a rate of 2° C/min to 310° C.

The reproducibility of the retention times is very important when the similarity indexes between chromatograms are calculated. If the retention times are not stable, peaks

belonging to different compounds could be compared by mistake. For GC separations that are correctly performed, the reproducibility of retention times is not a problem, and variations less than 0.1 min. are typical. However, in certain cases the variations can be large, such as, when attempts are made to compare chromatograms that were run several months apart and a drift in retention times is present. This drift can be caused, for example, by the modification of the stationary phase of a chromatographic column that has been subjected to constant use for a long period of time or by changes in operating parameters for the separation. Computer programs are available that can alter the real retention times of all peaks in one chromatogram and adjust them to correspond to those in the second chromatogram. This can be done by choosing reference peaks in both chromatograms and modifying one set of retention times in such a way that the reference peaks are forced to coincide. The procedure, which is named a "rubber band" correction, uses a polynomial transformation to the times from the chromatogram to be corrected.

The procedure can be explained considering chromatogram A with peaks at retention times $t_1, t_2, t_3 \dots t_n$, and chromatogram A' with corresponding peaks for the same compounds at retention times $t_1', t_2', t_3' \dots t_n'$. The proposed transformation will be applied to any retention time t_x' from chromatogram A', changing the old retention time t_x' into a new retention time $t_x'' = t_x$.

If a pair of corresponding peaks in the chromatograms A and A' have the retention times t_1 and t_1' , and the times in the second chromatogram are only shifted compared to the first one, then the times are related by the equation:

$$t_1 = a + t_1' \quad (53)$$

An adjustment can be done to t_1' by adding the coefficient a and transforming it into t_1'' , where:

$$t_1'' = a + t_1' = t_1 \quad (54)$$

This change, although valid for t_1' (which is changed by this operation into $t_1'' = t_1$), is not the common case because in practice the retention time variation is not only a shift but also can be an expansion or a contraction.

The procedure can be further developed for two pairs of peaks with the retention times t_1, t_2 in the first chromatogram and t_1', t_2' in the second chromatogram, following a similar scheme and writing formally:

$$\begin{aligned} t_1 &= a + b(t_1') \\ t_2 &= a + b(t_2') \end{aligned} \quad (55)$$

The coefficients a and b can be determined by solving the equation system (55) where t_1, t_2 and t_1', t_2' are reference peaks in the two chromatograms. Then, any retention time t_x' can be adjusted to t_x'' using the relation:

$$t_x'' = a + b(t_x') \quad (56)$$

This transformation will make $t_1'' = t_1$ and $t_2'' = t_2$, and possibly adjust some other peaks between t_1' and t_2' , but still will not necessarily be true for every retention time in

chromatogram A'. However, more corrections can be made, choosing for example five standards and solving (using a computer program) the equation system:

$$\begin{aligned} t_1 &= \mathbf{a} + \mathbf{b} (t_1') + \mathbf{c} (t_1' - t_1)^2 + \mathbf{d} (t_1' - t_1)^3 + \mathbf{e} (t_1' - t_1)^4 \\ t_2 &= \mathbf{a} + \mathbf{b} (t_2') + \mathbf{c} (t_2' - t_2)^2 + \mathbf{d} (t_2' - t_2)^3 + \mathbf{e} (t_2' - t_2)^4 \\ t_3 &= \mathbf{a} + \mathbf{b} (t_3') + \mathbf{c} (t_3' - t_3)^2 + \mathbf{d} (t_3' - t_3)^3 + \mathbf{e} (t_3' - t_3)^4 \\ t_4 &= \mathbf{a} + \mathbf{b} (t_4') + \mathbf{c} (t_4' - t_4)^2 + \mathbf{d} (t_4' - t_4)^3 + \mathbf{e} (t_4' - t_4)^4 \\ t_5 &= \mathbf{a} + \mathbf{b} (t_5') + \mathbf{c} (t_5' - t_5)^2 + \mathbf{d} (t_5' - t_5)^3 + \mathbf{e} (t_5' - t_5)^4 \end{aligned} \quad (57)$$

After the determination of the unknown coefficients **a**, **b**, **c**, **d**, **e**, any retention time t_x' can be adjusted to $t_x'' = t_x$ using the relation:

$$t_x'' = \mathbf{a} + \mathbf{b} (t_x') + \mathbf{c} (t_x' - t_x)^2 + \mathbf{d} (t_x' - t_x)^3 + \mathbf{e} (t_x' - t_x)^4 \quad (58)$$

By this procedure, it is very likely that peaks corresponding to the same compound will be compared. A mass spectral identification is commonly needed to validate the correspondence of the standards. Also, the standards chosen for adjusting retention times should be spread in the chromatogram, and the extremes should bracket the retention times to be corrected.

Besides simple similarity comparisons, more elaborate comparisons were also performed on Py-GC data [1]. Some of the techniques utilized to compare Py-GC data are similar to those used for the processing of Py-MS results that will be discussed in Section 5.5.

Collections of Py-GC results for a variety of polymers have been reported [43a]. However, because the goal of the chromatography is to obtain an optimum separation of the components, standard recommendations may generate inadequate chromatograms for particular experimental setups. The libraries of Py-GC data contain descriptive information and graphs of the pyrograms but are not adequate for matching an unknown chromatogram with those from the library [44].

The quantitative analysis using GC is based on the fact that the area under a chromatographic peak is proportional with the amount of the component generating that peak. Ideally, for a given volume of sample injected into the chromatograph, the peak areas are linearly dependent on the concentrations. Because the concentrations are of interest, they can be determined from the areas using the relation:

$$c_i = b A_i \quad (59)$$

and the value of **b** is determined from a calibration curve. This value (response factor) may be different for different compounds and for different types of detectors. Peak area measurement is commonly done electronically. This measurement raises a series of problems such as the choice of the baseline for a given portion of a chromatogram, integration of peaks which are merged and are not separated at the baseline, or integration of peaks appearing as shoulders on other peaks, etc. These kinds of problems are frequently detailed in the manuals associated with specific integrators (e.g. [29]). For very narrow peaks and for those with the shape close to a Gaussian curve, the peak height can also be used for quantitation.

The quantitation in Py-GC is not as much utilized as in the GC for liquid samples. The main problems are related to the complexity of the pyrograms, difficulties in getting calibrations for a given compound, as well as the inherited variability of pyrolysis and pyrolysate transfer processes. One possibility to compensate for some of these problems is the use of an internal standard in the material to be pyrolysed. One problem with the addition of an internal standard is the addition of the appropriate amount of standard. The samples in pyrolysis being small (commonly up to 1 mg), the standard should be in the range of 0.02 to 0.05 mg. It is therefore difficult to weigh this amount of internal standard with enough precision. A possibility to add an internal standard with better accuracy is to adsorb it first on a neutral support. As an example, dibromobenzene was adsorbed at 5% in pure alumina from a CH_2Cl_2 solution. Then, 1 mg of the alumina was added together with the precisely weighed sample [44a]. Dibromobenzene can be used in a variety of samples as a standard for pyrolysis at temperatures up to 700°C , showing no decomposition and generating a single chromatographic peak.

5.3. Mass Spectrometers as Detectors in Pyrolysis-Gas Chromatography.

Mass spectrometers are used as detectors in gas chromatography offering the capability of compound quantitation and identification with exceptionally good sensitivity. For this reason, pyrolysis-gas chromatography/mass spectrometry (PY-GC/MS) is an excellent tool for polymer analysis. When a pyrolyser is used at the front end of the chromatograph, no special problems related to the GC/MS analysis are really added. The only role of the pyrolyser is in this case to provide the pyrolysate to the GC. Because of the extensive use of Py-GC/MS as a technique in analytical pyrolysis and because mass spectrometry is a rather complex subject [37,38], a more detailed discussion is required.

GC/MS is a common analytical technique and a large amount of information is available regarding this subject [e.g. 38]. In GC/MS, the carrier gas containing the (separated) analytes from the GC is transferred to the mass spectrometer. The gas flow is commonly set between 0.1 to 3.0 mL/min. (at near atmospheric pressure). Because the mass spectrometers operate at 10^{-5} to 10^{-7} mbar, they are equipped with efficient pumps, which maintain inside the mass spectrometer a high vacuum.

- Ion generation.

The mass spectrometric analysis starts with an ionization process (see also Section 3.5). This ionization takes place in the ion source of the MS instrument, where the analyte is introduced as gas phase. There are two common ionization procedures used for GC/MS: electron ionization (EI) and chemical ionization (CI). Other ionization procedures are also used in mass spectroscopy (see below and Section 5.4). The EI process consists of an electron bombardment, which is commonly done with electrons having an energy of 70 eV. The electrons are usually generated by thermoionic effect from a heated filament and accelerated to the required energy. A schematic diagram of an EI source is shown in Figure 5.3.1.

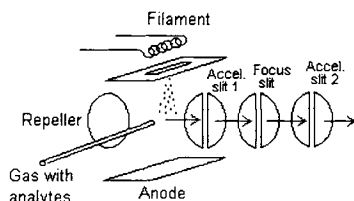
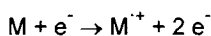
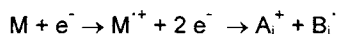


FIGURE 5.3.1. Schematic diagram of an EI source.

As described in Section 3.5, the electrons interact with the molecules M to eject an additional electron leaving a positively charged species that is a molecular ion of the type M^+ (odd-electron OE^+):

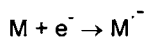


When the molecular ion obtains too high energy during the electron impact, there are fragments that are generated in the ion source. The fragment ions A_i^+ are commonly even electron ions EE^+ (odd-electron fragments OE^+ are also possible), while the rest of the molecule forms radicals B_i which are not detected in the mass spectrometer:



More than one fragmentation path is possible for a given molecule, but the nature and abundance of fragments is characteristic for a given compound. The fragment abundance represented versus m/z (mass/charge) generates a mass spectrum. The formation of molecular ions takes place with a range of internal energies. Those that have lower energies will not decompose before detection and will appear as M^+ in the spectrum. If they have higher internal energies, the M^+ ions can decompose by a variety of energy dependent reactions, each of which results in the formation of an ion and a neutral species. Some fragments still have enough energy to suffer further fragmentations.

Some compounds may also form negative radical ions under electron bombardment.

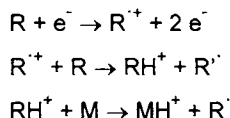


Negative ion operation (with detection and use for analytical purposes) involves altering the source, the focus potential, and some other parameters in order to allow negative ions to enter the ion separation section of the MS and then to be detected. For this reason, the MS instruments are set to work either in EI^+ or EI^- mode.

Besides the stable ions, metastable ions are also known to be formed in the ionization process. These ions have a short half-life. Some start dissociating in the ionization chamber, but a significant number will still be able to leave it, continuing to dissociate during their passage to the detector. They generate diffuse peaks in the mass spectra.

In chemical ionization, in addition to the carrier gas and the analytes coming from the GC, a reagent gas (methane, butane, ammonia, etc.) is injected in the ion source at a

typical pressure of 10^{-2} to 10^{-3} mbar. The initial step in the ionization takes place by the electron impact on the molecules of the reagent gas (which is in large excess compared to the analyte molecules) forming R^+ ions, assuming Cl^+ . Following this step, the R^+ ions react with other R molecules generating RH^+ ions (and radicals R^\cdot). These RH^+ ions further react with the analyte forming MH^+ ions:



The ions MH^+ tend to not fragment because they have a much lower energy than the ions M^+ generated by direct electron impact. Besides MH^+ ions, ion clusters containing the analyte molecule and one or more molecules of the reagent gas may be formed during chemical ionization. The ions A_i^+ , M^+ or MH^+ formed in the ion source are then accelerated and shaped by electric lenses into an ion beam. Some particular compounds are able to generate enough negative ions in chemical ionization that Cl^- operation mode is convenient. Several instrument parameters should be set up accordingly to work with negative ions.

- Separation of ions by their m/z ratio.

The ions from the ion beam are separated by their mass to charge ratio (m/z) (where commonly $z = 1$), providing the series $m_1/z_1, m_2/z_2, m_3/z_3, \dots, m_n/z_n$ that will give the mass spectrum. The ion separation can be done using special ion optics that differentiate the mass spectrometers as follows: magnetic sector instruments, quadrupole, time-of-flight, ion trap, Wein filter, ion cyclotron resonance, etc.

In a magnetic sector instrument, the ions generated in the ion source are sent through a magnetic field where they are deflected on an arc trajectory of the radius r given by the formula:

$$r = [(m/z) (2V / B^2)]^{1/2} \quad (1)$$

where B is the magnetic field strength and V is the accelerating potential applied to the ions leaving the ion source. A simplified diagram of this deflection is shown in Figure 5.3.2.

Rel. (1) indicates that different r are obtained for different m/z values (when B and V are constant), and this would disperse the ions of different masses. However, it is more convenient to have all ions focused at the same point but at different times (in cycle). This can be achieved by varying the field B with a precise rate in time (cycled) and keeping V constant such that the same value r for ions of different m/z is obtained.

This method requires that the ions leaving the ion source must have exactly the same kinetic energy. This is not entirely true in practice, and the focusing is not always very good. For this reason, besides the magnetic sector (B), the instruments also need an electric sector (ESA or E), which is a focusing and also energy dispersive device.

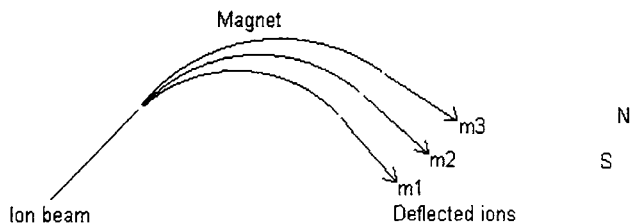


FIGURE 5.3.2. Trajectory of ions of different masses in a magnetic field perpendicular on the plane of deflection.

Combinations of the two types of field (EB, BE, or EBE) are used to achieve a good separation (in time) of ions of different mass and good convergence of the ion beam on one point, even if it has ions of different energies. At this point a slit allows the delivery to the detector of ions in a very narrow mass range. Figure 5.3.3 shows the schematics of a BE arrangement.

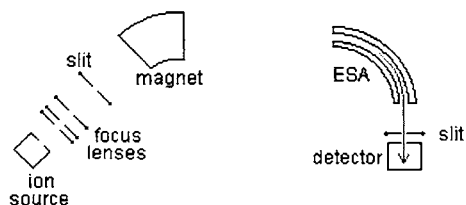


FIGURE 5.3.3. Schematics of a BE magnetic sector mass spectrometer.

In practice, typical values for the acceleration potential V are 3 to 10 kV (E is taken equal to V), and B is varied to cover a selected mass range (1 to 20000 Dalton or more). In typical scan mode, a certain mass range is chosen, and the magnetic field is cyclically swept to cover this range. This range can be chosen depending on the range of mass for the compounds of interest or to avoid the increase in background produced in the mass spectrometer by air and water. This procedure may leave undetected some low molecular weight compounds.

A typical cycle requires about 1 sec. The masses of the ions are detected with a certain resolution $m/\delta m$, where δm is the minimum difference required for two masses to be resolved. Magnetic sector instruments may work at low resolution (e.g. 1000) or at high resolution (10000 or higher). Magnetic sector systems can have excellent sensitivity ($5 \cdot 10^{-7} \text{ C } \mu\text{g}^{-1}$). Besides the scan mode, the mass spectrometers may work at a fixed m/z (or at a few selected m/z values), which is called single ion monitoring (SIM).

Quadrupole type mass spectrometers separate the ions by passing them along the central axis of four parallel equidistant rods that have a fixed voltage (DC) and an alternating (RF) voltage applied to them (see Figure 5.3.4). The field strengths (voltage) can be set such that only ions of one selected mass can pass through the quadrupole, while all other ions are deflected to strike the rods. By varying (with a precise rate) the

strength and frequencies of the electric fields, different masses can be filtered through the quadrupole. In practice, the following are typical values for the parameters of the electrical field: ω is about 1-2 MHz, $V_1 = 1000$ V, and $V_2 = 6000$ V.

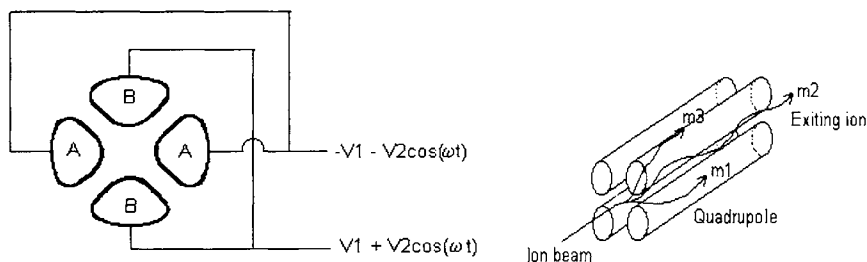


FIGURE 5.3.4. Trajectory of ions of different masses in a quadrupole with varying electric fields. The rods have a hyperbolic internal cross section exaggerated in the drawing.

With the quadrupole instruments a low-resolution type spectrum is obtained. For a $m/z = 200$ for example, the minimum mass difference of two peaks that can be separated could be around 0.2 mass units (resolution 1000). The mass range for the quadrupoles can go as high as 2000 Dalton, but common commercial quadrupole instruments have a mass range between 2 and 1000 (some only up to 650). The quadrupoles can work in both scan mode or in SIM mode.

The ion trap mass spectrometer (ITMS) consists of a hyperbolic cross-section center ring electrode (a doughnut) and two hyperbolic cross-section endcap electrodes (see Figure 5.3.5). The ion trap works also in cycles. A cycle starts with the application of a low RF amplitude and fixed frequency to the ring electrode (no DC), while the endcaps are grounded. A pulse of electrons is injected into the ion trap to ionize and fragment the gaseous sample coming from the transfer line. The ring electrode at low RF amplitude traps all the ions formed during the ionization pulse. The RF amplitude is then increased, and ions of increasing mass (in fact m/z) are sequentially ejected from the trap and detected. A key parameter to the operation is the gas pressure inside the trap (usually He), which must be maintained at 10^{-3} mbar by appropriate gas flow from the GC. This gas forces the ions toward the middle of the trap and provides a better sensitivity. A small AC voltage of fixed frequency and amplitude is also applied to the endcaps during the analysis part of the cycle. Then the process is repeated.

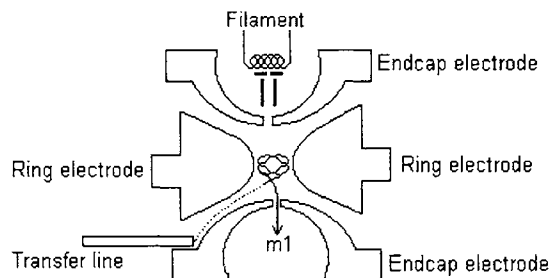


FIGURE 5.3.5. *Cross-section of an ion trap.*

The ion traps generate low-resolution mass spectra but can have very good sensitivity. Some problems have been reported regarding the similarity between the spectra generated by ion traps and other types of mass spectrometers when the concentration of a certain compound is high. For high concentration, some ion traps do not generate typical EI+ spectra.

The time-of-flight instruments (TOF) separate the ions of different m/z ratio based on the fact that the ions accelerated with a fixed potential have different velocities v . Therefore they travel a fixed distance in different amounts of time. The kinetic energy of an ion accelerated by the potential V is given by formula:

$$mv^2 / 2 = zV \quad (2)$$

and the "flight" time of this ion over a distance L is $t = L / v$ or

$$t = L m^{1/2} / (2zV)^{1/2} \quad (3)$$

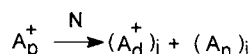
Time-of-flight spectrometers (TOF) work on scans using a pulsed ion source. The ions are sent through an electrostatic sector, which acts as a velocity filter going into a long *flight tube*. At the end of the flight tube the ions are detected based on their "arrival" time. Some TOF instruments utilize a variable accelerating potential, which allows the light ions, which are faster, to encounter a weaker field, and the heavier ions to encounter a stronger field, increasing in this way their separation. The frequency of pulses in a TOF instrument can be high, and the time of a scan can be much shorter than the time required for a cycle with a magnetic sector, quadrupole, or ion trap system. For GC/MS systems, it is useful to have more scans per chromatographic peak, and this can be better achieved using a time-of-flight spectrometer. Another advantage of TOF MS instruments is that their mass range can be very large, similar to those of magnetic sector instruments but at a lower cost.

- Ion detection.

After the separation by m/z , the ions are detected using different procedures. Two classes of detectors are known: point ion detectors, which detect the arrival of all ions sequentially at one point, and array detectors, which detect all ions simultaneously along a surface. These detectors record the number (abundance) of individual ions at each m/z . Several point ion detectors are available, such as Faraday cup, electron multiplier, and scintillator. The array detectors are commonly made of separate point detectors (of miniature dimensions) clustered together in the area exposed to the incoming ions. The array detectors have the advantage of collecting simultaneously the signal for a series of ions, but their dynamic range and sensitivity are usually lower. The signal from the detector is further processed (amplified and analyzed) by an electronic data system. Problems such as mass/time calibration, linearity of the detector response, etc. are usually transparent when using modern mass spectrometers, but they are very important in their construction. More details about the ion sources, ion optics, detectors or data processing systems of different mass spectrometers can be found in the literature dedicated to mass spectrometry [e.g. 38].

- *MS/MS systems.*

A special type of mass spectrometric system is an MS/MS (e.g. [45]). In an MS/MS system the ions are generated by any of the available procedures (common EI or CI ionizations are used). The process continues with the ion separation using one of the systems previously described. A particular ion A^+ (named parent ion) is then selected and further dissociated by collision with the molecules of a gas N (collision induced dissociation-CID or collision activated dissociation-CAD) in a reaction zone of the MS/MS system. The common reaction taking place in the CID zone can be described as follows:



The resulting A_d^+ ions (called daughter ions) are further separated in the second MS, which can be a quadrupole, magnetic sector, etc. As expected, the neutral fragments A_n cannot be seen in the second MS analysis. The fragmentation of the parent ion generates more than one daughter ion, and the fragmentation pattern is characteristic for a particular species A_p^+ .

The generation of the parent ions and the two ion analysis zones in a MS/MS system are not different from those described for standard MS systems. On the other hand, the collision zone is specific for the MS/MS systems. The parent ions resulting from the first separation zone may have high kinetic energies (KeV range), for example, when emerging from a sector instrument or may have low kinetic energy (eV range) when generated in a quadrupole instrument. These ions enter the collision zone, which can be a cell (of about 1 cm long) where the neutral collision gas is introduced (Ar, N₂, etc.). This cell is differentially pumped and can be held to a given potential. An RF-only quadrupole can also be used as a reaction region and as a focusing device at the same time. Alternative ways to CID were also investigated, such as photodissociation, electron induced dissociation, or solid surface induced dissociation of the parent ion.

A significant amount of work has been devoted to MS/MS techniques [e.g. 45], and numerous alternative procedures were proposed to perform MS/MS analysis. In particular, MS/MS analysis seems to be a possible means to reduce the need for chromatography in analyzing complex mixtures.

- *Data processing in Py-GC/MS.*

The chart showing the ion abundance versus m/z of the fragments of a compound is its mass spectrum. Usually, the abundance is normalized to the most abundant ion (base peak expressed as 100%), and it is also common that the mass peaks are shown as bar graphs (the real peaks in a mass spectrum have ideally a Gaussian shape). The mass assigned to each ion is usually expressed as an integer, although the first decimal is commonly obtained with accuracy even for low-resolution spectra. The mass spectrum can be used as a fingerprint leading to the identification of the molecular species that generated it. The fragmentation (when done in standard MS conditions) generates typical patterns that allow the identification of each compound, either based on interpretation rules or by matching it with standard spectra found in mass spectral

libraries. The development of large libraries with standard spectra (over 275,000) and of algorithms for automatic library searches made the use of these tools for spectra interpretation routine. The algorithms for automatic library searches use several criteria for evaluating the quality of a match between the unknown spectrum and a reference spectrum. One well-known algorithm is the Probability Based Matching (PBM) system. This algorithm compares the unknown with all the spectra in the library and has two characteristic features: it weights the mass peaks and performs a reverse search. The weighting of the mass peaks refers to the fact that the mass peaks corresponding to higher masses are given more importance in the search than the peaks with lower mass. This action is necessary because the larger molecular fragments have in general a lower probability of occurrence than lower mass peaks. An empirical rule shows that when dealing with a large number of spectra, the probability of appearance of m/z values have a Log (constant + normal Gaussian) distribution, as shown in Figure 5.3.6.

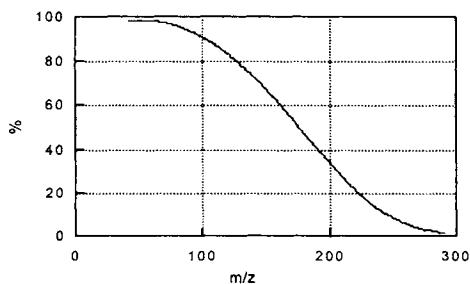


FIGURE 5.3.6. *The Log (constant + normal Gaussian) distribution of masses for a large number of spectra.*

The reverse search refers to the fact that the algorithm checks whether a peak from the reference spectrum is present in the unknown (and in the appropriate abundance) and not the other way around. In this way, the reverse search ignores peaks in the unknown that are not present in the reference. The mass library searches are, in fact, much more elaborate, and provide at the end a list of possible matches and for each of them a calculated percentage match.

The rules for explaining the fragmentation of particular structures that were developed to interpret mass spectra without the help of library searches are now more useful for choosing the correct structure from a list of possible compounds identified as candidates by the library search or for obtaining molecular information when the library search does not give a proper answer. Some spectra are, however, easier to interpret, while it is very difficult for others. In each spectrum, there are some "characteristic ions" that are diagnostic for a certain compound. The number of characteristic ions may vary. A compilation of eight peaks of mass spectra for a significant number of compounds has been published [45a]. As little as three characteristic ions are sometimes reported for compound identification. An example of an informative spectrum is that of the TMS derivative of hydroxymethylfuranboxaldehyde, which is shown in Figure 5.3.7.

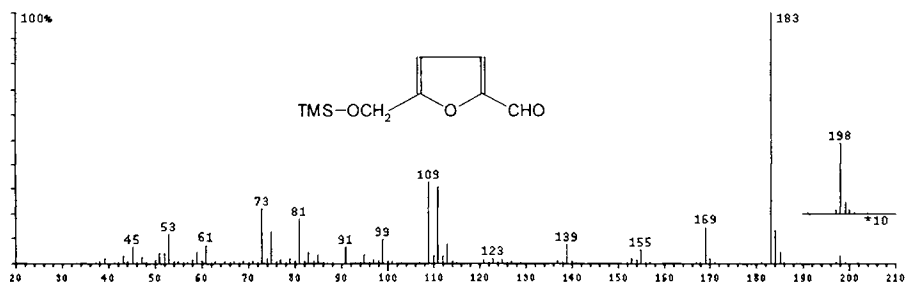


FIGURE 5.3.7. *EI* spectrum of trimethylsilyl derivative of hydroxymethylfuran-carboxaldehyde.

This spectrum shows the ion with m/z 73, which is typical (although not specific) for a TMS group. The ion with $m/z = 198$ can be assumed to be the molecular ion. The loss of a CH_3 group from TMS generating the ion $m/z - 15$ is also typical for silylated compounds. Indeed, the ion 183 is the base peak in the spectrum. The loss of the O-TMS group generating $m/z - 89 = 109$ is also present. It is clear that the compound is a silylated compound, and from the ratio of isotope intensities of ions with m/z 183/184 and 183/185, it can be concluded that it contains only one silyl group. (For each Si atom, $m/z + 1$ is 5.1% and $m/z + 2$ is 3.4% from the intensity of m/z ; for each C atom, $m/z + 1$ is 1.1% from the intensity of m/z , and $m/z + 2$ can be practically neglected.) The loss of a CHO group, which generates the ion 169, indicates an aldehyde. The ion 81 will correspond to $\text{C}_4\text{H}_3\text{O}-\text{CH}_2^+$, and it is typical for furylalkyl type compounds.

For other compounds, the spectrum is less informative. As an example, the spectrum of 1,6-anhydro- β -D-glucopyranose (levoglucosan), given in Figure 5.3.8, shows little structural features. In addition to the problem of relating a certain fragment to the original structure, some fragments are common to a large number of compounds (such as the ion with $m/z = 60$, which is common in amides, some acids, nitro compounds, etc.).

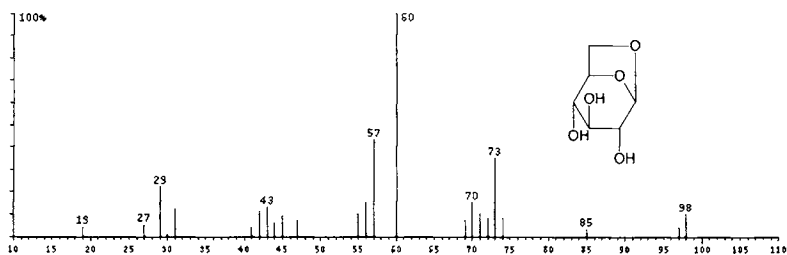


FIGURE 5.3.8. *EI* spectrum of 1,6-anhydro- β -D-glucopyranose (levoglucosan).

Spectra interpretation can also be done by utilizing additional information, such as CI spectral information for the same compound, etc. One useful procedure applied for example for the analysis of the pyrolysate of cellulose [45b] is to use derivatization with BSTFA and derivatization with d9-BSTFA. The retention times in the GC/MS trace are practically not different for the material silylated by the two reagents. However, the two spectra corresponding to one derivatized material are different, and the difference

indicates the number of trimethylsilyl groups attached ($\Delta m/z = 9$ corresponding to one TMS group). As an example, the spectrum of tri-TMS levoglucosan is shown in Figure 5.3.9, and the spectrum of tri-d₉-TMS levoglucosan is shown in Figure 5.3.10.

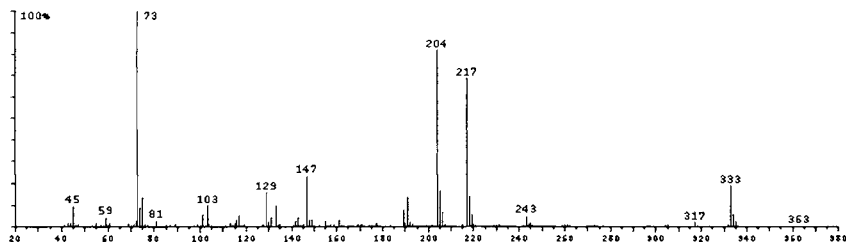


FIGURE 5.3.9. *EI* spectrum of tri-TMS levoglucosan.

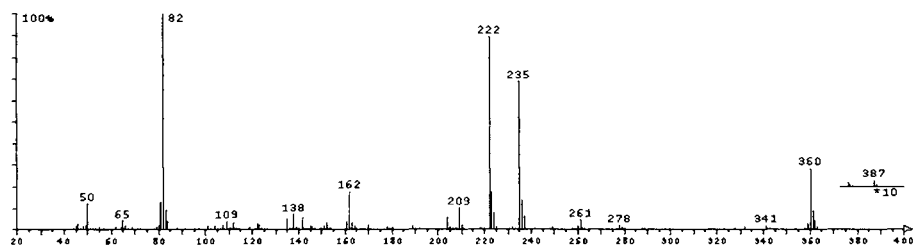


FIGURE 5.3.10. *EI* spectrum of tri-d₉-TMS levoglucosan.

The peak at $m/z = 333$ corresponds to the peak at $m/z = 360$ in the deuterated compound, indicating the presence of three TMS groups ($\Delta m/z = 27$) in the derivatized levoglucosan.

The CI MS spectra interpretation is more difficult because of the lack of fragmentation and because the reproducibility of CI spectra is more affected by the experimental conditions in which they are generated. However, CI spectra provide valuable information regarding the molecular mass, and this can be extremely useful in combination with EI spectral information. As an example, the CI spectrum of levoglucosan obtained using butane as collision gas is shown in Figure 5.3.11. The spectrum shows the ion $m/z = 163$, which corresponds to $M+1$ for levoglucosan.

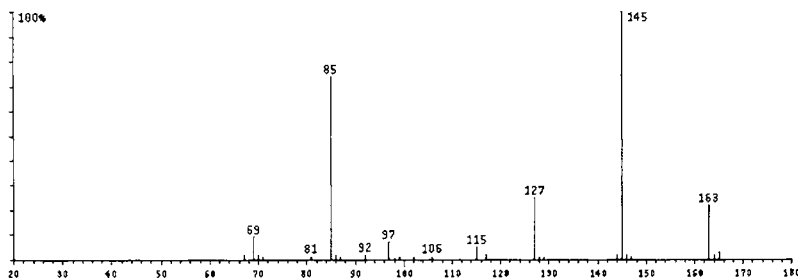


FIGURE 5.3.11. *CI* spectrum of levoglucosan (butane collision gas).

For the GC/MS, when the mass spectrometer is used as a detector during the chromatographic process in scan mode, the chromatogram can be displayed as a total ion chromatogram (TIC) or extracted (reconstructed) ion chromatogram for a specific m/z value. When the acquisition of the mass spectra has been done in SIM mode, a single ion chromatogram can be displayed.

A total ion chromatogram is a plot of the total ion count (detected and processed by the data system) as a function of time. The single ion chromatogram (extracted or SIM) plots the intensity of one ion (m/z value) as a function of time. These chromatograms have a discrete structure being made from scans (the scan number is linearly dependent of time). When the points of the chromatogram are close to each other, this gives a continuous aspect of the graph. Each scan has an associated spectrum for the TIC, and therefore the TIC has in fact a tridimensional structure. Tridimensional plots are available with certain data systems, although their practical utility is rather limited. Most data systems display the TIC and spectra for chosen scan numbers.

Figure 5.3.12 shows a small portion of the TIC for the pyrolysate of a melanoidin polymer (from the reaction of glucose and ammonia) covering the scans 2410 to 2426 and the spectra corresponding to scans 2415 to 2419. There are two compounds that generated the chromatographic peaks in Figure 5.3.12, namely 1,2-benzoxazole and 1-phenyl ethanone. Due to an incomplete chromatographic separation, scan 2417 shows a mixture of fragment ions corresponding to both compounds.

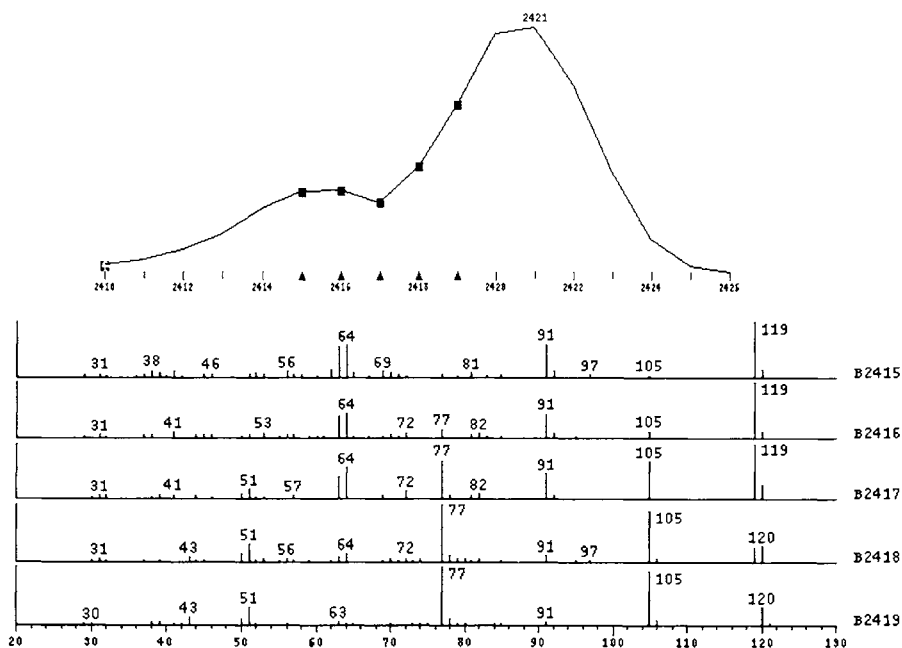


FIGURE 5.3.12. Portion of the TIC (scans 2410 to 2426) for the pyrolysate of a melanoidin polymer, and the spectra corresponding to scans 2415 to 2419. The two compounds generating the peaks are benzoxazole and 1-phenyl ethanone.

Both compounds were identified using the mass-library search. However, the spectrum for the 1-phenyl ethanone is quite diagnostic. The molecular ion corresponds to $m/z = 120$, loss of a $-CH_3$ group gives the ion with $m/z = 105$, and the loss of $-CH_3CO$ group gives the ion with $m/z = 77$, which indicates aromatic character.

The use of Py-GC/MS is frequent for both qualitative and quantitative purposes. Its use as a quantitative tool is done mainly for comparisons, but also for identifications and characterizations together with qualitative analysis. Computer programs known as target compound software are available, combining the stability of retention times in a given separation with the identification of specific compounds based on several characteristic mass ions. These software packages have the general purpose of quantitation of specific compounds in GC/MS chromatograms and can be applied to Py-GC/MS results.

Because the sensitivity of the GC/MS is exceptionally good reaching down to ppb level in a 1-mg (1- μ L) sample, the technique is irreplaceable in the analysis of complex mixtures that have some volatility. Combined with pyrolysis, it becomes an ideal tool for the analysis of non-volatile materials. Py-GC/MS allows the identification of specific compounds in pyrolysates, and numerous practical applications were reported. Typical such applications are sample comparisons, compound identification and quantitation, analysis for obtaining structural information, analysis for determining purity or for detecting impurities (contaminants) in a sample, etc.

Spectra interpretation for Cl^+ results is less standardized than for EI^+ spectra. Depending on the experimental conditions and on the specific molecule, the CI spectrum may show the molecular ion with or without some fragmentation or as clusters with the chemical ionization agent. However, CI spectra are commonly utilized for the confirmation of a specific compound. In Py-MS, where a simpler spectrum is desirable for the interpretation of the results, CI is a common ionization mode (see Section 5.4).

A different procedure to process Py-GC/MS data is to generate a sum of all spectra of all the peaks in a chromatogram [45c]. Particular peak information is lost in this technique, but characteristic cumulative spectra can be generated for different polymers. Examples of cumulative spectra for cellulose, CMC, and hydroxypropylmethyl cellulose (10% substitution with hydroxypropyl and 30% substitution with methyl) are shown in Figures 5.3.13 to 5.3.15, respectively.

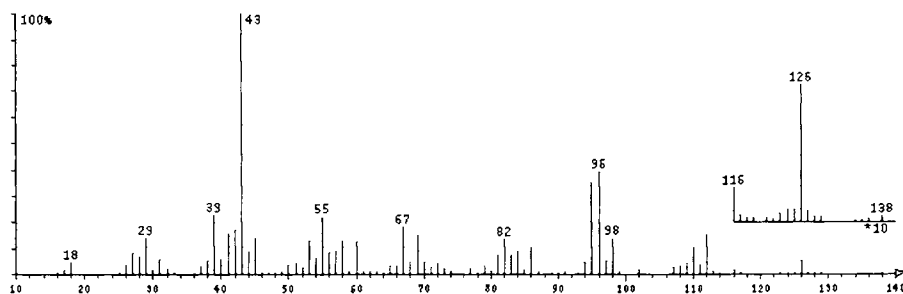


FIGURE 5.3.13. *Cumulative spectrum for cellulose.*

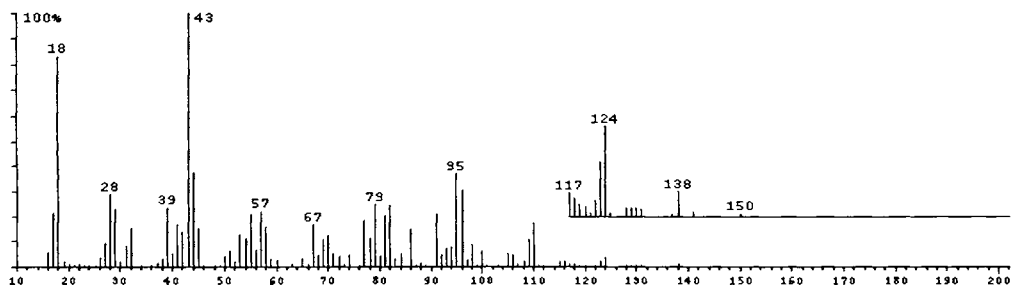


FIGURE 5.3.14. Cumulative spectrum for CMC.

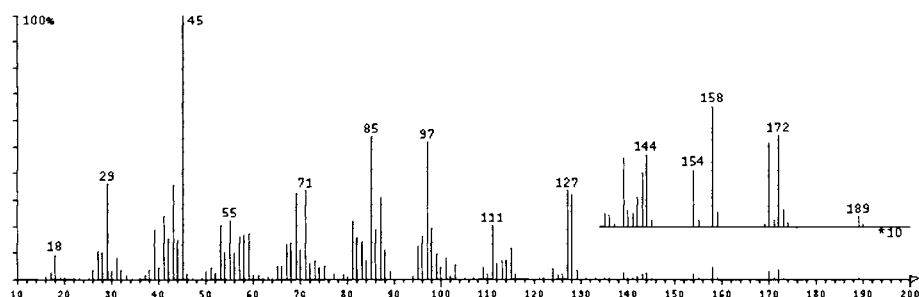


FIGURE 5.3.15. Cumulative spectrum for hydroxypropylmethyl cellulose.

These cumulative spectra provide fingerprint information, generate some structural hints such as the typical ions for furfural in the cumulative spectrum of cellulose, and seem to be quite independent of the chromatographic conditions utilized for the separation [45c]. However, they are similar to Py-MS spectra (see section 5.4) where the chromatography step is completely eliminated and the analysis time is much shorter.

The reproducibility of Py-GC/MS is also very good. Some care must be taken regarding the control of the pyrolysis process as well as in maintaining good chromatographic practices. The only possible disadvantage of this technique is the relatively long time required for the GC separation (which can reach several hours) unless fast chromatographic procedures are applied. Some examples of TIC traces generated by Py-GC/MS were already given in Section 5.2.

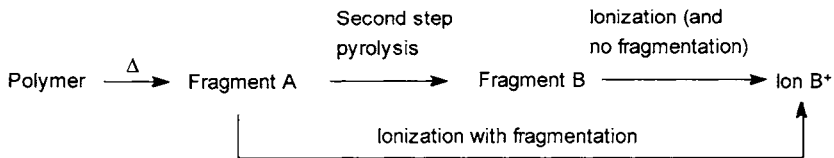
5.4. Pyrolysis - Mass Spectrometric (Py-MS) Techniques.

Historically, pyrolysis-mass spectrometry (Py-MS) was applied to the analysis of biopolymers before Py-GC [45]. However, the first application utilized an off-line setup. In time, several on-line procedures were developed and they became more common. In Py-MS the pyrolysate is directly transferred to the mass spectrometer and analyzed, generating a complex spectrum (sometimes also called a pyrogram, although this should not be confused with the chromatogram of a pyrolysate, also called pyrogram). The ionization process that takes place in the ion source of the mass spectrometer can

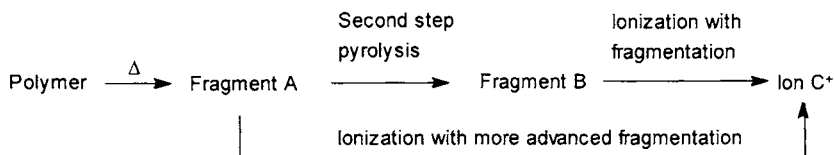
be carried out by standard ionization procedures such as EI or CI or by other special techniques (desorption ionization, etc.). In Py-MS, in addition to the decomposition of the sample by heat in the pyrolyser, the pyrolysate suffers fragmentations in the MS during the process of ion formation. The ions generated from all the fragments are detected and produce the mass spectrum. The abundance of each mass in the spectrum is the sum of the contributions of all species having charged fragments for that specific mass. This adds significant complexity to the resulting mass spectrum, which requires special interpretation that is not always straightforward.

The extreme complexity of the spectrum generated without separation by Py-MS can be estimated (for the worst case) considering that the pyrolysate contains between 20 to 400 compounds (in different proportions) and that the mass spectrum of any of these compounds can have between 15 to 40 peaks. The resulting mass spectrum of the pyrolysate without a GC separation can be the combination of 300 to 16000 contributions. For a mass range between 30 to 330 mass units, it is therefore very likely that every mass unit is generated by more than one contribution. The result is that very little molecular information can be obtained from such a spectrum and also that some averaging will take place and the resulting spectrum will not display enough characteristic features to be useful even as a diagnostic fingerprint. This problem is more obvious when trying to differentiate compounds that have similar features, such as the same monomeric unit in two polymers.

Some simplification of the previously described picture results from the fact that the fragmentation due to the ionization procedure in a mass spectrometer (such as the electron impact) may generate similar fragments as pyrolysis (see Section 3.5). Therefore some of the ions seen in the mass spectrometer are generated either by pyrolysis and not fragmented in the mass spectrometer (seen as molecular ions) or by the fragmentation of larger molecules due to the ionization alone. Schematically the process can be described as follows:



Or it is possible that the combination of pyrolysis and ionization will generate at the end the same fragments, as shown below:



In order to reduce the complexity of the Py-MS spectrum, various experimental procedures were developed. One procedure to reduce fragmentation in the MS system is the use of low energy EI ionization, where the electron beam has energies of 14–15

eV (instead of 70 eV). These energy values are only a few eV above the ionization potential of most molecules, and the fragmentation at these voltages is lower (but not absent). However, even these energies may produce too much fragmentation, and also small variations in the electron energy are reported to lead to large differences in the mass spectral fingerprints [47].

As an example, the Py-EI MS spectra of glycogen and of cellulose using an electron impact energy for ion generation in the mass spectrometer of 14 eV [47] and with pyrolysis done at 510° C are shown in Figure 5.4.1 (A) and Figure 5.4.1 (B) respectively. Glycogen is formed from polycondensed α -D-glucosyl units interconnected by α -glucosidic (1 \rightarrow 4) links and with a certain percent of branching at C-6 OH groups (it has some (1 \rightarrow 6)- α -D- links), while cellulose is a linear homopolysaccharide consisting of β -D-glucosyl units interconnected by β -glucoside (1 \rightarrow 4) links. As shown in Figures 5.4.1 (A) and 5.4.1 (B), the differences in the spectra are not major, and any structural information is difficult to obtain. Significant fragmentation may have continued after pyrolysis, and this is typical of EI spectra of numerous organic compounds containing -OH groups. The fragmentation can be strong even when the ionization is rather mild and not performed at 70 eV, which is the standard. Cellulose Py-MS spectrum shows a small 162 ion, which indicates the dehydrated glucose ($C_6H_{10}O_5$) group.

Only limited molecular information can be obtained with this technique on polymer molecules. In contrast, when a chromatographic separation is interposed between the pyrolyser and the MS, the fragmentation of each compound eluting in the MS is useful. This fragmentation (when done in standard MS conditions with ionization energy of 70 eV) generates library searchable spectra that allow the identification of many compounds.

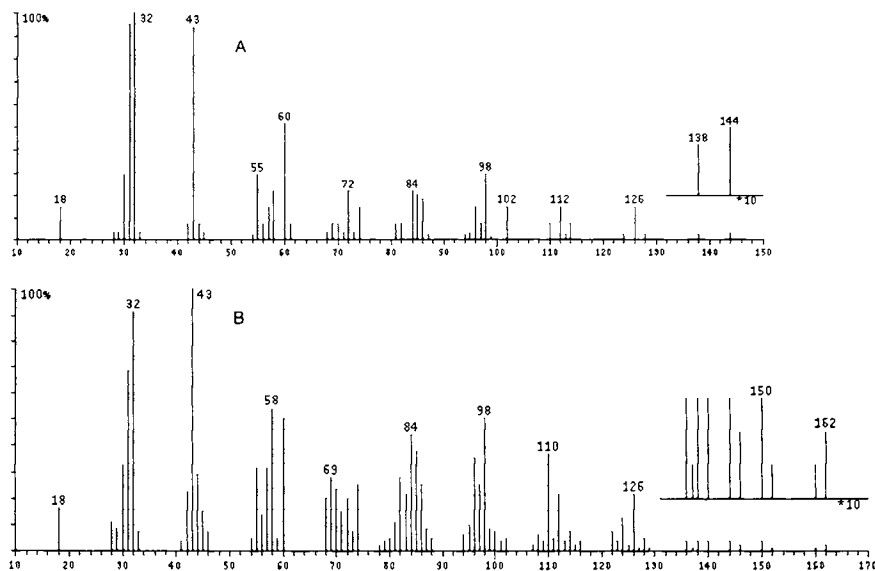


FIGURE 5.4.1. Py-EI MS spectra (14 eV electron energy) of glycogen (A) and of cellulose (B) obtained at 510° C using a Curie point pyrolyser [47].

The structural information that can be obtained from a molecule in EI type ionization differs significantly from molecule to molecule. For example, as indicated in Section 5.3, the MS spectrum of a compound such as levoglucosan is not very informative regarding the molecule structure. When levoglucosan is an important pyrolysis product, such as in the case of glycogen or cellulose, it is understandable why the Py-EI MS spectrum offers little structural information. For this reason, it was suggested that softer ionization techniques with less or no fragmentation are more appropriate for analyzing pyrolysates generated in Py-MS (with no separation).

In order to obtain even simpler MS spectra that will counteract a number of drawbacks in the common EI ionization procedures applied in Py-EI MS, several special ionization techniques were applied. One of them is CI ionization, but also field ionization (FI), field desorption (FD), and photoionization (PI) were utilized to obtain simplified mass spectra for pyrolysates. Also, MS/MS techniques were utilized for the analysis in attempts to substitute at least in part for the need of a separation.

Some success was obtained using CI ionization because this technique allows the generation of spectra containing mainly the molecular ion (usually MH^+) with little fragmentation. As an example, the Py-CI MS spectrum for cellulose using NH_3 as a collision gas is shown in Figure 5.4.2.

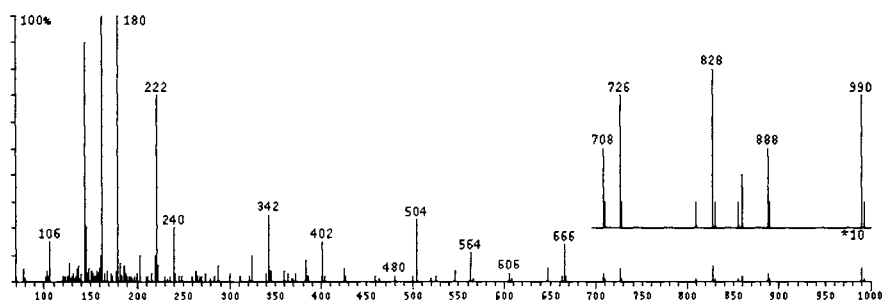


FIGURE 5.4.2. *Py-CI MS spectrum for cellulose using NH_3 as a collision gas.*

The CI spectrum shows interesting features proving the presence of oligosaccharides in the pyrolysate. Also, the ions $(162)_n + 14$ (162 corresponding to $C_6H_{10}O_5$ and 14 corresponding to NH_4) such as 180, 342, 504, 666, and 828 indicated the groups $(C_6H_{10}O_5)_n$. However, the differentiation regarding other structural features was difficult.

Py-MS has been developed as a practical technique in analytical pyrolysis because of rapid analysis and high transfer efficiency of the sample to the mass spectrometer, which can be translated into high sensitivity. Although in constant conditions the reproducibility of Py-MS is also good, a series of factors may affect the mass spectral information obtained by Py-MS. Besides the type of ionization (which certainly influences the spectra), type of instrumentation, heating rate, ion source pressure, presence of oxygen during pyrolysis, as well as typical parameters such as temperature and sample load produce significant variation in the spectral information [47a]. To these affecting factors, some others must be added, such as sample homogeneity, sample preparation, type of deposition on the heating device, as well as sample matrix. Instrumentation reproducibility determined by factors such as cleanliness of ionization

source, pyrolysate transferability and condensation on cool parts, etc. should also be considered. All these factors must be kept constant to obtain reproducible Py-MS results. Result transferability from one experimental setup to another or from laboratory to laboratory can be a problem in Py-MS if all the appropriate conditions are not maintained.

Some comparisons between Py-MS, Py-GC, and Py-GC/MS are shown in Table 5.4.1.

TABLE 5.4.1. *Some comparisons between Py-MS, Py-GC, and Py-GC/MS.*

Parameter	Py-MS	Py-GC	Py-GC/MS
Transfer efficiency	good	average (poor for some compounds)	same as Py-GC
Analysis time	short (1 min.)	long (hours)	long (hours)
Reproducibility	very good (not for direct probe)	good	good
Fingerprint capability	yes	yes	yes
Molecular information	poor	possible with standards	excellent
Quantitation	poor	good	good
Automation capability	yes	yes	yes

Two aspects of Py-MS will be discussed further:

- Pyrolysis instrumentation adapted for Py-MS studies, and
- Softer ionization MS techniques applicable to Py-MS.

In addition, special data interpretation of Py-MS results will be detailed in the next section (see Section 5.5).

- Sample preparation in Py-MS.

The sample preparation in Py-MS plays an important role in the reproducibility of this technique. Because Py-MS is used mainly as a tool for comparing samples between themselves and with standards more than as a tool for obtaining structural information, the reproducibility is of extreme importance. In most cases the sample is deposited on the heating element of the pyrolyser in a very thin layer and usually in very low amount (1–100 μg). When the sample is soluble, a solvent, which is subsequently removed, can be used to apply the sample. For insoluble samples, a liquid carrier containing the sample as a suspension is frequently utilized allowing the application of a very small amount of analyte but requiring the handling of a larger (although still small) volume of liquid. The choice of the carrier liquid depends on the sample, and water, methanol, and CS_2 are common. Sometimes a buffered solvent/carrier is used, and in these cases the pH and the ionic strength should be controlled. It was reported that a change in the carrier might influence the pattern of the Py-MS spectrum [47].

The amount of analyte used in Py-MS also may influence the reproducibility. It is therefore strongly recommended to use the same amount of sample (such as 20 μg) when reproducibility is important, although little variation was reported [47] when the sample was between 2 to 20 μg . This small amount of sample sometimes presents significant challenge, mainly in the case of non-homogeneous samples (such as plant

tissue). As indicated previously (see Section 4.1), careful sampling is a critical step in analytical pyrolysis.

- Direct probe and filament Py-MS techniques.

The simplest pyrolysis procedure used as a Py-MS technique is probably the direct (insertion) probe (into the MS). Direct insertion probe (DIP) is a common feature for mass spectrometers, used for sample introduction. The probe itself has the capability of heating and of introducing the pyrolysate directly into the ion source of the mass spectrometer. The heating of the DIP can go to temperatures of 500° C or more and can be controlled with relatively good precision. Both isothermal and gradient capabilities are commonly available. However, the heating rate of DIP systems is usually done at slow rates and is not designed for flash pyrolysis. This makes the direct probe isothermal procedure work in fact as a relatively rapid gradient, having too long TRT to be considered flash pyrolysis. Gradient direct probe can be used for the analysis of compounds that are generated (predominantly) at different temperatures from a given sample. This is a useful tool for time-resolved pyrolysis studies. The reproducibility of both procedures may vary at different instrument models, and it is not uncommon to have some problems.

Some MS systems have, besides a temperature controlled probe, a heated-filament probe. This type of probe allows a more direct heating of the sample when it is deposited directly on the filament [48]. However, most of these probes still operate within common values for the current intensity and voltage and have a TRT that is longer than those used for flash pyrolysis. True flash pyrolysis using a resistively heated filament requires boosted current or boosted voltage for achieving a rapid heating (see Section 4.3), and such systems are commercially available.

By scanning the temperature in a filament pyrolyser, the technique allows the separation of non-polymeric impurities from a polymer or composite material. Time-resolved filament pyrolysis has a series of useful applications as an analytical tool or even in some structure elucidations. As an example, it can be used [48] to differentiate the existence of more labile groups in a polymer structure. A typical variation of the total ion trace in a time-resolved pyrolysis MS for a composite material is shown in Figure 5.4.3.

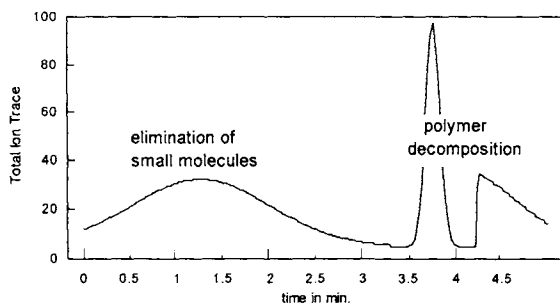


FIGURE 5.4.3. Total ion trace (TIT) of a time-resolved filament pyrolysis MS for a composite material.

The volatile components or the labile groups from a polymer will be released at lower temperatures (or at the beginning of the heating time), while the polymer backbone will decompose at higher temperatures. Each point in the total ion trace (TIT) has an associated mass spectrum that allows the characterization of this process. Thermal analysis (TA) associated with the MS analysis of the evolving pyrolysates is a useful tool for polymer analysis, but the main focus in this process is not related to an actual pyrolysis.

Once transferred to the ion source of the mass spectrometer, the pyrolysate must be ionized. The ionization procedure can be done either by EI or CI or by using softer ionization techniques with less or no fragmentation. Without a GC separation, when using hard ionization techniques, the chemical composition of the pyrolysate for polymers is difficult to determine, and the mass spectrum is utilized mainly as a fingerprint. However, DIP with CI ionization (Py-DCl MS) was successfully utilized for the analysis of several polymeric carbohydrates [48a] with the possibility of making meaningful assignments of the fragments containing two monosaccharide residues.

- *Curie point Py-MS technique.*

The need for flash pyrolysis-MS led to the construction of MS systems having a Curie point pyrolyser included as a sample introduction capability. The characteristics of a Curie point pyrolyser were already discussed (see Section 4.2), and this type of system is capable of heating the sample to a stable temperature with very short TRT values. The cooling in vacuum, however, is not as quick as in a stream of helium. For this reason, differences may be seen between common Curie point pyrolysis and the one attached to an MS system that works in high vacuum. An additional feature of the Curie point Py-MS systems is the need for an expansion chamber. The pyrolytic process generates gases, and these are released in a burst. This may alter the vacuum in the MS system, and for this reason the expansion chamber is needed. A schematic diagram of a Curie point Py-MS system is shown in Figure 5.4.4.

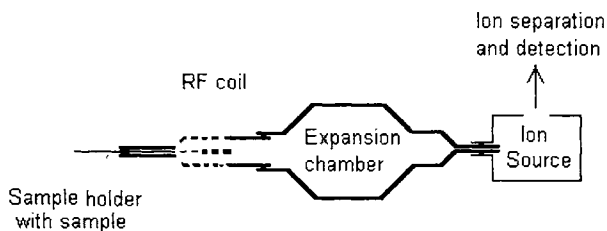


FIGURE 5.4.4. *Schematic diagram of a Curie point Py-MS system.*

The walls of the expansion chamber as well as those of the RF region must be inert (glass or gold-coated), and the expansion chamber should be heated (at moderate temperatures 150–200° C) to reduce condensation. Common problems for this type of pyrolyser are condensations on the cool portion of the system. On the other hand, heating the walls of the sample region (with resistors) may generate decomposition of the sample before pyrolysis. Also, the expansion chamber extends the time for the sample to be introduced in the mass spectrometer ion source and therefore the time

available for MS analysis. In this way, more than a few scans can be taken by the MS system acquiring the corresponding spectra for the sample. Also, the expansion chamber maintains a certain pressure during pyrolysis such that the results are closer to a Curie point pyrolysis performed in an inert gas atmosphere. Several experimental designs have been described for adjusting the TRT time in a Curie point Py-MS system or for modifying the temperature (or volume) of the expansion chamber. By modifying the TRT to values as long as 1.5 s by attenuating the RF power, time-resolved studies were done with Curie point pyrolysers [49]. These time-resolved studies are useful for the study of thermal stability of certain polymers and also for simplifying the composition of the pyrolysate generated at a certain temperature (point in time during the heating of the sample).

A different approach in using Curie point Py-MS is to remove the expansion chamber and to use samples of extremely small size in order not to affect the vacuum. Although this does not seem to be a radical difference compared to the expansion chamber design, high-vacuum pyrolysis [50] takes place in these conditions. In high-vacuum pyrolysis, intermolecular collisions are significantly diminished, and experiments done with small molecules [51] showed that in this experimental setup the intermolecular reactions between pyrolysis fragments are eliminated. The number of scans acquired using this technique is lower than in the case of using the expansion chamber.

- Laser Py-MS techniques.

Lasers have been used as a source of energy for pyrolysis, and several experimental systems were described in Section 4.5. The main use of lasers in mass spectral analysis is associated with several desorption techniques where the pyrolysis is an undesired process. However, laser pyrolysis is also used in direct coupling with an MS system, and a schematic diagram of a laser Py-MS system is shown in Figure 5.4.5.

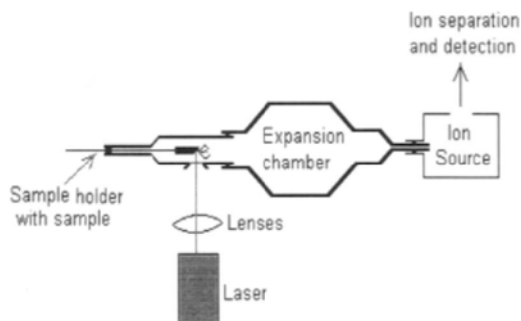


FIGURE 5.4.5. Schematic diagram of a laser Py-MS system.

Similarly to Curie point Py-MS, the expansion chamber may be needed for buffering the emission of the pyrolysate and for allowing a longer time for the MS to acquire scans (spectra). Different types of lasers, combinations of lasers, or other experimental setups were reported [52, 53] as utilized in Py-MS.

The processes taking place in laser Py-MS are not well characterized because more than one effect may happen when the sample is irradiated with the laser beam—laser induced desorption (LID), melting, pyrolysis, ionization, etc. These processes depend on the laser intensity and energy (wavelength) and on the substrate and sample composition. Also, the vacuum in the MS system may play a role regarding the result of irradiation by diminishing any secondary reactions of the pyrolysate.

For example, microprobe analysis of complex samples (laser microprobe mass analysis LAMMA) was performed by using a setup with no expansion chamber and by focusing the laser beam on a small area on the surface of the sample. Although coal and shale samples were successfully analyzed using LAMMA [52], the nature of the bonding in these types of materials cannot be evaluated because it is not clear if a certain compound is the result of desorption or of pyrolysis. More successfully analyzed were the inorganic components of such composite materials where the thermal decomposition was not a concern.

As indicated previously, one problem in Py-MS is the complexity of the generated spectrum and the impossibility of determining if a given mass in the spectrum is a molecular ion from a fragment generated by pyrolysis or is a fragment ion generated by the ionization process in the MS. An interesting method of differentiating between the two types of fragments was reported [54, 55]. This can be achieved with a technique using a modulated molecular beam. In this technique, the molecules that are vaporized with the laser are sent as a molecular beam to the ionization chamber of a mass spectrometer. However, this molecular beam is mechanically chopped before ionization, and phase spectrometry is used for the analysis. A schematic of the instrumentation is shown in Figure 5.4.6.

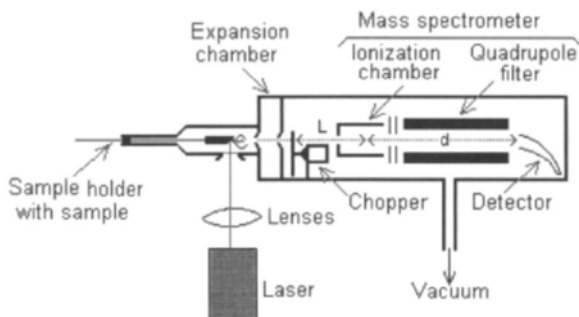


FIGURE 5.4.6. Schematic diagram of a laser Py-MS system using a modulated molecular beam.

If a standard synchronous detection technique is used, the unmodulated background can be subtracted from the signal generated by the molecular beam. Some differentiation can also be made between the fragments generated during pyrolysis and fragments formed in the ionization chamber. For this purpose, it should be noted that the flight time of the neutral molecules t_n between the chopper and the ionization point is

$$t_n = L / v_n \quad (1)$$

and the transit time for the ions through the mass analyzer t_i is

$$t_i = d / v_i \quad (2)$$

In rel. (1) and (2) L is the distance from the chopper to the ionization point, v_n is the velocity of the molecules, d is the length of the ion path, and v_i ion velocity (see Figure 5.4.7). If ω is the modulation frequency of the chopper, then the phase of the ion signal (in deg.) for the system is given by

$$\phi = \omega (t_n + t_i) = \omega (L / v_n + d / v_i) \quad (3)$$

The inverse velocities for both neutral and ionic species can be estimated as being proportional with the square root of the mass of the given particle, or

$$1 / v_n \approx A' (m_n)^{1/2} \quad \text{and} \quad 1 / v_i \approx B' (m_i)^{1/2} \quad (4)$$

This leads to the relation:

$$\phi = A (m_n)^{1/2} + B (m_i)^{1/2} \quad (5)$$

where A and B are some appropriate constants. Since for the molecular ions $m_n = m_i$, but $m_n > m_i$ for fragment ions, for a given m_i/z value (only the ions are detected), a larger ϕ will correspond to a fragment ion compared to a molecular ion (because that ion has a larger associated m_n).

For a series of molecular ions where $m_n = m_i$, a plot of the ion signal phase (in deg.) as a function of $(m_i)^{1/2}$ for different m_i values will show a linear dependence. For a series of ions generated from the same parent molecule, the value of $(m_n)^{1/2}$ in rel. (5) is a constant, and the plot of the ion signal phase as a function of $(m_i)^{1/2}$ will also show a linear dependence but of a different slope. The slope for molecular ions will be $A + B$, while the slope for fragments will be B with the intercept $A m_n$. Plots as shown in Figure 5.4.7 will be generated. Using a plot of the type shown in Figure 5.4.7, it is possible to differentiate parent ions, which are assumed to be generated during pyrolysis, from fragment ions that are generated during the ionization process. Although this technique looks promising, very few results were reported [54, 55], possibly due to experimental difficulties in measuring ion signal phase.

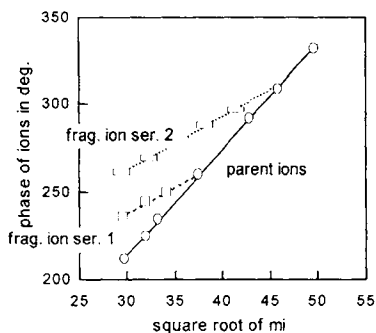


FIGURE 5.4.7. Dependence of the ion signal phase ϕ on $(m_i)^{1/2}$ for molecular ions and for fragment ions.

- Field ionization (FI) and field desorption (FD) techniques used in Py-MS.

Electron impact (EI) and chemical ionization (CI) techniques are commonly utilized as ionization techniques for Py-GC/MS as well as for Py-MS. However, when the pyrolysate is a complex mixture, the use of EI as an ionization technique generates a spectrum that is usually too complex. One ionization technique helping with the data interpretation is CI, which commonly generates much simpler spectra than EI. Besides MH^+ ions (see Section 5.3), the CI ionization may also produce some fragmentation (for example when the pressure of the reagent gas is not high enough) or may generate some cluster ions. For example, when CH_4 is used as reagent gas, besides the quasimolecular ion $M+1$ (corresponding to MH^+), ions with masses $M+29$ or $M+41$ can be seen. Nevertheless, the total spectrum of a pyrolysate obtained by Py-MS analysis with CI ionization will still be simpler and sometimes easier to interpret and utilize than EI spectra.

A different ionization technique sometimes utilized to generate ions in Py-MS is field ionization (FI). Field ionization is a very mild ionization technique that generates M^+ or M^- ions from molecules M with low or no fragmentation. This technique consists of placing the compound of interest in an intense electric field. This electric field is created by applying a large electric potential (8–10 kV) between a wire covered with extremely sharp micro-needles (whiskers) and a planar electrode, which also has an exit slit for the ions. The micro-needles can be obtained, for example, by decomposing benzonitrile on a hot tungsten wire. A high charge density is generated at the tip of the micro-needles, and subsequently an intense electrical field (with a gradient of about 10^8 V cm^{-1}) is generated. The intensity of an electric field of a conductor is numerically equal to the variation of the potential per unit of length considered in the direction of the normal n to the equipotential surface. In other words:

$$E = - \lim_{\Delta n \rightarrow 0} \frac{\Delta V}{\Delta n} = - \frac{dV}{dn} \quad (6)$$

For a conductor (at constant potential) with sharp protrusions, the variation of the derivative in rel. (6) may take large values generating a high electric field. The ionization takes place when electrons are transferred from the molecules (in positive potential) or to the molecules (in negative potential) via a process called quantum tunneling, generating M^+ or M^- ions respectively. The process takes place with very little vibrational excitation from the electric field, and therefore few or no fragment ions are generated. The ions formed by FI are ejected to the ion separation/detection system of the mass spectrometer. Several studies were reported with the use of Py-FI MS of certain biological materials [56-58]. The disadvantages of Py-FI MS are related to common problems in Py-MS such as condensations and losses of the labile fragments. A schematic diagram of a Curie point pyrolysis system with field ionization is shown in Figure 5.4.8.

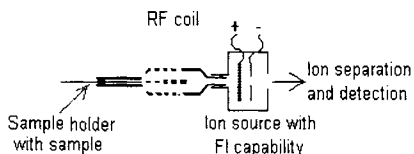


FIGURE 5.4.8. Schematic diagram of a Curie point pyrolysis system for sub-microgram quantities of sample, with field ionization in the MS ion source.

When the sample is directly deposited on the wire covered with the micro-needles, a desorption of the ions formed from the deposited compounds may take place, and the process is called field desorption (FD) [59]. The FD process can be associated with the heating of the wire holding the sample, which is in very low amount (~ 10 ng), and pyrolysis of the material can be achieved simultaneously with the desorption process. In addition to the low amount of sample, the high vacuum and the intense electric field cause this process to lack secondary pyrolysis effects. The Py-FD MS generates mainly molecular ions (or $M+1$ ions) from the primary pyrolysis products, and it can be more informative than other Py-MS techniques. As a comparison, the Py-FI MS spectrum of glycogen with the pyrolysis done by Curie point heating system at 770°C and its Py-FD MS spectrum [1] are shown in Figures 5.4.9 (A) and (B) respectively. The spectrum shown in Figure 5.4.9 (A) for Py-FI MS of glycogen is in fact not completely different from the one shown in Figure 5.4.1 (A) obtained using Py-EI MS.

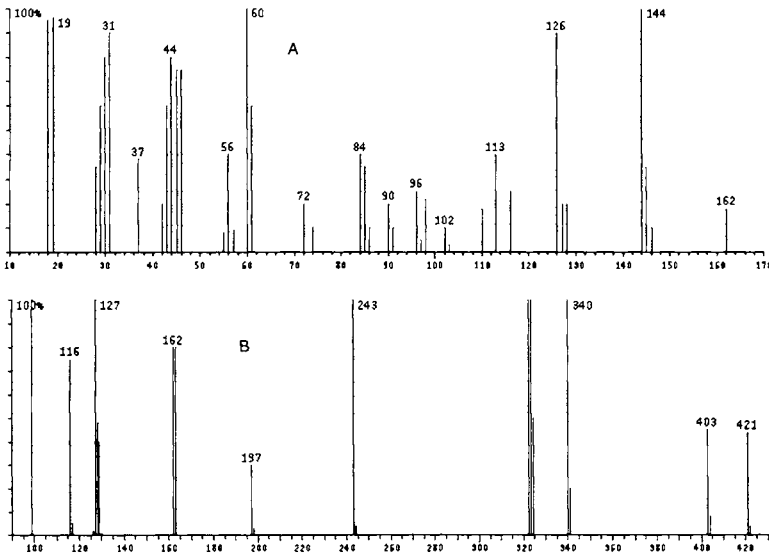


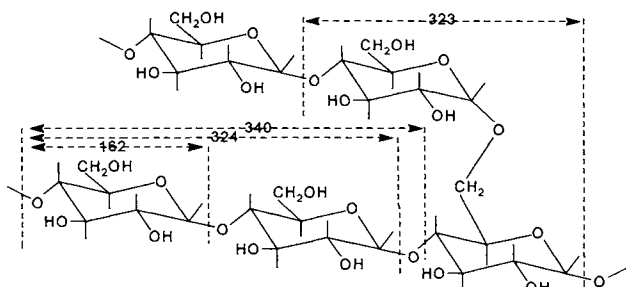
FIGURE 5.4.9. *Py-FI MS spectrum of glycogen (A) and Py-FD MS spectrum of glycogen (B).*

On the other hand, Py-FI MS spectrum is known to generate little fragmentation, and therefore the fragments seen in this spectrum come mainly due to pyrolysis (not because of the ionization) and they can be assigned to specific compounds [57]. Based on this information, some ion assignments can be done as seen in Table 5.4.2.

TABLE 5.4.2. Ions seen in Py FI MS spectrum of glycogen and their assignment [57].

Ion	Ion type	Compound assigned
18	M	water
19	M+1	water
28	M	CO, ethane
29	fragment	CHO
30	M	formaldehyde
31	M+1	formaldehyde
42	M	ketene, propene
43	M+1	ketene
44	M	acetaldehyde
45	M+1	acetaldehyde
46	M	formic acid
55	fragment	C3H3O
56	M	acrolein
57	fragment	C4H7 ?
60	M	hydroxyacetaldehyde
61	M+1	hydroxyacetaldehyde
72	M	pyruvaldehyde
74	M	hydroxypropanone
84	?	
85	?	
86	M	butandione
90	M	glyceraldehyde
91	M+1	glyceraldehyde
96	M	furancarboxaldehyde
97	M+1	furancarboxaldehyde
98	M	furfuryl alcohol
102	?	
103	?	
110	M	methylfurancarboxaldehyde
113	?	
116	?	
126	M	levoglucosenone
127	M+1	levoglucosenone
128	M	1,6-anhydro-3-deoxy-β-D-threo-hex-3-enopyranose
144	M	1,4:3,6-dianhydro-α-D-glucopyranose
145	M+1	1,4:3,6-dianhydro-α-D-glucopyranose
146	?	
162	M	levoglucosan

Even less fragmentation can be seen in the Py-FD MS spectrum (Figure 5.4.9 (B)), which indicates clearly the fragments $C_6H_{10}O_5$ MW = 162, $C_{12}H_{19}O_{10}$ MW = 323, $C_{12}H_{20}O_{10}$ MW = 324, etc. This is due to the low temperature of the desorption process. Some possible fragmentations are shown below:



Part of the cause of showing large fragments in Py-FD MS is the soft ionization. However, pyrolysis conditions as well as transfer efficiency of larger molecules into the ionization chamber play an important role in explaining this result. HPLC studies of pyrolysis products of polymeric carbohydrates such as cellulose obtained at temperatures around 500° C indicated the presence of anhydrocellobiose (C₁₂H₂₀O₁₀, 4-O-β-glucopyranosyl-1,6-anhydroglucose) as well as other anhydrocello-n-oses (n = 3, 4, 5, 6) [60] in the pyrolysate. This shows that these compounds may be present even if the pyrolysis is performed at relatively high temperatures. Also the EI or FI ionization can be done for large molecules. At the same time lack of volatility and condensation on cold spots of the polar, larger molecules is a common effect seen in pyrolysis, and this may explain the absence of the ions corresponding to these large pyrolysate components in the Py-EI or Py-FI MS spectra.

- Photoionization used in Py-MS.

Photoionization is not a common technique in mass spectrometry, but it was reported to be utilized for both Py-GC/MS [61, 62] and for Py-MS [61]. Compared to EI spectra, for which extended mass spectral libraries are available, the photoionization (PI) spectra are not standard and therefore not library searchable. However, the ionization being softer, the molecular ion is commonly more intense providing additional information in certain cases when the EI mass spectrum is not diagnostic.

A photoionization system usually consists of a windowless, differentially pumped rare gas resonance lamp coupled with the ionization chamber of the mass spectrometer. Argon, krypton, or other inert gases are used in the lamp. Energies of 11.6 and 11.8 (Ar I) eV are produced by argon, and 10.0 and 10.6 (Kr I) eV for krypton. The pressure inside the ion source is usually about 10⁻² Torr.

The technique has some few advantages over EI because of the perfectly stable energies the lamps can emit. Although the ionization efficiency obtained at higher energies is much lower than that of EI, photoionization is efficient at low ionization energies. Different photon energies are available by use of different rare gases in the resonance lamp. Also, while the EI ionization cross-section of molecules rises approximately linearly from a certain threshold to higher energies, photoionization cross-sections show a more step-function type behavior. This allows selective detection of classes of compounds depending on their ionization potentials, as well as fragmentation reduction by choosing a photon energy close to the ionization threshold of the compound of interest.

As an example, in the case of Py-GC/MS of amylose (formed from α -D-glycosyl units interconnected by α -glucosidic (1 \rightarrow 4) links) [61], it was found that Kr I radiation leads to more pronounced molecular ions than Ar I for compounds such as levoglucosenone, 5-hydroxy-2-furaldehyde, 1,4-dideoxy-D-glycero-hex-1-enopyranos-3-ulose and levoglucosan. The Kr I mass spectra of the first three compounds showed a substantial reduction in formation of fragment ions relative to the molecular ion in comparison to the Ar I spectra and to spectra obtained at 14 eV by electron impact. The photoionization (PI) spectra obtained with Ar I radiation are similar to the low-voltage EI spectra and contain enough fragment ions for comparison with existing libraries of EI spectra at higher energies. When used in a Py-GC/MS system, the choice of different ionization energies adds the ionization potential as a third dimension to the GC MS analysis of the pyrolysate. (Other experimental parameters such as the ion source temperature may play a role in the mass spectra generated by PI.)

The Py-MS applications of PI are still rather limited. The intensity of molecular ions in the spectra is higher, but fragmentation still takes place. As an example, comparison between different spectra of amylose is shown in Figures 5.4.10 (A) to 5.4.10 (C). Figure 5.4.10 (A) displays the low-voltage (14 eV) EI mass spectrum (pyrolyser-mass spectrometer equipped with expansion chamber) for amylose analyzed from a sodium phosphate buffer matrix using a Curie-point temperature of 510 $^{\circ}$ C. The spectra for the same sample (amylose pyrolysate) and the Ar I and Kr I PI spectra are shown in Figures 5.4.10 (B) and 5.4.10 (C).

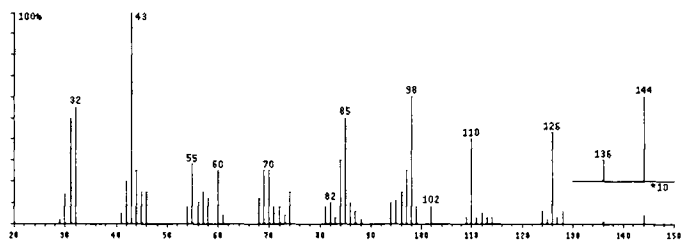


FIGURE 5.4.10 (A). *Py-EI MS spectrum at 14 eV electron energy of amylose.*

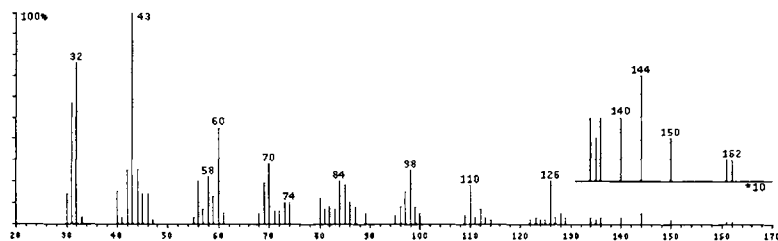


FIGURE 5.4.10 (B). *Cumulative Py-GC/PI MS spectrum using Ar I for amylose.*

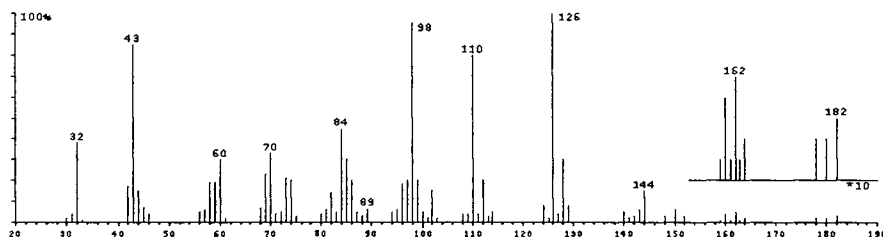


FIGURE 5.4.10 (C). Cumulative Py-GC/PI MS spectrum using Kr I for amylose.

These spectra are in fact cumulative spectra from Py-GC/MS, but they are a close equivalent to Py-MS spectra. As seen in Figures 5.4.10 (A), (B), and (C), except for the intensities of the ions, the fragments seen in the pyrolysate are not too different. In fact, the EI spectrum and Ar I PI spectrum of amylose are quite similar, and only the Kr I PI spectrum shows differences.

- Other techniques used in MS and their relation to pyrolysis.

Besides EI, CI, FI or FD techniques for generating ions in the mass spectrometer, some other ionization techniques have been reported. One such technique is metastable atom bombardment (MAB), which is based on Penning ionization. In MAB a metastable ion beam generated outside the ion volume is used to bombard the sample. The energy available for ionization is discrete (quantified) and can be fixed by the choice of the rare gas used in the atom gun (He, Ne, Ar, Kr, Xe). This energy ranges from 8 to 20 eV. Use of an appropriate rare gas allows the control of the internal energy transferred to the ions formed, and fragmentation can be diminished or made more significant. By eliminating extensive fragmentation during ion formation, MAB can be used in connection with Py-MS. MAB can also be used in combination with MS/MS analysis of the pyrolysates.

Another MS technique used in connection to pyrolysis is MIMS (membrane introduction mass spectrometry). MIMS is in fact a special inlet for the mass spectrometer, where a membrane (usually silicone, non-polar) lets only certain molecule types enter the ionization chamber of the MS. This allows, for example, direct analysis of certain volatile organic compounds from air. The system makes possible the coupling of atmospheric pyrolysis to a mass spectrometer [61a] allowing direct sampling of the pyrolysate. Other parts of the mass spectrometer do not need to be changed when using MIMS.

Some other techniques are oriented toward the analysis of large molecules, but fragmentation is not a desired objective. However, molecular cleavage may take place during the process of energy transfer to the sample, and this can be related to a pyrolytic process. Because of this association with pyrolysis, some of these techniques will be mentioned. For example, as indicated previously, lasers can be used to produce sample pyrolysis, which can be followed by mass spectral analysis of the resulting fragments. When using a laser, it was shown that if the energy transferred to the molecule is sufficiently high, the energy cannot be dissipated fast enough and the large molecules pyrolyse generating fragments (small stable molecules may melt and vaporize). From these fragments, some electrons can be ejected to form ions that are

further analyzed in the MS. However, the pyrolytic process is sometimes undesirable, especially when molecular information is needed. The reduction of pyrolysis effects, while maintaining the capability of desorption and ion formation from a certain analyte, can be achieved by using a special matrix for the sample and laser pulses for a very short period of time. This technique is called MALDI (matrix assisted laser desorption ionization). Commonly sinapic acid (3,5-dimethoxy-4-hydroxycinnamic acid) or nicotinic acid is used as matrix material for the sample. Also, the lasers that are typically used are tunable lasers emitting in either ultraviolet or infrared where most molecules absorb radiation. Large molecules such as proteins are analyzed using MALDI, and molecules with masses up to 1,000,000 Dalton were reported to be desorbed by this technique [63]. An appropriate MS system (usually TOF) also needs to be utilized for the detection of large masses. Through certain adjustments such as the choice of the matrix, the wavelength of the laser, or the pulse time, the laser energy can be used in MALDI mainly for providing the energy needed for the desorption of molecules, diminishing the pyrolysis as much as possible. This can be realized based on the fact that the absorption of the laser energy depends on the laser wavelength and the absorption spectrum of the matrix. In this way, the analyte molecules do not absorb directly the laser energy.

The theory of a simple thermoionic process [64] has been adapted to find the number of desorbed particles from a given surface covered with an organic layer that does not absorb the laser energy. However, the heat flux in the substrate, which absorbs the energy, heats the sample to the same temperature as the substrate. This number N is given by relation:

$$N = 2\pi C n^l \int_0^{\infty} \int_0^{\infty} \exp[-\Delta E / k T(r,t)] r dr dt \quad (7)$$

where

$$T(r,t) = T_0 + \Delta T(r,t) \quad (8)$$

where C is a constant, n is the number of particles per unit area, l is the reaction order in a Polanyi-Wigner model of desorption [65], k is the Boltzmann constant ($k = 13.805 \cdot 10^{-24} \text{ J deg}^{-1}$), T is expressed in deg. Kelvin, ΔE is the desorption energy, and $\Delta T(r,t)$ is given by rel. (3), Section 4.5. Rel. (7) can be approximated by

$$N = A \exp(-\Delta E^* / k T_{\max}) \quad (9)$$

where A is a constant, ΔE^* is the effective desorption energy, which has a value within $\pm 20\%$ from the theoretical ΔE (ΔE can be in the range of 0.1 to 1 eV, which is equivalent with $1.60218 \cdot 10^{-20}$ to $1.60218 \cdot 10^{-19} \text{ J}$). Figure 5.4.11 shows the variation of $\exp(-\Delta E^* / k T)$ as a function of $T^\circ \text{C}$ for $\Delta E^* = 0.25 \text{ eV}$ (curve A) and for $\Delta E^* = 0.5 \text{ eV}$ (curve B).

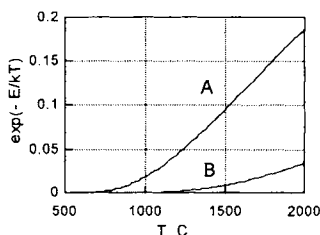


FIGURE 5.4.11. The variation of $\exp(-\Delta E^* / k T)$ as a function of $T^\circ \text{C}$ for $\Delta E^* = 0.25 \text{ eV}$ (curve A) and for $\Delta E^* = 0.5 \text{ eV}$ (curve B).

By modifying the laser wavelength (and intensity) or using a second laser, a photoionization process may be included (LPI) to generate ions from the analyte that will be further separated and detected in the mass spectrometer. When the ion formation from the plume of the first laser is low, some other secondary ionization techniques such as CI can also be used.

There are other MS ionization techniques applied to analyze pyrolysates such as secondary ion mass spectrometry (SIMS) [66], californium plasma desorption [67], or fast atom bombardment (FAB) [68].

In SIMS, accelerated ions bombard the sample, commonly put in a liquid matrix (LSIMS). The process may generate heat and thermal fragmentation when applied to larger molecules. Similar processes take place in FAB, where the source of energy consists of accelerated atoms, or in californium plasma. Ionization techniques working at very high temperatures (glow discharge and inductively coupled plasma) are also known, but they are used for elemental analysis, being able to generate ions for all metal atoms and for some nonmetallic ones that could be present in the sample.

5.5. Data Interpretation in Pyrolysis - Mass Spectrometry (Py-MS).

Data analysis in Py-MS is utilized for both qualitative and quantitative purposes. It is done for a variety of purposes such as sample classification for taxonomic purposes, study of complex biological samples for the estimation of pathologic modifications (clinical applications), chemical interpretation of sample differences in soil humic compounds and in fossil biomaterials, fermentation monitoring, etc. Some of this work required only qualitative differentiation between samples, and therefore notable effort was done for enhancing the capability of recognizing results with significant differences from those displaying only random fluctuations. Quantitative evaluations were also possible through statistical data analysis for the determination of the level of particular constituents in complex mixtures.

Data processing in Py-MS evolved in a special manner because the pyrolysis component and MS component are integral parts of a unique technique. This is different from the case of Py-GC and Py-GC/MS where the pyrolysis side can be considered just a convenient way to process the sample for analysis. Py-MS also has specific applications, having been proven to be an excellent tool for comparison of biopolymer samples and composite materials, but less useful for obtaining structural information or for studying the presence of impurities in a polymer.

Collections of Py-MS spectra were published [47], and also specific interpretation techniques were adapted to process Py-MS data, mainly developed for providing pertinent comparisons. Most techniques are oriented toward comparing multi-component fingerprint information. Therefore, the stability of the results (reproducibility) is an important quality that must be maintained when performing Py-MS work. It was shown [47] that variability of 1–3% in peak intensities can be noticed for replicates within 1 day of work and up to 10–11% in long term (one month).

A typical multivariate set of data is generated when performing Py-MS. Each Py-MS trace is formed from a considerable number of peaks and each peak can be considered a measurable variable. The results from a set of samples to be evaluated by considering all these variables will generate a typical *data matrix*. The data matrix can be studied using *multivariate* data analysis. However, simple *univariate* data analysis can be applicable by selecting for analysis one single m/z value.

- *Data pretreatment in Py-MS.*

One goal in comparing complex samples is to eliminate any possible sources of variation except for the nature of the sample. This can be done by carefully evaluating the sources of fluctuation in reproducibility of Py-MS data of replicate samples and trying to eliminate them. One such source is the variation in the sample size. The low amount of sample (such as 2 to 20 μg) utilized in Py-MS is not easy to apply consistently. Another problem can be the instrument sensitivity, which may drift in time. These problems should be reduced as much as possible by controlling the experimental setup. If they still occur, they may be somewhat compensated by expressing the mass peaks as normalized to the base peak. This is common in mass spectrometry (base peak is always taken 100%). When all mass peaks are more intense (or less intense) proportionally from replicate to replicate, the normalization to the base peak excludes, in part, sample loading fluctuations or the drift in the MS sensitivity. If the peak intensities are expressed in counts, the intensity of each mass can be normalized by the sum of the counts of all peaks in the spectrum using the formula:

$$x_i = I_i / \sum I_i \quad (1)$$

or by a chosen peak (such as the base peak) using formula:

$$x_i = I_i / I_B \quad (2)$$

If an internal standard with a peculiar peak at a m/z value uncommon for any other component in the pyrolysate is present, the normalization can be done with this peak using rel. (2) where I_B is replaced by the intensity of the standard.

Another problem that should be taken into consideration before starting comparisons in Py-MS is the selection of appropriate peaks to be processed. Some mass peaks are common to numerous compounds, and their selection for comparison may diminish the chances of an appropriate differentiation. By inspecting, for example, the spectra for glycogen and cellulose shown in Figures 5.4.1 (A) and (B), it can be seen that by selecting the peaks with m/z = 18, 32, 43, 60, 72, 126, 144 for a comparison, the result will be that the two spectra are similar. On the contrary, by selecting the peaks with m/z = 58, 69, 82, 96, 110, 124, 162, significant differences can be noticed between the spectra. Sometimes, peaks with structural significance (as opposed to fingerprint significance only) may be chosen for spectra comparison. If these peaks can be recognized in the Py-MS trace, they may provide more information in a comparison than simple fingerprint peaks. Peaks with larger fluctuations in replicates should be excluded in order to achieve pertinent comparisons. Such peaks may lead to false results indicating differences between samples when the samples are in fact identical or similar. This shows that an estimation of the variability between replicates of Py-MS results can

be very useful. A variety of possibilities for this estimation will be further discussed, but a simple estimation can be done for any one particular mass peak using simple error analysis procedures.

Based on the peak differentiation, as discussed previously, each peak in the Py-MS pyrogram can be selected for a different normalization. Proper normalization of the spectrum intensities is of crucial importance. Two types of normalization have been applied: pattern scaling and feature scaling. Pattern scaling is performed to compensate for overall variations in ion intensities caused by sample size or instrument sensitivity, and this may not be necessary if the system automatically takes the largest peak as 100% and the others are normalized accordingly. However, a very few large peaks sometimes vary more significantly from sample to sample, and they can be eliminated before normalizing the rest of the peaks to the remaining base peak. Feature scaling consists of scaling the relative intensity of selected peaks, for example to enhance the weight of the characteristic part of the pyrolysis patterns. This normalization procedure can be carried out in an iterative manner using computer programs. The normalized data can then be analyzed by multivariate statistical analysis using other available computer packages. However, it should be noted that this normalization type may introduce artificial information into the data.

- Py-MS data analysis with univariate statistical techniques.

Sometimes, peaks with structural significance (as opposed to fingerprint significance only) can be chosen for spectra comparison. If these peaks can be recognized in the Py-MS trace, they may provide more information in a comparison than simple fingerprint peaks. Also if it is possible to identify peaks that are rather constant in all spectra, this may provide a reference for the results. By plotting the intensities of an ion with structural significance against a constant ion, a scatter plot can be obtained, sometimes providing relevant information. An example is shown in Figure 5.5.1, where the intensity of the ion with $m/z = 125$ is represented as a function of ion with $m/z = 43$ for a series of polymeric carbohydrates some containing amino-sugars.

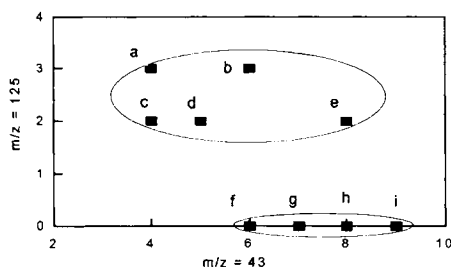


FIGURE 5.5.1. A scatter plot of the intensity of ion with $m/z = 125$ as a function of ion with $m/z = 43$ for: (a) chitin, (b) chondroitin sulfate, (c) chitosan, (d) capsular polysaccharide from *Neisseria meningitidis* [47], (e) teichuronic acid from *Bacillus subtilis* [47], (f) carrageenan, (g) alginic acid, (h) amylose, (i) agarose.

It can be clearly seen that the samples are separated into two groups, only one group containing amino-sugars. This type of plot was reported to indicate differences between

complex samples such as normal and dystrophic muscle biopsy samples [47], but it also can be used to differentiate plant materials, etc. Numerous computer packages are also available for displaying data and allowing visual differentiation of groups of samples.

Py-MS analyses not requiring a long time to complete can be rather easily repeated, thereby generating more than one result for a given sample (specimen). The results are commonly affected by fluctuation, and statistical data analysis is frequently needed. The usefulness of univariate data analysis seems to be limited when analyzing Py-MS results because in each spectrum there is a significant number of peaks, each representing a measurement. However, if one mass peak is properly selected from the Py-MS spectrum, this can be used as a unique measurement for the given specimen, and univariate data analysis can be quite informative. Also, any peak can be selected separately, one at a time, for evaluation. This type of approach is less informative than multivariate data analysis, but has the advantage of being simpler.

Before discussing some applications, a few basic aspects on univariate statistics will be presented. A large amount of information exists regarding this field, and more details can be found in the original literature (e.g. [70,71]). Also a variety of computer packages performing statistical data analysis is available (e.g. [71a]).

The typical approach for the study of errors is to classify them as systematic (or determinate) or random. Systematic errors are generated by a specific cause, and it is assumed that by removing the cause, the systematic error is also eliminated.

Random errors are studied using statistical evaluation. It can be assumed that random errors are scattered within a continuous range of values. Therefore, the measurement of one variable x in a set of analyses can generate any values in a continuous range. Any obtained set of measurements $\{x_1, x_2, \dots, x_n\}$ is defined in statistics as a *sample* of this continuous range of values. Only all possible measurements (which must be infinite in number to cover the whole range) would generate the real set, which is called *population*. (The statistical term *sample* can easily be confused in analytical chemistry with the term sample = specimen, as the term *population* may also have a different meaning. To avoid this confusion, the statistical terms *sample* and *population* will always be italicized.)

Considering for example a set of Py-MS analyses, a single m/z value for all Py-MS traces can be selected. For each analysis "j", the measurement of the peak intensity at the chosen m/z generates a value x_j . If the number of measurements is n , they will generate the *sample* $\{x_1, x_2, \dots, x_n\}$. The *average* (or the *mean*) of these measurements, and the *standard deviation* (which shows the distribution of measurements about the mean) are given by the formulas:

$$m = \frac{\sum_{j=1}^n x_j}{n} \quad s = \sqrt{\frac{\sum_{j=1}^n (x_j - m)^2}{(n-1)}} \quad (3)$$

The value s^2 (variance) is sometimes used instead of s . If a series of *sample* sets, each containing n data, are taken randomly from a *population*, the mean of each set will also be a random variable but will show less and less scatter as n increases. The standard

deviation of the mean of each set, called *standard error* of the mean s_m , is given by the formula:

$$s_m = s / n^{1/2} \quad (4)$$

The values m and s describe the *sample*, but they are not necessarily the same for the *population*. For the *population*, μ will replace the average m , and σ will replace the standard deviation s (when $n \rightarrow \infty$, then $m \rightarrow \mu$ and $s \rightarrow \sigma$).

One important question regarding the distribution of measurements about their mean is the expected frequency of occurrence of an error as a function of the error magnitude. The most commonly utilized function, which describes well the *relative frequency of occurrence of random errors* in large sets of measurements, is given by Gauss formula (see also rel. (9) Section 5.2):

$$f(x) = (2\pi \sigma^2)^{-1/2} \exp [- (x - \mu)^2 / 2\sigma^2] \quad (5)$$

This frequency function shows that the point of maximum frequency is obtained for the mean (when $x = \mu$), the distribution of positive and negative errors is symmetrical, and as the magnitude of the deviation from the mean increases, an exponential decrease in the frequency takes place. The errors with the relative frequency of occurrence given by rel. (5) have a so-called *normal distribution* $\mathbf{N}(\mu, \sigma)$. Using the substitution:

$$z = (x - \mu) / \sigma \quad (6)$$

and assuming that the variable x has a normal distribution $\mathbf{N}(\mu, \sigma)$, then z will have a distribution $\mathbf{N}(0, 1)$. The value $(x - \mu)$ is a so-called *mean centered value*, and by dividing it by σ , it is expressed in σ units (or it is *standardized*). Mean centered standardized variables (*standardized variates*) are commonly used in statistical data processing. The area under the curve $f(x)$ for $x < \alpha$ will give a *cumulative frequency distribution* expressed by

$$F(\alpha) = \int_{-\infty}^{\alpha} f(x) dx \quad (7)$$

where $f(x)$ is the distribution function given by rel. (5). This cumulative frequency distribution is equal to the probability P for x to have a value below α in any measurement, and the integral over the whole space gives $P = 1$. The values of function $F(\alpha)$ are known and tabulated (e.g. [71]) or present in computer statistical packages.

The mean of a *sample* of n values $\{x_1, x_2, \dots, x_n\}$, as indicated previously, is also a random variable. Assuming that x has a normal distribution $\mathbf{N}(\mu, \sigma)$, the mean m takes a continuous range of values with a normal distribution $\mathbf{N}(\mu, \sigma/n^{1/2})$ and the variable

$$z = (m - \mu) / (\sigma/n^{1/2}) \quad (8)$$

has an $\mathbf{N}(0, 1)$ distribution. It is possible now to evaluate how close the values of μ and m are for a certain *population* and an experimental m . For the variable z given by rel. (8), two values $z_{\alpha/2}$ and $z_{1-\alpha/2}$ can be found such that the probability for z of being outside the interval $(z_{\alpha/2}, z_{1-\alpha/2})$ is equal to α (area under the curve). Therefore, the probability P will be $P = 1 - \alpha$ when

$$z_{\alpha/2} < (m - \mu) / (\sigma/n^{1/2}) < z_{1-\alpha/2} \tag{9}$$

Because $z_{\alpha/2} = -z_{1-\alpha/2}$, rel. (9) is equivalent to

$$\mu - z_{1-\alpha/2} (\sigma/n^{1/2}) < m < \mu + z_{1-\alpha/2} (\sigma/n^{1/2}) \tag{9a}$$

The values for P(z) and z can be obtained from tables [71]. Using rel. (9) it is easy to obtain the maximum possible differences between m and μ . Figure 5.5.2 shows the curve N(0,1) with two values $z_{\alpha/2}$ and $z_{1-\alpha/2}$ such that the probability for z of being outside the interval $(z_{\alpha/2}, z_{1-\alpha/2})$ is equal to α (area under the curve). The larger α is, the smaller is P and the smaller is the value for $z_{1-\alpha/2}$.

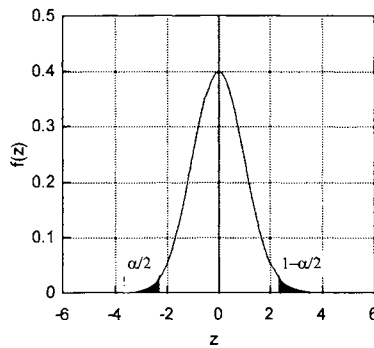


FIGURE 5.5.2. Gaussian curve N(0,1), showing two values $z_{\alpha/2}$ and $z_{1-\alpha/2}$ such that the probability for z of being outside the interval $(z_{\alpha/2}, z_{1-\alpha/2})$ is equal to α (area under the curve).

For small sets of measurements it was found that the relative frequency of occurrence of random errors is not described so well by Gaussian distribution as by another frequency function named “t” or Student function, $f(t, \nu)$ (where $\nu = n - 1$ represents the degree of freedom of the sample) with a known expression [71]:

$$f(t, \nu) = \frac{1}{\sqrt{\nu \pi}} \frac{\Gamma[(\nu + 1) / 2]}{\Gamma(\nu / 2)} (1 + t^2 / \nu)^{-(\nu+1)/2}$$

where

$$\Gamma(z) = \int_0^{\infty} t^{(z-1)} \exp(-z) dt$$

For the Student distribution, the values of cumulative frequency F(t, ν) are also known and tabulated [72] (or present in computer packages). Figure 5.5.3 shows the dependence between the cumulative frequency distribution F(x) and x for a N(0,1) distribution (trace A) and the dependence between the cumulative frequency distribution F(x, 3) and x for a Student distribution (trace B).

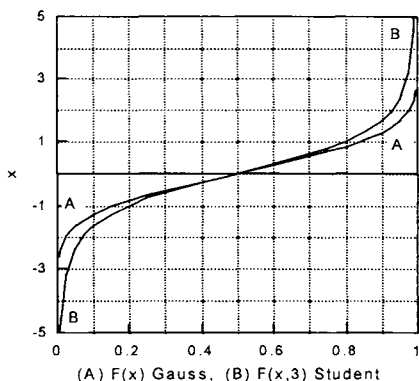


FIGURE 5.5.3. The dependence between the cumulative frequency distribution $F(x)$ and x for an $N(0,1)$ distribution (trace A) and between $F(x, 3)$ and x for a Student distribution (trace B).

Besides the distribution functions of Gauss and Student, some other functions were proposed for describing the expected frequency of occurrence for errors. For example, for a set of random variables $x^{(1)}, x^{(2)} \dots x^{(k)}$, each having a $N(0,1)$ distribution, the variable:

$$\chi^2 = \sum_{i=1}^k (x^{(i)})^2 \quad (10)$$

has a special distribution $f(\chi^2, \kappa)$ with a known expression [71], where $\kappa = k - 1$ is the number of degrees of freedom. This is a so-called χ^2 distribution, and the values for its cumulative frequency $F(\chi^2, \kappa)$ are also known and tabulated [72].

Several applications of univariate statistical analysis for data evaluation in Py-MS are known [73]. One such application is the evaluation of reproducibility of a replicate of an analysis for the peak intensity at a given m/z value. If a series of measurements are made on identical specimens, this will provide a *sample* $\{x_1, x_2 \dots x_n\}$. This *sample* will allow the calculation of parameters such as the mean m and the standard deviation s . By comparing the value s for different m/z values it is possible to select those m/z that are more reproducible (smaller s).

The univariate statistical theory is used, for example, for rejecting one extreme value in a set of scattered results in a given *sample*. For this purpose, the extreme value x_e is temporarily eliminated from the *sample*. Then, from the *sample* $\{x_1, x_2 \dots x_n\} - x_e$ there are calculated m , s and the value:

$$L = \frac{m - x_e}{s \sqrt{\frac{n}{(n-1)}}} \quad (11)$$

If the variable x has a Gaussian distribution, it can be shown that L has a Student distribution with $\nu = n - 2$ degrees of freedom. It is possible now to decide if x_e should be accepted or rejected by reasoning in the same manner as for evaluating how close

are the values of μ and m (see rel. (9)). For a desired probability P chosen for this decision (such as $P = 0.95$ or 95%), a value $\alpha = 1 - P$ is obtained, and then an interval $(t_{\alpha/2, v}, t_{1-\alpha/2, v})$ is found from the tables containing $F(t, v)$ and t values for the particular v . The value x_e should be accepted in the *sample* if

$$t_{\alpha/2, v} < L < t_{1-\alpha/2, v} \quad (12)$$

Another utilization of statistical theory is to decide if two specimens are the same or different when the measurements performed on each specimen generate the two *samples* $\{x_1, x_2 \dots x_n\}$ and $\{x'_1, x'_2 \dots x'_k\}$ containing scattered values. For this purpose, the two averages m and m' and the two standard deviations s and s' are calculated. It can be shown that if the *samples* are large enough, the variable:

$$H = \frac{m - m'}{\sqrt{s^2/n + s'^2/k}} \quad (13)$$

has an $N(0,1)$ distribution. Again, reasoning in the same manner as for evaluating how close are the values of μ and m (see rel. (9)) and selecting a desired probability P for this decision, a value $\alpha = 1 - P$ is obtained, and then an interval $(z_{\alpha/2}, z_{1-\alpha/2})$ is found from the tables containing $F(z)$ and z for Gaussian distribution. The two specimens (the two samples) are not different if

$$z_{\alpha/2} < H < z_{1-\alpha/2} \quad (14)$$

In the case of *samples* with a low number of measurements, instead of a Gaussian distribution, a Student distribution can be assumed for the variable T , where

$$T = \frac{m - m'}{s'' \sqrt{1/n + 1/k}}, \quad s'' = \sqrt{\frac{(n-1)s^2 + (k-1)s'^2}{n+k-2}} \quad (15)$$

For the desired probability P chosen for the decision, a value $\alpha = 1 - P$ is obtained, and then an interval $(t_{\alpha/2, v}, t_{1-\alpha/2, v})$ is found from the tables for the particular $v = n + k - 2$. The two specimens (the two samples) are not different if

$$t_{\alpha/2, v} < T < t_{1-\alpha/2, v} \quad (16)$$

A statistical data evaluation was, for example, applied on a Py-GC determination of the level of ethylcellulose in specially treated paper. Two levels of ethylcellulose were expected. Based on the content of ethanol in the pyrolysate, the calculated level of ethylcellulose generated the plot shown in Figure 5.5.4a. The data were initially arranged in increasing level of ethyl cellulose content, to illustrate better the extreme values. The result is shown in Figure 5.5.4b.

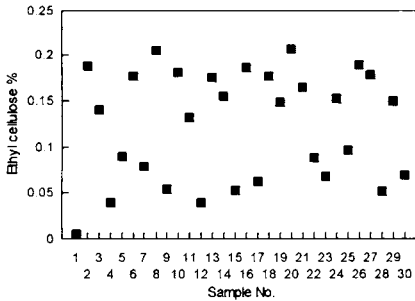


FIGURE 5.5.4a. Calculated level of ethylcellulose from the ethanol content in the pyrolysate.

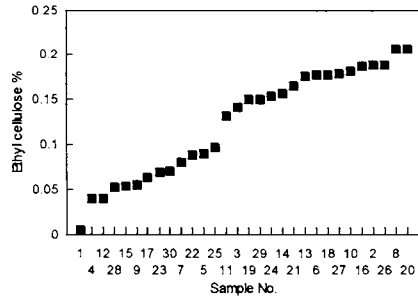


FIGURE 5.5.4b. The same data as in Figure 5.5.4a arranged in increasing order.

It was questioned if sample #1 belongs to the visually separated first group of 13 samples. For a chosen $\alpha = 0.05$ and $v = 11$, it can be found from appropriate tables that $t_{1-\alpha/2, v} = 2.201$. Using rel. (11) from the first set, the value $L = 3.03$ is obtained and therefore the measurement for sample #1 must be rejected. The same calculation was applied to sample #20 to see if it belongs to the second set. For the same $\alpha = 0.05$ and for $v = 15$, the tables gave $t_{1-\alpha/2, v} = 2.131$ and the calculations showed $L = -1.781$. This indicated that the sample #20 should not be discarded. The second step was to see if the two groups are significantly different. The calculation of the value T based on rel. (15) gave $T = 13.7$ and for $\alpha = 0.05$ and $v = 28$ from tables it can be found that $t_{1-\alpha/2, v} = 2.048$. This indicated that the two groups are different and that the Py-GC can be used for sample differentiation.

Some other common statistical tests (many available in computer packages) can also be applied to process Py-MS univariate data. Besides tests for deciding if a result belongs to a certain group or if two groups of results showing some scattered values describe the same sample or are statistically different, quantitative analyses are also performed using Py-MS results. The common procedure for quantitative analysis is to use the values of the intensities x_j at a chosen m/z for a series of standard samples with known concentrations c_j , and generate a calibration line using a linear regression dependence of the form:

$$c = \alpha + \beta x \quad (17a)$$

where

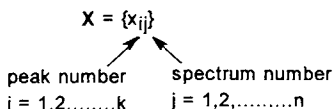
$$\beta = \left[\sum_{j=1}^n (x_j - \bar{x})(c_j - \bar{c}) \right] / \left[\sum_{j=1}^n (x_j - \bar{x})^2 \right] \quad \text{and} \quad \alpha = \bar{c} - \beta \bar{x} \quad (17b)$$

Using the calibration line, results can be obtained for the unknown samples from the intensities at the selected mass. The choice of the mass peak for quantitation was proven important for obtaining good results, and this can be done by evaluating one by one the masses in a set of selected m/z values.

- *Multivariate data sets.*

Multivariate data analysis has been developed as an independent field of statistics and has numerous practical and theoretical applications. This explains the existence of a variety of printed materials and of different computer programs available for multivariate data processing [71a]. Only some aspects of multivariate data analysis with application to the processing of Py-MS data will be discussed here.

The common case encountered in practice for Py-MS data is a typical multivariate problem, with a number of "p" specimens generating (through replicate measurements) a total of "n" Py-MS results, each consisting of "k" peaks. Although it is possible that the number of peaks varies from spectrum to spectrum when analyzing different specimens (samples), a maximum number k of peaks can be assumed for all spectra. Also, each of the p samples can be analyzed a number of times to generate replicates, with the number of replicates equal or different from sample to sample (commonly taken equal). The intensity of a peak in a Py-MS result will be noted with x, and a *data matrix* will be generated such that its elements are the intensities $x_{i,j}$ and the matrix can be noted $\{x_{i,j}\}$ or X . The first index in $\{x_{i,j}\}$ designates the peak $i = 1, 2 \dots k$, and the second index designates the result spectrum $j = 1, 2 \dots n$:



Each spectrum can be considered a point in a "k" dimensional space. An illustration of a typical data matrix obtained in a Py-MS study is shown in Table 5.5.1.

TABLE 5.5.1. *Illustration of a data matrix in Py-MS.*

Specimens	Results	m/z ₁	m/z ₂	m/z ₃	m/z _k
1	1	x _{1,1}	x _{2,1}	x _{3,1}		x _{k,1}
	2	x _{1,2}	x _{2,2}			x _{k,2}
	3	x _{1,3}				
2						
.						
.						
p						
.						
.						
n		x _{1,n}				x _{k,n}

In univariate statistics a key question discussed previously was to evaluate how close the values of μ and m are for a certain *population* and an experimental m . The answer to this question is used as a model for significance tests. One main tool used to evaluate statistical data is the distribution function, which describes the distribution of measurements about their mean. In other words, the distribution function gives the

expected frequency of occurrence of an error as a function of the error magnitude. Gaussian *normal* density function in more than one dimension is commonly utilized to describe the *relative frequency of occurrence of random errors* in large sets of multivariate data. For example, the bivariate normal density function for two variables X_1 and X_2 is given by relation:

$$f_2(X_1, X_2) = \frac{1}{2\pi\sigma_1\sigma_2(1-\rho^2)^{1/2}} \exp \left\{ -\frac{1}{2(1-\rho^2)} \left[\frac{(X_1 - \mu_1)^2}{\sigma_1^2} - \frac{2\rho(X_1 - \mu_1)(X_2 - \mu_2)}{\sigma_1\sigma_2} + \frac{(X_2 - \mu_2)^2}{\sigma_2^2} \right] \right\} \quad (18)$$

where σ_1 and σ_2 are the standard deviations, μ_1 and μ_2 are the means for X_1 and X_2 , respectively, and ρ is the product moment correlation:

$$\rho = \frac{\text{cov}(X_1, X_2)}{\sigma_1\sigma_2} = \frac{\sum_{i=1}^n (X_{1i} - \mu_1)(X_{2i} - \mu_2)}{n - 1} \quad (18a)$$

(s_1, s_2, m_1, m_2 are approximations for $\sigma_1, \sigma_2, \mu_1, \mu_2$ respectively). The bivariate normal density function has a bell shape form, and it is centered at the point (μ_1, μ_2) that represents the centroid of the distribution. A multivariate normal distribution can be defined similarly to a bivariate normal distribution.

Different applications regarding the evaluation of Py-MS data as shown for one single peak (univariate data) can be extended to the data matrix. One such application is the rejection of an extreme value in a set of replicates for the same specimen. For this purpose, a variable H_j^2 should first be calculated:

$$H_j^2 = \left[\sum_{i=1}^k (x_{ij} - m_i') / m_i' \right]^2 \quad (19)$$

where m_i' is the average of the peak i intensities in all replicates, excluding spectrum j . This variable has a χ^2 distribution, with $\kappa = k - 1$ degrees of freedom. For a desired probability P chosen for the decision, a value $\alpha = 1 - P$ is obtained, and then an interval $(\chi_{\alpha/2, \kappa}^2, \chi_{1-\alpha/2, \kappa}^2)$ is found from the tables of cumulative frequency $F(\chi^2, \kappa)$. The spectrum j should be retained if

$$\chi_{\alpha/2, \kappa}^2 < H_j^2 < \chi_{1-\alpha/2, \kappa}^2 \quad (20)$$

- Measures for comparing multivariate Py-MS data.

Common ways to compare two (or more) Py-MS results are those based on different types of measures. A particular case of multivariate data analysis is that of two samples to be compared. The comparison can be done, for example, by simple procedures such as subtracting the peaks obtained in the second spectrum from the corresponding ones obtained in the first spectrum and plotting the result. The spectra subtraction is commonly performed with the electronic capabilities of data processing available in modern instrumentation. As an example, Figure 5.5.5 shows the subtracted spectrum of cellulose from glycogen (glycogen - cellulose) [73a]. The peak intensities were reported to the total ion intensity in the spectrum.

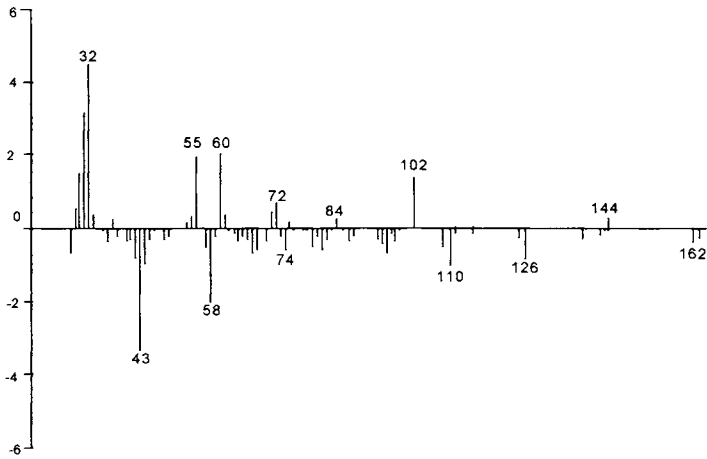


FIGURE 5.5.5. *Subtracted Py-MS spectrum of cellulose from glycogen (glycogen - cellulose).* The peak intensities were normalized to the total ion intensity in the spectrum.

The peaks predominant in glycogen will show positive, while those predominant in cellulose will show negative values. The smaller are the differences in the graph, the less difference is expected between the samples.

More complicated techniques derived from multivariate data analysis are also utilized for data comparison, and these can be based on different types of measures such as:

- similarity,
- distance-type parameters, and
- correlation-type parameters.

A similarity index for two Py-MS results (see also Section 5.2), A and B, each with a maximum of k peaks, can be calculated based on the ratios of peak intensities for each m/z_i ion. Assuming that A_i and B_i , $i = 1, 2, \dots, k$, are the pair peak intensities in the two samples, first are calculated the ratios:

$$R_i = A_i / B_i \text{ or } R_i = B_i / A_i \text{ such that } R_i < 1 \quad (21a)$$

and $R_i = 0$ for each missing corresponding peak. The similarity is then calculated using the formula:

$$SI = \left(\sum_{i=1}^k R_i \right) / k \quad (21b)$$

Another possibility [69] (which was also used for the comparison of chromatograms) applies the formula:

$$F = 100 \left\{ 1 - \frac{\sum (A_i - B_i)^2}{\sum [(A_i)^2 + (B_i)^2]} \right\} \quad (22)$$

where A_i and B_i are peak intensities for the same m/z_i , and i takes values from 1 to the total number of peaks k . A perfect fit in rel. (22) gives a factor $F = 100\%$, and no match gives $F = 0\%$.

A measure of similarity can also be calculated based on the concept of Euclidean distance. For this purpose, the differences:

$$\Delta_i = A_i - B_i \quad (23a)$$

are first calculated. The next step is to calculate the distance D using the formula:

$$D = \left[\sum_{i=1}^k (\Delta_i)^2 \right]^{1/2} \quad (23b)$$

This type of calculation is affected by the absolute difference between peaks, and the large peaks have, as a rule, larger differences than the small peaks. Because of this, the variation in the large peaks dominate the value of D, but sometimes their difference is not relevant for the nature of the sample. A weighing factor w_i can be introduced to improve this situation by using a relation of the type:

$$D = \left[\sum_{i=1}^k (\Delta_i)^2 w_i / \sum_{i=1}^k w_i \right]^{1/2} \quad (23c)$$

The choice of the weighing factor is critical in determining the utility of this type of approach.

The correlation coefficient can also be utilized as a parameter for comparing two results. Taking the intensities A_i as the values for a variable A and the intensities B_i as the values for a the variable B, a linear dependence of the type given by rel. (17a) can be sought, or

$$B = \alpha + \beta A \quad (17c)$$

and a correlation coefficient R can be calculated for the dependence:

$$R = \left[\sum_{i=1}^k (A_i - \bar{A})(B_i - \bar{B}) \right] / \left[\sum_{i=1}^k (A_i - \bar{A})^2 \sum_{i=1}^k (B_i - \bar{B})^2 \right]^{1/2} \quad (24)$$

For identical samples $R = 1$, and R is lower when the samples are different. This coefficient can be used as a measure of similarity. The similarity results are further utilized to decide if the Py-MS results on two samples are different enough to indicate that the samples are different indeed or only the analytical fluctuations are the cause of imperfect similarity. A threshold of similarity (distance, or correlation) is commonly used for this decision.

For larger sets of samples, using the data matrix it is also possible to calculate parameters for the comparison of the results for classification purposes or for establishing identity or difference among samples. Similarly, distance or regression as defined for the two-sample case can be extended to the case of multiple samples.

For any pair of spectra or of samples it is possible, for example, to calculate an Euclidean distance, using a relation similar to rel (23c). For this purpose, the mean intensities must be calculated first, (with rel. 3) for each peak and in each sample using

its replicates. A set of average intensities $\{\bar{x}_{ij}\}$ where $i = 1, 2, \dots, k$ and $j = 1, 2, \dots, p$ ($p < n$) is generated. Then, the differences $\bar{\Delta}_{jh}(i)$ for each peak i are calculated for any pair of samples (j, h) using the formula:

$$\bar{\Delta}_{jh}(i) = \bar{x}_{ij} - \bar{x}_{ih} \quad (25a)$$

Then, the Euclidean distance is obtained using the formula:

$$\bar{D}_{jh} = \left[\sum_{i=1}^k (\bar{\Delta}_{jh}(i))^2 w_i / \sum_{i=1}^k w_i \right]^{1/2} \quad (25b)$$

If the distance between spectra (and not samples) needs to be calculated, rel. (25a) will be replaced by

$$\Delta_{jh}(i) = x_{ij} - x_{ih} \quad (26a)$$

and

$$D_{jh} = \left[\sum_{i=1}^k (\Delta_{jh}(i))^2 w_i / \sum_{i=1}^k w_i \right]^{1/2} \quad (26b)$$

It is certainly expected that the D_{jh} values for replicates of the same sample should be very small.

In addition to the Euclidean distance, a "city block" distance can be calculated. The formula giving a city block distance between spectra j and h is

$$B_{jh} = \sum_{i=1}^k |x_{ij} - x_{ih}| \quad (27)$$

It is possible to estimate now a weighing factor to be used in the calculation of distances using rel. (26b) or rel. (23c) based on the results in a data matrix. For this purpose, the standard deviation is calculated (with rel. 3) for each peak using the replicates of each sample. In this way, a set of standard deviations $\{s_{ij}\}$ is generated where $i = 1, 2, \dots, k$ are the peaks and $j = 1, 2, \dots, p$, ($p < n$) are the samples. A weighing parameter r_i (which can be used as w_i and is called inner variance) can be calculated [1] with the formula:

$$r_i = \left[\left(\sum_{j=1}^p s_{ij} \right) / p \right]^{-1} \quad (28)$$

such that the peaks with larger standard deviations will have smaller weights.

Another weighing factor can be calculated either from the set of average intensities, $\{\bar{x}_{ij}\}$ where $i = 1, 2, \dots, k$, and $j = 1, 2, \dots, p$, ($p < n$), or from the total data matrix $\{x_{ij}\}$ where $i = 1, 2, \dots, k$ and $j = 1, 2, \dots, n$. For the calculation of this weighing factor, a total mean peak intensity \bar{x}_i must be obtained by averaging all the x_{ij} values for each peak i . The weighing parameter q_i (which can be used as w_i) is then calculated [1] using the formula:

$$q_i = \left[\left(\sum_{j=1}^p (\bar{x}_{ij} - \bar{x}_i)^2 \right) / p \right] \quad \text{or}$$

$$q_i = \left[\left(\sum_{j=1}^n (x_{ij} - \bar{x}_i)^2 \right) / n \right] \quad (29)$$

This weighing factor, called outer variance term, favors the peaks with larger differences from the average. A *characteristicity* coefficient c_i can be obtained as a product of the two weighing parameters:

$$c_i = r_i q_i \quad (30)$$

and used as w_i when calculating distances between sets of Py-MS results (pyrograms), each set generated by a sample.

The Euclidean distance D_{jh} can be used to obtain a similarity value S_{jh} using the formula:

$$S_{jh} = 1 - (D_{jh} / D_{jh \max}) \quad (31)$$

where $D_{jh \max}$ is the maximum value obtained for D_{jh} .

Other distance formulas may involve ranking [1] followed by a distance calculation or generalized distances of the type:

$$D = \left[\sum_{i=1}^k (\Delta_i)^q \right]^{1/q} \quad (32)$$

More sophisticated distance measures such as Mahalanobis D^2 measure (named after its developer) are also utilized to process pyrolysis results [74,75]. Mahalanobis D^2 measure is calculated between two groups of samples U and V using the relation:

$$D^2_{UV} = \mathbf{x}' \mathbf{S}^{-1} \mathbf{x} \quad (33)$$

where \mathbf{x}' is a row vector (and \mathbf{x} is its transposed \mathbf{x}'), calculated as a difference between the average intensities for each m/z value, between group U and group V and where the matrix \mathbf{S} is calculated from the pooled within group covariances for the group U and group V. This measure will be described for a simplified case of eight points in a tridimensional space with the data matrix given in Table 5.5.2.

TABLE 5.5.2. Model data matrix for two sets of samples each with four replicates and three MS peaks.

Specimens	Results	m/z_1	m/z_2	m/z_3
U	1	$x_{1,1}$	$x_{2,1}$	$x_{3,1}$
	2	$x_{1,2}$	$x_{2,2}$	$x_{3,2}$
	3	$x_{1,3}$	$x_{2,3}$	$x_{3,3}$
	4	$x_{1,4}$	$x_{2,4}$	$x_{3,4}$
	average	$x_{1,U}$	$x_{2,U}$	$x_{3,U}$
V	1	$x_{1,5}$	$x_{2,5}$	$x_{3,5}$
	2	$x_{1,6}$	$x_{2,6}$	$x_{3,6}$
	3	$x_{1,7}$	$x_{2,7}$	$x_{3,7}$
	4	$x_{1,8}$	$x_{2,8}$	$x_{3,8}$
	average	$x_{1,V}$	$x_{2,V}$	$x_{3,V}$

The vector \mathbf{x}' will be calculated as

$$\mathbf{x}' = \left[\begin{array}{ccc} x_{1,U} - x_{1,V} & x_{2,U} - x_{2,V} & x_{3,U} - x_{3,V} \end{array} \right] \quad (34)$$

The next step in the calculation consists of generating the matrix of within-group deviations (the matrix of mean centered values for each group). A *mean centered (or corrected) value* for an element x_{ij} from the group U ($j \in U$) (first four rows of elements in this example) is calculated as the difference:

$$\underline{x}_{ij} = x_{ij} - x_{iU} \quad (35)$$

and a similar relation is used for the elements in the group V, replacing x_{iU} with x_{iV} (last four rows of elements in this example). With these values, the matrix $\underline{\mathbf{X}}$ will be generated:

$$\underline{\mathbf{X}} = \begin{bmatrix} \underline{x}_{1,1} & \underline{x}_{2,1} & \underline{x}_{3,1} \\ \underline{x}_{1,2} & \underline{x}_{2,2} & \underline{x}_{3,2} \\ \underline{x}_{1,3} & \underline{x}_{2,3} & \underline{x}_{3,3} \\ \underline{x}_{1,4} & \underline{x}_{2,4} & \underline{x}_{3,4} \\ \underline{x}_{1,5} & \underline{x}_{2,5} & \underline{x}_{3,5} \\ \underline{x}_{1,6} & \underline{x}_{2,6} & \underline{x}_{3,6} \\ \underline{x}_{1,7} & \underline{x}_{2,7} & \underline{x}_{3,7} \\ \underline{x}_{1,8} & \underline{x}_{2,8} & \underline{x}_{3,8} \end{bmatrix} \quad (36)$$

The next step is to calculate the 3 x 3 matrix of *pooled within groups* sums of (mean corrected) squares and cross products (SSCP) by the formula:

$$\mathbf{W} = \underline{\mathbf{X}}' \underline{\mathbf{X}} \quad (37)$$

where $\underline{\mathbf{X}}'$ is the transpose of matrix $\underline{\mathbf{X}}$.

From matrix \mathbf{W} , matrix \mathbf{S} can be calculated by dividing each element of the matrix by the number of elements in $\underline{\mathbf{X}}$ less 2, using the formula:

$$\mathbf{S} = (i \cdot j - 2)^{-1} \mathbf{W}, \text{ or for this } 3 \times 8 \text{ case, } \mathbf{S} = (3 \cdot 8 - 2)^{-1} \mathbf{W} = 1/22 \mathbf{W} \quad (38)$$

Considering that the product of two matrices $\mathbf{A} = \{a_{ij}\}$ and $\mathbf{B} = \{b_{ij}\}$ is the matrix $\mathbf{C} = \{c_{ij}\}$

where $c_{ij} = \sum_{h=1}^n a_{ih} \cdot b_{hj}$, and the covariance between two *samples* $X = \{x_1, x_2, \dots, x_n\}$ and

$X' = \{x'_1, x'_2, \dots, x'_n\}$ with the averages m and m' respectively is given by the formula

$\text{cov}(X, X') = \sum_{i=1}^n (x_i - m)(x'_i - m') / (n - 1)$, it can be shown that the matrix \mathbf{S} contains

pooled within group covariances (see e.g. [74]).

To obtain D^2_{UV} the next steps are to calculate \mathbf{S}^{-1} and the product $\mathbf{x}' \mathbf{S}^{-1} \mathbf{x}$. By replacing \mathbf{S} with the identical matrix $\mathbf{1}$ in rel. (33), it can be seen that D^2_{UV} distance is reduced to the square of the Euclidean distance.

- Cluster analysis of Py-MS data.

Once a parameter measuring the similarity, distance, or regression has been calculated for a set of samples (possibly using dedicated computer programs), a next step is frequently required for the interpretation of the results. The distance, similarity or regression calculations within a set of samples will generate a matrix $D = \{d_{ij}\}$. The interpretation of the results in this matrix is commonly done using techniques known as cluster analysis. Clustering algorithms can be classified as hierarchical or non-hierarchical.

Hierarchical algorithms are characterized by the construction of a tree-like structure. A *single linkage* algorithm starts with placing in the first cluster the two nearest points. At the next stage, a third point joins the already formed cluster of two if its shortest distance to the members of the first cluster is smaller than to any other point. Otherwise, two unclustered points are placed in a new cluster. The procedure continues until all points end up in a single large cluster. The distance between two clusters is defined as the shortest distance between a point in the first cluster and a point in the second cluster. This technique will be exemplified for the similarity matrix from Table 5.5.3.

TABLE 5.5.3. Similarity matrix in % (SI %) for eight samples of pyrolysed plant material, each pair similarity calculated using rel. (17).

Sample	2	3	4	5	6	7	8
1	93	86	65	61	56	53	45
2		89	64	56	48	39	44
3			44	43	51	56	50
4				87	54	48	49
5					52	51	54
6						78	82
7							85

The clustering procedure described above generated the tree shown in Figure 5.5.6

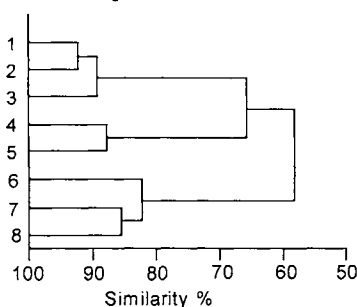


FIGURE 5.5.6. Dendrogram with complete linkage clustering based on Table 5.5.3 similarities.

Other hierarchical algorithms are also known, such as that using the *average linkage* option. In this algorithm, the first set of clusters is done in the same way as previously described. However, the addition of the third element to a cluster considers the average distance to the elements in the previously formed cluster, and the distance between clusters is the average distance from points in the first cluster and the second cluster.

Non-hierarchical algorithms start with a cluster center, and all elements are grouped within a threshold of values in this cluster. Then, a new cluster center is selected, which is outside of the first cluster based on the chosen threshold, and the process is repeated for the remaining unclustered points. As an example, the data from Table 5.5.4 could be clustered using a threshold of 85% similarity and form the clusters {1,2,3}, {4,5}, {6}, and {7,8}. These clusters differ from the result obtained using the hierarchical technique only by the fact that sample {6} does not belong to the group {7,8}. For another chosen threshold, such as 82% similarity, the clusters would be the same. Depending on the data matrix **D** and threshold, the algorithms may generate the same or different results. It is common that the clustering is done using dedicated computer programs available in statistical packages.

Another procedure applied in classifying distances obtained from Py-MS data is the use of the d plots [1]. This procedure consists of choosing two points of larger distance from the matrix **D** and representing all the distances reported to these points on an orthogonal system of axes. The procedure is illustrated for the similarities given in Table 5.5.3. The chosen reference samples are spl. #1 and spl. #7 for one representation, and spl. #5 and spl. #2 for another representation. The results are shown in Figure 5.5.7 (A) and Figure 5.5.7 (B). The three obvious clusters are the same for the two d plots and the same as those indicated by the previous clustering procedures. A different choice of the reference samples shows, however, different images which may emphasize or diminish the clustering. Also, there are known methods to emphasize the separation between classes.

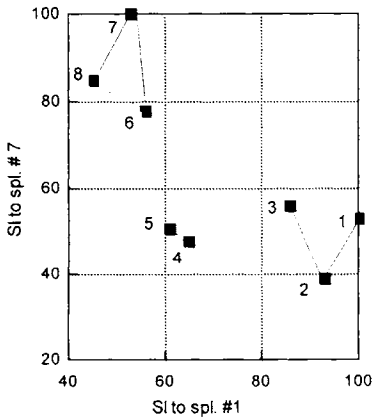


FIGURE 5.5.7 (A). Plot of SI values from Table 5.5.3 using spl. #1 and spl. #7 as references, illustrating a d plot.

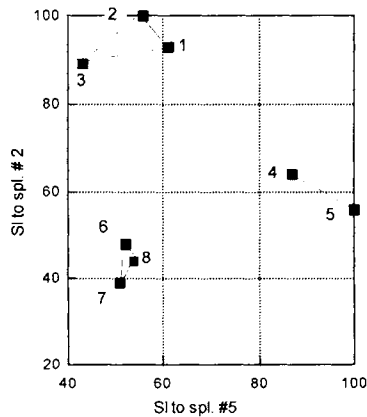


FIGURE 5.5.7 (B). Plot of SI values from Table 5.5.3 using spl. #5 and spl. #2 as references, illustrating a d plot.

This type of data processing and display is commonly done using computer packages for statistical data evaluations (e.g. [76]).

- Discriminant analysis applied to Py-MS data.

The multivariate set of data that results from Py-MS analysis usually contains a large number of variables. Some of these variables may convey the same information, and others may have no real informative value. The aim of discriminant analysis is to find a linear composite (*canonical variates*) of the predictor variables with the property to maximize the ratio of the variations between groups to that within groups of sample replicates. Other composites are computed such that the accounted-for variation appears in decreasing order. The plot of the first two canonical variates displays the maximum discrimination of the groups in two dimensions. After the calculation of the canonical variates, these can be tested (using statistical criteria) to find if the group centroids are indeed different. Also, it is possible to find which predictors contribute the most to discriminating among groups. Each linear composite can be expressed as

$$z_{hj} = \bar{x}_{h1} b_{1j} + \bar{x}_{h2} b_{2j} + \bar{x}_{h3} b_{3j} + \dots + \bar{x}_{hn} b_{nj} \quad (39)$$

where the coefficients $\{b_{ij}\}$ are the so-called *loadings* and \bar{x}_{ij} are the mean corrected values for the elements from a certain group. The values of $\{b_{ij}\}$ (where $\{b_{ij}\}$ form matrix **B**) are calculated by solving an eigenvalue problem of the form:

$$(\mathbf{W}^{-1} \mathbf{A} - \lambda \mathbf{I}) \mathbf{B} = 0 \quad (40)$$

where **W** is the pooled within groups (mean corrected) SSCP matrix given by rel (37), and **A** is the between groups (mean corrected) SSCP matrix. Canonical correlation for multivariate data is commonly done using dedicated computer programs [74]. Large loadings reflect the importance to the discrimination of a particular mass in a given canonical variate.

Sometimes the interpretation of the canonical variates cannot be done with the coefficients b_{ij} only. A tool for interpretation is the so-called *factor spectrum* with intensities b_{ij} . In the case of a binary mixture, the positive part of the factor spectrum can be interpreted as the differences in mass spectrum of one component and the negative part as the differences in the spectrum of the other component. This can be illustrated for the factor spectrum for a mixture of pectin and methylated pectin [76a]. The first canonical variates contained $m/z = 31, 32$ (coming from methanol) and $m/z = 85$ attributed to a lactone ion also formed from the methylated pectin. The low DM factor spectrum contains five major masses common to furaldehyde. This spectrum is shown in Figure 5.5.8.

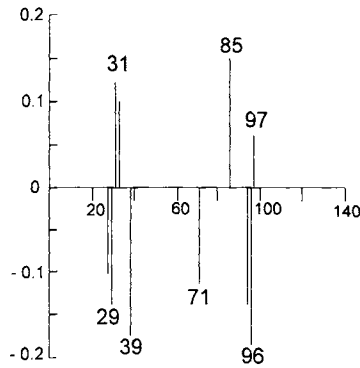


FIGURE 5.5.8. Factor spectrum for the first canonical variate for pectin related to the degree of methylation (DM). The upper spectrum shows high DM values while the lower spectrum shows low DM.

- Factor analysis applied to Py-MS data.

Attempting to find a smaller number of variables (dimensions) that retain most of the information in the original data matrix is very useful for a better and easier understanding of results. This approach of multivariate data treatment is known as *factor analysis*.

There are several factor analysis procedures that result in a reduction in dimensionality. One such procedure simply eliminates some of the variables, which in Py-MS case would be the peaks for certain m/z values. To prevent the loss of valuable information in this procedure, an appropriate rule for this procedure must be established. Dedicated computer programs are available to perform such procedures, and commonly they have the following steps:

- The matrix of distances \mathbf{D} is first calculated with the initial data matrix \mathbf{X} , and the values are ordered in a decreasing row: $d_1, d_2, d_3 \dots d_z$, such that $d_1 > d_2 > d_3 \dots > d_z$. (each $d_1, d_2 \dots$ being one of the d_{jn} values in matrix \mathbf{D}).
- One or more dimensions (columns) in the data matrix \mathbf{X} are eliminated and a new matrix \mathbf{X} with fewer columns is obtained. A new distance matrix \mathbf{D} is calculated from \mathbf{X} with the values d_{jn} .
- The new values are also ordered in a decreasing row: $d_1, d_2, d_3 \dots d_z$. If the two rows $\{d_n\}$ and $\{d_n\}$ show the same order of elements (for example, when $d_{ij} > d_{kl}$, also $d_{ij} > d_{kl}$), then the eliminations in the matrix \mathbf{X} do not affect the results and are justified.
- An index of the goodness of fit was developed for this procedure, which requires minimization of the value:

$$S = \left[\sum (d_{ij} - \underline{d}_{ij})^2 / \sum (d_{ij})^2 \right]^{1/2} \quad (41)$$

The above described procedure can be combined with “moving” points in a certain dimension to maintain the order of the distances. For example, if $d_{ij} > d_{kl}$ but $\underline{d}_{ij} < \underline{d}_{kl}$, the coordinates x_{ij} of a point “j” can be “corrected” (in dimension “i”) to achieve $\underline{d}_{ij} < \underline{d}_{kl}$. This type of technique was extensively used for processing Py-MS data for the classification of microorganisms and bioorganic samples [76, 76b].

Another common method in factor analysis is *principal component analysis*. Principal component method can be considered a development of the previous procedure and commonly proceeds in a sequence of steps [74] as follows:

- Instead of using the initial configuration of variables, use a *linear composite* of it (with the same dimensionality) such that the new set exhibits the largest differences between the samples in the first dimension, followed by next largest differences in the second dimension, etc. The new set of variables should be uncorrelated with each other. This operation is called a *rotation*.
- Reduce the dimensionality by discarding dimensions that have low significance in differentiating the samples.
- Find a new orientation in the reduced space that makes the retained dimensions more interpretable.

The first factor, defined as the linear combination of the original variables, obtained by the above described procedure will account for more of the variance in the data set than any other combination of variables. The second factor will be the linear combination of variables that accounts for most of the residual variance after the effect of the first factor has been removed from the data. Subsequent factors are defined similarly until all variance in the data is exhausted. In case the original variables are uncorrelated, the factor analysis solution requires as many factors as there are variables. However, in most data sets, many variables are more or less correlated and the variance in the data can be described by a smaller set of factors than there are variables. Therefore the data reduction is applicable.

Mathematically the procedure uses the possibility to write a matrix \mathbf{A} (with k columns and n rows, $\mathbf{A}_{(k \times n)}$) as a product of three matrices:

$$\mathbf{A}_{(k \times n)} = \mathbf{P}_{(k \times r)} \Delta_{(r \times r)} \mathbf{Q}_{(r \times n)}' \quad (42)$$

where \mathbf{P} is the orthonormal matrix of eigenvectors of the matrix $\mathbf{A}\mathbf{A}'$ (of order $k \times k$), \mathbf{Q} is the orthonormal matrix of eigenvectors of $\mathbf{A}'\mathbf{A}$ (of order $n \times n$), and Δ is a diagonal matrix with the elements on the main diagonal equal to the square roots of the diagonal elements of the matrix Δ^2 . The matrix Δ^2 contains the first r ordered positive eigenvalues of matrix $\mathbf{A}\mathbf{A}'$ (or $\mathbf{A}'\mathbf{A}$) [74].

It is common to express the data matrix \mathbf{X} as its standardized variate \mathbf{X}_s . If the average of each column in the data matrix \mathbf{X} is \bar{x}_i and the standard deviation of each column is s_i , then the matrix \mathbf{X}_s will have the elements:

$$(\underline{x}_{ij})_s = (x_{ij} - \bar{x}_i) / s_i \quad (43)$$

Applying to the matrix \mathbf{X}_s rel. (42), it will be obtained:

$$\mathbf{X}_s = \mathbf{P} \Delta \mathbf{Q}' \quad (44)$$

or by multiplying to the right with \mathbf{P}' it results:

$$\mathbf{P}' \mathbf{X}_s = \Delta \mathbf{Q}' = \mathbf{Y} \quad (45)$$

which can be considered a rotation of the matrix \mathbf{X}_s with the direction cosines given by the rows of matrix \mathbf{P}' (see e.g. [77]). The dimensionality of the new matrix \mathbf{Y} depends on the retained dimension r in the matrix Δ , and based on rel. (42) it will be $(r * n)$. If, for example, $r = 3$, only three new variables made from the combination of intensities for different m/z values will be associated with each point (spectrum). If a new set of, for example, three new variables are generated, y_{1j} , y_{2j} , y_{3j} , these are the components of a vector $\mathbf{y}_j = | y_{1j}, y_{2j}, y_{3j} |$ for each sample and they are expressed as

$$\begin{aligned} y_{1j} &= a_{11} x_{1j} + a_{12} x_{2j} + a_{13} x_{3j} \dots + a_{1k} x_{kj} \\ y_{2j} &= a_{21} x_{1j} + a_{22} x_{2j} + a_{23} x_{3j} \dots + a_{2k} x_{kj} \\ y_{3j} &= a_{31} x_{1j} + a_{32} x_{2j} + a_{33} x_{3j} \dots + a_{3k} x_{kj} \end{aligned} \quad (46)$$

The next possible step in factor analysis after the reduction of the number of components is a second rotation of the resulting matrix \mathbf{Y} with the purpose to improve the interpretability of the solution.

By multiplying rel. (44) to the left with \mathbf{Q} it results:

$$\mathbf{X}_s \mathbf{Q} = \mathbf{P} \Delta = \mathbf{Z} \quad (47)$$

The dimensionality of the new matrix \mathbf{Z} also depends on the retained dimension r in the matrix Δ , and based on rel. (42) it will be $(k * r)$. Matrix \mathbf{Z} is made from a number of factors, $\mathbf{z}_j' = | z_{1j}, z_{2j}, \dots, z_{kj} |$. Each factor can be expressed as

$$z_{hj} = x_{h1} b_{1j} + x_{h2} b_{2j} + x_{h3} b_{3j} \dots + x_{hn} b_{nj} \quad (48)$$

where the coefficients $\{b_{ij}\}$ are the so-called loadings.

One additional step in factor analysis that helps the interpretation of the results is *factor scaling*. One scaling that is appropriate for Py-MS results interpretation is the adjustment of the principal components so that their variances are equal to unity. This is accomplished by means of the transformation:

$$\mathbf{Z}_s = \mathbf{X}_s \mathbf{Q} \mathbf{D}^{-1/2} \quad (49)$$

where \mathbf{Z}_s is the matrix with *unit variance component scores* and $\mathbf{D}^{-1/2}$ is a diagonal matrix that scales the matrix \mathbf{Z} . It is convenient to write:

$$\mathbf{F} = \mathbf{Q} \mathbf{D}^{-1/2} \quad (50)$$

where matrix \mathbf{F} gives the component loadings.

Another process utilized for better interpretation of the factor analysis results is *factor rotation*. A much easier interpretation can be done if a new rotation is done such that only a few variables have weights different from zero in matrix \mathbf{Z} or \mathbf{Z}_s . Considering for example the matrix \mathbf{Z}_s , this process can be achieved formally by replacing matrix \mathbf{F} with matrix \mathbf{G} such that:

$$\mathbf{G} = \mathbf{F} \mathbf{J} \quad (51)$$

and the columns of matrix \mathbf{G} contain as many near-zero loadings as possible, \mathbf{J} being an orthogonal matrix of rotations. This can be exemplified for a hypothetical variable x_1 with the loadings plotted in the plane of two principal components f_1 and f_2 . If the initial axis f_1 goes to the position of g_1 and f_2 goes to g_2 , then the length of the projection of x_1 on g_1 and on g_2 will be, respectively,

$$g_1(x_1) = \ell(x_1) \cos \theta \quad (52a)$$

$$g_2(x_1) = \ell(x_1) \sin \theta \quad (52b)$$

(where $\ell(x_1)$ is the length of the vector x_1) and one new projection can be chosen smaller, the other one becoming larger than the initial ones, as shown schematically in Figure 5.5.9.

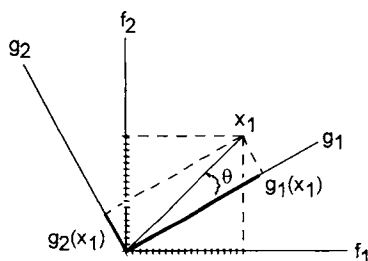


FIGURE 5.5.9. Projection of a vector x_1 on two systems of orthogonal axes such that its projection can be small on one new axis and large on the other one.

Computer programs are available obtaining a matrix \mathbf{G} to optimize the requirement of as many near-zero elements as possible [74]. Although it is common that the factors are determined using computer algorithms, the results of principal component analysis may be interpretable. In the application of factor analysis to a set of mass spectra, the factors are linear combinations of the intensities of different masses [78]. The coefficients b_{ij} are the loadings of the peak intensities x_{ij} , to describe their contribution to z_{ij} , and a large loading of one variable has to be accompanied by high loading of variables strongly correlated with that variable. As an example, pectin pyrolysis with different degrees of methylation was studied [76a] using principal component analysis. Figure 5.5.10 shows the plot of principal component mass loadings for the first vs. the second principal component. Figure 5.5.10 shows that the analysis is dominated by two pairs of ions: the pair $m/z = 95$ and 96 and the pair $m/z = 85$ and 86 . Masses $m/z = 95$ and 96 can be attributed to furancarboxaldehyde, which dominated the spectrum of pectin with low DM values, while the mass $m/z = 85$ is related to the 4-(hydroxymethyl)-1,4-butyrolactone.

A correlation between two variables can be either positive or negative. The interpretation of the factors in terms of patterns in the samples is the most difficult part and not always possible. However, a particular combination of m/z values in a mass spectrum can be indicative of the presence of a chemical compound in the sample. A tool for interpretation, similar to that utilized to interpret canonical variates, is the *factor spectrum* with intensities $s_i b_{ij}$ (where s_i is the standard deviation of each column in the data matrix X). This spectrum, plotting the values $s_i b_{ij}$ at m/z_i , shows the part of the intensity change described by the factor. In other words, such a spectrum will show those masses that contribute the most to the discrimination of the samples. Because the loadings b_{ij} generally can be either positive or negative, the factor spectrum exhibits positive and negative intensities.

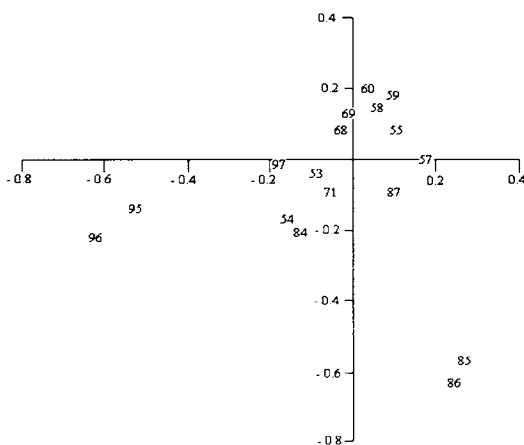


FIGURE 5.5.10. The plot of m/z loadings for the first vs. the second principal component in a Py-MS analysis of pectin methylation.

An interesting utilization of the factors can be obtained from the assumption that any variable x_{ij} is influenced by various factors that are more or less shared by other variables. In this approach each of the variables can be described in terms of these factors:

$$x_{hj} = c_{j1} z_{h1} + c_{j2} z_{h2} + c_{j3} z_{h3} \dots + c_{jr} z_{hr} \quad (53a)$$

or in matrix notation:

$$X_s = Z_s F' \quad \text{or} \quad X_s = Z_s G' \quad (53b)$$

According to these equations the intensities in a pyrolysis mass spectrum can be divided into a number of contributions from different factors, possibly different chemical components [81, 82]. The intensity of a factor in a particular mass spectrum, called the *factor score*, can be obtained from rel. (53a or 53b). The coefficients c_{ji} are a measure of the relative contribution of the individual factors to the intensities at a given m/z value. The factor scores of the first factor show the largest variation in the set of spectra [83, 84]. Score plots of one of the factors for each mass "h" (see rel. 53a) allow sometimes a differentiation of the masses with specific contribution from classes of compounds [85]. Also, scattered score plots of the first two discriminant factors may reveal

structural characteristics in the sample [78]. Computer programs are available for this type of data processing and for the visualization of the results [81]. Data processing performed as previously described has been applied to numerous practical problems (e.g. [76a], [78a]).

The most useful result of multivariate analysis procedures is the reduction in apparent dimensionality of the data. From an initial collection of several hundred mass peaks, the data are reduced to only a few factors, each of which is by definition a linear combination of the original mass peak intensities. By plotting these linear combinations in the form of spectra, significant information about the chemical components underlying the factors can be obtained. Often this requires rotation of the factors in order to optimize the chemical component patterns.

Most of the procedures using multivariate data processing were used for qualitative purposes such as classification and identification of microorganisms, differentiation of capsular polysaccharides of different bacteria, or fossil biomaterials, etc. Quantitation was also possible in identifying adulteration of several foods [86].

- Other techniques utilized in the analysis of Py-MS data.

An alternative approach to the use of multivariate data analysis for the processing of Py-MS results is the use of artificial neural networks, which were proven useful in revealing nonlinear relationships in multivariate data. The advantage of neural networks comes from the fact that it is possible to "train" them. Training is effected by presenting the networks with "known" inputs and outputs and modifying the connection weights between the individual nodes of the network and the biases according to a back-propagation algorithm (normally using nonlinear weighting function or activation function) until the output nodes of the network match the desired outputs with a certain degree of accuracy. A neural network consisting of only one hidden layer, with an arbitrarily large number of nodes, can learn any nonlinear mapping of a continuous function to an arbitrary degree of accuracy. The most common architecture is the fully interconnected feed-forward artificial neural networks (ANNs).

The network effectiveness during training is usually determined in terms of the root-mean square error between the actual and the desired outputs averaged over the training set. The ANN is then fed with unknown inputs and will then immediately output the globally optimal best fit to the outputs. If the outputs from the previously unknown inputs are accurate, the trained ANN is said to be generalized. The method is useful for the quantitative analysis of Py-MS data because ANNs are considered to be relatively robust to noisy data such as those that may be generated by Py-MS. Fully interconnected feed-forward ANNs were utilized, for example, in a study attempting to quantitate the number of microorganisms in a mixture with glycogen [87].

Genetic programming (GP) is another technique using computers for processing Py-MS data. This technique is a computerized procedure that uses the concepts of Darwinian selection to generate and optimize a desired function or mathematical expression. An initial random population of individuals, each encoding a function or expression, is generated, and their fitness to reproduce the desired output is assessed. New individuals are generated either by mutation (the introduction of one or more random

changes to a single parent individual) or by crossover (randomly rearranging functional components between two or more parent individuals). The fitness of the new individuals is assessed, and the best individuals from the total population become the parents of the new generation. This process is repeated until either the desired result is achieved or the rate of improvement in the population becomes zero. It has been shown that if the parent individuals are chosen according to their fitness values, the genetic method can approach the theoretical optimum efficiency for a search algorithm. This type of approach was utilized to process Py-MS data for food analysis [87].

5.6 Infrared Spectroscopy (IR) Used as a Detecting Technique for Pyrolysis.

Infrared spectroscopy has been used in combination with different thermal experiments as a convenient tool of analysis. For example, IR-EGA (infrared evolved gas analysis) was used for obtaining information on different thermal and combustion processes [89]. A simple IR attachment where the sample can be pyrolysed close to the IR beam is available (Pyroscan/IR available from CDS Analytical). A gas stream can be controlled to flush the pyrolysate.

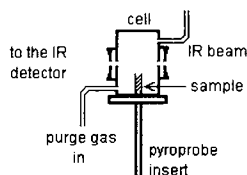


FIGURE 5.6.1. Schematic diagram of a pyrolysis IR attachment (based on CDS PyroScan/IR system)

Infrared (IR) spectrometers, particularly Fourier transform infrared (FTIR) instruments have also been used as detectors in gas chromatography [90] offering the capability of compound quantitation and identification similarly to MS instruments, although with lower sensitivity. When a pyrolyser is used at the front end of the chromatograph, it usually acts just as a convenient way of sample transformation/injection into the GC/FTIR. A few basic concepts related to IR instrumentation are given below.

The IR absorption of electromagnetic energy is caused by the capability of specific parts of molecules to vibrate with certain frequencies. Such a frequency (in wavenumbers) can be expressed by the relation:

$$\bar{\nu} = (2\pi c)^{-1} [\kappa (m_1 + m_2) / m_1 m_2]^{-1/2} \quad (1)$$

where κ is a force constant, c speed of light, and m_1 , m_2 are the masses of the atoms forming the bond which vibrates. The vibrational energy of the molecule is obtained from quantum theory and can be expressed as

$$E_{\text{vib}} = \sum_{k=1}^s hc [(v_k + 1/2) - (v_k - 1/2)^2 \chi] \bar{\nu}_k \quad (2)$$

where the sum is taken over all normal vibrations, h is Planck's constant, χ is an anharmonicity constant, v_k is the vibrational quantum number ($v_k = 1, 2, 3, \dots$), and $\bar{\nu}_k$ is

the “classical” or “equilibrium” frequency (in wavenumbers) for each normal vibration (see e.g. [77]). The transitions between different energy levels E_{vib} of the molecule (if they are not forbidden by the selection rules) will give the frequency the molecule can absorb. The transition between ground state (all $\nu_k = 0$) and the state with one of the $\nu_k = 1$ are so called fundamental vibrations. These are more intense in the spectra, which commonly appear as broadened bands due to the rotational transitions associated with each vibration.

The common IR spectrophotometers generate an *absorption* (or *transmission*) *spectrum*, which gives the variation of the IR absorption (transmission) of a sample as a function of frequency in a range (expressed in wavenumbers) between about 300 cm^{-1} to 4000 cm^{-1} . The IR spectrum can be used for compound identification (as a fingerprint) or for quantitation (commonly using a specific frequency). The quantitation is based on Beer's law, which shows that the absorption is proportional with the concentration of the analyte absorbing at a given frequency.

The common IR systems consist of an IR source (with a continuous spectrum), a light dispersive device, a sample holder, and a detector. The “classical” technique to select a specific frequency (with a narrow bandwidth) is done with a monochromator using gratings or prisms made from KBr, NaCl, etc. The Fourier transform IR is based on a different principle, and the FTIR instruments have a different design. The instrument contains a Michelson interferometer with a moving mirror traveling in the direction x , back and forth, starting at a point where the two beams have zero path difference (see Figure 5.6.2).

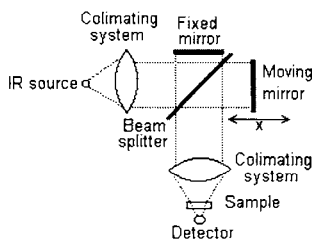


FIGURE 5.6.2. Schematic diagram of a Michelson interferometer used in the FTIR instruments.

The intensity $I(x)$ measured by the detector depends on the position of the moving mirror, and it is given by the relation:

$$I(x) = \int_{-\infty}^{\infty} I(\nu) \cos 2\pi\nu x \, d\nu \quad (3a)$$

This x depending intensity $I(x)$ is numerically changed (using a computer program) into frequency depending intensity using the inverse Fourier transform:

$$I(\nu) = 1/2\pi \int_{-\infty}^{\infty} I(x) \cos 2\pi\nu x \, dx \quad (3b)$$

The plot of $I(\nu)$ is in fact the IR spectrum. The FTIR has significant advantages over “classical” IR, mainly related to the capability to record a spectrum in a very short time

interval. This allows FTIR to be hyphenated with GC (and other separation techniques). Two different procedures were utilized in GC/FTIR:

- the lightpipe procedure, and
- sample collection on a moving, cooled surface.

The lightpipe procedure passes the eluting materials from the GC through a low volume lightpipe, which is commonly heated and is coated inside with a reflecting material (gold). The lightpipe acts as an on-line gas cell, and the IR spectrum is recorded in scans as frequently as the FTIR can measure a spectrum. The results can be processed as usual IR spectra, although the regular IR spectra are measured at room temperature and not in gas phase. Some differences are seen from standard IR spectra for certain compounds, but libraries with prerecorded spectra in standard conditions can still be used for sample identification.

The other procedure uses a "trapping" system of the GC eluting materials on a moving surface that is cooled at sufficiently low temperature. The collection is commonly done on a cold zinc selenide plate. This plate moves at a constant speed, such that a given point on the plate corresponds to a given time during the chromatographic process. The plate is then inspected using FTIR microscopy (see e.g. [91]), and the IR spectrum is recorded. Some procedures involve the addition of a make-up gas (such as argon) together with the GC eluting materials, and the analytes are trapped in a solid argon matrix (for this purpose the cooling must be appropriate). The IR spectra of cooled materials (with or without the argon matrix) also can show some differences from standard IR spectra due to the reduction of rotational energy that leads to narrower bands in IR.

Although the IR detectors are not as popular as the MS, pyrolysis-gas chromatography / Fourier transform IR (Py-GC/FTIR) occasionally has been used in polymer analysis. Such applications have been commonly related to the analysis of certain gases such as CO₂, CO, CH₄, NH₃, etc., where the MS analysis is less successful. Py-GC/FTIR has been applied in several studies of plant materials [92] and in analysis of peat [93]. Py-GC/FTIR was utilized, for example, for the analysis of humic substances and their metal derivatives [94], starch derivatives [94a], and for synthetic polymer analyses [38a].

5.7 Other Analytical Techniques in Pyrolysis.

As indicated previously (see Section 1.2) pyrolysis must be associated with an analytical technique in order to provide information on a sample. Several common analytical techniques such as GC, GC/MS or GC/FTIR have been utilized either hyphenated with pyrolysis or off-line and were described previously. Less frequently, techniques such as HPLC, preparative LC, TLC, SFE/SFC, or NMR also have been used for the analysis of pyrolysates. These types of techniques are commonly applied off-line. They are used mainly for obtaining information on that part of the pyrolysate that is difficult to transfer directly to an analytical system such as a GC or for the analysis of materials associated with the char. However, the analysis of the non-volatile part of pyrolysates is frequently neglected, although this leads to an incomplete picture regarding the chemical composition of pyrolysates.

The HPLC (high performance liquid chromatography) technique is widely applied for the analysis of numerous analytes, and a large amount of information is available regarding the subject (e.g. [95]). HPLC has also been utilized as an off-line [96] or as an on-line [96a] technique for the analysis of pyrolysates of different materials. The technique consists of extracting the pyrolysate (off-line or on-line) with an appropriate solvent, followed by HPLC separation and analysis. In HPLC, the chromatographic separation takes place in a column filled with a stationary phase while a liquid mobile phase is pumped through the column. Similarly to the GC separation, the partition of each analyte between the two phases is different, leading to different retention times for the components of the mixture. The block diagram of an HPLC system is given in Figure 5.7.1.

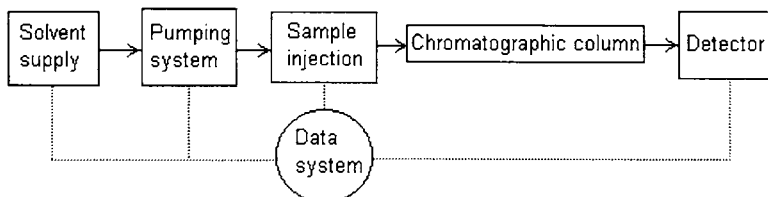


FIGURE 5.7.1. Block diagram of an HPLC system.

An on-line system utilized for lignin pyrolysate analysis [96a] consists of a Curie point pyrolyser connected on-line with an HPLC system. The pyrolysis is performed in argon, and then a system of switching valves allows a solvent to flush the pyrolysing chamber, dissolve the pyrolysate, and carry it to the chromatographic system. The switching valves allow two positions A and B, as shown in Figure 5.7.2. The operation is performed in three stages, A-B-A. In the first stage A, the sample is pyrolysed while the pump 2 delivers eluent to the precolumn and the analytical column (for equilibration). In stage B, the solvent is flushed through the pyrolysing chamber, dissolves the pyrolysate, and carries it to the precolumn where it is completely adsorbed. This process takes a certain period of time, and it is necessary to focus the analytes at the beginning of the precolumn. In the second stage A, the analytes are back flushed from the precolumn and sent to the analytical column and further to the detection system.

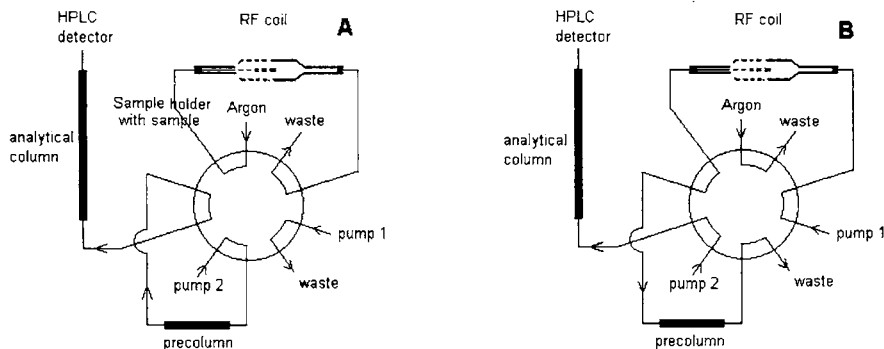


FIGURE 5.7.2. On-line Py-HPLC system which works in three stages A-B-A [96a]. First stage A, pyrolysis. Stage B, flush the pyrolysing chamber and carry the analytes to the precolumn. Second stage A, the analytes are back flushed and sent to the analytical column.

The theory of chromatographic separation in HPLC is not too different from the theory for GC separation. A series of concepts already described for GC in Section 5.2 are applicable to HPLC, such as: capacity factor (rel. 5, Section 5.2), number of theoretical plates (rel. 17a, Section 5.2), separation factor (rel. 30, Section 5.2), resolution (rel. 31 and rel. 34, Section 5.2), peak capacity (rel. 44, Section 5.2), etc. Although most chromatographic columns used in HPLC are packed columns and the associated number of theoretical plates is much smaller than in GC (on the order of several thousands), the solvents used can cover a wide variety and solvent mixtures can also be utilized as a mobile phase. In addition to this, solvent gradients (with a variable composition during separation) can also be used in HPLC. The temperature influences the HPLC separation less than the GC one, although some techniques require temperature control of the chromatographic column. A wide variety of stationary phases are used in HPLC, and they are classified in two general groups:

- direct phases, which are polar (commonly silica covered with water and -OH groups, or polar chemically bonded phases on silica) and are utilized with non-polar solvents such as CH_2Cl_2 , hexane, etc. and
- reverse phases, which are practically non-polar (hydrocarbon chains chemically attached to a solid support that can be silica, zirconia, or organic polymeric materials) and are utilized with polar solvents such as water, CH_3OH , CH_3CN , etc.

Besides standard columns, a variety of other column types are known, such as those used for size exclusion, ion exchange, etc.

The detectors used in HPLC also can be of different types based on the measurement of the refractive index, UV-visible absorption, fluorescence, etc. LC/MS utilizing special sample introduction systems is also common for the analysis of the eluents from the HPLC systems. The most common detector in HPLC is probably the one using UV-visible absorption. However, some compounds such as those generated from the pyrolysis of carbohydrates have low UV-visible absorption. For this reason, derivatization techniques are sometimes applied to attach chromophoric groups to the sugar molecule. For example, in a study of pyrolysis products of cellulose and amylose, the pyrolysate was first per-O-benzoylated and then separated by HPLC with UV-visible detection; then fractions were collected and analyzed by MS for peak identification [96]. Another example is the off-line LC/MS analysis of the pyrolysis products of a melanoidin polymer obtained from ammonia and glucose [97]. Compound identification is less straightforward in LC/MS due to the lack of fragmentation in typical LC/MS spectra. As an example, the LC/MS spectrum of deoxyfructosazine (MW = 304) obtained using thermospray ionization is shown in Figure 5.7.3. No fragmentation is seen in this spectrum, and the ion with $m/z = 328$ (possibly due to a cluster with Na) adds no structural information. The spectrum identification was done using the standard compound.

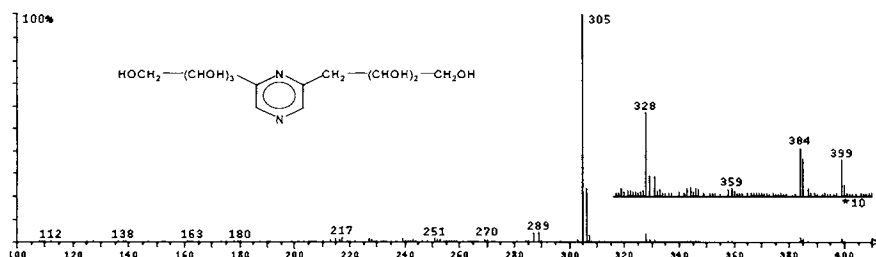


FIGURE 5.7.3. LC/MS spectrum of 2,6-deoxyfructosazine.

Other ionization techniques were also utilized in LC/MS such as FAB, which puts the sample in a liquid matrix such as glycerol and uses fast atom bombardment as the source of energy for the ions. This technique practically does not heat the sample, allowing the formation of molecular ions for certain unstable molecules. An example of a FAB spectrum for syringoresinol detected in lignin pyrolysis is given in Figure 5.7.4.

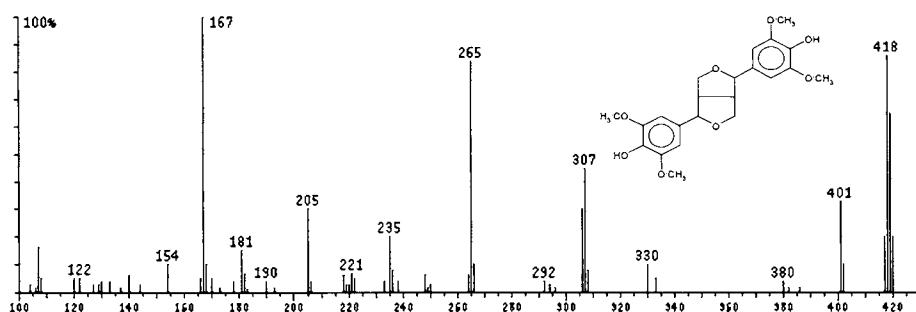


FIGURE 5.7.4. LC continuous FAB mass spectrum of syringoresinol.

Besides thermospray and FAB, other LC/MS ionization techniques are known such as electrospray, or atmospheric pressure ionization (APCI). As LC/MS becomes more common, more studies on pyrolysates using these techniques are likely to be done.

Another chromatographic technique utilized for the analysis of pyrolysates is thin layer chromatography (TLC) [98, 98a]. TLC can be utilized as an off-line simple technique for the analysis of pyrolysates, with the possibility to visualize the presence of species that do not elute through the stationary phase and remain at the start line of the TLC plate. Supercritical fluid extraction (SFE) and supercritical fluid chromatography (SFC) also have been utilized for the off-line analysis of pyrolysates [99]. The procedure consists of placing off-line the pyrolysate in the extractor, followed by capillary SFC separation and FID detection of the extract.

Nuclear magnetic resonance (NMR) studies on pyrolysates also have been performed [100]. In NMR the sample absorbs electromagnetic radiation in radio-frequency region when placed in an external uniform magnetic field and irradiated with radio frequency. The nuclear spin of a variety of atoms is different from zero (such as for ^1H , or ^{13}C), and these nuclei can be aligned in the same direction in a (strong) magnetic field (only a small fraction of nuclei is in fact aligned because of thermal disorder). The atoms with

spin 1/2, for example, can assume two energy levels corresponding to the spin in the direction of the field (low energy) and in the opposite direction of the field. The difference in energy between these two levels is given by the relation:

$$\Delta E = h\nu = \mu H_o / I \quad (1)$$

where h is Planck's constant, H_o is the strength of the magnetic field (in gauss), μ is the nuclear magnetic moment, and I is the spin number. The values for μ are significantly different for different atom types, and a single type of nuclei can be studied in a given NMR experiment (such as protons).

As far as rel. (1) indicates, for one atomic species such as ^1H , or ^{13}C , one single precise frequency will be absorbed. However, the nuclei are shielded from an external magnetic field by their electron cloud. The electron density around each nucleus may vary from molecule to molecule [101], and this variation modifies the absorbed frequency as given by rel. (1). The difference in the absorbing frequency of a particular atom from a reference atom is called *chemical shift*. The result field H_o , which determines the resonance behavior of the nucleus, will be, therefore, different from the applied field H_{appl} , and using a *shielding parameter* σ it can be written:

$$H_o = H_{\text{appl}} - \sigma H_{\text{appl}} \quad (2)$$

The most generally used reference compound in NMR is tetramethylsilane (TMS). This substance absorbs at higher field than almost all organic compounds for both ^1H (used in proton NMR) or for ^{13}C (used in ^{13}C NMR). In a relative NMR scale, TMS is set at 0 Hz at the right edge of the scale. A chemical shift parameter can be calculated using this reference. Applying rel. (2) to the reference and to a sample, it results:

$$\sigma_{\text{ref}} = (H_{\text{ref}} - H_o) / H_{\text{ref}} \quad \text{and} \quad \sigma_{\text{spl}} = (H_{\text{spl}} - H_o) / H_{\text{spl}} \quad (3)$$

From rel. (3), a chemical shift parameter δ expressed in ppm can be obtained as

$$\delta = (\sigma_{\text{ref}} - \sigma_{\text{spl}}) 10^6 \quad (4a)$$

or introducing the values for σ_{ref} and σ_{spl} given by rel. (3), it can be obtained:

$$\delta = (H_{\text{ref}} - H_{\text{spl}}) / H_{\text{ref}} 10^6 \quad (4b)$$

The quantity δ is dimensionless and expressed in ppm. The value of δ varies up to about 10 units for different types of protons depending on the chemical structure of the compound. The range for different types of ^{13}C is up to about 220 units.

The resonance absorbance peaks for a given substance corresponding to different values of the chemical shift of atoms in different surroundings will generate the NMR spectrum. Empirical correlations are available between the structural arrangements of organic groups and the chemical shift parameter δ for both proton and ^{13}C NMR. The absorption of the energy for a certain δ being proportional with the number of the absorbing atoms in the molecule, peak areas may indicate the relative number of atoms of a specific kind. NMR analysis is widely used for structural determinations.

Modern instruments are Fourier transform NMR, which use a constant magnetic field commonly produced by a superconducting magnet and a strong radio-frequency pulse that irradiates the sample. The *free induction decay* signal emission of the sample is

detected as a function of time, and its Fourier transform is a frequency function, which represents the NMR spectrum.

NMR has not been very frequently associated with pyrolysis. An example is the use of NMR to understand the modification in lignin during pyrolysis. The NMR spectrum of a lignin pyrolysate is shown in Figure 5.7.5 [100].

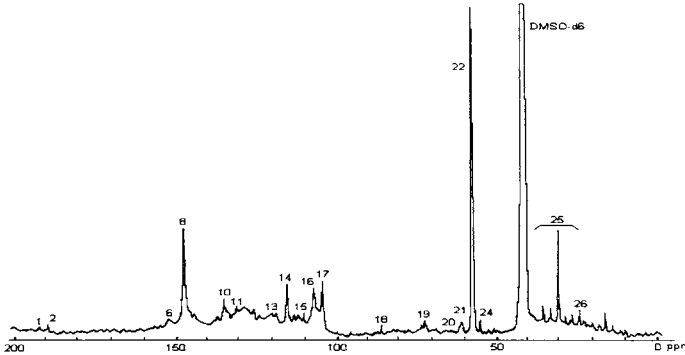


FIGURE 5.7.5. ^{13}C NMR spectrum of a lignin pyrolysate [100]. Some peak assignments are given in Table 5.7.1.

TABLE 5.7.1. Assignments for the most important peaks in the ^{13}C NMR spectrum of pyrolytic lignin.

Peak No.	Chemical shift	Assignment*
1	~ 193	α -CHO
2	~ 191	γ -CHO in cinnamaldehyde
6	~ 152	C3-C5 in syringyl (etherified)
8	148.3	C3-C5 in syringyl (non-etherified) C, in guaiacyl
10	135.4	C, in guaiacyl (etherified)
11	131.7	C β in cinnamaldehyde
13	~119	C6, in guaiacyl (etherified)
14	115.5	C5 in guaiacyl (non-etherified) C3 / C5 in p-hydroxyphenyl
15	~111	C2 in guaiacyl (etherified)
16	107.2	C2 / C6 in syringyl with α -CHO
17	104.3	C2 / C6 in syringyl
18	~ 86	C β , in β -O-4
19	~72	C α , in β -O-4
20, 21	~60 62	C γ , in β -O-4 and phenylcoumaran
22, 23	56.3	Methoxyl in syringyl and guaiacyl. resp.
24	~ 54	C β in phenylcoumaran units
25, 26	15-45	Saturated aliphatic side chain

*The term etherified refers only to the link at C4 and not to methoxyls. Some assignments were tentative.

Even electrochemical methods have been used for monitoring pyrolysis products. As an example, the volatile pyrolysis products of pine needles were analyzed using simultaneously oxidation-reduction potentiometry, pH-metry, and conductometry [102].

References 5.

1. I. Ericsson, *J. Anal. Appl. Pyrol.*, 8 (1985) 73.
- 1a. W. J. Irwin, *Analytical Pyrolysis*, Marcel Dekker Inc., New York, 1982.
2. M. M. Mulder, J. J. Boone, *Nederlands Tijds. voor Natuurkunde*, B56 (1990) 73.
3. J. Hetper, M. Sobera, *J. Chromatog. A*, 776 (1997) 337.
4. S. Tsuge, *Trends in Anal. Chem.*, 1 (1981) 87.
5. M. Neeman, *Tetrahedron* 6 (1959) 36.
6. A. E. Pierce, *Silylation of Organic Compounds*, Pierce Chemical Co., Rockford, 1968.
7. R. B. Watts, R. G. O. Kekwick, *J. Chromatog.*, 88 (1974) 15.
8. A. Zlatkis, B. C. Petitt, *Chromatographia*, 2 (1969) 484.
9. M. Donike, *J. Chromatog.*, 78 (1973) 273.
10. D. R. Knapp, *Handbook of Analytical Derivatization Reactions*, Wiley, New York, 1979.
11. D. E. Bradway, T. Shafik, *J. Chromatog. Sci.*, 15 (1977) 322.
12. T. M. Tulp, O. Hutzinger, *J. Chromatog.*, 139 (1977) 51.
13. F. K. Kawahara, *Anal. Chem.*, 40 (1968) 2073.
14. I. C. Cohen, *J. Chromatog.*, 44 (1969) 251.
15. J. F. Laurence, *J. Agr. Food Chem.*, 22 (1974) 936.
16. R. B. Bruce, W. R. Maynard, *Anal. Chem.*, 41 (1969) 977.
17. R. E. Weston, B. B. Wheals, *Analyst* 95 (1970) 680.
18. A. C. Moffat, E. C. Horning, *Anal. Lett.*, 3 (1970) 205.
19. L. D. Matcalfe, A. A. Schmitz, *Anal. Chem.*, 33 (1961) 363.
20. D. T. Downing, *Anal. Chem.*, 39 (1967) 218.
21. P. A. Biondi, M. Cagnasso, *J. Chromatog.*, 109 (1975) 389.
22. C. W. Gehrke, K. Leimer, *J. Chromatog.*, 57 (1971) 219.
23. T. P. Mawhinney, R. S. Robinett, A. Atalay, M. A. Madison, *J. Chromatog.*, 358 (1986) 231.

24. D. Roach, C. W. Gehrke, *J. Chromatog.*, 43 (1969) 303.
25. J. Korolczuk, *J. Chromatog.*, 88 (1974) 177.
26. Y. Hoshika, Y. Takata, *J. Chromatog.*, 120 (1976) 379.
27. E. Nakamura et al., *J. Am. Chem. Soc.*, 98 (1976) 2346.
28. J. A. Lomax, J. M. Commandeur, P. W. Arisz, J. J. Boon, *J. Anal. Appl. Pyrol.*, 19 (1991) 65.
29. R. L. Grob, *Modern Practice of Gas Chromatography*, J. Wiley, New York, 1995.
30. F. Reif, *Statistical Physics*, McGraw Hill Book Co., New York, 1967.
31. M. J. E. Golay, *Gas Chromatography* ed. by V. J. Coates, H. J. Noebels, I. S. Fagerson, Academic Press, New York, 1958.
32. L. S. Ettre, *Open Tubular Columns in Gas Chromatography*, Plenum, New York, 1965.
33. J. C. Giddings, *J. Chromatog.*, 4 (1960) 11.
34. J. C. Giddings, in *Gas Chromatography* ed. by N. Brenner, J. E. Callen, M. D. Weiss, Academic Press, New York 1962.
35. *Alltech Chromatography Catalog 350*, Alltech Assoc. Inc., Deerfield, 1995.
- 35a. J. B. Forehand, S. C. Moldoveanu, unpublished results.
36. K. Grob, *Classical Split and Splitless Injection in Capillary GC*, Heuting, Heidelberg, 1986.
- 36a. R. P. W. Scott, *Introduction to Analytical Gas Chromatography*, M. Dekker Inc., New York, 1997.
37. R. Buffington, M. K. Wilson, *Detectors for Gas Chromatography*, Hewlett-Packard, 1987.
38. J. H. Beynon, *Mass Spectrometry and its Applications to Organic Chemistry*, Elsevier, Amsterdam, 1960.
- 38a. R. Oguchi, A. Shimizu, S. Yamashita, K. Yamaguchi, P. Wylie, *J. High Res. Chromatog.*, 14 (1991) 412.
39. F. W. McLafferty, *Interpretation of Mass Spectra*, Univ. Science Books, Mill Valley, 1980.
40. K. J. Hyver, ed., *High Resolution Gas Chromatography*, Hewlett-Packard, 1989.
- 40a. H. J. Cortes, *Multidimensional Chromatography*, M. Dekker, Inc. New York, 1990.

- 40b. J. K. Whelan, J. M. Hunt, A. Y. Huc, *J. Anal. Appl. Pyrol.*, 2 (1980) 79.
- 40c. S. A. Liebman, E. J. Levy, *Pyrolysis and GC in Polymer Analysis*, M. Dekker, New York, 1985.
- 40d. S. C. Moldoveanu, unpublished results.
41. E. Kovats, *Helv. Chim Acta*, 41 (1958) 1915.
42. L. S. Ettre, *Anal. Chem.*, 36 (1964) 31A.
- 42a. P. G. Vincent, M. M. Kulik, *Appl. Microbiol.*, 20 (1970) 957.
43. W. Jennings, T. Shibamoto, *Qualitative Analysis of Flavor and Fragrance Volatiles by Glass Capillary Gas Chromatography*, Academic Press, New York, 1980.
- 43a. C. G. Smith, *J. Anal. Appl. Pyrol.*, 15 (1989) 209.
44. F. C-Y. Wang, *Anal. Chem.*, 69 (1997) 667A.
- 44a. J. B. Forehand, S. C. Moldoveanu, unpublished results.
45. K. L. Bush, G. L. Glish, S. A. McLuckey, *Mass Spectrometry/Mass Spectrometry: Techniques and Applications of Tandem Mass Spectrometry*, VCH, New York, 1988.
- 45a. *Eight Peak Index of Mass Spectra*, The Royal Soc. of Chem., Cambridge, UK, 1991.
- 45b. J. B. Forehand, N. P. Kulshreshtha, S. C. Moldoveanu, 49th TCRC, Lexington, 1996.
- 45c. CDS Analytical Inc. polymer library of global spectra.
46. P. D. Zeman, *Anal. Chem.*, 24 (1952) 1709.
47. H. L. C. Meuzelaar, J. Haverkamp and F. D. Hileman, *Pyrolysis Mass Spectrometry of Recent and Fossil Biomaterials*, Elsevier, Amsterdam, 1982.
- 47a. A. P. Snyder, G. A. Eiceman, W. Windig, *J. Anal. Appl. Pyrol.*, 13 (1988) 243.
48. K. Qian, W. E. Killinger, M. Casey, *Anal. Chem.*, 68 (1996) 1019.
- 48a. R. J. Helleur, R. Guevremont, *J. Anal. Appl. Pyrol.*, 15 (1989) 85.
49. W. Winding, P. G. Kistemaker, J. Haverkamp, H. L. C. Meuzelaar, *J. Anal. Appl. Pyrol.*, 1 (1979) 39.
50. P. P. Schmidt, W. Simon, *Anal. Chim. Acta*, 89 (1977) 1.
51. M. A. Posthumus, N. M. M. Nibering, A. J. H. Boerboom, *Org. Mass. Spectrom.*, 11 (1976) 907.

52. N. Vanderborgh, R. Jones, *Anal. Chem.*, 55 (1983) 527.
53. H. L. C. Meuzelaar, P. G. Kistemaker, M. A. Posthumus, *Biomed. Mass Spectrom.*, 4 (1975) 139.
54. R. M. Lum, *Thermochimica Acta*, 18 (1977) 73.
55. R. M. Lum, *Amer. Lab.*, 10 (1978) 47.
56. H. D. Beckey, H.-R. Schulten, in *Mass Spectrometry, Part A*, C. Merritt Jr., C. N. Evans (Ed.) M. Dekker Inc., New York, 1979, p. 145.
57. H.-R. Schulten, W. Gortz, *Anal. Chem.*, 50 (1978) 428.
58. H.-R. Schulten, H. D. Beckey, H. L. C. Meuzelaar, A. J. H. Boerboom, *Anal. Chem.*, 45 (1973) 191.
59. H.-R. Schulten, in *Analytical Pyrolysis*, C. E. R. Jones, C. A. Cramers Ed., Elsevier, Amsterdam, 1977, p. 17.
60. A. D. Pouwels, G. B. Eijkkel, P. W. Arisz, J. J. Boon, *J. Anal. Appl. Pyrol.*, 15 (1989) 71.
61. W. Genuit, J. J. Boon, *J. Anal. Appl. Pyrol.*, 8 (1985) 25.
- 61a. A. D. Hendricker, F. Basile, K. J. Voorhees, *J. Anal. Appl. Pyrol.*, 46 (1998) 65.
62. N. Washida, H. Akimoto, H. Tagaki, M. Okuda, *Anal. Chem.*, 50 (1978) 910.
63. C. Fenselau, *Anal. Chem.*, 69 (1997) 661A.
64. G. J. Q. van der Peyl, J. Haverkamp, P. G. Kistemaker, *Intern. J. Mass Spectrom. Ion Phys.*, 42 (1982) 125.
65. D. A. King, *Surf. Sci.*, 47 (1975) 384.
66. I. V. Blestos, D. M. Hercules, D. Graifendorf, A. Benninghoven, *Anal. Chem.*, 57 (1985) 2384.
67. D. F. Torgerson, R. P. Skowronsky, R. D. MacFarlane, *Biochem. Biophys. Res. Commun.*, 60 (1974) 616.
68. A. Bellistreri, D. Gorozzo, M. Giuffrida, G. Montaudo, *Anal. Chem.*, 59 (1987) 2024.
69. J. C. Huges, B. B. Wheals, M. J. Whitehouse, *Forensic Sci.*, 10 (1977) 334.
70. C. Liteanu, I. Rica, *Teoria si Metodologia Statistica a Analizei Urmelor*, Ed. Scrisul Romanesc, Craiova, 1979.
71. E. L. Crow, F. A. Davis, M. W. Maxfield, *Statistics Manual*, Dover, New York, 1960.

- 71a. Solution for Science vol. 39, SciTech, Chicago, 1997, e-mail: science@scitechint.com.
72. D. L. Massart, A. Dijkstra, L. Kaufman, *Evaluation and Optimization of Laboratory Methods and Analytical Procedures*, Elsevier, Amsterdam, 1978.
73. D. W. Poxon, R. G. Wright, *J. Chromatog.*, 61 (1971) 142.
74. P. E. Green, *Analyzing Multivariate Data*, The Dryden Press, Hinsdale, 1978.
75. H. J. H. MacFie, C. S. Gutteridge, J. R. Norris, *J. Gen. Microbiol.*, 104 (1978) 67.
76. W. Eshius, P. G. Kistemaker, H. L. G. Meuzelaar, in *Analytical Pyrolysis*, C. E. R. Jones, C. A. Cramers Ed., Elsevier, Amsterdam, 1977, p. 151.
- 76a. R. E. Aries, C. S. Gutteridge, W. A. Laurie, J. J. Boon, G. B. Eijkel, *Anal. Chem.*, 60 (1988) 1489.
- 76b. H. J. H. MacFie, C. S. Gutteridge, *J. Anal. Appl. Pyrol.*, 4 (1982) 175.
77. S. C. Moldoveanu, *Aplicatiile Teoriei Grupurilor in Chimie*, Ed. Stiintifica si Enciclopedica, Bucharest, 1975.
78. A. van der Kaaden, J. J. Boon, J. Haverkamp, *Biomed. Mass. Spectrom.*, 11 (1984) 486.
79. W. Windig, P. G. Kistemaker, J. Haverkamp, H. L. C. Meuzelaar, *J. Anal. Appl. Pyrol.*, 2 (1980) 7.
80. W. Windig, P. G. Kistemaker, J. Haverkamp, *J. Anal. Appl. Pyrol.*, 3 (1982) 199.
81. H. L. C. Meuzelaar, W. Winding, A. M. Harper, S. M. Huff, W. H. McClennen, J. M. Richards, *Science*, 226 (1984) 268.
82. W. Windig, J. Haverkamp, P. G. Kistemaker, *Anal. Chem.*, 55 (1983) 81.
83. R. Hoogerbrugge, S. J. Willig, P. G. Kistemaker, *Anal. Chem.*, 55 (1983) 1710.
84. L. V. Vallis, H. J. MacFie, C. S. Gutteridge, *Anal. Chem.*, 57 (1985) 704.
85. W. Windig, H. L. C. Meuzelaar, *Anal. Chem.*, 56 (1984) 2297.
86. R. E. Aries, C. S. Gutteridge, in *Applications of Mass Spectrometry in Food Science*, J. Gilbert Ed., Elsevier, London, 1986.
87. R. Goodacre, N. J. Neal, D. B. Kell, *Anal. Chem.*, 66 (1994) 1070.
88. R. J. Gilbert, R. Goodacre, A. M. Woodward, D. B. Kell, *Anal. Chem.*, 69 (1997) 4381.

89. S. A. Liebman, D. H. Ahlstrom, P. R. Griffiths, *Appl. Spectrosc.*, 30 (1976) 355.
90. R. White, *Chromatography/Fourier Transform Infrared Spectroscopy and its Applications*, M. Dekker, New York, 1991.
91. G. W. Ewing, *Analytical Instrumentation Handbook*, M. Dekker Inc., New York, 1997.
92. J. O. Lephardt, R. A. Fenner, *Appl. Spectrosc.*, 34 (1980) 174.
93. G. D. Calvert, J. S. Esterle, J. R. Durig, *J. Anal. Appl. Pyrol.*, 16 (1989) 5.
94. X. Q. Lu, A. M. Vassallo, W. D. Johnson, *J. Anal. Appl. Pyrol.*, 43 (1997) 103.
- 94a. K. C. Patel, R. D. Patel, *Chem. Era*, 2 (1978) 30.
95. G. Szepesi, *How to Reverse Phase HPLC*, VCH Pub. Inc., New York, 1992.
96. P. W. Arisz, J. A. Lomax, J. J. Boon, *Anal. Chem.*, 62 (1990) 1519.
- 96a. E. R. E. van der Hage, J. J. Boon, *J. Chromatog. A*, 736 (1996) 61.
97. S. C. Moldoveanu, unpublished results.
98. F. Shafizadeh, R. H. Furneux, T. T. Stevenson, T. G. Cochran, *Carbohydrate Res.*, 61 (1978) 1519.
- 98a. S. Yamaguchi, J. Hirano, Y. Isoda, *J. Anal. Appl. Pyrol.*, 16 (1989) 159.
99. J. H. Raymer, C. S. Smith, E. D. Pellizzari, G. Velez, *J. Liquid Chromatog.*, 13 (1990) 1261.
100. D. St. A.G. Radlein, J. Piskorz, D. S. Scott, *J. Anal. Appl. Pyrol.*, 12 (1987) 51.
101. S. C. Moldoveanu, A. Savin, *Aplicatii in Chimie ale Metodelor Semiempirice de Orbitali Moleculari*, Ed. Academiei R. S. Romania, Bucuresti, 1980.
102. S. Liodakis, D. Gakis, M. Statheropoulos, N. Tzamtzis, A. Pappa, *J. Anal. Appl. Pyrol.*, 43 (1997) 139.

This Page Intentionally Left Blank

PART 2.

Analytical Pyrolysis of Organic Biopolymers

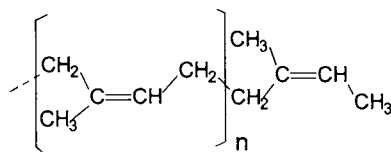
This Page Intentionally Left Blank

Chapter 6. Analytical Pyrolysis of Polyterpenes

6.1 Natural Rubber.

Rubber is a natural product that exists as a colloidal dispersion named latex in the sap of certain plants from various families such as Moraceae, Compositae or Euphorbiaceae. From this last family, *Hevea brasiliensis* is the most common plant that produces natural rubber for practical use. The latex has rather large colloidal particles (in aqueous medium) with diameters up to 5 μm (although the average is 0.5 μm). These particles are made from aggregates of 10^6 to 10^8 macromolecules of polyisoprene. The presence of the isoprene molecule in the structure of natural rubber makes it part of the polyterpenes family of compounds [1].

The stability of latex is due to a thin layer of proteins on particles, which acts as a colloid stabilizer. Natural rubber is practically obtained by the precipitation and drying of the latex. The precipitation is done with acids (acetic acid is commonly used for this purpose) when the isoelectric point of the protecting protein is reached ($\text{pH} \approx 4.6$). The macromolecules have a MW between $5 \cdot 10^4$ to $3 \cdot 10^5$ Dalton and contain between 600 to 50,000 units of isopentene. Due to the double bond, both *cis* and *trans* isomers are possible for the monomer units. It was determined that natural rubber is an isotactic polymer formed exclusively from *cis* units and has the following (idealized) structure (in reality the polymer is not perfectly planar):



A natural polymer formed from *trans* isopentene units is found in some plants from Sapotaceae family and is known as gutta-percha (or balata when it comes from a South American plant from the same family).

Natural rubber is rather stable below 200° C although some decomposition starts at about 150° C. In the interval between 200° C and 300° C (in the absence of oxygen), some volatile hydrocarbons are generated, but at prolonged heating the main change takes place in the viscosity of rubber, which becomes more viscous and finally sets into an inelastic solid. This solid is assumed to contain cross-linking bonds. The longer this preheating takes place, the less isoprene is generated when the material is pyrolysed. Significant decomposition with formation of smaller molecules takes place only beginning at 290–300° C. The main pyrolysis product, depending on temperature, is DL-limonene (or dipentene) when the pyrolysis is done below 450° C and isoprene (2-methyl-1,3-butadiene) when the pyrolysis is done above this temperature [2]. The yield of isoprene as a function of temperature during the pyrolysis in a microfurnace [3] gave the results shown in Figure 6.1.1. The dependence on temperature of the ratio of isoprene/(isoprene dimer) was shown in Figure 4.1.2.

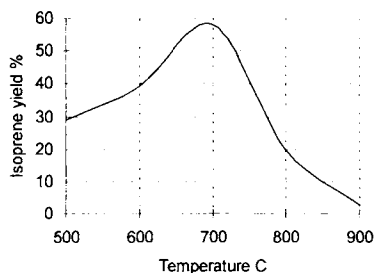


FIGURE 6.1.1. Yield of isoprene as a function of temperature in the pyrolysis of natural rubber in a microfurnace.

Other pyrolysis products besides isoprene and its dimer are also formed from rubber. The more volatile compounds with the maximum of five carbon atoms generated from the pyrolysis of natural rubber at 700° C are indicated in Table 6.1.1.

TABLE 6.1.1. Volatile pyrolysis products (C_5 or lower) from natural rubber.

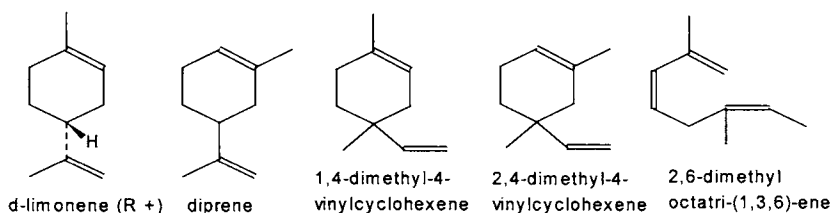
Compound	Formula	MW
methane	CH ₄	16
ethene	C ₂ H ₄	28
ethane	C ₂ H ₆	30
propene	C ₃ H ₆	42
propane	C ₃ H ₈	44
1,3-butadiene	C ₄ H ₆	54
1-butene	C ₄ H ₈	56
2-methylpropene	C ₄ H ₈	56
2-butene (<i>cis</i>)	C ₄ H ₈	56
2-butene (<i>trans</i>)	C ₄ H ₈	56
methylpropane	C ₄ H ₁₀	58
butane	C ₄ H ₁₀	58
isoprene	C ₅ H ₈	68
3-methyl-1-butene	C ₅ H ₁₀	70
1-pentene	C ₅ H ₁₀	70
2-methyl-1-butene	C ₅ H ₁₀	70
2-pentene (<i>trans</i>)	C ₅ H ₁₀	70
2-pentene (<i>cis</i>)	C ₅ H ₁₀	70
2-methyl-2-butene	C ₅ H ₁₀	70

A pyrolysis study done at 384° C [4] showed that isoprene is about 28% (by weight) and 60% is DL-limonene. Other compounds with more than five carbon atoms were also detected in natural rubber pyrolysate. Some of them are shown in Table 6.1.2.

TABLE 6.1.2. *Compounds heavier than C₅ from the pyrolysis of natural rubber.*

Compound	Formula	MW
3-methyl-1,3-pentadiene	C ₆ H ₄	76
toluene	C ₇ H ₈	92
2,3-dimethylcyclopentene	C ₇ H ₁₂	96
m-xylene	C ₈ H ₁₀	106
2,3-dimethylcyclohexene	C ₈ H ₁₄	110
octene	C ₈ H ₁₆	112
1,5-dimethyl-5-vinylcyclohexene	C ₉ H ₁₄	122
1-methyl-4-ethylcyclohexene	C ₉ H ₁₆	124
dipentene	C ₁₀ H ₁₆	136
Hydrocarbon ?	C ₁₁ H ₁₈	150
Hydrocarbon ?	C ₁₂ H ₁₈	162
Hydrocarbon ?	C ₁₅ H ₂₄	204
Hydrocarbon ?	C ₁₆ H ₂₆	218

Besides DL-limonene, other isomers were also identified in the rubber pyrolysates [5], including a linear compound:



Pyrolysis-field ionization MS performed on natural rubber at 315° C [6] generated the spectrum shown in Figure 6.1.2. The results from Py-FI MS show that the main pyrolysis compounds are oligomers of isoprene corresponding to $m/z = (68)_k$ where $k = 1, 2, \dots, 19$. However, at trace level other series are present [6] such as $m/z = (68)_k + 2$, $m/z = (68)_k - 2$, $m/z = (68)_k + 12$, $m/z = (68)_k - 12$, $m/z = (68)_k + 14$, $m/z = (68)_k - 14$. The series $m/z = (68)_k + 2$ corresponding to $C_5H_9-(C_5H_8)_k-C_5H_9$ and the series $m/z = (68)_k - 2$ corresponding to $C_5H_7-(C_5H_8)_k-C_5H_7$ may come from disproportionation of the free radicals. Series $m/z = (68)_k + 12$, $m/z = (68)_k - 12$, $m/z = (68)_k + 14$, and $m/z = (68)_k - 14$ may come from the free radicals formed by random scission of the chain, as exemplified in Section 2.6, reaction B. *Cis-trans* isomerizations may also occur during pyrolysis, but the isomers are not distinguished by Py-FI MS. As seen in the spectrum, the ion corresponding to $m/z = 136$ is the most abundant. Limonene was found to account for most of this peak.

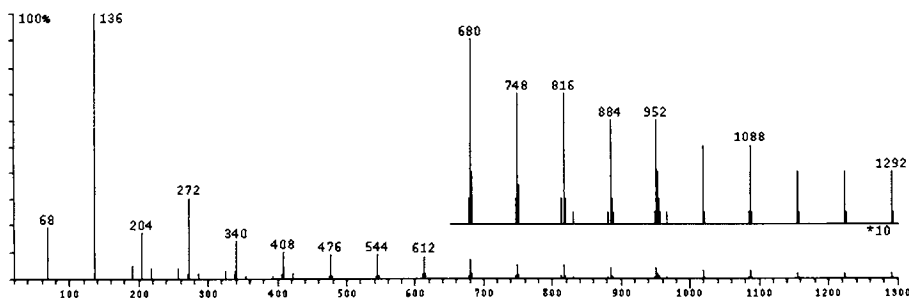


FIGURE 6.1.2. *Py-field ionization MS spectrum of natural rubber at 315° C [6].*

A Py-GC study [7] with pyrolysis done at 500° C showed numerous peaks corresponding to the isoprene dimers, trimers . . . up to hexamers eluting in clusters of peaks. The separation was done on a methyl silicone 5% phenyl silicone type column with FID detection. The results from a Py-GC/MS study [8] where natural rubber was pyrolysed at 580° C in a Curie point Py-GC/MS on-line system showed similar results. The TIC trace of the pyrolysate with the separation done on a 60 m Carbowax column, 0.32 mm i.d., 0.25 μ m film thickness, with the temperature gradient of the GC oven between 40° C and 240° C, is shown in Figure 6.1.3. Some peak identifications are shown in Figure 6.1.3.

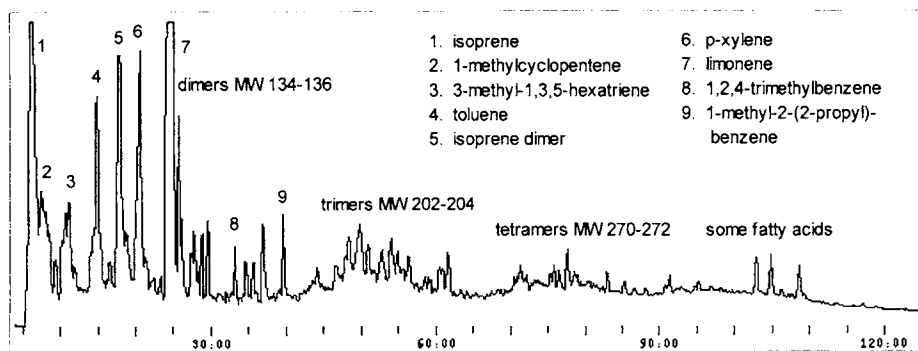
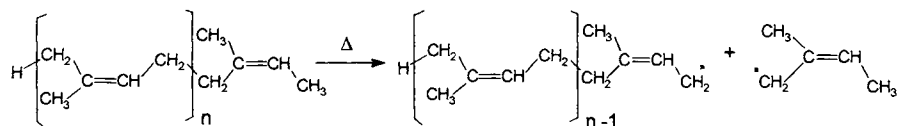


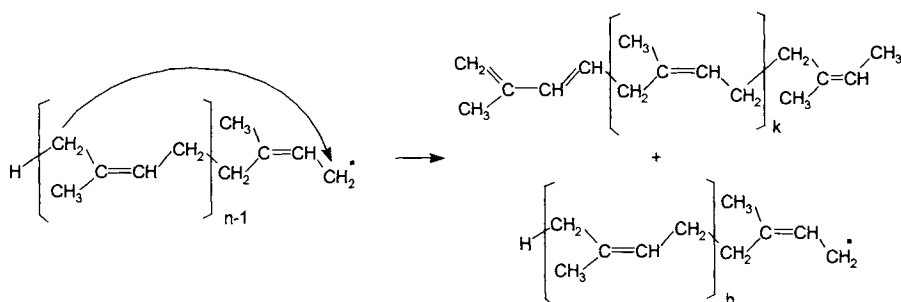
FIGURE 6.1.3. *TIC chromatogram obtained by Py-GC/MS of natural rubber at 580° C.*

Among the compounds identified besides isoprene and its oligomers are several aromatic hydrocarbons. Also, a few fatty acids were identified. Low levels of aldehydes were detected in the fresh rubber latex, and the presence of the acids in the pyrolysate is not unexpected [9]. However, these acids may also come from contaminants in the pyrolysis experiment. The peaks corresponding to pentamers and hexamers were not obvious in Figure 6.1.3, possibly due to the separation conditions or due to a higher pyrolysis temperature. Some compounds other than those indicated in Figure 6.1.3 were reported to be present in natural rubber pyrolysate [4,10], but their detection may depend on specific pyrolysis conditions and on the sensitivity of the analytical procedure.

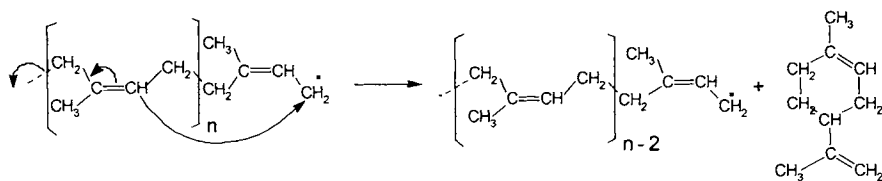
The pyrolysis of natural rubber takes place by a free radical mechanism as described in Section 2.6. The β -chain scission is the dominant initiation process and the bond dissociation reaction was estimated to be about $61.5\text{--}63 \text{ kcal mol}^{-1}$:



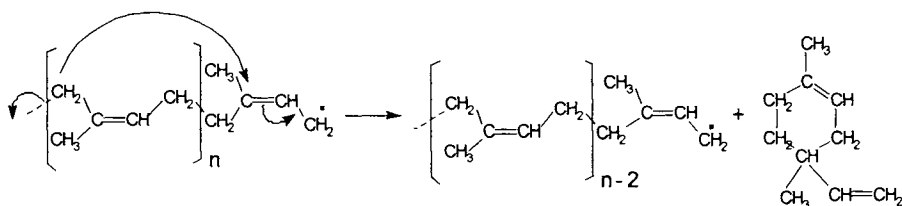
The main series of oligomers can be explained by the reactions where an intramolecular radical transfer takes place:



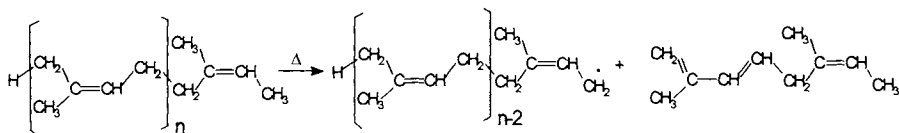
The compounds with the formula $\text{C}_5\text{H}_7\text{--}(\text{C}_5\text{H}_8)_k\text{--C}_5\text{H}_9$ will have the molecular weight $(68)_k$ where $k = 0, 1, 2, \dots$. The formation of 1-methyl-4-isopropenylcyclohexene (DL-limonene) during the pyrolysis of polyisoprene also comes from an intramolecular transfer step:



Other cyclic dimers can be formed by the following scheme:



The linear dimer may be formed directly from the polymer by chain scission under the influence of heat:



Besides the main series, each of the minor series can be explained by the depolymerization and disproportionation reactions as shown in Section 2.6, associated with C-C scissions of the radicals.

The rate of pyrolysis has been also reported [4]. First order overall kinetics was demonstrated, and the \log_{10} of the rate constant as a function of temperature is shown in Figure 6.1.4.

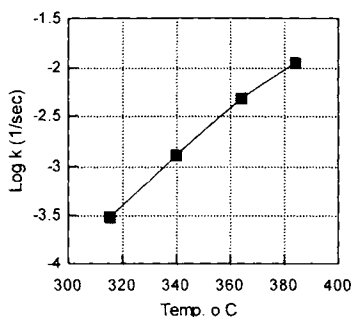
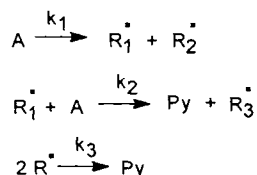


FIGURE 6.1.4. \log_{10} of the rate constant as a function of temperature.

Representing the free radical chain scission by the reactions:



the rate of pyrolysis k is expressed by

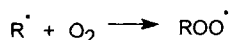
$$k = k_2 (k_1 / k_3) [Py] \quad (1)$$

and the activation energy is

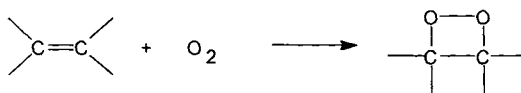
$$\Delta E = \Delta E_2 + 1/2 \Delta E_1 + 1/2 \Delta E_3 \quad (2)$$

From pyrolysis kinetics data it was calculated that $\Delta E \approx 41 \text{ kcal mol}^{-1}$. By estimating $\Delta E_2 \approx 18 \text{ kcal mol}^{-1}$, $\Delta E_1 \approx 62 \text{ kcal mol}^{-1}$, $\Delta E_3 \approx 9 \text{ kcal mol}^{-1}$, the calculated ΔE is $44.5 \text{ kcal mol}^{-1}$.

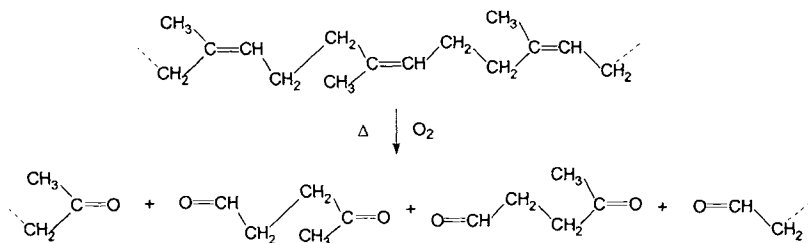
Natural rubber was also studied regarding pyrolysis in the presence of oxygen. Thermal oxidation of natural rubber is assumed always to be associated with scission, although photo-oxidation at low temperature may involve peroxide formation without scission. The effect of oxygen is to increase the reaction rate of scission and therefore to decrease the temperature where the scission starts. The oxidation may take place after the initial formation of a free radical that reacts with oxygen:



The peroxide radical can go to a product by abstraction and generate for example an acid and another radical. Commonly, acetic acid and also formic acid are formed in considerable amount during oxidative pyrolysis. The previous mechanism can probably explain the formation of these small molecules. The oxygen (singlet oxygen) may also react with the double bond forming a dioxetane intermediate:



The O-O bond is weak (30–50 kcal/mol) and may break with the formation of aldehydes or ketones. One main product in scission/oxidation of rubber is levulinialdehyde, and formally its formation can be written as:



The main oxidation products found during oxidative pyrolysis of natural rubber are given in Table 6.1.3.

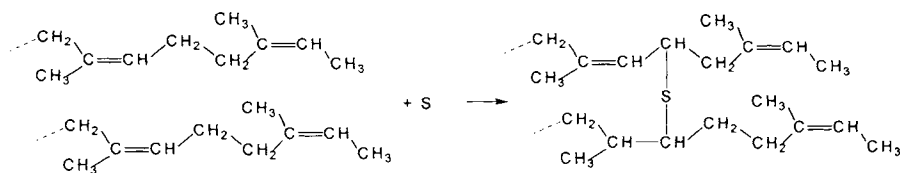
Several applications of analytical pyrolysis on natural rubber have been reported. One such application is the determination of particles of rubber in atmospheric dust [11]. In this work, isoprene peak was utilized for rubber identification in a Py-GC system, the pyrolysis being performed at 740° C. Most other applications were related to the determination of natural rubber in complex mixtures [3] and synthetic rubber mixtures.

TABLE 6.1.3. *Oxidative pyrolysis products of natural rubber.*

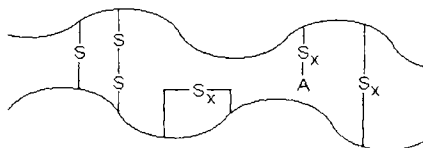
Compound	Formula	MW
water	H ₂ O	18
carbon monoxide	CO	28
carbon dioxide	CO ₂	44
formic acid	CH ₂ O ₂	46
methanol	CH ₄ O	32
acetaldehyde	C ₂ H ₄ O	44
acetic acid	C ₂ H ₄ O ₂	60
methyl formate	C ₂ H ₄ O ₂	60
ethanol	C ₂ H ₆ O	46
pyruvaldehyde	C ₃ H ₄ O ₂	72
acetone	C ₃ H ₆ O	58
propionaldehyde	C ₃ H ₆ O	58
methyl acetate	C ₃ H ₆ O ₂	74
butenone	C ₄ H ₄ O	70
2-methylpropenaldehyde	C ₄ H ₆ O	70
butanone	C ₄ H ₈ O	72
2-methylfuran	C ₅ H ₆ O	82
β-angelica lactone (5-methyl-2(5H)-furanone)	C ₅ H ₆ O ₂	98
levulinialdehyde	C ₅ H ₈ O ₂	100
γ-valerolactone	C ₅ H ₈ O ₂	100
hexanedione	C ₆ H ₈ O ₂	112

6.2 Vulcanized Rubber.

In practice, the most important chemical modification of natural rubber is vulcanization. Vulcanization is applied for the modification of mechanical properties of natural rubber, mainly regarding the temperature range of elasticity, which is considerably extended. The process consists of a chemical reaction with sulfur (1–3%), which takes place at 130–145° C. Besides sulfur, a reaction at room temperature with S₂Cl₂ is sometimes used for vulcanization. The reaction takes place as follows:



The final product may contain sulfur in cyclic or pendent groups or may contain polysulfide bridges as suggested in the following scheme:



A larger amount of sulfur added to natural rubber (20–30%) generates a different product, vulcanite. Besides sulfur, during the vulcanization process other chemical compounds are commonly added to rubber. One group of such compounds consists of *vulcanization accelerators* (A in the previous scheme). Substances such as diphenylguanidine, mercaptobenzothiazole, tetramethythuram disulfide, N-oxidiethylene-2-benzothiazolylsulfenamide, and cyclohexylbenzothiazolylsulfenamide are utilized as accelerators.

Also, antioxidants were found to decrease the aging rate of natural rubber. Among the *antioxidants* more frequently used are N-phenyl- β -naphthylamine, 2,6-di-tert-butyl-4-methyl-1-hydroxybenzene (BHT), N-isopropyl-N'-phenyl-p-phenylenediamine, N-(1,3-dimethylbutyl)-N'-p-phenylenediamine, and poly-(2,2,4-trimethyl-1,2-dihydroquinoline).

Other materials commonly added to vulcanized rubber are plasticizer agents, such as stearic acid or other long chain fatty acids, waxes, long chain hydrocarbons, etc. Also a significant amount of carbon black, some mineral oxides (ZnO), etc. are added to modify the mechanical properties of rubber.

Pyrolysis of vulcanized rubber generate the same compounds as natural rubber [10, 12] (see Section 6.1) and in addition H_2S , SO_2 , CH_3SH . Also, the temperatures at which vulcanized rubber starts decomposing are higher.

A typical Py-mass spectrum of vulcanized rubber is given in Figure 6.2.1 [13]. The values $m/z = 32, 34, 48$ and 64 are probably with contribution from sulfur compounds.

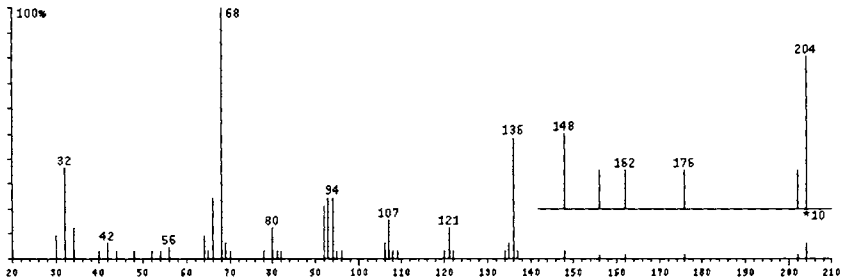
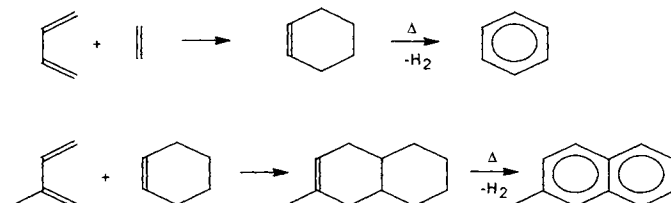


FIGURE 6.2.1. *Py-mass spectrum of vulcanized rubber.*

Vulcanized rubber pyrograms frequently show, in addition to the compounds generated by the pyrolysis of polyisoprene, other compounds such as benzothiazole, which are generated by the pyrolysis of the additives.

One important industrial application of vulcanized rubber pyrolysis is related to the processing of used tires (which are generated worldwide at a rate of over 5 million tons per year). The shredded scrap tires are commonly pyrolysed between 450 and 600° C, generating char (37–38 wt.%), oils (53–58 wt.%), and gases (4–9 wt.%) [14, 15]. The gases are composed mainly of H_2 , CH_4 , C_4H_6 , CO , CO_2 . Other aliphatic hydrocarbons were also detected in gases. The oils contain a mixture of hydrocarbons, with DL-limonene as a main component (see Table 6.1.2). However, of special interest was the

evaluation of the level of aromatic hydrocarbons and of polynuclear aromatic hydrocarbons (PAH) in the pyrolysis oils. The concentration of light aromatic hydrocarbons in pyrolysis oils as a function of temperature is indicated in Table 6.2.1. The formation of aromatic hydrocarbons during rubber pyrolysis can be explained by a combination of Diels Alder condensations and pyrolytic dehydrogenations of the type:



or by rearrangements followed by small molecule eliminations of the type

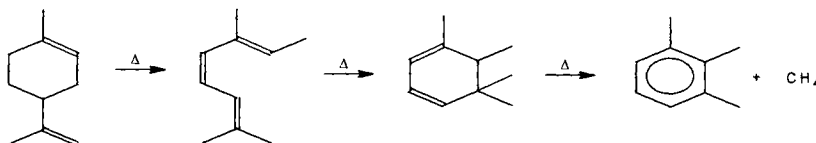


TABLE 6.2.1. The concentration (in ppm) of light aromatic hydrocarbons in tire pyrolysis oils as a function of temperature.

Name of the compound	Temperature					
	450° C	475° C	500° C	525° C	560° C	600° C
benzene	<5	55	770	2950	70	605
toluene	2250	3200	6095	17740	7770	5070
ethylbenzene	250	235	120	405	370	190
1,2-dimethylbenzene	2780	3190	3345	5710	5875	3530
1,4-dimethylbenzene	2750	2665	3620	6880	8350	3120
styrene	1205	1705	1950	3545	3635	1915
1,3-dimethylbenzene	920	1020	1325	2450	2570	1040
trimethylbenzene	840	825	1255	085	1285	820
trimethylbenzene	1050	1265	1670	1240	1530	1200
trimethylbenzene	1550	1350	2370	2320	3210	1450
methylstyrene	730	570	1090	1145	1590	715
trimethylbenzene	1075	1070	1325	1295	1395	1095
4-methylstyrene	730	570	1090	1145	1590	715
trimethylbenzene	370	440	490	675	320	330
methylstyrene	6020	6025	7630	8865	9030	6950
limonene	31320	30330	29010	28965	24590	25130
indene	2190	2630	3175	3090	3105	1560

The formation of PAHs can be easily explained from further dehydrogenations and eliminations of aromatic compounds with a lower number of aromatic rings. A few structures of these compounds detected in tire pyrolysis oils are given below, and the concentration of PAHs in this material as a function of temperature [14] is indicated in Table 6.2.2.

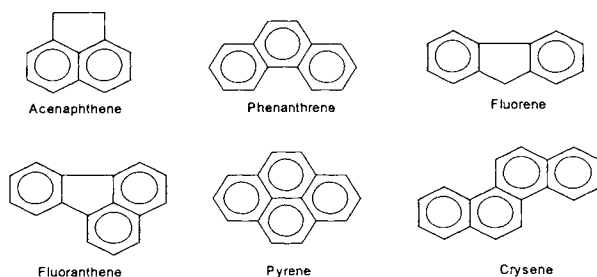


TABLE 6.2.2. *The concentration (in ppm) of polynuclear aromatic hydrocarbons in tire pyrolysis oils as a function of temperature.*

Name of the compound	Temperature					
	450° C	475° C	500° C	525° C	560° C	600° C
naphthalene	465	420	725	1115	665	1630
2-methylnaphthalene	650	570	730	770	1005	2365
1-methylnaphthalene	460	490	625	645	895	1570
biphenyl	1030	1040	1630	885	1320	3000
1-ethylnaphthalene	430	510	690	830	745	1335
2,6-dimethylnaphthalene	565	565	855	755	995	1990
1,7-dimethylnaphthalene	550	440	365	1020	700	560
1,6-dimethylnaphthalene	275	600	595	715	485	1085
1,5-dimethylnaphthalene	190	305	375	1440	635	880
1,2-dimethylnaphthalene	770	405	600	450	460	1385
acenaphthene	560	580	635	700	620	1070
trimethylnaphthalene	765	470	670	1050	605	825
trimethylnaphthalene	665	515	425	330	830	1570
trimethylnaphthalene	155	175	220	695	430	710
fluorene	280	210	325	290	295	605
methylfluorene	65	180	135	90	240	585
2-methylfluorene	115	245	220	175	335	745
1-methylfluorene	260	340	370	310	450	555
?-methylfluorene	135	200	170	320	195	280
phenanthrene	95	230	200	125	195	315
anthracene	85	160	125	135	225	295
dimethylfluorene	215	425	425	165	320	465
2-methylphenanthrene	595	495	315	470	815	1240
2-methylanthracene	455	640	500	1010	720	1140
4-methylphenanthrene	355	200	140	275	605	730
1-methylphenanthrene	505	890	470	585	600	555
dimethylphenanthrene	745	1200	520	650	760	1290
2,7-dimethylphenanthrene	1255	1300	1740	525	1060	1075
dimethylphenanthrene	105	120	455	350	1260	540
fluoranthene	120	325	325	355	790	1100
dimethylphenanthrene	730	>5	490	445	1490	1210
dimethylphenanthrene	440	385	305	615	5195	370
pyrene	530	105	120	425	225	115
trimethylphenanthrene	530	400	600	470	520	940
trimethylphenanthrene	30	35	65	35	30	150
chrysene	30	15	35	>5	30	60
Total (%)	1.53	1.52	1.72	1.92	2.67	3.43

The level of PAHs in tire pyrolysate is relatively high. Compounds such as benzo [b]fluoranthene, benzo[a]pyrene, dibenz[a,h]anthracene, and dibenz[a,c]anthracene were not reported [14], although they are likely to be present at levels below 1–2 ppm.

Among other applications of pyrolytic techniques in the study of rubber vulcanizates is the evaluation of cross-linking density. Pyrolytic data can be correlated with total crosslink density. A set of results were reported for the correlation between the cross-linking density and the score of the canonical variate function obtained from the pyrolysis data set. The correlation coefficient for this correlation was very good (0.954), proving the possibility to evaluate cross-linking density from pyrolysis data [13]. The results are illustrated in Figure 6.2.2. Similar results were obtained when the cross-linking values were correlated to the ratio of the peak areas or peak heights of dipentene and 3-methyl-1,3-pentadiene detected in the vulcanized rubber pyrolysates [10].

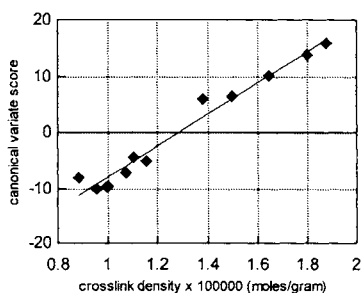
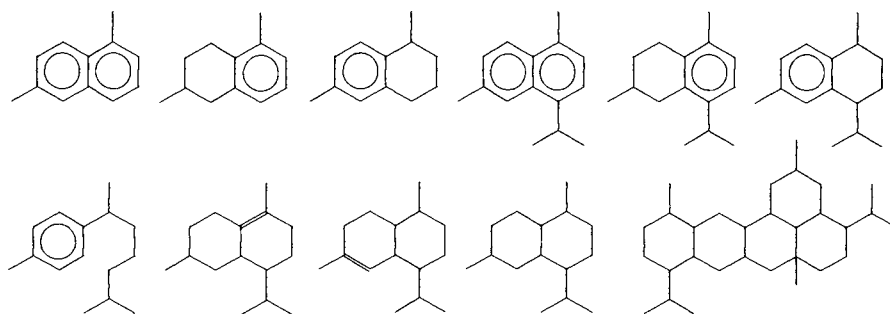


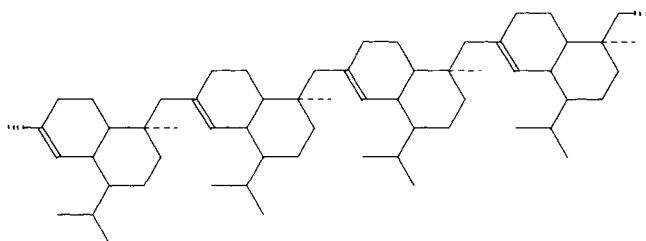
FIGURE 6.2.2. *The correlation between cross-linking density of vulcanized rubber and the canonical variate score.*

6.3 Other Polyterpenes.

Other polymeric terpenes are also known in nature. One such material is the resin called dammar (recent or fossil), generated by the trees from the family Dipterocarpaceae. Pyrolytic studies were performed on this polymer [16] after separation in two fractions, one soluble in CH_2Cl_2 and the other insoluble. Three different pyrolysis techniques were used to obtain information on the insoluble polymer, flash pyrolysis, open isothermal furnace pyrolysis and closed system isothermal pyrolysis. Several compounds separated and identified in pyrolysates by GC/MS are shown below:



Pyrolysis results showed that the basic structural unit in the polymer is cadin-5,6-ene and that the bond between monomers takes place in position C-1 to C-13'. The following structure was proposed for the polymer:



References 6.

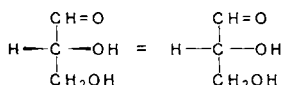
1. 3. C. D. Nenitzescu, *Chimie Organica*, vol. 2 Ed. Technica, Bucuresti, 1958.
2. G. C. Williams, *J. Chem. Soc.*, 15 (1862) 110.
3. A. Krishen, *Anal. Chem.*, 44 (1972) 494.
4. J. C. W. Chien, J. K. Y. Kiang, *Eur. Polym. J.*, 15 (1979) 1059.
5. M. Galin, *J. Macromol. Sci. Chem.*, A7 (1973) 873.
6. R. P. Latimer, *J. Anal. Appl. Pyrol.*, 39 (1997) 115.
7. S. A. Groves, R. S. Lehrle, M. Blazso, T. Szekely, *J. Anal. Appl. Pyrol.*, 19 (1991) 301.
8. J. B. Forehand, S. C. Moldoveanu, unpublished results.
9. D. Craig, A. E. Juve, W. L. Davidson, *J. Polymer Sci.*, 6 (1951) 13.

10. J. Xigao, L. Huiming, *J. Anal. Appl. Pyrol.*, 3 (1981) 49.
11. Y-K. Lee, M. G. Kim, K-J. Whang, *J. Anal. Appl. Pyrol.*, 16 (1989) 49.
12. E. M. Bevilacqua, *Rubber Chem. Technol.*, 38 (1965) 1214.
13. J. L. Savoca, R. Lattimer, J. M. Richards, W. Winding, H. L. C. Meuzelaar, *J. Anal. Appl. Pyrol.*, 9 (1985) 19.
14. A. M. Cunliffe, P. T. Williams, *J. Anal. Appl. Pyrol.*, 44 (1998) 131.
15. F. Cataldo, *J. Anal. Appl. Pyrol.*, 44 (1998) 121.
16. B. G. K. van Aarssen, J. W. de Leeuw, B. Horsfield, *J. Anal. Appl. Pyrol.*, 20 (1991) 125.

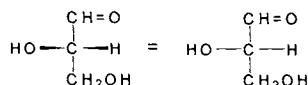
Chapter 7. Analytical Pyrolysis of Polymeric Carbohydrates

7.1. Monosaccharides, Polysaccharides, and General Aspects of their Pyrolysis.

Polymeric carbohydrates (polysaccharides) are built by bonding monosaccharide residues through the elimination of a water molecule and the formation of an ether bond. The general formula for monosaccharides is $C_nH_{2n}O_n$ ($n=3$ for trioses, $n=4$ for tetroses, $n=5$ for pentoses,...). They contain a carbonyl group (aldehyde or ketone) and two or more $-OH$ groups. Glyceraldehyde together with dihydroxyacetone can be considered the simplest monosaccharides. Glyceraldehyde has one asymmetric carbon. Consequently, there are two possible enantiomers, R (or D) and S (or L):

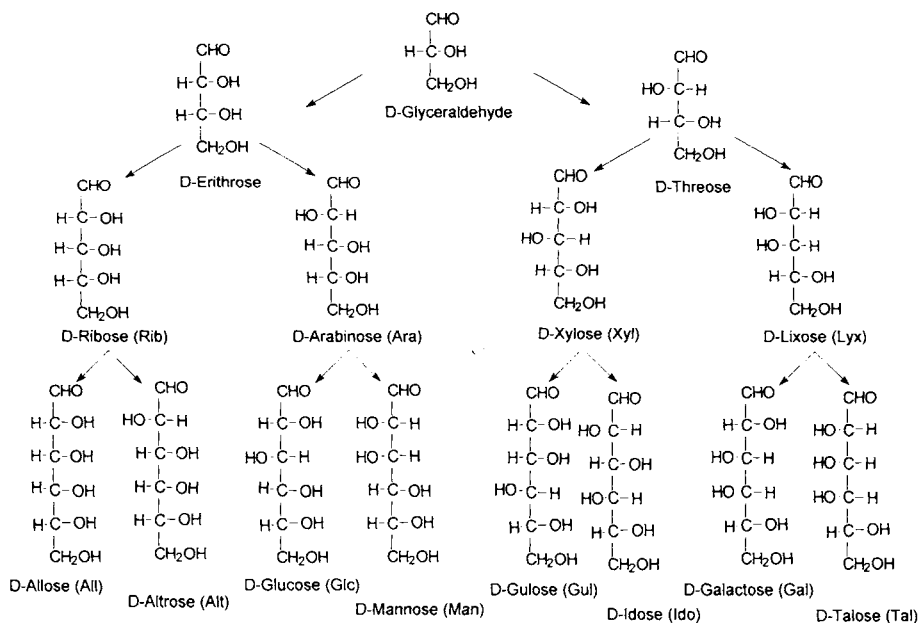


D-Glyceraldehyde



L-Glyceraldehyde

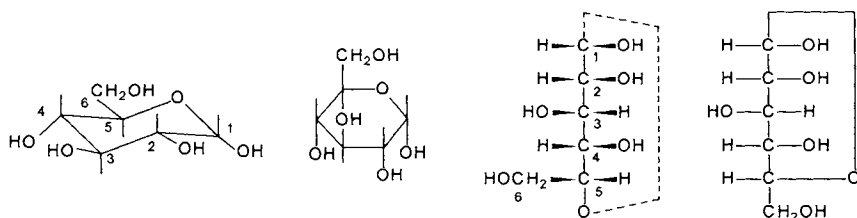
All monosaccharides with a larger number of carbons can be conventionally derived from glyceraldehyde or dihydroxyacetone by adding more $\text{H}-\text{C}-\text{OH}$ groups to the existent one(s). Glyceraldehyde will generate aldoses, while dihydroxyacetone will generate ketoses. The aldoses with the same stereochemistry as D-glyceraldehyde at the asymmetric carbon that is the most distant from the carbonyl group will form a D-series. The D-series of aldoses is shown below.



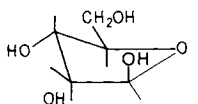
The monosaccharides with the same stereochemistry as L-glyceraldehyde at the most distant asymmetric carbon will form the L-series of aldoses.

For the monosaccharides with $n > 4$, it is common that the carbonyl group forms a cyclic hemiacetal with one of the -OH groups. An example of a common aldohexose is glucose. This substance exists almost entirely in its six-membered cyclic form (glucopyranose). The open chain (linear) form of glucose can be found in water solutions only as a small proportion of the dissolved glucose. Linear glucose is (2R,3S,4R,5R)-2,3,4,5,6-pentahydroxyhexanal. D-Glucopyranose has five asymmetric carbons, four of them with precise steric assignment. For C-1 there are two possible steric forms (two anomers), namely α and β corresponding to S and R configurations, respectively.

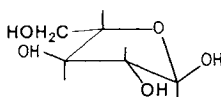
The configurations of monosaccharides are described by several types of formulas. As an example, the following formulas are shown for α -D-glucopyranose: structural, Haworth, modified Fischer, and Fischer. In Fischer formulas the -H or -OH groups are above or below the plane formed by the hemiacetal bonds and the carbon chain (-H bonds are shown shorter).



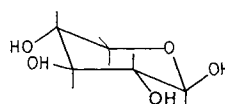
Because polysaccharides are natural macromolecules occurring in all living organisms, the structure of some polysaccharides can be much more complex, as they are not made only from simple monosaccharides. In the composition of natural polymeric carbohydrates, a wide variety of sugars are found. Among these, the most common are pentoses and hexoses. The structural formulas of three common pentoses are shown below. They frequently form cyclic structures with five-member rings (furanoses).



β -D-Ribofuranose (Ribf)

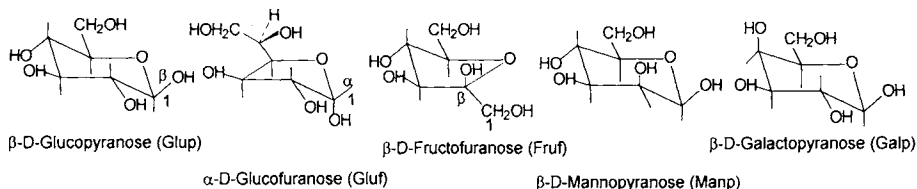


α -L-Arabinofuranose (Araf)



β -D-Xylopyranose (Xylp)

The structural formulas of several common hexoses are shown below.



β -D-Glucopyranose (Glup)

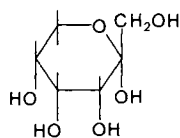
α -D-Glucopyranose (Gluf)

β -D-Fructofuranose (Fruf)

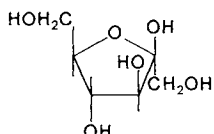
β -D-Mannopyranose (Manp)

β -D-Galactopyranose (Galp)

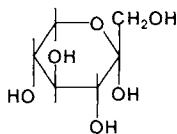
The above structures include fructose, which is a ketohexose. In addition to fructose, there are three other ketohexoses, which are shown below (also with fructose):



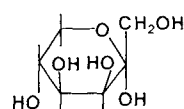
α -D-Psicopyranose



β -D-Fructofuranose

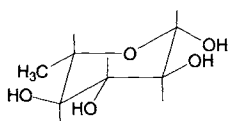


α -D-Sorbose

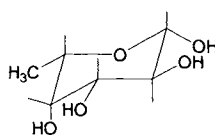


α -D-Tagatose

Besides simple monosaccharides, a large number of associated compounds are found in the structure of natural polysaccharides. Among these are the deoxysugars. The structural formulas of two common deoxyhexoses are shown below:

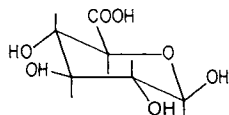


6-Deoxy- β -L-mannopyranose
L-Rhamnopyranose (Rhap)

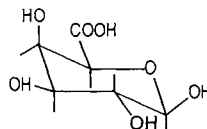


6-Deoxy- β -L-galactopyranose
L-Fucopyranose (Fucp)

Acids related to monosaccharides are also common for the formation of natural polysaccharides. There are three types of acids associated with monosaccharides: aldonic acids generated by the oxidation of the aldehyde group of a monosaccharide, uronic acids generated by the replacement of the primary alcohol group of a monosaccharide by a carboxyl group, and saccharic acids generated by simultaneous oxidation and replacement. Aldonic acids have a marked tendency to eliminate water and form lactones. The structural formulas of two common hexuronic acids are

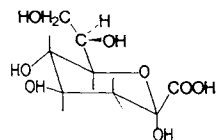


β -D-Glucopyranuronic acid (GlcA)

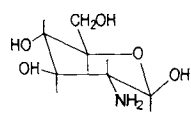


β -D-Galactopyranuronic acid (GalA)

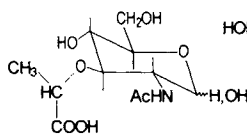
More complicated compounds related to monosaccharides are also implicated in the formation of certain polysaccharides. Acid esters, acids derived from deoxysugars, aminosugars, N-acetylated aminosugars, sialic acids (nonulosaminic acids which are N- or O- substituted derivatives of neuraminic acid), etc., are not uncommon as components in natural polysaccharides. A few of these monosaccharide-related compounds are shown below.



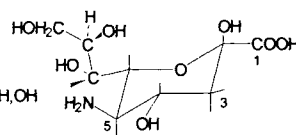
3-Deoxy- β -D-manno-octopyranulosonic acid (KDO)



2-Amino-2-deoxy- β -D-galactopyranose



2-Acetamido-2-deoxy-muramic acid



5-Amino-3,5-dideoxy-D-glycero- α -D-galacto-2-nonulopyranonic acid (Neuraminic acid)

- Pyrolysis of monosaccharides.

Pyrolysis of monosaccharides is relevant for the pyrolysis of polysaccharides that they form as monomeric units. Analytical pyrolysis has been used in several studies to characterize monosaccharides [1, 2]. It was shown for example that some individual monosaccharides give characteristic peaks in Py-MS analysis and that it is possible to distinguish hexoses, pentoses, hexouronic acids and deoxysugars by Py-MS. The technique can also provide evidence for the presence of carbohydrate substituents such as O- or N-acetyl groups, amino groups, or pyruvate substituents [3]. However, Py-MS with EI type ionization does not distinguish well between structural isomers. This is mainly due to the fact that different isomers of anhydro-sugars, which are important pyrolysis products and maintain the steric configuration of the initial monosaccharide, produce similar electron-impact mass spectra [1,2].

There are several classes of compounds formed from rapid pyrolysis of carbohydrates. Besides anhydrosugars, they are carbonyl compounds, furan derivatives, lactones, pyran derivatives, phenols, acids and acid esters, and other compounds. In general, the presence of a substantial quantity of 5-hydroxymethylfuraldehyde in the pyrogram indicates that a hexose is present. Substantial amounts of furaldehyde and the absence of 5-hydroxymethylfuraldehyde in the pyrolysis products indicate the presence of a pentose. However, these markers are not diagnostic for a specific hexose or pentose.

In many instances, the Py-MS of simple sugars were indistinguishable. Many of the pyrolysis products identified from sugars are common to all saccharides. For example, when glucose and galactose are sampled from water, they give similar pyrograms. Only sampling from aqueous boric acid solutions [7] permits their characterization based on the comparison of product peak ratios because of the selective complex reactions of sugars with boric acid.

Because a large number of isomeric products are formed from the pyrolysis of carbohydrates, GC must be used in order to separate and identify isomers by the differences in the retention times. The use of Py-GC or Py-GC/MS for the identification of simple carbohydrates is, however, infrequent. Another problem in the analysis of the pyrolysis product of monosaccharides is that numerous compounds are polar because they partially retain -OH groups from the initial monosaccharide. The analysis of some of these compounds using on-line GC-MS is not always successful. Compounds containing -OH groups are commonly analyzed after derivatization with reagents such as BSTFA (see Section 5.1). A more complete analysis is done by applying two chromatographic techniques, one direct on-line PY-GC/MS and the other off-line pyrolysis followed by GC/MS of the derivatized pyrolysate.

An example of the previously described procedure of using two chromatographic separations is given below for the analysis of the pyrolysates of glucose and of fructose. A typical on-line Py-GC/MS chromatogram for a glucose pyrolysate is given in Figure 7.1.1. The separation was performed on a Carbowax type column, 60 m long, with 0.32 mm i.d. and 0.25 μm film thickness. The temperature for the GC separation was varied between 40° C and 240° C.

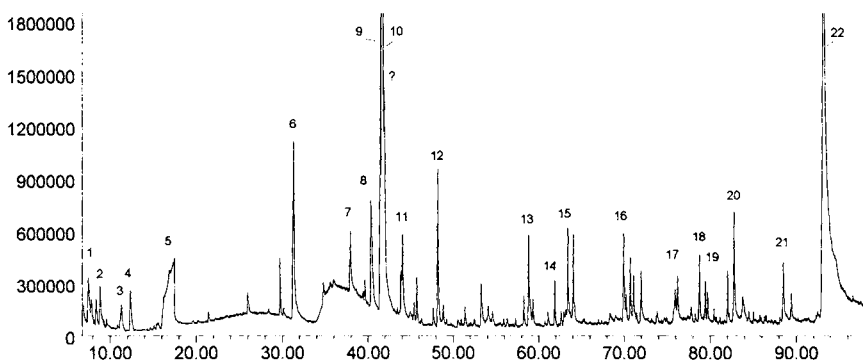


FIGURE 7.1.1. Chromatogram for the pyrolysate of glucose obtained by on-line Py-GC/MS. The peak assignments are #1 furan, #2 2-methylfuran, #3 2,5-dimethylfuran, #4 3-methyl-2-butanone, #5 water, #6 1-hydroxypropanone, #7 hydroxyacetaldehyde, #8 acetic acid, #9 oxopropanoic acid methyl ester, #10 furancarboxaldehyde, #11 1-(2-furanyl)-ethanone, #12 5-methyl-2-furfural, #13 2-hydroxycyclopent-2-en-1-one, #14 2-hydroxy-3-methyl-2-cyclopenten-1-one, #15 2,3-dihydro-5-hydroxy-6-methyl-4H-pyran-4-one, #16 2-methyl-1,3-benzendiol, #17 2,5-dimethyldioxane, #18 2-hydroxy-3-pentanone, #19 5-formyl-2-furfurylmethanoate, #20 2,3-dihydro-3,5-dihydroxy-6-methyl-4H-pyran-4-one, #21 1,4,3,6-dianhydro- α -D-glucopyranose, #22 5-(hydroxymethyl)-furancarboxaldehyde.

A typical chromatogram for a fructose pyrolysate done by on-line Py-GC/MS is given in Figure 7.1.2. The conditions for the separation were similar to those for glucose.

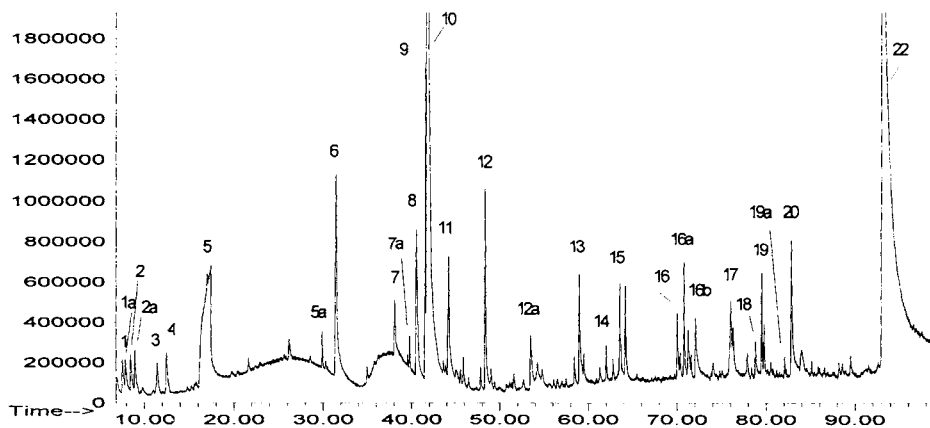


FIGURE 7.1.2. Chromatogram for the pyrolysate of fructose obtained by on-line Py-GC/MS. The peak assignments are the same as in Figure 7.1.1. Peak 21 is missing. In addition, the following peaks were identified: #1a acetaldehyde, #2a propanone, #5a 2,3-butanedione, #7a 5-methyl-2(3H)-furanone, #12a furanmethanol, #16a methyl 2-furoate, #16b 2,5-dimethyl-4-hydroxy-3(2H)-furanone, #19a 1,3,5-benzenetriol.

The peak identification in Figures 7.1.1 and 7.1.2 was done based on mass spectral library search. A list of some characteristic mass peaks, most of them found in both chromatograms, are given in Table 7.1.1.

TABLE 7.1.1. *Characteristic mass peaks for the compounds identified in Figures 7.1.1 and 7.1.2 for glucose and fructose pyrolysates, respectively.*

Peak No.	Compound	MW	Characteristic ions (with relative intensity)
1	furan	68	39(100), 68(62), 58(5)
1a	acetaldehyde	44	29(100), 44(75), 43(32)
2	2-methylfuran	82	82(100), 53(80), 81(75)
2a	propanone	58	43(100), 58(33)
3	2,5-dimethylfuran	96	96(98), 95(80), 81(40)
4	3-methyl-2-butanone	86	43(100), 86(21), 41(15)
5	water	18	18(100), 17(21)
5a	2,3-butanedione	86	43(100), 86(50), 28(42)
6	1-hydroxypropanone	74	43(100), 74(25), 31(20)
7	hydroxyacetaldehyde	60	31(100), 32(48), 60(7)
7a	5-methyl-2(3H)-furanone	98	55(100), 98(95), 43(85), 70(16)
8	acetic acid	60	60(100), 45(85), 43(80)
9	oxopropanoic acid methyl ester	102	43(100), 102(32), 59(4)
10	furancarboxaldehyde	96	96(100), 95(91), 39(40)
11	1-(2-furanyl)-ethanone	110	95(100), 110(44), 39(13)
12	5-methyl-2-furfural	110	110(100), 109(95), 53(40)
12a	furanmethanol	98	98(100), 97(60), 81(60), 69(40)
13	2-hydroxycyclopent-2-en-1-one	98	98(100), 55(63), 42(55), 69(31)
14	2-hydroxy-3-methyl-2-cyclopenten-1-one	112	112(100), 97(15), 83(20), 69(22)
15	2,3-dihydro-5-hydroxy-6-methyl-4H-pyran-4-one	128	128(100), 43(50), 72(35), 85(15)
16	2-methyl-1,3-benzendiol	124	124(100), 123(59), 95(19), 107(8)
16a	methyl 2-furoate	126	95(100), 126(26), 39(29)
16b	2,5-dimethyl-4-hydroxy-3(2H)-furanone	128	43(100), 57(45), 128(17), 85(10)
17	2,5-dimethyldioxane	116	42(100), 45(91), 116(61), 101(29)
18	2-hydroxy-3-pentanone	102	45(100), 57(94), 29(99), 102(2)
19	5-formyl-2-furfurylmethanoate	154	126(100), 79(64), 109(44), 154(19)
19a	1,3,5-benzenetriol	126	126(100), 69(31), 85(22), 97(14)
20	2,3-dihydro-3,5-dihydroxy-6-methyl-4H-pyran-4-one	144	43(100), 44(75), 144(37), 101(31)
21	1,4:3,6-dianhydro- α -D-glucopyranose	144	69(100), 57(38), 98(19), 144(5)
22	5-(hydroxymethyl)-furancarboxaldehyde	126	126(90), 97(100), 41(65), 109(15)

The chromatograms of glucose and fructose shown in Figures 7.1.1 and 7.1.2 are quite similar, except for a few differences such as the absence of 1,4:3,6-dianhydro- α -D-glucopyranose in the fructose pyrolysate. More notable differences can be seen in the yield and nature of less volatile compounds, which are better analyzed as silylated pyrolysates. In addition, specific stereo-configuration of the parent sugar molecule can be observed only in anhydrosugars, which are also seen in silylated pyrolysates. The anhydrosugars are, for this reason, the most important pyrolysis products for successful application of Py-GC in the characterization of carbohydrates. The chromatographic trace shown in Figure 7.1.3 was obtained from a glucose pyrolysate generated at 590° C followed by off-line derivatization with bis(trimethylsilyl)trifluoroacetamide (BSTFA). The separation of the silylated pyrolysate was done on a chromatographic column with methyl silicone and 5% phenyl silicone stationary phase, 60 m long, 0.32 mm i.d., 0.25 μ film thickness.

The 1,6-anhydrohexoses are commonly found in large quantities only in the pyrolysis products of aldohexoses (as well as from polysaccharides [4]), but only small amounts of anhydrosugars (i.e., 1% yield) have been detected from the pyrolysis of ketohexoses [5]. The pyrogram of fructose, for example, reveals the presence of very small amounts of 2,6-anhydrofructofuranose. Aldopentoses pyrolyse in the same manner as their

hexose counterparts and form their characteristic anhydrosugars. For example, 1,4-anhydro-arabinopyranose is formed from arabinose. Furaldehyde and an uncharacterized product [6], a structural isomer of anhydropentose, are also present in pyrograms of pentoses.

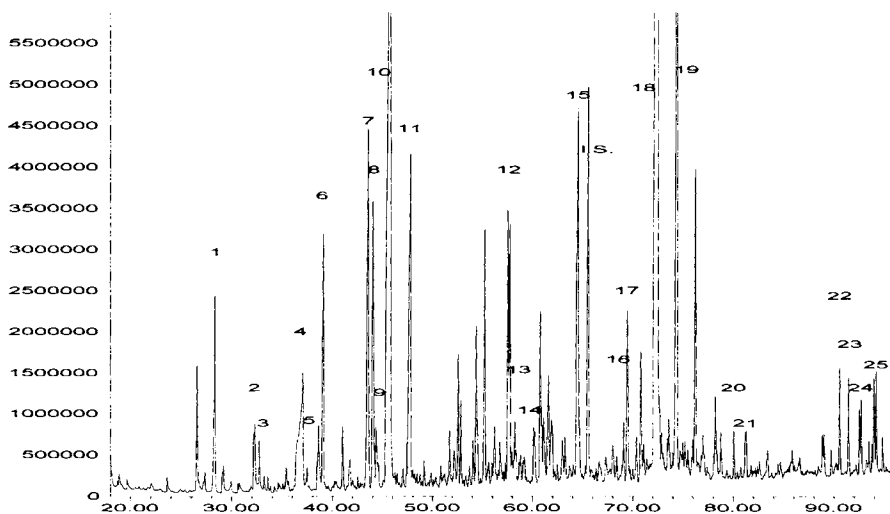


FIGURE 7.1.3. Chromatogram for the pyrolysate of glucose obtained by pyrolysis followed by off-line derivatization with BSTFA and GC/MS analysis. The peak assignments are #1 glycolic acid 2TMS, #2 oxopentanoic acid 2TMS, #3 2-hydroxy-cyclopenten-1-one TMS, #4 reagent, #5 benzoic acid TMS, #6 dihydroxyacetone 2TMS, #7 1,4-dioxan-2,5-diol 2TMS, #8 an isomer of dioxandiol 2TMS, #9 2-furanhydroxyacetic acid 2TMS, #10 5-(hydroxymethyl)furanicarboxaldehyde TMS, #11 an anhydro-deoxy-sugar 1TMS, #12 trihydroxybenzene 3-TMS, #13 4-hydroxycyclohexylcarboxylic acid 2TMS, #14 an anhydrosugar 2TMS, #15 2-hydroxycyclohexylcarboxylic acid 2TMS, #16 an anhydrosugar 3TMS, #17 an anhydrosugar 3 TMS, #18 levoglucosan 3TMS, #19 glucopyranose 5TMS ?, #20, #21, #22, #23, #24, #25 anhydrosugars xTMS.

The peak identification in Figure 7.1.3 was also done based on mass spectral library search. Some characteristic mass peaks used for compound identifications are given in Table 7.1.2.

Fructose was also pyrolysed in similar conditions with glucose, with the purpose to identify similarities and differences between the two substances. The chromatographic trace for fructose pyrolysate is shown in Figure 7.1.4. The results were obtained as in the case of glucose by off-line derivatization and GC/MS analysis.

TABLE 7.1.2. Characteristic mass peaks for the compounds identified in Figure 7.1.3 for glucose pyrolysate.

Peak No.	Compound	MW	Characteristic ions (with relative intensity)
1	glycolic acid 2TMS	220	73(100), 147(78), 66 (20), 205(17), 177(11)
2	oxopentanoic acid 2TMS	262	73(100), 147(50), 131(38), 205(11), 247(7)
3	2-hydroxy-cyclopenten-1-one TMS	170	155(100), 81(25), 75(17), 73(17)
4	reagent	?	99(100), 69(25), 168(4)
5	benzoic acid TMS	194	179(100), 105(75), 135(48), 77(45), 194(8)
6	dihydroxyacetone 2TMS	234	73(100), 103(44), 189(10), 219(4)
7	1,4-dioxan-2,5-diol 2TMS	264	117(100), 161(79), 73(76), 191(8), 263(1)
8	an isomer of dioxandiol (dioxolan ?) 2TMS	264	117(100), 161(87), 73(82), 231(22), 191(6)
9	2-furanhydroxyacetic acid 2TMS	286	169(100), 73(58), 147(30), 243(13), 286(3)
10	5-(hydroxymethyl)furanicarboxaldehyde TMS	198	183(100), 109(34), 111(28), 169(14), 198(4)
11	an anhydro-deoxy-sugar 1TMS	?	129(100), 73(57), 147(37), 103(27), 217(11)
12	trihydroxybenzene 3-TMS	342	73(100), 239(100), 342(54), 327(10)
13	4-hydroxycyclohexylcarboxylic acid 2TMS	288	73(100), 147(70), 273(46), 103(20)
14	an anhydro-deoxy-sugar 2TMS	?	217(100), 73(82), 147(35), 191(21)
15	2-hydroxycyclohexylcarboxylic acid 2TMS	288	73(100), 81(83), 273(64), 129(62), 75(60)
16	an anhydrosugar 3TMS	?	73(100), 147(40), 217(29), 103(29)
17	an anhydrosugar 2TMS	?	204(100), 217(57), 191(51), 333(6)
18	levoglucosan 3TMS	378	73(100), 204(48), 217(42), 147(18), 333(9)
19	glucopyranose 5TMS ?	540	73(100), 204(88), 191(64), 217(21), 435(3)
20	anhydrosugar xTMS.	?	217(100), 73(49), 116(13), 129(8), 191(5),
21	anhydrosugar 3TMS	?	73(100), 217(99), 204(57), 103(48), 333(1)

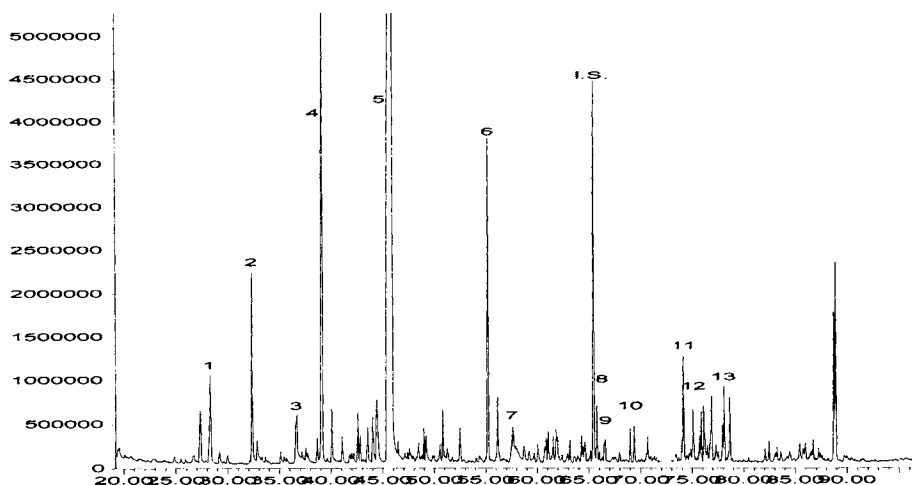


FIGURE 7.1.4. Chromatogram for the pyrolysate of fructose obtained by pyrolysis followed by off-line derivatization with BSTFA and GC/MS analysis. The peak assignments are: #1 glyoxylic acid 3TMS, #2 a diol 2TMS, #3 reagent, #4 dihydroxyacetone 2TMS, #5 5-(hydroxymethyl)furanicarboxaldehyde TMS, #6 4-hydroxy-cyclohexylcarboxylic acid 2TMS, #7 an anhydrosugar 2TMS, #8 dihydroxyacetone dimer 4TMS ?, #9 2-deoxy-D-erythro-pentofuranose 3TMS, #10 an anhydrosugar 3TMS, #11, #12 pentofuranoses 3TMS ?, #13 2,6-anhydrofructofuranose 3TMS ?.

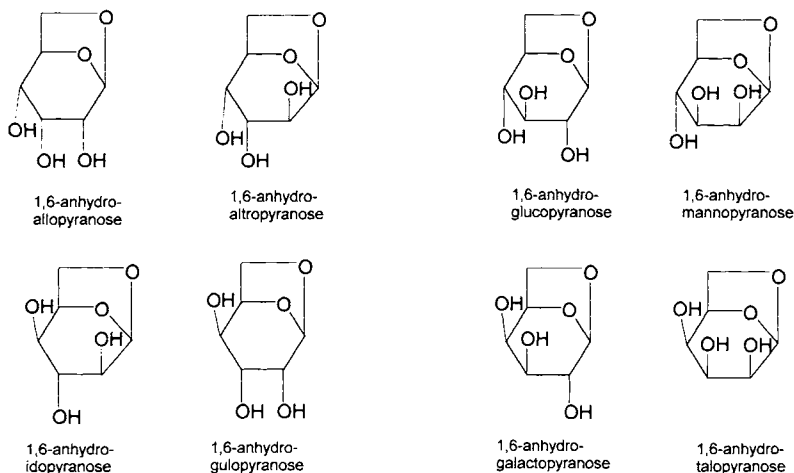
A more successful approach in the analysis of monosaccharides [6, 6a] was applied based on the partial polycondensation of monosaccharides, which has been found to occur at temperatures between 200° C and 250° C. This reaction forms random polymers with linkages involving the C-1 glycosidic carbon [8]. By further pyrolysis, anhydrosugars are formed by transglycosidation involving the glycoside bonds of the polysaccharides. In this way, characteristic 1,6-anhydrohexoses were formed from aldohexoses, 1,4-anhydropentoses from aldopentoses, or 2,6-anhydroketoses from ketohexoses [9]. The formations of some of the characteristic anhydrosugars are illustrated in Table 7.1.3. It is thought that the uncondensed portion of the monosaccharide contributes mainly to the formation of the dehydration products such as 5-hydroxymethylfuraldehyde and furaldehyde. Attempts to analyze different monosaccharides by pyrolysis at lower temperatures (358° C) and differentiation of their lower molecular weight pyrolysis products also have been reported [10].

TABLE 7.1.3. *Some characteristic anhydrosugars generated in monosaccharide pyrolysis.*

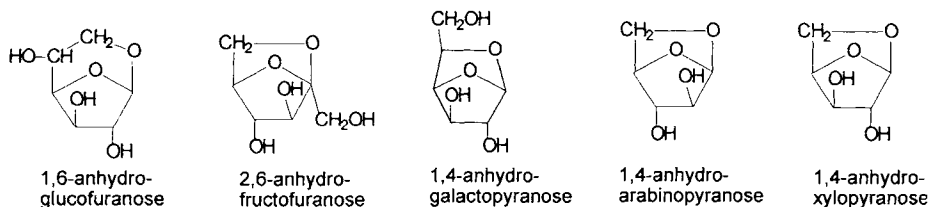
Aldopentoses	Characteristic pyrolysis product
arabinose	1,4-anhydroarabinopyranose and a pyranone*
xylose	1,4-anhydroxylopyranose and a pyranone
ribose	1,4-anhydroribopyranose and a pyranone*
lyxose	1,4-anhydrolyxopyranose and a pyranone
Aldohexoses	Characteristic pyrolysis product
glucose	1,6-anhydroglucopyranose 1,6-anhydroglucofuranose
galactose	1,6-anhydrogalactopyranose 1,4-anhydrogalactopyranose 1,6-anhydrogalactofuranose
mannose	1,6-anhydromannopyranose 1,6-anhydromannofuranose
allose	1,6-anhydroallopyranose 1,6-anhydroallofuranose
talose	1,6-anhydrotalopyranose 1,4-anhydrotalopyranose 1,6-anhydrotalofuranose
Ketohexoses	Characteristic pyrolysis product
fructose	2,6-anhydrofructofuranose
tagatose	2,6-anhydrotagatofuranose

* This pyranone is the same for arabinose and ribose, but different from that generated from xylose and lyxose.

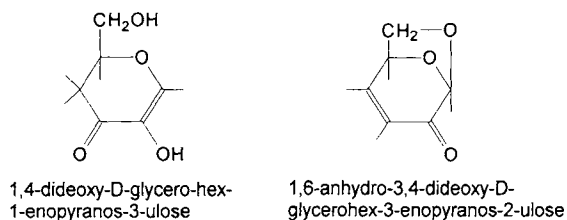
The structures of the 1,6-anhydrosugars generated from different aldohexoses, indicating the steric arrangement of different OH groups, are shown below (C-H bonds not shown).



Some structures for other anhydrosugars generated in monosaccharide pyrolysis are shown below (C-H bonds not shown).



Some other molecules generated in sugar pyrolysis, while maintaining the initial monosaccharide cycle, do not show any stereoisomers. This is the case for 1,4-dideoxy-D-glycero-hex-1-enopyranos-3-ulose (1-hydroxymethyl-5-hydroxy-2,3-dihydropyranone) and for 1,6-anhydro-3,4-dideoxy-D-glycero-hex-3-enopyranos-2-ulose (levoglucosenone) (showing C-H bonds):



The formation of different anhydrosugars from different initial sugars is illustrated in Figure 7.1.5. This figure shows the interval between 40 min. to 50 min. for four chromatographic traces of the silylated pyrolysate of mannose (trace a), allose (trace b), galactose (trace c), and glucose (trace d) (pyrolysis done at 590°C). In this time interval, the main anhydrosugars are eluted. As seen in Figure 7.1.5, each sugar has pyrolysis products with different retention times.

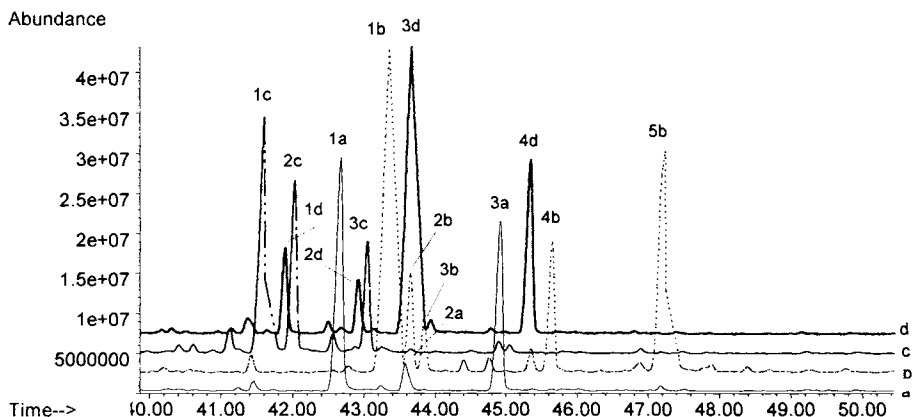


FIGURE 7.1.5. Four traces of silylated pyrolysate: (a) mannose, (b) allose, (c) galactose, and (d) glucose. Peak identification is given in Table 7.1.4.

The assignments for the peaks shown in Figure 7.1.5 are given in Table 7.1.4.

TABLE 7.1.4. Peak assignments for several compounds found in monosaccharide pyrolysates shown in Figure 7.1.5.

Saccharide	Peak	Assignment
mannose	1a	1,6-anhydromannopyranose
	2a	1,6-anhydromannofuranose
	3a	1,4-anhydromannopyranose
allose	1b	1,6-anhydroallopyranose
	2b	1,6-anhydroglucopyranose (impurity in allose)
	3b	an anhydrofuranose ?
	4b	1,6-anhydroallofuranose
	5b	1,4-anhydroallopyranose
galactose	1c	1,6-anhydrogalactopyranose
	2c	1,6-anhydrogalactofuranose
	3c	1,4-anhydrogalactopyranose
glucose	1d	1,6-anhydroglucofuranose
	2d	1,4-anhydroglucopyranose type ?
	3d	1,6-anhydroglucopyranose (levoglucosan)
	4d	1,4-anhydroglucopyranose

A significant difference can be seen in Figure 7.1.5 between the retention times for the same type of compound but generated from a different initial monosaccharide. For example, the 1,6-anhydropyranoses are the peaks 1a, 1b, 1c, and 3d. The 1,6-anhydrofuranoses are the peaks 2a, 4b, 2c, and 1d. The 1,4-anhydropyranoses are the peaks 3a, 5b, 3c and 4d.

Some differences are also seen in the EI spectra for the same type of compound but generated from a different initial monosaccharide. However, these differences are sometimes more difficult to interpret, as the identifications rely on mass spectral library searches. The spectrum for tri-TMS 1,6-anhydroglucopyranose was shown in Figure

5.3.8, and for comparison the spectra of 1,6-anhydropyranoses from allose and galactose are given in Figures 7.1.6 and 7.1.7 respectively.

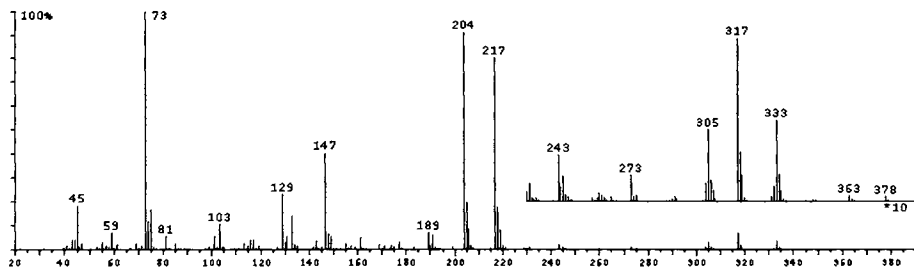


FIGURE 7.1.6. *El spectrum of tri-TMS 1,6-anhydroallopyranose.*

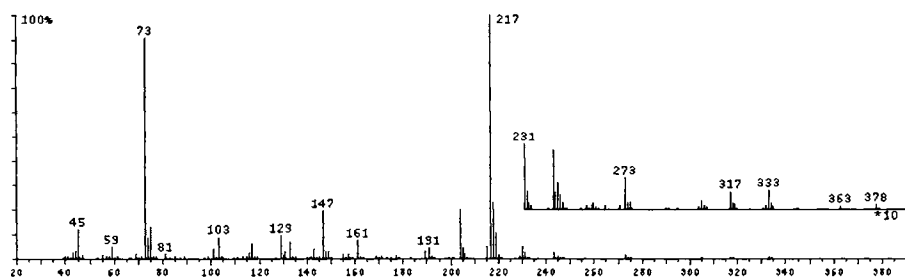


FIGURE 7.1.7. *El spectrum of tri-TMS 1,6-anhydrogalactopyranose.*

The spectra of other anhydrosugars are given in Figure 7.1.8 and 7.1.9. Figure 7.1.8 shows the spectrum of tri-TMS 1,6-anhydromannofuranose, and Figure 7.1.9 shows the spectrum of tri-TMS 1,4-anhydromannopyranose. Significant differences can be seen in the peak intensities between these two spectra; however the m/z values in the spectrum are not very different.

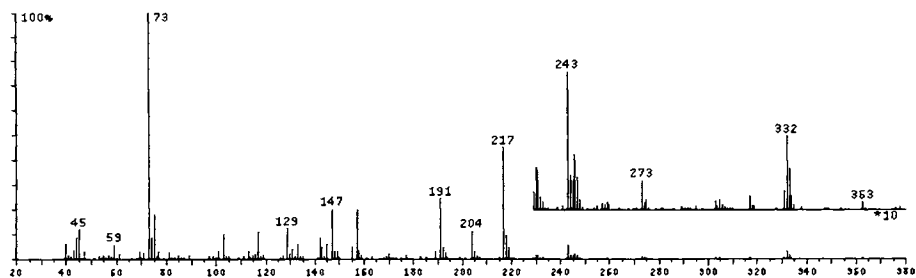


FIGURE 7.1.8. *El spectrum of tri-TMS 1,6-anhydromannofuranose.*

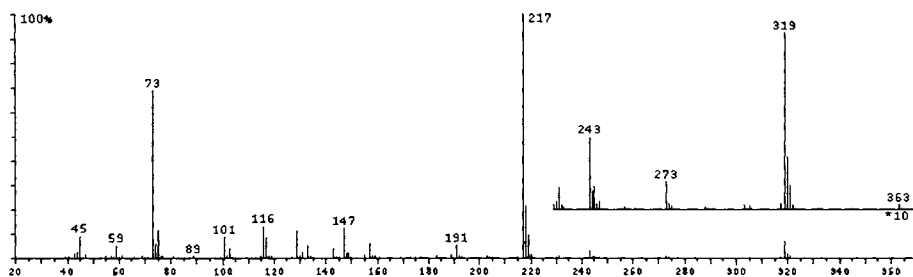
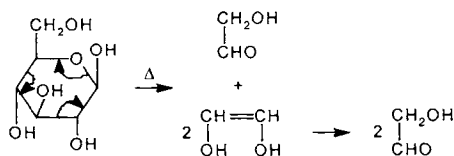


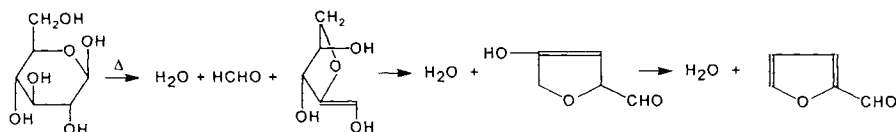
FIGURE 7.1.9. EI spectrum of tri-TMS 1,4-anhydromannopyranose.

It is interesting to note that, as a rule, the uronic acids and the neutral sugars from which they derive form similar small compounds. The anhydrosugars are not characteristic for uronic acids pyrolysis products. Uronic acids can be identified mainly based on the presence of furancarboxylic acid, which gives no information regarding the stereochemistry of the original saccharide.

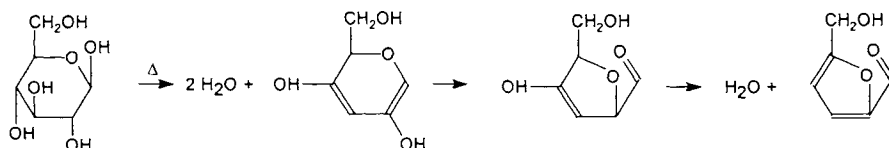
Several mechanisms were proposed for the formation of smaller molecules from monosaccharides. The formation of hydroxyacetaldehyde for example is one of the reactions that may take place by a retro-aldolization (C-H bonds not shown):



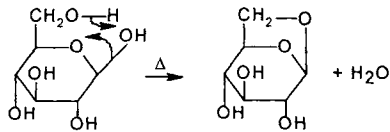
Other reactions may take place with elimination of water and other small molecules such as formaldehyde and the formation of furancarboxaldehyde, which is very abundant in the pyrolysis of most sugars:



The formation of 5-hydroxymethyl-2-furancarboxaldehyde (hydroxymethylfurfural) can be explained by the reaction:



The formation of levoglucosan is a simple water elimination:



- *Classification of polymeric carbohydrates.*

Some natural polysaccharides are homopolysaccharides and they consist of a unique monomeric unit interconnected by identical links. Among these are cellulose, amylose, amylopectin, chitin, and glycogen, which are very common in nature. Polysaccharides can be formed from pentoses or hexoses with different types of ether links. Table 7.1.5 shows the type of links in some natural homopolysaccharides. However, many natural polysaccharides are formed from two or more types of residues and they are heteropolysaccharides.

A practical classification of natural polysaccharides is based on their source. This kind of classification recognizes the following groups:

- plant polysaccharides such as cellulose, amylose and amylopectin, pectins, gums and mucilages, hemicelluloses;
- algal polysaccharides;
- microbial polysaccharides and lipopolysaccharides;
- fungal polysaccharides; and
- animal polysaccharides such as glycogen and chitin.

The problem with this classification is that some polysaccharides are very common in nature. A group such as plant polysaccharides is much larger than others such as fungal polysaccharides. Therefore, for a large group, a more detailed classification is needed. One such classification following the previous one, but also considering how common in nature are the individual polysaccharides, recognizes the following groups:

- cellulose and its derivatives;
- amylose, amylopectin, starch and their derivatives;
- pectins;
- gums and mucilages including plant exudates such as gum arabic, gum ghatti, gum karaya, gum tragacanth, and seed gums such as guar gum, locust bean gum, tamarind kernel powder, etc.;
- hemicelluloses and other plant polysaccharides such as larch arabinogalactan;
- algal polysaccharides such as agar, alginic acid, carrageenan, fucoidan, furcellaran, laminaran;
- microbial polysaccharides and biosynthetic gums such as xanthan, dextran;
- lipopolysaccharides from the cell surface of bacteria;
- fungal polysaccharides;
- glycogen;
- chitin; and
- proteoglycans.

The above classification is adopted for the present book.

TABLE 7.1.5. *Linkage type of several natural homopolysaccharides.*

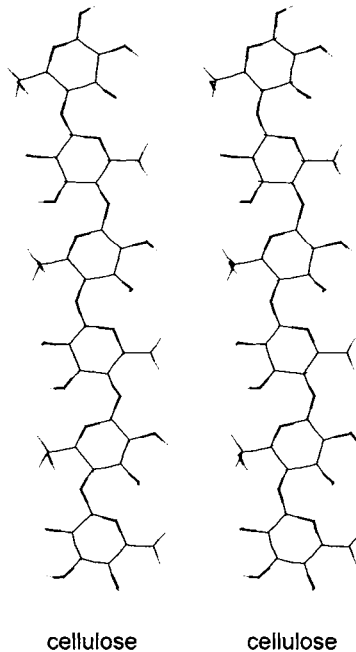
Type of bond	Common name
L-Arabinans (1 → 3)- α -L-, (1 → 5)- α -L- branched	Plant pectins
D-Fructans (2 → 1)- β -D- linear	Inulin
(2 → 6)- β -D- linear	Levans
(2 → 6)- β -D-, (2 → 1)- β -D- branched	Levans
L-Fucans (1 → 2)- α -L-, (1 → 4)- α -L- branched	Fucoidan
D-Galactans (1 → 3)- β -D-, (1 → 4)- α -D- linear	Carrageenan
(1 → 3)- β -D-, (1 → 6)- β -D-branched	
(1 → 4)- β -D- linear	Plant pectins
(1 → 5)- β -D- linear	Galactocarlose
D-Galacturonans (1 → 4)- α -D- linear	Pectic acid
D-Glucans (1 → 2)- β -D- linear	
(1 → 3)- α -D-, (1 → 4)- α -D- linear	Nigeran, isolichenan
(1 → 3)- β -D- linear	Laminaran
(1 → 3)- β -D-, (1 → 6)- β -D- branched	Scieroglucan
(1 → 3)- β -D-, (1 → 4)- β -D- linear	Lichenan
(1 → 4)- α -D- linear	Amylose
(1 → 4)- α -D-, (1 → 6)- α -D. linear	Pullulan
(1 → 4)- α -D-, (1 → 6)- α -D- branched	Glycogen, amylopectin
(1 → 4)- β -D- linear	Cellulose
(1 → 6)- β -D-, (1 → 3)- α -D- branched	Dextran
(1 → 6)- β -D- linear	Pustulan
2-Amino-2-deoxy-D-glucans (1 → 4)- β -D- linear	Chitin
D-Mannans (1 → 2)- α -D-, (1 → 6)- α -D- branched	
(1 → 4)- β -D- linear	
D-Xylans (1 → 3)- β -D- linear	Rhodymenan
(1 → 3)- β -D-, (1 → 4)- β -D- linear	
(1 → 4)- β -D- linear	

Polysaccharide structure can be described similarly to protein structure. A primary structure refers to the sequence of connected sugars. However, this is more complicated than in proteins, because the bonding of the sugar units can be done at different points and can also involve branching.

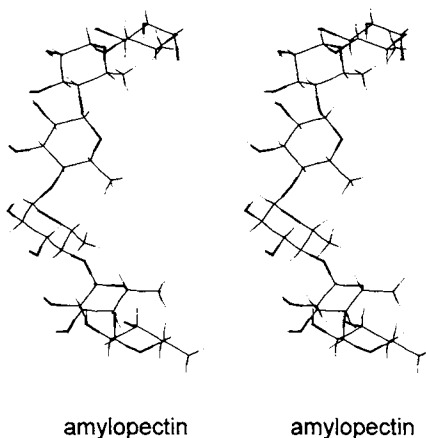
A secondary structure refers to the spatial relationship of near neighbors, which is a result of the geometry of each individual sugar and their intermolecular type interactions such as van der Waals interactions and hydrogen bonding.

A tertiary structure represents gross folding of the chain, which brings together groups that are separated along the chain by large distances. Polysaccharides have four main types of tertiary structure: extended ribbon, helix, crumpled ribbon, and flexible coil. Finally, a quaternary structure refers to aggregation of polysaccharide chains.

As an example, the steric structure of cellulose is given below (one sheet of white paper held perpendicular to the page is needed to separate the two fields of vision to see the structure). The primary (1 → 4)- β -glucosidic structure, the secondary arrangement, as well as the extended ribbon tertiary structure can be seen.



For comparison, the steric structure of amylopectin is given below. Besides the (1 → 4)- α -glucosidic structure, the secondary arrangement and the beginning of the coiling tertiary structure can be seen.



- Summary of the features of pyrolysis of polysaccharides.

Through the use of pyrolysis, polysaccharides can be characterized regarding their component monosaccharide units and also regarding the type of linkage between the residues. Therefore, the primary structure of polysaccharides can be well studied using pyrolysis. The assignment of the type of linkage is more difficult, as there are numerous possible linkages between monosaccharide units (e.g. 15 theoretical possibilities between hexopyranoses). The tertiary and the quaternary structures cannot be analyzed directly using pyrolysis, although for polysaccharides formed from aggregates, pyrolysis has been utilized for the characterization of different components.

A variety of small molecules are formed during pyrolysis of polysaccharides, and hydroxyacetone, 2-furaldehyde, 2-hydroxycyclopent-2-en-1-one, 5-hydroxymethyl-2-furaldehyde and 1,5-anhydro-4-deoxy-glycero-hex-1-en-3-ulose are more common pyrolysis products. However, only the anhydrosugars, also formed in significant proportion during pyrolysis, are diagnostic for a specific monosaccharide unit because the stereoisomerism is not lost during pyrolysis.

One approach utilized in carbohydrate pyrolysis is Py-MS. Py-MS using EI type ionization does not differentiate well between anhydrosugar stereoisomers, and its utilization to obtain structural information on carbohydrates is rather limited. However, there are reports [10a] where the type of bond between monosaccharide units can be differentiated using Py-EI MS. As an example, the Py-EI MS results are shown for a (1 → 2)-β-glucan and for a (1 → 3)-β-glucan (laminaran).

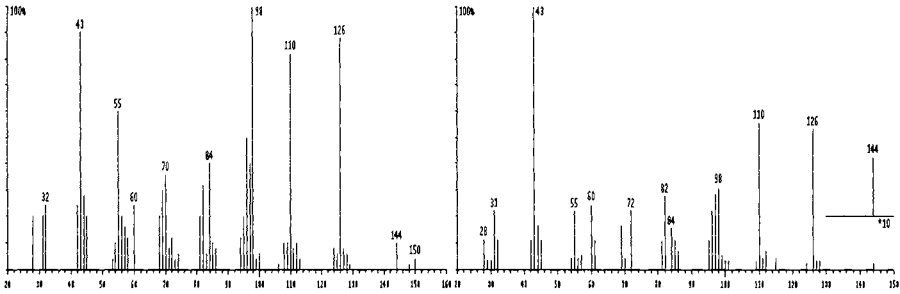


FIGURE 7.1.9 A. Py-EI MS results for a (1 → 2)-β-glucan.

FIGURE 7.1.9 B. Py-EI MS results for a (1 → 3)-β-glucan (laminaran).

Figure 7.1.10 shows the score plot of the first two discriminant functions of the Curie point Py-MS data on several glucans and one mannan (five replicates of each sample). A good separation of each polysaccharide is obtained.

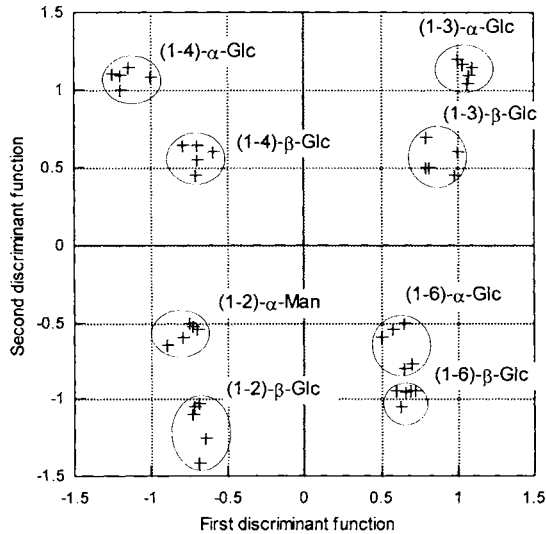


FIGURE 7.1.10. Score plot of the first two discriminant functions of the Curie point Py-MS data on several glucans and one mannan (five replicates of each sample) [10a].

Using Py-FI MS, even better results were obtained [3] for the differentiation of the type of bonds. Using oven pyrolysis at 500° C and evaporation of the sample in the MS source, different spectra were generated from 1,3-α-mannan, 1,3-β-mannan, 1,4-β-mannan, 1,2-α-mannan [3], and are shown in Figures 7.1.11 (A) to 7.1.11 (D).

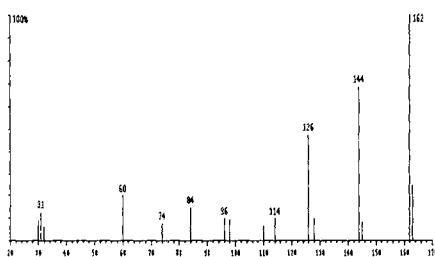


FIGURE 7.1.11 A. *Py-FI mass spectrum of 1,3- α -mannan.*

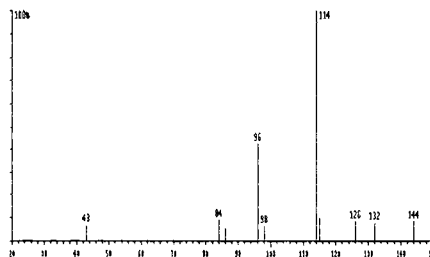


FIGURE 7.1.11 B. *Py-FI mass spectrum of 1,3- β -mannan.*

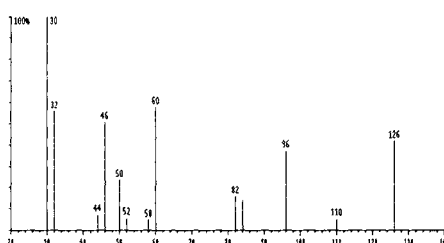


FIGURE 7.1.11 C. *Py-FI mass spectrum of 1,4- β -mannan.*

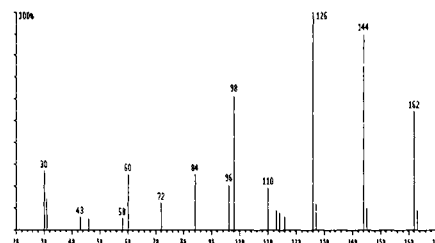
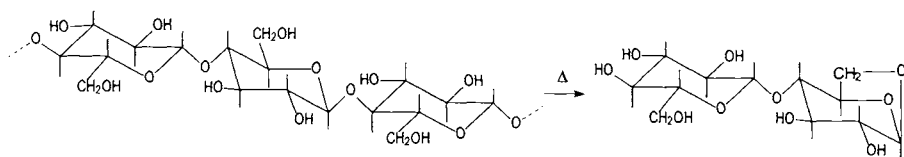


FIGURE 7.1.11 D. *Py-FI mass spectrum of 1,2- α -mannan.*

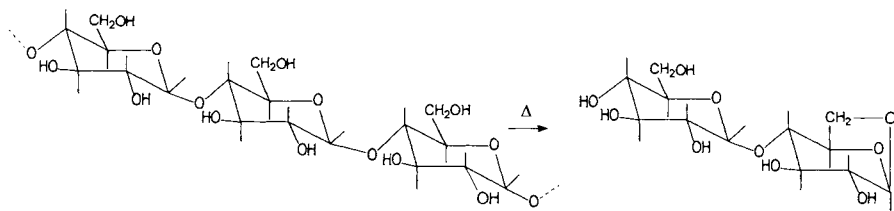
It was noted that Curie-point pyrolysis of the same compounds generated different spectra. Furanoid products with $m/z = 96$, $m/z = 110$, $m/z = 82$ are present in the spectra; however, depending on the material stability, the ions $m/z = 162$ and $m/z = 144$ (corresponding to the anhydrosugars) show different intensities.

As indicated above, Py-MS with EI ionization cannot differentiate well between anhydrosugar stereoisomers, and only Py-GC or Py-GC/MS can successfully identify the compounds based on their retention time (and mass spectrum). For example, the pyrograms of galactose-containing polysaccharides reveal that galactosyl units form all three anhydro sugars that were detected in galactose pyrolysis. The largest amount and most stable anhydro sugar is 1,6-anhydro-galactopyranose. In general, glucosyl units pyrolyse to form 1,6-anhydro-glucopyranose product along with small amounts of 1,6-anhydro-glucofuranose. In contrast to glucosyl and galactosyl units, mannosyl units produce 1,6-anhydro-mannopyranose only. The pyrograms of polysaccharides that contain arabinose and xylose monomeric units form the corresponding 1,4-anhydropyranose product.

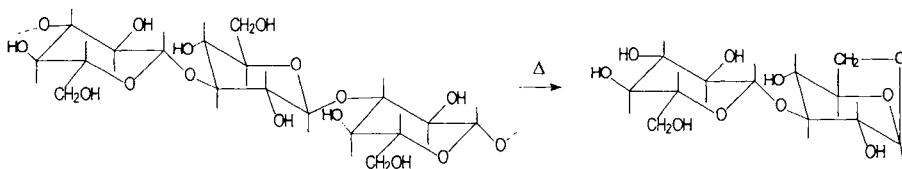
Regarding the linkage assignment based on pyrolysis data, there are numerous attempts to establish a correlation from Py-MS data, and some results will be presented in the discussion of specific classes of polysaccharides. One interesting possibility is the analysis of the anhydrosugars containing two monomeric units that result from polymeric carbohydrate pyrolysis. For example, cellulose generates cellobiosan ($C_{12}H_{20}O_{10}$, 4-O- β -glucopyranosyl-1,6-anhydroglucose) during pyrolysis:



It is likely that amylose will generate 4-O- α -glucopyranosyl-1,6-anhydroglucose (maltosan):



Maltosan was tentatively identified in a Py-DCl-MS study on starch [3a]. A polysaccharide such as laminaran, which is a (1 \rightarrow 3)- β -D-glucan, is likely to generate 3-O- β -glucopyranosyl-1,6-anhydroglucose:



The possibility to explore the links between monosaccharide units using the analysis of the anhydrosugars with two monomeric units was little investigated because these compounds are more difficult to analyze by simple GC (or GC/MS). Either HPLC or GC with derivatization must be used for this type of analysis. Differences between the type of bond in the disaccharide were reported using Py-DCl-MS/MS. Analyzing the daughter ions from the ion 342 in the pyrolysate of laminaran, which is a β -(1 \rightarrow 3)-glucan, and from starch, which is a α -(1 \rightarrow 4)-glucan, different fragmentations were obtained as shown in Figures 7.1.12 A and B [3a].

The influence of inorganic compounds on polysaccharide pyrolysis has been extensively investigated. More detailed information is further provided in connection to the description of pyrolysis of each polymeric carbohydrate. As a general rule, inorganic compounds increase the formation of small molecules generated in pyrolysis, thereby reducing the number of larger molecules that would provide better structural information. In Py-MS, addition of KOH to the initial polysaccharide results in a loss of information. Also addition of calcium ions (as CaCl_2) increases the decarboxylation. At the same time retro-aldolization reactions are diminished.

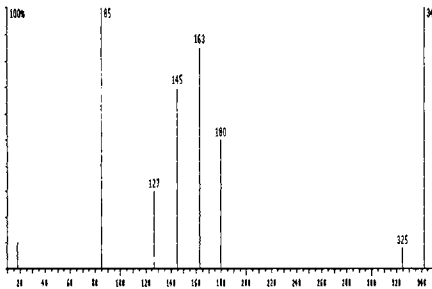


FIGURE 7.1.12 A. Daughter ions from the ion 342 in the pyrolysate of laminaran.

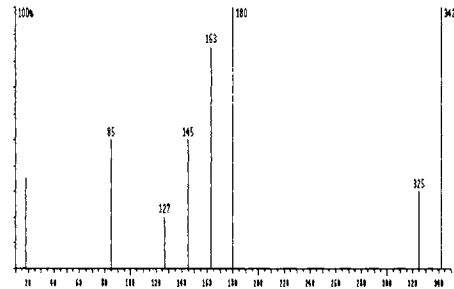


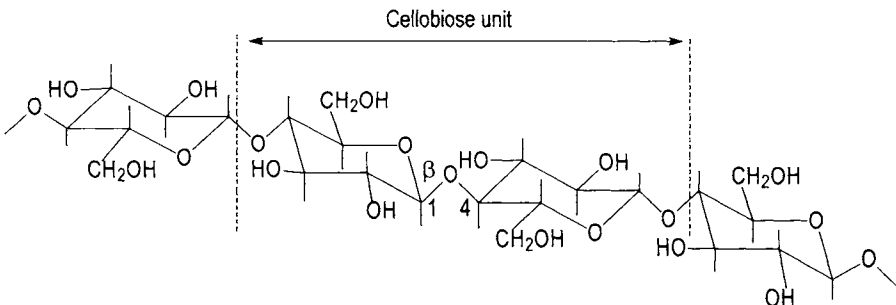
FIGURE 7.1.12 B. Daughter ions from the ion 342 in the pyrolysate of starch.

Pyrolysis products of polysaccharides as well as of some of their derivatives can be analyzed for a variety of purposes including identification, structure determination, or for a series of commercial applications, and details on particular classes are presented in the following sections.

7.2 Cellulose.

Cellulose is the structural compound of plant cells and is very common in nature. It is found in plant material usually mixed with other polysaccharides and with lignin, resins, fats, and inorganic substances. However, several vegetal fibers such as cotton or flax contain fairly pure cellulose. Pure cellulose (microcrystalline) obtained by the purification of natural cellulose is also readily available. Although cellulose can be obtained with high purity, the quality of the material may vary depending on the degree of polymerization (DP), moisture content, etc.

Cellulose is a well-characterized homopolysaccharide consisting of β -D-glucose monomeric units interconnected by β -glucoside (1 \rightarrow 4) links:



The disaccharide cellobiose could also be considered the repeating unit of cellulose, but the DP value is measured by the number of glucose units in the macromolecule. This number varies from about 200 for purified cellulose, which suffers some

depolymerization during the purification process, to about 3000 glucose units for cotton fibers, or even higher, up to 10,000.

Cellulose pyrolysis has been studied in detail from a variety of points of view mainly related to chemical utilization of wood pyrolysis products or to fire related problems. Analytical pyrolysis of cellulose is not often used as a tool for cellulose detection, but it is a common procedure for studying the pyrolysis products. A variety of analytical procedures have been applied for this study, pyrolysis/gas chromatography/mass spectrometry (Py-GC/MS) being the most common [11-16]. Besides Py-GC/MS, other analytical procedures also have been utilized, such as Py-MS [17,18], Py-IR [19], and off-line Py followed by HPLC [20]. The Py-MS spectrum of cellulose was shown in Figure 5.4.1 (B). Some procedures applied GC/MS on derivatized pyrolysis products (off-line), the derivatization being done by silylation [21], permethylation, perbenzoylation [22], etc. Information about cellulose also has been obtained from the analysis of pyrolysis products of several cellulose derivatives, such as O-substituted cellulose [23]. Also the study of cellulose crystalline structure with X-ray during pyrolysis has been used [23a] to generate information about the pyrolysis mechanism.

The analytical technique applied for the analysis of the pyrolysate must be chosen appropriately because each technique searches for only a limited range of compounds. In a GC separation, for example, only more volatile compounds are eluted and analyzed. The non-volatile compounds such as cellobiosan can be seen only in an HPLC procedure or after the derivatization of the pyrolysate.

Cellulose is relatively stable when heated in an inert atmosphere. The adsorbed water on cellulose is probably the first compound eliminated when cellulose is heated. However, this process is not considered a pyrolysis. Between 200° C and 220° C cellulose loses some more water. By monitoring the IR spectra of cellulose during this water loss, the formation of some double bonds was noted. It was concluded that the water elimination around 220° C comes from the glucose units without depolymerization [23a] and not just from some adsorbed water. A thermogravimetric study [24] showed that a more significant weight loss starts only around 300° C with the modification of the skeletal structure of the polymer. A large variety of molecules are generated during cellulose pyrolysis above this temperature. These are commonly classified as gases, tar (a liquid pyrolysis residue), and char (a carbonaceous residue). However, this classification seems to omit some compounds that are solid but not pure carbon. Depending on temperature some compounds are part of the tar, but larger molecules are part of the char.

The yield of different pyrolysis products depends on the cellulose quality such as the average value for DP, the proportion of low molecular weight polymer, crystallinity, as well as the water content and the acidity of the sample. The experimental conditions influencing the chemistry of the pyrolysate include the equilibrium temperature T_{eq} , temperature rise time (TRT), total heating time (THT) (see Section 4.1), and pyrolysis experimental setup [25,26]. A variation in pyrolysis products depending on cellulose type is exemplified in Table 7.2.1. This table gives the yield of gases, tar, char, and water for two commercially available celluloses [13].

TABLE 7.2.1. The yield of gases, tar, char, and water in % for two commercially available celluloses pyrolysed in nitrogen at 500° C [13].

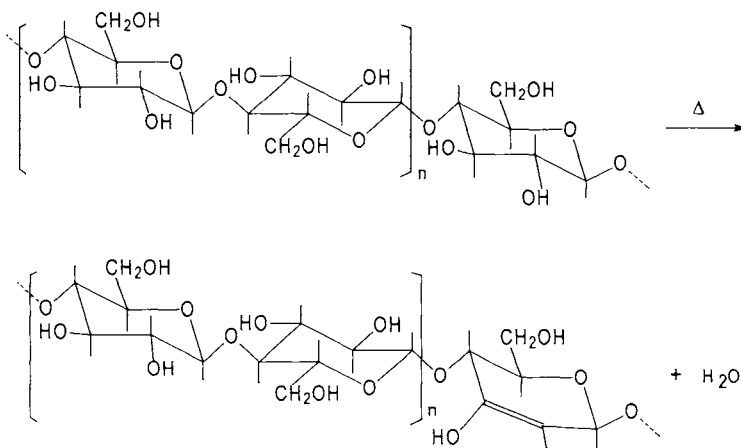
	S & S cellulose	Baker cellulose
gas	14.2	5.1
tar	73.6	90.1
water	8.0	4.6
char	4.2	1.0

- Initial pyrolytic reactions during cellulose pyrolysis.

The decomposition process seems to start with three competing reactions followed by further decompositions. The main initial pyrolysis mechanisms probably are

- side group Ei elimination of water (E),
- chain scissions by transglycosidation (T), and
- chain scissions with reverse aldolization (retroaldolization) (R).

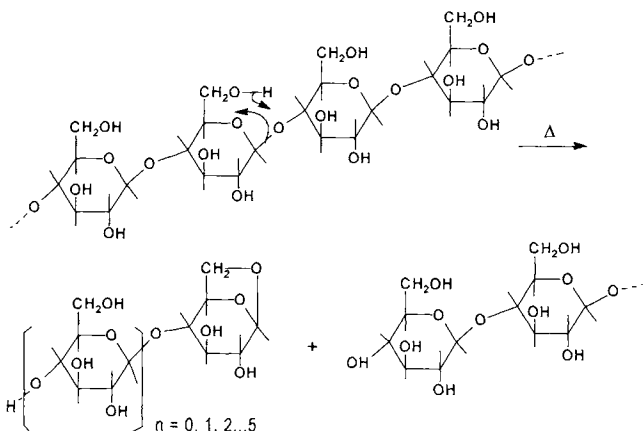
The side group reactions with water elimination take place at lower temperatures of about 350° C, while chain scissions are predominant at higher temperatures. The Ei water elimination reaction can be written as follows (see Section 2.1):



Besides the water elimination from the position 2,3 of the glucose unit as indicated above, other elimination positions such as 1,2 or 3,4 or 3,6 are possible. Because the side group elimination does not affect the DP value of the polymer, this reaction must be followed by the cleavage of the polymeric bonds to generate smaller molecules. These small molecules are the ones identified in cellulose pyrolysis products by techniques such as Py-GC/MS.

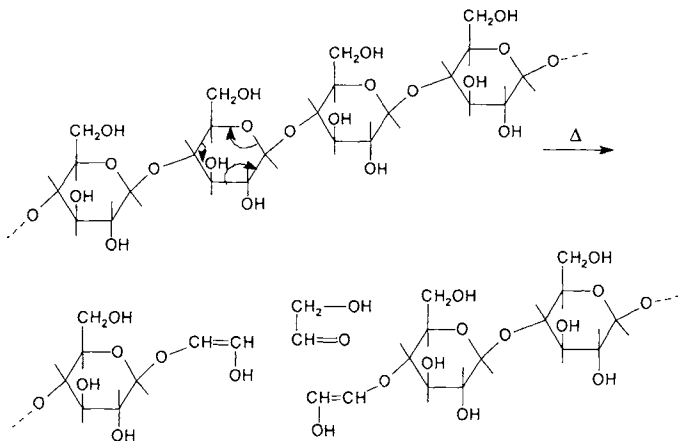
The chain scission by transglycosidation can take place with the formation of several smaller molecules. The most common product of depolymerization is 1,6-anhydro- β -D-glucose ($C_6H_{10}O_5$, levoglucosan), but anhydrocellobiose ($C_{12}H_{20}O_{10}$, 4-O- β -glucopyranosyl-1,6-anhydroglucose) or cellobiosan, as well as several anhydrocello-noses ($n = 3, 4, 5, 6$) have been detected in the pyrolysate [12]. The depolymerization by

transglycosidation is important because it is considered one of the main initial reactions in cellulose pyrolysis. By monitoring the yield of levoglucosan as a function of cellulose depolymerization [23a], this yield is 15% to 20% for cellulose with a DP > 200 and increases to about 44% for cellulose with DP < 200. This would show that the formation of small molecules is preceded by depolymerization with the formation of large oligomers. Using Haworth projection formulas, the transglycosidation reaction can be written as follows (levoglucosan is formed when $n=0$ and cellobiosan when $n=1$):



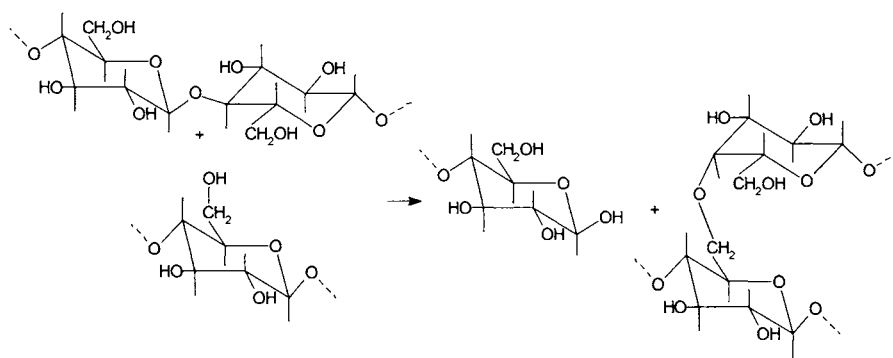
Further decomposition of levoglucosan and cellobiosan generates smaller molecules in cellulose pyrolysate. The reaction of levoglucosan formation is one of the main paths in pyrolytic decomposition of cellulose above 400°C , although the pyrolysis conditions such as the presence of acids or bases may favor other mechanisms. The yield of 1,6-anhydro- β -D-glucose in the pyrolysate was reported [13,27] to vary from traces to 40% or more.

The chain scission with reverse aldolization takes place as follows:



The yield of hydroxyacetaldehyde can be significant in cellulose pyrolysis depending on pyrolysis conditions and was reported to vary from 7% to 19%. Mono and disaccharides with an attached C₂ cleavage fragment [such as 1-(2-hydroxyethenyl)- α -glucopyranoside] were also identified in cellulose pyrolysis products.

An interesting process that may take place during cellulose pyrolysis is the inter-chain ether formation. This process is very unlikely for hydroxyl groups at C-2, C-3 or C-4 of the glucose units by water elimination between two chains. However, from energy considerations a displacement process involving one of the acetal oxygens seems possible:



This process would generate a three-dimensional polymer more stable than cellulose because the new ether bonds are more stable than the acetal-ether bonds. The increased thermal stability may allow further dehydration and possible dehydrogenation with less chain depolymerization and may be a step toward the char formation in cellulose pyrolysis. The above reaction may explain some structural modifications seen in cellulose by X-rays and by thermogravimetric analysis around 280° C. The char formation in cellulose pyrolysis as well as in other polymer pyrolysis is not always well understood. The analysis of char is rather difficult as this material is not soluble and does not contain small molecules. The amount of carbon in char is high, but this does not exclude the existence of a specific macromolecular structure. A parallel between char formation in pyrolysis and the coalification of wood, although rather remote, may suggest the type of structures that are possible components of char. The coalification process seen in fossil wood (see Section 14.2), although it involves lignin and other wood components in addition to cellulose, generates polynuclear aromatic hydrocarbon structures and these may be a likely component of char.

- Further pyrolytic reactions during cellulose pyrolysis.

Subsequent to the first step in pyrolysis, more decompositions take place. The paths of these decompositions strongly depend on pyrolysis conditions and may yield a wide variety of products. It is not clear which sequence is followed by the pyrolysis process, and depending on pyrolysis conditions there are variations in the amount and in the nature of the generated substances.

The influence of pyrolysis temperature on the qualitative chemical composition of the cellulose pyrolysate can be illustrated by comparing the pyrograms generated at different temperatures. This is shown in Figures 7.2.1, 7.2.2 and 7.2.3, which give the total ion chromatograms (TIC) generated by a GC/MS system for the trimethylsilylated pyrolysate of cellulose obtained at three different temperatures between 450° C and 850° C.

The chromatographic trace shown in Figure 7.2.1 was obtained from the cellulose pyrolysate generated at 590° C followed by off-line silylation with bis(trimethylsilyl) trifluoroacetamide (BSTFA).

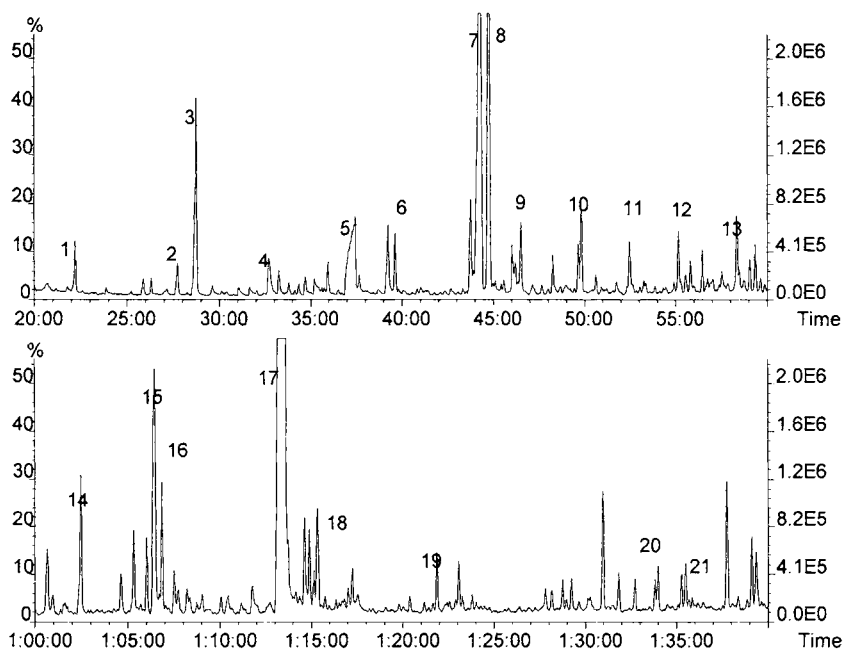


FIGURE 7.2.1. Cellulose pyrolysate obtained at 590° C and trimethylsilylated. The separation was done on a methyl silicone with 5% phenyl silicone type column. #1 1,2-dihydroxyethane, #2 2-hydroxypropionic (lactic) acid, #3 hydroxy acetic (glycolic) acid, #4 furanmethanol, #5 peak from silylation reagents, #6 1,3-dihydroxypropanone, #7 1,4-dioxane-2,5-diol, #8 1,3-dioxolane-4,5-diol, #9 1,3-dihydroxybenzene, #10 2-methyl-1,4-dioxane-2,5-diol, #11 1,4-dihydroxybenzene, #12 3-hydroxy-2-(hydroxymethyl)-2-cyclopenten-1-one, #13 2-hydroxy-5-(hydroxymethyl)-4(H)-pyran-4-one, #14 1,2,3-trihydroxybenzene, #15 internal standard, #16 an anhydrosugar, #17 levoglucosan (1,6-anhydro- β -D-glucopyranose), #18 a monosaccharide, #19 an anhydrosugar, #20 an anhydrosugar, #21 1,6-anhydro- β -D-glucopyranose ?.

The separation of the silylated pyrolysate was done on a methyl silicone with 5% phenyl silicone chromatographic column, 60 m long, 0.32 mm i.d., 0.25 μ film thickness. Some of the peaks in these chromatograms were identified. However, a significant number of peaks remained unidentified or only tentatively identified. Most peak identifications were done based only on the mass spectra library search (see Section 5.3).

The chromatographic trace given in Figure 7.2.2 was obtained from the cellulose pyrolysate generated at 850° C. The separation of the trimethylsilylated pyrolysate was done on the same column as for 590° C pyrolysis. At first look, most major compounds generated at 850° C are the same as for 590° C pyrolysis, and a significant overlapping in the chemical composition is indeed present. Only some peak intensities are different. However, a more detailed analysis indicates that besides the typical pyrolysis products obtained at 590° C, several other compounds start to be formed at higher temperatures. Above 800–850° C, in addition to the compounds that are generated at lower temperatures, smaller and more stable molecules such as aromatic compounds are formed.

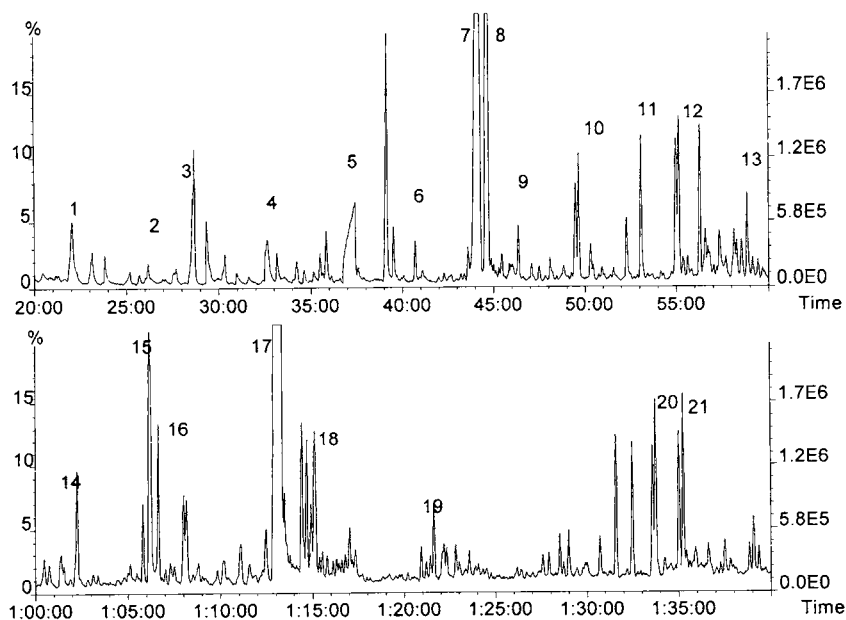


FIGURE 7.2.2. Cellulose pyrolysate obtained at 850° C and trimethylsilylated. The separation was done on the same column as for 590° C pyrolysis. The numbers correspond to the chemical names indicated for Figure 7.2.1.

At lower pyrolysis temperature, namely around 450° C, the pyrolysate composition becomes less complex. This can be seen by comparing the chromatograms shown in Figures 7.2.1 or 7.2.2 with the chromatogram shown in Figure 7.2.3.

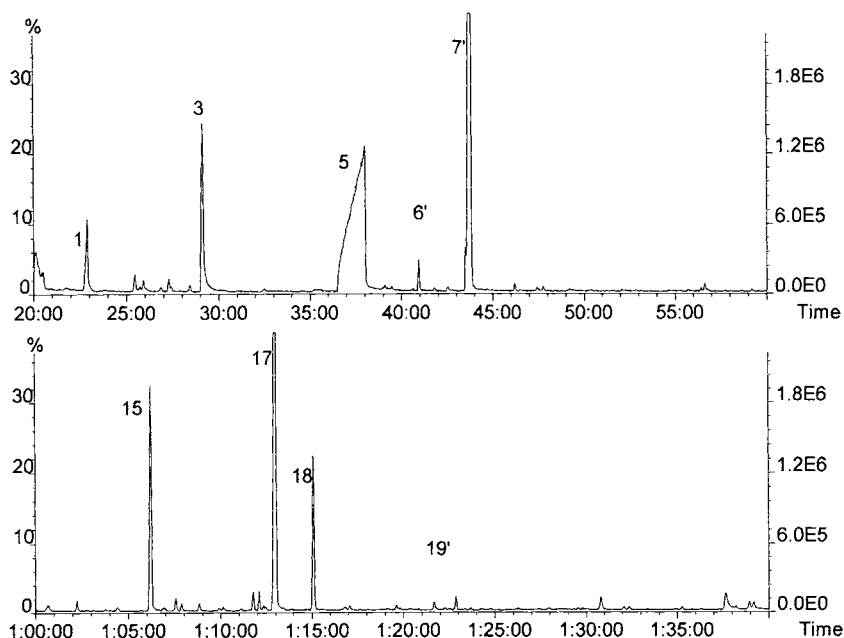


FIGURE 7.2.3. Cellulose pyrolysate obtained at 450° C and trimethylsilylated. The separation was done on the same column as for 850° C. Several numbers correspond to the chemical names indicated for Figure 7.2.1. Some peaks are, however, different: #6' diethyleneglycol, #7' glycerin, #19' inositol.

The characteristic ions for some peaks shown in Figures 7.2.1, 7.2.2 and 7.2.3, which were identified in the silylated pyrolysates of cellulose, are given in Table 7.2.2.

The type of analysis utilized to determine the composition of a pyrolysate is important because only a certain group of compounds can be seen in one type of analysis. The identification of more volatile compounds found in cellulose pyrolysate can be done very conveniently by on-line Py-GC/MS analysis. The TIC traces of cellulose pyrolysate obtained at 590° C and separated on a Carbowax or on a methyl-phenyl silicone type column were already given in Section 5.2 (Figures 5.2.10, 5.2.11 and 5.2.13). As indicated in Section 5.2, in these chromatograms compounds such as formaldehyde, methanol, or CO were not seen because the mass spectrometer used for the analysis had the mass range detection with a low cut-off at $m/z = 32$.

TABLE 7.2.2. *Some peak identifications and their characteristic ions for the silylated pyrolysates of cellulose shown in Figures 7.2.1 to 7.2.3.*

Peak No.	Compounds	Formula	MW	Characteristic ions
1	1,2-dihydroxyethane 2 TMS	C ₈ H ₂₂ O ₂ Si ₂	206	147(100), 73(63), 103(21), 191(19)
2	2-hydroxypropionic (lactic) acid 2 TMS	C ₉ H ₂₂ O ₃ Si ₂	234	73(100), 117(92), 147(86), 190(15), 191(14), 219(8)
3	hydroxy acetic (glycolic) acid 2 TMS	C ₈ H ₂₀ O ₃ Si ₂	220	73(100), 147(78), 66 (20), 205(17), 177(11)
4	furanmethanol TMS	C ₈ H ₁₄ O ₂ Si	170	81(100), 155(51), 73(20), 170(8)
5	peak from silylation reagents	?	?	99
6	1,3-dihydroxypropanone 2 TMS	C ₉ H ₂₂ O ₃ Si ₂	234	73(100), 103(44), 189(10), 147(8), 219(4)
6'	diethyleneglycol 2 TMS	C ₁₀ H ₂₆ O ₃ Si ₂	250	73(100), 117(39), 116(18), 147(9), 191(1)
7	1,4-dioxane-2,5-diol 2 TMS	C ₁₀ H ₂₄ O ₄ Si ₂	264	117(100), 161(79), 73(76), 191(8), 263(1)
7'	glycerol 3 TMS	C ₁₂ H ₃₂ O ₃ Si ₃	308	73(100), 147(35), 205 (22), 117(21), 103(21), 218(5)
8	1,3-dioxolane-4,5-diol 2 TMS	C ₉ H ₂₂ O ₄ Si ₂	250	117(100), 73(94), 161(86), 101(19), 231(6), 249(1)
9	1,3-dihydroxybenzene 2 TMS	C ₁₂ H ₂₂ O ₂ Si ₂	254	73(100), 254(18), 45(9)
10	2-methyl-1,4-dioxane-2,5-diol 2 TMS	C ₁₁ H ₂₆ O ₄ Si ₂	278	73(100), 131(92), 175(47), 265(12), 278(2)
11	1,4-dihydroxybenzene 2 TMS	C ₁₂ H ₂₂ O ₂ Si ₂	254	239(100), 254(76), 73(50)
12	3-hydroxy-2-(hydroxymethyl)-2-cyclopenten-1-one 2 TMS	C ₁₂ H ₂₄ O ₃ Si ₂	272	257(100), 73(55), 272(9)
13	2-hydroxy-5-(hydroxymethyl)-4(H)-pyran-4-one 2 TMS	C ₁₂ H ₂₂ O ₄ Si ₂	286	271(100), 73(26), 147(22), 286(2)
14	1,2,3-trihydroxybenzene 3 TMS	C ₁₅ H ₃₀ O ₃ Si ₃	342	73(100), 239(92), 342(52)
15	internal standard			
16	an anhydrosugar			205(100), 191(86), 73(85), 147(52)
17	levoglucosan (1,6-anhydro-β-D-glucopyranose) 3 TMS	C ₁₅ H ₃₄ O ₅ Si ₃	378	73(100), 204(48), 217(42), 147(18), 333(9)
18	a monosaccharide ?	C ₂₁ H ₅₂ O ₆ Si ₅	540	217(100), 73(62), 117(12), 319(6)
19	an anhydrosugar			73(100), 147(51), 217(44), 191(28), 286(12)
19'	inositol 6 TMS ?	C ₂₄ H ₆₀ O ₆ Si ₆	612	73(100), 318(40), 147(38), 217(35), 367(5), 433(4)
20	an anhydrosugar			73(100), 204(44), 217(38), 205(36), 191(18)
21	1,6-anhydro-β-D-glucofuranose ?			73(100), 204(54), 205(52), 217(40), 191(20)

- *Compounds identified in cellulose pyrolysates.*

The compounds found in the pyrolysate formed in the common range of pyrolysis temperatures, between 500 to 650° C, that can be analyzed by GC/MS with or without derivatization (e.g. TMS) and shown in Figures 7.2.1 to 7.2.3 and in Figures 5.2.10, 5.2.11 and 5.2.13 can be classified as follows:

- monosaccharides (glucose),
- anhydrosugars (shown in Table 7.2.3),
- carbonyl compounds (shown in Table 7.2.4),
- furans and lactones (shown in Table 7.2.5),
- pyrans (shown in Table 7.2.6),
- phenols (shown in Table 7.2.7),
- acids and acid esters (shown in Table 7.2.8), and
- other compounds (shown in Table 7.2.9).

TABLE 7.2.3. *Anhydrosugars* generated in cellulose pyrolysis.*

MW	Name	Formula
126	levoglucosenone (6,8-dioxabicyclo(3.2.1)oct-2-en-4-one), (1,6-anhydro-3,4-dideoxy-D-glycerohex-3-enopyranos-2-ulose)	C6H6O3
144	1,4:3,6-dianhydro- α -D-glucopyranose	C6H8O4
144	1,4-dideoxy-D-glycero-hex-1-enopyranos-3-ulose	C6H8O4
144	3,4-dihydroxy-6,8-dioxabicyclo(3.2.1)oct-1-ene	C6H8O4
162	levoglucosan (1,6-anhydro- β -D-glucopyranose)	C6H10O5
162	5,6-anhydro- β -D-glucopyranose	C6H10O5
162	1,6-anhydro- β -D-glucofuranose	C6H10O5
162	1,4-anhydro- β -D-glucopyranose	C6H10O5

* Several anhydrodisaccharides, and anhydrocello-n-oses ($n = 3, 4, 5, 6$) have been detected in the pyrolysate, but they were not seen in regular GC/MS separations due to their low volatility. They cannot be detected even after derivatization as trimethylsilyl derivatives (TMS). These substances can be detected, however, in the pyrolysate using an LC procedure or using off-line permethylation of the pyrolysate [22], which increases the volatility more than trimethylsilylation.

TABLE 7.2.4. *Carbonyl compounds generated in cellulose pyrolysis.*

MW	Name	Formula
30	formaldehyde	CH ₂ O
44	acetaldehyde	C ₂ H ₄ O
60	hydroxyacetaldehyde	C ₂ H ₄ O ₂
56	2-propenal	C ₃ H ₄ O
58	propanal	C ₃ H ₆ O
58	propanone	C ₃ H ₆ O
72	propenedialdehyde	C ₃ H ₄ O ₂
74	3-hydroxypropanal	C ₃ H ₆ O ₂
74	hydroxypropanone	C ₃ H ₆ O ₂
90	2,3-dihydroxypropanal	C ₃ H ₆ O ₃
90	dihydroxypropanone	C ₃ H ₆ O ₃
84	but-3-enal-2-one	C ₄ H ₄ O ₂
100	3-carboxy-2-propenal	C ₄ H ₄ O ₃
70	2-butenal (cis)	C ₄ H ₆ O
70	2-butenal (trans)	C ₄ H ₆ O
86	2,3-butanedione	C ₄ H ₆ O ₂
102	2-hydroxybutanedialdehyde	C ₄ H ₆ O ₃
72	butanal	C ₄ H ₈ O
72	butanone	C ₄ H ₈ O
88	1-hydroxybutan-2-one	C ₄ H ₈ O ₂
88	1-hydroxybutan-3-one	C ₄ H ₈ O ₂
96	cyclopent-1-ene-3,4-dione	C ₅ H ₄ O ₂
82	2,4-pentadienal	C ₅ H ₆ O
82	cyclopent-1-ene-2-one	C ₅ H ₆ O
82	1,4-pentadien-3-one	C ₅ H ₆ O
98	1-pentene-3,4-dione	C ₅ H ₆ O ₂
98	pent-4-enal-2-one	C ₅ H ₆ O ₂
98	hydroxycyclopentenone	C ₅ H ₆ O ₂
98	1,3-cyclopentandione	C ₅ H ₆ O ₂
114	dihydroxypentenone	C ₅ H ₆ O ₃
84	2-methyl-1-buten-3-one	C ₅ H ₈ O
84	pent-3-en-2-one	C ₅ H ₈ O
84	cyclopentanone	C ₅ H ₈ O
100	2,3-pentanedione	C ₅ H ₈ O ₂

TABLE 7.2.4. *Carbonyl compounds generated in cellulose pyrolysis (continued).*

MW	Name	Formula
116	1-acetyloxypropan-2-one	C5H8O3
86	pentanal	C5H10O
86	2-pentanone	C5H10O
96	2-methyl-2-cyclopenten-1-one	C6H8O
112	2-hydroxy-3-methyl-2-cyclopenten-1-one	C6H8O2
112	3-hydroxy-2-methyl-2-cyclopenten-1-one	C6H8O2
128	3-hydroxy-2-(hydroxymethyl)-2-cyclopenten-1-one	C6H8O3
128	6-methyl-1,4-dioxaspiro[2,4]heptan-5-one	C6H8O3
144	1-hydroxy-3,6-dioxabicyclo[3.2.1]octan-2-one	C6H8O4
114	2-methylcyclopentanone	C6H10O
114	3-methylcyclopentanone	C6H10O
130	2,3-dihydroxyhex-1-en-4-one	C6H10O3
106	benzaldehyde	C7H6O
122	3-hydroxybenzaldehyde	C7H6O2
138	3,4-dihydroxybenzaldehyde	C7H6O3
138	2,4-dihydroxybenzaldehyde	C7H6O3
110	2,3-dimethyl-2-cyclopenten-1-one	C7H10O
126	3,5-dimethylcyclopentan-1,2-dione	C7H10O2
112	1-cyclopentylethanone	C7H12O
114	3-methyl-2-hexanone	C7H14O
152	3,5- or 4,5-dihydroxyacetophenone	C8H8O3

TABLE 7.2.5. *Furans and related substances generated in cellulose pyrolysis.*

MW	Name	Formula
68	furan	C4H4O
70	2,3-dihydrofuran	C4H6O
84	(2H)-furan-3-one	C4H4O2
84	(5H)-furan-2-one	C4H4O2
84	(3H)-furan-2-one	C4H4O2
86	tetrahydrofuran-3-one	C4H6O2
96	2-furancarboxaldehyde	C5H4O2
96	3-furancarboxaldehyde	C5H4O2
82	2-methylfuran	C5H6O
82	3-methylfuran	C5H6O
98	2-(hydroxymethyl)furan	C5H6O2
98	2,3-dihydro-5-methylfuran-2-one	C5H6O2
98	2,5-dihydro-5-methylfuran-2-one	C5H6O2
98	3-(hydroxymethyl)-furan	C5H6O2
98	2-methyl-2,3-dihydrofuran-3-one	C5H6O2
114	3-methyltetrahydrofuran-2,4-dione	C5H6O3
100	4-methyltetrahydrofuran-3-one	C5H8O2
100	2-methyl-3-hydroxy-2,3-dihydrofuran	C5H8O2
100	2-methoxy-2,3-dihydrofuran	C5H8O2
100	2-methoxy-2,5-dihydrofuran	C5H8O2
102	tetrahydro-2-furanmethanol	C5H10O2
102	2-methoxytetrahydrofuran	C5H10O2
110	2-acetylfuran	C6H6O2
110	5-methyl-2-furancarboxaldehyde	C6H6O2
126	furfuryl formate	C6H6O3
126	2-furoic acid methyl ester	C6H6O3

TABLE 7.2.5. *Furans and related substances generated in cellulose pyrolysis (continued).*

MW	Name	Formula
126	5-(2-hydroxyethylidene)-(5H)-furan-2-one	C6H6O3
126	5-hydroxymethyl-2-furancarboxaldehyde	C6H6O3
126	3-ethyl-2,4(3H,5H)-furanone	C6H6O3
96	2,5-dimethylfuran	C6H8O
128	5-acetyltetrahydrofuran-2-one	C6H8O3
144	5-hydroxymethyl-2-tetrahydrofuran-3-one	C6H8O4
114	5-ethylidihydro-2(3H)-furanone	C6H10O2
138	2-(propane-2,3-dione)-furan	C7H6O3
128	2-(propan-2-one)-tetrahydrofuran	C7H12O2
144	5-ethyl-3-hydroxy-4-methyl-tetrahydrofuran-2-one	C7H12O3

TABLE 7.2.6. *Pyrans and related substances generated in cellulose pyrolysis.*

MW	Name	Formula
112	5,6-dihydropyran-2,5-dione	C5H4O3
98	2,4-dihydropyran-3-one	C5H6O2
114	4-hydroxy-5,6-dihydro-(2H)-pyran-2-one	C5H6O3
126	3-hydroxy-6-methyl-(2H)-pyran-2-one	C6H6O3
126	3-hydroxy-2-methyl-(4H)-pyran-4-one	C6H6O3
142	2-hydroxy-5-(hydroxymethyl)-4(H)-pyran-4-one	C6H6O4
142	3,5-dihydroxy-2-methyl-(4H)-pyran-4-one	C6H6O4
112	a methylidihydropyranone	C6H8O2
112	a methylidihydropyranone	C6H8O2
128	2-hydroxymethyl-2,3-dihydropyran-4-one	C6H8O3
130	4-(hydroxymethyl)-tetrahydropyran-3-one	C6H10O3
138	methyl-formyl-(4H)-pyran-4-one	C7H6O3
126	a dimethylidihydropyranone	C7H10O2
126	a dimethylidihydropyranone	C7H10O2

TABLE 7.2.7. *Phenols generated in cellulose pyrolysis.*

MW	Name	Formula
94	phenol	C6H5O
110	1,2-dihydroxybenzene	C6H6O2
110	1,3-dihydroxybenzene	C6H6O2
110	1,4-dihydroxybenzene	C6H6O2
126	1,2,3-trihydroxybenzene	C6H6O3
108	3- or 4-methylphenol	C7H8O
108	2-methylphenol	C7H8O
124	4-methyl-1,2-dihydroxybenzene	C7H8O2
124	3-methyl-1,2-dihydroxybenzene	C7H8O2
124	4-methyl-1,3-dihydroxybenzene	C7H8O2
124	2-methyl-1,4-dihydroxybenzene	C7H8O2
124	3-methoxyphenol	C7H8O2
120	p-vinylphenol	C8H8O
122	2,4-dimethylphenol	C8H10O
122	2,6-dimethylphenol	C8H10O
122	3,5-dimethylphenol	C8H10O
122	ethyl-phenol	C8H10O
154	2,6-dimethoxyphenol	C8H10O3
136	3,4,5-trimethylphenol	C9H12O
144	1-naphthol	C10H8O

TABLE 7.2.8. *Acids and acid esters generated in cellulose pyrolysis.*

MW	Name	Formula
46	formic acid	CH ₂ O ₂
60	acetic acid	C ₂ H ₄ O ₂
76	hydroxyacetic acid	C ₂ H ₄ O ₃
88	2-oxopropanoic acid	C ₃ H ₄ O ₃
74	propionic acid	C ₃ H ₆ O ₂
90	lactic acid	C ₃ H ₆ O ₃
86	3-butenic acid	C ₄ H ₆ O ₂
102	pyruvic acid methyl ester	C ₄ H ₆ O ₃
102	hydroxyacetic acid vinyl ester	C ₄ H ₆ O ₃
86	crotonic acid	C ₄ H ₆ O ₂
88	butyric acid	C ₄ H ₈ O ₂
100	but-3-enoic acid methyl ester	C ₅ H ₈ O ₂
180	2-deoxygluconic acid	C ₆ H ₁₂ O ₆
158	4,6-dihydroxyhepta-4,6-dien-1-carboxylic acid	C ₇ H ₁₀ O ₄

TABLE 7.2.9. *Other compounds generated in cellulose pyrolysis.*

MW	Name	Formula
2	hydrogen	H ₂
18	water	H ₂ O
12	carbon	C
28	carbon monoxide	CO
44	carbon dioxide	CO ₂
16	methane	CH ₄
32	methanol	CH ₄ O
28	ethylene	C ₂ H ₄
30	ethane	C ₂ H ₆
62	ethylene glycol	C ₂ H ₆ O ₂
106	1,3-dioxolane-4,5-diol	C ₃ H ₆ O ₄
84	1,4-dioxadiene	C ₄ H ₄ O ₂
102	acetic anhydride	C ₄ H ₆ O ₃
120	1,4-dioxane-2,5-diol	C ₄ H ₈ O ₄
120	1,4-dioxane-2,3-diol	C ₄ H ₈ O ₄
122	1,2-butandiol	C ₄ H ₁₀ O ₂
66	1,3-cyclopentadiene	C ₅ H ₆
116	4-cyclopenten-1,2,3-triol	C ₅ H ₈ O ₃
80	5-methyl-1,3-cyclopentadiene	C ₆ H ₈
80	2-methyl-2,3-hexadiene	C ₆ H ₈
180	inositol	C ₆ H ₁₂ O ₆

- *Cellulose pyrolysis at higher temperatures.*

Besides the typical pyrolysis products listed in Tables 7.2.3–7.2.9, several other pyrolysis products were identified at higher temperatures (small molecules are formed even at temperatures below 600° C [28]). Table 7.2.9 lists a series of aromatic [29] and polynuclear aromatic hydrocarbons generated from the pyrolysis of cellulose at 850° C [30]. Numerous other compounds were also reported as formed during cellulose burning, due to cellulose pyrolysis [31–36]. Some of the polynuclear aromatic compounds, such as benzo(a)pyrene, are present only in traces but their detection in the pyrolysate is important due to their known carcinogenic properties. Besides the compounds shown in Table 7.2.9, some other polynuclear aromatic hydrocarbons (PAH) are present in cellulose pyrolysates. This can be inferred from Figure 7.2.4, which shows the extracted single ion chromatograms corresponding to the molecular ions of some polynuclear aromatic hydrocarbons.

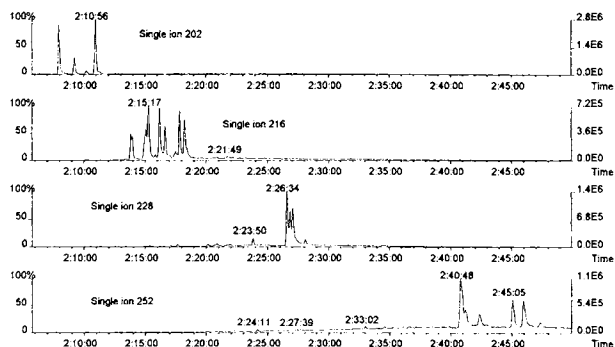


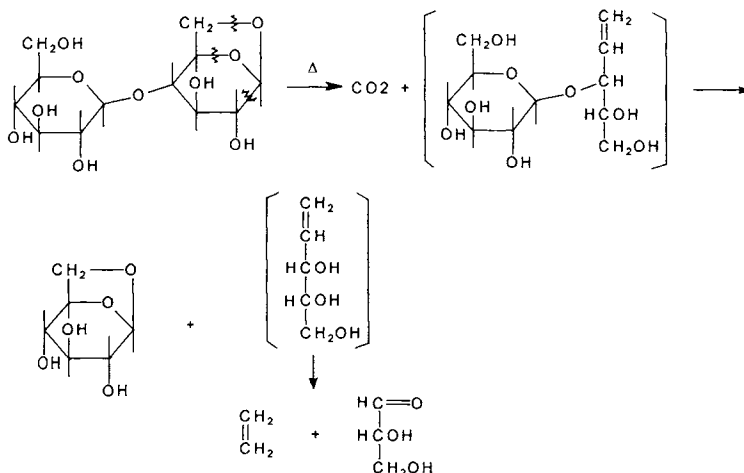
FIGURE 7.2.4. GC/MS traces for extracted single ion chromatograms corresponding to masses 202, 216, 228, 252 in a cellulose pyrolysate subjected to clean-up and preconcentration for PAH analysis [21].

More peaks can be seen for a known mass (202, 216, 228 or 252) than the number of compounds with the corresponding mass listed in Table 7.2.10. The formation of these hydrocarbons is the result of advanced pyrolysis of some of the compounds previously listed. Due to the higher thermal stability of the compounds listed in Table 7.2.10, their concentration increases in the pyrolysates as the temperature increases.

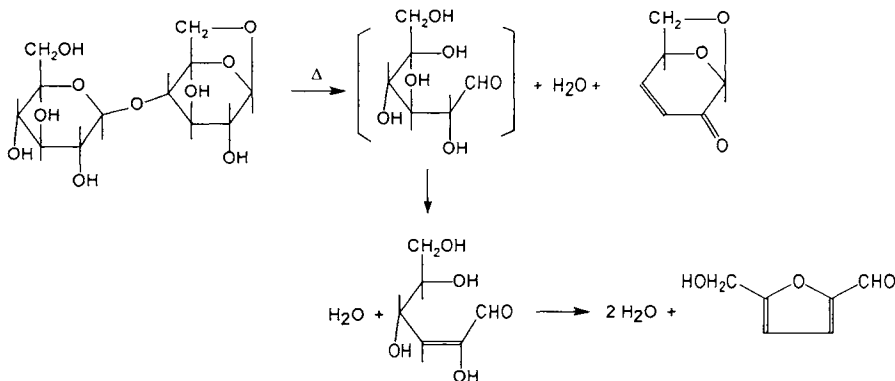
TABLE 7.2.10. Aromatic hydrocarbons generated from pyrolysis of cellulose at 850°C.

MW	Compound name	Formula
78	benzene	C ₆ H ₆
92	toluene	C ₇ H ₈
104	styrene	C ₈ H ₈
106	ethylbenzene	C ₈ H ₁₀
106	xylene (o, m, p)	C ₈ H ₁₀
116	indene	C ₉ H ₈
118	4-methylstyrene	C ₉ H ₁₀
128	naphthalene	C ₁₀ H ₈
142	methylnaphthalene	C ₁₁ H ₁₀
152	acenaphthylene	C ₁₂ H ₈
154	biphenyl	C ₁₂ H ₁₀
166	fluorene	C ₁₃ H ₁₀
178	phenanthrene	C ₁₄ H ₁₀
178	anthracene	C ₁₄ H ₁₀
190	methylphenanthrene	C ₁₅ H ₁₂
202	fluoranthene	C ₁₆ H ₁₀
202	pyrene	C ₁₆ H ₁₀
216	2,3-benzofluorene	C ₁₇ H ₁₂
228	1,2-benzanthracene	C ₁₈ H ₁₂
228	chrysene	C ₁₈ H ₁₂
252	benzo(b)fluoranthene, benzo(k)fluoranthene	C ₂₀ H ₁₂
252	benzo(e)pyrene	C ₂₀ H ₁₂
252	benzo(a)pyrene	C ₂₀ H ₁₂
252	perylene	C ₂₀ H ₁₂
276	benzoperylene	C ₂₂ H ₁₂
278	dibenzanthracene	C ₂₂ H ₁₄
300	coronene	C ₂₄ H ₁₂

Cellobiosan can also be taken as a starting source of some of the smaller molecules (including levoglucosan) identified in the pyrolysate:



The pyrolytic process of cellobiosan can also explain the formation of levoglucosenone and hydroxymethylfurfural:



Cellobiosan may generate by pyrolysis other anhydrosugars such as 1,4-anhydro- β -D-glucopyranose or 5,6-anhydro- β -D-glucopyranose. However, these anhydrosugars can be generated from cellulose itself by a similar mechanism as levoglucosan.

The pyrolysis of levoglucosan or cellobiosan does not generate all the compounds found in cellulose pyrolysis. The chromatographic profile of cellulose and levoglucosan pyrolysates obtained at 590°C are not identical [37] although they have significant similarities [37a]. This can be seen by comparing the upper and the lower trace in Figure 7.2.5. The upper trace (A) is the TIC for a cellulose pyrolysate at 590°C and is the same trace shown in Figure 7.2.1 on a different time scale (some peak

identifications can be obtained by comparing the retention times and the shape of the chromatograms). The lower trace (B) is the TIC for levoglucosan pyrolysate obtained at 590° C (silylated). The differences seen in the two chromatograms indicate that levoglucosan is not the only intermediate in cellulose degradation.

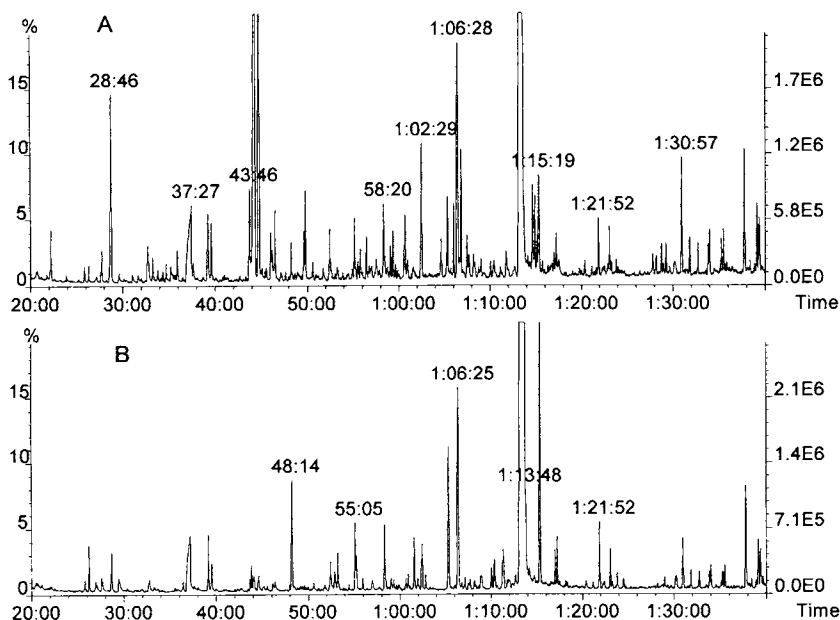
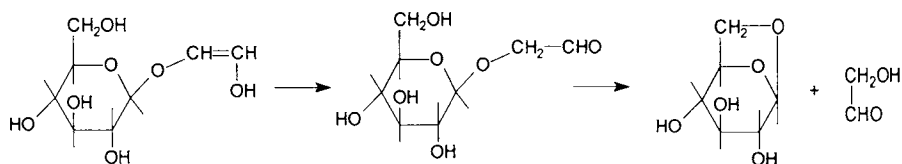
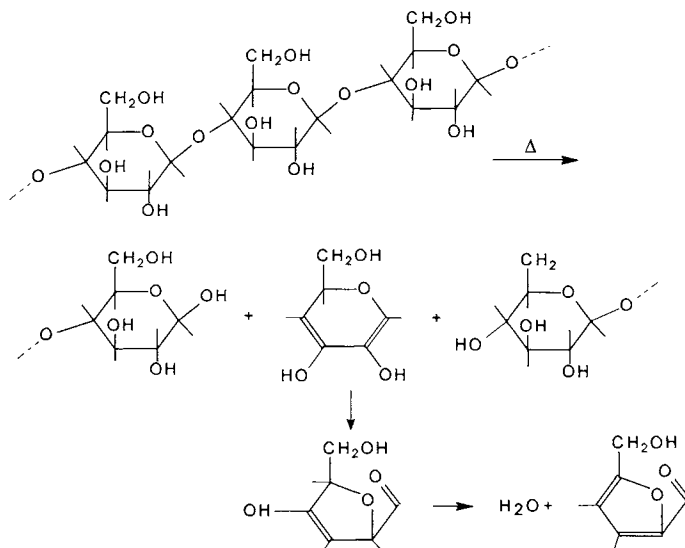


FIGURE 7.2.5. Upper trace A: TIC for cellulose pyrolysate obtained at 590° C and silylated, identical to the trace shown in Figure 7.2.1 (some peak identifications can be obtained by comparing the retention times and the shape of the chromatograms). Lower trace B: TIC for levoglucosan pyrolysate (silylated).

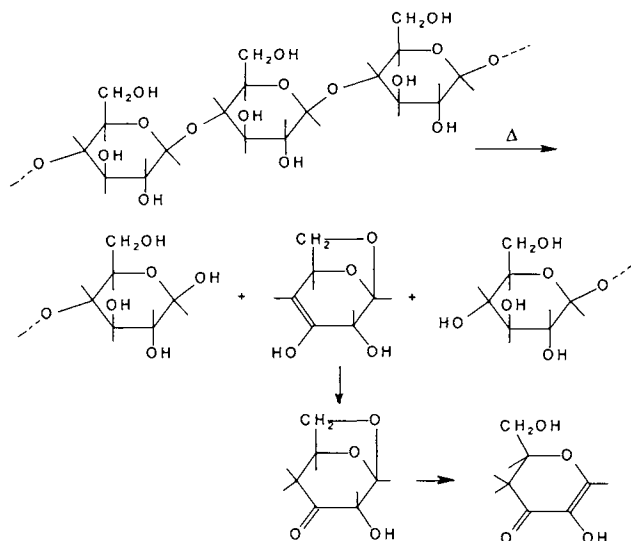
It is likely that many of the pyrolysis products of cellulose are generated by more than one reaction path. It is difficult to determine from the available experimental data which path is dominant. Even condensation reactions of the pyrolysis products are not excluded as additional possibilities to generate substances identified in the pyrolysate. The explanation of the formation of the same known pyrolysate constituents can start, for example, with 1-(2-hydroxyethenyl)- α -glucopyranoside and subsequent generation of levoglucosan:



Also, compounds that are very abundant in the pyrolysate such as hydroxymethylfurfural can be formed directly from cellulose:



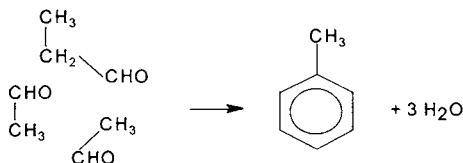
By a similar mechanism it is likely that 1,4-dideoxy-D-glycero-hex-1-enopyranos-ulose is formed:



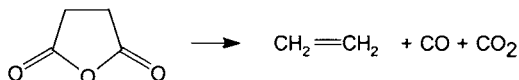
Formation of compounds such as dioxanediols can be explained by subsequent condensation reactions of the type:



The formation of aromatic hydrocarbons at more elevated pyrolysis temperatures can be explained by reactions of the type:



The formation of radicals at elevated temperatures from the mononuclear aromatic compounds, followed by condensations between them, may explain the presence of polynuclear aromatic compounds in the pyrolysate, as shown in Section 2.4. The generation of small molecules at higher pyrolysis temperatures can be explained by reactions of the type:



- Cellulose pyrolysis in acidic or basic conditions or in the presence of salts.

The influence of acidic conditions or basic conditions also has been studied extensively for cellulose [38,39]. Both bases and acids increase the formation of char and gases on the account of liquid pyrolytic products (pyrolytic oil) and accelerate the rate of pyrolysis compared to pyrolysis of pure cellulose at equal temperatures. The addition of potassium hydroxide clearly favors the retroaldolization mechanism. Lewis acids, such as ZnCl_2 , also accelerate the rate of pyrolysis compared to pyrolysis of pure cellulose at equal temperatures [40]. Other salts, like MgCl_2 or even NaCl , accelerate the decomposition but to a lower extent. The mechanism for the salt effects and the role of the inorganic ions is not clear [38]. Higher inorganic ion concentrations seem to favor hydroxyacetaldehyde formation associated with the decrease of levoglucosan. In spite of the accelerated rate of pyrolysis produced by some salts and bases, the same types of substances are used as flame retardants. This is explained by the role of these compounds in modifying the heat flux through the burning cellulose, char formation, non-combustible gas formation, etc., and does not indicate a decrease in the rate of cellulose pyrolysis.

Cellulose pretreated with acids, such as sulfuric acid or hydrochloric acid followed by a wash of the sample to neutrality also shows an increased rate of decomposition but generates more liquid pyrolytic products. These samples produce higher yields of levoglucosan associated with the decrease of hydroxyacetaldehyde. Inorganic ions SO_4^{2-} or Cl^- are found incorporated in the acid-pretreated and washed cellulose [38] (see also Section 7.3).

Cellulose pyrolysis in the presence of salts, acids, or bases may be used as a model of cellulose pyrolysis in a wood matrix. A series of differences are usually seen during pyrolysis of microcrystalline cellulose and wood, even considering only those components of wood that are generated by cellulose pyrolysis. The differences can be explained by the influence of inorganic components in wood, but also by the presence of chemical bonding of cellulose with lignin and hemicelluloses (xylans, etc.).

- Pyrolysis of cellulose in air.

Another aspect of cellulose pyrolysis is the pyrolysis in air (at non-flaming temperatures). This type of pyrolysis was studied mainly in connection with the stability to heating of different commercial cellulosic fibers [19]. It was determined that the main result of the presence of air is a more rapid decomposition. Oxygen acts mainly as a catalyst, and the chemical composition of the pyrolysate is not significantly different from the one obtained in an inert gas [41]. Cellulose of higher crystallinity is less influenced by the presence of air than the more amorphous one. It was suggested that some oxidation may take place at the macromolecular chain ends, but the crystallinity decreases the accessibility of oxygen to the macromolecular chain. In the presence of air, the yield of levoglucosan resulting from chain scission increases with crystallinity indicating the absence of the oxidative process.

- Kinetics of cellulose pyrolysis.

The kinetics of cellulose pyrolysis was extensively studied, mainly for practical purposes. As shown in Sections 3.2 and 3.3, cellulose pyrolysis can be approximated either by a reaction of first order (pseudo first order) or by more elaborate models. Assuming a first order reaction for example, the weight variation of a cellulose sample during pyrolysis is given by the relation (see rel. 15, Section 3.2):

$$W = W_0 \exp \left[-9.6 \cdot 10^5 \exp \left(-\frac{100700}{8.3146 \cdot T} \right) \cdot t \right] \quad (1)$$

where T is the temperature in °K and t is the time in sec. Other models are mainly utilized for describing the pyrolysis of larger quantities of cellulose, commonly for producing gases or pyrolytic oil for industrial purposes or related to fire problems as previously discussed in Section 3.3.

Several analytical applications of cellulose pyrolysis related to plant materials will be discussed in Part 3 of this book.

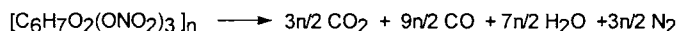
7.3 Chemically Modified Celluloses.

A variety of derivatives of cellulose are known and some of these have a large commercial production and use. Certain classes of cellulose derivatives can easily be recognized:

- inorganic esters (nitrate, sulfate, phosphate, etc.),
- organic esters (acetate, other aliphatic acids, benzoate, etc.),
- alkali cellulose,
- ethers (methyl, ethyl, carboxymethyl, hydroxypropyl, benzyl, etc.), and
- xanthates.

- *Pyrolysis of cellulose nitrate, sulfate, and phosphate.*

Cellulose nitrate (named also nitrocellulose) is the most important inorganic ester of cellulose. It can be obtained by the direct reaction of cellulose with HNO_3 , but for industrial purposes the reaction is done frequently in the presence of H_2SO_4 or H_3PO_4 (in addition to HNO_3). The nitration mechanism is that of a common esterification. Several degrees of esterification with HNO_3 can be obtained and are measured by the nitrogen content in cellulose. Depending on the intended use (lacquers, plastics, smokeless gunpowder), the nitrogen content varies between 10.0 to 13.5%. The product with 12.5–13.5% nitrogen is mainly used as smokeless gunpowder. The completely trisubstituted product corresponds to a theoretical nitrogen content of 14.14%. The decomposition of cellulose nitrate used as smokeless gunpowder starts at a low temperature (around 200°C) and, theoretically, takes place with the formation of H_2O , CO , CO_2 and N_2 , by the reaction:

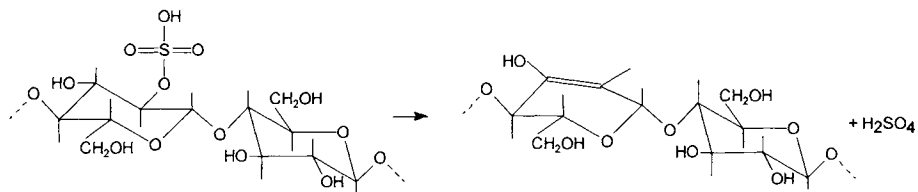


However, besides these compounds, several other compounds indicated in Table 7.3.1 were identified in the pyrolysate at 750°C [42].

TABLE 7.3.1. *Compounds identified in the pyrolysate of cellulose nitrate.*

MW	Name	Formula
28	nitrogen	N_2
30	nitrogen monoxide	NO
44	nitrous oxide	N_2O
46	nitrogen dioxide	NO_2
18	water	H_2O
27	hydrogen cyanide	HCN
28	carbon monoxide	CO
30	formaldehyde	CH_2O
44	carbon dioxide	CO_2
44	acetaldehyde	$\text{C}_2\text{H}_4\text{O}$
56	propenal (acrolein)	$\text{C}_3\text{H}_4\text{O}$
58	acetone	$\text{C}_3\text{H}_6\text{O}$

Cellulose sulfate has significantly fewer applications than the nitrate. The pyrolysis of cellulose treated with sulfuric acid and containing residual sulfate groups was previously discussed (see Section 7.2). The pyrolysate of this material has a chemical composition similar to that of cellulose pyrolysate. However, the existence of residual sulfate groups favors the reaction:



This reaction is supposed to have an E2 mechanism [32]. Further decomposition of the dehydrated cellulose results in an increased yield of water, char, gases and carbonyl compounds and a simultaneous decrease in levoglucosan formation as compared to pure cellulose pyrolysis.

Cellulose phosphate also has been studied regarding its stability to thermal degradation [42a]. It was determined that cellulose phosphate decomposes faster than pure cellulose, but it forms a highly condensed and cross-linked carbonaceous material containing polycyclic aromatic groups. This material acts as an effective flame retardant. The probable mechanism for the formation of this char is intermolecular condensation followed by further dehydration of the material. Cellulose phosphate complexes with a series of transitional metals also have been studied using PY-FI MS with the purpose of evaluating cellulose flameproofing [42b]. Thermal degradation of these compounds leads to the formation of metal phosphates and dehydrated cellulose that may further produce cross-linked char.

- Cellulose acetate.

Among the esters with organic acids, cellulose acetate is the most important one. Cellulose acetate has numerous uses such as manufacture of yarn, photographic films, lacquers, etc. Cellulose can be acetylated starting with lower levels of esterification up to the formation of cellulose triacetate. The acetate is obtained from the reaction of cellulose with acetic anhydride, usually in the presence of a catalyst such as H₂SO₄ or HClO₄. Numerous industrial procedures are known for this process [43].

Pyrolysis of cellulose acetate has been applied for analytical purposes of the fibers [44], structural elucidation [45], study of thermal stability [46], etc. The main pyrolysis product of cellulose acetate is acetic acid. Several compounds typical in cellulose pyrolysis such as 5-hydroxymethyl-2-furancarboxaldehyde can be seen as its ester with acetic acid. Also, some compounds tentatively identified as dihydroxydioxanes and dihydroxydioxolanes in cellulose pyrolysate are found as acetic acid esters in the pyrolysate of cellulose acetate. Depending on the degree of substitution (D.S.), for D.S. < 3, free -OH groups are still present in cellulose. This allows the formation of compounds typical for cellulose pyrolysate in addition to the compounds resulting from

the decomposition of totally acetylated glucose units. Some hydrolysis reactions may also occur, replacing acetyl groups with H.

The pyrolysate of cellulose acetate contains both volatile and less volatile compounds. In order to identify a wider range of compounds with different volatilities by GC analysis, it is common to apply two chromatographic conditions, one for the analysis of more volatile compounds and another for more polar and less volatile ones. The second technique may be associated with derivatizations. The results for the pyrolysis of a cellulose acetate sample at 590° C followed by GC/MS with the separation on a polar chromatographic column are shown in Figure 7.3.1. This particular separation was done on a 60 m Carbowax column with 0.32 mm i.d., 0.25 μ film thickness.

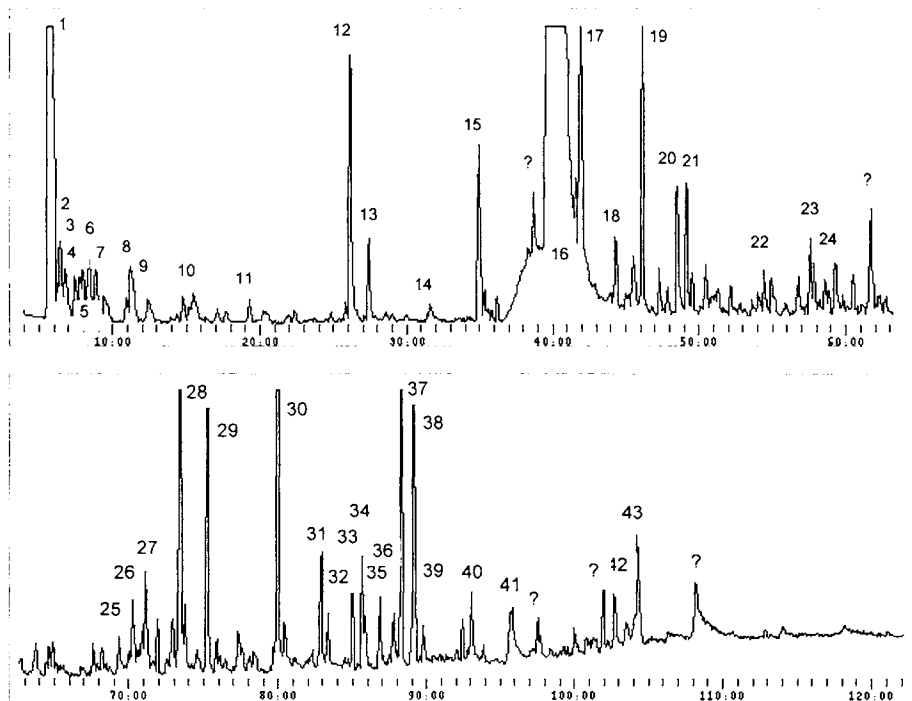


FIGURE 7.3.1. Total ion chromatogram for pyrolysed cellulose acetate separated on a Carbowax column. Peak # corresponds to the identification given in Table 7.3.2.

A list of the compounds identified by MS library searches in this pyrolysate is given in Table 7.3.2. Water and formaldehyde are absent from the chromatogram shown in Figure 7.3.1 and from the list of compounds given in Table 7.3.2 because the acquisition range of the mass spectrometer was set above $m/z = 32$. However, both water and formaldehyde are present in the pyrolysate.

TABLE 7.3.2. MS identification of the chromatographic peaks for pyrolysed cellulose acetate shown in Figure 7.3.1.

Peak #	Compound	Formula	MW
1	carbon dioxide	CO ₂	44
2	acetaldehyde	C ₂ H ₄ O	44
3	2-methyl-1-buten-3-yne	C ₅ H ₆	66
4	furan	C ₄ H ₄ O	68
5	acetone	C ₃ H ₆ O	58
6	2-propenal	C ₃ H ₄ O	56
7	3-methylfuran	C ₅ H ₆ O	82
8	3-buten-2-one	C ₄ H ₆ O	70
9	2,5-dimethylfuran	C ₆ H ₈ O	96
10	2,3-dihydrofuran	C ₄ H ₆ O	70
11	1-buten-4-ol acetate	C ₆ H ₁₀ O ₂	114
12	2-methylfuran	C ₅ H ₆ O	82
13	acetic anhydride	C ₄ H ₆ O ₃	102
14	1-hydroxy-2-propanone	C ₃ H ₆ O ₂	74
15	1,4-dioxaspiro[4,4]non-6-ene	C ₇ H ₁₀ O ₂	126
16	acetic acid	C ₂ H ₄ O ₂	60
17	furancarboxaldehyde	C ₅ H ₄ O ₂	96
18	furanylethanone	C ₆ H ₆ O ₂	110
19	furfuryl acetate	C ₇ H ₈ O ₃	140
20	methylfurancarboxaldehyde	C ₆ H ₆ O ₂	110
21	4-cyclohexene-1,3-dione	C ₅ H ₄ O ₂	96
22	5-methyl-2(5H)-furanone (angelica lactone)	C ₅ H ₆ O ₂	98
23	1,4-benzenediol	C ₆ H ₆ O ₂	110
24	2(H)-pyran-2-one	C ₅ H ₄ O ₂	96
25	1,4-benzenediol monoacetate	C ₈ H ₈ O ₃	152
26	2-furanmethanol	C ₅ H ₆ O ₂	98
27	phenol	C ₆ H ₆ O	94
28	2-penten-1,4-diol diacetate	C ₉ H ₁₄ O ₄	186
29	3-penten-1,4-diol diacetate	C ₉ H ₁₄ O ₄	186
30	5-acetoxymethyl-2-furancarboxaldehyde	C ₈ H ₈ O ₄	168
31	1,4-benzenediol diacetate	C ₁₀ H ₁₀ O ₄	194
32	1,2-diacetoxycyclohexane	C ₁₀ H ₁₆ O ₄	200
33	tetrahydro-2H-pyran-2,5-diol diacetate	C ₉ H ₁₄ O ₅	202
34	tetrahydro-2H-pyran-3,5-diol diacetate	C ₉ H ₁₄ O ₅	202
35	4-hydroxy-5-oxohexanoic acid lactone	C ₆ H ₈ O ₃	128
36	1,2-benzenediol diacetate	C ₁₀ H ₁₀ O ₄	194
37	acetylated anhydrosugar		
38	acetylated anhydrosugar		
39	benzoic acid	C ₇ H ₆ O ₂	122
40	1,3-benzenediol monoacetate	C ₈ H ₈ O ₃	152
41	3-ethyl-2-hydroxy-2-cyclopenten-2-one acetate	C ₉ H ₁₂ O ₃	168
42	anhydrosugar acetate		
43	anhydrosugar acetate		

In order to identify less volatile compounds, the pyrolysis of cellulose acetate sample (at 590° C) can be followed by an off-line derivatization with bis-(trimethylsilyl)-trifluoroacetamide (BSTFA). Typically the derivatized pyrolysate is analyzed by GC/MS on a non-polar column. The results of this type of analysis (separation on a 60 m DB-5 column 0.32 mm i.d. and 0.25 μ film thickness) is shown in Figure 7.3.2 and the peak identification is given in Table 7.3.3.

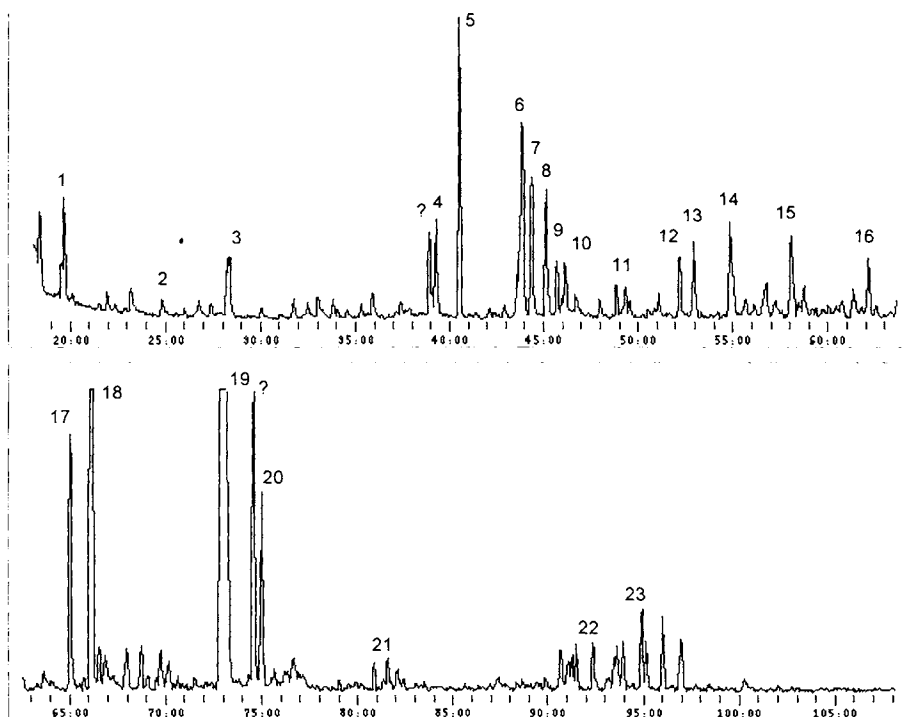


FIGURE 7.3.2. Total ion chromatogram for pyrolysed cellulose acetate with silylation and separation on a DB5 column. Peak # corresponds to the identification given in Table 7.3.3.

TABLE 7.3.3. MS identification of the chromatographic peaks for cellulose acetate pyrolysate shown in Figure 7.3.2.

Peak No.	Compound	Formula	MW
1	reagent		
2	lactic acid di-TMS	C ₉ H ₂₂ O ₃ Si ₂	234
3	hydroxyacetic acid di-TMS	C ₈ H ₂₀ O ₃ Si ₂	220
4	dihydroxyacetone di-TMS	C ₉ H ₂₂ O ₃ Si ₂	234
5	3-oxy-butanoic acid TMS	C ₁₀ H ₂₄ O ₃ Si ₂	248
6	1,3-dioxolane-x,y -diol di-TMS ?	C ₉ H ₂₂ O ₄ Si ₂	250
7	1,4-dioxane-x,y-diol di-TMS ?	C ₁₀ H ₂₄ O ₄ Si ₂	264
8	1,3-dioxolane-x,y -diol di-TMS ?	C ₉ H ₂₂ O ₄ Si ₂	250
9	1,4-dioxane-x,y-diol di-TMS ?	C ₁₀ H ₂₄ O ₄ Si ₂	264
10	1,4-dihydroxybenzene di-TMS	C ₁₂ H ₂₂ O ₂ Si ₂	254
11	2,4-dimethyl-2-(TMS-oxy)-cyclopent-2-en-1-one	C ₁₀ H ₁₈ O ₂ Si	198
12	1,2-dihydroxybenzene di-TMS	C ₁₂ H ₂₂ O ₂ Si ₂	254
13	1,4-dioxane-x,y-diol di-TMS type		
14	dioxaheptanoic acid tri-TMS ?	C ₁₆ H ₃₄ O ₄ Si ₃	374
15	2-hydroxy-5-(hydroxymethyl)-4Hpyran-4-one di-TMS	C ₁₂ H ₂₂ O ₄ Si ₂	286
16	1,2,3-trihydroxybenzene tri-TMS	C ₁₅ H ₃₀ O ₃ Si ₃	342
17	2-isopropyl-3-ketobutyrate di-TMS ?	C ₁₃ H ₂₈ O ₃ Si ₂	288
18	2,3,5-trihydroxybenzene tri-TMS	C ₁₅ H ₃₀ O ₃ Si ₃	342
19	levoglucosan tri-TMS	C ₁₅ H ₃₄ O ₅ Si ₃	378
20–23	sugar or anhydrosugar x-TMS		

TABLE 7.3.4. *Main pyrolysis products of ethyl cellulose at 590° C.*

MW	Name	Formula
44	acetaldehyde	C2H4O
46	ethanol	C2H6O
56	propenal	C3H4O
58	propanal	C3H6O
68	furan	C4H4O
86	2,3-butandione	C4H6O2
72	ethoxyethene	C4H8O
88	ethoxyacetaldehyde	C4H8O2
104	ethoxyacetic acid	C4H8O3
90	ethoxyethanol	C4H10O2
66	1,3-cyclopentadiene	C5H6
82	cyclopentenone	C5H6O
82	methylfuran	C5H6O
84	cyclopentanone	C5H8O2
86	ethoxypropene	C5H10O
102	ethoxypropanal	C5H10O2
126	trihydroxybenzene	C6H6O3
126	levoglucosenone	C6H6O3
126	(hydroxymethyl)furanaldehyde	C6H6O3
112	ethoxyfuran	C6H8O2
128	ethoxyfuranone	C6H8O3
128	(hydroxymethyl)dihydrofuranaldehyde	C6H8O3
100	methylpentenol	C6H12O
134	1-hydroxy-ethyleneglycoldiethylether	C6H14O3
142	3-ethoxy-5-hydroxymethylfuran	C7H10O3
142	2-ethoxy-5-hydroxymethylfuran	C7H10O3
138	ethoxyphenol	C8H10O2
154	(ethoxymethyl)furanaldehyde	C8H10O3
154	dihydroxyethoxybenzene	C8H10O3
156	2,5-diethoxyfuran	C8H12O3
156	2,3-diethoxyfuran	C8H12O3
172	diethoxyfuranone	C8H12O4
218	diethylated levoglucosan	C10H18O5
264	triethylated glucose	C12H24O6
	several ethylated disaccharides	

For high substitution of ethyl cellulose, levoglucosan is practically absent and only triethylated levoglucosan is seen in the pyrolysate. Table 7.3.4 shows the main pyrolysis products of ethyl cellulose with D.S. \approx 3 at 590° C.

Sodium carboxymethyl cellulose, $R_{Cell}O-CH_2COO^- Na^+$ (CMC), is another common cellulose ether. The degree of substitution (D.S.) that can be obtained for this product usually ranges between D.S. = 0.1 to D.S. = 1.2. As a by-product, sodium glycolate can be formed in the synthesis. Pure CMC is commercially available. Carboxymethyl cellulose in itself is a weak acid that can be precipitated from CMC solutions with a mineral acid. The pH of precipitation varies between 6 for low substitution values to 1 for high substitution (D.S of about 0.9).

As indicated previously, when a GC/MS procedure is applied for the analysis of a pyrolysate, it is difficult to detect the variety of compounds generated during the pyrolysis by using only one chromatographic procedure. Two chromatographic techniques are, however, able to cover a wide range of volatility. The CMC pyrolysate

can be well analyzed by using on-line Py-GC/MS with the separation on a polar chromatographic column [50] and, as a second procedure, using off-line derivatization of the pyrolysate with BSTFA followed by GC/MS analysis. In the on-line Py-GC/MS experiment, the more polar molecules are not seen because they do not elute from the chromatographic column. At the same time, the second procedure does not detect smaller and non-polar molecules.

A total ion chromatogram (TIC) obtained by on-line Py-GC/MS of pyrolysed CMC (Hercules 12M31; D.S. 1.2) at 590° C is shown in Figure 7.3.3. The separation was done on a Carbowax column 60 m long, 0.32 mm i.d. and 0.25 μ film thickness. Water is again not shown in the chromatogram given in Figure 7.3.3 and is absent from Table 7.3.5 because the acquisition range of the mass spectrometer was set above 18. Water is, however, present in the pyrolysate of CMC.

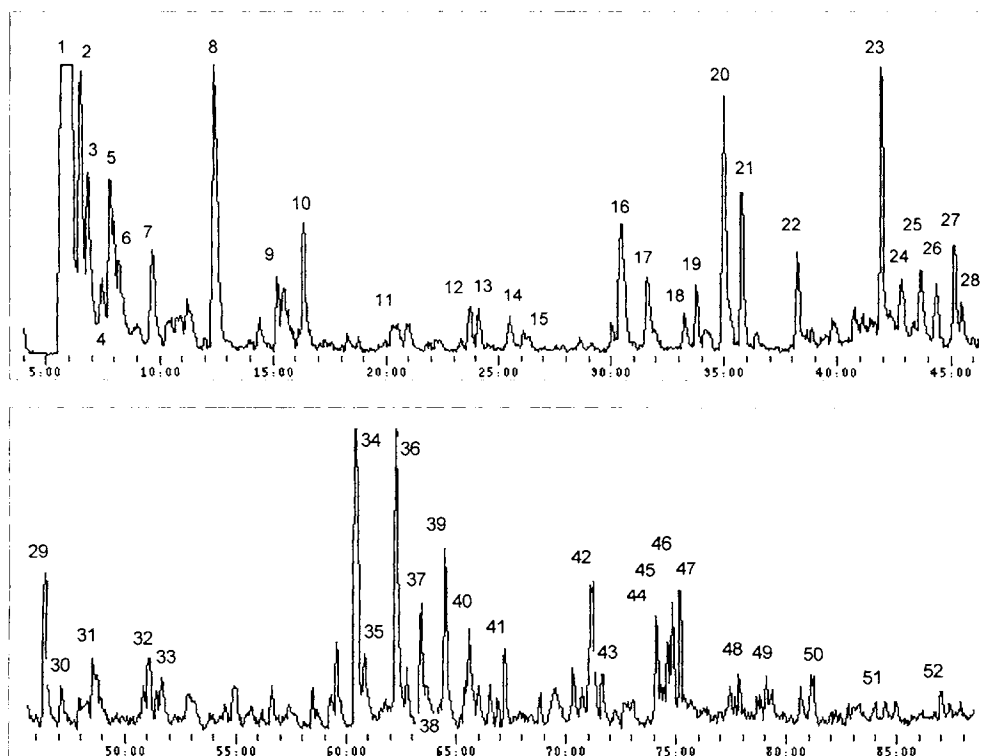


FIGURE 7.3.3. Total ion chromatogram for pyrolysed CMC by on-line Py-GC/MS with separation on a Carbowax column.

A series of compounds identified in the TIC shown in Figure 7.3.3 are listed in Table 7.3.5. As seen in Table 7.3.5, several cyclopentadiene derivatives were identified in CMC pyrolysate, similar to those from cellulose pyrolysate.

TABLE 7.3.5. Peaks identified in the TIC of CMC pyrolysate separated on a Carbowax column.

Peak #	Compound	Formula	MW
1	carbon dioxide	CO ₂	44
2	acetaldehyde	C ₂ H ₄ O	44
3	cyclopentadiene	C ₅ H ₆ O	82
4	furan	C ₄ H ₄ O	68
5	acetone	C ₃ H ₆ O	58
6	5-methyl-1,3-cyclopentadiene	C ₆ H ₈	80
7	butanone	C ₄ H ₈ O	72
8	2,3-butanedione	C ₄ H ₆ O ₂	86
9	toluene	C ₇ H ₈	92
10	2,3-pentandione	C ₅ H ₈ O ₂	100
11	m-xylene	C ₈ H ₁₀	106
12	cyclopentanone	C ₅ H ₈ O	84
13	2-methylcyclopentanone	C ₆ H ₁₀ O	98
14	3-ethyl-2,5-dihydrofuran	C ₆ H ₁₀ O	98
15	1,2,3-trimethylbenzene	C ₉ H ₁₂	120
16	3-hydroxy-2-butanone	C ₄ H ₈ O ₂	88
17	1-hydroxy-2-propanone	C ₃ H ₆ O ₂	74
18	1-methylcyclohexene	C ₇ H ₁₂	96
19	2,5-dimethyl-2-cyclopentenone	C ₇ H ₁₀ O	110
20	2-cyclopenten-1-one	C ₅ H ₆ O	82
21	2-methyl-2-cyclopenten-1-one	C ₆ H ₈ O	96
22	2,5-furandione	C ₄ H ₂ O ₃	98
23	furancarboxaldehyde	C ₅ H ₄ O ₂	96
24	4,4-dimethyl-2-cyclopenten-1-one	C ₇ H ₁₀ O	110
25	2,3,4-trimethyl-2-cyclopenten-1-one	C ₈ H ₁₂ O	124
26	furanyl ethanone	C ₆ H ₆ O ₂	110
27	3-methyl-2-cyclopenten-1-one	C ₆ H ₈ O	96
28	benzaldehyde	C ₇ H ₆ O	106
29	2,3-dimethyl-cyclopent-2-en-1-one	C ₇ H ₁₀ O	110
30	2,3,4-trimethyl-cyclopent-2-en-1-one	C ₈ H ₁₂ O	124
31	5-methylfurancarboxaldehyde	C ₆ H ₆ O ₂	110
32	tetrahydro-2H-pyran-2-one	C ₅ H ₈ O ₂	100
33	3,4,5-trimethyl-cyclopent-2-en-1-one	C ₈ H ₁₂ O	124
34	2,4-dimethyl-2-hydroxycyclopent-2-en-1-one	C ₇ H ₁₀ O ₂	126
35	2-ethyl-3-methoxy-2-cyclopenteneone	C ₈ H ₁₂ O ₂	140
36	2-hydroxy-3-methyl-2-cyclopenten-1-one	C ₆ H ₈ O ₂	112
37	2,3-dimethyl-cyclopentenol-one	C ₇ H ₁₀ O ₂	126
38	1-methoxy-6,6-dimethyl-cyclohexene	C ₉ H ₁₆ O	140
39	2,3,4,5-tetramethylcyclopent-2-en-1-ol	C ₉ H ₁₆ O	140
40	3-ethyl-2-hydroxy-2-cyclopenten-2-one	C ₇ H ₁₀ O ₂	126
41	3,5-diethyl-2-hydroxy-2-cyclopent-2-en-1-one	C ₉ H ₁₄ O ₂	154
42	2-methylphenol	C ₇ H ₈ O	108
43	2,3-dihydro-1H-inden-2-one	C ₉ H ₈ O	132
44	4-hydroxy-5-oxohexanoic acid lactone	C ₆ H ₈ O ₃	128
45	2,5-dimethylphenol	C ₈ H ₁₀ O	122
46	2,3-dimethylphenol	C ₈ H ₁₀ O	122
47	3-methylphenol	C ₇ H ₈ O	108
48	3,5-dimethylphenol	C ₈ H ₁₀ O	122
49	4-ethylphenol	C ₈ H ₁₀ O	122
50	2,4,6-trimethylphenol	C ₉ H ₁₂ O	136
51	3-ethyl-5-methylphenol	C ₉ H ₁₂ O	136
52	1(3H)-isobenzofuranone	C ₈ H ₆ O ₂	134

The TIC obtained using off-line pyrolysis of CMC (D.S. 1.2) done at 590° C followed by derivatization with BSTFA and separation on a non-polar column is shown in Figure 7.3.4.

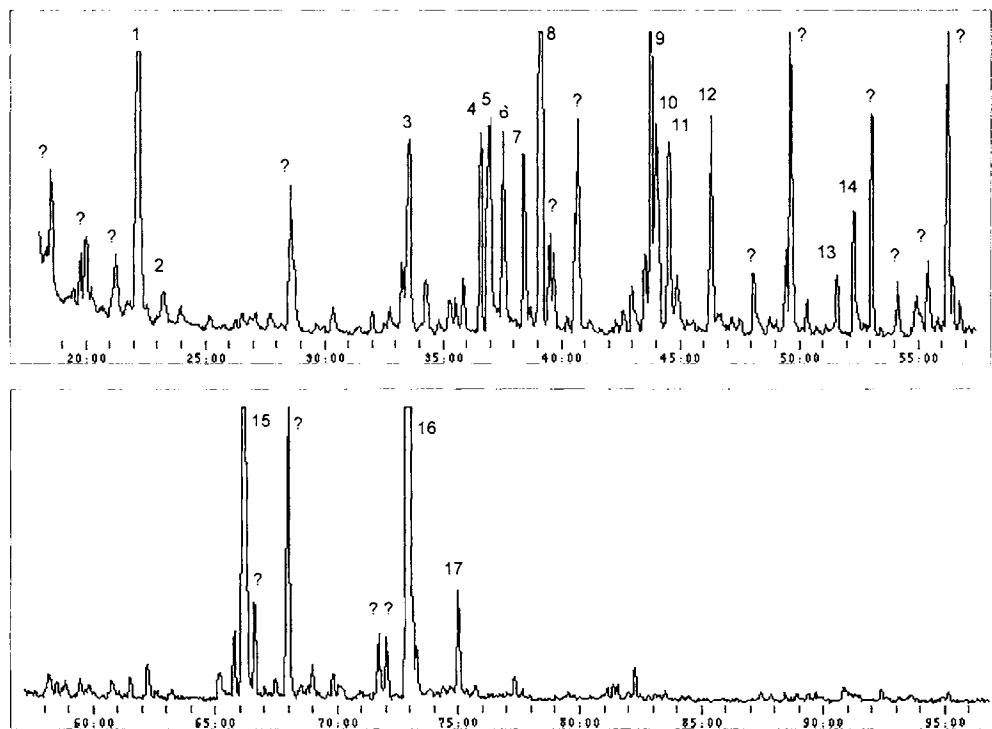


FIGURE 7.3.4. Total ion chromatogram for pyrolysed CMC at 590° C with silylation and separation on a DB5 column.

The column used in this case was a DB5 column, 60 m long, 0.32 mm i.d. and 0.25 μ film thickness. The GC oven program was varied between 50° C to 300° C. A series of compounds identified in the chromatogram after silylation are given in Table 7.3.6. Levoglucosan is still a major pyrolysis product. Several compounds seen in CMC pyrolysate are also generated during pyrolysis of microcrystalline cellulose (see Section 7.2). This is due to the fact that the D.S. for CMC is not close to 3 (it is far from a complete substitution of -OH groups with -O-CH₂COONa) and numerous free -OH groups are still present in CMC.

TABLE 7.3.6. Peaks identified in the TIC of CMC silylated pyrolysate separated on a DB5 column.

Peak #	Compound	Formula	MW
1	ethylene glycol di-TMS	C ₈ H ₂₂ O ₂ Si ₂	206
2	butandiol di-TMS	C ₁₀ H ₂₆ O ₂ Si ₂	234
3	2-(TMS-oxy)-TMS-butanoic acid	C ₁₀ H ₂₄ O ₃ Si ₂	248
4	1,3-propandiol-di-TMS	C ₉ H ₂₄ O ₂ Si ₂	220
5	reagent		ion 99
6	2-(TMS-oxy)-3-methyl-2-cyclopenten-1-one	C ₉ H ₁₆ O ₂ Si	184
7	2,4-dimethyl-2-(TMS-oxy)-cyclopent-2-en-1-one	C ₁₀ H ₁₈ O ₂ Si	198
8	bis-(TMS-oxy)-TMS-acetic acid	C ₁₁ H ₂₈ O ₄ Si ₃	308
9	glycerol tris-(TMS)	C ₁₂ H ₃₂ O ₃ Si ₃	308
10	bis-O-(TMS)-1,4-dioxan-2,5-diol	C ₁₀ H ₂₄ O ₄ Si ₂	264
11	bis-O-(TMS)-1,3-dioxolane-4,5-diol	C ₉ H ₂₂ O ₄ Si ₂	250
12	bis-(TMS)-(bis-1,2-oxy-phenylene)	C ₁₂ H ₂₂ O ₂ Si ₂	254
13	4-methyl-bis-(TMS)-(bis-1,2-oxy-phenylene)	C ₁₃ H ₂₄ O ₂ Si ₂	268
14	bis-(TMS)-(bis-1,4-oxy-phenylene)	C ₁₂ H ₂₂ O ₂ Si ₂	254
15	internal standard		
16	levoglucosan-tri-TMS	C ₁₅ H ₃₄ O ₅ Si ₃	378
17	TMS-monosaccharide ?		

A series of other ethers of cellulose also have practical applications, and their pyrolysis products can be used for analytical purposes such as their identification in modified paper, in lacquers and varnishes, etc. Hydroxyethyl celluloses are frequently utilized as protective colloids.

During the synthesis process of hydroxyethyl celluloses involving ethylenoxide, the free -OH groups of cellulose can be replaced with -O-CH₂CH₂OH, with -O-CH₂CH₂-O-CH₂CH₂OH or with -(O-CH₂CH₂)_n-O-CH₂CH₂OH (n = 2, 3, ...). The pyrolysis products [12] generate a series of compounds similar to those found in cellulose pyrolysate with substitution on some of the -OH groups, as well as significant amounts of polyethylene glycols, polyethylene glycol aldehydes and their derivatives obtained by the elimination of water:

H-(O-CH₂CH₂)_n-O-CH₂CH₂OH (n = 0, 1, 2, 3, ...) MW = 62, 106, 150, etc.

H-(O-CH₂CH₂)_n-O-CH₂CHO (n = 1, 2, 3, ...) MW = 104, 148, 192, etc.

CH₂=CH-(O-CH₂CH₂)_n-O-CH₂CHO (n = 0, 1, 2, 3, ...) MW = 86, 130, 174, etc.

Several pyrolysis studies have been done on O-(2-hydroxyethyl) celluloses [50a]. In one such study, Py-MS was used to determine the degree of substitution per glucosyl residue [50a] and also to obtain some information about the pyrolysis mechanism of this material.

Hydroxypropyl methyl cellulose analyzed by using on-line Py-GC/MS with the separation on a polar chromatographic column [50] gives the TIC shown in Figure 7.3.5. This particular material had about 10% substitution with hydroxypropyl and 30% substitution with methyl on the OH groups.

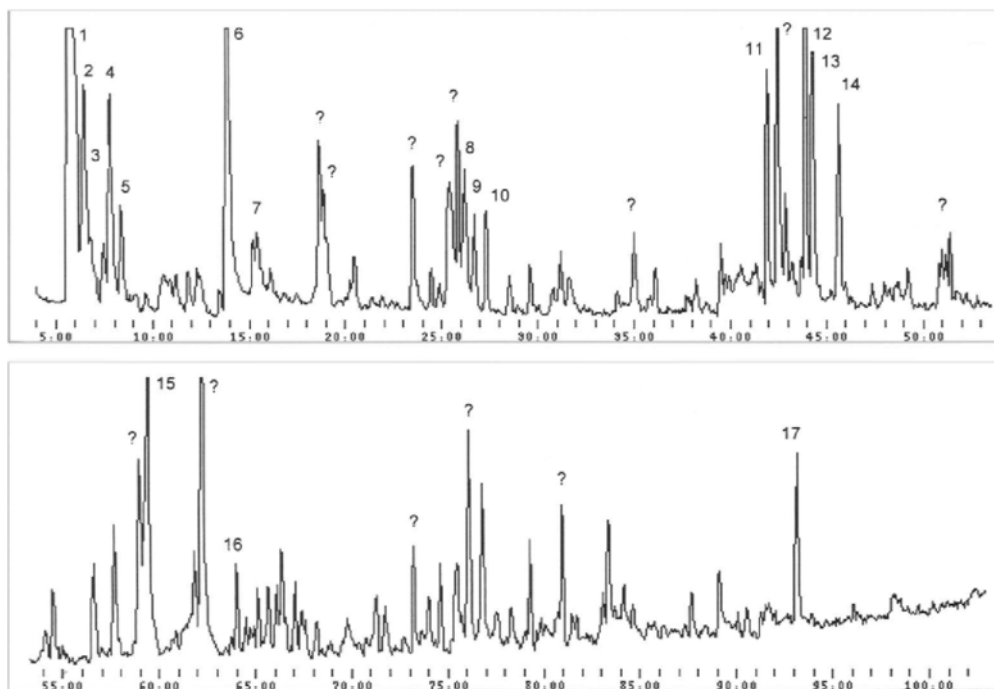


FIGURE 7.3.5. Total ion chromatogram for pyrolysed hydroxypropyl methyl cellulose by on-line Py-GC/MS at 590° C with separation on a Carbowax column.

A series of compounds identified in the TIC of hydroxypropyl methyl cellulose pyrolysate are listed in Table 7.3.7. Water, CO, formaldehyde, and most importantly methanol are not shown in the chromatogram although present in the pyrolysate.

TABLE 7.3.7. Peaks identified in the TIC of hydroxypropyl methyl cellulose pyrolysate separated on a Carbowax column.

Peak #	Compound	Formula	MW
1	carbon dioxide	CO ₂	44
2	acetaldehyde	C ₂ H ₄ O	44
3	furan	C ₄ H ₄ O	68
4	acetone	C ₃ H ₆ O	58
5	2-propenal	C ₃ H ₄ O	56
6	methoxyacetaldehyde	C ₃ H ₆ O ₂	74
7	2-butenal	C ₄ H ₆ O	70
8	2-methylfuran	C ₅ H ₆ O	82
9	5-methylcyclopenten-3-one	C ₆ H ₈ O ₂	112
10	2-(methoxymethyl)-furan	C ₆ H ₈ O ₂	112
11	furancarboxaldehyde	C ₅ H ₄ O ₂	96
12	2-(1',2'-dihydroxyethyl)-furan ?	C ₆ H ₈ O ₃	128
13	dihydrofuroic acid methyl ester ?	C ₆ H ₈ O ₃	128
14	1,1'-biindenyl ?	C ₁₈ H ₁₄	230
15	methoxydihydrofuroic acid methyl ester	C ₇ H ₁₀ O ₄	158
16	2-methoxyphenol	C ₇ H ₈ O ₂	124
17	2-(dihydropyranon-yl)-acetic acid methyl ester	C ₈ H ₁₀ O ₄	170

The TIC obtained using off-line pyrolysis of hydroxypropyl methyl cellulose followed by derivatization with BSTFA and separation on a non-polar column is shown in Figure 7.3.6. The column used for the separation was a DB5 column, 60 m long, 0.32 mm i.d. and 0.25 μ film thickness. The GC oven program was varied between 50° C to 300° C.

The compound identifications are more difficult in this case due to the possibility of having together compounds generated from glucose units with little or no substitution, units substituted with methyl groups, and units substituted with hydroxypropyl. By derivatization, all the active hydrogens from the -OH groups are substituted with O-TMS groups. This will also take place for the fragments containing hydroxypropyl groups.

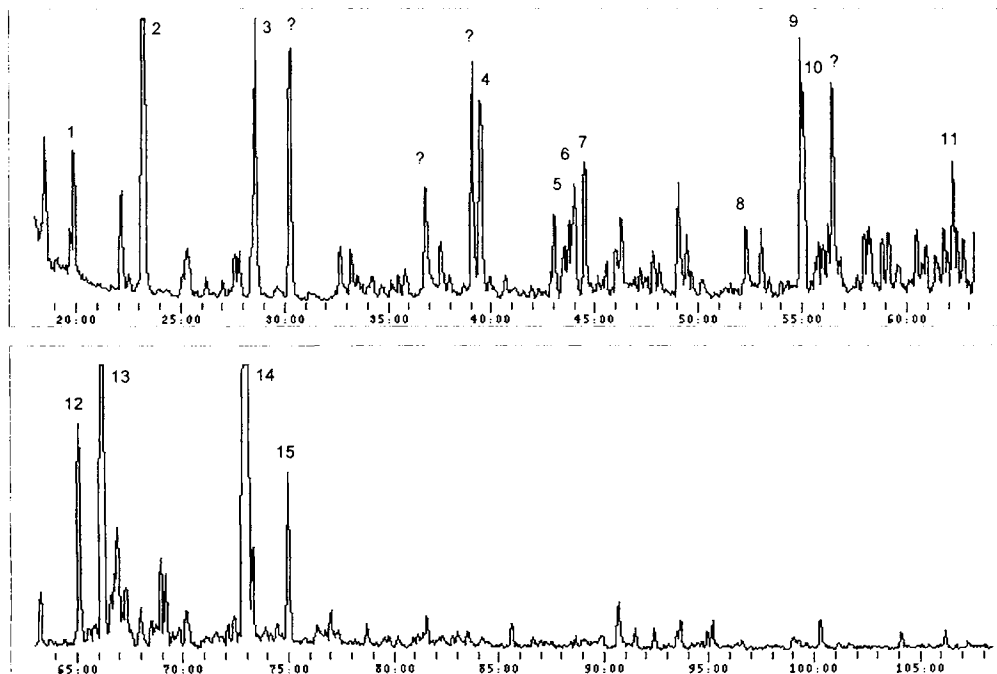


FIGURE 7.3.6. Total ion chromatogram for pyrolysed hydroxypropyl methyl cellulose silylated and separated on a DB5 column.

Some peak identifications for Figure 7.3.6 found in trimethylsilylated hydroxypropyl methyl cellulose pyrolysate are given in Table 7.3.8.

TABLE 7.3.8. Peaks identified in the TIC of hydroxypropyl methyl cellulose pyrolysate silylated and separated on a DB5 column.

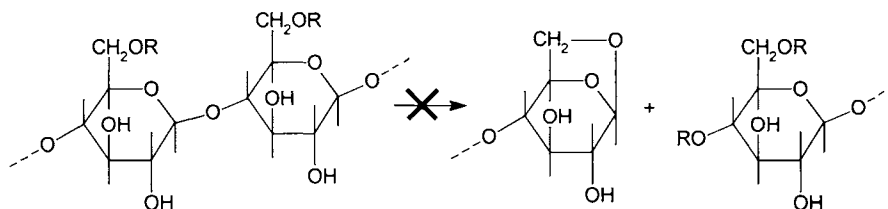
Peak #	Compound	Formula	MW
1	reagent		
2	ethylene glycol di-TMS	C ₈ H ₂₂ O ₂ Si ₂	206
3	hydroxyacetic acid di-TMS	C ₈ H ₂₀ O ₃ Si ₂	220
4	dihydroxyacetone di-TMS	C ₁₃ H ₂₂ O ₃ Si ₃	234
5	glycerin tri-TMS	C ₁₂ H ₃₂ O ₃ Si ₃	308
6	1,3-dioxolane-x,y -diol di-TMS ?	C ₉ H ₂₂ O ₄ Si ₂	250
7	1,4-dioxane-x,y-diol di-TMS ?	C ₁₀ H ₂₄ O ₄ Si ₂	264
8	1,2-dihydroxybenzene di-TMS	C ₁₂ H ₂₂ O ₂ Si ₂	254
9	2,5-di(hydroxymethyl)-furan di-TMS	C ₁₂ H ₂₄ O ₃ Si ₂	272
10	2-hydroxy-5-(hydroxymethyl)-furan di-TMS	C ₁₁ H ₂₂ O ₃ Si ₂	258
11	2,3,5-trihydroxybenzene tri-TMS	C ₁₅ H ₃₀ O ₃ Si ₃	342
12	2-isopropyl-3-ketobutyrate di-TMS	C ₁₃ H ₂₈ O ₃ Si ₂	288
13	2,3,5-trihydroxybenzene tri-TMS	C ₁₅ H ₃₀ O ₃ Si ₃	342
14	levoglucosan tri-TMS	C ₁₅ H ₃₄ O ₅ Si ₃	378
15	sugar or anhydrosugar x-TMS		

- Mechanisms in the pyrolysis of cellulose derivatives.

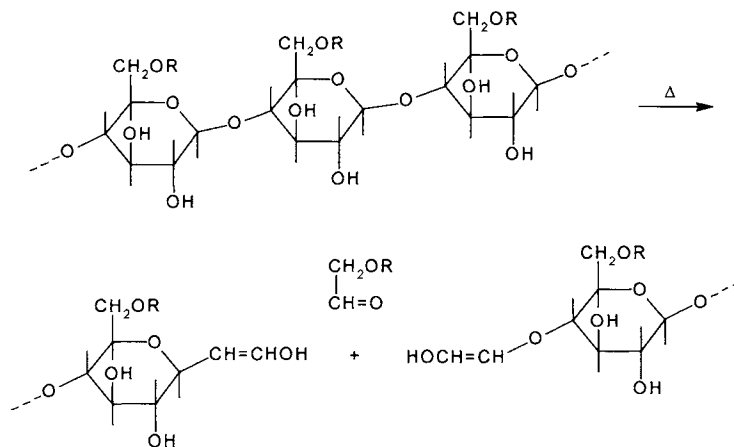
As it was indicated for cellulose, the pyrolysis of cellulose ethers may also take place in two steps:

- first step having the polymer as starting material and generating smaller molecules (with the three proposed mechanisms: transglycosidation, reverse aldolization and elimination).
- second step consisting of further pyrolysis of the products generated in the first step (with a variety of mechanisms).

Compared to cellulose and the possible mechanisms taking place during the first step in its pyrolysis, for the ethers of celluloses the transglycosidation is of much lower importance [23].



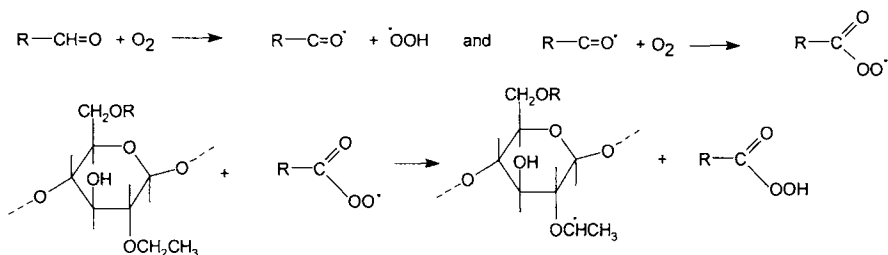
At the same time, the reverse aldolization and the elimination seem to occur in the same manner as for cellulose. The elimination reaction for ethyl cellulose was shown previously (see Section 2.1). The reverse aldolization (shown for cellulose) probably occurs as follows:



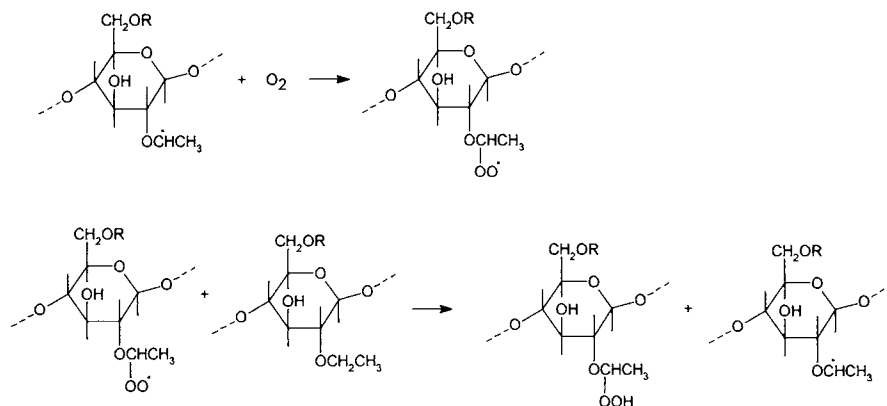
Regarding the further steps in pyrolysis, common reactions such as water elimination, fragmentations and possible condensations may take place from the small molecules.

The pyrolysis of modified celluloses is a rather complex process [46]. One additional element of complexity for these materials is brought by the variety of substitutions on the cellulose backbone. For a material with the D.S. lower than 3, a mixture of cellulose pyrolysate and modified cellulose pyrolysate is generated. This complicates the understanding of the pyrolysis mechanism. It is, however, likely that the same pyrolysis mechanisms as for cellulose will function for substituted celluloses.

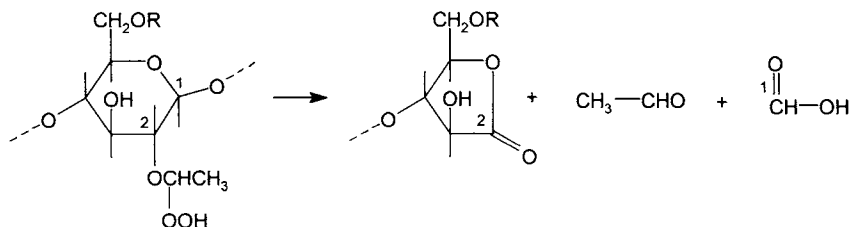
For the oxidative pyrolysis (pyrolysis in the presence of oxygen around 100° C to 150° C, namely below the ignition temperature), it was shown that in contrast to cellulose, substituted celluloses degrade oxidatively [23a]. This was evaluated in more depth for ethyl cellulose [51]. The reaction starts probably with the initiation step at the free aldehyde groups:



Subsequent to the initiation, the propagation may take place with the formation of a hydroperoxide at the ethoxy group:



Studies with labeled carbon [52] indicate that to a considerable extent the decomposition of the hydroperoxide takes place with the scission of C-1 to C-2 bond.



Besides formic acid and acetaldehyde, the oxidative pyrolysis also generates ethanol, ethyl formate, ethane, CO_2 , CO , etc.

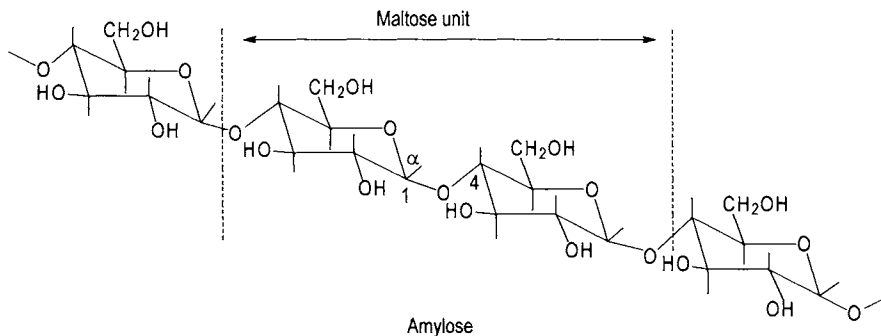
Other substituted celluloses were found to behave similarly to ethyl cellulose. An oxidation susceptibility order was established [23a]: allyl cellulose > CMC > benzyl cellulose > ethyl cellulose > cyanoethyl cellulose. The cellulose ethers were found to be less resistant to oxidation than the esters.

The pyrolytic oxidation of the esters generates mainly the esterifying acid and, when the acid has a longer chain, some aldehydes and acids with shorter chain length but which are formed from the esterifying acid. Formaldehyde, formic acid, CO_2 , CO , etc. are formed from the glucose units.

7.4 Amylose and Amylopectin.

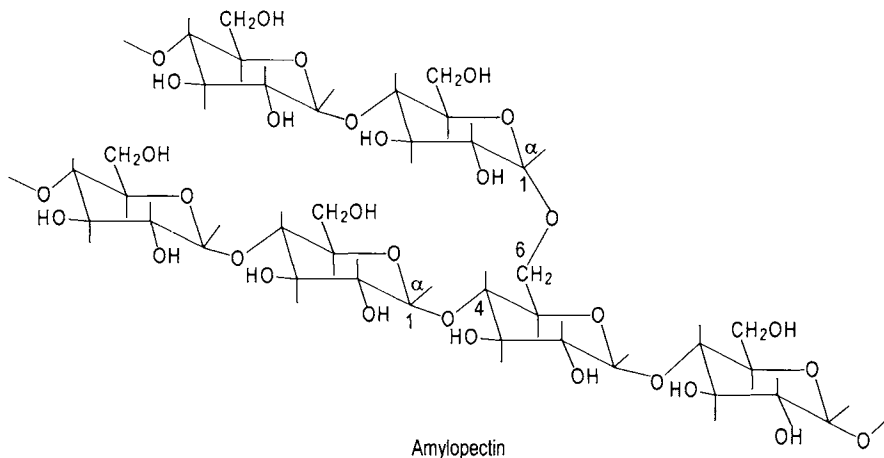
Amylose and amylopectin are the two main constituents of starch. Similarly to cellulose, starch is very common in plant cells. The proportion of amylose and amylopectin in starch varies, and cornstarch for example contains about 27% amylose and 73% amylopectin.

Amylose is formed from α -D-glycosyl units interconnected by α -glucosidic (1 \rightarrow 4) links (cellulose has β -glucosidic (1 \rightarrow 4) links).



Chemical procedures for the determination of the DP values of amylose indicate 200-300 glucose units, while light scattering and ultracentrifugation indicate a DP of about 6000.

Amylopectin has a similar structure but does have some branching at C-6 OH groups [it has (1 \rightarrow 6)- α -D- links] and a higher DP. The length of the branches is estimated to be 17 to 26 glucose units and the DP is about 10^6 D-glycosyl units.

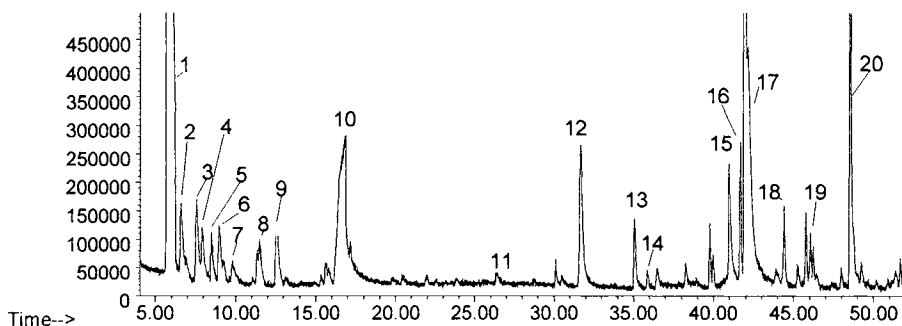


- Pyrolysis of starch.

Because of its practical importance, significant effort was made to understand the pyrolysis of starch rather than one of its components. Data are also available on amylose pyrolysis alone, but much less on amylopectin. However, the pyrolysis products of these compounds are expected to be the same. Starch pyrolysis generates

compounds analogous to those from cellulose. Similarly to cellulose, starch generates carbonaceous char as a residue, gases, water, and tar. Compared to cellulose there are, however, variations in peak intensities and even some variation in the nature of components in the pyrolysate. A TIC for starch (with an unknown ratio of amylose and amylopectin) pyrolysate obtained at 590° C by on-line Py-GC/MS is given in Figure 7.4.1.

Abundance



Abundance

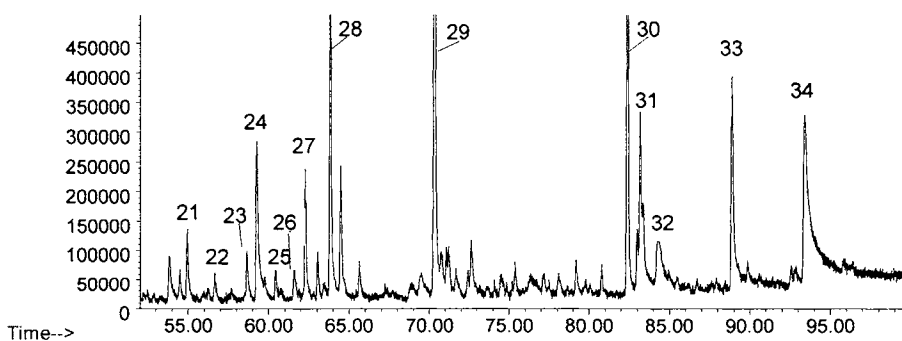


FIGURE 7.4.1. Starch pyrolysate at 590° C and separated on a Carbowax column. Peak identification (by mass spectra library search) is indicated in Table 7.4.1.

The separation was done on a Carbowax column, 60 m long, 0.32 mm i.d. and 0.25 μ film thickness. The temperature of the GC oven had a gradient between 35° C and 240° C. The identification of the peaks shown in Figure 7.4.1 was done by mass spectral library search and the results are given in Table 7.4.1.

TABLE 7.4.1. *Peak identification for starch pyrolysate separated on a Carbowax column and shown in Figure 7.4.1.*

Peak #	Compound	Formula	MW
1	carbon dioxide	CO ₂	44
2	acetaldehyde	C ₂ H ₄ O	44
3	furan	C ₄ H ₄ O	68
4	acetone	C ₃ H ₆ O	58
5	2-propenal	C ₃ H ₄ O	56
6	2-methylfuran	C ₅ H ₆ O	82
7	2-butanone	C ₄ H ₈ O	72
8	2,5-dimethylfuran	C ₆ H ₈ O	96
9	2,3-butanedione	C ₄ H ₆ O ₂	86
10	water	H ₂ O	18
11	3-methylfuran	C ₅ H ₆ O	82
12	hydroxypropanone	C ₃ H ₆ O ₂	74
13	2-cyclopenten-1-one	C ₅ H ₆ O	82
14	2-methyl-2-cyclopenten-1-one	C ₆ H ₈ O	96
15	acetic acid	C ₂ H ₄ O ₂	60
16	methyl pyruvate	C ₄ H ₆ O ₃	102
17	furfural (furan carboxaldehyde)	C ₅ H ₄ O ₂	96
18	1-(2-furyl)-ethanone	C ₆ H ₆ O ₂	110
19	1-acetyloxy-2-butanone	C ₆ H ₁₀ O ₃	130
20	5-methylfurfural	C ₆ H ₆ O ₂	110
21	3-methyl-5-methylene-2(5H)-furanone	C ₆ H ₆ O ₂	110
22	3-methyl-2(5H)-furanone	C ₅ H ₆ O ₂	98
23	2(5H)-furanone	C ₄ H ₄ O ₂	84
24	2-hydroxy-cyclopent-2-en-1-one	C ₅ H ₆ O ₂	114
25	3,4-dimethyl-2-hydroxy-cyclopenten-2-en-1-one	C ₇ H ₁₀ O ₂	128
26	1,2,3-trihydroxy-4-cyclopentene	C ₅ H ₈ O ₃	116
27	2-hydroxy-3-methyl-2-cyclopenten-1-one	C ₆ H ₈ O ₂	112
28	2,3-dihydro-5-hydroxy-6-methyl-4H-pyran-4-one	C ₆ H ₈ O ₃	128
29	methoxyfuran	C ₅ H ₆ O ₂	98
30	hydroxy-methoxy-furan	C ₅ H ₆ O ₃	114
31	2,3-dihydro-3,5-dihydroxy-6-methyl-4H-pyran-4-one	C ₆ H ₈ O ₄	144
32	3,4-dihydroxy-2-methyl-4H-pyran-4-one	C ₆ H ₆ O ₄	142
33	1,4:3,6-dianhydro- α -D-glucopyranose	C ₆ H ₈ O ₄	144
34	5-(hydroxymethyl)-2-furan carboxaldehyde	C ₆ H ₆ O ₃	126

Some less volatile compounds formed in starch pyrolysis at 590° C were seen, as expected, only in the trimethylsilylated pyrolysate. Figure 7.4.2 shows the chromatogram of a starch pyrolysate performed at 590° C off-line, followed by trimethylsilylation (with BSTFA) and separated on a DB5 column (60 m long, 0.32 mm i.d. and 0.25 μ film thickness).

As seen in Figure 7.4.2, levoglucosan is the major pyrolysis product of starch. Other studies show the same result, although the exact profile of the pyrogram may differ for different experimental setups or with the origin of the starch. Most pyrolysis studies were performed using GC as an analytical technique, and the anhydrosugar(s) containing two or more monomeric units are not detected although they may be present. It is likely that an anhydrosugar analogous to cellobiosan is present in starch pyrolysate.

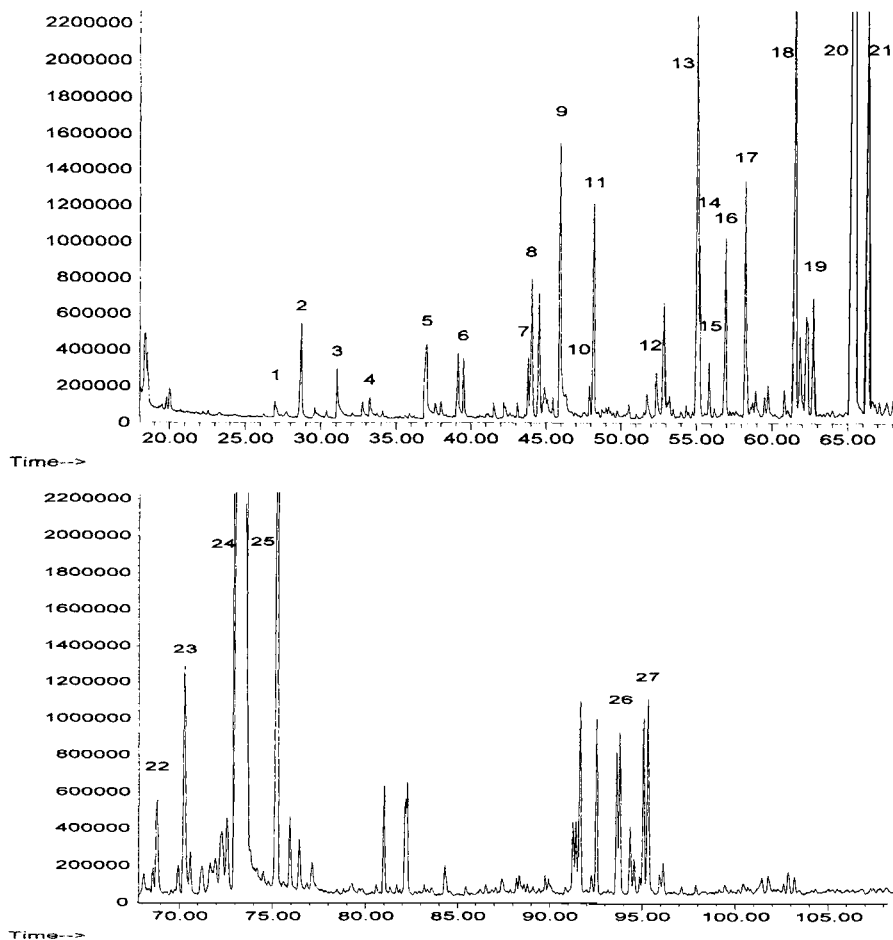


FIGURE 7.4.2. Starch pyrolysate at 590° C derivatized (silylated) and separated on a DB5 column. Peak identification is indicated in Table 7.4.2.

Table 7.4.2. Peak identification for starch pyrolysate silylated and separated on a DB5 column as shown in Figure 7.4.2.

Peak #	Compound	Formula	MW
1	lactic acid-di-TMS	C ₉ H ₂₂ O ₃ Si ₂	234
2	hydroxyacetic acid-di-TMS	C ₈ H ₂₀ O ₃ Si ₂	220
3	methoxy furan	C ₅ H ₆ O ₂	98
4	2-(TMS-oxy)-2-cyclopenten-1-one	C ₈ H ₁₄ O ₂ Si	170
5	reagent		ion 99
6	dihydroxyacetone di-TMS	C ₉ H ₂₂ O ₃ Si ₂	234
7	glycerol tris-(TMS)	C ₁₂ H ₃₂ O ₃ Si ₃	308
8	triethylene glycol-2-TMS	C ₁₂ H ₃₀ O ₄ Si ₂	294
9	2-methyl-3-(TMS-oxy)-pyranone	C ₉ H ₁₄ O ₃ Si	198
10	dihydroxypropanoic acid-tri-TMS	C ₁₂ H ₃₀ O ₄ Si ₃	322
11	cyclopentanecarboxylic acid-TMS ?	C ₉ H ₁₈ O ₂ Si	186

Table 7.4.2. Peak identification for starch pyrolysate silylated and separated on a DB5 column as shown in Figure 7.4.2 (continued).

Peak #	Compound	Formula	MW
12	dihydroxybenzene-di-TMS	C ₁₂ H ₂₂ O ₂ Si ₂	254
13	dihydroxymethylfuran-di-TMS	C ₁₁ H ₂₂ O ₃ Si ₂	258
14	hydroxy-(hydroxymethyl)furan-di-TMS	C ₁₁ H ₂₂ O ₃ Si ₂	258
15	pyranone	C ₅ H ₄ O ₂	96
16	hydroxycyclopentadiene carboxylic acid-di-TMS	C ₁₂ H ₂₂ O ₃ Si ₂	270
17	(hydroxymethyl)-furoic acid-di-TMS	C ₁₂ H ₂₂ O ₄ Si ₂	286
18	hydroxy-(hydroxymethyl)-cyclopentenone-di-TMS	C ₁₂ H ₂₆ O ₂ Si ₂	258
19	2,3,5-trihydroxybenzene tri-TMS	C ₁₅ H ₃₀ O ₃ Si ₃	342
20	hydroxy-cyclohexanoic acid-di-TMS	C ₁₃ H ₂₈ O ₃ Si ₂	288
21	Internal Standard		
22	1,4:3,6-dianhydro- α -D-glucopyranose-tri-TMS	C ₁₅ H ₃₂ O ₄ Si ₃	360
23	deoxyhexonic acid- γ -lactone-tri-TMS	C ₁₅ H ₃₄ O ₅ Si ₃	378
24	levoglucosan-tri-TMS	C ₁₅ H ₃₄ O ₅ Si ₃	378
25	anhydrosugar x-TMS		
26	monosaccharide 5-TMS	C ₂₁ H ₅₂ O ₆ Si ₅	540
27	monosaccharide 5-TMS	C ₂₁ H ₅₂ O ₆ Si ₅	540

Besides the compounds indicated in Tables 7.4.1 and 7.4.2, there are several other pyrolysis products of starch (and amylose) reported in literature [53]. They were either not seen in the pyrograms from Figures 7.4.1 and 7.4.2 or not identified. A complementary list of compounds detected in amylose pyrolysate [53] obtained in similar conditions (510^o C) as those for Tables 7.4.1 or 7.4.2 are given in Table 7.4.3.

TABLE 7.4.3. Complementary list of compounds reported [43] to be present in starch pyrolysate.

Compound	Formula	MW
carbon monoxide	CO	28
ethane	C ₂ H ₆	28
ketene	C ₂ H ₂ O	42
propene	C ₃ H ₆	42
2-propenal	C ₃ H ₄ O	56
ethandial	C ₂ H ₂ O ₂	58
hydroxyacetaldehyde	C ₂ H ₄ O ₂	60
cyclopentadiene	C ₅ H ₆	66
2,3-dihydro-5-methylfuran	C ₅ H ₈ O	84
benzene	C ₆ H ₆	78
2-methylbutanal	C ₅ H ₁₀ O	86
2-methylcyclobutanone	C ₅ H ₈ O	84
2-hydroxy-3-oxobutanal	C ₄ H ₆ O ₃	102
furanmethanol	C ₅ H ₆ O ₂	98
angelica lactone (5-methyl-2(3H)-furanone)	C ₅ H ₆ O ₂	98
phenol	C ₆ H ₆ O	94
3-hydroxy-2-penteno-1,5-lactone	C ₅ H ₆ O ₃	114
5-(2hydroxyethylidene)-2(H)-furanone	C ₆ H ₆ O ₃	126
3-oxopentanoic acid	C ₅ H ₈ O ₃	116
2-furyl hydroxymethyl ketone	C ₆ H ₆ O ₃	126
levoglucosenone	C ₆ H ₆ O ₃	126
3-hydroxy-6-methyl-2(H)-pyran-2-one	C ₆ H ₆ O ₃	126
3-hydroxy-2-methyl-4(H)-pyran-4-one	C ₆ H ₆ O ₃	126
5-hydroxy-2-methyl-4(H)-pyran-4-one (one of the three isomers seen as TMS derivative)	C ₆ H ₆ O ₃	126
several anhydrohexoses	C ₆ H ₈ O ₄	144
1,4-dideoxy-D-glycero-hex-1-enopyranos-3-ulose	C ₆ H ₈ O ₄	144

Besides the small molecules that are identified in starch pyrolysates, certain studies [20, 54] determined that oligosaccharides and oligosaccharides with attached sugar ring cleavage fragments were generated in starch or in amylose pyrolysis. The first study [20] showed that in amylose pyrolysate analyzed by CI with NH_3 as ionization gas (see Section 5.4) a series of ions with $m/z = (162)_n + 14$ can be seen. The mass 162 corresponds to the fragment $\text{C}_6\text{H}_{10}\text{O}_5$ and 14 corresponds to NH_4 and $n = 1, 2 \dots 6$. This indicates the presence of up to six anhydrosaccharide units in the pyrolysates. The results were confirmed by analyzing the perbenzoylated products using HPLC. The MS analysis of different collected fractions showed that ring cleavage products can be associated with the anhydrosaccharide units corresponding to mass 60 (probably $\text{C}_2\text{H}_4\text{O}_2$) or mass 42 (probably $\text{C}_2\text{H}_2\text{O}$). It was shown that the group $\text{C}_2\text{H}_4\text{O}_2$ has two derivatizable OH groups, while the group $\text{C}_2\text{H}_2\text{O}$ has one derivatizable OH group. The second study proved by Py-CI MS using ammonia as a collision gas the presence of oligomers up to nonamer ($m/z = 1476$ corresponding to nine anhydrosaccharide units + ammonia).

A study [53] regarding the influence of different additives to the pyrolysis products of starch indicated that inorganic acids, bases, or salts such as Na_2CO_3 or ZnCl_2 as well as sea salt matrices influence the yield of different compounds in starch pyrolysate. The acids were found to increase the production of furans and anhydrohexoses. The presence of phosphates appeared to increase the yield of cyclization reactions with the formation of more pyranones. Alkaline matrices generated more carbonyl compounds, acids, and lactones. Strongly alkaline matrices generated unsaturated hydrocarbons and aromatic compounds. The neutral salts that can act as Lewis acids favor dehydration and elimination reactions. Addition of KOH (50 mM) to the amylose during pyrolysis was demonstrated [54] to generate extensive fragmentation in the pyrolysate. The highest oligomer that can be seen from the pyrolysis of pure amylose was up to nine anhydrosaccharide units, while only much lower oligomers are seen after KOH addition. The highest distinctive peak in the pyrogram is at $m/z = 180$, followed by a peak at $m/z = 162$, and the base peak at $m/z = 134$.

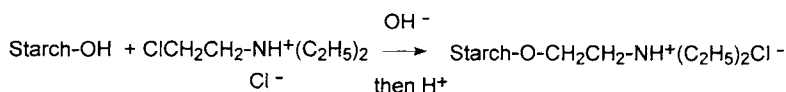
- Modified starches.

Starch can be subject to a variety of chemical modifications aimed to improve functionality for practical applications. Among starch modifications, the following are common:

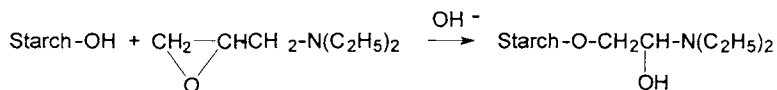
- Acid conversions when starch is treated with an acid such as HCl or H_2SO_4 at 40–60°C (commonly a starch slurry with 35–40% solids is treated with 0.2–0.5 N HCl for a few hours). Following the acid conversion, the acid is neutralized. In this process, the DP value decreases (and several physical properties are modified). Although chemical studies show that the $\alpha\text{-D-(1}\rightarrow\text{4)}$ links are more sensitive to hydrolysis than $\alpha\text{-D-(1}\rightarrow\text{6)}$ links, it was determined that due to starch crystallinity more $\alpha\text{-D-(1}\rightarrow\text{6)}$ links are hydrolyzed [55]. This happens because the $\alpha\text{-D-(1}\rightarrow\text{6)}$ links are in the amorphous regions and they are more accessible to the reagent (less hydrogen bonds). This explains why the DP of amylose is reduced less than that of the amylopectin component.
- Oxidation of starch, which is commonly done with sodium hypochlorite and generates carboxyl groups at the aldehyde end groups and at some OH groups from C-6

positions. Possibly some C-2 and C-3 OH groups are also oxidized to aldehydic then carboxylic groups. The water solubility and stability of starch pastes are modified.

- Pyroconversion, which consists of heating dry starch at temperatures between 100 to 200° C generating dextrans. Some depolymerization takes place in this process associated with dehydration and transglycosidation reactions. The α -D-(1 \rightarrow 4) bond cleavage is followed by recombination of the fragments with nearby free hydroxyl groups to form branched structures. This explains the increase in water solubility and this modification allows the use of dextrin in binding and adhesive applications.
- Cross-linking of starch, which is done by reacting starch with small amounts of reagents with bifunctional groups such as epichlorohydrin, acid anhydrides, etc.
- Acetylation of starch, which is commonly done with acetic anhydride and can reach a D.S. between 2 and 3. Highly acetylated starches are soluble in organic solvents and become insoluble in water. They are used for their capability to form films and coatings.
- Hydroxyethylation of starch, which is obtained from starch and ethylene oxide. This compound has been utilized in papermaking for sizing and coating, in textile manufacturing, and as a blood plasma extender. Hydroxypropylated starch has also practical applications.
- Reaction of starch with polyphosphates or phosphorus containing reagents, which is utilized in paper, adhesives, and textiles.
- Preparation of cationic starches, done with reagents such as 2-diethylaminoethyl chloride, 2,3-epoxypropyldiethylamine, or by cross-linking starch with epichlorohydrin in the presence of ammonia. The reaction with 2-diethylaminoethyl chloride is done at pH 11 to 12, followed by neutralization with acids.

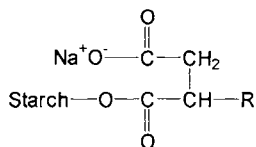


The reaction with 2,3-epoxypropyldiethylamine takes place as follows:



Cationic starches have numerous applications in paper industry, in textiles, as flocculating agents, in cosmetics, adhesives, etc.

- Preparation of starch succinate or alkenylsuccinates by reaction with succinic anhydride or its derivatives. The general structure of these compounds is



Starch succinates have numerous applications in food and pharmaceuticals.

- Preparation of grafted starches on synthetic polymers. Ce^{+4} salts are used to oxidize starch and generate free radicals that react with certain monomers (methyl methacrylates, acrylonitrile, vinyl acetate, acrylamide, etc.)

A few pyrolysis data are available for modified starches [56,57]. Interesting results were reported on starch cross-linked with epichlorohydrin (SE), starch cross-linked with epichlorohydrin in the presence of ammonia (SEA), and starch cross-linked with epichlorohydrin in the presence of ammonia and 3-chloro-2-hydroxypropyltrimethylammonium chloride (SQEA) [57]. The resulting cross-linked starches are used as ion exchangers. The presence of ammonia and of 3-chloro-2-hydroxypropyltrimethylammonium chloride generates cationic starches. For these materials, the pyrolysis was performed at 600° C for 10 s using 0.5 mg substance. The separation was done on a DB-5ms column 30 m long, 0.25 mm id, 0.25 μ m film thickness. The GC system used a temperature gradient of 5° C/min., between 50° C and 300° C. The compounds identified in the pyrolysate of the four materials are given in Table 7.4.4. The results showed a series of nitrogen compounds in the cationic starches. Cross-linked starch showed fewer peaks in the pyrograms than starch, indicating an increased stability of starch after cross-linking. Also, less levoglucosan was produced. More peaks were present in the mixture obtained by Py-GC/MS of SEA sample. This indicated less cross-linked material in comparison to SE. The SQEA sample gave a more complicated TIC profile than SEA. Although the study [57] did not provide direct proof of the existence of linkages to starch of hydroxypropyl, poly-(hydroxypropyl-amine), and trimethylammoniumhydroxypropyl groups, the results indirectly supported the existence of such linkages.

TABLE 7.4.4. *Compounds identified in the pyrolysate of starch, cross-linked starch with epichlorohydrin, and in two cationic starches (SEA and SQEA).**

Compound	In starch	In SE	In SEA	In SQEA
pyridine	-	-	C	C
3-furaldehyde	S	S	S	-
?-methyl pyridine	-	-	-	C
4-methyl pyridine	-	-	C	C
2-furaldehyde	S	S	S	S
2-furanmethanol	S	S	S	-
3-methyl pyridine	-	-	C	C
cyclopent-1-ene-3,4-dione	S	S	S	-
2-acetylfuran	S	S	S	S
2(5H)-furanone	S	S	S	-
2,5-dimethyl pyrimidine	-	-	C	C
2,3-dimethyl pyrazine	-	-	C	C
5-methyl-2-(3H)-furanone	S	S	S	-
5-methylfurfural	S	S	S	-
4-oxopentanal	S	S	S	-
phenol	S	S	S	-
3-methyl-5-methyliden-2(5H)-furanone	S	S	S	S
5,6-dihydropyran-2,5-dione	S	S	S	-
2-ethyl-6-methyl pyrazine	-	-	-	C
4-hydroxy-5,6-dihydro-(2H)-pyran-2-one	S	-	S	-
trimethyl pyrazine	-	-	C	C
3-hydroxy-2-methyl-2-cyclopenten-1-one	S	S	S	-
2,3,5-trimethyl-1H-pyrrole	-	-	C	C
3-methyl-1,2-cyclopentanedione	S	S	S	-
2,4-dihydropyran-3-one	S	S	S	-

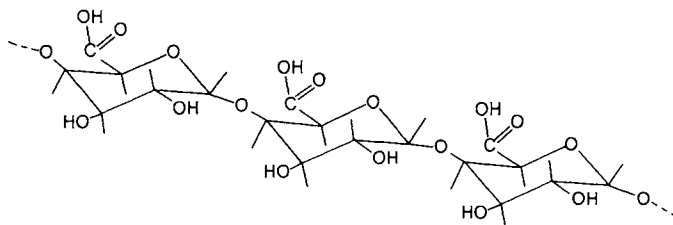
TABLE 7.4.4. *Compounds identified in the pyrolysate of starch, cross-linked starch with epichlorohydrin, and in two cationic starches (SEA and SQEA)* (continued).*

Compound	In starch	In SE	In SEA	In SQEA
2-ethyl-3,5-dimethyl-pyrazine	-	-	C	C
2-furoic acid methyl ester	S	S	S	-
2,6-diethyl pyrazine	-	-	-	C
tetrahydrofuran-2-propan-2-one	S	S	S	-
2-methyl-3-propylpyrazine	-	-	C	C
maltol	S	S	S	-
2,3,4,5-tetramethyl-1H-pyrrole	-	-	C	C
5H-5-methyl-6,7-dihydrocyclopentanpyrazine	-	-	-	C
3,5-dihydroxy-2-methyl-5,6,-dihydro-4H-pyran-4-one	S	-	S	-
3,4-dihydroxy benzaldehyde	S	S	S	-
2-ethyl-3,4,5-trimethyl-1H-pyrrole	-	-	-	C
3,5-dihydroxy-2-methyl-4H-pyran-4-one	S	-	S	-
2-allyl-5-methyl pyrazine	-	-	C	C
2,5-dimethyl-3-cis-propenylpyrazine	-	-	-	C
6,7-dihydro-2,5-dimethyl-5H-cyclopentapyrazine	-	-	-	C
5-hydroxymethylfurfural	S	S	S	-
2-methyl quinoxaline	-	-	-	C
3-methoxy-5-methyl-2(5H)-furanone	S	-	-	-
1,4-dideoxy-D-glycero-hex-1-enopyranos-3-ulose	S	S	S	-
2,3,6-trimethyl-4(3H)-pyrimidinone	-	-	C	C
1,6-anhydro- β -D-glucopyranose	S	S	S	-
1,6-anhydro- β -D-glucofuranose	S	-	S	-

* S indicates origin from the starch; C indicates origin from the cationic component.

7.5 Pectins.

The pectins cover a range of polysaccharides commonly found in cell walls and intercellular layers of land plants but not in their woody tissues. Sources of pectins are apples (making up to 15% of dry apples), citrus fruits (up to 30% of dry rinds of citrus fruits), tobacco, beets, etc. Pectins have the capability to form gels and are used commercially in preserves, jellies, etc. The MW of pectins may vary between 20,000 to 400,000. Pectic substances include homopolysaccharides such as (1 \rightarrow 4)- α - linear D-galacturonans, (1 \rightarrow 4)- β - linear D-galactans, and (1 \rightarrow 3)- α -, (1 \rightarrow 5)- α - branched L-arabinans. Other pectins are heteropolysaccharides containing both neutral and acidic sugars. Pectins rich in D-galacturonic acid are also called pectic acids and those rich in methyl esters of D-galacturonic acid are called pectinic acids. Some pectins are present in plants as their calcium salts. An idealized structure for pectin as (1 \rightarrow 4)- α -linked poly-D-galacturonic acid is shown below.



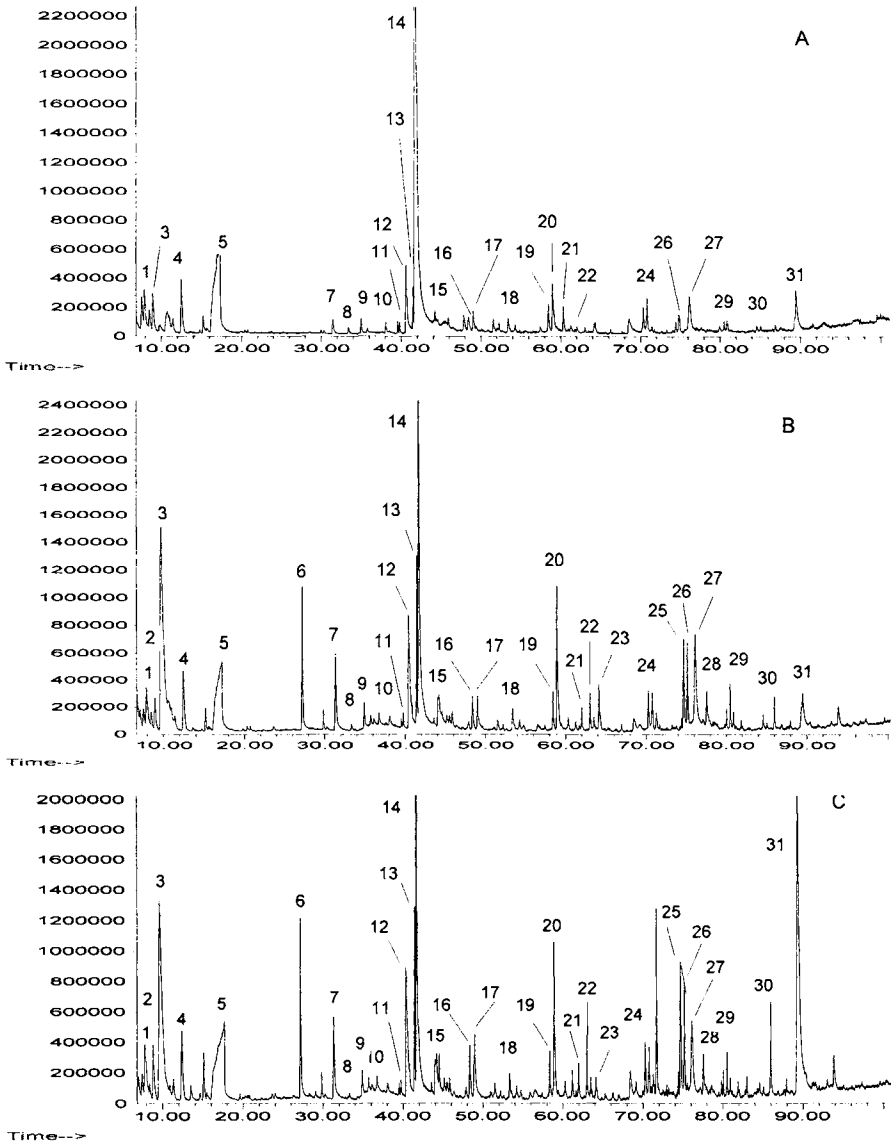


FIGURE 7.5.1. TIC traces for pyrolysates obtained at 590° C from polygalacturonic acid (trace A), apple pectin (trace B), and citrus pectin (trace C). Peak identifications are shown in Table 7.5.1.

TABLE 7.5.1. *Some peak identifications from pectin pyrolysate at 590° C.*

Peak No.	Compound	MW	Characteristic ions (relative intensity in parentheses)
1	propanone	58	43(100), 58(33)
2	2-methylfuran	82	82(100), 53(80), 81(75)
3	3-methyl-2-butanone	86	43(100), 86(21), 41(15)
4	methylbenzene	92	91(100), 92(73), 65(11)
5	water	18	18(100), 17(21)
6	2-oxopropanoic acid methyl ester ?	102	43(100), 102(14), 59(8)
7	1-hydroxy-2-propanone	74	43(100), 74(25), 31(20)
8	2,3-dihydro-1,4-dioxin	86	86(100), 29(42), 57(48), 30(10)
9	2-cyclopenten-1-one	82	82(100), 39(40), 54(32), 53(30)
10	3-methyl-2-cyclopenten-1-one	96	96(100), 67(88), 81(45), 53(28)
11	5-methyl-2(3H)-furanone	98	55(100), 98(88), 43(86)
12	acetic acid	60	60(100), 45(85), 43(80)
13	3-oxopropanoic acid methyl ester	102	43(100), 102(32), 59(4)
14	furancarboxaldehyde	96	96(100), 95(91), 39(40)
15	1-(2-furanyl)-ethanone	110	95(100), 110(44), 39(13)
16	5-methyl-2-furfural	110	110(100), 109(95), 53(40)
17	4-cyclopenten-1,3-dione	96	96(100), 42(83), 68(82), 54(50)
18	furanmethanol	98	98(100), 97(60), 81(60), 69(40)
19	2(5H)-furanone	84	55(100), 84(76), 27(65)
20	2-hydroxycyclopent-2-en-1-one	98	98(100), 55(63), 42(55), 69(31)
21	2-hydroxy-3-methyl-2-cyclopenten-1-one	112	112(100), 97(15), 83(20), 69(22)
22	unknown	128 ?	113(100), 128(93), 58(90), 87(55)
23	unknown	114	114(100), 58(90), 85(5)
24	phenol	94	94(100), 66(34), 65(26)
25	unknown	154 ?	123(100), 154(60), 95(24), 39(15)
26	2-butendioic acid diethyl ester	172	128(100), 99(61), 54(29)
27	5-ethylidihydro-2-(3H)-furanone	114	85(100), 42(18), 57(12), 114(11)
28	butandioic acid dimethyl ester	146	115(100), 55(62), 59(45)
29	3-methyl-2,4-(3H, 5H)-furanone	114	114(100), 56(92), 28(78), 85(12)
30	butandioic acid monomethyl ester	132	101(100), 55(42), 45(25)
31	mix: 2-furancarboxylic acid, benzoic acid and 2-hydroxypyridine in traces B and C		112, 95 and 122, 105

The amidation (which may come from pectin processing) is present in citrus pectin and at a lower extent in apple pectin [59]. As indicated for example in Table 7.5.1, peak # 31 is a mixture, and in the pyrolysates of citrus pectin and apple pectin this peak consists mainly of 2-hydroxypyridine. Citrus pectin pyrolysate also contains a significant level of pyrrolcarboxaldehyde (peak at 71.6 min. in Figure 7.5.1 C).

As indicated previously, a particular GC/MS analysis shows only a given range of compounds present in the pyrolysate, and depending on the chosen conditions, this range can be wider or narrower. It is frequently necessary to use more than one technique to see a wider range of compounds present in the pyrolysates. A second set of chromatograms generated by a GC/MS system for the trimethylsilylated pyrolysates of polygalacturonic acid and two pectins indicated above are shown in Figures 7.5.2 A, B and C. The pyrolysates were also generated at 590° C followed by off-line silylation with BSTFA. The separation of the silylated pyrolysates was done on a methyl silicone with 5% phenyl silicone chromatographic column, 60 m long, 0.32 mm i.d., 0.25 µ film thickness. The GC separation was performed using a temperature gradient of 2° C/min. between 50° C and 300° C. Some peak identifications are shown in Table 7.5.2. Numerous peaks in the chromatograms for pectins are common to other polysaccharides.

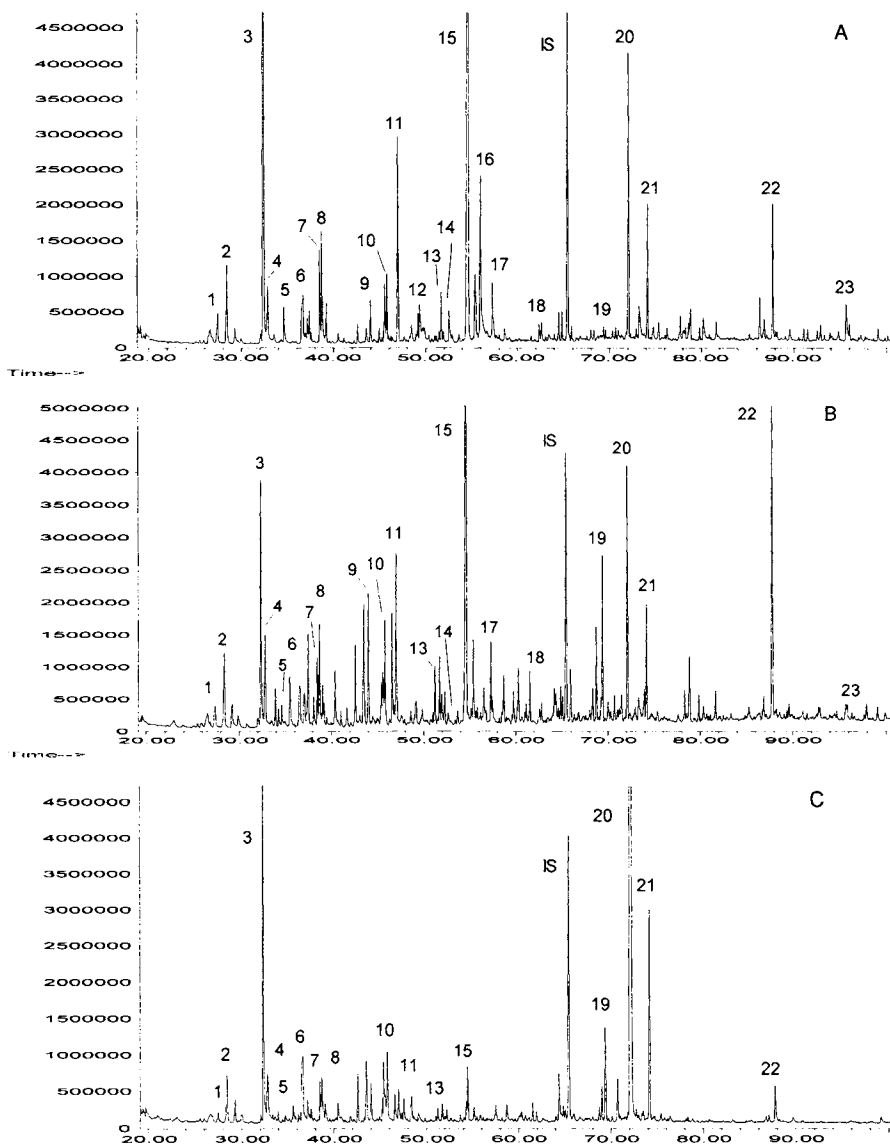
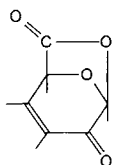


FIGURE 7.5.2. TIC traces for silylated pyrolysates obtained at 590° C from polygalacturonic acid (trace A), apple pectin (trace B), and citrus pectin (trace C). Peak identification shown in Table 7.5.2.

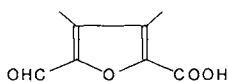
TABLE 7.5.2. *Some peak identifications for the silylated pyrolysates of polygalacturonic acid, apple pectin, and citrus pectin.*

Peak No.	Compound	Formula	MW	Characteristic ions (relative intensity in parentheses)
1	lactic acid 2-TMS	C ₉ H ₂₂ O ₃ Si ₂	234	73(100), 117(85), 147(80), 191(7), 219(5)
2	glycolic acid 2 TMS	C ₈ H ₂₀ O ₃ Si ₂	220	147(100), 73(90), 205(10), 177(8)
3	furan carboxylic acid TMS	C ₈ H ₁₂ O ₂ Si	168	125(100), 169(83), 95(45), 184(8)
4	hydroxy-2-cyclopenten-1-one TMS	C ₈ H ₁₄ O ₂ Si	170	155(100), 81(20), 170(5)
5	reagent	ion 99		99 (100)
6	propandioic acid 2-TMS	C ₉ H ₂₀ O ₄ Si ₂	248	147(100), 73(76), 233(6), 248(1)
7	α-hydroxy-2-furanacetic acid 2 TMS ? or isomer of # 8	C ₁₂ H ₂₂ O ₄ Si ₂ ?	286	169(100), 73(62), 243(12), 271(3)
8	3-methyl-4-hydroxycyclopenten-1-one 1TMS	C ₉ H ₁₆ O ₂ Si	184	169(100), 73(18), 184(12), 170(10)
9	2-butendioic acid 2-TMS	C ₁₀ H ₂₀ O ₄ Si ₂	260	147(100), 73(84), 245(16), 45(12)
10	1,2-dihydroxybenzene 2 TMS	C ₁₂ H ₂₂ O ₂ Si ₂	254	73(100), 254(28), 45(4)
11	dihydroxycyclopentenone 2-TMS ?	C ₁₁ H ₂₂ O ₃ Si ₂	258	147(100), 73(95), 243(90), 258(22)
12	dimethyl-4-hydroxy-2-cyclohexen-1-one TMS	C ₁₁ H ₂₀ O ₂ Si	212	197(100), 153(92), 123(14), 212(8)
13	1,3-dihydroxyphenol 2-TMS	C ₁₂ H ₂₂ O ₂ Si ₂	254	239(100), 254(80), 73(31)112(12)
14	2-hydroxyacetophenone TMS	C ₁₁ H ₁₆ O ₂ Si	208	193(100), 208(51), 151(22), 165(20)
15	2,3-dihydroxy-3-cyclopenten-1-one 2-TMS	C ₁₁ H ₂₂ O ₃ Si ₂	258	243(100), 73(34), 244(22), 258(10)
16	2-acetyl-5-hydroxy-3-cyclopenten-1-one or 5-carboxy-2-furfural TMS	C ₁₀ H ₁₆ O ₃ Si or C ₉ H ₁₂ O ₄ Si	212	197(100), 73(28), 198(14), 212(10)
17	dihydroxycyclopentenone isomer of #16	C ₁₁ H ₂₂ O ₃ Si ₂	258	73(100), 147(88), 243(76), 258(29), 230(17)
18	3-hydroxybenzoic acid 2-TMS	C ₁₃ H ₂₂ O ₃ Si ₂	282	267(100), 73(51), 282(48), 193(47), 223(33)
19	3-methyl-2-hydroxybenzoic acid 2-TMS	C ₁₄ H ₂₄ O ₃ Si ₂	296	281(100), 73(41), 191(29), 282(25), 296(1)
20	levoglucosan 3-TMS (not from pectin ?)	C ₁₅ H ₃₄ O ₅ Si ₃	378	204(100), 217(93), 73(91), 147(28), 333(20)
21	1,4-anhydrogalactopyranose 3TMS	C ₁₅ H ₃₄ O ₅ Si ₃	378	217(100), 73(34), 191(5), 319(7)
22	bis-(hydroxycyclopenten)-1,4-dioxin	C ₁₆ H ₂₄ O ₄ Si ₂	336	321(100), 322(26), 323(12)
23	unknown			267(100), 193(52), 336(49), 73(26), 293(14)

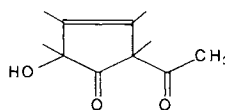
As seen from the peak assignment shown in Table 7.5.2, even levoglucosan is present in all pectins and in polygalacturonic acid pyrolysate. It is likely that this compound comes from sucrose or starch added to the pectin that was used to generate the pyrograms shown in Figures 7.5.2A to 7.5.2C. Some compounds in the pyrolysis of pectins were postulated from Py-MS studies. For example, 6-oxolevoglucosan and 6-oxolevoglucosenone are hypothetical compounds formed from the uronic acid residue in a similar manner as levoglucosan and levoglucosenone are formed from the neutral sugars. 6-Oxolevoglucosenone has the same molecular weight (MW = 140) as 5-carboxy-2-furfural and also as 2-acetyl-5-hydroxy-3-cyclopenten-1-one. The identification using GC/MS analysis of 6-oxolevoglucosan and of 6-oxolevoglucosenone in the pyrograms shown in Figures 7.5.1 and 7.5.2 was not positive. In the silylated pyrolysate, both 5-carboxy-2-furfural and 2-acetyl-5-hydroxy-3-cyclopenten-1-one are strongly suspected to be present, although the peak assignment is not certain. Two peaks corresponding to the molecular ion $m/z = 212$ ($139 + \text{Si}(\text{CH}_3)_3$) are present in the chromatogram of the silylated pyrolysate.



6-oxo-levoglucosenone
C₆H₄O₄ MW = 140



5-carboxy-2-furfural
C₆H₄O₄ MW = 140



2-acetyl-5-hydroxy-3-cyclopenten-1-one
C₇H₈O₃ MW = 140

Less volatile compounds are also formed in the pyrolysis of pectins. However, their identification based on their mass spectra is more difficult. For example, the compound with the characteristic ions 73(100), 147(50), 412(32), 441(32), 133(12), 456(8), or the compound with the ions 267(100), 193(52), 336(49), 73(26), 137(17), 293(14), 233(7), 409(1), are present in pectin spectra but were not identified.

The degree of methylation (DM) of pectin [60] can be estimated using a Py-MS technique. The application of principal component analysis and canonical variate analysis to the Py-MS data (see Section 5.5) showed a linear relationship between DM and the first canonical variate score of the data as shown in Figure 7.5.3.

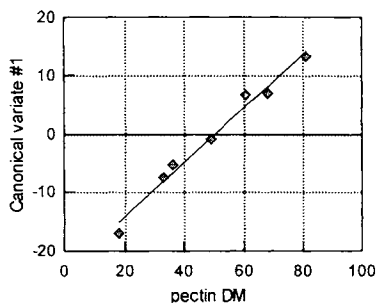


FIGURE 7.5.3. *Linear relationship between DM and the first canonical variate score for pectin.*

The following equation can be utilized for DM determination:

$$DM = 2.13 Y + 50 \quad (1)$$

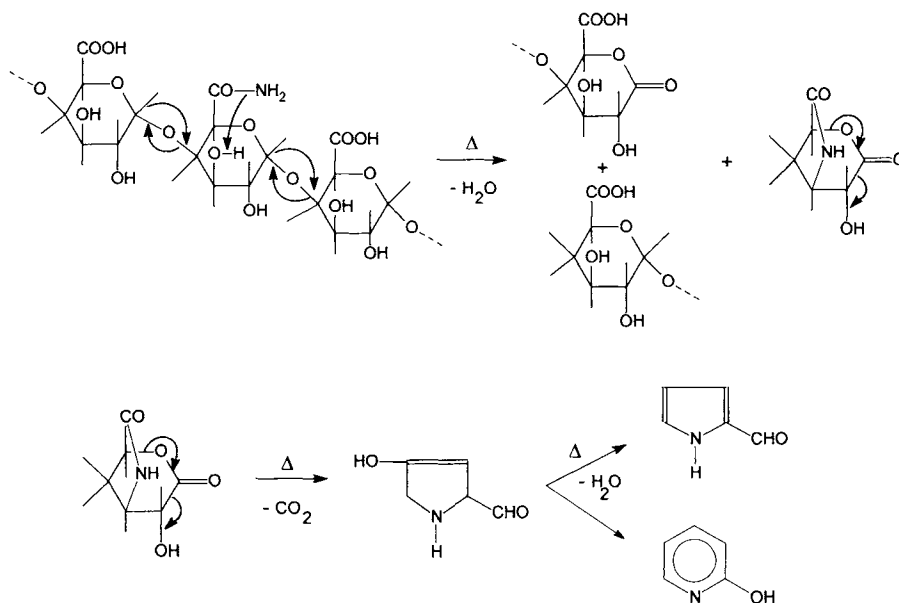
Using this linear dependence, the DM values for new unknown samples can be established. A similar study has been done on amidated pectin [61].

- *Mechanisms in the formation of small molecules in pectin pyrolysates.*

The formation of small molecules during pectin pyrolysis was in part addressed in Section 2.6. Experimental findings showed that the formation of 6-oxolevoglucosan and 6-oxolevoglucosenone is not likely in polygalacturonic acid pyrolysis. Probably the elimination of water between positions 6 and 1 does not take place at temperatures where decarboxylation or formation of furan cycles is already under way at appreciable

rates. The main pyrolysis products are furancarboxaldehyde (see Section 2.6), furancarboxylic acid, acetic acid, etc. Several other compounds formed with considerable yield are several hydroxycyclopentenones and levoglucosan. It is not clear if levoglucosan shown in pectin pyrolysates in Figures 7.5.1 and 7.5.2 is generated from the existing galactans in the pectin or from added sucrose (which is common in commercial pectin).

From the methylated pectin, the main pyrolysis compound seems to be 4-(hydroxymethyl)-butyrolactone. Two main nitrogenous compounds are formed from amidated pectin, hydroxypyridine and pyrrol-2-carboxaldehyde. Their formation can be explained by the following reactions:

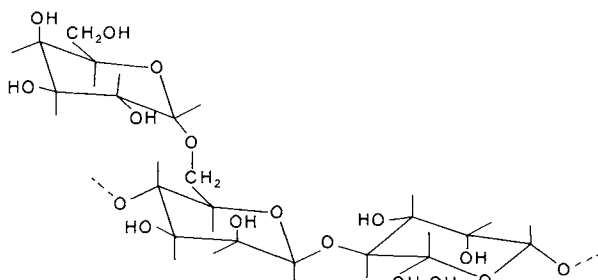


These reactions are similar to those involved in the formation of furancarboxaldehyde from galacturonic acid. The intermediate shown as 2-hydroxy-4-oxa-8-azabicyclo[3.2.1]octane-2,6-dione is not a stable molecule and continues to decompose with the formation of another unstable compound, which eliminates water.

7.6 Gums and Mucilages.

The plant gums are plant exudates or seed gums and are polysaccharides made mainly from hexuronic acid residues and neutral monosaccharides residues sometimes esterified. (Unlike the other gums, tamarind kernel powder does not have uronic acids in its structure, but only neutral sugars such as glucose, galactose and xylose.) Among the more common plant exudates are gum arabic, gum ghatti, gum karaya, and gum tragacanth. The common seed gums are guar gum, locust bean gum, and tamarind.

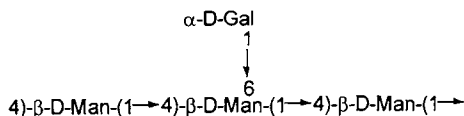
The structure of gums is usually branched. Gum arabic contains for example a chain of (1→3) linked β -D-galactopyranosyl groups to which side chains of D-glucopyranosyluronic acid, L-arabinofuranosyl, and L-rhamnopyranosyl residues are attached. Guar gum has as the main component (about 85%) a well-characterized galactomannan, guaran. This contains a main backbone of (1→4)-linked β -D-mannopyranosyl units with α -D-galactopyranosyl attached by (6→1) links as shown below.



Mucilages are gelatinous substances that have the ability to retain water. Mucilages coat quince seeds, psyllium seeds, and okra seeds. D-galacturonic acid is also a characteristic component of mucilages. A typical mucilage may have a chain of (1→3) and (1→4) linked β -D-xylopyranosyl groups to which side chains of L-arabinofuranosyl and D-galactopyranosyluronic acid residues are attached.

Pyrolysis-GC of the galactomannan from guar gum [62] indicated the existence of mannopyranose units by the presence of 1,6-anhydromannopyranose in the pyrolysate. The galactose unit was identified in the same manner. The ratio of Man/Gal suggested from Py-GC data indicated more mannose units than the theoretical 2:1.

There are numerous gums of industrial interest, and some have been analyzed using pyrolysis. As an example, locust bean gum has considerable commercial value as a sizer for textiles and as a component of foods, pharmaceuticals, and cosmetics. Its idealized structure is that of a galactomannan with the main chain of D-mannosyl units linked through the 1 and 4 positions as shown below:



The side chain is a single unit of α -D-galactose. The proportion of manno to galacto residues can vary between 3:1 and 4:1 depending on the source of the gum. Small amounts of glucan and pentosan have been detected in some preparations. The Py-GC analysis of a locust bean gum preparation [6a] showed pyrolysis products associated with the galactosyl and mannosyl units. Even the peak area ratio of the peak corresponding to 1,6-anhydromannopyranose and the peak corresponding to 1,6-anhydrogalactopyranose was found to be roughly 3:1. The pyrogram also showed the

TABLE 7.7.1. *Polysaccharides with less common structure isolated from plants.*

Common Name	Structure	Source
Lichenan	(1→3)-β-D-, (1→4)-β-D- linear glucan	Iceland moss, cereal grains
Nigeran	(1→3)-α-D-, (1→4)-α-D- linear glucan	<i>Aspergillus niger</i> , Iceland moss
Pustulan	(1→6)-β-D- linear glucan	Lichens
Inulin	(2→1)-β-D- linear fructan	Dandelions, dahlias
Levans	(2→6)-β-D- linear fructan	Various grasses
Levans	(2→6)-β-D-, (2→1)-β-D- branched fructan	Plants and bacteria

Several Py-MS studies were done on homoglycans. A Py-FI MS study on a (1→4)-β-xylan [2] showed several characteristic ions such as $m/z = 132$ (associated with the monomer unit $C_5H_8O_4$), the ion $m/z = 96$ (associated with furfural, $C_5H_4O_2$), and the ion $m/z = 114$ (probably associated with 3-hydroxy-2-penteno-1,5-lactone, $C_5H_6O_3$). The study showed that retro-aldolization between C-1 and C-2 atoms does not take place. Smaller ions seen in the spectrum were probably generated from further pyrolysis of the initially formed fragments.

In general, the extraction of hemicelluloses from wood is not a simple process. Two fractions are commonly obtained initially, the lignin and the holocellulose. Lignin is a high molecular weight random polymer, consisting of an irregular array of differently bonded hydroxy- and methoxy-substituted phenylpropane units. Holocellulose is defined as the water-insoluble carbohydrate fraction, including cellulose and hemicelluloses. It can be prepared by removing the lignin with sodium chlorite, but other methods for delignification of wood are also known. Because the complete removal of lignin leads to extensive degradation of the polysaccharides, incomplete delignification is common, but it leaves a considerable amount of residual lignin-like material in the holocellulose. The further separation of holocellulose into cellulose and hemicelluloses can be done with aqueous solutions of potassium or sodium hydroxide. However this treatment leads to considerable uncertainty about the actual composition of the initial material due to undesired chemical modifications that take place.

An example of a Py-GC/MS study on holocellulose and hemicelluloses of beech wood [63] started with a repeated treatment of the wood chips with 0.5 M sodium chlorite at pH 4 to remove lignin. The residue was the holocellulose fraction. The xylan fraction was further obtained by extraction of the holocellulose with 4.5% sodium hydroxide solution. This xylan as well as the holocellulose contained residual lignin and part of this was chlorinated due to the treatment with sodium chlorite. In addition to this xylan, a technical xylan fraction was also isolated from chopped wood using an extraction with water after exposure to steam for 10 min. at 170° C. Classical chemical methods for wood analysis indicate that beech wood contains 24% lignin and 75.1% holocellulose. This holocellulose contains about 43% cellulose and 31% hemicelluloses. An important constituent of beech wood hemicelluloses is O-acetyl-4-O-methylglucuronoxylan (acetylglucuronoxylan). The xylose content of beech wood is about 19%, with 4.8% of 4-O-methylglucuronic acid. Hemicelluloses are coupled to the lignin macromolecule by ether and ester linkages through the hemicellulose side-chain groups arabinose, galactose, and 4-O-methylglucuronic acid. This makes impossible the separation of lignin without modification of the chemical composition of the sample. The results of Py-GC/MS analysis are given in Table 7.7.2. This table shows the chemical composition of the pyrolysate of holocellulose (A), xylan fraction (B) and technical xylan (C). The technical xylan contained a higher level of lignin, but no chlorinated lignin was present.

TABLE 7.7.2. *Chemical constituents of the pyrolysate of holocellulose (A), a xylan fraction (B), and technical xylan (C) from beech wood [64].* (The origin from lignin of certain compounds is also indicated in the table.)

MW	Compound	Source	Lignin
44	carbon dioxide	A, B, C	
30	formaldehyde	A	
42	propene	C	
42	ketene	A	
50	chloromethane	A, C	
44	acetaldehyde	A, B, C	
56	2-methylpropene	A, B, C	
48	ethanethiol	C	
56	2-propenal	A, B, C	
72	pyruvaldehyde	A, C	
68	furan	A, B, C	
60	glyceraldehyde	C	
46	dimethyl ether	C	
74	methyl acetate	A, B, C	
66	1,3-cyclopentadiene	A, B, C	
60	hydroxyacetaldehyde	C	
70	2,5-dihydrofuran	A, B, C	
84	1-penten-3-one	B	
86	2,3-butanedione	A, B, C	
72	1-butanal	A, B	
72	butan-2-one	B, C	
86	pentan-3 one	B	
82	2-methylfuran	A, B, C	
82	3-methylfuran	A, B	
70	cis-2-butenal	B	
60	acetic acid	A, B, C	
80	cyclohexadiene	C	
74	hydroxypropanone	A, B	
60	1-propanol	B	
78	benzene	A	
84	2-methyl-1-buten-3-one	A, C	
98	1-pentene-3,4-dione	A, B, C	
84	2 keto-3-butenal	B	
86	pentan-2 one	A, B	
100	2,3-pentanedione	A, B, C	
89	2-hydroxy-3-butanone	A	
86	cyclopentanol	B	
74	2-hydroxypropanal	A	
88	1-pentene-3,4-dione	A	
96	(2,5)-dimethylfuran	A, C	
96	methylfuran	B	
94	2-vinylfuran	C	
94	3-penten-2-one	B, C	
86	3-pentanone	C	
74	3-hydroxypropanal	C	
88	1-hydroxy-2-butanone	A, C	
102	methylpyruvate	A, C	
102	2-hydroxybutanal-3 one	A, B, C	
92	toluene	A, B, C	
84	2H-furan-3-one	A, B, C	
90	2,3-dihydroxypropanal	A	
96	3-furaldehyde	A, B, C	

TABLE 7.7.2. *Chemical constituents of the pyrolysate of holocellulose (A), a xylan fraction (B), and technical xylan (C) from beech wood [64] (continued).* (The origin from lignin of certain compounds is also indicated in the table.)

MW	Compound	Source	Lignin
96	2-furaldehyde	A, B, C	
98	methylpentynol	A, B	
108	2-methyl-5-vinylfuran	A, C	
102	2-hydroxymethyltetrahydrofuran	B	
116	acetolacetate	A, B, C	
98	2-hydroxymethylfuran	A, B, C	
96	cyclopentenedione	A, B	
106	dimethylbenzene	B	
106	dimethylbenzene	B, C	
94	5H-furan-2-one	B	
100	2-pentenoic acid	B	
96	2-methyl-2-cyclopenten-1-one	A, B, C	
104	vinylbenzene	B, C	L
110	2-acetylfuran	C	
110	2-ethyl-5-methylfuran	A, B	
98	β -angelica lactone	A, B, C	
98	α -angelica lactone	A, B, C	
110	2,5-dimethylcyclopentenone	B	
110	5-methyl-2-furaldehyde	A, C	
96	3-methyl-2-cyclopenten-1-one	A, B, C	
106	benzaldehyde	A	L
126	2-acetyl-3-hydroxyfuran	C	
94	phenol	A, B, C	
112	pyrane-2,5-dione	A, B, C	
114	3-hydroxy-1,5-pentenolactone	A, B, C	
110	dimethylcyclopentenone	B	
112	2-hydroxy-3-methyl-2-cyclopenten-1-one	A, B, C	
120	trimethylbenzene	B	L
112	3-hydroxy-2-methyl-2-cyclopenten-1-one	A, B, C	
110	dimethylcyclopentenone	A, C	
124	2,4-furandialdehyde	A, B	
108	2-methylphenol	A, B, C	L
108	2-methyl-1,3-cyclopentanedione	A, B	
112	2-furoic acid	C	
110	2-propylfuran	B	
120	4-methylbenzaldehyde	B	L
108	3-methylphenol	A, B	L
96	cyclohex-2-en-1-one	A, C	
124	2-methoxyphenol	A, B, C	L
126	2-methyl-3-hydroxy-4H-pyran-4-one	A, B, C	
122	2,3-dimethylphenol	B	L
122	2,4-dimethylphenol	B	L
126	methylhydroxypyranone	C	
122	ethylphenol	B	L
126	3-hydroxy-6-methyl-3,4-dihydro-2H-pyran-2-one	A, B	
122	3,5-dimethylphenol	B	L
122	2,6-dimethylphenol	B	L
144	3,5-dihydroxy-2-methyl-5,6-dihydro-4H-pyran-2-one	C	
122	3,4-dimethylphenol	A, B, C	L
122	ethylphenol	B	L
122	2,5-dimethylphenol	B	L
136	methylethylphenol	B	L

TABLE 7.7.2. *Chemical constituents of the pyrolysate of holocellulose (A), a xylan fraction (B), and technical xylan (C) from beech wood [64] (continued).* (The origin from lignin of certain compounds is also indicated in the table.)

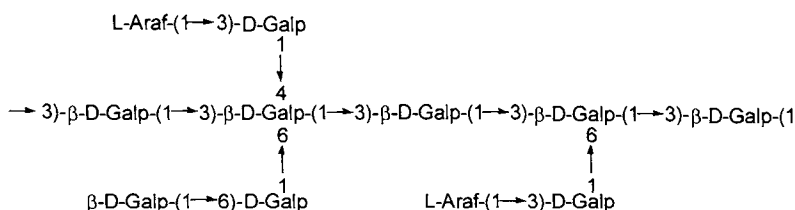
MW	Compound	Source	Lignin
110	dihydroxybenzene	A	L
110	1,2-dihydroxybenzene	A, B, C	L
110	1,2-dihydroxybenzene	A, B, C	L
138	2-methoxy-4-methylphenol	B, C	L
126	5-hydroxymethyl-2-furaldehyde	A, C	
132	anhydropentose	C	
138	hydroxybenzoic acid	B	L
136	methylethylphenol	B	L
136	methylethylphenol	B	L
132	1,6-anhydroxylofuranose	A, B, C	
124	dihydroxymethylbenzene	A, B, C	L
110	1,3-dihydroxybenzene	A	L
140	2-methoxy-4-hydroxyphenol	A, B, C	L
132	indan-1-one	A	
136	hydroxyacetophenone	B	L
152	2-methoxy-4-ethylphenol	A, C	L
132	methylethylphenol	B	L
124	α -hydrindone	A, B	
122	3-hydroxybenzaldehyde	A, B	L
144	1,4-dideoxy-D-glycerohex-1-enopyranos-3-ulose	A, B	
132	anhydropentose	C	
146	1,2-dimethylindane	B	
162	1,6-anhydrogalactose	C	
150	2-methoxy-4-vinylphenol	A, B, C	L
146	methylindanone	B	
124	dihydroxymethylbenzene	B	L
132	7-methylbenzofuran	A	
154	2,6-dimethoxyphenol	A, B, C	L
138	dihydroxydimethylbenzene	B	L
154	2-methoxy-4-hydroxymethylphenol	A	L
136	methoxybenzaldehyde	B, C	L
152	2-methoxy-4-formylphenol	A, C	L
136	methoxybenzaldehyde	B	L
138	dihydroxydimethylbenzene	B	L
150	4-formylbenzenecarboxylic acid	B	
168	2,6-dimethoxy-4-methylphenol	A, B, C	L
166	2-methoxy-4-ethanalphenol	A, B, B	L
168	2-methoxy-4-(1-hydroxyethyl)phenol	B	L
166	2 methoxy-4-acetylphenol	A, B	L
188	2,6-dimethoxy-3-chlorophenol	A, B	L
162	1,6-anhydroglucose	A, C	
166	2-methoxy-4-hydroxyvinylphenol	A, B	L
194	2 methoxy-6-chloro-4-vinylphenol	B	L
182	vanillic acid methyl ester	A	L
180	2-methoxy-4-(propan-2-one)phenol	A, B, C	L
182	2,6-dimethoxy-4-ethylphenol	A, C	L
162	1,6-anhydromannopyranose	A, C	
168	2-methoxy-4-carboxyphenol	A	L
180	2,6-dimethoxy-4-vinylphenol	A, B, C	L
178	2-methoxy-4-(prop-1-en-3-one)phenol	A, B	L
184	2,6-dimethoxy-4-hydroxymethylphenol	C	L
202	2,6 dimethoxy-3-chloro-4-methylphenol	A, B	L

TABLE 7.7.2. Chemical constituents of the pyrolysate of holocellulose (A), a xylan fraction (B), and technical xylan (C) from beech wood [64] (continued). (The origin from lignin of certain compounds is also indicated in the table.)

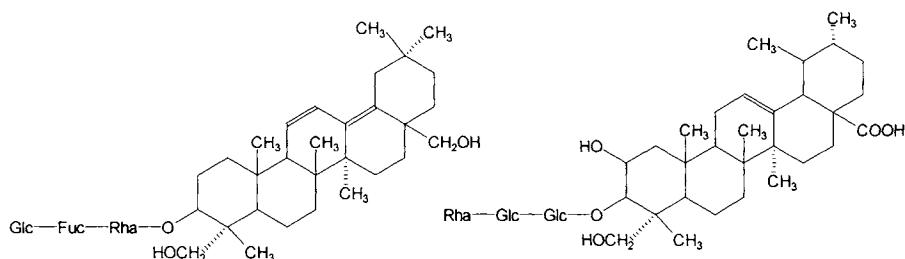
MW	Compound	Source	Lignin
194	2,6-dimethoxy-4-(prop-1-enyl)phenol	A, C	L
162	anhydrohexose	C	
182	2,6-dimethoxy-4-formylphenol	A, B, C	L
216	2-methoxy-3-chloro-4-(hydroxy-propyl)phenol	A, B	L
196	2,6-dimethoxy-4-ethanalphenol	A, C	L
194	2,6-dimethoxy-4-(prop-2-enyl)phenol	C	L
214	2-methoxy-6-chloro-4-(1-hydroxypropyl)phenol	B	L
214	2,6-dimethoxy-chloro-4-vinylphenol	A, B	L
196	2-methoxy-4-(3-hydroxypropan-2-one)phenol	A	L
196	2-methoxy-4-(1-hydroxypropan-2-one)phenol	C	L
196	2,6-dimethoxy-4-acetylphenol	A, B	L
228	2-methoxy-4-(prop-2-enal)phenol	A	L
210	2,6-dimethoxy-4-(propan-2-one)phenol	A, B, C	L
216	2,6-dimethoxy-3-chloro-4-formylphenol	A, B	L
198	2,6-dimethoxy-4-carboxyphenol	A, C	L
224	2,6-dimethoxy-4-(2,3-propanedione)phenol	A, C	L
210	2,6-dimethoxy-4-propanalphenol	A	L
230	2,6-dimethoxy-3-chloro-4-acetylphenol	A	L
228	2,6-dimethoxy-3-chloro-4-(prop-2-enyl)phenol	A, B	L
230	2,6-dimethoxy-3-chloro-4-ethanalphenol	B	L
244	2,6-dimethoxy-3-chloro-4-(1-hydroxy-prop-2-enyl)phenol	A	L
212	2,6-dimethoxy-4-(1-hydroxypropyl)phenol	C	L
244	2,6-dimethoxy-3-chloro-4-(propan-2-one)phenol	B	L
246	2,6-dimethoxy-3-chloro-4-(1-hydroxypropyl)phenol	A	L
244	2,6-dimethoxy-3-chloro-4-(1-hydroxyprop-2-enyl)phenol	A	L
226	2,6-dimethoxy-4-(1-carboxypropyl)phenol	A, C	L
208	2,6-dimethoxy-4-(prop-2-enal)phenol	A	L
242	2,6-dimethoxy-3-chloro-4-(prop-2-enal)phenol	A	L
244	2,6-dimethoxy-3-chloro-4-(prop-2-enyl)phenol	A	L

Among the pyrolysis products, specific carbohydrate pyrolysis products are 1,6-anhydro-D-glucopyranose, 1,4-dideoxy-D-glycerohex-1-enopyranos-3-ulose, and 1,6-anhydrogalactose indicating the presence of glucose and galactose residues in the material. The xylan markers are considered 3-hydroxy-2-penteno-1,5-lactone and anhydroxylose. The presence of a large amount of acetic acid was caused by de-esterification of the acetylated methylglucuronoxylan during pyrolysis. The abundance of acetic acid in the technical xylan fraction was higher than in the other polysaccharide fractions probably because the technique used for its isolation caused less de-acetylation of the acetylglucuronoxylan.

Some hemicelluloses have practical applications such as larch arabinogalactan, which is a water-soluble gum found in the heartwood of trees from *Larix* genus, and which is used in processed food as an emulsifier, or in pudding mixes, etc. A Py-GC/MS study of arabinogalactan from larch wood indicated the presence of the galactose unit and of arabinose unit in the ratio 6:1, as it is known in this material. The arabinose units were identified mainly by the formation of 1,4-anhydro-L-arabinopyranose, which elutes faster than the corresponding hexoses. The structure shown below was therefore confirmed by Py-GC/MS [64].



Besides typical plant polysaccharides, Py-MS was also applied for the study of certain plant glycosides [65] from the group of β -amyryne (cyclic triterpenes) such as:



Py-MS with chemical ionization (using NH_3 as collision gas) was utilized for the characterization of the sugar moiety of these compounds.

7.8 Algal Polysaccharides.

Some of the polysaccharides found in algae are identical or very similar to those found in land plants. Starch is one of them. Algal starches have, however, smaller molecules (lower DP) as compared to starch from land plants. Cellulose and several hemicelluloses are also found in algae.

Other polysaccharides found in algae are less common in land plants. One example is laminaran, which is a (1→3)- β -D- linear glucan with some (1→6)-linkages as branches. Laminaran has only 2 or 3 branches per molecule with an average chain length of 7 to 11 D-glucopyranosyl units, which leads to a DP of about 30. Alginate is another typical algal polysaccharide. It is made from (1→4)-linear linked β -D-mannopyranosyluronic acid and α -L-gulopyranosyluronic acid residues. The compound seems to have regions with uniform composition containing one or the other hexuronic acid residue, interconnected with regions containing a mixture of both. Alginate is used mainly in the food industry as a foam stabilizer or thickening agent.

Some algae also contain sulfated polysaccharides, the more common of these being agar and carrageenan. Agar is formed from three types of interconnected polymeric chains: (1→3)-linked β -D-galactopyranosyl and (1→4)-linked 3,6-anhydro- α -L-galactopyranosyl residues, which form the agarose, an agarose with the galactopyranosyl residues with the C-4 and C-6 participating in an acetal with pyruvic

acid, and a sulfated galactan with no 3,6-anhydro- α -L-galactopyranosyl residues. Carrageenan is commonly made from (1 \rightarrow 3)-linked β -D-galactopyranosyl and (1 \rightarrow 4)-linked α -L-galactopyranosyl groups with different degrees of sulfation at the OH from C-2, C-4 or C-6.

Several other less common polysaccharides were isolated from algae [62] and are indicated in Table 7.8.1. Some of these polysaccharides also have a certain degree of sulfation.

TABLE 7.8.1. *Polysaccharides with less common structure isolated from algae.*

Common Name	Structure	Source
Rhodymenan	(1 \rightarrow 3)- β -D- linear xylan	green seaweed
Fucoidan	(1 \rightarrow 2)- α -L-, (1 \rightarrow 4)- α -L- branched fucan	brown seaweed
Xylan	(1 \rightarrow 3)- β -D-, (1 \rightarrow 4)- β -D- linear xylan	red seaweed

Pyrolysis of polysaccharides from algae was performed using both Py-MS and Py-GC/MS techniques (e.g. [2, 3, 64]). Py-MS studies [2] showed it was possible to obtain structural information on the primary and secondary structure of the polysaccharide from specific ions in its spectrum. Particularly EI spectra at 14 eV ionization energy were used for compound differentiation. Four examples of such spectra are shown below in Figure 7.8.1.

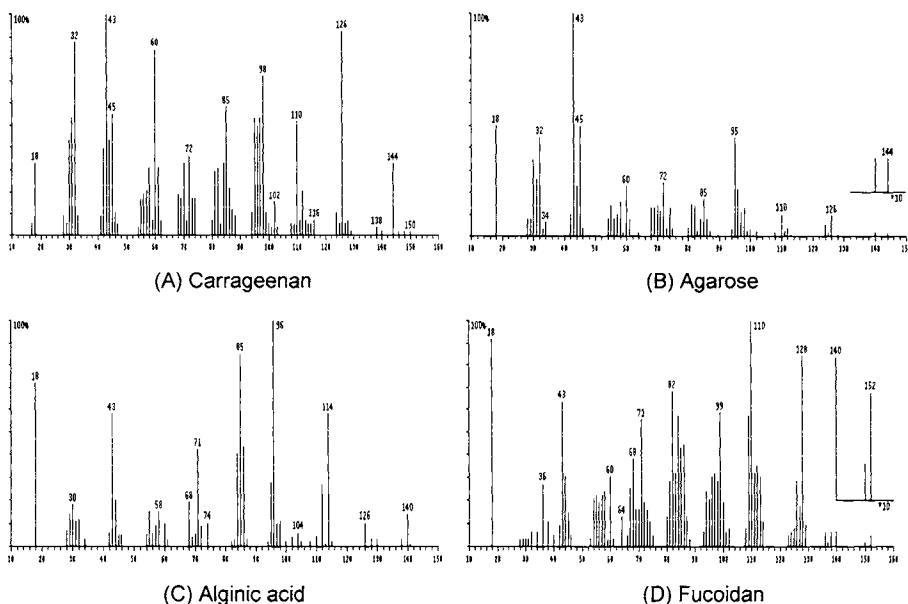


FIGURE 7.8.1. *Py-MS spectra at 14 eV of several algal polysaccharides [3].*

The interpretation of the peaks in different polysaccharide spectra is not always straightforward. The ion $m/z = 64$ is a marker for sulfation. Higher intensity for the mass peak ion $m/z = 64$ indicates higher sulfation, as seen in Figure 1 (D). The peaks

$m/z = 45$ and 95 are, in general, markers for 3,6-anhydrohexoses. Fucoidan, being a polydeoxy-sugar, has a more peculiar Py-MS spectrum. Py-GC/MS study of fucoidan [6a] indicated clearly the presence in the chromatogram of 1,4-anhydro-6-deoxy-galactopyranose, which can be considered a good marker for this material.

Even MS/MS analyses (with initial Py-DIP and CI in the mass spectrometer) were performed on some algal polysaccharides [3a] with successful differentiation between several starting materials (see also Section 7.1).

FI mass spectra were proven informative in algal polysaccharide analysis [2]. Characteristic Py-FI mass spectra were reported for agarose, alginic acid, laminaran, etc. Also, Py-GC/MS studies were done on algal polysaccharides [64a,64b]. The identification of pyrolysis products for several polysaccharides from red algae showed, as expected, compounds commonly obtained during polysaccharide pyrolysis. A list of several compounds found in these pyrolysates is shown in Table 7.8.2.

TABLE 7.8.2. *Common pyrolysis products in some polysaccharides from red algae (Rhodophyta).*

Compound	MW
methanol	32
2-butanone	72
hydroxy-acetaldehyde	60
acetic acid	60
1-hydroxy-2-propanone	74
2-methylfuran	92
2(3H)-furanone	84
2-furaldehyde	96
1-(2-furanyl)-ethanone	110
1-(3-hydroxy-2-furanyl)-ethanone	126
5-methyl-2-furaldehyde	110
phenol	94
2-furyl hydroxymethyl ketone	126
5-(methoxymethyl)-2-furaldehyde	140
1,6-anhydro-3,4-dideoxy- β -D-glycero-hex-3-enopyranos-2-ulose (levoglucosenone)	126
6-O-methyl-hexose	158
5-(hydroxymethyl)-2-furaldehyde	126
1,5-anhydro-4-deoxy-D-glycero-hex-1-en-3-ulose	144
1-deoxy-3,6-anhydro-lyxo-hexopyranos-2-ulose	144
anhydro-deoxy-galactopyranose	144
1,4-anhydro-6-O-methyl-galactopyranose	176
1,6-anhydro-4-O-methyl-galactopyranose	176
1,6-anhydro- β -D-galactopyranose	162
2-O-methyl-3,6-anhydro-galactose	176

Although no unexpected compounds were seen in the pyrograms of algal polysaccharides, the chromatographic profile of each material was quite distinctive, suggesting the possibility the use of pyrograms for taxonomic purposes. The presence of the sulfate groups in the algal polysaccharide affects the pyrolysis such that more levoglucosenone and anhydro-deoxy-galactopyranose are generated, probably because dehydration is favored compared with other decomposition pathways.

7.9 Microbial Polysaccharides.

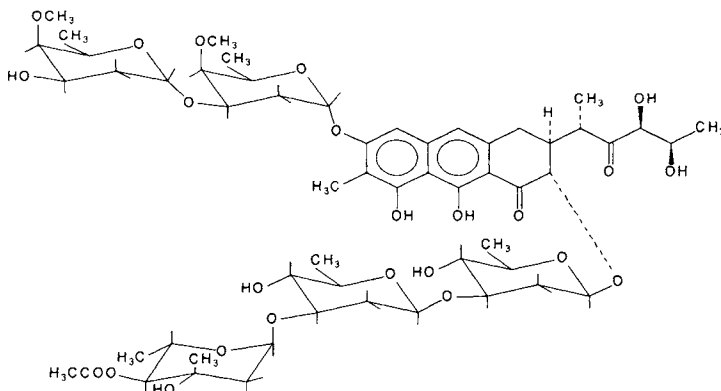
Microbial polysaccharides comprise a wide variety of carbohydrate macromolecules, some of them with considerable structural complexity. Three main types of microbial polysaccharides are known:

- those generated in culture media;
- those which are part of bacterial cell walls; and
- those which form a capsule surrounding the microbial cell.

The microbial polysaccharides generated in culture media, or extracellular polysaccharides, may be similar to some of the plant or algae polysaccharides such as cellulose, levans, alginic acid, etc. Some polysaccharides are more specific to microorganisms, such as the dextrans produced by certain bacteria growing on a sucrose substrate. The structure of dextrans is characterized by a (1→6)- α -D-glucopyranosyl chain. Branches may occur at (1→6)- or (1→3)-linked points. Xanthan gum is another extracellular polysaccharide. Its structure consists of (1→4)-linearly linked β -D-glucopyranosyl residues to which are attached trisaccharide side chains consisting of α -D-mannosyl and D-glucosyluronic acid residues in the ratio 2:1. Some of the mannosyl groups have the OH from C-4 and C-6 participating in an acetal with pyruvic acid.

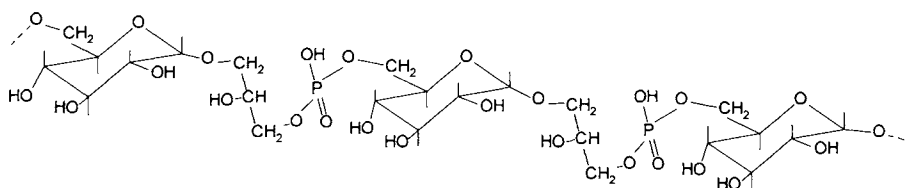
Several Py-MS and Py-GC/MS studies were done on extracellular microbial polysaccharides [6a, 64, 66]. The dextrans being connected in 1→6 positions generate less levoglucosan than cellulose or starch. Otherwise, typical pyrolysis results for a polyhexose were reported [66]. The pyrolysis of xanthan gum showed that the presence of metal cations (Na^+ , Ca^{2+}) at the uronic residue will diminish the relevant information from pyrograms. However, after treating the material with a strong ion exchange resin in H^+ form, its pyrolysate was much more informative revealing the presence of glucosyl and mannosyl groups in the correct proportion existing in the polysaccharide. A marker for the glucuronic acid was also reported, tentatively identified as 1-deoxy-glucofuranosylfuro-3,6-lactone.

A special group of extracellular microbial polysaccharides are certain compounds with antibiotic properties such as chromomycins. The structure of chromomycin A_3 shows several carbohydrate units, although the substance cannot be considered a true polymer.

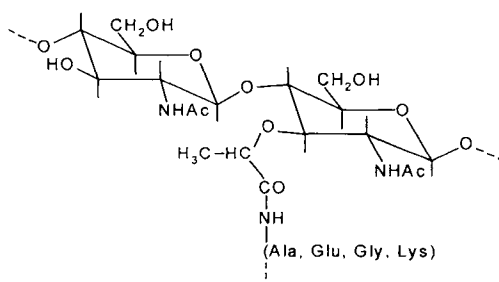


Pyrolysis of compounds with aromatic cycles will be dominated by aromatic compounds, as their stability is significantly higher than that of sugars.

A group of polymers containing phosphate and known as teichoic acids was isolated from the cell wall of Gram-positive bacteria. A typical representative of this group of compounds is built from 10 to 50 ribitol phosphate units joined through the phosphodiester linkages or from glycerol phosphate units joined through the phosphodiester linkages. Carbohydrate residues are present in these types of teichoic acids only as substituents at some of the OH groups of ribitol or glycerol, but residues of amino acids such as D-alanine are also present. Other teichoic acids are built from monosaccharide or oligosaccharide phosphate units. A model structure of such a compound is given below:

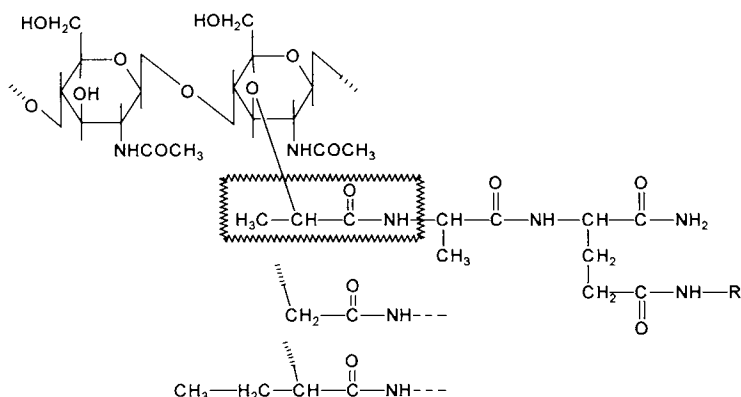


Highly branched biopolymers consisting of polysaccharide chains cross-linked by peptide bridges form a group of biopolymers known as peptidoglycans or mureins, which are common in the cell wall of bacteria. The polysaccharides from peptidoglycans typically contain 2-acetamido-2-deoxy-D-glucose and 2-acetamido-3-O-(1-carboxyethyl)-2-deoxy-D-glucose (2-acetamido-2-deoxymuramic acid). The linkage to the amino acids (alanine, D-glutamic acid, L-lysine, etc.) is done through the carboxyl group of the 2-acetamido-3-O-(1-carboxyethyl)-2-deoxy-D-glucose:



Py-MS results on peptidoglycans (including the peptide and the polysaccharide) from several microorganisms were reported [3]. These Py-MS spectra showed differences depending on the source of the peptidoglycan and indicated that these spectra can be utilized for the differentiation of certain microorganisms. One specific study [66a], done to identify the source of propionamide in the pyrolysate of bacteria, identified peptidoglycans lactyl-peptide bridge as a source for this compound. This was found by pyrolyzing a series of model compounds including a 2-acetamido-2-deoxy-muramyl dipeptides, its carboxymethyl analogue, and its carboxypropyl analogue (muramic acid is 3-O-(1-carboxyethyl)-D-glucose). A significantly larger amount of propionamide was generated from the muramyl dipeptide than from the other model compounds, although

the other potential sources of propionamide such as the amino acids were the same in these models. This suggested that the elimination of propionamide takes place from the lactyl-peptide bridge of the molecule that is indicated below [66a]:



In the cell wall of Gram-positive organisms, teichoic acids are usually connected through a phosphodiester unit to cell wall peptidoglycans. Teichoic acids are replaced in certain conditions in Gram-positive organisms by teichuronic acids, which are polymers containing D-glucuronic acid and 2-acetamido-2-deoxy-D-galactose with structures of the type $\rightarrow 4\text{-}\beta\text{-D-GlcA-(1}\rightarrow 3\text{)-}\alpha\text{-}\beta\text{-D-GalNAc-(1}$. A Py-MS spectrum obtained using 14 eV excitation energy [3] of teichuronic acid from *Bacillus subtilis* is shown in Figure 7.9.1.

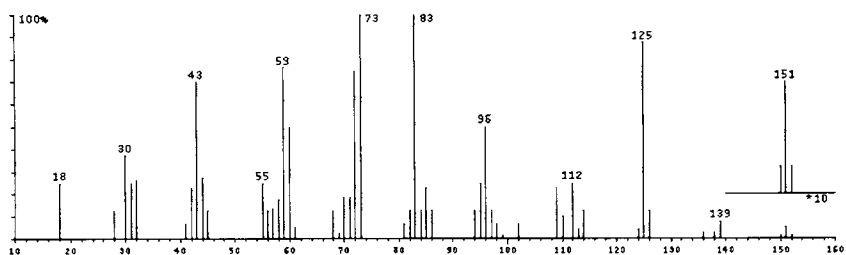
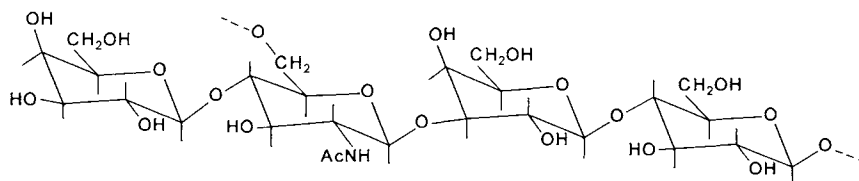


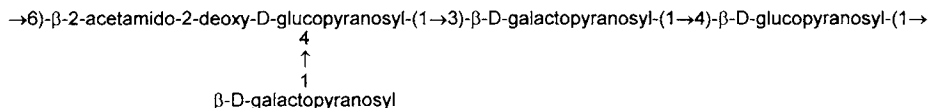
FIGURE 7.9.1. Py-MS spectrum obtained using 14 eV excitation energy [3] and 510°C pyrolysis for teichuronic acid from *Bacillus subtilis*.

In this spectrum, the ions 59, 73, 83, and 125 are assumed to come from the GalNAc units, while the ions 60, 96, 102, 112 are assumed to come from the GlcA units.

Bacterial capsular polysaccharides also have complex structures and may contain neutral or acidic monosaccharide residues as well as aminosugar residues (the most common being 2-amino-2-deoxy-D-glucose). Some of these contain less common monosaccharide residues such as deoxysugars, heptoses, octoses, sugar ethers, or aminouronic acids. Over 70 types of polysaccharides have been identified in the capsules that cover the cells, and frequently they have immunological properties similar to the O-antigen part of lipopolysaccharides. The structure of a simple polysaccharide from a bacterial capsule containing a tetrasaccharide repeating unit [62] is shown below:



or



Both Py-MS [3] and Py-GC/MS studies were performed on capsular polysaccharides isolated from microorganisms. As an example, a Py-GC/MS study on the capsular polysaccharides from different *Klebsiella* bacteria indicated that they generate characteristic pyrograms [6a] and this can be used for fingerprinting. Elimination of the metal ions (by treatment with ion exchangers in H^+ form) was useful for obtaining more characteristic traces that can be used for the differentiation of microorganisms. The ratio of different monosaccharide units from each bacterium polysaccharide was reflected in the peak height of the corresponding anhydrosugar seen in the pyrogram. Capsular polysaccharides from different microorganisms were also analyzed by Py-MS (with 14 eV ionization, 510° C Curie point pyrolysis [3]) and characteristics were found for each particular microorganism evaluated. Py-MS results on a capsular polysaccharide from *Neisseria meningitidis* [3] are shown in Figure 7.9.2. Specific peaks also seen in KDO (3-keto-3-deoxy-manno-octulosonic acid or 3-deoxy-manno-octopyranulosonic acid) Py-MS spectrum ($m/z = 110, 112, 122, 140$) were identified in the pyrolysates, indicating its presence in the biopolymer structure. Also a large peak with $m/z = 60$ characteristic for aliphatic acids (and higher than the one seen in KDO spectrum) is present in the spectrum, which may indicate that this material could contain lipopolysaccharides (see Section 7.10).

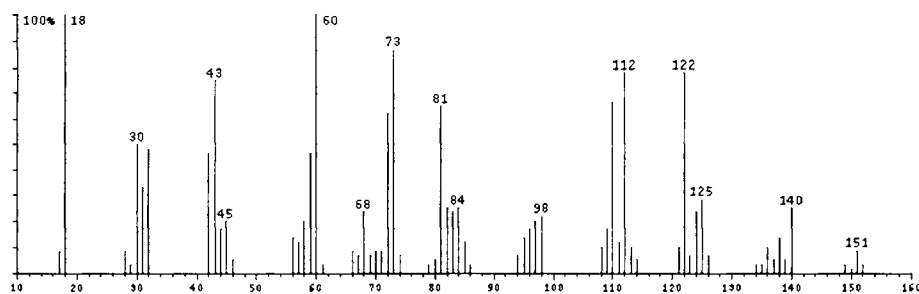
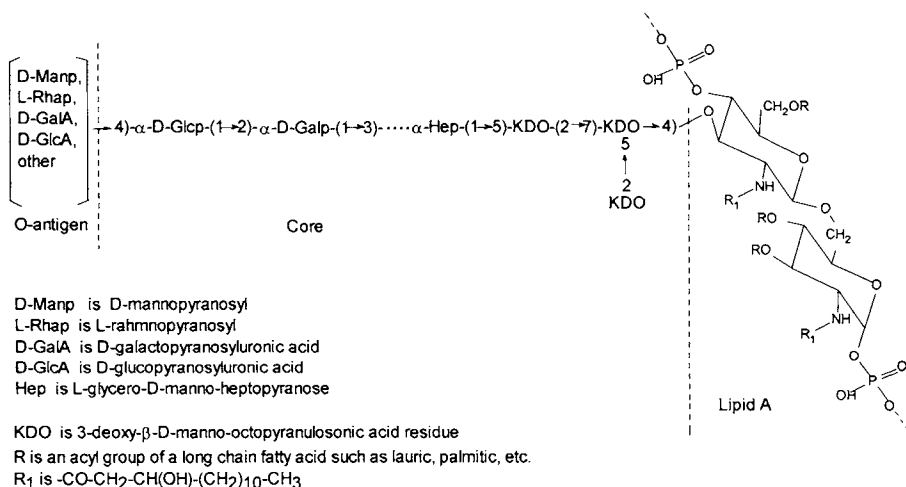


FIGURE 7.9.2. Py-MS spectrum obtained using 14 eV excitation energy [3] and 510° C for the capsular polysaccharide from *Neisseria meningitidis*.

A significant amount of work also has been done on direct Py-MS of a variety of microorganisms with the purpose of their rapid identification and classification [3]. No separation of the polysaccharide from the whole microorganism was done for this purpose, but the polysaccharide pyrolysis products are main components of the pyrolysate. Some of these applications are described in Part 3 of this book.

7.10 Lipopolysaccharides from the Cell Surface of Bacteria.

Lipopolysaccharides are complex macromolecules containing carbohydrate residues. They are commonly found on the cell surface of bacteria and are responsible for type specific immunological reactions. Their structure shows three distinct parts: O-antigen, core, and lipid A. The O-antigen portion is the outer part of the capsule. It is usually a complex polysaccharide although a number of common repeating oligosaccharides formed from D-mannopyranosyl, D-galactopyranosyluronic acid, or D-glucopyranosyluronic acid residues can be present. Less common monosaccharide residues such as aminosugars, deoxysugars, heptoses, octoses, sugar ethers, or aminouronic acids complicate this portion of the lipopolysaccharide. The core polysaccharide is usually simpler and consists of a linear chain with few short branches, containing D-glucose, D-galactose, and 2-acetamido-2-deoxy-D-glucose. The core is connected to the lipid A portion by a heptose and an octose (still part of the core). The lipid A consists of repeating units of an amido-disaccharide connected through phosphodiester bonds. This disaccharide has O- and N-substitution with long chain fatty acids. A typical lipopolysaccharide can be represented by the structure:



Few pyrolysis studies were performed on particular components of bacterial lipopolysaccharides. Py-MS results on KDO were reported [3]. The Py-MS studies on individual lipopolysaccharides may encounter problems caused by the difficulty of obtaining pure compounds from this class. As previously indicated, a significant amount of work has been done on direct Py-MS of a variety of whole microorganisms with the purpose of their rapid identification and classification [3].

7.11 Fungal Polysaccharides.

Fungal polysaccharides include homopolysaccharides as well as heteropolysaccharides including D-galacto-D-mannans, D-xylo-D-mannans, etc. Scleroglucan is used as an industrial gum. Several homopolysaccharides found in fungi are shown in Table 7.11.1.

TABLE 7.11.1. *Some homopolysaccharides found in fungi.*

Common name	Structure	Source
scleroglucan	(1 → 3)-β-D-, (1 → 6)-β-D- branched glucan	fungi
pullulan	(1 → 4)-α-D-, (1 → 6)-α-D. linear glucan	fungi
galactocarolose	(1 → 5)-β-D- linear galactan	penicillin mould
curdlan, pachyman	(1 → 3)-β-D- linear glucan	fungi and yeasts
	(1 → 2)-α-D-, (1 → 6)-α-D- branched mannan	yeasts

A few pyrolysis studies done on yeasts and yeast-like fungi did not attempt to analyze individual polysaccharides but to obtain a fingerprint characterization [67]. It was also common to use statistical techniques such as factor analysis for the data interpretation. It was not unusual to find N-acetylamino sugar units in fungal polysaccharides. These units showed characteristic peaks in Py-MS that allowed the distinction of different materials.

7.12 Glycogen.

Glycogen is the most common polysaccharide present in animals and its purpose is to provide a means to store glucose. Glycogen has a structure similar to amylopectin but with a higher degree of branching. The length of a unit chain was estimated to have 12 glycosyl units. As expected, glycogen pyrolysis generates products similar to those obtained from amylopectin (or starch). A Py-FI MS using high resolution MS [16] allowed some identifications in the pyrogram, and the compounds identified are shown in Table 7.12.1.

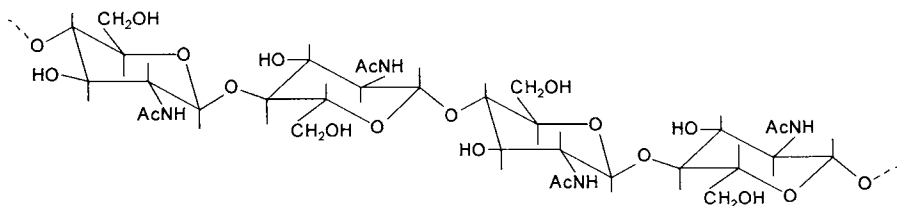
TABLE 7.12.1. *Ions identified in the Py-FI high-resolution mass spectrum of glycogen performed by Curie point pyrolysis at 770° C and their molecule assignment.*

Mass	Compound	Formula
18.011	water	H ₂ O
27.997	carbon monoxide	CO
28.031	ethene	C ₂ H ₄
30.011	formaldehyde	CH ₂ O
42.010	ketene	C ₂ H ₂ O
42.047	propene	C ₃ H ₆
43.990	carbon dioxide	CO ₂
44.026	acetaldehyde	C ₂ H ₄ O
46.006	formic acid	CH ₂ O ₂
56.026	acrolein	C ₃ H ₄ O
60.021	hydroxyacetaldehyde	C ₂ H ₄ O ₂
72.021	pyruvaldehyde	C ₃ H ₄ O ₂
74.036	hydroxypropanone	C ₃ H ₆ O ₂
86.037	2,3-butanedione	C ₄ H ₆ O ₂
90.032	glyceraldehyde	C ₃ H ₆ O ₃
90.032	dihydroxypropane	C ₃ H ₈ O ₃
96.021	2-furaldehyde	C ₅ H ₄ O ₂
98.036	furfuryl alcohol	C ₅ H ₆ O ₂
98.036	1,5-anhydro-2,3-dideoxy-β-D-(pent-2-enofuranose)	C ₅ H ₆ O ₂
110.037	5-methyl-2-furaldehyde	C ₆ H ₆ O ₂
126.032	levoglucosenone	C ₆ H ₆ O ₃
126.032	5-hydroxymethyl-2-furaldehyde	C ₆ H ₆ O ₃
128.047	1,6-anhydro-3-deoxy-O-β-D-threo-hex-3-enopyranose)	C ₆ H ₈ O ₃
144.042	unknown	C ₆ H ₈ O ₄
162.052	levoglucosan	C ₆ H ₁₀ O ₅

As seen in Table 7.12.1, the same compounds were identified in starch pyrolysis (see Tables 7.4.1, 7.4.2, and 7.4.3). Glycogen pyrolysis was utilized in a series of studies to identify this compound in biological samples and in mixtures with other biopolymers (see Part 3). Studies were also done to determine the influence of the matrix on the Py-MS results for glycogen [68a].

7.13 Chitin.

Chitin is a polysaccharide containing amino type monosaccharide residues. It occurs as a structural polysaccharide in the exoskeleton of crustacea and it is also present in some fungi and algae. Chitin is a homopolysaccharide consisting of 2-acetamido-2-deoxy- β -D-glucopyranose residues interconnected by β -glucoside (1 \rightarrow 4) links. This structure is similar to that of cellulose, except for the acetamido groups replacing the OH groups at C-2 position of the glucose residue.



Chitin pyrolysis has been studied by different pyrolytic techniques [69–70] such as Curie point Py-MS, Curie point Py-GC/MS, micro oven Py-MS, etc., and with different types of ionization techniques in the mass spectrometer such as EI^+ , CI and FI (see Section 5.4). The main pyrolysis products identified in chitin pyrolysis at a temperature of about $500^\circ C$ are shown in Table 7.13.1.

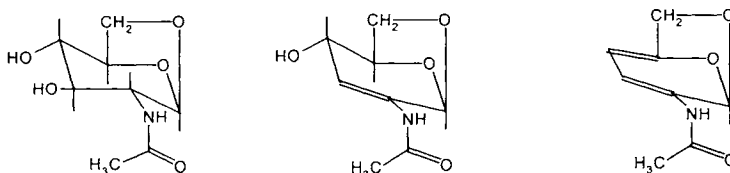
TABLE 7.13.1. *The main pyrolysis products identified in chitin pyrolysis at a temperature of about $500^\circ C$.*

MW	Compound	Formula
60	acetic acid	$C_2H_4O_2$
59	acetamide	C_2H_5NO
83	methyloxazol	C_4H_5NO
84	2-methyl-2-imidazolone	$C_4H_8N_2$
92	$C_5H_4O_2$?	$C_5H_4O_2$
79	pyridine	C_5H_5N
111	$C_5H_5NO_2$?	$C_5H_5NO_2$
110	1-(1H-pyrazol-4-yl)-ethanone	$C_5H_6N_2O$
82	2-methylfuran	C_5H_6O
78	benzene	C_6H_6
126	levoglucosenone	$C_6H_6O_3$
93	3-methylpyridine	C_6H_7N
93	2-methylpyridine	C_6H_7N
109	3-hydroxy-4-methylpyridine	C_6H_7NO
108	2,5-dimethylpyrazine	$C_6H_8N_2$
108	2,3-dimethylpyrazine	$C_6H_8N_2$

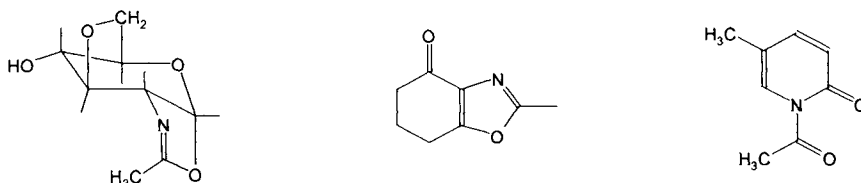
TABLE 7.13.1. *The main pyrolysis products identified in chitin pyrolysis at a temperature of about 500° C (continued).*

MW	Compound	Formula
96	2,5-dimethylfuran	C ₆ H ₈ O
96	2-methyl-2-cyclopentenone	C ₆ H ₈ O
111	C ₆ H ₉ NO ?	C ₆ H ₉ NO
122	4-methyl-1,3-benzenediamine	C ₇ H ₁₀ N ₂
137	3-acetoxypyridine	C ₇ H ₇ NO ₂
137	C ₇ H ₇ NO ₂ ?	C ₇ H ₇ NO ₂
153	C ₇ H ₇ NO ₃ ?	C ₇ H ₇ NO ₃
92	toluene	C ₇ H ₈
107	N-methylbenzenamine	C ₇ H ₉ N
122	2,3,5-trimethylpyrazine	C ₇ H ₁₀ N ₂
146	4-hydroxyquinazoline	C ₈ H ₆ N ₂ O
104	ethenylbenzene	C ₈ H ₈
151	6-methyl-3-pyridinol acetate	C ₈ H ₉ NO ₂
151	methyl-N-acetyl-2-pyridinone	C ₈ H ₉ NO ₂
151	6,7-dihydro-2-methyl-4(5H)-benzoxazolone	C ₈ H ₉ NO ₂
167	C ₈ H ₉ NO ₃ ?	C ₈ H ₉ NO ₃
149	N-(2-hydroxyphenyl)-acetamide	C ₈ H ₉ N ₂ O
165	N-(2,4-dihydroxyphenyl)-acetamide	C ₈ H ₉ N ₂ O ₂
167	trianhydro-2-acetamido-2-deoxyglucose	C ₈ H ₉ NO ₃
153	C ₈ H ₁₁ NO ₂ ?	C ₈ H ₁₁ NO ₂
185	oxazoline structure ?	C ₈ H ₁₁ NO ₄
185	dianhydro-2-acetamido-2-deoxyglucose	C ₈ H ₁₁ NO ₄
123	butylpyrrole	C ₈ H ₁₃ N
203	1,6-anhydro-2-acetamido-2-deoxyglucose	C ₈ H ₁₃ NO ₅
130	benzenepropanenitrile	C ₉ H ₈ N
137	1-(1-cyclopenten-1-yl)-pyrrolidine	C ₉ H ₁₅ N
228	tetradecanoic acid	C ₁₄ H ₂₈ O ₂
142	pentadecanoic acid	C ₁₅ H ₃₀ O ₂
256	hexadecanoic acid	C ₁₆ H ₃₂ O ₂
282	eicosane	C ₂₀ H ₄₂

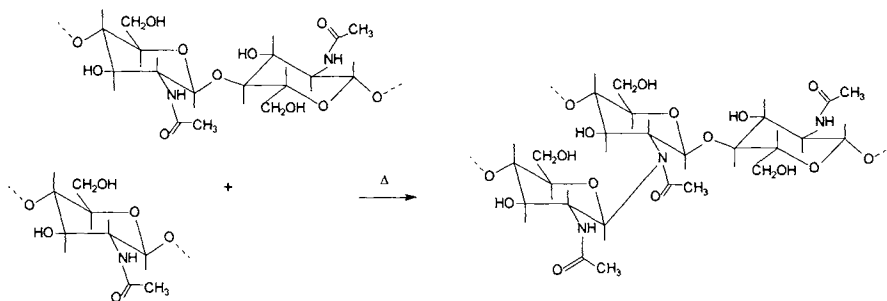
The list of compounds given in Table 7.13.1 contain some long chain fatty acids (tetradecanoic acid, pentadecanoic acid, hexadecanoic acid) that probably are not generated from chitin itself but from associated materials present in the chitin sample (chitin purification is difficult due to its insolubility). The main pyrolysis mechanism seems to be similar to that of cellulose. 1,6-Anhydro-2-acetamido-2-deoxyglucose seems to be a major component in the pyrolysate as are further dehydrated hexosamines.



Dehydrations involving the acetamido group also take place, and this explains the formation of oxazoline type compounds and pyridinone type compounds.

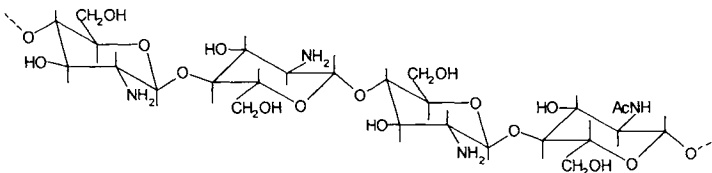


Condensation reactions with the initial formation of tridimensional polymer structures are also possible. This may take place by reactions of the type:



This type of reaction may generate structures containing -N-C-C-N- bonds. Further dehydration and fragmentation at higher temperatures of these compounds can explain the formation of pyrazines in the chitin pyrolysate [71].

Treatment of chitin with bases such as NaOH has the effect of hydrolyzing the N-acetyl groups (about 70 to 85% of them) and generating a polymer known as chitosan:



Several derivatized chitosans have practical applications. Py-GC and Py-MS have been used for the evaluation of free amine content in several chitosan samples [72,73].

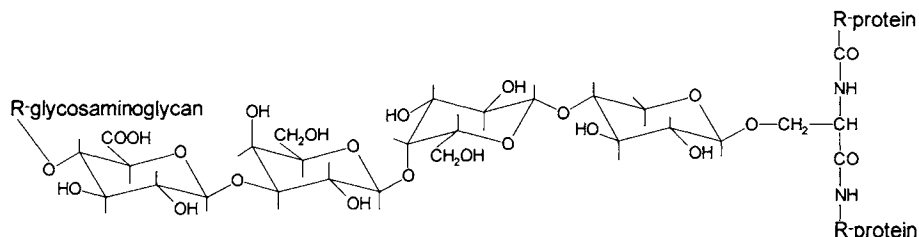
7.14 Proteoglycans.

A significant number of biopolymers found in animals contain both a protein chain and carbohydrates in the same molecule. These biopolymers are classified as either glycoproteins or proteoglycans. The differentiation of the two classes is based on the number of carbohydrate units per unit length of protein backbone, with the protein predominant in glycoproteins and carbohydrate predominating in proteoglycans. A third

class, carbohydrate-protein complexes, is also known, but in these compounds the protein and the carbohydrates are not covalently linked, and certain separation procedures can be applied without destroying the molecular entities.

Glycoproteins will be discussed in some detail in Section 12.4. The carbohydrate components of proteoglycans are known as glycosaminoglycans. Proteoglycans are essential parts of the connective tissue in mammals and are also present to some extent in fish and bacteria (peptidoglycans from the cell wall of bacteria are different biopolymers and were discussed in Section 7.9). The term mucopolysaccharide was used in the past to describe polysaccharide materials of animal origin containing 2-amino-2-deoxyhexoses.

The proteoglycans are formed from a protein chain, a linkage (carbohydrate) region and a considerably large glycosaminoglycan region, connected as shown below:

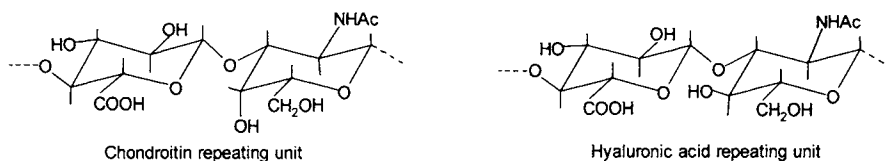


Eight main glycosaminoglycans have been identified [62] in proteoglycans and are indicated in Table 7.14.1.

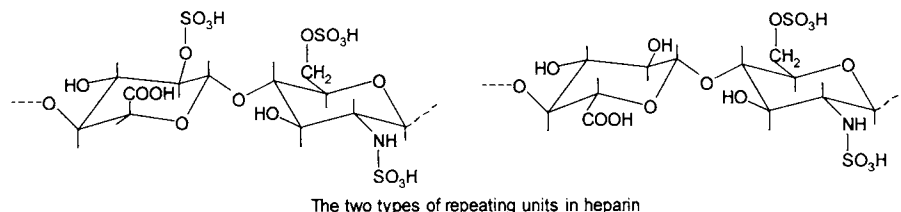
TABLE 7.14.1. *Classification of glycosaminoglycans.*

Common name	Semi-systematic name
chondroitin	galactosaminoglucuronan
chondroitin 4-sulfate	galactosaminoglucuronan
chondroitin 6-sulfate (with different sulfation deg.)	galactosaminoglucuronan
dermatan sulfate	galactosaminoiduronan
heparin	glucosaminoglucuronoiduronan
heparan sulfate	glucosaminoglucuronoiduronan
hyaluronic acid	glucosaminoglucuronan
keratan sulfate	glucosaminogalactan

Different glycosaminoglycans are not very different in structure. For example, the repeating unit in chondroitin is $\rightarrow 4$)-O-(β -D-glucopyranosyluronic acid)-(1 \rightarrow 3)-O-(2-acetamido-2-deoxy- β -D-galactopyranosyl)-(1 \rightarrow . The number of units varies but can be in the range of hundreds. Hyaluronic acid has a rather similar structure, $\rightarrow 4$)-O-(β -D-glucopyranosyluronic acid)-(1 \rightarrow 3)-O-(2-acetamido-2-deoxy- β -D-glucopyranosyl)-(1 \rightarrow , as shown below:



Chondroitin 4-sulfate and chondroitin 6-sulfate have sulfate groups in positions 4 and 6 respectively of the acetamido-2-deoxy-D-galactosyl groups of the polysaccharide repeating unit. Dermatan sulfate is isomer to chondroitin 4-sulfate, with L-iduronic acid replacing the D-glucuronic acid. Keratan sulfate contains no hexuronic acid residue and has the repeating unit $\rightarrow 3\text{-O-}\beta\text{-D-galactopyranosyl-(1}\rightarrow 4\text{)-O-(2-acetamido-2-deoxy-}\beta\text{-D-glucopyranosyl 6-sulfate)-(1}\rightarrow$. Heparin is a mixture of two repeating units. One unit consists of L-iduronic acid 2-sulfate and 2-deoxy-2-sulfamido-D-glucose 6-sulfate. The second unit is D-glucuronic acid and 2-deoxy-2-sulfamido-D-glucose 6-sulfate.



Heparan sulfate has less frequent O-sulfate groups on 2-deoxy-2-sulfamido-D-glucopyranosyl residue compared to heparin and may be N-acetylated.

Besides the typical structures previously indicated, irregularities may also be present in the repeating units. Glycosaminoglycans contain numerous anionic groups (carboxyl, sulfate) and in nature they may be present as sodium, potassium, etc. forms, which is not always possible to know because of the modifications suffered during the purification process.

Pyrolysis work on glycosaminoglycans as well as on proteoglycans was mainly done by Py-MS [3] using Curie point pyrolysis at 510°C and with EI ionization at 14 eV. Because glycosaminoglycans do not have significant structural differences, their Py-MS spectra are also similar. As an example, the Py-MS results for hyaluronic acid potassium salt and for chondroitin 6-sulfate sodium salt are shown in Figures 7.14.1 and 7.14.2 respectively [3].

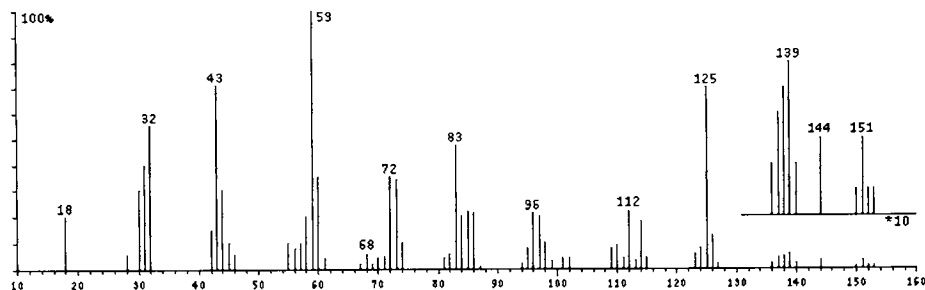


FIGURE 7.14.1. Py-MS results for hyaluronic acid pyrolysed at 510°C and analyzed after ionization at 14 eV [3].

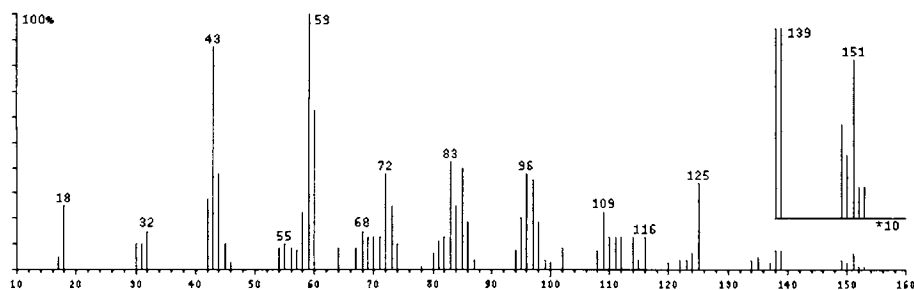


FIGURE 7.14.2. Py-MS results for chondroitin 6-sulfate pyrolysed at 510° C and analyzed after ionization at 14 eV [3].

The ions with $m/z = 59, 73, 83, 97, 109, 125, 137, 139, 151$ in the two spectra were attributed to the presence of acetamido-2-deoxy-glycosyl residues, while the ions with $m/z = 60, 68, 96, 112, 114, 126$ were attributed to the presence of uronic acid residues. The ion with $m/z = 64$ is the only ion generated by SO_2 and is a marker for sulfation. The Py-MS study on several glycosaminoglycans [3] showed that the sample purity (separation from the protein) plays an important role in the spectrum appearance. Also, the fact that these compounds were pyrolysed in salt form may have reduced some of the potential differences in the spectra.

References 7

1. H. -R. Schulten, U. Bahr, H. Wagner, H. Herman, *Biomed. Mass Spectrom.*, 9 (1982) 115.
2. H. -R. Schulten, U. Bahr, W. Gortz, *J. Anal. Appl. Pyrol.*, 3 (1981/1982) 229.
3. H. L. C. Meuzelaar, J. Haverkamp, F. D. Hileman, *Pyrolysis Mass Spectrometry of Recent and Fossil Biomaterial*, Elsevier, Amsterdam, 1982.
- 3a. R. J. Helleur, R. Guevremont, *J. Anal. Appl. Pyrol.*, 15 (1989) 85.
4. R. D. Guthrie, in W. Pigman and D. Horton (eds.), *The Carbohydrates: Chemistry and Biochemistry*, Academic Press, New York, 1972, p. 423.
5. P. Koll, S. Deyhim, K. Heyns, *Chem. Ber.*, 111 (1978) 2909.
6. D. R. Budgell, E. R. Hayes, R. J. Helleur, *Anal. Chim. Acta*, 192 (1987) 243.
- 6a. R. J. Helleur, *J. Anal. Appl. Pyrol.*, 11 (1987) 297.
7. S. L. Morgan, C. A. Jacques, *Anal. Chem.*, 54 (1982) 741.
8. J. W. Liskowitz, B. Carroll, *Carbohydr. Res.*, 5 (1967) 245.
9. P. Koll, S. Deyhim, K. Heyns, *Chem. Ber.*, 106 (1973) 3565.

10. N. Mitsuo, N. Nakayama, H. Matsumoto, T Satoh, Chem. Pharm. Bull., 37 (1989) 1624.
- 10a. A. Van der Kaaden, J. J. Boon, J. Haverkamp, Biomed Mass Spectrom., 11 (1984) 486.
11. A. D. Pouwels, G. B. Eijkel, J. J. Boon, J. Anal. Appl. Pyrol., 14 (1989) 237.
12. A. D. Pouwels, G. B. Eijkel, P. W. Arisz, J. J. Boon, J. Anal. Appl. Pyrol., 15 (1989) 71.
13. J. Piskorj, D. Radlein, D. S. Scott, J. Anal. Appl. Pyrol., 9 (1986) 121.
14. F. Shafizadeh, Y. L. Fu, Carbohydrate Res., 29 (1973) 113.
15. F. Sharizadeh, Adv. Carbohydr. Chem. Biochem., 23 (1968) 419.
16. H. -R. Schulten, W. Gortz, Anal. Chem., 50 (1978) 428.
17. H. -R. Schulten, U. Bahr, W. Gortz, J. Anal. Appl. Pyrol., 3 (1981) 137.
18. H. -R. Schulten, U. Bahr, W. Gortz, J. Anal. Appl. Pyrol., 3 (1981) 229.
19. A. Basch, M. Levin, J. Polym. Sci., 11 (1973) 3095.
20. P. W. Arisz, J. A. Lomax, J. J. Boon, Anal. Chem., 62 (1990) 1519.
21. S. C. Moldoveanu, unpublished results.
22. J. A. Lomax, J. M. Commandeur, P. W. Arisz, J. J. Boon, J. Anal. Appl. Pyrol., 19 (1991) 65.
23. P. W. Arisz, J. J. Boon, J. Anal. Appl. Pyrol., 25 (1993) 371.
- 23a. R. T. Conley, *Thermal Stability of Polymers*, M. Dekker Inc., New York 1970, chap. 12.
24. A. E. Pavlath, K. S. Gregorski, J. Anal. Appl. Pyrol., 8 (1985) 41.
25. T. Funazukuri, R. R. Hudgins, P. L. Silveston, J. Anal. Appl. Pyrol., 9 (1986) 139.
26. T. Funazukuri, R. R. Hudgins, P. L. Silveston, J. Anal. Appl. Pyrol., 10 (1986) 25.
27. F. Shafizadeh, R.H. Fumeaux, T.G. Cochran, J.P. Scholl, Y. Sakai, J. Appl. Polym. Sci., 23 (1979) 3525.
28. G. M. Simmons, M. Gentry, J. Anal. Appl. Pyrol., 10 (1986) 25.
29. O. T. Chortyk, W. S. Schlotzhauer, Beitrage zur Tabakforschung, 7 (1973) 165.
30. J. B. Forehand, S. C. Moldoveanu, unpublished results.

31. H. Sakuma, M. Kusama, S. Sato, S. Sugawara, *Agr. Biol. Chem.*, 40 (1976) 2013.
32. H. Sakuma, M. Kusama, S. Ishiguro, N. Shimojima, S. Sugawara, *Agr. Biol. Chem.*, 40 (1976) 2021.
33. H. Sakuma, N. Shimojima, S. Sugawara, *Agr. Biol. Chem.*, 42 (1978) 359.
34. H. Sakuma, T. Ohsumi, S. Sugawara, *Agr. Biol. Chem.*, 43 (1979) 2619.
35. H. Sakuma, T. Ohsumi, S. Sugawara, *Agr. Biol. Chem.*, 44 (1980) 555.
36. H. Sakuma, S. Munakata, S. Sugawara, *Agr. Biol. Chem.*, 45 (1981) 443.
37. J. B. Forehand, S. C. Moldoveanu, unpublished results.
- 37a. S. Glassner, A. R. Pierce III, *Anal. Chem.*, 37 (1965) 525.
38. F. Shafizadeh, R. H. Furneux, T. T. Stevenson, T. G. Cochran, *Carbohydrate Res.*, 61 (1978) 1519.
39. S. Julien, E. Chornet, R. P. Overend, *J. Anal. Appl. Pyrol.*, 27 (1993) 25.
40. V. G. Randall, M. S. Masri, A. E. Pavlath, *Proc. 7th Int. Conf. Therm. Anal.*, Kingston, ON, vol. II, 1982, p. 1190.
41. R. F. Schwenker Jr., L. R. Beck, *J. Polym. Sci.*, C2 (1963) 331.
42. L. Huwei, F. Ruonong, *J. Anal. Appl. Pyrol.*, 14 (1988) 163.
- 42a. B. Kaur, I. S. Gur, H. L. Bhatnagar, *Angew. Makromolekulare Chem.*, 147 (1987) 157.
- 42b. B. Kaur, R. K. Jain, I. S. Gur, H. L. Bhatnagar, *J. Anal. Appl. Pyrol.*, 9 (1986) 173.
43. E. Ott, H. M. Spurlin, M. W. Grafflin, *Cellulose and Cellulose Derivatives*, Interscience Inc., New York, 1954.
44. T. Mitsui, M. Hida, Y. Fujimura, *Bunseki Kagaku*, 39 (1990) 427.
45. J. M. Chalinor, *J. Anal. Appl. Pyrol.*, 16 (1989) 323.
46. R. K. Jain, K. Lal, H. L. Bhatnagar, *J. Anal. Appl. Pyrol.*, 8 (1985) 359.
47. J. Marton, *Tappi J.*, 11 (1990) 139.
48. T. Yano, H. Ohtani, S. Tsuge, T. Obokata, *Analyst*, 117 (1992) 849.
49. S. C. Moldoveanu, unpublished results.
- 49a. W. Baltes, H. -J. Schmahl, *Z. Lebensm. Unters. Forsch.*, 171 (1980) 286.

50. W. P. Brown, C. F. H. Tipper, *J. Appl. Polymer Sci.*, 22 (1978) 1459.
- 50a. P. W. Arisz, G. B. Eijkel, J. J. Boon, *J. Anal. Appl. Pyrol.*, 33 (1995) 21.
51. L. F. McBurney, *Ind. Eng. Chem.*, 41 (1949) 1251.
52. O. P. Koz'mina, A. K. Khripunov, V. I. Kurlyankyna, *Vysokomolekul. Soedin.*, 5 (1963) 492.
53. A. Van der Kaaden, J. Haverkamp, J. J. Boon, J. W. de Leeuw, *J. Anal. Appl. Pyrol.*, 5 (1983) 199.
54. M. A. Scheijen, J. J. Boon, *Rapid Commun. Mass Spectrom.*, 3 (1989) 238.
55. O. Wurzburg, *Modified Starches: Properties and Uses*, CRC Press, Boca Raton, 1986.
56. K. C. Patel, R. D. Patel, *Chem. Era*, 2 (1978) 30.
57. I. Simkovic, B. A. Francis, J. B. Reeves, *J. Anal. Appl. Pyrol.*, 43 (1997) 145.
58. M. Souty, A. Perret, *Ann. Technol. Agric.*, 19 (1970) 41.
59. J. C. E. Reitsma, W. Pilnik, *Carbohydr. Polym.*, 10 (1989) 315.
60. R. E. Aries, C. S. Gutteridge, W. A. Laurie, J. J. Boon, G. B. Eijkel, *Anal. Chem.*, 60 (1988) 1489.
61. J. H. Lauterbach, S. C. Moldoveanu, 45th. TCRC conf. vol. 45 (1991).
62. J. F. Kennedy, C. A. White, *Bioactive Carbohydrates In Chemistry, Biochemistry and Biology*, E. Horwood Lim., Chicester 1983.
63. A. D. Pouwels, A. Tom, G. B. Eijkel, J. J. Boon, *J. Anal. Appl. Pyrol.*, 11 (1987) 417.
64. R. J. Helleur, D. R. Budgell, E. R. Hayes, *Anal. Chim. Acta*, 192 (1987) 367.
- 64a. R. J. Helleur, E. R. Hayes, J. S. Craigie, J. L. McLachlan, *J. Anal. Appl. Pyrol.*, 8 (1985) 349.
- 64b. R. J. Helleur, E. R. Hayes, W. D. Jamieson, J. S. Craigie, *J. Anal. Appl. Pyrol.*, 8 (1985) 333.
65. K. P. Madhusudanan, P. Pant, D. S. Bakhuni, *Indian J. Chem.*, 26B (1987) 790.
66. A. C. Tas, A. Kerkenaar, G. F. LaVos, J. Van der Greef, *J. Anal. Appl. Pyrol.*, 15 (1989) 55.
- 66a. L. W. Eudy, M. D. Walla, J. R. Hudson, S. L. Morgan, *J. Anal. Appl. Pyrol.*, 7 (1985) 231.

67. W. Windig, G. S. De Hoog, J. Haverkamp, *J. Anal. Appl. Pyrol.*, 3 (1981/1982) 213.
68. A. van der Kaaden, J. J. Boon, J. W. de Leeuw, F. de Lange, P. J. W. Schuyf, H. -R. Schulten, U. Bahr, *Anal. Chem.*, 56 (1984) 2160.
- 68a. A. P. Snyder, J. H. Kremer, H. L. C. Meuzelaar, W. Windig, *J. Anal. Appl. Pyrol.*, 13 (1988) 77.
69. R. Marbot, *J. Anal. Appl. Pyrol.*, 39 (1997) 97.
70. D. Knorr, T. P. Wampler, R. A. Teutonico, *J. Food Sci.*, 50 (1985) 1762.
71. W. S. Schlotzhauer, O. T. Chortyk, P. R. Austin, *J. Agric. Food. Chem.*, 24 (1976) 177.
72. G. S. Lal, E. R. Hayes, *J. Anal. Appl. Pyrol.*, 6 (1984) 183.
73. J. Mattai, E. R. Hayes, *J. Anal. Appl. Pyrol.*, 3 (1982) 327.

This Page Intentionally Left Blank

Chapter 8. Analytical Pyrolysis of Polymeric Materials with Lipid Moieties

8.1 Classification of Complex Lipids and Analytical Pyrolysis of Simple Lipids.

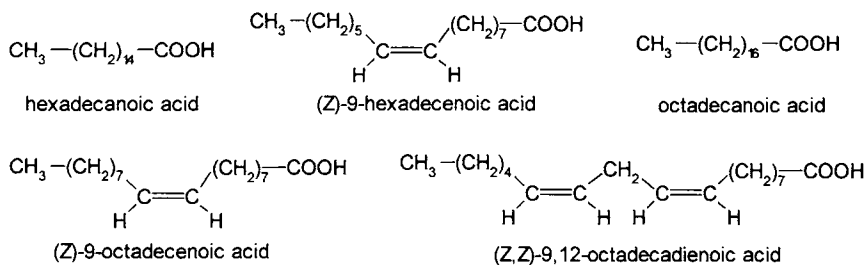
Lipids are bioorganic substances related to fatty acid esters and include a variety of compounds such as glycerol esters, waxes, phosphoglycerides, sphingolipids, natural hydrocarbons, some vitamins, etc. This diversity of compounds is explained by the fact that initially the term *lipids* was used to describe natural bioorganic substances soluble in hydrocarbons and insoluble in water. Lipids include both small molecules and polymeric materials. Because some simple lipids are not polymeric, their pyrolysis will be discussed only to the extent of being associated with the pyrolysis of complex lipids. However, non-polymeric lipids are commonly associated with polymeric ones, and pyrolytic techniques were frequently applied on the whole lipid without separation for purposes such as classification or identification of microorganisms based on the pyrolysis pattern of their lipids [1].

- Classification of lipids.

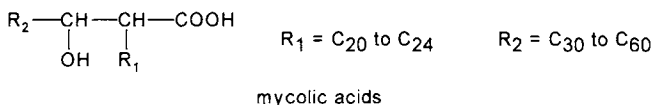
Several classifications of lipids are available. Based on their chemical composition lipids can be classified as follows:

- simple lipids, which include glycerol esters, cholesterol esters, waxes, hydrocarbons, some vitamins, etc.;
- phosphoglycerides, which include phosphatidic acids, phosphate diesters with choline, ethanolamine, serine, etc., and phosphate triesters;
- sphingolipids, which include sphingomielins, cerebrosides, gangliosides, sulfatides, etc.;
- glycolipids;
- peptidolipids; and
- peptidoglycolipids.

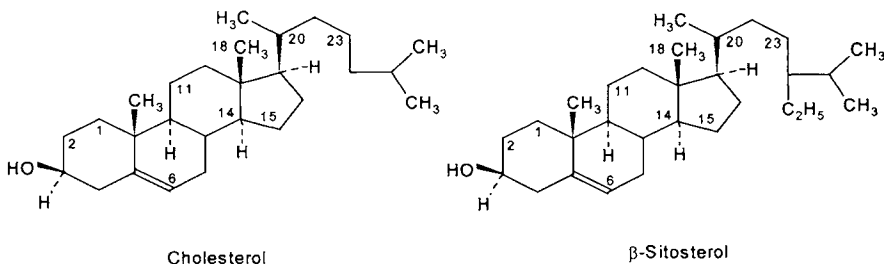
One important group of compounds that are classified as simple lipids consists of glycerol esters. These substances are very common in plants and animals. Glycerol esters include mono-, di-, or triglycerides, as glycerol has three OH- esterifying groups. The acids that esterify glycerol are fatty acids. There are significant differences in the distribution of acids in fats between land animals, aquatic animals, microorganisms, plants, etc. and even between different species [1a]. The acids comprise both saturated and unsaturated acids, commonly with C₁₄ to C₂₀ carbon atoms. Among the most common ones are (Z)-9-octadecenoic acid (oleic acid), hexadecanoic acid (palmitic acid), octadecanoic acid (stearic acid), (Z)-9-hexadecenoic acid (palmitoleic acid), and (Z,Z)-9,12-octadecadienoic acid (linoleic acid).



The variety of fatty acids found in lipids is extremely large. Acids containing a wider range of carbon atoms between C_4 to C_{34} or higher are also found as glycerides. Besides simple acids, more complex ones such as branched and/or hydroxylated acids are also common mainly in microorganisms. One group of such acids is, for example, the mycolic acids:

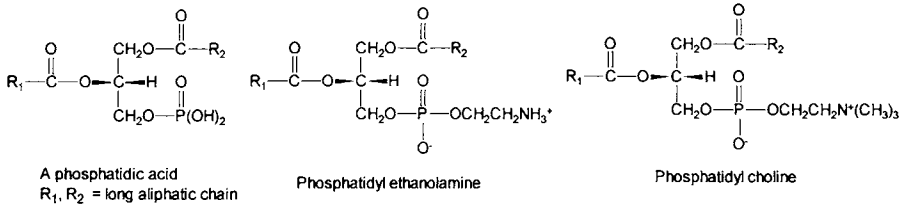


Among the simple lipids are also the cholesterol and cholesterol esters with acids such as palmitic, stearic, or oleic. These compounds are common compounds in most animal cells, although not in plants. Besides cholesterol, other zoosterols are known [1a]. Several sterols are also present in plants (phytosterols), the most common being the sitosterol(s) and stigmasterol.



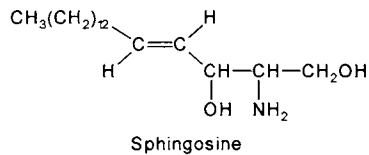
The waxes include a variety of esters of long chain aliphatic acids with long chain aliphatic alcohols, more frequently containing C_{12} to C_{34} carbon atoms. Some other simple compounds are included in this group of lipids [1a].

Phosphoglycerides are fats in which glycerol is esterified with two fatty acids and one phosphoric acid. (Glycerol esters of phosphoric acid containing a free OH- glycerol group and only one fatty acid, as well as compounds with an ether linkage at one OH- glycerol group named plasmalogens, are also known.) The phosphoric acid moiety can be further esterified (phosphoric acid is a tribasic acid). This esterification can be done with ethanolamine (in cephalins), choline (in lecithins), serine, inositol, etc.



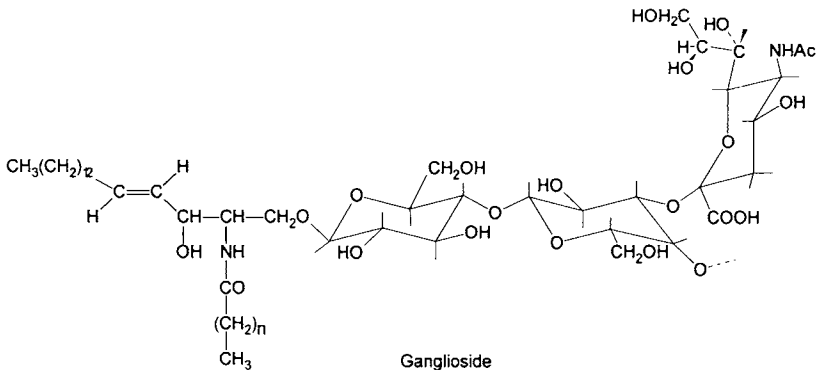
Phosphoglycerides with the phosphoric acid moiety further esterified with inositol may generate more complex compounds, as inositol can be connected with other glycosyl residues.

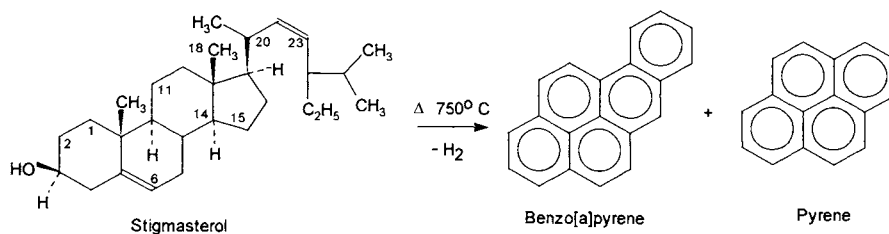
Sphingolipids form a lipid class that does not contain glycerol. In this class are included sphingomyelins, cerebroside, gangliosides, and sulfatides. The compounds from this class can be considered as derived from sphingosine or related substances such as dehydrosphingosine (sphinganine), 4-hydroxy-sphinganine, etc.



For example, sphingomyelins are sphingosine phosphatides where the amino group in sphingosine is acylated with a fatty acid radical such as stearyl, palmityl, etc., and the primary alcohol group forms a phosphatide (primary alcohol is esterified with a phosphoric unit itself esterified with choline at the second site).

Cerebroside (glycosylceramides) are formed from sphingosine where the amino group is acylated with a fatty acid radical (like in sphingomyelins), but the primary alcohol group forms an ether bond with a sugar residue. Di-, tri- and tetraglycosylceramides are found in mammalian tissues, mainly in the central nervous system. When the glycosylceramides contain residues of N-acetylneuraminic acid, the substances are considered to form a separate class known as gangliosides.





Not only the analysis of triglycerides can be done using GC/MS. The EI+ mass spectra of other lipids with relatively small molecules are known. As an example, Figure 8.1.2 shows the mass spectrum for dipalmitoylphosphatidylethanolamine in EI+ standard conditions.

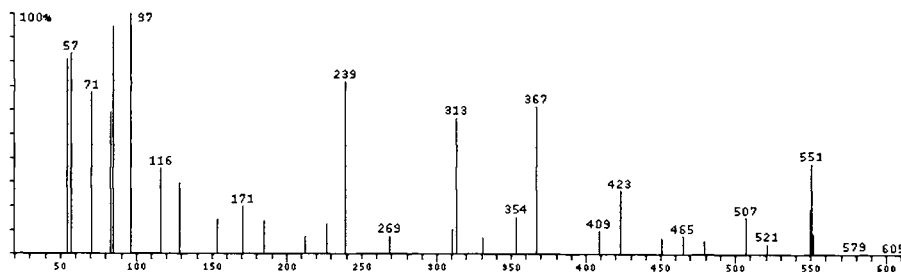


FIGURE 8.1.2. The mass spectrum (EI+ standard conditions) for dipalmitoylphosphatidylethanolamine.

Comparing the spectrum from Figure 8.1.2 with the spectrum from Figure 8.1.1, it can be seen that they are rather similar, differing only in peak intensities, as it is known that the spectra of phospholipids are similar to those of triglycerides [11]. Spectra for analogous compounds but with serine or choline replacing ethanolamine or with different fatty acids are also known. As an example, Figure 8.1.3 shows the mass spectrum for distearylphosphatidylcholine.

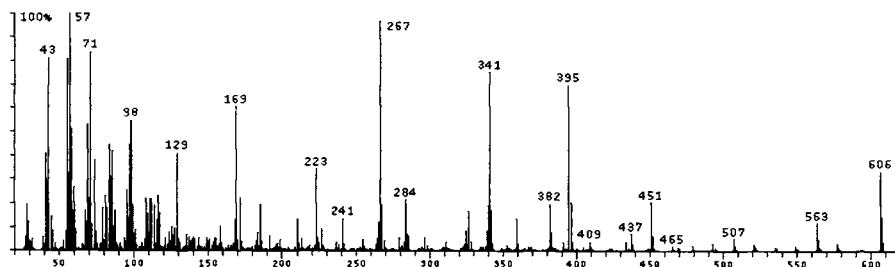


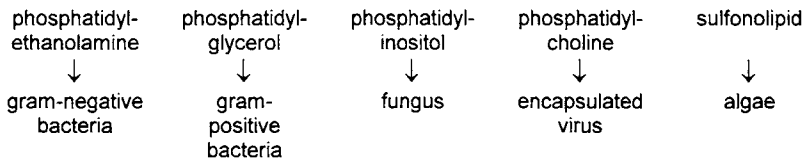
FIGURE 8.1.3. The mass spectrum (EI+ standard conditions) for distearylphosphatidylcholine.

Analysis of lipid pyrolysates using Py-GC/MS was performed [12], but it lacked a good separation that would have shown the individual compounds. Extracted ion

chromatograms generated from the pyrograms were used as markers for a specific microorganism rather than for the detection of a lipid type.

8.2 Complex Lipids.

Pyrolysis studies on complex lipids were done mainly with the purpose of microorganism characterization [13]. Besides DNA and proteins, the lipids are considered valuable markers with chemotaxonomic utility for microorganisms. The association of a certain predominant lipid and a specific group of microorganisms is indicated below [13].



In addition, the analysis of the fatty acids in a complex lipid may provide a view of the nutritional and metabolic history of the microorganism (see also Section 16.1). Also, problems in bacterial taxonomy were solved based on fatty acid distribution, which was used as a fingerprint for different bacteria.

Several pyrolytic techniques were utilized for the analysis of lipids, such as:

- simple Py-MS studies with some sort of mathematical processing of data [11],
- Py-GC/MS with EI ionization and the direct analysis of the pyrolysate [12],
- Py-MS with linear temperature programming, CI ionization [9], and
- Py-GC/MS with derivatization using TMAH or related compounds [5,14].

Associated with these techniques, which are oriented toward practical purposes, there are results on individual lipids. The lipid moiety is not always significant for Py-MS spectra. As an example, the Py-MS spectrum of a ganglioside (trisialosyl-tetraglycosylceramide seen in Section 8.1) [15] is given in Figure 8.2.1.

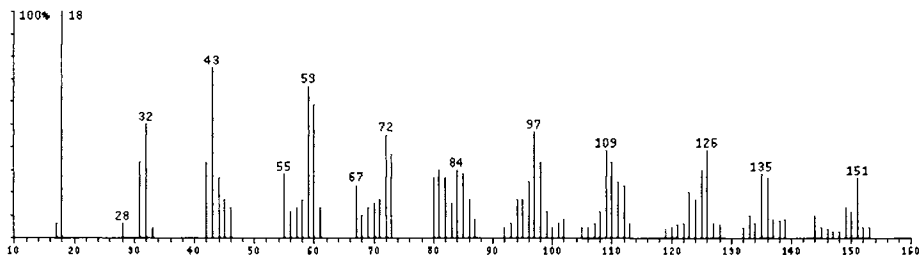


FIGURE 8.2.1. Py-MS spectrum of a ganglioside [15].

The ions typical for the aminosugar are seen in the spectrum from Figure 8.2.1, while the lipid moiety is difficult to detect. Other techniques may show more clearly the fatty acid moiety. For example, for the analysis of several types of *Salmonella*, a Py-MS

study with methane chemical ionization was performed on lipid preparations from their cell envelope [9]. A Py-CH₄ CI MS spectrum of lysophosphatidyl ethanolamine is shown in Figure 8.2.2 A for comparison, and the Py-CH₄ CI MS spectrum obtained at 217.6° C from the lipid extract of *Salmonella typhimurium* TA-100, is shown in Figure 8.2.2 B.

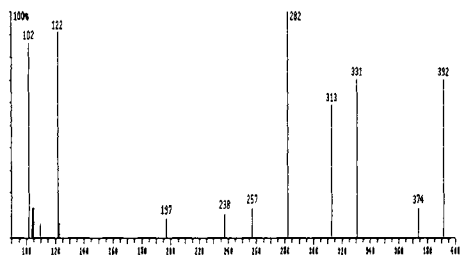


FIGURE 8.2.2 A. Py-CH₄ CI MS spectrum of lysophosphatidyl ethanolamine [9].

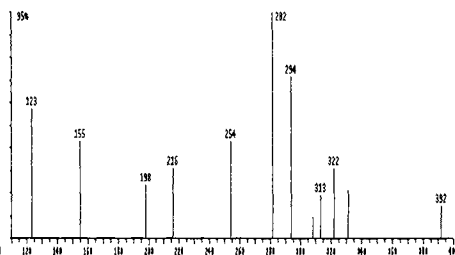
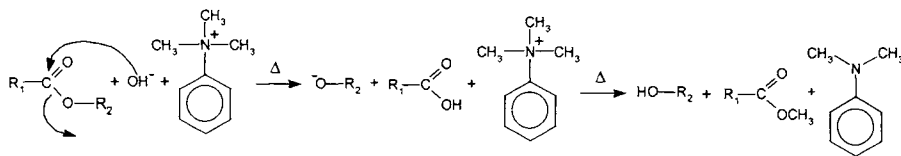


FIGURE 8.2.2 B. Py-CH₄ CI MS spectrum obtained at 217.6° C from a lipid extract of *Salmonella typhimurium* [9].

As seen in Figures 8.2.2 A and 8.2.2 B, the two spectra have significant similarities indicating the presence of lysophosphatidyl ethanolamine in the lipid extract. The lysophosphatidyl ethanolamine (lysocephalin) can be obtained from an appropriate material (egg yolk, bovine liver, or bovine brain) using a phospholipase. The fatty acids in this lysophosphatidyl ethanolamine are primarily palmitic and stearic acids.

The technique that seems to show best the fatty acid constituents is pyrolysis in the presence of a methylating agent (such as TMAH). Both Py-MS and Py-GC/MS studies were done using this procedure [5,14]. This reaction seems to be a transesterification (with typical nucleophilic mechanism) where R₁ is the long hydrocarbon chain of the fatty acid and R₂ is the glycerol (or an alternative) residue.



A number of studies were done on lipid fatty acids determination using pyrolytic techniques (some using TMAH) on whole cell microorganisms for characterization and differentiation [16-27].

References 8

1. J. Asselineau, *The Bacterial Lipids*, Hermann, Paris, 1962.
- 1a. H. J. Deuel, *The Lipids*, Interscience Pub., New York, 1951.
2. J. F. Kennedy, C. A. White, *Bioactive Carbohydrates In Chemistry, Biochemistry and Biology*, E. Horwood Lim., Chicester, 1983.

3. D. B. Shina, W. L. Gaby, *J. Biol. Chem.*, 239 (1964) 3668.
4. J. M. Challinor, *J. Anal. Appl. Pyrol.*, 37 (1996) 185.
5. S. DeLuca, E. W. Sarver, P. de B. Harrington, K. J. Voorhees, *Anal. Chem.*, 62 (1990) 1465.
6. W. A. Hartgers, J. S. Sinninghe Damste, J. W. de Leeuw, *J. Anal. Appl. Pyrol.*, 34 (1995) 191.
7. D. T. Downing, R. S. Greene, *Anal. Chem.*, 40 (1968) 827.
8. Y. S. Stein, M. J. Antal, M. Jones, *J. Anal. Appl. Pyrol.*, 4 (1983) 283.
9. J. A. Adkins, T. H. Risby, J. J. Scocca, R. E. Yasbin, J. W. Ezzell, *J. Anal. Appl. Pyrol.*, 7 (1984) 35.
10. H. L. Frederickson, J. W. de Leeuw, A. C. Tas, J. van der Greef, G. F. LaVos, J. J. Boon, *Biomed. Envir. Mass Spectrom.*, 18 (1989) 96.
- 10a. P. Bernfeld, *Biogenesis of Natural Compounds*, Pergamon, Oxford, 1963.
11. S. DeLuca, E. W. Sarver, K. J. Voorhees, *J. Anal. Appl. Pyrol.*, 23 (1992) 1.
12. A. P. Snyder, W. H. McClennen, J. P. Dworzansky, H. L. C. Meuzelaar, *Anal. Chem.*, 62 (1990) 2565.
13. C. Fenselau, ed., *Mass Spectrometry for the Characterization of Microorganisms*, ACS Symposium Ser. 541, ACS, Washington DC, 1994.
14. J. P. Dworzansky, L. Berwald, W. H. McClennen, H. L. C. Meuzelaar, *J. Anal. Appl. Pyrol.*, 21 (1991) 2211.
15. H. L. C. Meuzelaar, J. Haverkamp, F. D. Hileman, *Pyrolysis Mass Spectrometry of Recent and Fossil Biomaterial*, Elsevier, Amsterdam, 1982.
16. F. Basile, K. J. Voorhees, T. L. Hadfield, *Appl. Environ. Microbiol.*, 61 (1995) 1534.
17. S. J. DeLuca, F. W. Sarver, P. DeB. Harrington, K. J. Voorhees, *Anal. Chem.*, 62 (1990) 1465.
18. J. P. Anhalt, C. Fenselan, *Anal. Chem.*, 47 (1975) 219.
19. A. C. Tas, J. De Waart, J. Bouwman, M. C. Ten Noever De Brauw, J. Van Der Greef, *J. Anal. Appl. Pyrol.*, 11 (1987) 329.
20. K. J. Voorhees, S. L. Durfee, D. M. Updegraaf *J. Anal. Appl. Pyrol.*, 8 (1988) 315.

21. K. J. Voorhees, S. L. Durfee, J. R. Holtzclaw, G. C. Enke, M. R. Bauer, *J. Anal. Appl. Pyrol.*, 14 (1988) 7.
22. S. J. DeLuca, F. W. Sarver, K. J. Voorhees, *J. Anal. Appl. Pyrol.*, 23 (1992) 1.
23. G. Holzer, T. F. Bourne, W. Bertsch, *J. Chromatog.*, 468 (1989) 181.
24. J. P. Dworzanski, L. Berwald, H. L. C. Meuzelaar, *Appl. Environ. Microbiol.*, 56 (1990) 1717.
25. H. Engman, H. T. Mayfield, T. Mar, W. Bertsch, *J. Anal. Appl. Pyrol.*, 6 (1984) 137.
26. F. B. Smith, A. P. Snyder, *J. Anal. Appl. Pyrol.*, 24 (1992) 23.
27. A. A. Garaibeh, K. J. Voorhees, *Anal. Chem.*, 68 (1996) 2805.

Chapter 9. Analytical Pyrolysis of Lignins

9.1. Lignin.

Lignin is the second most important component of wood, making up 15% to 36% of its dry weight. It appears in nature together with cellulose from which it is difficult to separate due to the fact that besides physical mixing some covalent bonds seem to exist between lignin and cellulose. Elemental analysis of lignin indicates that its composition shows differences for different types of wood. Table 9.1.1 shows the content in C, H, and O for three different lignins [1]:

TABLE 9.1.1. *Elemental composition % in C, H, and O of different lignins.*

Lignin	C	H	O
Spruce (<i>Picea abies</i>)	62.59	6.07	31.34
Beech (<i>Fagus silvatica</i>)	60.12	6.42	33.46
Bamboo (<i>Bambusa spec.</i>)	61.96	5.67	32.37

Common procedures for obtaining lignin are of two types [2]. One type is based on the hydrolysis and/or solubilization of cellulose with the lignin left as an amorphous material insoluble in water. The second type is based on the removal of lignin by dissolving it with specific solvents or reagents followed by reprecipitation. Some of these procedures cause a significant chemical modification of lignin.

In the first type of technique, which attempts to solubilize the cellulosic material, there are several procedures generating lignin:

- Sulfuric acid dissolves cellulose (with hydrolysis) leaving a lignin called "Klason lignin," or "sulfuric acid lignin." Lignin is known to be sensitive to the action of strong acids, and therefore modifications from the natural form are expected.
- Hydrochloric acid also dissolves cellulose to generate "Willstätter lignin."
- Cellulose can be dissolved in cuprammonium hydroxide, generating "cuproxam lignin."
- Sugars including cellulose can be degraded with oxidative reagents such as periodate and separated from the insoluble lignin.
- Lignin can be enzymatically released by using enzymes or brown-rot microorganisms to degrade cellulose.

Among the second type of procedures, which solubilize the lignin followed by reprecipitation, are the following:

- A lignin fraction can be dissolved with ethanol at room temperature. This procedure generates a small amount of soluble lignin, which is not necessarily representative for the total "natural lignin." The lignin generated by this procedure is known as "Brown lignin."
- A procedure designed to increase the yield of soluble lignin is the "Milled-wood." In this procedure, the wood is ground in a mill for a long period of time and then extracted at room temperature with a solvent and reprecipitated as a "Milled-wood lignin" (MWL or MW lignin).

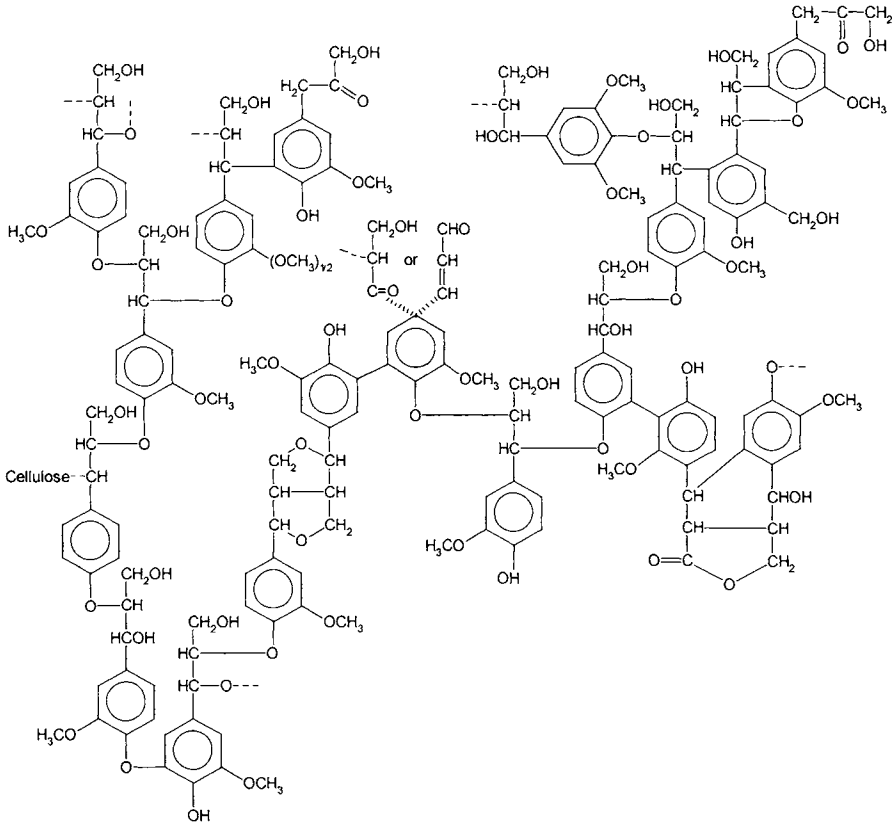
- Steam explosion was also used to increase the extractable lignin.
- A group of methods to obtain lignin are known as organosolv procedures. They consist of an extraction of wood sawdust with an alcohol (such as ethanol) and some acid (5% HCl) in stronger conditions (boiling under reflux) followed by the reprecipitation of lignin from the extract.
- In the organosolv procedures, dioxane or phenol can replace the alcohol, using a technique similar to "Brown's," standard organosolv, or "Milled-wood" procedures.
- Thioglycolic acid can be used for extracting lignin with better yields than alcohols.
- Organic acids, ethanolamine, dimethyl sulfoxide, etc. were also used as solvents for different extraction techniques.
- Alkali procedure uses NaOH to dissolve lignin. The process is common for obtaining cellulose free of lignin, but instead of using pure NaOH it was proven much more efficient to use NaOH and sodium sulfide (Na_2S , probably with some polysulfides). Lignin reprecipitated with acids is known as Kraft (kraft) lignin.
- Delignification with bisulfites (commonly used are $\text{Ca}(\text{HSO}_3)_2$ in solutions containing free SO_2) is also applied to generate lignin. The solutions are commonly precipitated as calcium lignosulfonate, etc.
- Detergents can also be used to remove lignin.

Because of its insolubility, only a small part of lignin from a certain type of wood can be obtained pure and not modified chemically. All the above procedures generate a "lignin" material which is a compromise between being representative for the whole lignin in a specific type of wood, not being mixed with cellulose and other components of wood, and not being chemically modified. Some lignins are specifically modified, such as kraft lignin, which contains sulfur bridges in its structure. Also, the bisulfite procedure generates a modified lignin (lignosulfonates).

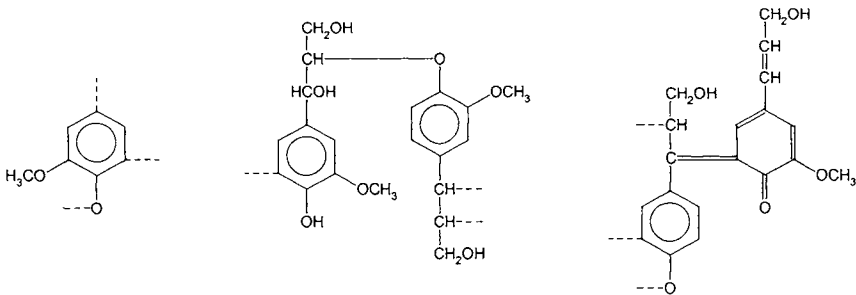
By their chemical composition, lignins are classified based on the predominance of the main phenylpropanes present in their structure. Three main phenylpropanes are common in lignins, namely 4-hydroxyphenylpropane (H), (4-hydroxy-3-methoxy)phenylpropane or guaiacylpropane (G), and (4-hydroxy-3,5-dimethoxy)phenylpropane or syringylpropane (S). Based on the occurrence of these basic units, lignins can be classified as G lignins or guaiacyl lignins (also known as type N), G/S lignins or guaiacyl-syringyl lignins (also known as type L), and H/G/S lignins.

Idealized structures for lignin were proposed [3], for example, as a polymer of coniferyl alcohol (4-hydroxy-3-methoxycinnamyl alcohol). However, lignin is not a repetitive polymer. Also, it is necessary to specify which lignin is considered when a specific structure is proposed.

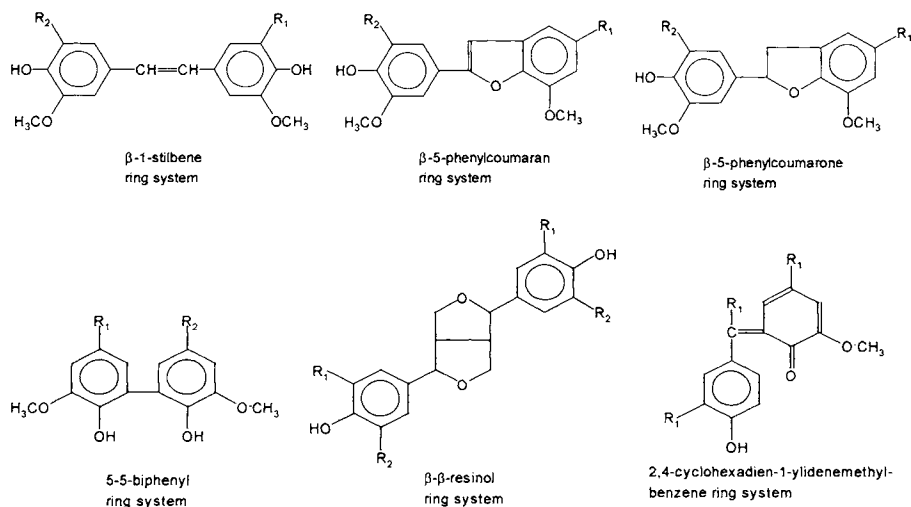
Combining the results regarding the type and number of functionalities in different lignins as determined by different analyses, several "model structures" were proposed such as "Freudenberg structure" which is shown below [2]:



Some other repeating units of lower importance were also indicated in lignin and they are shown below:



These idealized structures were generated based on lignin analysis, and they contain several dimer units:



In these dimer units R_1 indicates the rest of the polymer, while the substituents R_2 on the aromatic rings are H or O-CH_3 . These structures can be recognized as stable units and are also generated during lignin pyrolysis.

Lignin pyrolysis has been studied in detail from a variety of points of view most frequently related to chemical utilization of wood pyrolysis products, to fire related problems, and to waste problems related to paper mills. Also, as lignin may be generated in a variety of forms, lignin structure was studied using pyrolytic procedures [4,5]. Pyrolysis has also been extensively utilized to assess the degree of lignin purity (absence of cellulose, hemicellulose, proteins, etc). A variety of analytical procedures were applied for these studies, Py-GC/MS and Py-MS being, as usual, the most common [5-7]. Other analytical procedures were also utilized for the analysis of lignin pyrolysates, such as Py-IR [4] and on-line Py-HPLC/UV/MS [8].

Pyrolysis of lignin generates gases, tar, and char with yields depending on the lignin type and pyrolytic conditions. A typical result for kraft lignin pyrolysed at 650°C is shown in Table 9.1.2.

TABLE 9.1.2. Yield (wt.) % of different components from kraft lignin at 650°C in a filament pyrolyser.

Compound	% Yield wt.
H_2O	6.73
CO_2	8.22
Gases (excl. H_2O and CO_2)	14.36
Tar	33.99
Char	36.7

A Py-IR study of kraft lignin pyrolysis in a temperature gradient (FT-IR-EGA study) [4] showed the formation of different compounds evolving at certain temperature ranges as indicated in Figure 9.1.1.

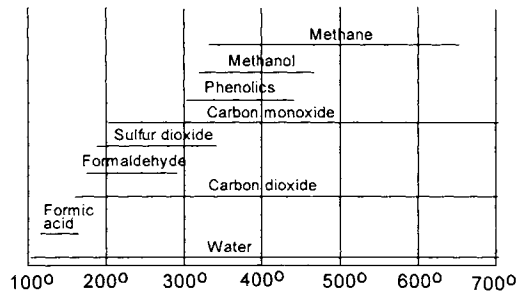


FIGURE 9.1.1. Evolution of gases from kraft lignin at different temperatures during linear gradient heating [4].

The gas evolution as monitored using FT-IR [4] generates curves similar to the one given in Figure 9.1.2, showing methanol evolution as a function of temperature.

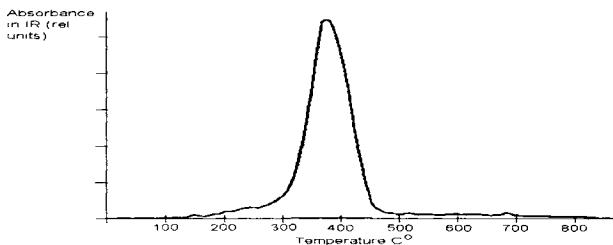


FIGURE 9.1.2. Methanol evolution as a function of temperature during kraft lignin pyrolysis [4].

The relative composition (% wt.) of gases (excluding H_2O and CO_2) generated by pyrolysis at $650^\circ C$ of kraft lignin is shown in Table 9.1.3.

TABLE 9.1.3. The relative composition (% wt.) of gases (excluding H_2O and CO_2) generated by pyrolysis at $650^\circ C$ of kraft lignin.

Compound	% Yield wt.
CO	40.88
CH ₄	30.92
C ₂ H ₄	7.52
CH ₃ OH	5.18
C ₆ H ₆	3.67
CH ₃ COOH	2.82
C ₂ H ₆	2.61
Other gases	2.00
C ₄ hydrocarbons	1.53
C ₃ H ₆	1.06
CH ₃ CHO	0.99
C ₃ H ₈	0.82

Numerous analyses of the tar generated during lignin pyrolysis were reported [6–8]. In one study [6] pyrolysis was used to determine the predominance of H, G, or S units in

lignin. Table 9.1.4 shows selected m/z values and the corresponding compounds indicating a certain unit (H, G, or S).

TABLE 9.1.4. Selected m/z values and the corresponding compounds indicating an H, G or S unit.

H		G		S	
m/z	compound	m/z	compound	m/z	compound
94	phenol	124	guaiacol	154	syringol
107	alkylphenols	135	vinylguaiacol	165	vinylsyringol
108	methylphenol	137	ethylguaiacol, homovanillin, coniferyl alcohol	167	ethylsyringol, syringylacetone, homosyringaldehyde
120	vinylphenol	138	methylguaiacol	168	methylsyringol
121	alkylphenols	151	vanillin, acetoguaiacone, propioguaiacone	181	syringaldehyde, acetosyringone, propiosyringone
134	propenylphenols	164	allyl and propenylguaiacol	194	allyl and propylsyringol
148	cumarylaldehyde	178	coniferylaldehyde	208	sinapinaldehyde

Some results regarding the content of H, G, and S in different lignins and wood samples obtained using Py-GC [6] are shown in Figure 9.1.3. The same figure shows for comparison the results obtained using a common chemical method (oxidation with nitrobenzene) and FTIR.

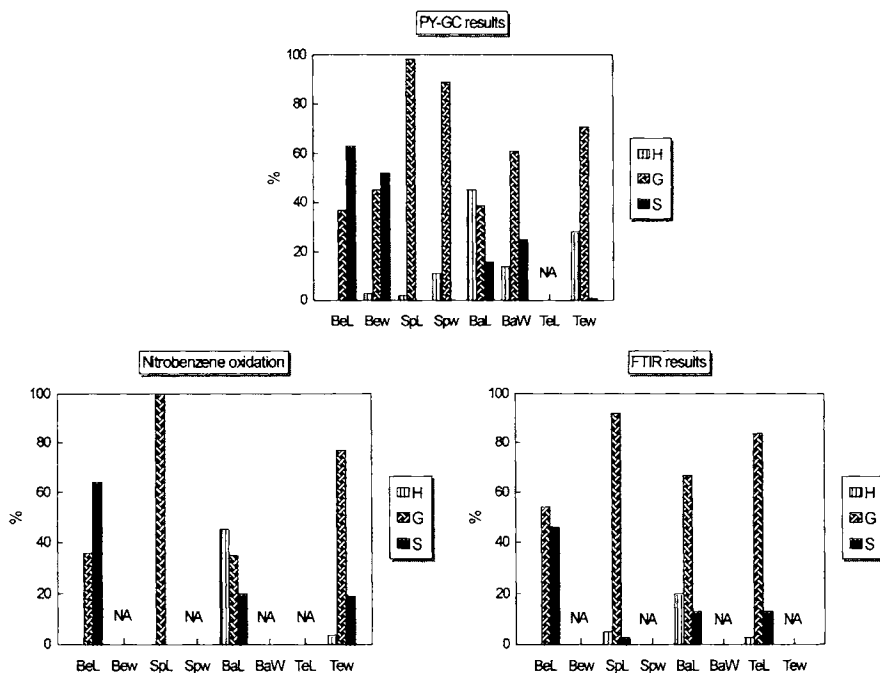


FIGURE 9.1.3. The content of H, G and S in different lignins and wood samples obtained using Py-GC, nitrobenzene oxidation, and FTIR. The samples are Bel= Beech MW lignin, Bew= Beech wood, SpL= Spruce MW lignin, Spw= Spruce wood, BaL= Bamboo MW lignin, BaW= Bamboo wood, TeL= Teak HCl lignin, Tew= Teak wood. (NA = not analyzed).

A series of compounds identified in several lignin pyrolysates at 510° C are given in Table 9.1.5 [6a]. The analyzed materials were cottonwood (*Populus deltoides*) milled wood lignin (MLW) from which the polysaccharide fraction was removed enzymatically, a steam exploded lignin from yellow poplar (*Liriodendron tulipifera*) extracted with NaOH and reprecipitated (StE.), a lignin purified by organosolv procedure (Org.) from mixed hardwoods, kraft lignin (Kraft) which was purified of inorganic salts, and a bagasse lignin (Bag.) obtained from steam treated material followed by NaOH extraction and precipitation [6a].

TABLE 9.1.5. *Pyrolysis products at 510° C of several lignins [6a].* The analyzed materials were milled wood lignin (MLW), steam exploded lignin (StE.), a lignin purified by organosolv procedure (Org.), kraft lignin (Kraft), and bagasse lignin (Bag.).

MW	Compound	Main ions (EI 70 eV) (with relative intensity)	Type of lignin
94	phenol	94 (100), 66 (35), 65 (30)	MWL, Kraft, Bag.
108	2-(or 3-)methylphenol	108 (100), 107 (88), 79 (37)	Kraft, Bag.
124	guaiacol	109 (100), 124 (90), 81 (69), 53 (25)	MWL, StE., Org., Kraft, Bag.
108	4-methylphenol	107 (100), 108 (86)	Kraft, Bag.
122	dimethylphenol	122 (100), 107 (83), 121 (47)	Kraft, Bag.
122	C2-alkylphenol	107 (100), 122 (47), 121 (44)	Kraft
138	methylguaiacol	123 (100), 138 (80), 77 (24)	MWL, StE., Org., Kraft
122	4-ethylphenol	107 (100), 122 (34), 77 (19)	Bag.
138	methylguaiacol	132 (100), 138 (78), 95 (25)	MWL, StE., Org., Kraft, Bag.
138	4-methylguaiacol	138 (100), 123 (97), 95 (36), 77 (26)	MWL, StE., Org., Kraft, Bag.
120	4-vinylphenol	120 (100), 91 (46), 119 (26)	MWL, Kraft, Bag.
136	trimethylphenol	121 (100), 136 (37)	Kraft, Bag.
152	4-ethylguaiacol	137 (100), 152 (49)	MWL, StE., Org., Kraft, Bag.
150	4-vinylguaiacol	150 (100), 135 (87), 77(43)	MWL, StE., Org., Kraft, Bag.
138	1,3-dimethoxybenzene	138 (100), 107 (40), 109 (34)	MWL, StE., Org., Kraft
154	syringol	154 (100), 139 (57), 96 (33)	MWL, StE., Org., Bag.
164	4-(prop-1-enyl)guaiacol	164 (100), 77 (39), 149 (35), 103 (33)	MWL, StE., Org., Kraft, Bag.
166	4-propylguaiacol	137 (100), 166 (23)	MWL, StE., Org., Kraft, Bag.
152	4-formylguaiacol	151 (100), 152 (97), 81 (31)	MWL, StE., Org., Kraft, Bag.
164	cis-4-(prop-2-enyl)guaiacol	164 (100), 77 (35), 149 (31), 103 (29)	MWL, StE., Org., Kraft
168	4-methylsyringol	168 (100), 153 (56), 125 (36), 53 (25)	MWL, StE., Org., Bag.
166	4-ethanalguaiacol	137 (100), 166 (26)	MWL, Kraft
164	trans-4-(prop-2-enyl)guaiacol	164 (100), 137 (53), 77 (45), 149 (41)	MWL, StE., Org., Kraft, Bag.
162	guaiacol (G-C ₃ H ₃) derivative	162 (100), 147 (97), 91 (47)	MWL, StE., Org., Kraft, Bag.
166	4-acetylguaiacol	151 (100), 166 (46), 123 (23)	MWL, StE., Org., Kraft, Bag.
182	4-carboxylguaiacol methylester	151 (100), 182 (47), 123 (16)	MWL, StE.
180	4-(propane-2-one)guaiacol	137 (100), 180 (35), 122 (17)	Kraft
182	4-ethylsyringol	167 (100), 182 (54), 137 (18)	MWL, StE., Org., Bag.
180	4-vinylsyringol	180 (100), 165 (50), 137 (40), 77 (26)	MWL, StE., Org., Bag.
178	4-(prop-1-en-3-one)guaiacol	151 (100), 178 (41), 123(20)	MWL, StE., Org.
138	3-hydroxybenzoic acid	121 (100), 138 (77), 93(26)	MWL, Kraft
194	4-(prop-1-enyl)syringol	194 (100), 91 (39), 119 (27)	Org., MWL, StE., Bag.
196	4-propylsyringol	167 (100), 196 (28)	Org., MWL, StE., Bag.
182	4-formylsyringol	182 (100), 181 (77), 111 (24)	Org., StE., Bag.
174	3-methoxy-2-naphthalenol	174 (100), 131 (82), 159 (29), 77 (23)	Kraft

TABLE 9.1.5. *Pyrolysis products at 510° C of several lignins [6a] (continued)*. The analyzed materials were milled wood lignin (MLW), steam exploded lignin (StE.), a lignin purified by organosolv procedure (Org.), kraft lignin (Kraft), and bagasse lignin (Bag.).

MW	Compound	Main ions (EI 70 eV) (with relative intensity)	Type of lignin
182	4-(methylcarboxyl)guaiacol	137 (100), 182 (37), 138 (33), 122 (12)	Kraft
192	syringol (S-C ₃ H ₃) derivative	192 (100), 131 (35), 177 (33)	MWL, StE., Org., Bag.
150	cis-coniferyl alcohol	137 (100), 124 (57), 180 (51), 91 (44)	MWL, StE.
194	cis 4-(prop-2-enyl)syringol	194 (100), 91 (36), 119 (22), 77 (21)	MWL, StE., Org., Bag.
196	4-ethanal syringol	167 (100), 196 (34)	MWL, StE.
194	trans-4-(prop-2-enyl)syringol	194 (100), 91 (47), 77 (31), 179 (27)	MWL, StE., Org., Bag.
196	4-acetylsyringol	181 (100), 196 (58), 43 (32)	MWL, StE., Org., Bag.
178	4-(prop-2-enal)guaiacol	178 (100), 135 (43), 147 (42), 107 (41)	MWL, StE., Org., Kraft, Bag.
180	trans-coniferyl alcohol	137 (100), 180 (57), 124 (56), 91 (39)	MWL, StE., Org., Kraft
210	4-(propane-2-one)syringol	167 (100), 210 (26)	MWL, StE., Org., Bag.
210	4-propanalsyringol	167 (100), 210 (33), 182 (31), 154 (22)	MWL, StE., Org.
210	4-(propyl-3-one)syringol	181 (100), 210 (19)	MWL, StE., Org., Bag.
208	4-(prop-1-en-3-one)syringol	208 (100), 55 (49), 181 (43), 165 (21)	MWL, StE., Org.
164	p-coumaric acid	164 (100), 147 (40), 119 (25)	Bag.
194	ferulic acid	194 (100), 179 (18), 133 (15)	Bag.
212	4-(1-hydroxypropyl)syringol	168 (100), 67 (93), 212 (61)	MWL, StE., Org.
210	cis-sinapyl alcohol	167 (100), 210 (93), 77 (42), 154 (41)	MWL, StE.
208	4-(prop-2-enal)syringol	208 (100), 165 (53), 137 (44), 77 (33)	MWL, StE., Org.
210	trans-sinapyl alcohol	167 (100), 210 (95), 154 (41), 77 (40)	MWL, StE., Org.
272	α,β -diguaiacyl ethene	272 (100)	MWL, StE., Org., Kraft, Bag.
302	guaiacyl, syringylethene	302 (100)	MWL, StE., Org., Bag.

The results obtained with different pyrolysis techniques (Py-GC/MS with EI ionization, temperature-resolved in-source Py-MS with low EI potential and ammonia CI [6]), showed that enzyme-treated cottonwood milled-wood lignin is a relatively homogeneous polymer with a large fraction of preserved alkyl-aryl ether linkages. Technical lignins, StE., Org., and Kraft, were found to be modified depending on the severity of the isolation procedure, and they contained large amounts of β -1-linked stilbene and β - β -linked resinol type structures. Bagasse lignin shows the most condensed polymer structure with a large proportion of ether-bonded p-coumaric acid and ferulic acid. These findings are summarized in Table 9.1.6, which shows the content of coniferyl alcohol and sinapyl alcohol (4-hydroxy-3,4-dimethoxycinnamyl alcohol) in % estimated by Py-GC/MS in different lignins [6].

Techniques such as Py-MS or Py-GC/MS are not always suitable for the identification of less volatile or highly polar compounds. HPLC analysis with MS detection provides a better tool in such cases, and it was successfully applied for lignin pyrolysate analysis (see Section 5.7). Pyrolysis products from a lignin sample from mixed hardwood, obtained using the organosolv procedure with ethanol/water and generated at 510° C in an on-line Curie point pyrolyser and analyzed by HPLC [8], indicated the presence of a series of compounds shown in Table 9.1.7.

TABLE 9.1.6. *The content of coniferyl alcohol and sinapyl alcohol in %, estimated in different lignins.*

Lignin	Coniferyl alcohol %	Sinapyl alcohol %
MWL	9.7	13.5
StE.	2.6	8.1
Org.	1.5	3.8
Kraft	4.9	-
Bagasse	0.8	1.1

TABLE 9.1.7. *Pyrolysis products from lignin from mixed hardwood generated at 510° C in an on-line Curie point pyrolyser and analyzed by HPLC.*

MW	Compound
212	4-(1-hydroxypropyl)syringol
182	4-formylsyringol
196	4-acetylsyringol
154	syringol
180	trans-coniferyl alcohol
210	trans-sinapyl alcohol
208	4 (prop-1-en-3-one)syringol
212	vanillic acid methyl ester
168	4-methylsyringol
418	syringaresinol
418	episyringaresinol
320	1,1-(disyringyl)methane
290	1,1-(guaiacyl, syringyl)methane
180	4-vinylsyringol
260	1,1-(diguaiacyl)methane
182	4-ethylsyringol
356	dihydroconiferyl alcohol
332	3,3',4,4'-tetramethoxy-4,4'-dihydroxystilbene (<i>trans</i>)
332	3,3',4,4'-tetramethoxy-4,4'-dihydroxystilbene (<i>cis</i>)
194	4-(prop-2-enyl)syringol (<i>cis</i>)
302	3,3',4-trimethoxy-4,4'-dihydroxystilbene (<i>trans</i>)
388	medioresinol
194	4-(prop-2-enyl)syringol (<i>trans</i>)
302	3,3',4-trimethoxy-4,4'-dihydroxystilbene (<i>cis</i>)
272	3,3'-dimethoxy-4,4'-dihydroxystilbene (<i>trans</i>)
164	4-(prop-2-enyl)guaiacol (<i>cis</i>)
272	3,3'-dimethoxy-4,4'-dihydroxystilbene (<i>cis</i>)
164	4-(prop-2-enyl)guaiacol (<i>trans</i>)
196	4-(propane)syringol
396	dihydro-dehydro-coniferylaldehyde-sinapylaldehyde isomer
386	dihydro-dehydro-coniferylaldehyde-sinapylaldehyde isomer
386	dihydro-dehydro-coniferylaldehyde-sinapylaldehyde isomer
356	dihydro-dehydro-diconiferylaldehyde isomer
386	dihydro-dehydro-coniferylaldehyde-sinapylaldehyde isomer
356	dihydro-dehydro-diconiferylaldehyde isomer
356	dihydro-dehydro-diconiferylaldehyde isomer

The results from Table 9.1.7 show the presence of several oligomers that provide useful information on lignin structure. In fact, a comparison of pyrolysis results with nitrobenzene oxidation of lignin (used for the determination of lignin structure) showed that pyrolysis is more informative [9] than the oxidation procedure. Based on pyrolysis studies [5] more progress was made in understanding the lignin structure and how to evaluate its purity and modifications due to preparation procedure. It was concluded for example that sulfuric acid lignin contains proteins, and the chlorite procedure used to remove lignin from carbohydrate materials does not remove all the lignin.

Numerous other results regarding lignin pyrolysis were reported, such those for lignin from wheat straw [10], barley straw [11], rice [11a], biodegraded lignin [12], olive stones [12a], or from several types of wood. Also a variety of techniques were utilized, mainly Py-GC/MS but also special Py-MS with photoionization mass spectra [13], NMR [13a], HPLC, etc. One successful approach in lignin pyrolysis study was the pyrolysis in the presence of tetramethylammonium hydroxide (TMAH) or tetrabutylammonium hydroxide (TBAH) [13b]. The use of a methylating (or butylating) agent allowed a better chromatographic separation of the many polar compounds found in lignin pyrolysate and the identification of several carboxylic acids not detected previously in lignin pyrolysis. The presence of 3-(4-hydroxyphenyl)-2-propenoic acid (*p*-coumaric acid), 3-(3-methoxy-4-hydroxyphenyl)-2-propenoic acid (ferulic acid), and 3-(3,5-dimethoxy-4-hydroxyphenyl)-2-propenoic acid (sinapic acid) can be easily inferred from their methylated derivatives. In the absence of a methylating agent, these acids may suffer further pyrolysis, although their presence has been reported in some pyrolysis studies of lignin [13c]. During pyrolysis, intermediate products such as *p*-coumaric acid, ferulic acid and sinapic acid are decarboxylated, generating products as shown in Table 9.1.8. During pyrolysis in the presence of TMAH, the corresponding methyl esters are seen in the pyrolysates.

TABLE 9.1.8. *Pyrolysis products of p-coumaric, ferulic and sinapic acid with and without methylation.*

Intermediate	Main pyrolysate	Pyrolysis / methylation
<i>p</i> -coumaric acid	4-vinyl phenol	3-(4-methoxyphenyl)-2-propenoic acid methyl ester
ferulic acid	4-vinyl-2-methoxyphenol	3-(3,4-dimethoxyphenyl)-2-propenoic acid methyl ester
sinapic acid	4-vinyl-2,6-dimethoxyphenol	3-(3,4,5-trimethoxyphenyl)-2-propenoic acid methyl ester

Three milled wood lignins, from bamboo (*Bambusa spec.*), pine (*Pinus pinea*) and beech (*Fagus silvatica*) were analyzed using Py-GC/MS with pyrolysis done at 500° C for 10 sec. in a filament pyrolyser in the presence of TMAH [13b]. The separation was done on a 30 m 0.25 mm i.d. DB-FFAP column with a temperature gradient for the GC between 40 to 250° C. The analysis was done using a mass spectrometer operated in standard conditions (70 eV). Significant differences were seen in the chromatographic profiles of the three lignins, and the results on peak identifications are given in Table 9.1.9.

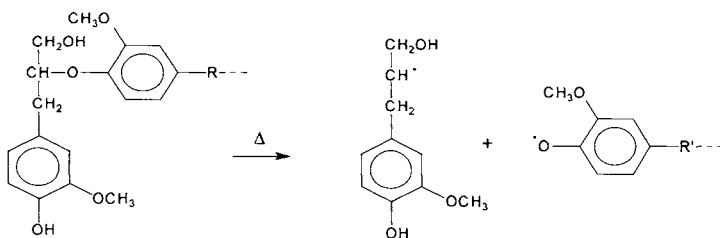
TABLE 9.1.9. *Compounds identified in the pyrogram performed in the presence of TMAH at 500° C [13b] for three milled wood lignins: bamboo, pine, and beech.*

Compound	Bamboo	Pine	Beech
1,2-dimethoxybenzene	-	+	-
3,4-dimethoxytoluene	-	+	-
1-(3,4-dimethoxyphenyl)ethanone	-	+	-
1,2,3-trimethoxybenzene	+	-	+
4-methoxybenzaldehyde	+	+	-
4-ethenyl-1,2-dimethoxybenzene	-	++	+
1-methyl-3,4,5-trimethoxybenzene	-	-	+
4-methoxybenzoic acid methyl ester	+	+	-
1-ethenyl-4-methoxybenzene	+	-	-
1-(3,4,5-trimethoxyphenyl)ethanone	-	-	+
3,4-dimethoxybenzenemethanol methyl ether	-	++	-
1-vinyl-3,4,5-trimethoxybenzene	-	-	++
benzenedicarboxylic acid dimethyl ester	-	-	+
benzenedicarboxylic acid dimethyl ester isomer	+	+	+
3,4-dimethoxybenzeneacetic acid methyl ester	-	++	-
1-(3,4,5-trimethoxy)benzenemethanol methyl ether	-	-	+
3,4-dimethoxybenzaldehyde	++	++	++
3-(4-methoxyphenyl)-2-propenoic acid methyl ester isomer	++	-	-
3,4-dimethoxybenzoic acid methyl ester	++	++	++
1-propenyl-3,4,5-trimethoxybenzene	-	+	+
1-(3,4-dimethoxyphenyl)propanone	-	+++	++
1-(3,4-dimethoxyphenyl)propanone isomer	-	+++	+
3,4,5-trimethoxybenzaldehyde	++	-	+++
1-(3,4-dimethoxyphenyl)glycerol trimethyl ether	-	+++	++
3-(4-methoxyphenyl)-2-propenoic acid methyl ester	+++	-	-
1-(3,4-dimethoxyphenyl)glycerol trimethyl ether isomer	-	+++	-
3,4,5-trimethoxybenzoic acid methyl ester	+++	-	+++
3-(3,4-dimethoxyphenyl)-2-propenol methyl ether	-	+	+
1-(3,4,5-trimethoxyphenyl)ethanone	+	-	+
3-(3,4,5-trimethoxyphenyl)-2-propenol methyl ether	-	-	+
1-(3,4,5-trimethoxyphenyl)propionaldehyde	-	-	+
3-(3,4,5-trimethoxyphenyl)-2-propenol methyl ether isomer	-	-	++
3-(3,4,5-trimethoxyphenyl)glycerol dimethyl ether	-	-	+++
3-(3,4,5-trimethoxyphenyl)propanone	-	-	+++
3-(3,45-trimethoxyphenyl)glycerol dimethyl ether isomer	++	-	++
3-(3,4-dimethoxyphenyl)-2-propenoic acid methyl ester	+	-	+++
3-(3,4,5-trimethoxyphenyl)-2-propenol methyl ether isomer	-	-	++
2,3,4,5-tetramethoxyphenyl acetic acid methyl ester	++	-	-
3-(3,4-dimethoxyphenyl)propanoic acid methyl ester	+	-	++
3-(3,4-dimethoxyphenyl)-2-propenoic acid methyl ester isomer	++	+	-
3-(3,4,5-trimethoxyphenyl)propanoic acid methyl ester	+	-	+
4,4'-dimethoxydimethylstilbene	-	-	++
3-(3,4,5-trimethoxy)benzenepropanol methyl ether	-	-	+
3-(3,4,5-trimethoxyphenyl)-2-propenoic acid methyl ester	+	-	++

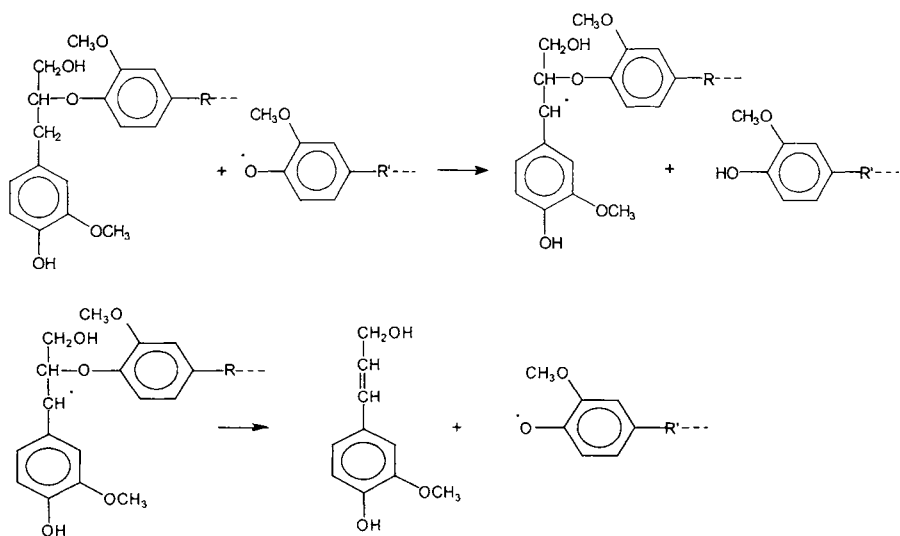
(-) not found; (+), (+ +), (+ + +) low, medium, high peaks respectively.

- Mechanisms in the formation of small molecules in lignin pyrolysis.

There are two proposed main mechanisms for lignin pyrolysis [6]. A free radical mechanism and a 6-center retro-ene reaction. The free radical mechanism probably starts with the following initiation reaction:

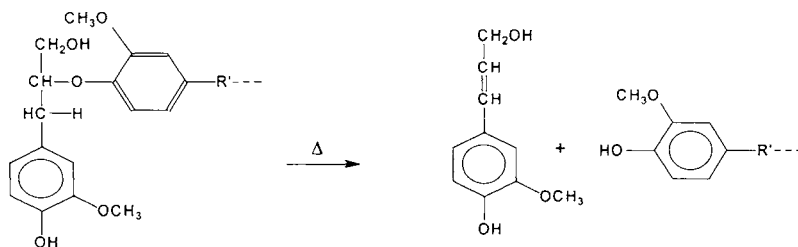


This process can be propagated and generates coniferyl alcohol with the following reaction:

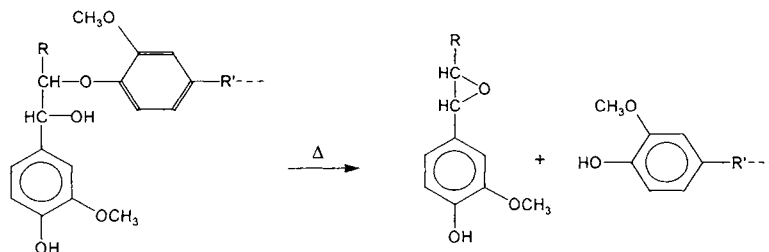


Other propagation reactions are also possible. Also, several termination reactions can be expected, generating guaiacol (2-methoxyphenol) or other related compounds.

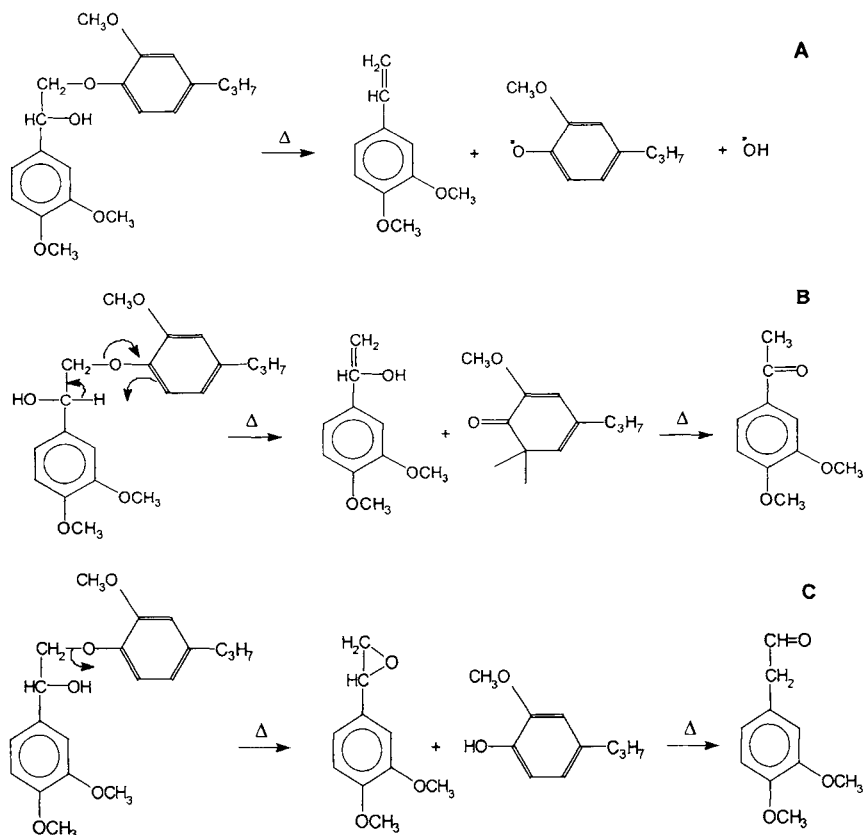
The second proposed main mechanism for the thermal degradation and formation of coniferyl alcohol is a 6-center retro-ene reaction (as indicated in Section 2.5):



Besides these two mechanisms, a third one, involving an oxirane intermediate was also proposed [14a].

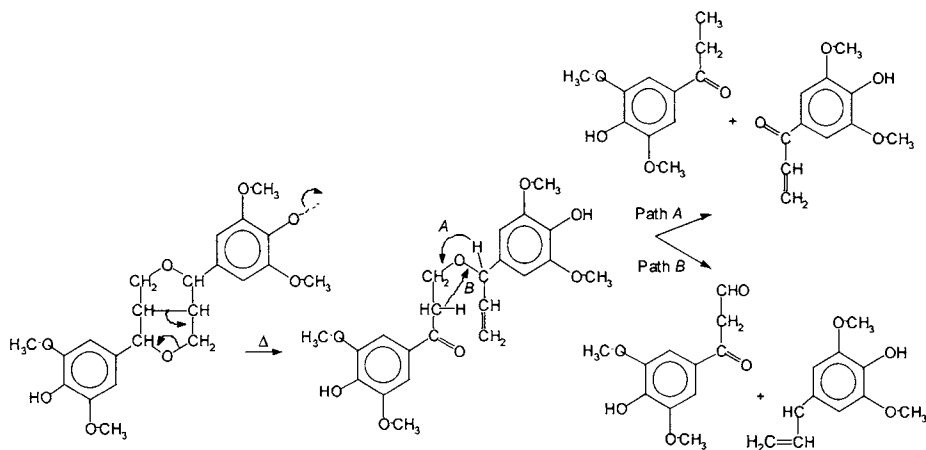


A study done on a model compound, 1-(3,4-dimethoxyphenyl)-2-(2-propylphenoxy)-1-ethanol, attempted to elucidate which mechanism is prevalent in lignin pyrolysis [14b]. The pyrolysis results of this model compound are expected to be different by the three mechanisms: the free radical one generating dimethoxyvinylbenzene (scheme A), the retro-ene mechanism generating dimethoxyacetophenone (scheme B), and the oxirane-forming mechanism generating dimethoxyphenylacetaldehyde (scheme C).



It was shown that the conventional pyrolysis of the model compound generated a mixture of compounds suggesting that the importance of the mechanisms is $A > B \gg C$. However, lignin provides a different matrix due to the "cage effect" of a large molecule. A simulation for this different matrix was the pyrolysis of the model compound in a tight sandwich with glass fiber. In these different conditions, from the yield of pyrolysis products it was concluded that the importance of the mechanisms in lignin pyrolysis can be $B > A > C$.

Other proposed mechanisms explain the formation of products from resinol type groups:



- Pyrolysis of lignin in the presence of acids, bases, or salts.

Unlike pyrolysis of carbohydrates, lignin pyrolysis is not significantly influenced by the addition of strong bases such as KOH [14]. However, the distribution of the yields of different pyrolysis products is influenced by the presence of acids. Also, the addition of salts such as $ZnCl_2$ decreased the abundance of coniferyl alcohol and increased the abundance of guaiacol and carbonyl containing compounds such as coniferyl aldehyde, homovanillin, etc. The acids (and Lewis acids) probably catalyze the dehydrogenation of the primary alcohol on the γ -carbon of the propylbenzene structure. Other studies of lignin pyrolysis in the presence of inorganic materials are also available [15,15a].

- Kinetics of lignin pyrolysis.

Kinetics of lignin pyrolysis has important practical applications, as lignin is a common by-product of paper and cellulose manufacturing. In fact, the "black liquor" generated by the kraft procedure to eliminate lignin from wood can be burned as an alternative to waste disposal. Lignin pyrolysis is a slightly endothermic process and has the characteristic that the sample weight decreases during pyrolysis to a lower limit, which depends on the heating temperature (T_{eq}), regardless how long the heating continues [16]. This residual weight W_∞ is shown for three temperatures in Figure 9.1.4.

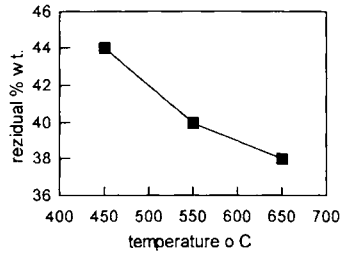


FIGURE 9.1.4. *Residual final weight of a kraft lignin sample at long pyrolysis time as a function of T_{eq} .*

A model for lignin thermal decomposition was developed assuming that the biomass is formed from a large number of fractions, each fraction starting to decompose at a characteristic temperature T_R [16,17] and not decomposing at a lower temperature. To determine the fraction of lignin that begins to decompose at a given temperature, a distribution function $C(T_R)$ was proposed [16]. The graph of $C(T_R)$ as a function of T_R is shown in Figure 9.1.5.

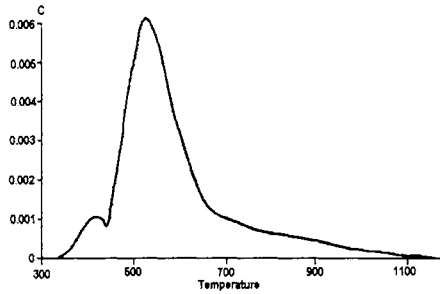


FIGURE 9.1.5. *The graph of $C(T_R)$ as a function of T_R .*

The kinetic equation for lignin decomposition can be established in this case only for small temperature intervals ΔT_R . For such an interval $(\Delta T_R)_i$, the following relation can be written:

$$\frac{dw_i}{dt} = -k(T_R) \exp \left[-\frac{E(T_R)}{RT} \right] (w_i - s) C_i \Delta T_R \quad (1)$$

where w_i is the lignin fraction weight, s is the yield of char at time infinity and highest temperature of operation, and $k(T_R)$ and $E(T_R)$ are kinetic parameters obtained to fit the experimental data. For kraft lignin heated at maximum 900° C, the following parameters were obtained [16]: $s = 0.368$, $\ln k(T_R) = 14.77 + 0.0208 (T_R - 273) \text{ sec}^{-1}$, and $E(T_R) = 52.64 + 0.173(T_R - 273) \text{ kJ mol}^{-1}$. Equation (1) was integrated using a numerical algorithm.

9.2. Lignocellulosic Materials.

As indicated previously (see Section 9.1), all the procedures used to obtain lignin are a compromise between being representative for the whole lignin in a specific type of wood, not being mixed with other wood components, and not being chemically modified. It was not possible to obtain a lignin that combines all the above attributes, probably due to its insolubility and sensitivity to reagents. Rather frequently lignin is obtained with some degree of impurities. These impurities are commonly of three types:

- cellulosic materials;
- proteinaceous materials; and
- small molecules from the plant cells.

Several pyrolysis studies were done on "lignin preparations" where a certain procedure for obtaining the lignin is selected and then the obtained material is evaluated. Pyrolysis techniques were proven to be a very efficient means for this type of characterization. As an example, several lignins were obtained from flue-cured and burley tobaccos (*Nicotiana tabacum*) and analyzed by Py-GC/MS [18,19] or Py-MS [19]. The results for the pyrolysis of Klason lignin from the flue-cured and burley lamina are shown in Table 9.2.1. The lignins were prepared by extracting the lamina with 80% ethanol/water followed by treatment with amylase and then elimination of the cellulosic material using 72% H₂SO₄.

TABLE 9.2.1. *Py-GC/MS identifications in two Klason lignins from flue-cured and burley lamina of Nicotiana tabacum.*

MW	Compound name	flue-cured	burley
27	hydrogen cyanide	x	x
64	sulfur dioxide	x	x
46	ethanol	x	
48	methanethiol	x	x
56	prop-2-enal	x	x
41	acetonitrile	x	
58	propanone	x	x
68	furan	x	x
68	2-methylbuta-1,3-diene	x	x
142	methyl iodide		x
62	dimethylsulphide		x
70	2-methylbut-2-ene	x	
66	cyclopentadiene	x	x
72	2-methylpropanal	x	x
86	buta-2,3-dione	x	x
46	formic acid		
72	butan-2-one	x	x
82	2-methylfuran	x	x
70	2,5-dihydrofuran	x	
86	3-methylbutanal	x	x
86	2-methylbutanal	x	x
78	benzene	x	x
85	1-methyl-tetrahydropyrrole	x	x
84	2-methyl-but-1-en-3-one	x	
60	acetic acid	x	x
74	hydroxypropanone	x	
100	penta-2,3-dione	x	

TABLE 9.2.1. *Py-GC/MS identifications in two Klason lignins from flue-cured and burley lamina of Nicotiana tabacum (continued).*

MW	Compound name	flue-cured	burley
62	glycol	x	
96	2,5-dimethylfuran	x	
94	2-vinylfuran	x	x
81	1-methylpyrrole	x	x
79	pyridine	x	x
67	(1H)-pyrrole	x	
92	toluene	x	x
102	pyruvic acid methyl ester	x	
84	(2H)-furan-3-one	x	
96	3-furaldehyde	x	
95	1-ethylpyrrole	x	x
93	2- (or 4-)methylpyridine		x
82	penta-2,4-dienal	x	x
94	aminopyridine	x	x
96	2-furaldehyde	x	x
81	2- or 3-methylpyrrole	x	x
108	benzylalcohol	x	x
93	2- or 4-methylpyridine		x
81	2- or 3-methylpyrrole	x	x
116	1-acetyloxypropan-2-one	x	x
98	2-hydroxymethylfuran	x	
93	3-methylpyridine	x	x
96	cyclopent-1-en-3,4-dione	x	
106	ethylbenzene	x	x
106	dimethylbenzene		x
86	dihydro-(3H)-furan-2-one		
84	(5H)-furan-2-one	x	x
104	vinylbenzene	x	x
110	2-acetylfuran	x	
70	N-cyano-N-methyl-methylamine		x
106	1,2-dimethylbenzene		x
95	2,4- (or 2,5-)dimethylpyrrole		x
99	2,3-dihydro-5-methylfuran-2-one	x	
130	4-hydroxymethyltetrahydropyran-3-one	x	
106	benzaldehyde	x	
130	2,3-dihydroxyhex-1-en-4-one	x	
110	5-methyl-2-furaldehyde	x	
107	dimethylpyridine or 3-ethylpyridine		x
105	3-vinylpyridine	x	x
94	phenol	x	x
114	4-hydroxy-5,6-dihydro-(2H)-pyran-2-one	x	
109	3-methoxypyridine		x
112	3-hydroxy-2-methylcyclopent-2-en-1-one	x	x
98	2,3-dihydropyran-4-one	x	
112	2-hydroxy-3-methylcyclopent-2-en-1-one	x	x
120	2-benzylethanal	x	
107	2-ethylpyridine		x
85	tetrahydropyrrol-2-one	x	x
120	acetylbenzene	x	x
108	4-methylphenol	x	x
124	2-methoxyphenol	x	x
126	3-hydroxy-6-methyl-(2H)-pyran-2-one	x	
121	3-acetylpyridine	x	x
95	pyridin-3-one	x	x

TABLE 9.2.1. *Py-GC/MS identifications in two Klason lignins from flue-cured and burley lamina of Nicotiana tabacum (continued).*

MW	Compound name	flue-cured	burley
126	3-hydroxy-2-methyl-(4H)-pyran-4-one	x	
117	benzylcyanide	x	
142	3,5-dihydroxy-2-methyl-(4H)-pyran-4-one	x	
122	4-ethylphenol		x
122	benzoic acid		x
139	4-methyl-2-methoxyphenol	x	x
144	1,4:3,6-dianhydro- α -D-glucose	x	
110	1,2-dihydroxybenzene	x	x
120	4-vinylphenol	x	x
136	phenylacetic acid	x	
181	2,4-di-(2-methyl)ethyl-3,4-dihydropyrrole-3,5-dione	x	x
110	1,3-(or 1,4-)dihydroxybenzene		x
181	3-(2-methyl)ethylidene-5-(2-methyl)ethyl-pyrrolidine-2,4-dione	x	x
140	4-hydroxy-2-methoxyphenol	x	x
172	n-nonanoic acid	x	
152	4-ethyl-2-methoxyphenol		x
117	indole	x	x
124	methyl-dihydroxybenzene		x
144	2-hydroxymethyl-5-hydroxy-2,3-dihydro-(4H)-pyran-4-one	x	
150	4-vinyl-2-methoxyphenol	x	x
195	4-(3-methyl)propyl-2-(2-methyl)ethyl-3,4-dihydro-(2H)-pyrrole-3,5-dione	x	x
195	2-(3-methyl)propyl-4-(2-methyl)ethyl-3,4-dihydro-(2H)-pyrrole-3,5-dione	x	x
195	3-(2-methyl)propylidene-5-(2-methyl)propylpyrrolidine-2,4-dione	x	x
154	2,6-dimethoxyphenol	x	x
195	3-(3-methyl)propylidene-5-(2-methyl)ethylpyrrolidine-2,4-dione	x	x
195	3-(2-methyl)propylidene-5-(2-methyl)ethylpyrrolidine-2,4-dione	x	x
164	4-(prop-1-enyl)-2-methoxyphenol	x	x
195	5-(3-methyl)propyl-3-(2-methyl)ethylidene-pyrrolidine-2,4-dione	x	x
162	nicotine	x	x
195	2-(2-methyl)propyl-4-(2-methyl)ethyl-3,4-dihydro-(2H)-pyrrole-3,5-dione	x	x
166	4-propyl-2-methoxyphenol	x	x
195	5-(2-methyl)propyl-3-(2-methyl)ethylidene-pyrrolidine-2,4-dione	x	x
164	4-(prop-2-enyl)-2-methoxy-phenol (cis)	x	x
146	myosmine	x	x
209	2,4-di-(3-methyl)propyl-3,4-dihydro-(2H)-pyrrole-3,5-dione	x	x
209	2-(3-methyl)propyl-4-(2-methyl)propyl-3,4-dihydro-(2H)-pyrrole-3,5-dione	x	x
168	4-methyl-2,6-dimethoxy-phenol	x	x
209	2-(3-methyl)propyl-2-(2-methyl)ethylidene-pyrrolidine-3,5-dione	x	x
209	2-(2-methyl)propyl-4-(3-methyl)propyl-3,4-dihydro-(2H)-pyrrole-3,5-dione	x	x
209	3-(2-methyl)propyl-5-(3-methyl)propyl-pyrrolidine-2,4-dione	x	x
164	4-(prop-2-enyl)-2-methoxy-phenol (trans)	x	x
160	methylmyosmine		x
155	4-phenylpyridine		x
209	2,4-di-(2-methyl)propyl-3,4-dihydro-(2H)-pyrrole-3,5-dione	x	x
209	3-(3-methyl)propylidene-5-(2-methyl)propylpyrrolidine-2,4-dione	x	x
209	3-(2-methyl)propylidene-5-(2-methyl)propylpyrrolidine-2,4-dione	x	x
158	5-phenyl-3-methylpyrazole	x	x
166	4-acetyl-2-methoxyphenol	x	x
162	1,6-anhydro- β -D-glucopyranose	x	
180	4-(propan-2-one)-2-methoxyphenol		x
182	4-ethyl-2,6-dimethoxyphenol		x
172	6,8-dimethylnaphthol		x

TABLE 9.2.1. *Py-GC/MS identifications in two Klason lignins from flue-cured and burley lamina of Nicotiana tabacum (continued).*

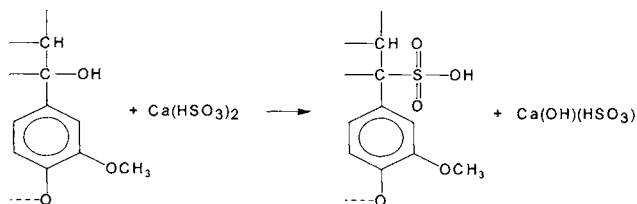
MW	Compound name	flue-cured	burley
156	3,3'-bipyridyl	x	x
162	levoglucofuranosan	x	
180	4-vinyl-2,6-dimethoxy-phenol		x
200	n-dodecanoic acid		x
210	4-propanal-2-methoxy-phenol		x
172	7,8-dimethylnaphthol		x
194	4-(prop-1-enyl)-2,6-dimethoxyphenol	x	x
170	biphenyl-2-ol or -4-ol		x
194	4-(prop-2-enyl)-2,6-dimethoxyphenol (cis)		x
196	2-acetyl-1-naphthol		x
194	4-(prop-2-enyl)-2,6-dimethoxyphenol (trans)	x	x
176	1-methyl-5-(3-pyridinyl)-tetrahydropyrrol-2-one	x	
186	biphenyl	x	
196	4-acetyl-2,6-dimethoxy-phenol	x	x
226	prist-1-ene	x	x
228	n-tetradecanoic acid	x	x
210	4-(propan-2-one)-2,6-dimethoxyphenol	x	
208	methylferulate		x
278	neophytadiene		x
-	5-substituted tetrahydropyrrole-3,6-piperazinedione	x	x
-	5-substituted tetrahydropyrrole-3,6-piperazinedione	x	x
-	5-substituted tetrahydropyrrole-3,6-piperazinedione	x	x
256	n-hexadecanoic acid		x

The results from Table 9.2.1 indicate that, although most peaks in the pyrogram of Klason lignin from tobacco are generated by lignin, other compounds are present. The flue-cured lignin showed the presence of anhydroglucopyranose, which is probably generated by cellulose, and both lignins showed the presence of pirrolidinopiperazinediones, which are characteristic for the pyrolysis of polypeptides. The presence of proteinaceous material in Klason lignin was also reported for other lignin preparations [9]. Besides carbohydrates and proteins, the study indicated the presence in the pyrolysate of small molecules such as nicotine, myosmine, and 3,3'-bipyridyl. These compounds are known to be present in tobacco leaf, but are supposed to be eliminated when the lamina is pre-extracted with 80% ethanol (as performed in the preparation of tobacco lignins). The presence of these small molecules indicates that it is difficult to penetrate the plant cells even under vigorous extraction procedures. Several other results on plant cell materials were reported with the same type of information as shown for tobacco lignins [20].

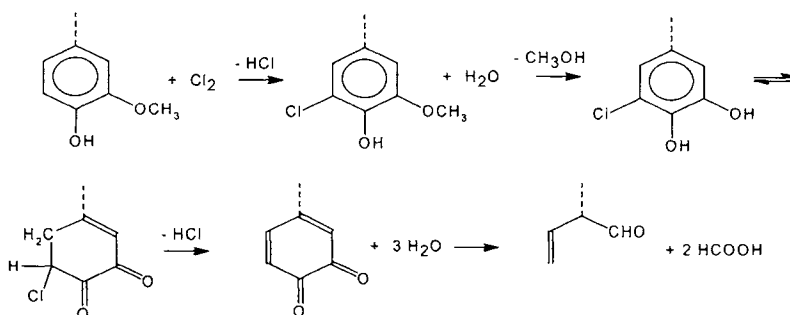
9.3. Chemically Modified Lignins.

Chemically modified lignins are the result of some procedures to prepare lignin (e.g. kraft lignin), but the main interest in these compounds arise from the fact that they are generated during paper and cellulose pulp manufacturing. Pulp mills commonly discharge effluents containing chlorolignins and lignosulfonates that raise an important environmental issue.

The pulping process consists of extraction of lignin from wood chips commonly by bisulfite pulping (kraft procedure using $\text{Na}_2\text{S} / \text{NaOH}$ is not so common today). During this process, which takes place at $135\text{--}150^\circ\text{C}$ at $4\text{--}6\text{ atm.}$, lignosulfonates are generated and dissolved to form a "black liquor." This is further removed from the wood pulp (with about 97% efficiency) and incinerated. The chemical reactions during bisulfite pulping are complex but can be basically described by the reaction:



Lignin content in wood is reduced from about 35% to 5%, and further processing is necessary to obtain whiter pulp. This consists of a series of bleaching steps using chlorine (C), alkali extraction (E), hypochlorite (H), and chlorine dioxide (D). The common sequence is CEHDED. The chlorination step C can be basically described by the reactions:



Alkali extraction removes the lignin degradation products, while the other steps produce further chlorination and/or oxidation. Besides small molecules in the bleaching process chlorinated lignins are generated.

The discharges from bisulfite pulping and bleaching produce the pulp mill effluents. They contain small molecules such as acids, mainly formic and acetic, chlorinated phenols and dioxines, neutral compounds such as methanol, chloroform, dichloromethane, terpenes, and sugars, as well as high molecular weight compounds. The high molecular weight compounds are chlorolignins and lignosulfonates (kraft lignins may be present if this process is used).

Analysis of chlorolignins and lignosulfonates is important in estimating the nature and the amount of compounds in pulp mill effluents. For this purpose, several analytical techniques were applied and among them Py-GC/MS [21-23]. The first step in the pyrolysis studies was the isolation of high molecular weight materials. This was done by ultrafiltration. The results of a Py-GC/MS study of chlorolignins and lignosulfonates collected from Rhine River [21] are shown in Table 9.3.1.

TABLE 9.3.1. *Main pyrolysis products of chlorolignins and lignosulfonates from pulp mill effluents.*

Mol. Wt.	Base peak	Compound	Abund.
44	44	carbon dioxide	++
64	6.4	sulfur dioxide	++
50	50	methyl chloride	++
44	44	acetaldehyde	++
56	41	butene	++
48	47	methanethiol	++
41	41	acetonitrile	++
56	56	2 propenal	++
58	43	2-propanone	+
68	68	furan	+
62	47	dimethylsulfide	++
76	76	carbon disulfide	+
66	66	cyclopentadiene	+
72	43	1-butanal	+
70	70	2 methyl-2-propenal	+
86	43	2,3-butanedione	++
72	43	2-butanone	+
92	82	2-methylfuran	+
92	82	3-methylfuran	+
89	57	propionic acid methyl ester	0
70	43	2-butenal	+
86	44	3-methylbutanal	+
74	43	acetic acid methyl ester	++
86	57	2-methylbutanal	+
78	78	benzene	+
84	84	thiophene	+
36.5	36	hydrochloric acid	++
73	73	methylisothiocyanate	+
100	43	2,3-pentadione	+
100	43	4-thiol 3-butyn-2-one (?)	0
90	43	1-thiol-2-propanone	+
96	96	2,5-dimethylfuran	+
60	43	acetic acid	+
78	48	(methylthio)methanol	+
94	94	2 vinylfuran	0
81	80	1-methyl-1H-pyrrole	+
84	69	2,3-dihydro-3-methylfuran	0
81	81	2-methylpyrrole	0
79	79	pyridine	+
94	94	dimethyldisulfide	+
100	69	2-butenic acid methyl ester	+
92	91	toluene	+
94	55	3,4-dihydro-2H-pyran	+
98	97	methylthiophene	0/+
98	97	2,3-dihydrofurfural	0
96	95	3-furaldehyde	+
110	95	3-acetylfuran	0
116	42	2,5-dimethyl-1,4-dioxane	+
78	63	dimethylsulfoxide	+
96	95	2-furaldehyde	+
81	80	methyl-1H-pyrrole	+
93	93	4-methylpyridin	0
106	91	C2-benzene	+

TABLE 9.3.1. *Main pyrolysis products of chlorolignins and lignosulfonates from pulp mill effluents (continued).*

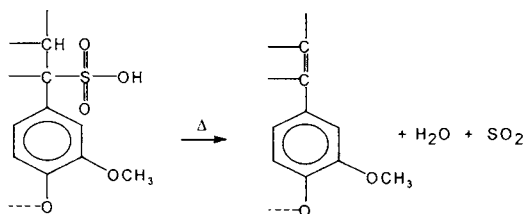
Mol. Wt.	Base peak	Compound	Abund.
106	91	C2-benzene	+
106	91	dimethylbenzene	+
112	111	2,4-dimethylthiophene	0
104	94	3-methyl-2-cyclopenten-1-one	+
106	91	dimethylbenzene	0
110	95	2-acetylfuran	+
110	110	5-methyl-2-furaldehyde	0
108	108	2,3-dimethylpyrazine	0
108	108	methoxybenzene	0
96	96	3-methyl-2-cyclopenten-1-one	+
110	110	5-methyl-2-furaldehyde	+
126	95	2-furancarboxylic acid methyl ester	+
94	94	phenol	+
118	118	benzofuran	0
120	105	trimethylbenzene	0
112	112	2-hydroxy-3-methylcyclopenten-1-one	+
116	116	1H-indene	0
108	108	2-methylphenol	+
108	108	4-methylphenol	+
124	109	guaiacol (2-methoxyphenol)	++
138	138	4-methylguaiacol	+
122	122	dimethylphenol	0
122	122	dimethylphenol	0
130	130	1-methyl-1-formyl-1H-imidazole	+
130	130	1-methyl-1H-indene	0
122	107	ethylphenol	+
122	107	ethylphenol	0
122	122	dimethylphenol	0
138	138	4-methylguaiacol	+
158	143	monochloroguaiacol	0
128	128	naphthalene	0
138	138	methylguaiacol	+
110	110	1,2-dihydroxybenzene	+
158	143	monochloroguaiacol	0
120	120	4-vinylphenol	+
152	152	dimethylguaiacol	+
140	140	methoxydihydroxybenzene	+
124	124	methoxyhydroxybenzene	+
158	143	monochloroguaiacol	0
152	137	4-ethylguaiacol	+
155	143	monochloroguaiacol	0/+
124	124	methyldihydroxybenzene	+
158	143	monochloroguaiacol	0
150	135	4-vinylguaiacol	+
172	172	chloro-4-methylguaiacol	0
142	142	2-methylnaphthalene	0
154	154	syringol (2,6-dimethoxyphenol)	+
164	164	4-(1-propenyl)guaiacol	+
152	152	4-formylguaiacol	+
172	172	chloro-1,2-dimethoxybenzene	0
172	172	chloro-4-methylguaiacol	0
164	164	4-(2-propenyl)guaiacol	+

TABLE 9.3.1. Main pyrolysis products of chlorolignins and lignosulfonates from pulp mill effluents (continued).

Mol. Wt.	Base peak	Compound	Abund.
144	144	chloro-1,2-dihydroxybenzene	0
168	168	4-methylsyringol	+
164	164	propenylguaiacol	++
166	166	1,2-dimethoxy-4-benzaldehyde	0
186	171	chloro-4-ethylguaiacol	0
166	151	4-propylguaiacol	+
192	192	dichloroguaiacol	0
166	151	4-ethanai guaiacol	+
162	162	propenyl-guaiacol	+
162	162	propenyl-guaiacol	+
178	178	4-(1-propenal)guaiacol	+
184	184	chloro-4-vinylguaiacol	0
180	137	4-(3-hydroxypropenyl)guaiacol	++
180	137	4-(propan-2-one)guaiacol	+
182	167	4-ethylsyringol	+
194	194	chloro-4-vinylguaiacol	0
226	211	trichloroguaiacol	0
194	151	4-(propane-dione)guaiacol	+
226	211	trichloroguaiacol	0
200	137	4-(2-chloro-2-ethanone)guaiacol	+
180	180	4-vinylsyringol	+
194	194	4-(1-propenyl)syringol	+
198	174	chloro-4-propenylguaiacol	0
182	137	4-ethoxyguaiacol	0
182	182	4-fomylsyringol	+
174	174	3-methoy-2-naphthalenol	0
214	171	chloro-4-(propanone)guaiacol	0
192	192	4-propenyl-syringol	+
186	186	biphenol	+
192	192	4-propenyl-syringol	+
226	211	trichloroguaiacol	0
194	194	propenylsyringol	++
178	178	4-(prop-1-en-3-yl)guaiacol	+
196	196	4-ethanalsyringol	+
210	210	4-(propanone)syringol	+
272	272	1,2-diguaiacyl ethene	+

Abundance: ++ → above 10%, + → 1% to 10%, and 0 → below 1%.

Among the compounds shown in Table 9.3.1, there are a few containing sulfur. This is because the main pyrolysis product containing sulfur of lignosulfonic acids seems to be SO₂. This is probably generated from sulfonated lignin by reactions of the type:



On the other hand, a significant number of chlorinated compounds were obtained in pyrolysis. This indicated that chlorinated fragments generated in the intermediate steps of the chlorination process are still present in lignin. They generate by pyrolysis compounds such as chloroguaiacols, chloromethylguaiacols, etc.

References 9.

1. F. Martin, C. Saiz-Jimenez, F. J. Gonzales-Vila, *Holzforschung*, 33 (1979) 210.
2. I. A. Pearl, *The Chemistry of Lignin*, M. Dekker, New York, 1967.
3. C. D. Nenitzescu, *Chimie Organica*, vol. 2 Ed. Technica, Bucuresti, 1958.
4. R. A. Fenner, J. O. Lephardt, *J. Agric. Food. Chem.*, 29 (1981) 846.
5. J. B. Reeves III, G. C. Galletti, *J. Anal. Appl. Pyrol.*, 24 (1993) 243.
6. O. Faix, D. Meier, I. Grobe, *J. Anal. Pyrol.*, 11 (1987) 416.
- 6a. E. R. E. van der Hage, M. M. Mulder, J. J. Boon, *J. Anal. Pyrol.*, 25 (1993) 149.
7. J. J. Boon, A. D. Powels, G. B. Eijkel, *Biochem. Soc. Trans.*, 15 (1987) 170.
8. E. R. E. van der Hage, J. J. Boon, *J. Chromatog. A*, 736 (1996) 61.
9. J. B. Reeves III, G. C. Galletti, *J. Anal. Appl. Pyrol.*, 25 (1993) 195.
10. R. Picaçlia, G. C. Galletti, P. Traldi, *J. High Resol. Chrom.* 13 (1990) 52.
11. A. K. Kivaisi, H. J. M. Op den Camp, H. J. Lubberding, J. J. Boon, G. D. Vogels, *Appl. Microbiol. Biotech.*, 33 (1990) 93.
- 11a. K. Kuroda, A. Suzuki, M. Kato, K. Imai, *J. Anal. Appl. Pyrol.*, 34 (1995) 1.
12. C. Saiz-Jimenez, J. W. de Leeuw, *Org. Geochem.* 6 (1984) 417.
- 12a. J. A. Caballero, A. Marcilla, J. A. Conesa, *J. Anal. Appl. Pyrol.*, 44 (1997) 75.
13. W. Genuit, J. J. Boon, O. Faix, *Anal. Chem.*, 59 (1987) 508.
- 13a. D. St. A.G. Radlein, J. Piskorz, D. S. Scott, *J. Anal. Appl. Pyrol.*, 12 (1987) 51.
- 13b. F. Martin, J. C. del Rio, F. J. Gonzalez-Vila, T. Verdejo, *J. Anal. Appl. Pyrol.*, 35 (1995) 1.
- 13c. R. D. Hartley, J. Haverkamp, *J. Sci. Food. Agric.*, 35 (1984) 14.
14. R. J. Evans, T. A. Milne, M. N. Soltys, *J. Anal. Appl. Pyrol.*, 9 (1986) 207.
- 14a. R. Brezny, V. Mihalov, V. Kovacik, *Holzforschung*, 37 (1983) 199.

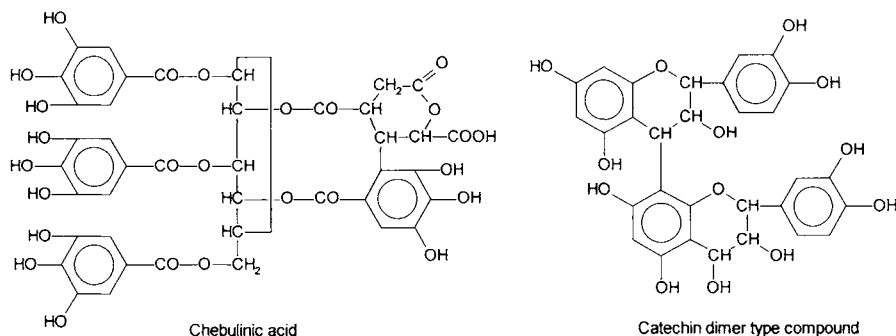
- 14b. K. Kuroda, *J. Anal. Appl. Pyrol.*, 35 (1995) 53.
15. K. Kuroda, Y. Inoue, K. Sakai, *J. Anal. Appl. Pyrol.*, 18 (1990) 59.
- 15a. M. Kleen, G. Gellerstedt, *J. Anal. Appl. Pyrol.*, 35 (1995) 15.
16. J. A. Caballero, R. Font, A. Marcilla, *J. Anal. Appl. Pyrol.*, 36 (1996) 159.
17. J. A. Caballero, R. Font, A. Marcilla, *J. Anal. Appl. Pyrol.*, 39 (1997) 161.
18. M. A. Scheijen, J. J. Boon, W. Hass, V. Heemann, *J. Anal. Appl. Pyrol.*, 15 (1989) 97.
19. M. A. Scheijen, J. J. Boon, *J. Anal. Appl. Pyrol.*, 19 (1991) 153.
20. M. Kleen, G. Lindblad, S. Backa, *J. Anal. Appl. Pyrol.*, 25 (1993) 209.
21. W. M. G. M. van Loon, J. J. Boon, B. de Groot, *J. Anal. Appl. Pyrol.*, 20 (1991) 275.
22. A. D. Pouwels, J. J. Boon, *J. Wood Chem. Technol.*, 7 (1987) 197.
23. W. M. G. M. van Loon, A. D. Pouwels, P. Veenendaal, J. J. Boon, *Intern. J. Environ. Anal. Chem.*, 38 (1990) 255.

This Page Intentionally Left Blank

Chapter 10. Analytical Pyrolysis of Polymeric Tannins

10.1. Polymeric Tannins.

The term tannin refers to substances of plant origin containing phenolic groups used in tanning, dyeing, the making of inks, or in medicine. A more restrictive term denotes a substance extracted from plants with the property of converting animal skins into leather. The natural tannins do not belong to a homogeneous chemical class. By their chemical properties they were classified into hydrolyzable and condensed tannins. Most tannins from both classes have a molecular weight between 1000 and 5000, although polymeric tannins may have larger molecules. A series of hydrolyzable tannins with smaller molecules were isolated, and some typical structures consist of sugar esters of polyphenolic carboxylic acids such as gallic acid (3,4,5-trihydroxybenzoic acid) ellagic acid, chebulic acid, etc. The condensed tannins may derive from flavan-3-ols such as catechin, flavan-3,4-diols, or from hydroxystilbenes. Two examples of smaller isolated tannins, one a hydrolyzable tannin (chebulinic acid) and one a condensed tannin (a dimer type compound from catechin), are shown below.



Polymeric tannins have more complicated structures including esterified oligosaccharide chains for the hydrolyzable ones or further polymerization of the flavonoid units for condensed ones. Because of their diversity including small molecules and polymers, characterization of natural tannins is not simple. The first step in their characterization is isolation. This has been done using several procedures such as ultrafiltration and gel permeation chromatography [2].

A variety of procedures were applied for the analysis of tannins [1], pyrolysis being one of them. Analytical results on pyrolysis products of different tannins were obtained using Py-MS, as well as Py-GC/MS and Py-GC/MS with the methylation using TMAH. Pyrolysis techniques were applied for the evaluation of catechol content of tannins from different plant materials [1,2], or for the quantitation of tannin content in products such as wine [2].

Tannin pyrolysis generates small molecules, and specific fragments were reported depending on the parent monomeric unit from tannin [3]. Representing a condensed tannin as shown in the formula below, the typical compounds identified in the pyrolysate are given in Table 10.1.1.

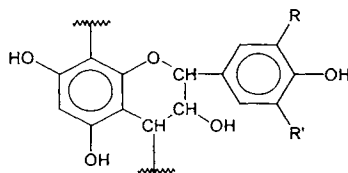


TABLE 10.1.1. *Typical compounds identified in the pyrolysate depending on R and R' in the tannin structure.*

Parent anthocyanin	Ring substituent R	Ring substituent R'	Pyrolysis fragment
pelargonidin	H	H	phenol
peonidin	OCH ₃	H	guaiacol
cyanidin	OH	H	catechol
petunidin	OH	OCH ₃	3-methoxycatechol
malvidin	OCH ₃	OCH ₃	2,6-dimethoxyphenol

In addition to the compounds indicated in Table 10.1.1, some other compounds were identified in tannin pyrolysis such as methylphenols, ethylphenols, vinylphenols, dimethoxyphenols, etc.

References 10.

1. G. C. Galletti, J. B. Reeves, *Org. Mass Spectrom.*, 27 (1992) 226.
2. C. G. Galletti, V. Modafferi, M. Poiana, P. Bocchini, *J. Agric. Food. Chem.*, 43 (1995) 1859.
3. R. D. Hartley, J. Haverkamp, *J. Sci. Food. Agric.*, 35 (1984) 14.

Chapter 11. Analytical Pyrolysis of Caramel Colors and of Maillard Browning Polymers

11.1 Pyrolysis of Caramel Colors.

Caramel colors are brown pigments produced by reaction of a saccharide with a "browning accelerator." They can be considered a "natural" material as caramels may be formed in food. Caramels are prepared as food colors by heating a solution of a sugar (commonly glucose or sucrose) with the accelerator. The caramels can be classified as one of four types [1] shown in Table 11.1.1.

TABLE 11.1.1. *Classification of caramels.*

Type	Name	Accelerator	Uses
1	Plain caramel	NaOH, Na ₂ CO ₃ , KOH, K ₂ CO ₃ , H ₂ SO ₄ , HCl	Alcoholic beverages
2	Caustic sulfite caramel	Na ₂ SO ₃ , K ₂ SO ₃ , NaOH + SO ₂ ,	(not common)
3	Ammonia caramel	(NH ₄) ₂ CO ₃ , Na ₂ CO ₃ + NH ₃ , NH ₃ , NH ₄ OH, etc.	Beer
4	Ammonium sulfite caramel	(NH ₄) ₂ SO ₃ , Na ₂ SO ₃ + NH ₄ OH, etc.	Soft drinks

The chemical composition of the caramels depends on the reagents utilized in their preparation as well as on the conditions of the reaction such as pH and heating temperature and time. Although only reducing sugars are supposed to be reactive enough to undergo condensation reactions, sucrose for example also was used for caramel preparation. It is likely that in stronger reaction conditions, sucrose may hydrolyze or decompose and form shorter chain hydroxy aldehydes that are reactive species. Besides the reagent used for the preparation of a certain caramel color, the nature of the anions present in the reaction, such as phosphate, carbonate, acetate, sulfite, etc. influences the reaction path. The caramels consist of a mixture of small molecules and polymeric colored compounds. Usually, they are used without further separation, although the caramel polymer alone can be obtained by dialysis or diafiltration as it commonly forms a colloidal solution.

The polymeric material from the plain caramel is generated from the condensation reactions of the aldehydes and ketones formed by heating the sugar with bases or acids. The ammonia caramel is formed in a Maillard type reaction [2] where carbonyl compounds react with amino groups or ammonia. This type of compound will be further presented in Sections 11.2 and 11.3. Sulfite caramel is also a Maillard type polymer. However, as hydrogen sulfites form stable adducts with aldehydes and ketones, the sulfite caramels include in their structure sulfite groups.

Because the information on the caramel composition is of practical importance, several procedures have been proposed for their analysis. One such analytical procedure is Py-GC/MS, which has been used for a rapid classification of caramels. The differentiation can be done based on the nature of the compounds generated by pyrolysis. Using GC/MS analysis [1,3] of the pyrolysates, the nature of the caramel can be obtained from the peak intensities, which vary as shown in Table 11.1.2.

TABLE 11.1.2. *Main pyrolysis products used for the identification of the type of caramel color.*

Compound	Caramel 1	Caramel 3	Caramel 4
pyrazine	-	++	++
pyridine	-	+	++
methylpyridine	-	+++	+
dimethylpyrazine	-	+	+
vinylpyrazine	-	+	+
furfural	+++	+	+++
cyclopentenone	+	+	+
methylvinylpyrazine	-	+	-
cyclopentene-1,3-dione	+	+	++
5-methylfurfural	++	+	+++
benzoxitrile	-	+	+
dihydrofuranone	+	++	+
2,5-furandialdehyde	++	+	+
2-hydroxymethyl-5-furfural	+++	-	+

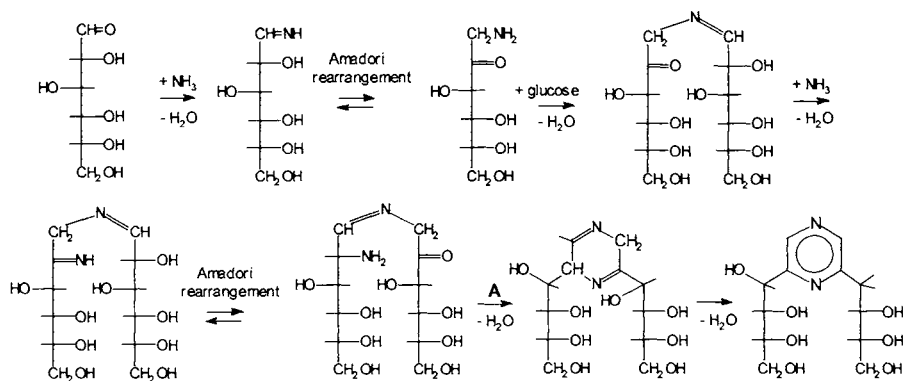
+ and - indicate the level of a compound in the pyrolysate, with +++ the highest level and - absent.

As seen in Table 11.1.2, the caramels of type 1 form mainly furans and cyclopentenones and do not show nitrogen containing compounds. Caramels of type 3 (ammoniated caramels) contain a variety of pyrazines and no hydroxymethylfurfural, while the type 4 caramels contain both pyrazines and furans. Pyrolysis of caramel colors of type 4 also generates a certain amount of SO₂.

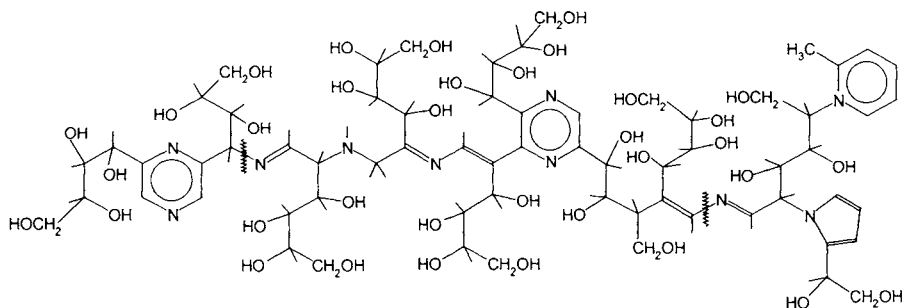
Besides standard Py-GC/MS, a faster procedure to identify the type of caramel color using a pyrolytic step has been developed [4,4a] using comparisons of cumulative mass spectra (see also Section 5.3). These were generated by adding the spectra obtained from a Curie point Py-GC/MS analysis.

11.2. Sugar-Ammonia and Sugar-Amines Browning Polymers.

The reaction of amino compounds with aldehydes or ketones associated with the formation of browning polymeric materials is known as Maillard condensation [2]. Maillard condensations cover a wide range of reactants from both groups of amino and carbonyl compounds. One class of Maillard condensation products comes from the reaction of ammonia with reducing sugars. This reaction takes place easily at mildly elevated temperatures and is common in a variety of food products [5] and tobacco [6,7]. The Maillard reaction generates a mixture of small molecules and polymers. By combining, for example, glucose with alcoholic ammonia [8], besides the browning polymer the major condensation product is 2-(D-arabino-tetrahydroxybutyl)-6-(D-erythro-2',3',4'-trihydroxybutyl)-pyrazine (2,6-deoxyfructosazine). In this reaction the Schiff base formed in the first step further generates an amino-carbonyl compound by a chemical transformation known as Amadori rearrangement. A possible path that explains the predominance of the 2,6 isomer vs. 2,5 isomer in this reaction of glucose with ammonia is the following:



The condensation reaction **A** from the above scheme is an internal cyclization. However, other paths are possible at this point (or after the first Amadori rearrangement step), the end result being the formation of a non-repetitive polymer with the following idealized structure [9].



The formation of 2,6-deoxyfructosazine from glucose, as well as of the browning polymer, are also functions of the pH, the presence of certain anions such as phosphate, acetate, sulfite, etc., or of the reaction medium (which can be water, ethylene glycol, propylene glycol, etc.). The molecular weight of the browning polymer may cover a wide range and depends on the concentration of the reagents, heating temperature during the reaction, reaction medium, etc. As an example, a browning polymer can be obtained by heating for two hours glucose and diammonium phosphate (which generates ammonia) in water solutions at 100°C . The polymer with the molecular weight between 10,000 and 100,000 can be separated by ultrafiltration or dialysis. The elemental composition of this browning polymer is rather close to that of deoxyfructosazine itself, as shown in Table 11.2.1.

TABLE 11.2.1. *Elemental composition of deoxyfructosazine and of a browning polymer made from glucose and diammonium phosphate, with $10,000 < \text{MW} < 100,000$.*

	C %	H %	N %	O %
deoxyfructosazine (theoretical)	47.37	6.57	9.21	36.85
deoxyfructosazine (experimental)	46.97	6.87	8.91	36.35
browning polymer (experimental)	49.74	6.3	8.7	35.05

From Table 11.2.1 it can be concluded that the ratio C/N in the browning polymer is about 1/(6.6), which is close to deoxyfructosazine, showing that one ammonia molecule reacts with one glucose, but one in ten glucose molecules may condense without involving a nitrogen atom.

The Py-GC/MS analysis of the browning polymer from glucose and ammonia (from diammonium phosphate) is shown in Figure 11.2.1. The pyrolysis was performed at 600° C for 10 sec. in a filament pyrolyser (CDS 1000), and the separation was done on a Carbowax column 60 m long, 0.32 mm i.d. and 0.25 μm film thickness, with temperature gradient of the GC oven between 40° C and 240° C.

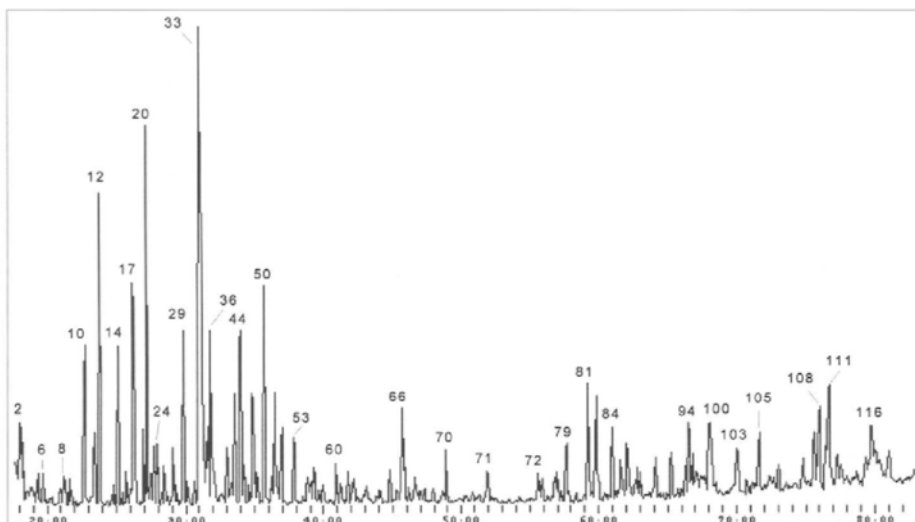
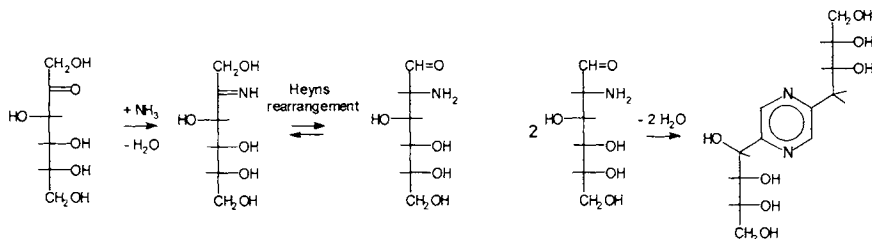


FIGURE 11.2.1. Pyrogram at 600° C of a browning polymer with MW between 10,000 and 100,000 made from glucose and diammonium phosphate in water at 100° C. Peak identification is given in Table 11.2.2.

Fructose also reacts with diammonium phosphate (or ammonium formate, acetate, etc.) to form predominantly 2,5-deoxyfructosazine and a browning polymer similar to the one obtained from glucose. A possible reaction path is the following:



The Py-GC/MS analysis of the browning polymer from fructose and ammonia (from diammonium phosphate) using the same separation conditions as for the pyrolysate of the glucose polymer is shown in Figure 11.2.2.

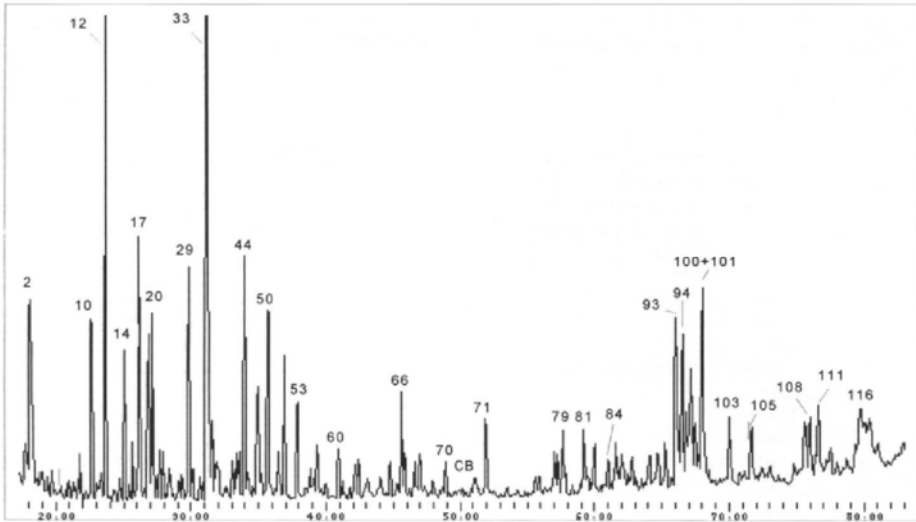


FIGURE 11.2.2. Pyrogram at 600° C of a browning polymer with MW between 10,000 and 100,000 made from fructose and diammonium phosphate in water at 100° C. Peak identification is given in Table 11.2.2.

The peak identifications from Figures 11.2.1 and 11.2.2 were done by MS library search and the results are given in Table 11.2.2. Most peaks are common in the two chromatograms; however, peak intensities are quite different.

TABLE 11.2.2. Peak identification of the compounds shown in Figures 11.2.1 and 11.2.2 from the pyrogram at 600° C of a sugar/ammonia browning polymer.

Peak No.	Name	Formula	MW
1	2,3-butandione	C ₄ H ₆ O ₂	86
2	acetonitrile	C ₂ H ₃ N	41
3	propanenitrile	C ₃ H ₅ N	55
4	crotonaldehyde	C ₄ H ₆ O	70
5	butenal + toluene	C ₃ H ₅ CHO + C ₆ H ₅ CH ₃	70 + 92
6	hex-2-en-4-ynal	C ₆ H ₆ O	94
7	3-penten-2-one	C ₅ H ₈ O	84
8	N-methylpyrrole	C ₅ H ₇ N	81
9	2-vinyl-5-methylfuran	C ₇ H ₈ O	108
10	pyridine	C ₅ H ₅ N	79
11	pyrazine	C ₄ H ₄ N ₂	80
12	2-methylpyridine	C ₆ H ₇ N	93
13	2,3-dimethylpyridine	C ₇ H ₉ N	107
14	2-methylpyrazine	C ₅ H ₆ N ₂	94
15	2-ethylpyridine	C ₇ H ₉ N	107
16	3-methylpyridine	C ₆ H ₇ N	93
17	1-hydroxy-2-propanone (acetol)	C ₃ H ₆ O ₂	74
18	aniline	C ₆ H ₇ N	93
19	2,5-dimethylpyrazine	C ₆ H ₈ N ₂	108
20	2,6-dimethylpyrazine	C ₆ H ₈ N ₂	108
21	ethylpyrazine	C ₆ H ₈ N ₂	108
22	3,5-dimethylpyridine	C ₇ H ₉ N	107

TABLE 11.2.2. *Peak identification of the compounds shown in Figures 11.2.1 and 11.2.2 from the pyrogram at 600° C of a sugar/ammonia browning polymer (continued).*

Peak No.	Name	Formula	MW
23	2,3-dimethylpyrazine	C6H8N2	108
24	2-cyclopenten-1-one	C5H6O	82
25	2-methyl-2-cyclopenten-1-one	C6H8O	96
26	2-ethyl-6-methylpyrazine	C7H10N2	122
27	2-ethyl-5-methylpyrazine	C7H10N2	122
28	(1-methylethoxy)-propanenitrile	C6H11NO	113
29	trimethylpyrazine	C7H10N2	122
30	2-vinylpyridine	C7H7N	105
31	β-angelica lactone	C5H6O2	98
32	2-vinylpyrazine	C6H6N2	106
33	acetic acid	C2H4O2	60
34	2,5-dimethyl-3-ethylpyrazine	C8H12N2	136
35	ions 43, 102	?	102
36	furfural	C5H4O2	96
37	acetyl acetate	C5H8O3	116
38	1,4-dioxadiene	C4H4O2	84
39	2,3-dimethyl-5-ethyl-pyrazine	C8H12N2	136
40	2-methyl-6-vinylpyrazine	C7H8N2	120
41	5-methyl-2-vinylpyrazine	C7H8N2	120
42	1-(2-furanyl)-ethanone	C6H6O2	110
43	2,4,6-trimethylpyridine	C8H11N	121
44	1H-pyrrole	C4H5N	67
45	3-methyl-2-cyclopenten-1-one	C6H8O	96
46	benzaldehyde	C7H6O	106
47	propanoic acid vinyl ester ?	C5H8O2	100
48	propanoic acid	C3H6O2	74
49	2,3-dimethyl-2-cyclopenten-1-one	C7H10O	110
50	2-methyl-1H-pyrrole	C5H7N	81
51	5-methyl furfural	C6H6O2	110
52	cyclopent-2-en-1,4-dione	C5H4O2	96
53	2,5-dimethylpyrrole	C6H9N	95
54	3-ethyl-1H-pyrrole	C6H9N	95
55	dihydro-2(3H)-furanone	C4H6O2	86
56	butyric acid	C4H8O2	88
57	propenoic acid	C3H4O2	72
58	N-methylacetamide	C3H7NO	73
59	3-methyl-3-hexen-2-one	C7H12O	112
60	2-furanmethanol	C5H6O2	98
61	5-methyl-2(5H)-furanone	C5H6O2	98
62	1-(6-methyl-2-pyrazinyl)-1-ethanone	C7H8N2O	136
63	2-acetyl-3-methylpyrazine	C7H8N2O	136
64	3-methyl-2(5H)-furanone	C5H6O2	98
65	2(5H)-furanone	C4H4O2	84
66	acetamide	C2H5NO	59
67	2-hydroxycyclopent-2-en-1-one	C5H6O2	98
68	2-butenic acid	C4H6O2	86
69	propanamide	C3H7NO	73
70	3-methyl-2-hydroxycyclopent-2-en-1-one	C6H8O2	112
71	2-pyridincarbonitrile	C6H4N2	104
72	2-hydroxy-3-methyl-4H-pyran-4-one (maltol) + 2-methylquinoxaline	C6H6O3 + C9H8N2	126
73	2-acetylpyrrole	C6H7NO	109
74	3-furancarboxylic acid	C5H4O3	112
75	2-furancarbonitrile+ ?	C5H3NO	93
76	pyrrolo[1,2-A]pyrazine	C7H6N2	118

TABLE 11.2.2. Peak identification of the compounds shown in Figures 11.2.1 and 11.2.2 from the pyrogram at 600° C of a sugar/ammonia browning polymer (continued).

Peak No.	Name	Formula	MW
77	4-methylpyrrolo[1,2-A]pyrazine	C8H8N2	132
78	1-methylpyrrolo[1,2-A]pyrazine	C8H8N2	132
79	phenol	C6H6O	94
80	1,3-dimethylpyrrolo[1,2-A]pyrazine	C9H10N2	146
81	2,5-dimethyl-4-hydroxy-3(2H)-furanone	C6H8O3	128
82	2-(2'-furyl)-6-methylpyrazine	C9H8N2O	160
83	2-(2'-furyl)-5-methylpyrazine	C9H8N2O	160
84	5-methyl-2-pyrazinmethanol	C6H8N2O	124
85	4-methylphenol	C7H8O	108
86	2-methyl-1H-pyrrolo[2,3-B]pyridine	C8H8N2	132
87	2-(2'-furyl)-3,5-dimethylpyrazine	C10H10N2O	174
88	3-methylpyrrolo[1,2-A]pyrazine	C8H8N2	132
89	1-methyl-1H-pyrrole-2-carboxaldehyde	C6H7NO	109
90	1,5-naphthiridin-4-amine ?	C8H7N3	145
91	1,4-dimethylpyrrolo[1,2-A]pyrazine	C9H10N2	146
92	3,6-dimethyl-4H-pyrido[1,2-A]pyrimidin-4-one ?	C10H10N2O	174
93	2,4-dimethyl-1H-pyrazole ?	C5H8N2	96
94	2-methyl-1H-benzimidazol	C8H8N2	132
95	1,3-dimethylpyrrolo[1,2-A]pyrazine	C9H10N2	146
96	2,2'-bipyridine	C10H8N2	156
97	1-ethyl-1-H-benzimidazol	C9H10N2	146
98	carbonyldiimidazol ?	C7H6N4O	162
99	trimethylpyrrolo[1,2-A]pyrazine ?	C10H12N2	170
100	1H-benzimidazol	C7H6N2	118
101	4-methyl-1H-imidazol ?	C4H6N2	82
102	2,3,4-trimethyl-2-cyclopenten-1-one	C8H12O	124
103	2,3-dihydro-3,5-dihydroxy-6-methyl-4H-pyran-4-one	C6H8O4	144
104	2,6-dimethyl-3-hydroxypyridine	C7H9NO	123
105	2-methyl-3-pyridinol	C6H7NO	109
106	3-(3,4-dihydro-2H-pyrrol-5-yl)-pyridine	C9H10N2	146
107	2-pyridincarboxylic acid	C6H5NO2	123
108	4-aminophenol	C6H7NO	109
109	3-aminophenol	C6H7NO	109
110	2-hydroxy-3-isobutylpyrazine	C8H12N2O	152
111	4-pyridinol	C5H5NO	95
112	benzoic acid	C7H6O2	122
113	2-aminophenol	C6H7NO	109
114	1H-indole	C8H7N	117
115	2,5-pyrrolidindione ?	C4H5NO2	99
116	2,5-dimethyl-3-isobutoxypyrazine ?	C10H16N2O	180
117	methyl-pyrazine-4-oxide ?	C5H6N2O	110
118	1-methyl-1H-imidazole-2-carboxaldehyde	C5H6N2O	110

The compounds indicated in Table 11.2.2 describe only a part of the pyrolysate composition because the more polar or less volatile compounds are not easily eluted from polar columns (Carbowax) and therefore are not detected.

One interesting finding regarding the pyrolysis products from the browning polymer (nondializable melanoidin) made from glucose (G polymer) and the one made from fructose (F polymer) is the predominance of the compounds with 2,6 substitution for the G polymer and the 2,5 substitution for the F polymer. This can be seen for example for the dimethylpyrazines generated during the pyrolysis of the two materials. Figures 11.2.3A and 11.2.3B show a portion of the trace of the extracted ion 108 for the

pyrolysate of the polymer G and the polymer F respectively. The peak corresponding to 2,5-dimethylpyrazine is significantly higher in the pyrolysate of the polymer F.

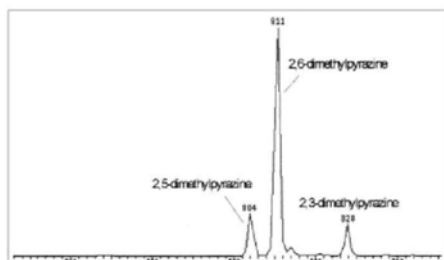


FIGURE 11.2.3A. Extracted ion 108 for the pyrolysate of the polymer G.

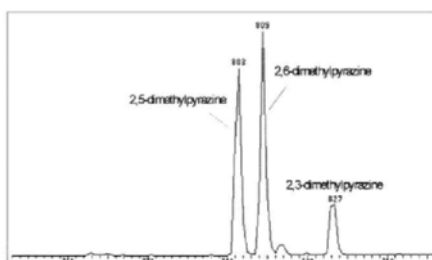


FIGURE 11.2.3B. Extracted ion 108 for the pyrolysate of the polymer F.

Figures 11.2.4A and 11.2.4B show a portion of the trace of the extracted ion 160 for the pyrolysate of the polymer G and the polymer F respectively. The peak corresponding to 2-(2'-furyl)-6-methylpyrazine and 2-(2'-furyl)-5-methylpyrazine have the intensities reversed for the polymer G compared to polymer F. This shows that the isomer structure of a polymer may be investigated using pyrolysis, the pyrolytic process preserving at least in part the type of substitution preexistent in the polymer structure.

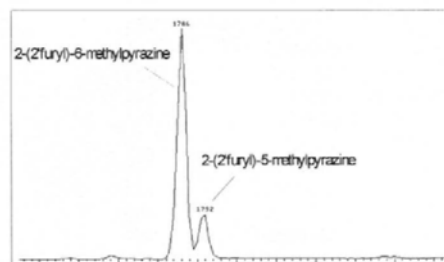


FIGURE 11.2.4A. Extracted ion 160 for the pyrolysate of the polymer G.

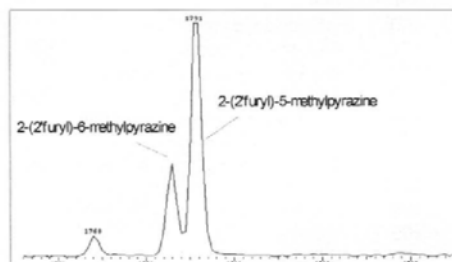


FIGURE 11.2.4B. Extracted ion 160 for the pyrolysate of the polymer F.

The prevalence of the formation of 2,6-deoxyfructosazine from glucose (or aldoses) in the reaction with ammonia (diammonium phosphate) and of 2,5-deoxyfructosazine from fructose (or ketoses) in the reaction with ammonia therefore is seen also in the position of substitutions in the structure of the browning polymers. However, from Figures 11.2.3 and 11.2.4 it can be seen that some 2,5 isomers are also present in the pyrolysate of the polymer G and some 2,6 isomers are present in the pyrolysate of polymer F. This can be either because the substitution in the polymer is not unique at certain positions and some mixing was already present in the structure of the polymer or due to the effect of pyrolysis that does not preserve well the initial position of the substitution. As a comparison, the extracted ion 108 (showing dimethylpyrazines) and the extracted ion 160 (showing furylmethylpyrazines) are given in Figures 11.2.5 and 11.2.6 for a pyrolysate of 2,6-deoxyfructosazine.

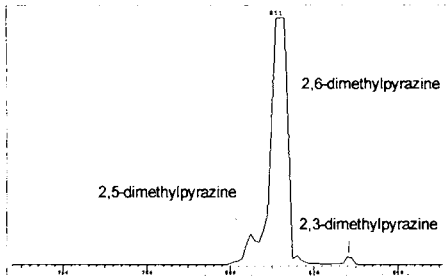


FIGURE 11.2.5. Extracted ion 108 for the pyrolysate of the 2,6-deoxyfructosazine.

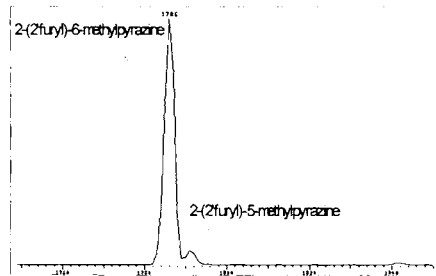
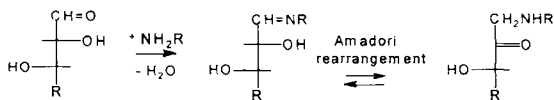


FIGURE 11.2.6. Extracted ion 160 for the pyrolysate of the 2,6-deoxyfructosazine.

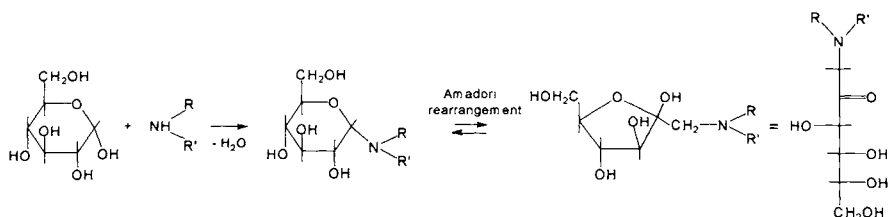
As seen in Figures 11.2.5 and 11.2.6, the pyrolysate of 2,6-deoxyfructosazine contains fewer 2,5-substituted compounds than the polymer G pyrolysate. This may be an indication that the polymer has some preexisting substructures with 2,5 substitution on pyrazine rings (or precursors), although the 2,6 substitution remains predominant. This result may be used as an argument in favor of the mechanism of Maillard condensation indicated above. Several other reaction paths for Maillard reaction were proposed, including the formation of very reactive α -dicarbonyl compounds in the early stages of the reaction. However, the results from pyrolysis of the browning polymers G and F indicate that in the case of the reaction of sugars with ammonia, the formation of α -dicarbonyl compounds cannot be significant. Such intermediates would generate equal proportion of the 2,5 and 2,6 substitutions regardless of the starting sugar being an aldose or a ketose.

Besides structure elucidation for the browning polymer, Py-GC/MS studies were also done in connection with food related problems [10] such as the use of sugar-ammonia browning polymers as food colors.

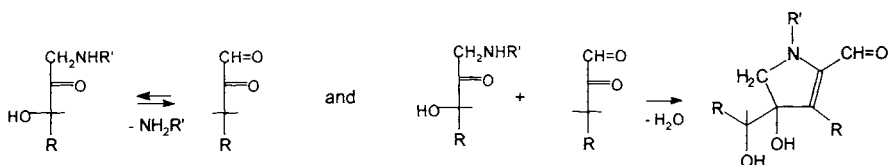
As indicated previously, primary and secondary amines can also react with carbonyl compounds to form a mixture of compounds containing small molecules and polymers. The small molecule compounds obtained from an aldose and an amine have the common name Amadori products because the Amadori rearrangement is involved in their formation. The compounds generated from ketoses and amines are known as Heyns products (although the differentiation Amadori/Heyns is not always considered). The mechanism for the reaction of primary amines with a reducing sugar can be formulated as follows:



The Amadori rearrangement in the reaction of a secondary amine with glucose can be formulated as follows:



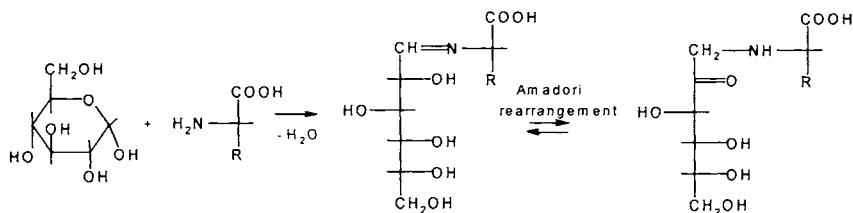
In this reaction the glycosylamines are transformed into the Amadori compounds. The elimination of the amine from the Amadori compounds may generate α -dicarbonyl compounds that are the source of further condensations and formation of browning polymers. This may be expressed by reactions of the type:



The new compounds formed from these reactions still contain reactive carbonyl groups that can continue the condensation and generate browning polymers. Pyrolysis studies were done on several Amadori compounds from this class [11–13], such as 1-deoxy-1-[(S)-2-(3-pyridyl)-1-pyrrolidiny]- β -D-fructose [11]. However, the nondialyzable melanoidin from this type of reaction received less interest.

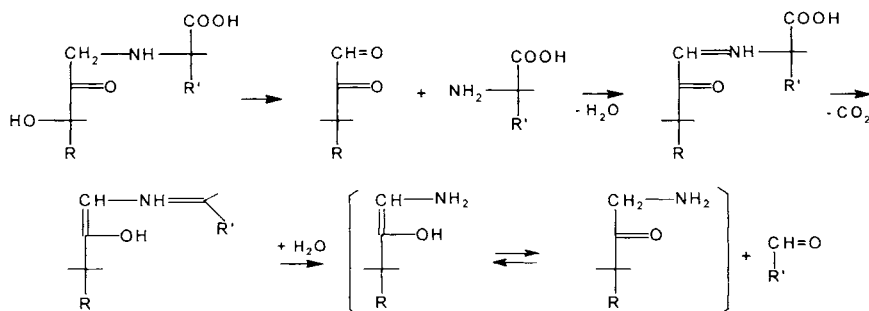
11.3. Sugar-Amino Acid Browning Polymers.

A class of Maillard condensation products even more common in nature than those coming from the reaction of ammonia or amines with reducing sugars is generated as a result of the reaction of amino acids with sugars or other carbonyl compounds. This reaction is of particular interest because it is related to food and nutrition and also may take place in live tissues. Maillard condensation of amino acids with carbonyl compounds generates a mixture of small molecules and polymeric browning materials similar to those generated from ammonia and sugars as described in Section 11.2. The reaction mechanisms of reaction of amino acids and sugars are in many cases similar to those already described in Section 11.2. The reaction between glucose and an amino acid with the formation of a typical Amadori compound can be written as follows:



Only proline (or hydroxyproline), being a secondary amine, will form Amadori compounds with a glycosylamine as an intermediate. Other amino acids contain primary amino groups, although secondary amines are present in some of them (tryptophan, histidine).

The reaction between amino acids and sugars leads not only to the formation of the Amadori compounds. Two types of secondary reactions may take place, one generating a variety of small molecules (with importance in the roast aroma associated with Maillard reaction) and the other generating browning polymers (nondializable melanoidins). Several schemes were proposed for these secondary reactions. As an example, the formation of α -dicarbonilic compounds or the formation of aldehydes from the amino acids by decarboxylation and deamination (Strecker degradation [5]) may take place generating reactive compounds, some with more than one reactive group.



Evidence was found that even free radicals may be formed in the first stages of the Maillard reaction [14]. The intermediates in Maillard reaction may produce small molecules or may further react and generate browning polymers [15].

A variety of results are available regarding the formation of small molecules during Maillard reaction [2,5]. However, pyrolysis of the Maillard polymer itself was less studied. One example of pyrolysis of a Maillard polymer is discussed below. The polymer has been obtained from the reaction of proline and fructose and separated from the reaction mixture by the extraction of small molecules accompanying the polymer with ethanol/*tert*-butyl methyl ether. The molecular weight is unknown for this polymer, as it was not obtained by dialysis or ultrafiltration, and no special measurement of MW was performed. However, the absence of the small molecules in the material was verified chromatographically. The pyrolysis has been performed in a filament system at 600° C and analyzed by on-line GC/MS on a Carbowax column (60 m long, 0.32 mm i.d., 0.25 μ m film thickness) [16]. For this analysis the GC separation was done using a temperature gradient between 35° C and 240° C. The obtained pyrogram is shown in Figure 11.3.1.

The peak identification obtained by MS library search for the pyrogram shown in Figure 11.3.1 is given in Table 11.3.1.

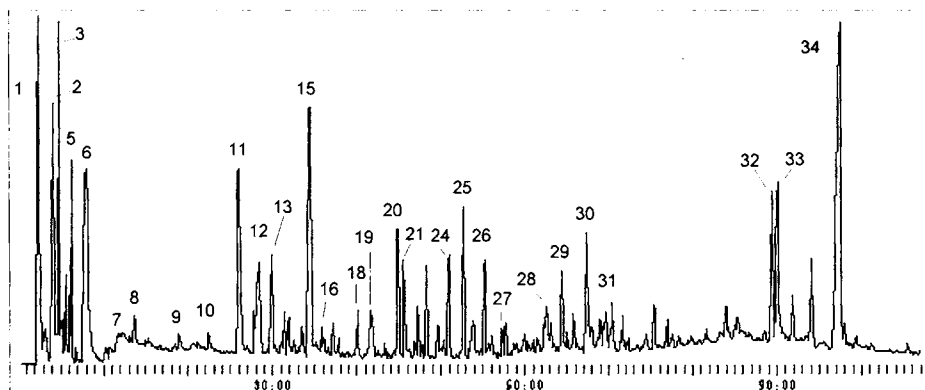


FIGURE 11.3.1. Pyrogram obtained at 600° C from fructose/proline browning polymer. Separation done on a Carbowax column followed by MS detection.

TABLE 11.3.1. Compounds identified in the pyrogram from Figures 11.3.1 of fructose/proline browning polymer (with the corresponding peak numbers).

Peak #	Compound	Formula	MW
1	1,2-propandiamine	C ₃ H ₁₀ N ₂	74
2	2-methoxy-2-methyl-propane	C ₅ H ₁₂ O	88
3	propanone	C ₃ H ₆ O	58
4	2-butanone	C ₄ H ₈ O	72
5	2,5-dimethyl-furan	C ₆ H ₈ O	96
6	pyrroline	C ₄ H ₇ N	69
7	3,4-dihydro-2H-pyran-2-methylbutenal	C ₅ H ₈ O	84
8	pyrrolidine	C ₄ H ₉ N	71
9	3-methylpyridine	C ₆ H ₇ N	93
10	2-methyl-2-cyclopenten-1-one	C ₆ H ₈ O	96
11	α-ethyl-2-piperidinmethanol	C ₈ H ₁₇ NO	143
12	acetic acid	C ₂ H ₄ O ₂	60
13	2-cyclohexylpiperidine	C ₁₁ H ₂₁ N	167
14	2-methyl-1H-pyrrole	C ₅ H ₇ N	81
15	1,2-propandiol	C ₃ H ₈ O ₂	76
16	2,3-1H-indole	C ₈ H ₉ H	119
16a	2-ethyl-3,5-dimethylpyridine	C ₉ H ₁₃ N	135
17	2-ethyl-6-methyl-benzenamine	C ₉ H ₁₃ N	135
18	mixture		
19	1-pyrrolidinecarboxaldehyde	C ₅ H ₉ NO	99
20	2-hydroxy-3-methyl-2-cyclopenten-1-one	C ₆ H ₈ O ₂	112
21	1-acetylpyrrolidine	C ₆ H ₁₁ NO	113
22	2,3-dihydro-3,3-dimethyl-imidazo[1,2-c]pyrimidindione	C ₈ H ₁₁ N ₃ O ₂	181
23	2-ethyl-6methyl-5-pyrimidinamine	C ₇ H ₁₁ N ₃	137
24	1-methyl-2-methanol-1H-imidazole	C ₅ H ₈ N ₂ O	112
25	2-(1-pyrrolidinyl)-2-cyclopenten-1-one	C ₉ H ₁₃ NO	151
26	3-methyl-2-(1-pyrrolidinyl)-2-cyclopenten-1-one	C ₁₀ H ₁₅ NO	165
27	piperidinone	C ₅ H ₉ NO	99
28	2,3-dihydro-3,5-dihydroxy-6-methyl-4H-pyran-4-one	C ₆ H ₈ O ₄	144
29	5,8-dimethyl-1,2,3,4-tetrahydroquinoxaline	C ₁₀ H ₁₄ N ₂	162
30	2-(1-pyrrolidinyl)-2-cyclopentan-1-ol	C ₉ H ₁₇ NO	155
31	1-(3,4,4A,5,6,7-hexahydro-2-naphthalenyl)-pyrrolidine	C ₁₄ H ₂₁ N	203
32	2-amino-3,4:5,6-bis(trimethylene)-pyridine	C ₁₁ H ₁₄ N ₂	174
33	tetrahydro-5-(2-methylpropyl)-4H-pyrrolo[1,2-a]pyrazine-2,4-dione	C ₁₁ H ₁₆ O ₂ N ₂	208
34	octahydro-5H,10H-dipyrrolo[1,2-a:1',2'-d]pyrazine-5,10-dione	C ₁₀ H ₁₄ N ₂ O ₂	194

The same polymer was also analyzed for less volatile components by performing the pyrolysis off line at 600° C in a filament system followed by off-line derivatization with BSTFA. The silylated pyrolysate was analyzed by GC/MS on a DB-5 column (60 m long, 0.32 mm i.d., 0.25 µm film thickness). For this analysis the GC separation was done using a temperature gradient between 50° C and 300° C. The chromatogram is shown in Figure 11.3.2.

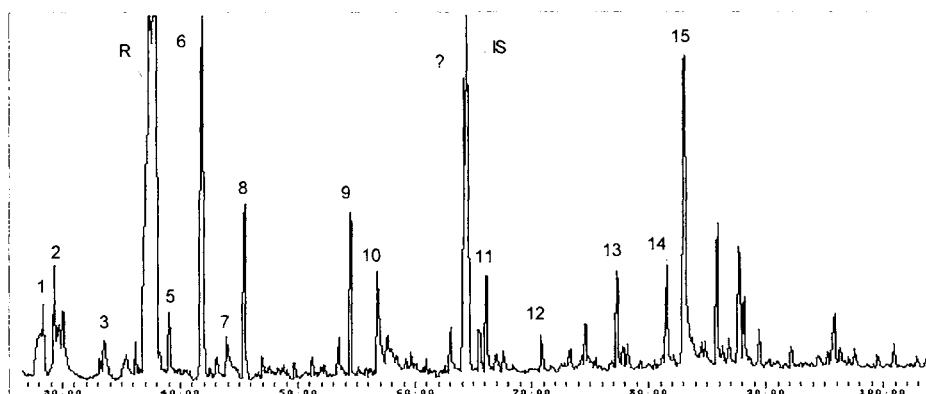


FIGURE 11.3.2. Chromatogram from a silylated pyrolysate obtained at 600° C from fructose/proline browning polymer. Separation done on a DB-5 column followed by MS detection.

The peak identification obtained by MS library search for the pyrogram shown in Figure 11.3.2 is given in Table 11.3.2.

TABLE 11.3.2. Compounds identified in the pyrogram from Figure 11.3.2 of a silylated pyrolysate obtained at 600° C from fructose/proline browning polymer (with the corresponding peak numbers).

Peak #	Compound	Formula	MW
1	lactic acid 2TMS	C9H22O3Si2	234
2	glycolic acid 2TMS	C8H20O3Si2	220
3	L-proline 2TMS	C11H25NO2Si2	259
4	2-ethyl-1-methyl-pyrrolidine	C7H15N	113
5	cyclohexancarboxylic acid TMS	C10H20O2Si	200
R	reagent		
6	2-(1-pyrrolidinyl)-2-cyclopentan-1-ol TMS	C12H25NOSi	227
7	4-hydroxy-piperidinyl carboxylate 2 TMS	C12H25NO3Si2	287
8	erythronic acid γ -lactone 2 TMS	C10H22O4Si2	262
9	4-hydroxy-cyclohexyl carboxylate 2 TMS	C13H28O3Si2	288
10	4-ethyl-1-isopropyl-2-pyrazolone ?	C8H16N2	140
11	(1-pyrrolidinyl)-cyclopentanol TMS isomer	C12H25NOSi	227
12	levoglucosan 3 TMS	C15H34O5Si3	378
13	glucosamine 4 TMS	C18H45NO5Si4	467
14	p-aminophenol 2 TMS	C12H23NOSi2	253
15	octahydro-5H,10H-dipyrrolo[1,2-a:1',2'-d]pyrazine-5,10-dione	C10H14N2O2	194

Pyrolysis products of the proline/fructose Maillard polymer show typical products for the pyrolysis of proline and of peptides containing proline. The sugar moiety is also shown by the presence of cyclopentenone derivatives (e.g. 2-hydroxy-3-methyl-2-cyclopenten-

1-one) or pyran derivatives. However, only a low level of levoglucosan is seen in the chromatograms.

The similarity between peptide pyrolysis products and the pyrolysis products of the corresponding Amadori polymer were also reported for other model melanoidins [17]. Figure 11.3.3 shows the Py-MS spectrum for the melanoidin obtained from glucose and tyrosine compared to the Py-MS spectrum for a polypeptide from tyrosine. Figure 11.3.4 shows the Py-MS spectrum for the melanoidin obtained from glucose and methionine compared to the Py-MS spectrum for a polypeptide from methionine, and Figure 11.3.5 shows the same pair for galactose and lysine.

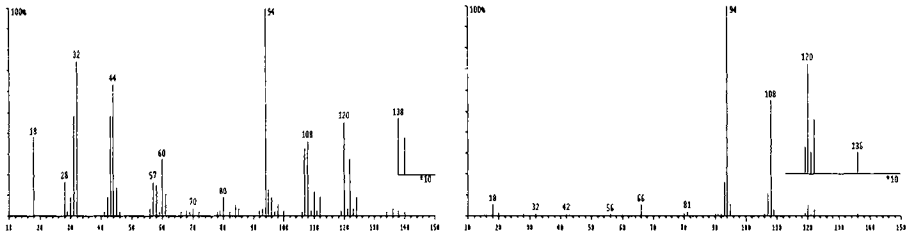


FIGURE 11.3.3. Py-MS spectrum for the melanoidin obtained from glucose and tyrosine, compared to the Py-MS spectrum for a polypeptide from tyrosine.

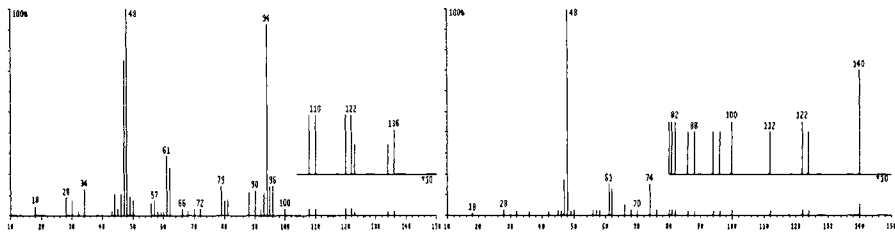


FIGURE 11.3.4. Py-MS spectrum for the melanoidin obtained from glucose and methionine, compared to the Py-MS spectrum for a polypeptide from methionine.

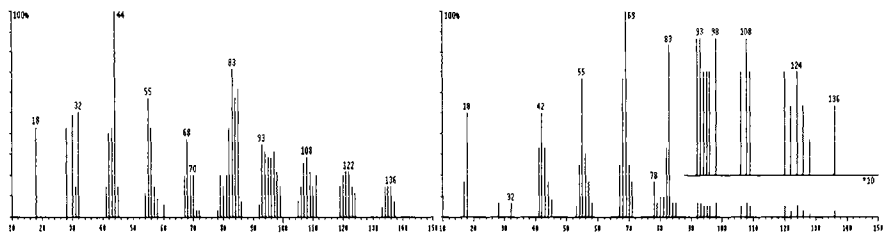
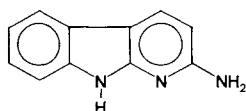


FIGURE 11.3.5. Py-MS spectrum for the melanoidin obtained from galactose and lysine, compared to the Py-MS spectrum for a polypeptide from lysine.

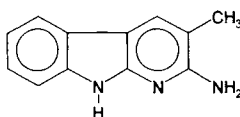
The similarity between the spectra of the melanoidin and the peptide is obvious. It is possible that the sugar moiety is modified substantially, which makes the melanoidin spectrum not resemble the sugar spectrum.

One more aspect of the polymer formation in the Maillard reaction between an amino acid and a reducing sugar, is the possibility that during the reaction, the amino acid undergoes decompositions (such as Strecker degradation or hydrolysis of the amide group for asparagine and glutamine) and generates in-situ ammonia. Ammonia is more reactive than amino acids in the reaction with reducing sugars, and polymers of the type described in Section 11.2 are likely to be formed.

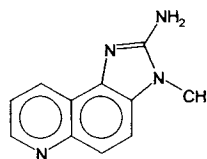
A special concern regarding the pyrolysis of Maillard polymers is the formation in this process of mutagenic compounds. Some of these compounds were isolated from pyrolysed food [5,6]. The formulas of several such compounds are shown below:



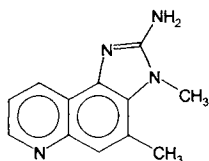
2-amino-9H-pyrido[2,3-b]indole (AαC), from soybean globulin pyrolysate



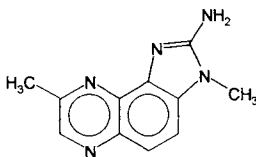
2-amino-3-methyl-9H-pyrido[2,3-b]indole, (MeAαC) from soybean globulin pyrolysate



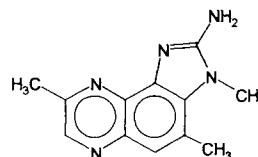
2-amino-3-methylimidazo[4,5-f]quinoline, (IQ) from broiled sardines



2-amino-3,4-dimethylimidazo[4,5-f]quinoline (MeIQ) from broiled sardines

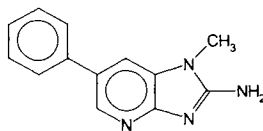


2-amino-3,8-dimethylimidazo[4,5-f]quinoxaline (MeIQx) from fried beef



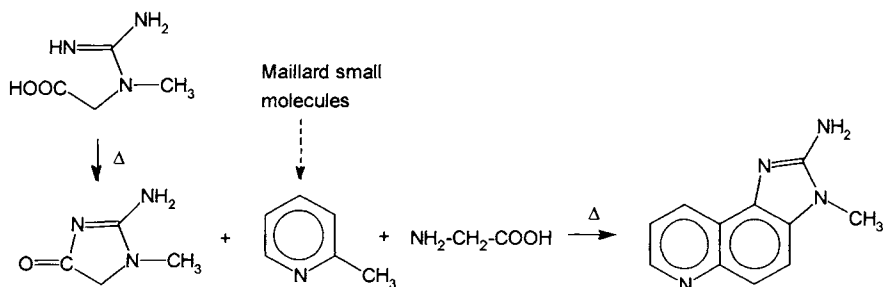
2-amino-3,4,8-trimethylimidazo[4,5-f]quinoxaline (4,8-diMeIQx) from fried beef

PhIP was detected in sidestream smoke of cigarettes [18]:



2-amino-1-methyl-6-phenylimidazo[4,5-b]pyridine (PhIP) from cigarette sidestream smoke

The association of Maillard polymer pyrolysis with the formation of these compounds is based on the correlation of the level of sugars and amino acids with the level of mutagen formation. Also, it was shown that the presence of creatinine (common in animals) may play an important role in the formation of these compounds, and a reaction path as shown below was proposed [19]:



In this reaction, creatine generates creatinine that reacts with a pyridine or a pyrazine (formed from the Maillard reaction) and an amino acid (glycine, alanine, etc.) to form the heterocyclic amine.

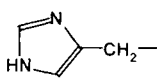
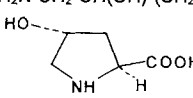
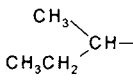
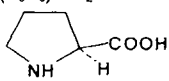
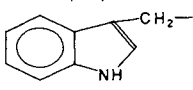
References 11.

1. W. Baltes, *J. Anal. Appl. Pyrol.*, 8 (1985) 533.
2. P. A. Finot, H. U. Aeschbacher, R. F. Hurrell (ed.), *The Maillard Reaction in Food Processing, Human Nutrition and Physiology*, Birkhauser Verlag, Basel, 1990.
3. W. Baltes, *Fresenius Z. Anal. Chem.*, 327 (1987) 220.
4. R. Hardt, H. Tschiersky, W. Baltes, *Fresenius Z. Anal. Chem.*, 331 (1988) 433.
- 4a. R. Hardt, W. Baltes, *Z. Lebensm.-Unters Forsch.*, 185 (1987) 275.
5. G. R. Waller, M. S. Feather (ed.), *The Maillard Reaction in Food and Nutrition*, ACS Simp. Ser. 215, Washington, 1983.
6. J. C. Leffingwell, *Recent Adv. Tob. Sci.*, 2 (1978) 1.
7. W. W. Weeks, M. P. Campos, S. C. Moldoveanu, *J. Agr. Food Chem.*, 41 (1993) 1321.
8. C. A. Lobry de Bruin, *Rec. Trav. Chim.*, 18 (1899) 72.
9. M. X. Wang, S. C. Moldoveanu, J. H. Lauterbach, unpublished results.
10. H. Tsuchida, M. Komoto, H. Kato, T. Kurata, M. Fujimaki, *Agr. Biol. Chem.*, 40 (1976) 2051.
11. W. W. Weeks, M. P. Campos, S. C. Moldoveanu, *J. Agr. Food Chem.*, 43 (1995) 2247.
12. R. Schrodter, W. Baltes, *J. Anal. Appl. Pyrol.*, 27 (1993) 145.

13. W. Hortig, W. Balthes, *J. Anal. Appl. Pyrol.*, 2 (1980/1981) 321.
14. T. Hayashi, M. Namiki, *Agr. Biol. Chem.*, 45 (1981), 933.
15. A. F. Ghiron, B. Quack, T. P. Mawhinney, M. Feather, *J. Agr. Food Chem.*, 36 (1988) 677.
16. S. C. Moldoveanu, N. P. Kulshreshtha, J. B. Forehand, unpublished results.
17. J. J. Boon, J. W. de Leeuw, Y. Rubinsztain, Z. Aizenshtat, P. Ioselis, R. Ikan, *Org. Geochem.*, 6 (1984) 805.
18. H. Kataoka, K. Kijima, G. Maruo, *Bull. Environ. Contam. Toxicol.*, 60 (1998) 60.
19. T. Sugimura, T. Kawachi, M. Nagao, T. Yahagi, Y. Sano, T. Okamoto, K. Shudo, T. Kosuge, K. Tsuji, K. Wakabayashi, Y. Iitake, A. Itai, *Proc. Japan Acad.*, 53B (1977) 58.

This Page Intentionally Left Blank

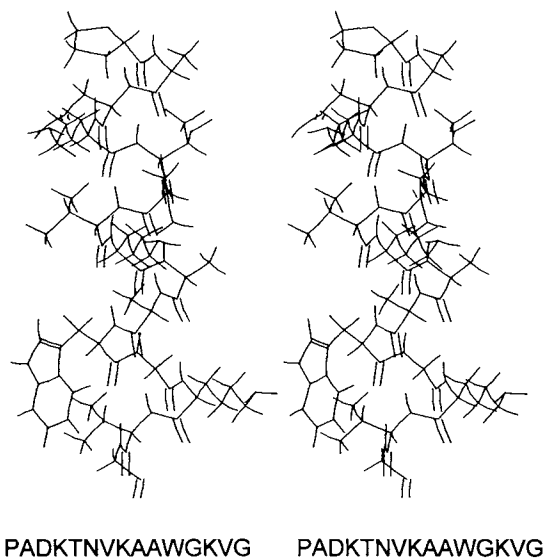
TABLE 12.1.1. *Amino acids present in proteins.*

Name	Abbrev. (three-letter)	Abbrev. (one-letter)	Radical R connected to the α -carbon (see Note)	MW	Formula
alanine	Ala	A	CH ₃ -	89.09	C ₃ H ₇ NO ₂
arginine	Arg	R	$\begin{array}{c} \text{HN} \\ \parallel \\ \text{C}-\text{NHCH}_2\text{CH}_2\text{CH}_2- \\ \\ \text{H}_2\text{N} \end{array}$	174.20	C ₆ H ₁₄ N ₄ O ₂
asparagine	Asn	N	H ₂ N-CO-CH ₂ -	132.12	C ₄ H ₈ N ₂ O ₃
aspartic acid	Asp	D	HOOC-CH ₂ -	133.10	C ₄ H ₇ NO ₄
cysteine	Cys	C	HS-CH ₂ -	121.16	C ₃ H ₇ NO ₂ S
cystine	Cys-Cys		-CH ₂ -S-S-CH ₂ -	240.30	C ₆ H ₁₂ N ₂ O ₄ S ₂
glutamic acid	Glu	E	HOOC-CH ₂ CH ₂ -	147.13	C ₅ H ₉ NO ₄
glutamine	Gln	Q	H ₂ N-CO-CH ₂ CH ₂ -	146.15	C ₅ H ₁₀ N ₂ O ₃
glycine	Gly	G	H-	75.07	C ₂ H ₅ NO ₂
histidine	His	H		155.16	C ₆ H ₉ N ₃ O ₂
hydroxylysine	Hyl		H ₂ N-CH ₂ -CH(OH)-(CH ₂) ₂ -	162.19	C ₆ H ₁₄ N ₂ O ₃
hydroxyproline	Hyp			131.13	C ₅ H ₉ NO ₃
isoleucine	Ile	I		131.17	C ₆ H ₁₃ NO ₂
leucine	Leu	L	(CH ₃) ₂ CHCH ₂ -	131.17	C ₆ H ₁₃ NO ₂
lysine	Lys	K	H ₂ N-(CH ₂) ₄ -	146.19	C ₆ H ₁₄ N ₂ O ₂
methionine	Met	M	CH ₃ SCH ₂ CH ₂ -	149.21	C ₅ H ₁₁ NO ₂ S
phenylalanine	Phe	F	(C ₆ H ₅)-CH ₂ -	165.19	C ₉ H ₁₁ NO ₂
proline	Pro	P		115.13	C ₅ H ₉ NO ₂
serine	Ser	S	HO-CH ₂ -	105.09	C ₃ H ₇ NO ₃
threonine	Thr	T	CH ₃ -CH(OH)-	119.12	C ₄ H ₉ NO ₃
tryptophan	Trp	W		204.22	C ₁₁ H ₁₂ N ₂ O ₂
tyrosine	Tyr	Y	HO-(C ₆ H ₄)-CH ₂ -	181.19	C ₉ H ₁₁ NO ₃
valine	Val	V	(CH ₃) ₂ CH-	117.15	C ₅ H ₁₁ NO ₂

Note: whole formulas are shown for proline and hydroxyproline.

Proteins are basically formed from one or more chains of polypeptides (with a particular primary structure). The chains of amino acids in proteins, being very long, can coil and fold. This spatial arrangement of amino acids is described by the secondary and tertiary structures of proteins. The arrangement of the amino acids that are near one another in the linear sequence is described by the secondary structure. For example, the amino acids may generate a helical structure (α -helix) such that the amino acids chain forms a tridimensional rod, and the amino acids that are four units apart can have hydrogen bonds between their N-H and C=O groups. An example of a stereo view of an α -helix

with the sequence PADKTNVKAAWGKVG, which is a portion of one of the hemoglobin polypeptide chains, is shown below (one sheet of white paper kept perpendicular on the page is needed to separate the two fields of vision for a stereo view):



The same amino acid sequence is shown in Figure 12.1.1 with the α helix indicated by a ribbon.

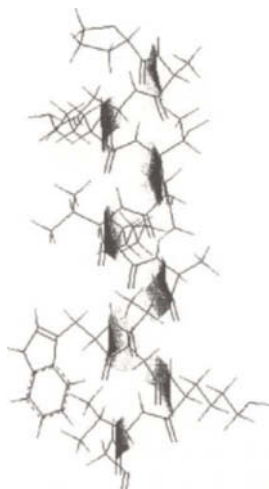


FIGURE 12.1.1. α -helix made by the sequence of amino acids PADKTNVKAAWGKVG.

Another typical secondary structure is the β -sheet. Tertiary structure describes the spatial arrangement of amino acid residues that are far apart (such as folding of parts of the protein connected by disulfidic bonds).

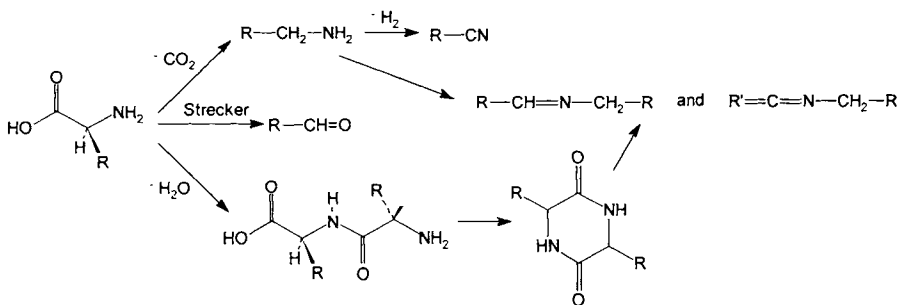
For proteins that are made from more than one chain, information on a quaternary structure is needed to describe the position of each subunit. Under the influence of heat, organic solvents, or salts, protein molecules may undergo changes in secondary, tertiary, or quaternary structures that can be irreversible. This process is called denaturation of proteins and is not exhibited by polypeptides, being one common criterion for their differentiation.

Pyrolysis studies on proteins have been done for a variety of purposes. One of these is to obtain information on the primary structure of proteins (amino acid sequence) [1]. Also pyrolysis has been used for differentiating different proteinaceous materials such as enzymes or microorganisms. Also, the generation of mutagenic compounds by pyrolysis of proteins has been of significant interest related to food and consumer products [2].

- Pyrolysis of amino acids.

The amino acid pyrolysis is relevant for protein pyrolysis because certain compounds in the pyrolysate are the same when the substance to be pyrolysed is the amino acid or a peptide formed from that specific amino acid (see Section 13.2). The main pyrolysis products of several amino acids are given in Table 12.1.2 [3,4].

The mechanisms of generating the compounds shown in Table 12.1.2 were already discussed in Section 3.5. The main mechanisms are the decarboxylation by CO_2 elimination or the water elimination with the formation of a dipeptide and further of the diketopiperazines. By Strecker degradation, amino acids may also be converted to aldehydes.



Other reactions are also possible. For example, R-H type compounds may be generated, and this is characteristic mainly for the aromatic amino acids. Smaller molecules, some unsaturated, are also formed by further decompositions. The compounds of the type $\text{R}-\text{CH}=\text{N}-\text{CH}_2-\text{R}$ and $\text{R}'=\text{C}=\text{N}-\text{CH}_2-\text{R}$ are formed mainly from aliphatic amino acids (Ala, Val, Leu, Ile).

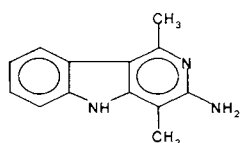
TABLE 12.1.2. *The main pyrolysis products of several amino acids.*

Alanine	MW	Formula
methylamine	31	CH ₅ N
3,4-dimethylpiperazin-2,5-dione	142	C ₆ H ₁₀ N ₂ O ₂
Arginine	MW	Formula
pyrroline	69	C ₄ H ₇ N
3-amino-2-piperidone	114	C ₅ H ₁₀ ON ₂
Asparagine	MW	Formula
maleimide	97	C ₄ H ₃ O ₂ N
succinimide	99	C ₄ H ₅ O ₂ N
Cysteine	MW	Formula
methylpyridine	93	C ₆ H ₇ N
methylthiazolidine	103	C ₄ H ₉ NS
methylethylthiazole	127	C ₆ H ₉ NS
Glutamine	MW	Formula
pyrrole	67	C ₄ H ₅ N
2,3-dehydro-2-piperidone	83	C ₄ H ₅ ON
methyl-2,3-dehydro-2-piperidone	97	C ₅ H ₇ ON
Hydroxyproline	MW	Formula
pyrroline	69	C ₄ H ₇ N
pyrrole	67	C ₄ H ₅ N
2-ethylpyrrole	95	C ₆ H ₉ N
1H-2,3-dihydropyrrole-2-carboxylic acid	113	C ₅ H ₇ O ₂ N
1,2-dipyrrolylethane	160	C ₁₀ H ₁₂ N ₂
1,3-dipyrrolylpropane	174	C ₁₁ H ₁₄ N ₂
diketodipyrrole	186	C ₁₀ H ₆ O ₂ N ₂
Isoleucine	MW	Formula
butanenitrile	69	C ₄ H ₇ N
2-methylbutene	70	C ₅ H ₁₀
2-methylbutanal	86	C ₅ H ₁₀ O
2-methylbutyronitrile	83	C ₅ H ₉ N
2-methylbutylamine	87	C ₅ H ₁₃ N
1-butanamine-2-methyl-N-(2-methylbutylidene)	155	C ₁₀ H ₂₁ N
3,6-(2-methylpropyl)-2,5-diketopiperazine	226	C ₁₂ H ₂₂ O ₂ N ₂
Leucine	MW	Formula
butanenitrile	69	C ₄ H ₇ N
3-methylbutene	70	C ₅ H ₁₀
3-methylbutanal	86	C ₅ H ₁₀ O
3-methylbutyronitrile	83	C ₅ H ₉ N
3-methylbutylamine	87	C ₅ H ₁₃ N
1-butanamine-3-methyl-N-(3-methylbutylidene)	155	C ₁₀ H ₂₁ N
3,6-diisobutyl-2,5-diketopiperazine	226	C ₁₂ H ₂₂ O ₂ N ₂

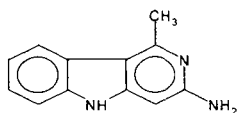
TABLE 12.1.2. *The main pyrolysis products of several amino acids (continued).*

Lysine	MW	Formula
pyrroline	69	C ₄ H ₇ N
3-aminohexahydroazepinone	128	C ₆ H ₁₂ O ₂ N ₂
Methionine	MW	Formula
methanethiol	48	CH ₄ S
vinyl-1-methylthioether	74	C ₃ H ₆ S
propane-1-methylthioether	90	C ₄ H ₁₀ S
3-methylthio-1-propylamine	105	C ₄ H ₁₁ NS
1-propanamine-N-(3-methylthiopropylidene)	145	C ₇ H ₁₅ NS
Phenylalanine	MW	Formula
toluene	92	C ₇ H ₈
ethylbenzene	106	C ₈ H ₁₀
ethenylbenzene	104	C ₈ H ₈
benzene-ethaneamine	121	C ₈ H ₁₁ N
phenylacetoneitrile	117	C ₈ H ₇ N
diphenylethane	182	C ₁₄ H ₁₄
Proline	MW	Formula
pyrroline	69	C ₄ H ₇ N
pyrrolidine	71	C ₄ H ₉ N
2,5-diketopiperazine	194	C ₁₀ H ₁₄ O ₂ N ₂
Tryptophan	MW	Formula
indole	117	C ₈ H ₇ N
3-methylindole	131	C ₉ H ₉ N
3-ethenylindole	143	C ₁₀ H ₉ N
3-ethylindole	145	C ₁₀ H ₁₁ N
2,3-dimethylindole	145	C ₁₀ H ₁₁ N
indole-3-ethanamine	160	C ₁₀ H ₁₂ N ₂
indolylacetoneitrile	170	C ₁₁ H ₁₀ N ₂
Tyrosine	MW	Formula
phenol	94	C ₆ H ₆ O
4-methylphenol	108	C ₇ H ₈ O
4-ethylphenol	122	C ₈ H ₁₀ O
4-ethenylphenol	120	C ₈ H ₈ O
phenyl-acetaldehyde	120	C ₈ H ₈ O
4-hydroxyphenetylamine	137	C ₈ H ₁₁ ON
Valine	MW	Formula
isobutene	56	C ₄ H ₈
2-methylpropanal	72	C ₄ H ₈ O
2-methylpropionitrile	69	C ₄ H ₇ N
2-methyl-1-propanamine	73	C ₄ H ₁₁ N
methylamine-N-(2-methylpropylidene)	85	C ₅ H ₁₁ N
ethylamine-N-(2-methylpropylidene)	99	C ₆ H ₁₃ N
2-methylpropylamine-N-(2-methylpropylidene)	127	C ₈ H ₁₇ N
3-isopropyliden-2,5-diketopiperazine	154	C ₇ H ₁₀ O ₂ N ₂
3,6-diisopropyl-2,5-diketopiperazine	198	C ₁₀ H ₁₈ O ₂ N ₂

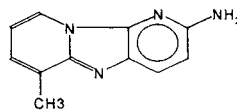
Besides the determination of major pyrolysis products for amino acids, a special issue is the formation of several mutagenic compounds (heterocyclic amines) during pyrolysis. These types of compounds were detected in traces in the pyrolysates of amino acids, and the finding is very important as the amino acids are components of proteins and are present in food. Some of these compounds isolated from pyrolysates performed at 550° C from several amino acids [5,6] are shown below:



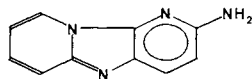
3-amino-1,4-dimethyl-
5H-pyrido[4,3-b]indole
(from tryptophan), Trp-P-1



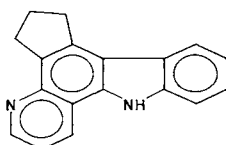
3-amino-1-methyl-
5H-pyrido[4,3-b]indole
(from tryptophan), Trp-P-2



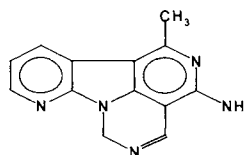
2-amino-6-methylpyrido-
[1,2-α:3',2'-d]imidazole
(from glutamic acid) Glu-P-1



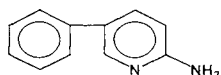
2-aminodipyrido-
[1,2-α:3',2'-d]imidazole
(from glutamic acid), Glu-P-2



3,4-cyclopentenopyrido-
[3,2-α]carbazole
(from lysine), Lys-P-1

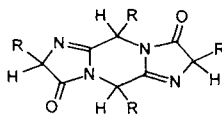
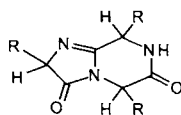


4-amino-6-methyl-1H-
2,5,10,10b-tetraaza-
fluoranthene
(from ornithine), Orn-P-1



2-amino-5-phenylpyridine
(from phenylalanine), Phe-P-1

The mechanism of formation of heterocyclic amines from amino acid pyrolysis has been studied on several model compounds [7,8]. Also, as indicated in Section 12.3, the interaction with sugars and creatinine may favor the formation of these heterocyclic amines. A variety of other conditions may influence the formation of these compounds. During pyrolysis plant materials generate lower amounts of mutagenic compounds as compared to animal materials, possibly due to the absence of creatine in plants. However, a mutagen 2-amino-1-methyl-6-phenylimidazo[4,5-b]pyridine was detected in cigarette smoke [8]. Also, it has been shown that thermal decomposition of amino acids at 250° C on a silica support generates condensation products of the type:



(Ala) R = CH₃

(Val) R = CH(CH₃)₂

(Leu) R = CH₂CH(CH₃)₂

The hexahydroimidazo[1,2-a]pyrazine-3,6-dione (with R = CH₃) was also identified in a pyrolysate of alanine in a pyrolytic reactor at 500° C [8a]. These types of compounds are generated through formation of linear dipeptides that were also identified in the pyrolysate.

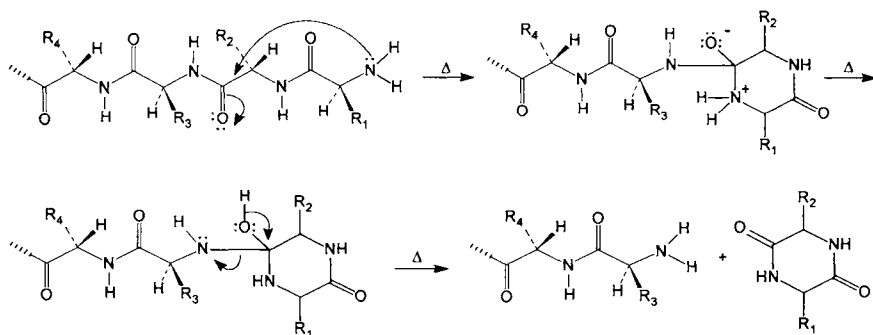
12.2. Peptides.

Pyrolysis of simple peptides offers models for understanding the pyrolysis results of larger polypeptides and proteins. Also, special types of peptides of practical interest are those with antibiotic properties such as the actinomycins containing peptide side-chains, etc. Their pyrolysis has been proven to be useful for structure elucidation and identification [9]. Other polypeptides with therapeutic use such as lypressin and felypressin were also studied by pyrolysis [10].

Among the simple peptides for which pyrolysis studies have been performed [11–13] are Gly-Gly, Gly-Pro [11, 11a], Val-Pro, Pro-Val, Ala-Pro, Pro-Ala, Ala-Gly, Gly-Ala [13], Phe-Leu-Met, Met-Leu-Phe, Phe-Met-Leu, Tyr-Tyr-Phe, Leu-Leu-Leu, Ala-Phe-Leu-Met, Ala-Met-Leu-Phe, Ala-Phe-Leu-Met-Tyr, Ala-Tyr-Leu-Met-Phe, Ala-Tyr-Leu-Met-Phe-Phe, Ala-Phe-Leu-Met-Tyr-Phe, Phe-Ala-Phe-Leu-Met-Tyr [13].

One type of compound generated by pyrolysis of simple peptides consists of small molecules similar to those obtained from the pyrolysis of component amino acids such as hydrocarbons (aromatic hydrocarbons from peptides containing Phe or Tyr), aldehydes, pyrrole, pyrroline, indole (from peptides containing TRP), some aliphatic amines, etc.

Another main type of pyrolysis products for peptides includes the diketopiperazines (DKP) and their secondary fragmentation products. The formation of DKP from oligopeptides showed that the generation of DKPs always takes place from neighboring amino acids. The mechanism of DKP formation seems to be the following:



For dipeptides the eliminated molecule is water, for tripeptides it is an amino acid, from tetrapeptides a dipeptide, etc. This explains the formation of DKPs as shown in Table 12.2.1.

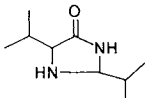
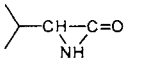
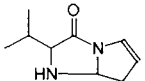
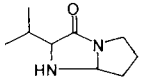
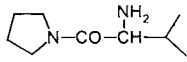
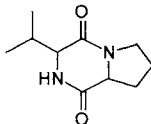
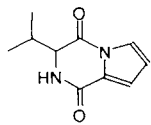
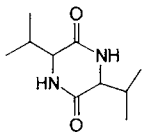
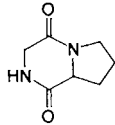
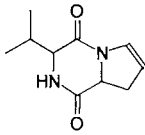
The type of DKP formed and the amount that can be detected in the pyrolysate may also be influenced by the nature and stability of the R group of a particular amino acid in the peptide sequence. In addition to this, the pyrolysis conditions were found to influence the amount of DKPs. Milder pyrolytic conditions favored more DKP formation, while higher temperatures of pyrolysis generated more small molecules, as expected.

TABLE 12.2.1. DKP formation noticed from different oligopeptides [9].

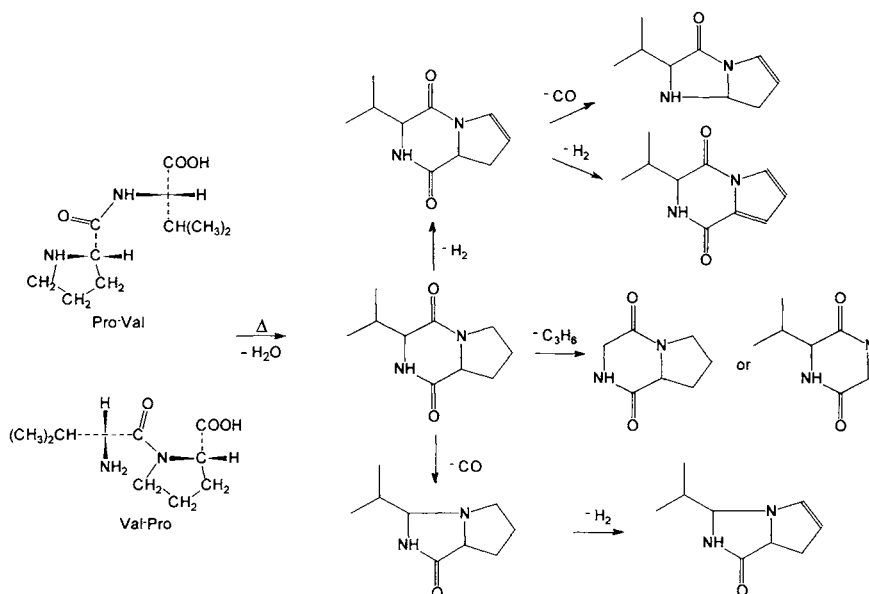
Oligopeptide	DKP type
A-B	A-B
A-B-C	A-B and smaller amount of B-C
A-B-C-D	A-B and C-D (B-C not observed [13])
A-B-C-D-E	A-B, C-D, etc.
A-B-C-D-E-F	A-B, C-D, E-F

The production of DKPs when one amino acid is proline leads to the formation of bicyclic compounds. As an example, several pyrolysis products for Val-Pro and Pro-Val obtained by Curie point pyrolysis at 510° C are given in Table 12.2.2.

TABLE 12.2.2. Several pyrolysis products for Val-Pro and Pro-Val.

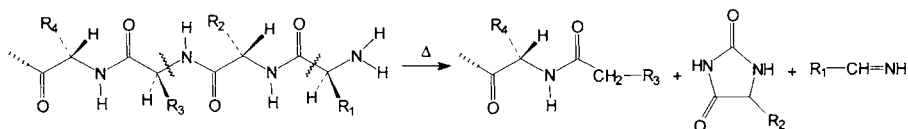
Product	MW	Product	MW
acetone	58		170
imidazole	68		99
pyrroline	69	cyanopyrrole	92
pyrrole	67		166
isobutyramide	87		168
	170		196
	192		198
	154		194

The compounds shown in Table 12.2.2 are generated by reactions of the type:

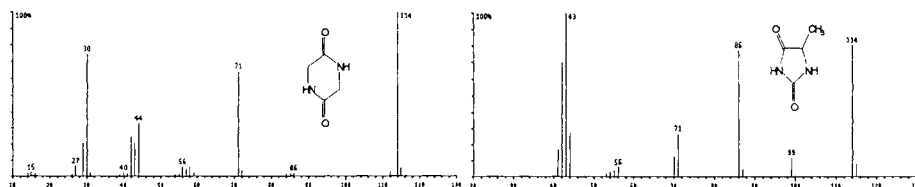


Direct pyrolysis of the DKPs corresponding to Pro-Val or Val-Pro was proven to generate the same types of compounds shown in Table 12.2.2. This is a proof that DKPs are the main primary pyrolysis products of these dipeptides. However, the pyrolysis of the dipeptides and their corresponding DKP does not generate identical pyrograms (chromatographic profiles of the pyrolysates). Therefore, some other processes may take place during the pyrolysis of each compound.

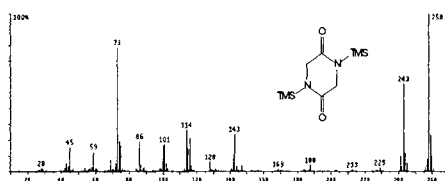
An alternative route for dipeptide pyrolysis may be the formation of substituted imidazolindiones.



The formation of imidazolindiones was not confirmed as coming from further thermal decomposition of diketopiperazines [11]. The identification of diketopiperazines was commonly done based on their mass spectra. The mass spectra of DKPs are different from the spectra of substituted 2,4 imidazolindiones as it can be seen in the spectra of diketopiperazine and 5-methyl-2,4-imidazolindione (both with MW = 114) that are shown in Figures 12.2.1a and 12.2.1b respectively.

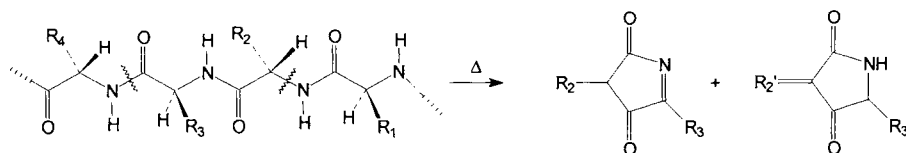
FIGURE 12.2.1a. *MS of diketopiperazine.*FIGURE 12.2.1b. *MS of 5-methyl-2,4-imidazolindione.*

When the GC/MS analysis is done following a derivatization such as silylation, the differentiation of the two types of compounds is not simple because only a limited number of spectra for derivatized compounds is available. For example, in common mass spectral libraries (NBS, Wiley) only the spectrum of the TMS derivative of (non substituted) diketopiperazine is reported (see Figure 12.2.2) and not that of the corresponding imidazolindione. Therefore, not knowing the spectrum it is difficult to decide if certain imidazolindiones are present or not together with DKPs in the chromatograms of silylated pyrolysates of peptides.

FIGURE 12.2.2. *MS of trimethylsilyl derivative of diketopiperazine.*

The mechanism with the formation of DKPs is probably the most common in peptide pyrolysis.

Besides substituted diketopiperazines and imidazolindiones, it was also proposed that disubstituted pyrrolidin-diones are formed in polypeptide pyrolysis. The reaction was presumed to take place as follows:



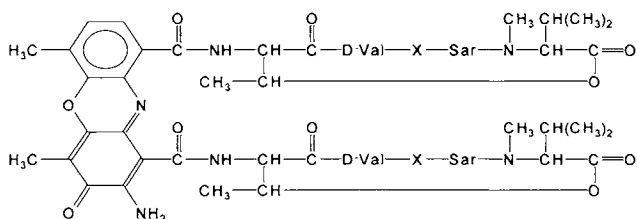
In this reaction, the formation of two series of compounds is proposed because in the chromatographic separations of polypeptide pyrolysates, an additional peak is noticed for each 3-alkenyl-5-alkyl-pyrrolidin-2,4-dione. This second peak is assigned to the corresponding 2,4-dialkyl-3,5-diketopyrroline (position isomers are not possible when R_2 and R_3 are identical) [1]. The list of different compounds from these two classes that may be formed during laser irradiation of different mammalian tissues [13a] due to peptide (protein) pyrolysis and the amino acid pair that can generate them is given in Table 12.2.3.

TABLE 12.2.3. 3-Alkenyl-5-alkyl-pyrrolidin-2,4-diones and 2,4-dialkyl-3,5-diketopyrrolines that can be formed from laser pyrolysis of mammalian tissues [13a].

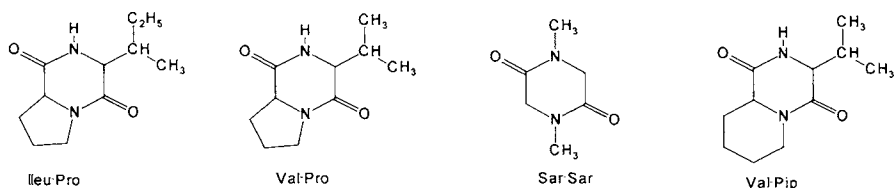
MW	Compound	Amino acid pair	Side-chain C
97	2H-pyrrole-3,5(3H)-dione	Gly-Gly	0
111	2-methyl-2H-pyrrole-3,5(3H)-dione	Ala-Gly	1
111	4-methyl-2H-pyrrole-3,5(3H)-dione	Gly-Ala	1
111	3-methylidene-pyrrolidine-2,4-dione	Gly-Ala	1
125	2,4-dimethyl-2H-pyrrole-3,5(3H)-dione	Ala-Ala	2
125	3-methylidene-5-methylpyrrolidine-2,4-dione	Ala-Ala	2
139	2-(2-methylethyl)-2H-pyrrole-3,5(3H)-dione	Val-Gly	3
139	4-(2-methylethyl)-2H-pyrrole-3,5(3H)-dione	Gly-Val	3
139	3-(2-methylethylidene)-pyrrolidine-2,4-dione	Gly-Val	3
153	4-(2-methylpropyl)-2H-pyrrole-3,5(3H)-dione	Gly-Leu	4
153	4-(3-methylpropyl)-2H-pyrrole-3,5(3H)-dione	Gly-Ileu	4
153	2-methyl-4-(2-methylethyl)-2H-pyrrole-3,5(3H)-dione	Ala-Val	4
153	4-methyl-2-(2-methylethyl)-2H-pyrrole-3,5(3H)-dione	Val-Ala	4
153	2-(2-methylpropyl)-2H-pyrrole-3,5(3H)-dione	Leu-Gly	4
153	2-(3-methylpropyl)-2H-pyrrole-3,5(3H)-dione	Ileu-Gly	4
153	3-methylidene-5-(2-methylethyl)-pyrrolidine-2,4-dione	Val-Ala	4
153	5-methyl-3-(2-methylethylidene)-pyrrolidine-2,4-dione	Ala-Val	4
153	3-(2-methylpropylidene)-pyrrolidine-2,4-dione	Gly-Leu	4
153	3-(3-methylpropylidene)-pyrrolidine-2,4-dione	Gly-Ileu	4
167	2-methyl-4-(2-methylpropyl)-2H-pyrrole-3,5(3H)-dione	Ala-Leu	5
167	2-methyl-4-(3-methylpropyl)-2H-pyrrole-3,5(3H)-dione	Ala-Ileu	5
167	2-(2-methylpropyl)-4-methyl-2H-pyrrole-3,5(3H)-dione	Leu-Ala	5
167	2-(3-methylpropyl)-4-methyl-2H-pyrrole-3,5(3H)-dione	Ileu-Ala	5
167	3-(2-methylpropylidene)-5-methyl-pyrrolidine-2,4-dione	Ala-Leu	5
167	3-(3-methylpropylidene)-5-methyl-pyrrolidine-2,4-dione	Ala-Ileu	5
167	3-methylene-5-(2-methylpropyl)-pyrrolidine-2,4-dione	Leu-Val	5
167	3-methylene-5-(3-methylpropyl)-pyrrolidine-2,4-dione	Ileu-Ala	5
181	2,4-bis(2-methylethyl)-2H-pyrrole-3,5(3H)-dione	Val-Val	6
181	3-(2-methyl)ethylidene-5-(2-methyl)ethyl-pyrrolidine-2,4-dione	Val-Val	6
195	2-(2-methylethyl)-4-(2-methylpropyl)-2H-pyrrole-3,5(3H)-dione	Val-Leu	7
195	2-(2-methylethyl)-4-(3-methylpropyl)-2H-pyrrole-3,5(3H)-dione	Val-Ileu	7
195	2-(2-methylpropyl)-4-(2-methylethyl)-2H-pyrrole-3,5(3H)-dione	Leu-Val	7
195	2-(3-methylpropyl)-4-(2-methylethyl)-2H-pyrrole-3,5(3H)-dione	Ileu-Val	7
195	3-(2-methylpropylidene)-5-(2-methylethyl)-pyrrolidine-2,4-dione	Val-Leu	7
195	2-(2-methylethyl)-4-(3-methylpropyl)-(2H)-pyrrole-2,4-dione	Val-Ileu	7
195	3-(2-methylethylidene)-5-(2-methylpropyl)-pyrrolidine-2,4-dione	Leu-Val	7
195	3-(3-methylethylidene)-5-(3-methylpropyl)-pyrrolidine-2,4-dione	Ileu-Val	7
209	3,5-bis(2-methylpropyl)-2H-pyrrole-3,5(3H)-dione	Leu-Leu	8
209	3-(2-methylpropyl)-5-(3-methylpropyl)-2H-pyrrole-3,5(3H)-dione	Ileu-Leu	8
209	3-(3-methylpropyl)-5-(2-methylpropyl)-2H-pyrrole-3,5(3H)-dione	Leu-Ileu	8
209	3,5-(3-methylpropyl)-2H-pyrrole-3,5(3H)-dione	Ileu-Ileu	8
209	3-(2-methylpropylidene)-5-(2-methylpropyl)-pyrrolidine-2,4-dione	Leu-Leu	8
219	3-(2-methylpropylidene)-5-(3-methylpropyl)-pyrrolidine-2,4-dione	Ileu-Leu	8
219	3-(3-methylpropylidene)-5-(2-methylpropyl)-pyrrolidine-2,4-dione	Leu-Ileu	8
219	3-(3-methylpropylidene)-5-(3-methylpropyl)-pyrrolidine-2,4-dione	Ileu-Ileu	8

Mass spectra of most of these compounds are not reported and therefore their identification by Py-GC/MS analysis is difficult. Only a small number of them were recognized in Curie point pyrolysates of peptides. A study on glycyl dipeptides [11a] showed that a common electron impact ionization shows the molecular ion of dipeptides, and also the ion $m/z = 113$ generated by the loss of substituents that takes place prior to ring fragmentation (except for Ala-Gly).

Polypeptide pyrolysis is important in connection with protein pyrolysis, but some studies were done on particular peptides such as actinomycins, which have antibiotic and cytostatic properties. Several actinomycins are known, the formulas for some of them being represented by:



where Sar = sarcosine (N-methyl glycine), X = proline in actinomycin D (C₁) and actinomycin C, X = sarcosine in actinomycin II, and X = piperolic acid (2-piperidinecarboxylic acid) in actinomycin Pip 2. Also, in actinomycin C, D-valine is replaced by D-allo-isoleucine. The structures of actinomycins have been investigated using pyrolytic techniques, and a series of diketopiperazines were identified in the pyrolysates [13b] such as those indicated below:

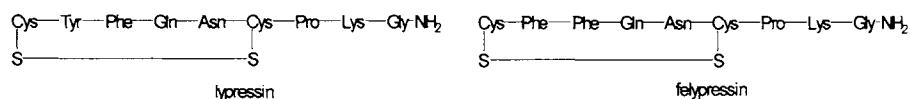


(where Pip = 2-piperidinecarboxylic acid).

Based on the structure of these diketopiperazines in each pyrolysate, it was possible to assign specific structures for actinomycins [13b].

As in many other cases, lower pyrolysis temperature has been proven to provide more information on the structure of the material that was pyrolysed. In the case of actinomycins, more informative results were obtained when the pyrolysis temperature was 400° C.

Regarding the use of pyrolysis to analyze lypressin and felypressin, the structure difference (absence of Tyr in felypressin) can be seen in the pyrolysate by the absence of cresol and phenol.



Another application of peptide pyrolysis is the study of silk. Pyrograms of minute pieces of fiber can be pyrolysed to identify the fingerprint of natural silk.

12.3. Simple Proteins.

Simple proteins (proteins) are formed from one or more chains of polypeptides. Although by hydrolysis they generate only amino acids, proteins can be extremely complex. Simple proteins are commonly classified based on their solubility, although this type of classification is far from perfect for such a complex group of compounds, mainly due to gradation in solubility. Based on their solubility proteins are classified as

- albumins (soluble in water, in dilute salts, acids, and bases, and precipitated with a 2M ammonium sulfate solution),
- globulins (insoluble in pure water but dissolved by dilute salts, acids or bases),
- glutelins (insoluble in neutral solvents including salt solutions, but dissolved by dilute acids or bases),
- prolamines (soluble in alcohol),
- scleroproteins (insoluble in most solvents),
- histones (basic proteins soluble in water but insoluble in a dilute ammonia solution), or
- protamines (similar to histones, but not coagulated by heat as are other soluble proteins).

The pyrolysis of simple proteins produces only compounds similar to those generated from peptides (see Section 12.2). This can be noticed for example in the pyrogram of two albumins [14], namely egg albumin, shown in Figure 12.3.1, and bovine serum albumin (crystallized, > 97% albumin), shown in Figure 12.3.2. Albumins contain low amounts of carbohydrates (however, they are not classified as glycoproteins). The pyrolysis of both egg albumin and bovine serum albumin were performed in a Curie point system at 510° C and analyzed by on-line GC/MS on a Carbowax column (60 m long, 0.32 mm i.d., 0.25 μm film thickness). For this analysis the GC separation was done using a temperature gradient between 35° C and 240° C.

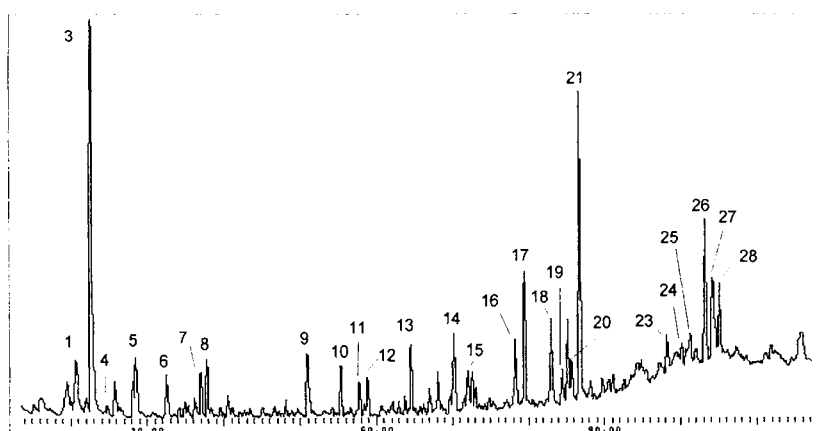


FIGURE 12.3.1. Pyrogram obtained at 510° C from egg albumin. Separation on a Carbowax column followed by MS detection.

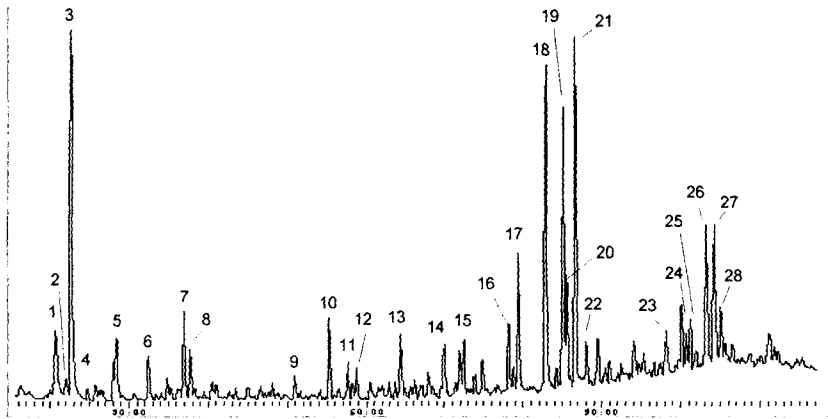


FIGURE 12.3.2. Pyrogram obtained at 510° C from bovine serum albumin. Separation on a Carbowax column followed by MS detection.

Table 12.3.1 shows some peak identifications for the pyrograms shown in Figures 12.3.1 and 12.3.2. In addition to these peaks, some other components such as CO or CO₂ are generated by pyrolysis. However, these very volatile molecules are not always captured in the TIC trace.

TABLE 12.3.1. Compounds identified in the pyrogram from egg and bovine serum albumin shown in Figures 12.3.1 and 12.3.2 (with the corresponding peak number).

Peak #	Compound	Formula	MW
1	acetonitrile	C ₂ H ₃ N	41
2	propanenitrile	C ₃ H ₅ N	55
3	toluene	C ₇ H ₈	92
4	water	H ₂ O	18
5	2-methyl-propanenitrile	C ₄ H ₇ N	69
6	pyridine	C ₅ H ₅ N	79
7	3-methylbutanenitrile	C ₅ H ₉ N	83
8	vinylbenzene	C ₈ H ₈	104
9	acetic acid	C ₂ H ₄ O ₂	60
10	pyrrole	C ₄ H ₅ N	67
11	2-methylpyrrole	C ₅ H ₇ N	81
12	3-methylpyrrole	C ₅ H ₇ N	81
13	methylbutanoic acid	C ₅ H ₁₀ O ₂	102
14	acetamide	C ₂ H ₅ NO	59
15	propanamide	C ₃ H ₇ NO	73
16	3-methylbutanamide	C ₅ H ₁₁ NO	101
17	benzenacetoneitrile	C ₈ H ₇ N	117
18	phenol	C ₆ H ₆ O	94
19	benzenepropanenitrile	C ₉ H ₉ N	131
20	4-methylpentanamide	C ₆ H ₁₃ NO	115
21	4-methylphenol	C ₇ H ₈ O	108
22	diphenylethane	C ₁₄ H ₁₄	196
23	piperidinone	C ₅ H ₉ NO	99
24	2,3-dihydrobenzofuran	C ₈ H ₈ O	120
25	pyridin carboxylic acid	C ₆ H ₅ NO ₂	123
26	1H-indole	C ₈ H ₇ N	117
27	2,5-pyrrolidindione	C ₄ H ₅ NO ₂	99
28	2-methyl-1H-indole	C ₉ H ₉ N	131

As can be seen from Figures 12.3.1 and 12.3.2 and from Table 12.3.1, the carbohydrate moiety is not detected because furfural, acetol, and other typical pyrolysis products from sugars are absent. However, in these pyrograms only the more volatile components can be seen. Several less volatile components can be seen in a GC analysis only after the pyrolysate is derivatized, for example, to generate trimethylsilyl derivatives (TMS). The chromatogram of the silylated pyrolysate (pyrolysis done at 510° C) from egg albumin is shown in Figure 12.3.3, and that from bovine serum albumin in Figure 12.3.4

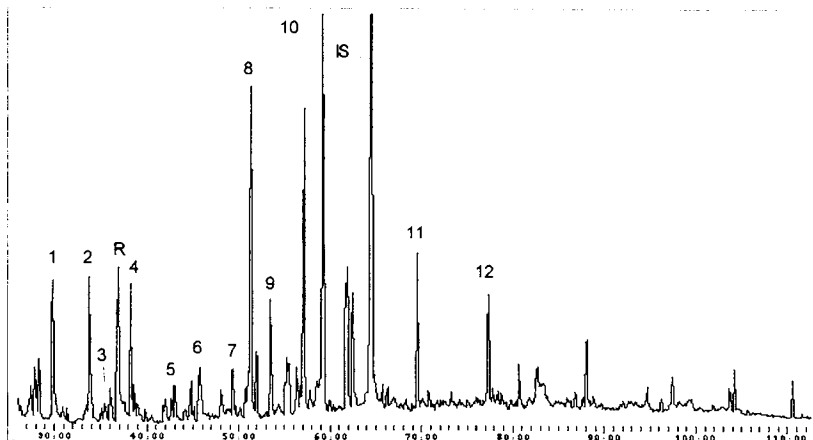


FIGURE 12.3.3. Chromatogram obtained from egg albumin pyrolysis at 510° C and silylation. Separation on a DB-5 column.

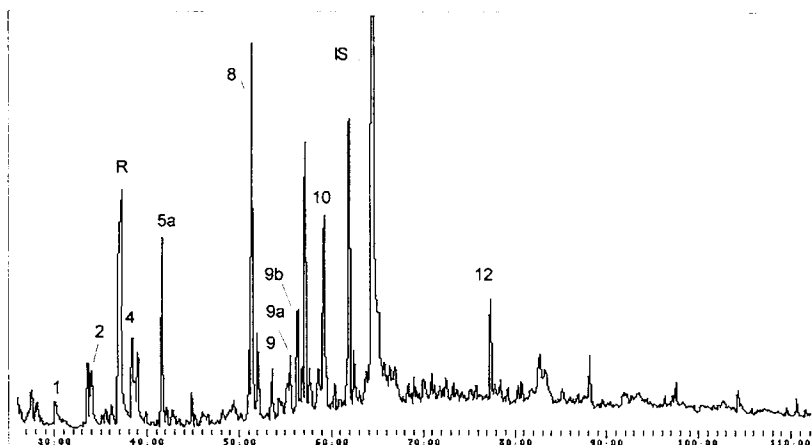


FIGURE 12.3.4. Chromatogram obtained from bovine serum albumin pyrolysis at 510° C and silylation. Separation on a DB-5 column.

The common procedure to generate silylated pyrolysates is to perform pyrolysis in a filament system followed by off-line derivatization with BSTFA. The chromatographic separation was done on a DB-5 column (60 m long, 0.32 mm i.d., 0.25 μ m film thickness) using a temperature gradient between 50° C and 300° C with detection by mass spectrometry. The compounds identified by mass spectral library search in the pyrograms from Figures 12.3.3 and 12.3.4 are listed in Table 12.3.2.

TABLE 12.3.2. *Compounds identified in the pyrograms from egg and bovine serum albumin shown in Figures 12.3.3 and 12.3.4.*

Peak #	Compound	Formula	MW
1	1H-pyrrole-2,5-dione TMS	C7H11NO2Si	169
2	4-methylphenol	C10H16OSi	80
3	3-methyl-1H-pyrrole-2,5-dione TMS	C8H13NO2Si	183
R	reagent ion 99		
4	3-methyl-2-(methylthio)-4(3H)-pyrimidinone	C6H8N2OS	156
5	3-vinylphenol TMS	C11H16OSi	192
5a	octanoic acid TMS	C11H24O2Si	216
6	pyrrol-2-carboxylic acid 2 TMS	C11H21NO2Si	255
7	4,5-dimethyl-2,6-dihydroxypyrimidine 2 TMS	C12H24N2O2Si2	284
8	dihydrouracyl 2 TMS	C10H22N2O2Si2	258
9	indole TMS	C11H15NSi	189
9a	parabanic acid 2 TMS	C9H18N2O3Si2	258
9b	dihydroxybenzene 2 TMS	C12H22O2Si2	254
10	5-oxoproline 2 TMS	C11H23NO3Si2	273
11	levoglucosan 3 TMS	C15H34O5Si3	378
12	glucosamine 4 TMS	C18H45NO5Si4	467

The silylated pyrolysate of the two albumins shows the presence of levoglucosan, which is a marker for the sugar moiety indicating the presence of carbohydrates. Besides the compounds seen by GC techniques, probably protein pyrolysates contain larger molecules, which are kept in the char that is formed in abundance in protein pyrolysis.

The similarity of the chromatograms from the two albumins showed significant differences. This proves the capability of Py-GC technique to differentiate between different types of proteins.

In protein analysis one important element is the purity of the enzyme and the procedure to obtain it. In many situations protein purification is not a simple step because of the lability of proteins. In many cases, the protein is associated with other components of the material from which it was obtained. As an example, the results for the analysis of the pyrolysate obtained from gluten at 510° C are discussed below. Gluten in this sample contained about 80% protein, 7% fats, and carbohydrates. The pyrolysis was first performed in a Curie point system and analyzed by on-line GC/MS on a Carbowax column in conditions similar to those previously described for the albumin analysis. The chromatogram is shown in Figure 12.3.5.

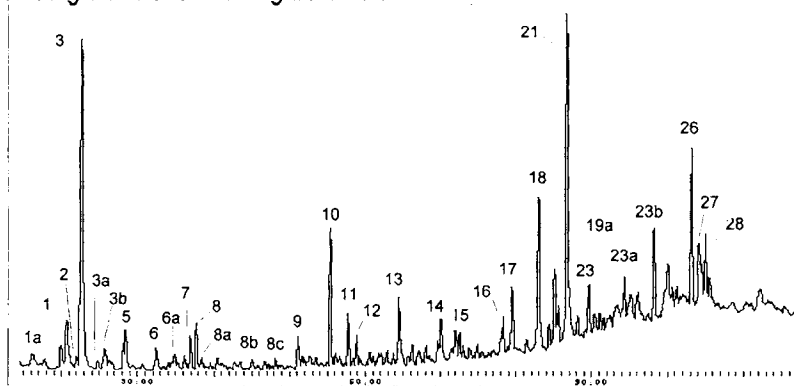


FIGURE 12.3.5. *Pyrogram obtained at 510° C from gluten. Separation on a Carbowax column.*

The compounds identified in the pyrogram from Figure 12.3.5 are similar to those found in albumin pyrolysates. However, some differences are noticed and the list of identified compounds is given in Table 12.3.3.

TABLE 12.3.3. *Compounds identified in the pyrogram of gluten shown in Figure 12.3.5.* The peak numbering was kept the same as in Figures 12.3.1 and 12.3.2, the additional peaks being labeled a, b, c....

Peak #	Compound	Formula	MW	*
1a	butanal	C4H8O	72	
1	acetonitrile	C2H3N	41	A
2	propanenitrile	C3H5N	55	A
3	toluene	C7H8	92	A
3a	dimehylsulfide	C2H6S2	94	
3b	2,3-dimethylbutandinitrile ?	C6H8N2	108	
5	2-methyl-propanenitrile	C4H7N	69	A
6	pyridine	C5H5N	79	A
6a	4-methylpyridine	C6H7N	93	
6b	4,4-dimethylvaleraldehyde ?	C8H14O	124	
7	3-methylbutanenitrile	C5H9N	83	A
8	vinylbenzene	C8H8	104	A
8a	methylpyrazine	C5H6N2	94	
8b	ethylpyridine	C7H9N	107	
8c	3-methylpyridine	C6H7N	93	
8d	1-propenylbenzene	C9H10	118	
9	acetic acid	C2H4O2	60	A
9a	piperidine	C5H11N	85	
10	pyrrole	C4H5N	67	A
11	2-methylpyrrole	C5H7N	81	A
12	3-methylpyrrole	C5H7N	81	A
12a	2,3-dimethylpyrrole	C6H9N	95	
13	methylbutanoic acid	C5H10O2	102	A
14	acetamide	C2H5NO	59	A
15	propanamide	C3H7NO	73	A
16	3-methylbutanamide	C5H11NO	101	A
17	benzenacetoneitrile	C8H7N	117	A
18	phenol	C6H6O	94	A
18a	hexanamide	C6H13NO	115	
19	benzenepropanenitrile	C9H9N	131	A
19a	pyrrolidinone	C4H7NO	85	
21	4-methylphenol	C7H8O	108	A
23	piperidinone	C5H9NO	99	A
23a	3,5-dihydroxybenzaldehyde	C7H6O3	138	
23b	2,6-piperidindione	C5H7NO	113	
23c	tetrahydro-5H-pyrrolo[1,2-a]pyrazindione	C7H10O2N2	154	
24	2,3-dihydrobenzofuran	C8H8O	120	A
26	1H-indole	C8H7N	117	A
27	2,5-pyrrolidindione	C4H5NO2	99	A
28	2-methyl-1H-indole	C9H9N	131	A

* A - Also detected in albumin pyrolysis.

As indicated previously for the albumins, in order to obtain more complete information on the pyrolysate from gluten, the material was also analyzed for less volatile components. For this purpose the gluten was pyrolysed at 510° C in a filament system and derivatized off-line with BSTFA. The silylated pyrolysate was analyzed by the same procedure as in the case of albumins. The chromatogram is shown in Figure 12.3.6.

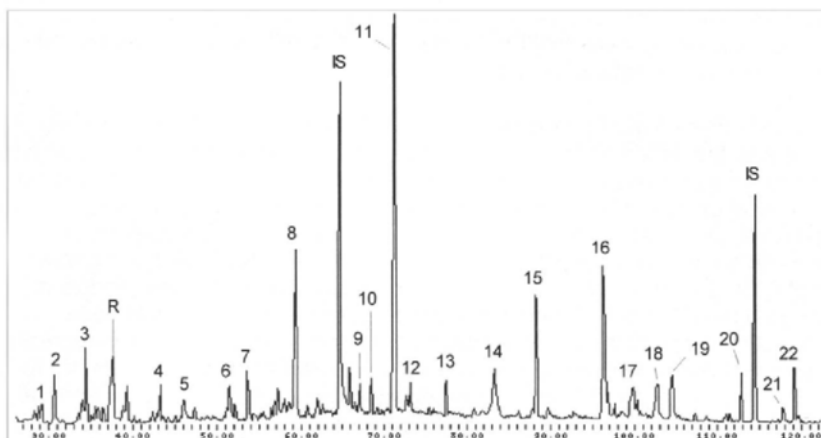


FIGURE 12.3.6. Chromatogram obtained after gluten pyrolysis at 510° C and silylation. Separation done on a DB-5 column.

The compounds identified in the pyrogram from Figure 12.3.6 are given in Table 12.3.4. The peaks are rather different from those identified in albumin pyrolysis.

TABLE 12.3.4. Compounds identified in the pyrogram of gluten with silylation shown in Figure 12.3.6.

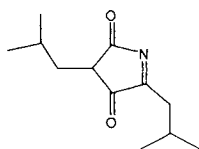
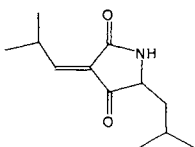
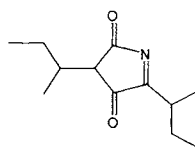
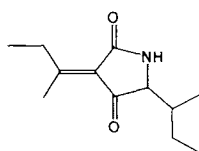
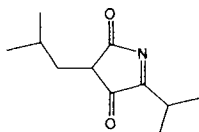
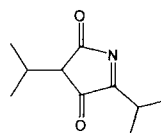
Peak #	Compound	Formula	MW
1	phenol TMS	C ₉ H ₁₄ O ₃ Si	166
2	1H-pyrrole-2,5-dione TMS	C ₇ H ₁₁ NO ₂ Si	169
3	4-methylphenol TMS	C ₁₀ H ₁₆ O ₃ Si	180
R	reagent	ion 99	
4	glycerol 3TMS	C ₁₃ H ₃₂ O ₃ Si ₃	308
5	3-ethyl-4-methyl-1H-pyrrole-2,5-dione TMS	C ₁₀ H ₁₇ NO ₂ Si	211
6	diketopiperazine 2 TMS (dihydrouracil 2 TMS ?)	C ₁₀ H ₂₂ N ₂ O ₂ Si ₂	258
7	indole TMS	C ₁₁ H ₁₅ NSi	189
8	5-oxoproline 2 TMS	C ₁₁ H ₂₃ NO ₃ Si ₂	273
IS	internal standard #1		
9	MW = 308		308
10	anhydrosugar 3 TMS	C ₁₅ H ₃₄ O ₅ Si ₃	378
11	levoglucosan 3 TMS	C ₁₅ H ₃₄ O ₅ Si ₃	378
12	monosaccharide 5 TMS ?	C ₂₁ H ₅₂ O ₆ Si ₅	540
13	2-amino-2-deoxy-D-glucose 4 TMS ?	C ₁₈ H ₄₅ NO ₅ Si ₄	467
14	octahydro-5H,10H-dipyrrolo[1,2-a:1',2'-d]pyrazin-5,10-dione	C ₁₀ H ₁₄ N ₂ O ₂	194
15	hexadecanoic acid TMS	C ₁₉ H ₄₀ O ₂ Si	328
16	9,12-octadecadienoic acid (Z,Z) TMS	C ₂₁ H ₄₀ O ₂ Si	352
17	octadecanoic acid TMS	C ₂₁ H ₄₄ O ₂ Si	356
18	3-benzyl-1,4-diaza-bicyclo[4,3,0]nonane-2,5-dione	C ₁₄ H ₁₆ N ₂ O ₂	244
19	3-benzyl-1,4-diaza-bicyclo[4,3,0]nonane-2,5-dione isomer	C ₁₄ H ₁₆ N ₂ O ₂	244
20	palmitic acid glycerin monoester 2 TMS	C ₂₅ H ₅₄ O ₄ Si ₂	474
IS	internal standard #2		
21	9-octadecenoic acid glycerin monoester 2 TMS	C ₂₇ H ₅₆ O ₄ Si ₂	500
22	9,12-octadecadienoic acid glycerin monoester 2 TMS	C ₂₇ H ₅₄ O ₄ Si ₂	498

Most compounds given in Tables 12.3.3 and 12.3.4 can be traced back to protein pyrolysates. However, two other groups of compounds were identified in the pyrograms,

one group generated by the pyrolysis of sugars (levoglucosan, acetic acid, etc.) and the other group generated by the pyrolysis of triglycerides and/or fatty acids. Neither of these groups is from proteinaceous material.

The compounds coming from protein and shown in Tables 12.3.1 to and 12.3.4 are small molecules, the amino acids (such as proline), or DKP type compounds. This type of information from protein pyrolysis has been commonly used for structure elucidation, protein identification, and differentiation between different proteinaceous materials (hair, microorganisms, etc.). However, the information on the protein structure is limited to amino acid content and to a certain extent to the amino acid sequence in the protein. For example, the generation of toluene, phenol, p-cresol, indole and methylindole is associated with the presence of aromatic amino acids in the protein. It has been possible to estimate the content of Phe based on the level of toluene in the pyrogram [4], the content of Tyr based on the level of phenol + p-cresol, and the amount of Trp based on the level of indole. Besides the aromatic amino acids, also Leu, Ile and Val were estimated based on the levels of 3-methylbutanal and 3-methylbutannitrile for Leu, 3-methylbutanal and 2-methylbutan-nitrile for Ile, and of 2-methylpropanal and 2-methylpropanitrile from Val.

The analysis of disubstituted diketopiperazines [11] and/or disubstituted pyrrolidindiones [1] was also shown to provide information on the amino acid sequence in proteins. Compounds as those indicated below show the presence of specific amino acids pairs in the protein.

Leu-Leu $m/z = 209$ Leu-Leu $m/z = 209$ Ile-Ile $m/z = 209$ Ile-Ile $m/z = 209$ Leu-Val $m/z = 195$ Val-Val $m/z = 181$

The pyrolysis generating the compounds indicated above was done at 510° C in a Curie point pyrolyser [1].

The pyrolysis of human hair [15] showed that diketopiperazine formation could provide information on the structure of proteins. This study utilized a Py-GC/MS/MS approach, assigning structures to the compounds generating different chromatographic peaks using the MS/MS capability with both EI and CI ionization techniques. Besides compounds of the type hexahydro-3-(2-methylpropyl)-pyrrolo[1,2-a]pyrazine (1,4-diazabicyclo[4,3,0]nonane-3-methylpropyl-2,5-dione, see Figure 3.5.6d), a second series of compounds with the same mass were noticed. The daughter ions of the two series of compounds were different, showing that pyrolysis of proteins does have in fact

In the insulin Py-MS spectrum, the sulfur bridges are indicated by the ion with m/z 34. The peaks with m/z 92 (toluene), 94 (phenol), and 108 (cresol) indicate the presence of Phe and Tyr. The ion with m/z 117 commonly comes from phenylacetonitrile when generated from Phe and from indole when generated from Tyr. The differentiation is difficult at this point, and usually the proteins containing Tyr have a stronger 117 ion than seen in this insulin spectrum. Other assignments can also be done by the spectrum inspection. This procedure can be applied for determining the amino acid composition of proteins.

Several other pyrolytic studies were done on proteins, some of these related to the identification of specific microorganisms (see Chapter 17). One example is the use of pyrolysis in connection with MIMS to detect proteins by pyrolysis of warfare pathogens in air at atmospheric pressure. This technique applied for example to ovalbumin with the pyrolysis performed at 450°C in air and in the presence of TMAH generated the spectrum shown in Figure 12.3.9.

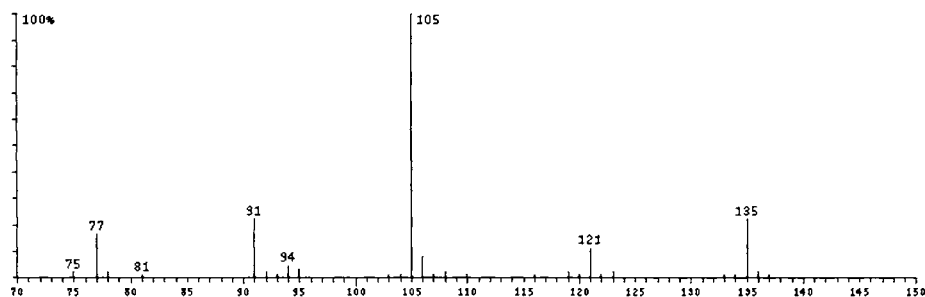


FIGURE 12.3.9. *Py-MS results for ovalbumin using pyrolysis at 450°C in air and in the presence of TMAH, detected with a MIMS system [14a].*

12.4. Conjugated Proteins.

The conjugated proteins cover a wide range of proteinaceous materials where other molecular structures (prosthetic groups) are covalently bound to a protein chain. The conjugated proteins can be classified as

- chromoproteins (such as hemoglobin, cytochrome, etc.),
- glycoproteins, where the protein is bound with carbohydrates,
- lipoproteins, which are combinations of proteins and lipids,
- nucleoproteins, which are combinations of proteins and nucleic acids, and
- phosphoproteins, where the protein is combined with phosphorus-containing compounds (other than nucleic acids or lecithin).

Several Py-MS and Py-GC/MS studies were performed on a variety of proteins. One common subject in these studies was determination of the amino acid composition of the protein. A number of studies were performed to determine the differences and similarities between proteins from a given class, such as hemoglobins of different origins or different enzymes, etc. [15–18].

Pyrolysis does not provide always the desired information on materials from this group. For example, several pyrolysis studies on hemoglobin [15,16], showed that the heme prosthetic group is not revealed in the mass spectrum due to its low contribution to the total mass of the molecule (about 1% [15]). The Py-MS result for hemoglobin from bovine erythrocytes obtained by Curie point pyrolysis at 510° C from a sample applied as a methanol suspension and analyzed by MS with EI ionization at 14 eV [15] is shown in Figure 12.4.1.

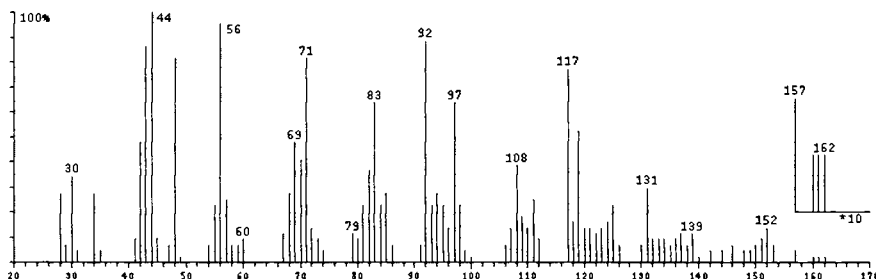


FIGURE 12.4.1. Py-MS result for a hemoglobin sample from bovine erythrocytes obtained using EI at 14 eV [15].

The spectrum in Figure 12.4.1 shows the existence of Cys and/or Cys-Cys by the presence of the ion with m/z 34, the existence of Met by the presence of the ion with m/z 48 (attributed to CH_3SH^+), the existence of Trp by the presence of the ion with m/z 117 (attributed to indole, although phenylacetonitrile may give the same peak) and by the presence of the ion with m/z 131 (skatole), etc. Pyrroline ($m/z = 69$) and pyrrole may be generated from both the porphyrin unit or from amino acids.

Probably the largest group of conjugated proteins is the glycoproteins. In this class are enzymes, food reserve proteins, hormones, plasma and body fluids, protective components of the body, structural proteins, proteic toxins, transport proteins, etc. Glycoproteins contain a protein chain with covalently attached carbohydrate segments usually made from hetero-oligosaccharides. These segments are usually branched and can contain neutral monosaccharides, basic monosaccharides (such as 2-amino-2-deoxy-D-glucose), and a unique nine-carbon sugar, 5-amino-3,5-dideoxy-D-glycero-D-galacto-2-nonulopyranuronic acid (neuraminic acid). Because the amino sugars in glycoproteins are frequently acetylated, glycoproteins are commonly slightly acidic due to the neuraminic acid. The presence of the carbohydrate moiety is again not always obvious in the Py-MS results. As an example, the Py-MS result for ceruloplasmin [15] (shown in Figure 12.4.2) does not have peaks diagnostic for the sugars (although the sample contained about 7% carbohydrate). The ions with m/z 60 and 43 may be interpreted as resulting from the sugar but also from other sources such as the acetyl groups from acetylneuraminic acid or from some acetates attached to the amino groups in the Lys or Arg residues.

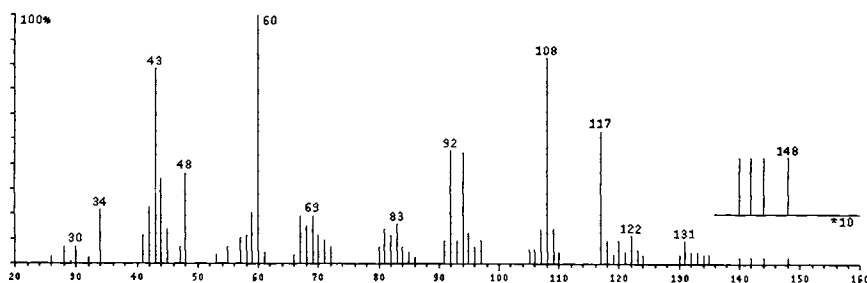


FIGURE 12.4.2. *Py-MS* result for a ceruloplasmin sample obtained using EI at 14 eV [15].

As seen in Section 12.3, pyrolysis coupled with more sensitive analytical techniques may detect the prosthetic groups, such as in the case of albumins analyzed by off-line Py-GC/MS with the derivatization of the pyrolysate.

Numerous studies done on conjugated proteins were oriented toward the differentiation of the material without performing special separations. For example, direct pyrolysis of several enzymes showed a significant difference in the chromatographic profile of the pyrolysate. The enzymes analyzed by this procedure included α -chymotrypsin, creatine kinase, lactate dehydrogenase, catalase, acetylcholinesterase, and urease [19,20].

Pyrolysis also has been used to evaluate the efficiency of removal of proteins from plant materials using enzymes [21].

References 12.

1. J. J. Boon, J. W. de Leeuw, *J. Anal. Appl. Pyrol.*, 11 (1987) 313.
2. K. Scog, *Food Chem. Toxicol.*, 31 (1993) 655.
3. G. Chiavari, G. Galletti, *J. Anal. Appl. Pyrol.*, 24 (1992) 123.
4. S. Tsuge, H. Matsubara, *J. Anal. Appl. Pyrol.*, 8 (1985) 49.
5. T. Sugimura, T. Kawachi, M. Nagao, T. Yahagi, Y. Sano, T. Okamoto, K. Shudo, T. Kosuge, K. Tsuji, K. Wakabayashi, Y. Iitake, A. Itai, *Proc. Japan Acad.*, 53B (1977) 58.
6. T. Yamamoto, K. Tsuji, T. Kosuge, T. Okamoto, K. Shudo, K. Takeda, Y. Iitake, K. Yamaguchi, Y. Seino, M. Nagao, T. Sugimura, *Proc. Japan Acad.*, 54B (1978) 248.
7. V. A. Basiuk, R. Navarro-Gonzalez, *J. Chromatog.*, 776 (1997) 255.
8. S. Manabe, K. Tohyama, O. Wada, T. Aramaki, *Carcinogenesis*, 12 (1991) 1945.
- 8a. V. A. Basiuk, R. Navarro-Gonzalez, E. Basiuk, *J. Anal. Appl. Pyrol.*, 45 (1998) 89.

9. A. B. Mauger, Chem. Commun., (1971) 39.
10. S. A. Liebman, E. J. Levy, ed., *Pyrolysis and GC in Polymer Analysis*, M. Dekker Inc., New York, 1985.
11. G. G. Smith, G. S. Reddy, J. J. Boon, J. Chem Soc. Perkin Trans. II, (1988) 203.
- 11a. A. D. Hendriker, K. J. Voorhees, J. Anal. Appl. Pyrol., 36 (1996) 51.
12. C. Merrit Jr., D. H. Robertson, J. Gas Chromatogr., 5 (1967) 96.
13. K. J. Voorhees, W. Zhang, A. D. Hendricker, B. Murugaverl, J. Anal. Appl. Pyrol., 30 (1994) 1.
- 13a. L. W. Weber, M. Spleiß, J. Anal. Appl. Pyrol., 39 (1997) 65.
- 13b. A. B. Mauger, Chem. Commun., 1971, 39.
14. T. O. Munson, D. D. Fetterolf, J. Anal. Appl. Pyrol., 11 (1987) 15.
- 14a. A. D. Hendricker, F. Basile, K. J. Voorhees, J. Anal. Appl. Pyrol., 46 (1998) 65.
15. H. L. C. Meuzelaar, J. Haverkamp, F. D. Hileman, *Pyrolysis Mass Spectrometry of Recent and Fossil Biomaterial*, Elsevier, Amsterdam, 1982.
16. A. P. Snyder, J. H. Kremer, H. L. C. Meuzelaar, W. Windig, J. Anal. Appl. Pyrol., 13 (1988) 77.
17. A. P. Snyder, G. A. Eiceman, W. Windig, J. Anal. Appl. Pyrol., 13 (1988) 243.
18. M. A. Ratcliff, E. E. Medley, P. G. Simmonds, J. Org. Chem., 39 (1974) 1481.
19. N. D. Danielson, J. L. Glajch, L. B. Rogers, J. Chromatog. Sci., 16 (1978) 455.
20. N. D. Danielson, L. B. Rogers, Anal. Chem., 50 (1978) 1680.
21. J. J. C. M. Van Arendonk, G. J. Niemann, J. J. Boon, J. Anal. Appl. Pyrol., 42 (1997) 33.

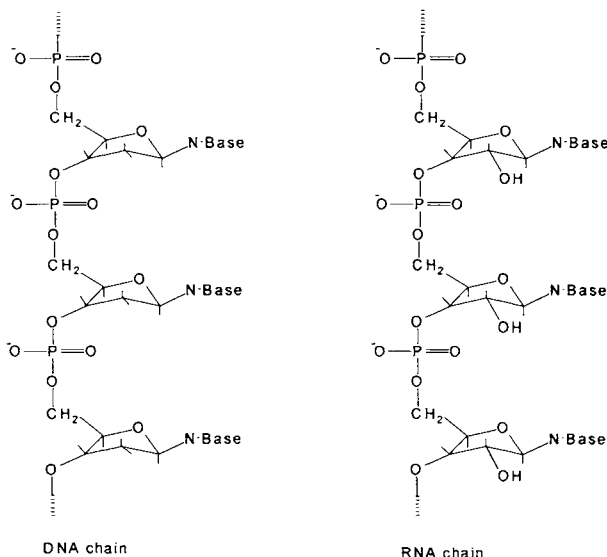
This Page Intentionally Left Blank

Chapter 13. Nucleic Acids

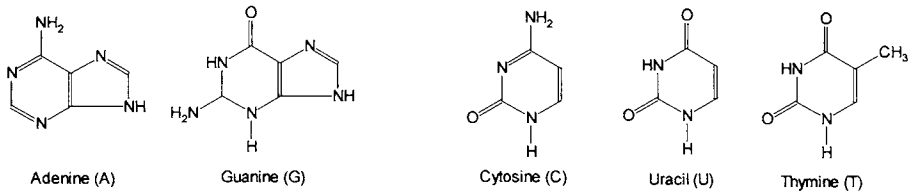
13.1 Classification of Nucleic Acids and Pyrolysis of Oligonucleotides.

Nucleic acids are biopolymers present in every living cell, with monomeric units consisting of a carbohydrate linked via a β -D-glycosidic bond to a heterocyclic base and interconnected by phosphodiester bonds at positions C-3 and C-5. The monomeric units of nucleic acids can be considered the nucleotides that are formed from a carbohydrate residue connected to the base by the β -D-glycosidic bond and to a phosphate group at C-5. The molecules derived from nucleotides by removing the phosphate group are the nucleosides.

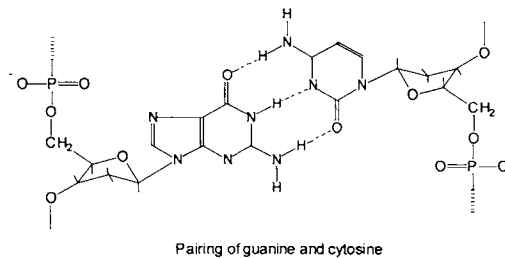
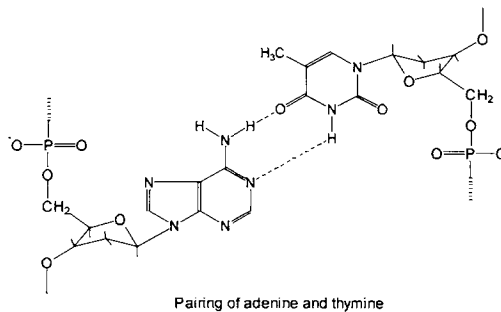
In deoxyribonucleic acid (DNA) the carbohydrate is 2-deoxy-D-ribose, while in ribonucleic acid (RNA) the carbohydrate residue is ribose. Three types of RNA were recognized, and they can be messenger RNA (mRNA), transfer RNA (tRNA), or ribosomal RNA (rRNA), which is the most abundant in cells. Values between 10^6 and 10^9 Dalton have been reported for the molecular weight of DNA, and the molecular weight is about 10^6 for rRNA, 10^5 for mRNA, and 10^4 for tRNA. The simplified structures of DNA and RNA are the following:



The heterocyclic bases present in nucleic acids are certain purines and pyrimidines. The bases always present in DNA are adenine, guanine, cytosine, and thymine, while in RNA the bases are adenine, guanine, cytosine, and uracil. Trace amounts of other bases are occasionally present in DNA and RNA. For example, DNA may contain 5-hydroxymethyl cytosine and several N-methyl purines. The tRNA may contain several unusual bases such as certain methyl purines or hydroxymethyl pyrimidines.



Similarly to proteins, both DNA and RNA have a secondary and a tertiary structure. The secondary structure of DNA shows two chains running in opposite directions, coiled in a left-handed (double) helix about the same axis. All the bases are inside the helix, and the sugar phosphate backbone is on the outside (see e.g. [1]). The chains are held together by hydrogen bonds between the bases with adenine always paired with thymine and guanine paired with cytosine. The base pairing in DNA is shown below:



A tertiary structure is also known for DNA, some DNA molecules assuming a circular or more complicated global shape (highly looped) in their intact state.

RNA molecules are commonly single stranded, but by the formation of loops RNA can also contain portions with double helical structure. The bases are typically paired in RNA only in about 50% of the molecule.

Several studies were done on pyrolysis of oligonucleotides [2–4]. For example, the monitoring of the synthesis of oligonucleotides by Py-MS during the solid phase synthesis (either by the phosphite procedure [5] or by the phosphate triester procedure [6]) was shown to be very useful. The pyrolysis can be done directly on a sample of support polymer containing the oligonucleotide, and the content in each base can be monitored based on specific ions generated by each base.

One possibility for understanding the Py-MS results for nucleic acids is to use a parallel between the mass spectral fragmentation and the pyrolysis fragmentation. This can be exemplified for the mass spectra of the silylated 2'-deoxyadenosine-5'-phosphate (deoxy-AMP) and adenosine-5'-phosphate (AMP), which are shown in Figure 13.1.1 and 13.1.2 respectively (EI spectra at 70 eV). The interpretation of several fragments in these spectra is given in Table 13.1.1.

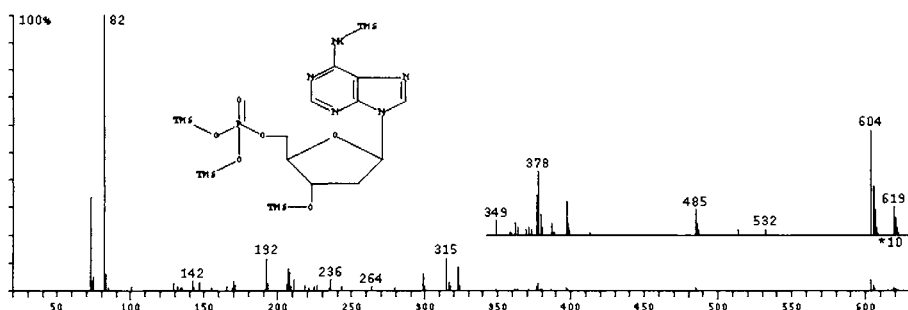


FIGURE 13.1.1. MS of silylated 2'-deoxyadenosin-5'-phosphate.

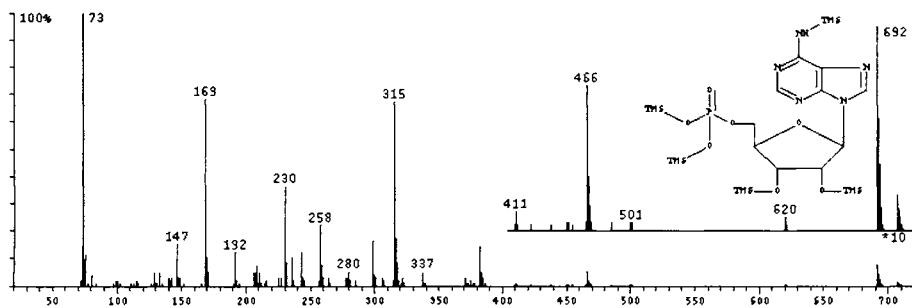
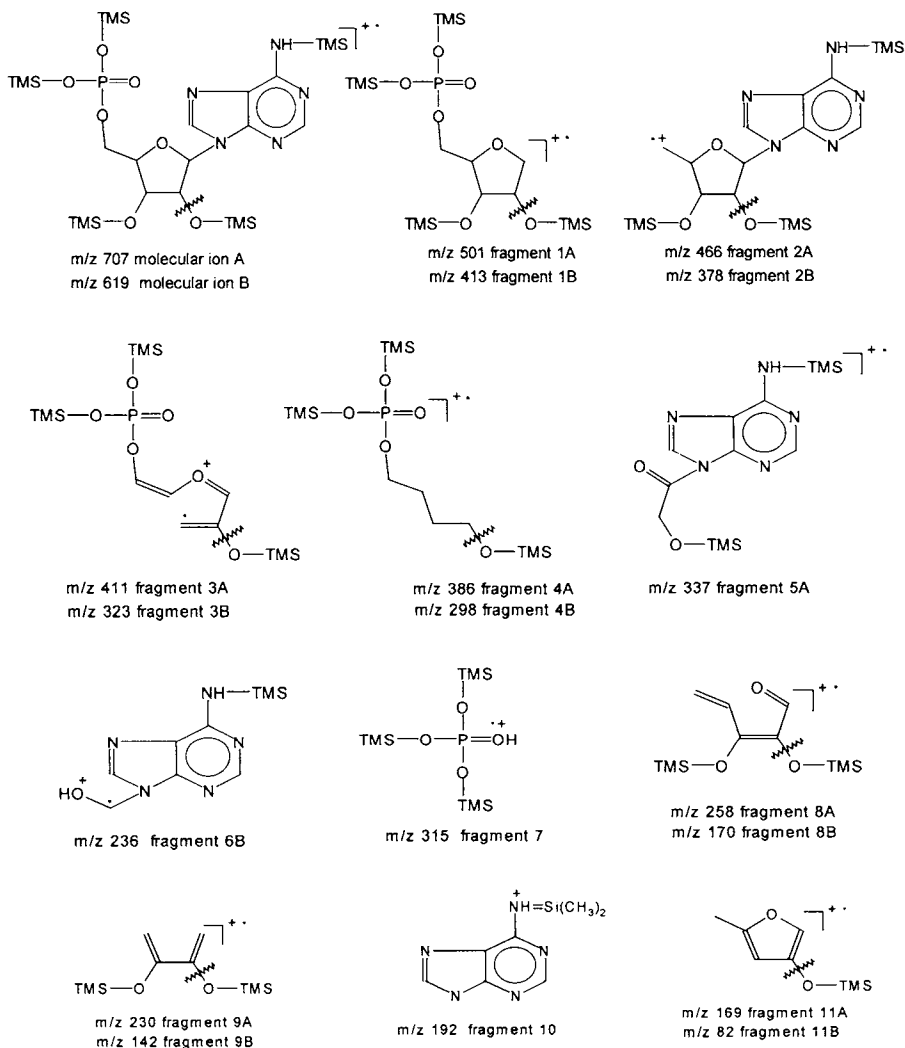


FIGURE 13.1.2 MS of silylated adenosin-5'-phosphate.

TABLE 13.1.1. Fragmentation in the mass spectra of silylated AMP and deoxy-AMP. A is used for fragments from AMP and B for deoxy-AMP.

Ion from AMP	ion from deoxy-AMP	Loss (from mol. ion)	Fragment Number	Source of the ion
707	619	-	mol. ion A, B	
692	604	15		loss of a CH ₃ from a silyl group
620	532	87		loss of NH-TMS
501	413	206	1A, 1B	loss of the adenine
486	398	206+15		loss of adenine and of a CH ₃ from a silyl group.
466	378	241	2A, 2B	loss of the phosphate group (silylated)
411	323	296	3A, 3B	loss of the base and some fragmentation
386	298	321	4A, 4B	loss of base-CH ₂ -CH-OH (silylated)
337		370	5A	loss of PO ₄ -CH ₂ -CH ₂ -CH-OH (silylated)
-	236	383	6B	loss of PO ₄ -CH ₂ -CH ₂ -CH-OH-CH ₂ (silylated)
315	315		7	loss of adenosine
258	170	449	8A, 8B	loss of base, phosphate and fragmentation
230	142	477	9A, 9B	loss of base, phosphate and fragmentation
192	192		10	ion from the base fragmentation
169	82	538	11A, 11B	loss of base, phosphate and fragmentation

In Table 13.1.1, the series "A" are the fragments for AMP and the series "B" are fragments for deoxy-AMP. The structure of these fragments is shown below:



The spectra of silylated AMP and deoxy-AMP show that the types of fragmentations that take place in the mass spectrometer are cleavage of the purine base and cleavage of the phosphate group, as well as a variety of fragmentations with the breaking of the ribose/deoxyribose ring. These fragments, although obtained from a silylated material, can be compared to those seen in the Py-MS of nucleic acids.

13.2 Pyrolysis of Nucleic Acids.

Earlier studies related to the pyrolysis of nucleic acids were done on whole microorganisms when it was shown that pyrolysis of DNA generates a significant proportion of furfuryl alcohol [2]. This compound was even used in a Py-GC/MS technique for the quantitation of DNA content in cultured mammalian cells [4].

Depending on the experimental conditions, the results on nucleic acids pyrolysis showed the dominance in the Py-MS spectra of the fragments either from the sugar moiety or from the base. The work done using a DI pyroprobe (DIP) [7] showed that the mass spectrum contains mainly the ions characteristic for the bases (N-Base) from the nucleic acids. On the other hand, using Curie point Py-MS [8] the ions characteristic for the sugar moiety are dominant in the spectrum. This allows the use of Curie point Py-MS for the differentiation between DNA and RNA but is less useful for the identification of the bases. The difference between the results of the two techniques seems to be generated by the condensation of the base-phosphate components on the walls of the pyrolysis chamber in the performance of standard Curie point Py-MS (see Section 5.4). Some role in the spectral characteristics may be played by the fact that the DCI experiments were in general performed at lower temperatures (280°–300° C). The influence of different pyrolytic conditions on the Py-MS results for DNA show that a series of parameters strongly influence the shape of the spectrum [9,10]. Among these parameters are the oxidative conditions, the type of pyrolysis probe (including the material of the sample holder), the heating rate (flash or programmed), the ion source pressure in the case of atmospheric pressure chemical ionization (APCI), the air flow over the heating zone, etc.

Two examples of Py-MS spectra dominated by the ions generated from the sugar moiety are the spectrum for a DNA sample from calf thymus obtained by Curie point Py-MS and EI at 14 eV [8] (shown in Figure 13.2.1) and the Py-MS spectrum for a RNA sample from baker's yeast generated in the same experimental conditions [8] (shown in Figure 13.2.2).

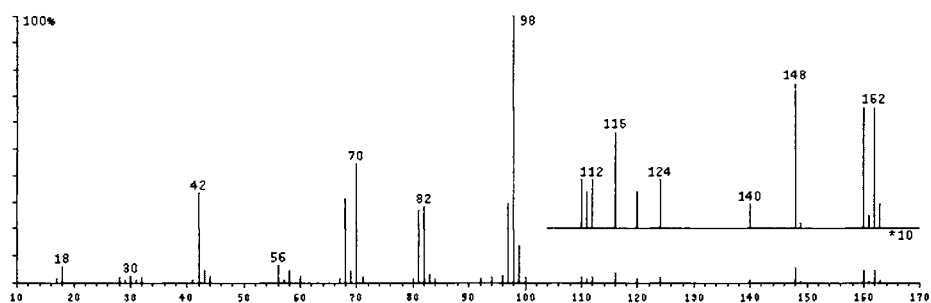


FIGURE 13.2.1 Py-MS spectrum for a DNA sample from calf thymus obtained with 14 eV EI [8].

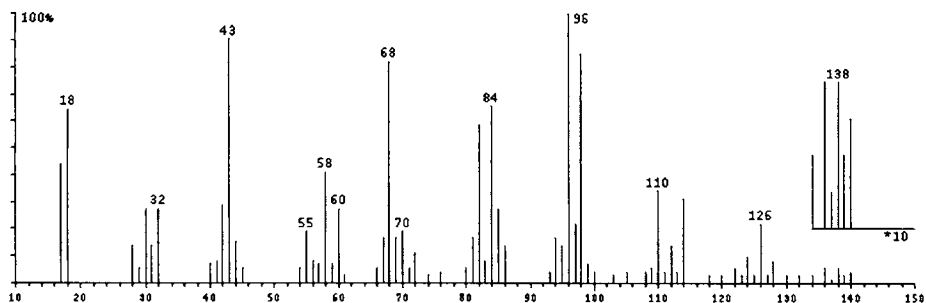


FIGURE 13.2.2 *Py-MS spectrum for an RNA sample from baker's yeast obtained with 14 eV EI [8].*

The two spectra shown in Figures 13.2.1 and 13.2.2 are dominated by the peaks of furan fragments (ions with m/z 96, 98) that are diagnostic for the sugar moiety (MW for furfuryl alcohol is 98).

More valuable information on nucleic acids has been obtained from pyrolysis data when it was possible to evaluate the nature and abundance of the purine/pyrimidine bases. The information on these bases is important for monitoring *in vitro* DNA synthesis [5,6], for the evaluation of chromosome modifications [7], and for the study of complex formation of DNA with cisplatin [11,12]. As indicated previously, the DIP technique was reported to be more useful for detecting the base component of the nucleic acid. However, some information on the bases can be obtained also by Curie point Py-MS, as it can be seen from the spectrum of NADPH (nicotinamide adenine dinucleotide phosphate) shown in Figure 13.2.3. The spectrum was obtained in similar conditions as spectra for DNA and RNA shown previously [8].

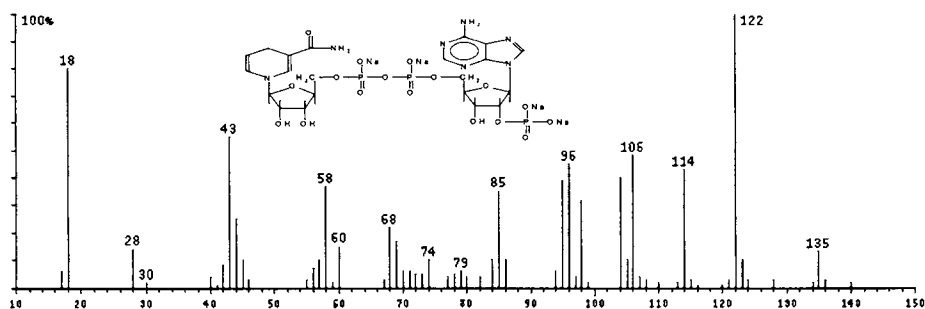
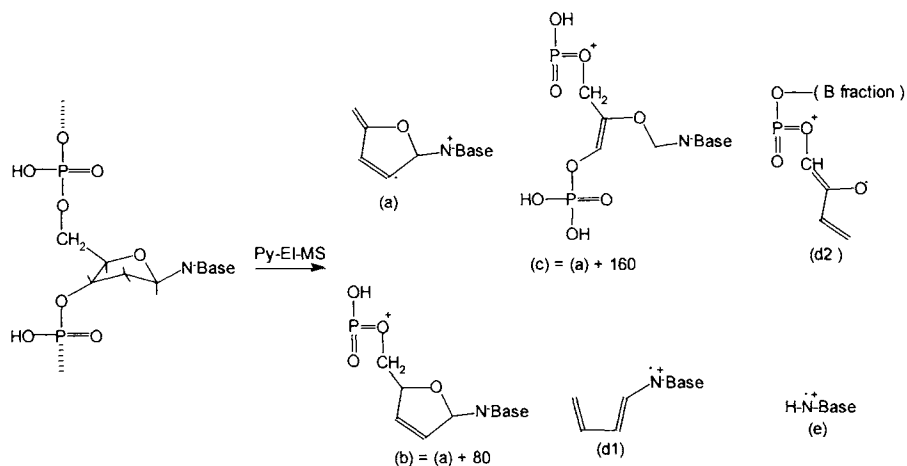


FIGURE 13.2.3 *Py-MS spectrum for NADPH obtained by Curie point Py-MS obtained with 14 eV EI [8].*

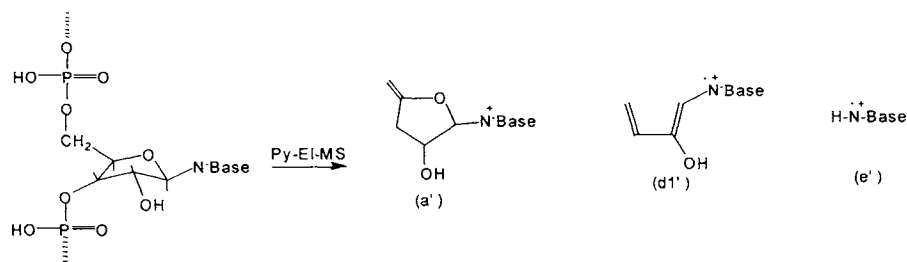
The spectrum is dominated by the peaks corresponding to nicotinamide (MW 124) and adenine (MW 135) showing that the nature of the base is also important for the spectrum features.

Several Py-MS fragmentations were reported for DNA when using DPI instrumentation, and they can be described by the following scheme [7]:



The process described in the above scheme covers two simultaneous processes, pyrolysis and mass spectral fragmentation. Therefore differences can be expected from the case of mass spectral fragmentation of silylated AMP and also some similarities (see Section 3.5). The scheme indicated above for DNA Py-MS appears to show that the purine base remains connected to most fragments. The EI spectra of the silylated nucleotide and the Py-MS using Curie-point instrumentation [8] seem to indicate that the phosphorylated sugar may play a more important role in the fragment formation. Probably depending on the experimental conditions, the spectrum is dominated by one type of fragment or the other. Negative ion CI probably would be a better ionization procedure for obtaining increased sensitivity for the base fragment detection.

The pyrolysis of RNA can be described by a similar scheme as for DNA and it is shown below [7]:



Based on Py-MS studies, it was possible to calculate the abundance of several bases in the nucleic acids and to obtain deviations between the composition of the nucleic acids of healthy and sick organs [7]. The abundance of the base expressed as deoxynucleoside dB % has been calculated from the ratio $\{(\text{BH}^+) \text{ peak height} / \sum [(\text{BH}^+) \text{ peak heights}]\}$ defined as Deflection %. The sum is taken over the peak for adenine (m/z 135), cytosine (m/z 111), guanine (m/z 151), and thymine (m/z 126). The

dependencies were chosen linear [7, 13], and calibration curves for base quantitation as shown in Figure 13.2.4 have been obtained [7].

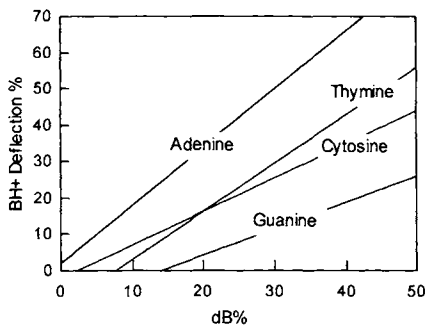


FIGURE 13.1.4. The dependence of base abundance dB% from the Deflection $I / (\Sigma I) \%$ for several nucleic acid bases [7].

13.3 Pyrolysis of Pt-DNA Complexes.

Py-MS analysis was also utilized for the investigation of the formation of complexes of DNA with Pt complexes $\text{cis-Pt}(\text{NH}_3)_2\text{Cl}_2$ (cisplatin), $\text{trans-Pt}(\text{NH}_3)_2\text{Cl}_2$, and $[\text{Pt}(\text{dien})\text{Cl}]\text{Cl}$. Cisplatin has antitumor activity, while the other two platinum compounds do not have therapeutic activity. Py-MS spectra for DNA from *Clostridium perfringens* were compared to the Py-MS results for the DNA complexes with the three Pt compounds. Specific ions were assigned for each base in the Py-MS spectrum. Insignificant differences were noted in the specific ions for different bases between the DNA sample and the DNA- $\text{trans-Pt}(\text{NH}_3)_2\text{Cl}_2$. For the DNA- $\text{trans-Pt}(\text{NH}_3)_2\text{Cl}_2$ complex, again no significant differences were seen in the characteristic peaks for the adenine and thymine. However, the spectra for guanine and cytosine were modified. As indicated previously, in DNA guanine and cytosine are coupled by strong hydrogen bonds. The variation in the spectra indicated that it is likely that cisplatin interacts with the DNA affecting the guanine/cytosine bond [11,12].

References 13.

1. L. Stryer, *Biochemistry*, Freeman, New York, 1988.
2. L. W. Eudy, M. D. Walla, J. R. Hudson, S. L. Morgan, *J. Anal. Appl. Pyrol.*, 7 (1985) 231.
3. R. Freeman, J. Wheeler, P. R. Sisson, A. C. Ward, H. Robertson, N. F. Lightfoot, *J. Anal. Appl. Pyrol.*, 28 (1994) 39.
4. R. S. Sahota, S. L. Morgan, K. E. Creek, *J. Anal. Appl. Pyrol.*, 24 (1992) 107.

5. H. M. Schiebel, H. -R. Schulten, *J. Anal. Appl. Pyrol.*, 5 (1983) 173.
6. L. Alder, A. Rosenthal, D. Cech, *Nucleic Acid Res.*, 11 (1983) 8431.
7. A. Frigerio (ed.), *Recent Developments in Mass Spectrometry in Biochemistry, Medicine and Environmental Research*, Elsevier, Amsterdam, 1983.
8. H. L. C. Meuzelaar, J. Haverkamp, F. D. Hileman, *Pyrolysis Mass Spectrometry of Recent and Fossil Biomaterial*, Elsevier, Amsterdam, 1982.
9. A. P. Snyder, G. A. Eiceman, W. Windig, *J. Anal. Appl. Pyrol.*, 13 (1988) 243.
10. A. P. Snyder, J. H. Kramer, H. L. C. Meuzelaar, W. Windig, *J. Anal. Appl. Pyrol.*, 13 (1988) 77.
11. J. P. Macquet, J. L. Butour, K. Jankowski, *Spectros. Int. J.*, 4 (1985) 75.
12. J. P. Macquet, K. Jankowski, J. L. Butour, *Biochem. Biophys. Res. Commun.*, 92 (1980) 68.
13. J. L. Wiebers, J. A. Shapiro, *Biochemistry*, 16 (1977) 1044.

This Page Intentionally Left Blank

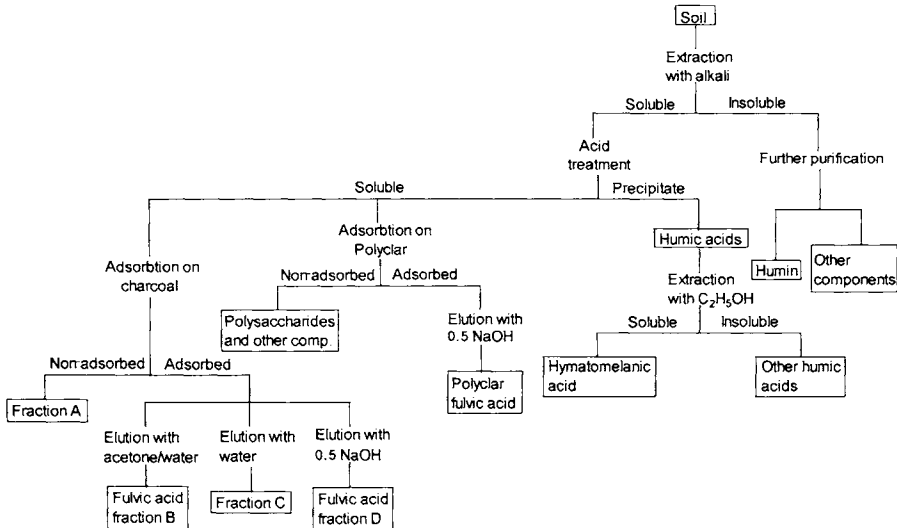
Chapter 14. Analytical Pyrolysis of Several Organic Geopolymers

14.1. Humins, Humic acids, and Fulvic Acids.

The organic matter left in soil is gradually converted into CO_2 , incorporated into microbial biomass from soil, or converted into more stable humic compounds. After one year in a temperate climate, about 70% of the incorporated carbon in plant residues is released as CO_2 . After 10 years only about 8% to 10% of the original organic carbon can still be found in soil [1]. The organic matter left in soil consists mainly of cellulose, lignin, proteins, fats, and low molecular weight plant components. Humic substances are formed from these compounds during numerous transformations. For this reason, humic materials include a variety of polymeric substances usually found in colloidal form. Although humic materials are not homogeneous, certain specific geopolymers are recognized and are classified in the following groups: humin, humic acids, and fulvic acids. Several schemes of separation of humic materials were proposed. These schemes have in common the separation into the three main fractions:

- humin, which is insoluble in bases but soluble in an organic solvent,
- humic acids, which are soluble in bases but precipitate with acids, and
- fulvic acids, which are soluble in both bases and acids.

The soluble compounds in these procedures are considered both those that form true solutions and also colloidal solutions. One such separation procedure is shown below [2]:

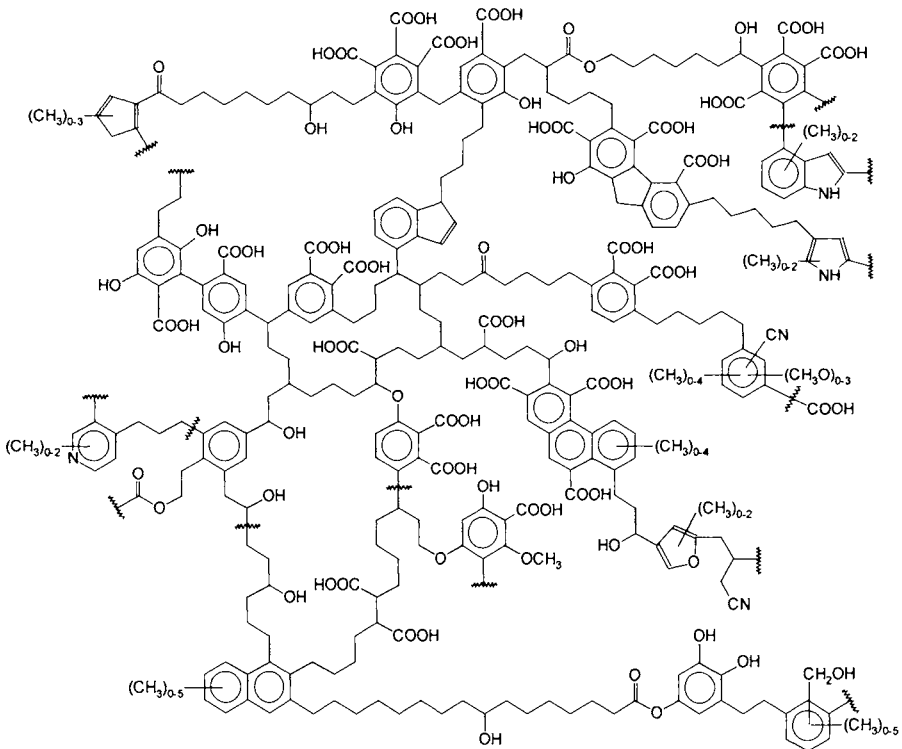


The above scheme provides further fractionation of humic acids allowing the separation of a fraction known as hymatomelanic acid and of fulvic acids in several fractions (B, D, etc.). Humin is commonly further purified of inorganic components. The elemental composition of the fractions obtained with this separation scheme from an uncultivated prairie brown soil (Typic Xerochrept) is given in Table 14.1.1.

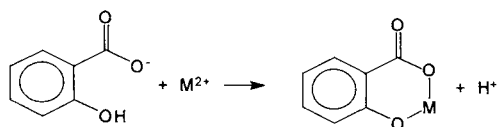
TABLE 14.1.1. *The composition of humic substances in uncultivated prairie brown soil [2].*

Compound	C%	H%	N%	O%	Ash%
polysaccharides and other compounds	37.8	6.8	2.1	53.3	22.0
humic acid	55.1	6.6	4.2	34.1	2.2
hymatomelanic acid	57.8	7.5	1.1	33.6	2.5
fulvic acid (Polyclar)	47.9	5.2	2.6	44.3	11.5
fulvic acid (fraction B)	49.9	6.3	1.4	42.4	6.5
fulvic acid (fraction D)	39.5	4.3	2.5	53.7	21.1

Although no specific chemical structure can be assigned to humic substances, several models were proposed, such as the one shown below for a humic acid [3]:



Although in the above structure no inorganic ions are indicated, the acids in soil can be present free or as their chelates with common ions such as Ca^{2+} , Mg^{2+} , $\text{Fe}^{2+,3+}$. The chelation property of humic acids [4] is shown in the formation of compounds of the form:



Pyrolysis of humic materials and of its components has been done for numerous purposes. One such purpose is structure elucidation. Also, as humic substances have more components that are of different origin (cellulose, lignin, plant cuticular materials), pyrolysis has been used to infer the source of each humic component and to assess its resistance to degradation in time [5]. Also, characterization of different types of soils has been done using pyrolysis studies [6,7].

Pyrolysis results of different humic components shown in Table 14.1.1 and the inferred origin of the material are indicated in Table 14.1.2 for the pyrolysis performed using an on-line Curie point system at 510°C with GC/MS separation and peak identification. The data from Table 2 indicate that different components of humic materials generate rather different pyrolysis products. The origin of most pyrolysis products can be traced back to carbohydrates, lignin, proteins, or lipids. The study of soils of different ages indicate that the proportion of pyrolysate constituents may vary, and it has been concluded that in time, carbohydrates are the first to decompose, followed by proteins and lignin. The most stable compounds are the highly aliphatic biopolymers originated probably in plant cuticles [5]. The degree of humification of the organic matter in soil has been evaluated from Py-GC/MS data based on the amount of protein remaining in soil, the protein level and composition being evaluated from pyrolysis data [8]. A special attention was given to the analysis of nitrogen-containing organic compounds in soil [8a]. Analyzed using a NPD detector, a significantly higher number of nitrogen-containing compounds were detected in soil pyrolysates than were found using FID or mass spectrometric detection [8a].

A successful technique applied for the analysis of humin and humic acids was the pyrolysis with on line methylation followed by GC/MS analysis [6,9]. In one such study [9] humin deashed by treatment with HCl and HF was pyrolysed and compared to humic acid obtained from the same soil, showing that humin contains larger amounts of carbohydrates and aliphatic compounds. This type of study also revealed the presence in the humin and humic acid pyrolysates of monocarboxylic acids with up to 32 carbon atoms, dicarboxylic acids, methoxymonocarboxylic acids with up to 26 carbon atoms, triterpenoid acids, etc. These compounds were not reported in other studies (e.g. [2]) where the chromatographic separation did not allow the detection of compounds difficult to elute due to their high boiling point and polarity.

Other studies of humic substances using pyrolysis were done for evaluating the seasonal variations in humic materials [10] in different soils, for the analysis of marine deposits [11], the analysis of composts [12] or of degraded lignins [3].

TABLE 14.1.2. Compounds identified in the pyrolysate of different humic components.

Compound	Polysaccharide	Humic acid	Hymatomelan	Fulvic Polyclar	Fulvic acid B	Fulvic acid D	Origin*	Compound	Polysaccharide	Humic acid	Hymatomelan	Fulvic Polyclar	Fulvic acid B	Fulvic acid D	Origin*
carbon monoxide	4	4	4	4	4	4	un	1,4-dioxan							1 un
carbon dioxide	4	4	4	4	4	4	un	hept-1-ene		1	1				un
methane							un	2,5-dimethylfuran	2	2	1		1	2	1 S
ethene							un	2,4-dimethylfuran		2			1		S
ethane							un	n-heptane							un
hydrogen sulfide							P	dimethylfuran		1	1				S
propene							un	vinylfuran	1		1	1			S
propane							un	N-methylpyrrole		1	1				P
methanol							S, L	pyridine		2	1			1	3 P
sulfur dioxide	3		3	2	2		un	5-methyl-2(5H)-furanone	1						S
acetaldehyde			3		3		S	pyrrole		1	1				P
2-methylprop-1-ene	2						un	toluene	1	3	2	1	2	2	1 P, L
but-1-ene			1				un	methylthiophene		1					un
buta-1,3-diene	2	2					un	γ-crotonolactone	3						S
n-butane							un	dihydropyran		1	1				S
methanethiol	1						P	oct-1-ene			1	1			1 Lp
trans-but-2-ene							un	oct-2-ene			1				Lp
3-methylpent-1-ene	1	1					un	3-furaldehyde	1	1		1			S
2-propenal	2				2		S	n-octane							Lp
acetone	1	2	2	1	1	3	1 S	n-C5 fatty acid methyl ester				1			Lp
pent-1-ene	1	1		1			un	2-furaldehyde	3	2	3	1	2	3	1 S
furan	1	1	1	1	1	3	1 S	acetamide		1					S
n-pentane							un	benzenemethanol	1	1	1		1	1	un
ethanethiol							P	methylpyrrole		1	1				P
cis-pent-2-ene	1						un	methylpyrrole		1	1				P
cyclopentadiene	1	1	1				S	furfuryl alcohol	2	1				1	1 S
2-methylpropenal	1	2	2	1		3	S	ethylbenzene				1	1	1	1 P, L
3-buten-2-one						2	S	methylpyridine							P
butane-2,3-dione	1				3		S	3-methylcyclopent-2-en-1-one	2						S
2-methylpentane	1						un	m- and/or p-xylene		2	1	1	1		1 P, L
cyclopentane	1						un	styrene	1	1	1	1	1		1 un
methylidihydrofuran	1						S	2-methylcyclopent-2-en-1-one	1					2	1 S
hex-1-ene	1		1				un	o-xylene		1	1				L
2-methylfuran	3	3	2	1	2	3	1 S	non-1-ene				1			Lp
n-hexane	1						un	C3-alkylfuran	1	1				1	S
3-methylfuran	1	1	1		1		S	furancarboxylic acid				1			S
hexatriene	1		1				un	C3-alkylfuran							1 S
hexadiene			1				un	n-nonane							Lp
3-methylbutanal	1	3	2	1		2	P	α-angelicalactone	1	1	1	1	1	1	1 S
2-methylbutanal	2	3	2	1		2	P	n-C6 fatty acid methyl ester				1			Lp
benzene	1	1	1	1	1	1	un	dimethylpyridine							1 P
thiophene	1					2	un	α-methylbenzenemethanol	1	1	1	1			un
acetic acid	3	1	2	1	1	2	S	C4-alkylfuran							S
2-methylcyclo butanone							S	benzaldehyde		1		1			L
cyclohexane							un	5-methyl-2-furaldehyde	3	3	3		3	3	3 S
cyclohexene	1		1				un	C3-alkylbenzene			1				un
ethylfuran	1			1			S	C3-alkylbenzene	1						un

*Peak intensities are rated 4, 3, 2, 1 for very high, high, medium, and low respectively. No number is assigned for traces. Origin is S = polysaccharide, L = lignin, P = protein, Lp = lipid, and un = undetermined.

TABLE 14.1.2. *Compounds identified in the pyrolysate of different humic components (continued).*

Compound	Origin*							Compound	Origin*								
	Polysaccharide	Humic acid	Humic acid	Hymatomelan	Fulvic Polyclar	Fulvic acid B	Fulvic acid D		Polysaccharide	Humic acid	Humic acid	Hymatomelan	Fulvic Polyclar	Fulvic acid B	Fulvic acid D		
4-hydroxy-5,6-dihydro-2H-pyran-2-one	3	1	1		1	2	3	S	n-undecane								Lp
phenol		1	1		3	3	2	un	n-C8 fatty acid methyl ester			1					Lp
trimethylcyclopentenone	1			1				S	methylpentane-1,5-dioate								Lp
α -methylstyrene		1		1				un	2,3-dihydro-3,5-dihydroxy-6-methyl-4H-pyran-4-one	2	1		1				S
dec-1-ene	1							Lp	ethylphenol	2	1	1		1			L
iso-C7 fatty acid methyl ester				1				Lp	C4-alkylbenzene						1		un
2-hydroxy-3-methyl-2-cyclopenten-1-one	2				1		1	S	C4-alkylbenzene				1	1			un
C3-alkylpyridine								P	C2-alkylphenol								L
n-decane								Lp	C2-alkylbenzene								un
n-C7 fatty acid methyl ester				1				Lp	C8H9NO2 (chitin pyrolysis product)		1						S
4-hydroxy-6-methyl-5,6-dihydro-2H-pyran-2-one	1	2	2		1	1	1	S	naphthalene								un
indene				1				un	n-C8 fatty acid			1					Lp
furan-2,5-aldehyde	1							S	C2-alkylphenol		3						L
o-cresol				1				L	methylguaiaicol	3		2	2				L
C3-alkylbenzene								un	3,5-dihydroxy-2-methyl-4H-pyran-4-one	1							S
C3-alkylbenzene						1		un	1,4:3,6-dianhydro- α -D-glucopyranose	2						2	S
5-(2-hydroxyethylidene)-2H-furanone	1							S	methylnaphthalene								un
hexane-2,3,4-trione		1						S	dodec-1-ene								Lp
3-hydroxy-6-methyl-3,4-dihydro-2H-pyran-2-one	1		1		1	1	1	S	iso-C9 fatty acid methyl ester	2		1					Lp
2-furyl hydroxymethyl ketone	1	1						S	vinylphenol			3	2	3	1		L
p-cresol		1			2	1		P, L	resorcinol	1							L
guaiaicol		2	1	1	3	2	1	L	2-methylthiophenol				1	1			un
levoglucosenone	3	1	2			1	2	S	anhydrohexose	1					1		S
3-hydroxy-6-methyl-2H-pyran-2-one	1	1						S	n-C9 fatty acid methyl ester								Lp
n-C7 fatty acid				1				Lp	methylhexane-1,6-dioate			1					Lp
ethylstyrene		1						L	5-(hydroxymethyl)-2-furaldehyde	1							S
3-hydroxy-2-methyl-4H-pyran-4-one	1		1		1			S	n-dodecane								Lp
3-acetoxypyridine		1					1	S	amino acid dimer		1	1					P
undec-1-ene	1			1				Lp	1-indanone							1	un
benzyl cyanide		1	1					P	amino acid dimer	2							P
5-hydroxy-2-methyl-4H-pyran-4-one	1							S	methylthiophenol								un

*Peak intensities are rated 4, 3, 2, 1 for very high, high, medium, and low respectively. No number is assigned for traces. Origin is S = polysaccharide, L = lignin, P = protein, Lp = lipid, and un = undetermined.

TABLE 14.1.2. *Compounds identified in the pyrolysate of different humic components (continued).*

Compound	Polysaccharide	Humin	Humic acid	Hymatomelan	Fulvic Polyclar	Fulvic acid B	Fulvic acid D	Origin*	Compound	Polysaccharide	Humin	Humic acid	Hymatomelan	Fulvic Polyclar	Fulvic acid B	Fulvic acid D	Origin*
C6-alkylbenzene								un	iso-C11 fatty acid methyl ester				1				Lp
ethylguaiaicol				1	1		1	L	amino acid dimer								P
n-C9 fatty acid			1					Lp	cis-isoeugenol	1	1						L
indole		1	1					P	tetradec-1-ene								Lp
C8H9NO2 (chitin pyrolysis product)		1						S	methylphthalic anhydride						1		un
iso-C10 fatty acid methyl ester								Lp	amino acid dimer								P
1,4-dideoxy-D-glycero-hex-1-enopyranos-3-ulose	3	1						S	n-tetradecane								Lp
vinylguaiaicol		3	3	1	2	3	1	L	n-C11 fatty acid methyl ester								Lp
tridec-1-ene								Lp	methyloctane-1,8-dioate				1				Lp
Indan-1,3-dione							1	un	4-methyl-2,6-dimethoxyphenol								1 L
1(3H)-isobenzofuranone	1					1		un	amino acid dimer		1	1	1				P
n-tridecane								Lp	levoglucosane (mannose ?)	3	1	2					1 S
C7H7NO3/C8H11NO2 (chitin pyrolysis product)	1							S	phthalide								1
n-C10 fatty acid methyl ester				1				Lp	amino acid dimer								S
methylheptane-1,7-dioate				1				Lp	trans-isoeugenol	2	1		1				L
amino acid dimer		1						P	amino acid dimer	1							P
amino acid dimer			1					P	amino acid dimer								P
2,6-dimethoxyphenol			2		2		1	L	ethyl- α -ethyl hexanoate								Lp
amino acid dimer								P	acetoguaiacone	2	2	1	1	2	1		L
amino acid dimer								P	trianhydro-2-acetamido-2-deoxyglucose (C8H9NO3)	2							S
amino acid dimer								P	n-C11 Fatty acid				1				Lp
eugenol	1	1	1					L	levoglucosane (glucose)	3	3	3		1			1 S
benzenepropionic acid						2		L	C8H9NO3 (chitin pyrolysis product)	1	1						S
C8H9NO2 (chitin pyrolysis product)	1							S	3,4-dimethoxyacetophenone				1				L
levoglucosane (galactose?)	3		2			3	1	S	iso-C12 fatty acid methyl ester					1			Lp
amino acid dimer		1	1					P	methyl vanillate				1				L
methylindole		3	1					P	4-ethyl-2,6-dimethoxyphenol								L
n-C10 fatty acid								Lp	(4-hydroxy-3-methoxy)phenylpropan-2-one		1	1		1	1	1	L
biphenyl								L	n-pentadecane		1	1					Lp
vanillin				1	1	2		L	n-C12 fatty acid methyl ester								Lp

*Peak intensities are rated 4, 3, 2, 1 for very high, high, medium, and low respectively. No number is assigned for traces. Origin is S = polysaccharide, L = lignin, P = protein, Lp = lipid, and un = undetermined.

TABLE 14.1.2. *Compounds identified in the pyrolysate of different humic components (continued).*

Compound	Polysaccharide	Humic acid	Hymatomelan	Fulvic Polyclar	Fulvic acid B	Fulvic acid D	Origin*	Compound	Polysaccharide	Humic acid	Hymatomelan	Fulvic Polyclar	Fulvic acid B	Fulvic acid D	Origin*
methylnonane-1,9-dioate			1				Lp	heptadec-1-ene		1	1				Lp
C8H11NO4 (chitin pyrolysis product)	1						S	n-heptadecane							Lp
4-vinyl-2,6-dimethoxyphenol	1	2	3	1	1		L	n-C14 fatty acid methyl ester			3				Lp
n-C12 fatty acid		1	1	1	1		Lp	methylundecane-1,11-dioate							Lp
propionguaiacone			1	1		1	L	C9-alkylphenol					1		un
vanillic acid		1			1	1	L	4-propenol-2,6-dimethoxyphenol							L
dihydroxydimethylbenz aldehyde	1						L	4-propanol-2,6-dimethoxyphenol							L
4-allyl-2,6-dimethoxyphenol							L	C9-alkylphenol							un
iso-C13 fatty acid methyl ester				1			Lp	prist-1-ene		2	2	2			Lp
anti-iso-C13 fatty acid methyl ester							Lp	n-C14 fatty acid	1	2	1		1	1	Lp
dianhydro-2-acetamido-2-deoxyglucose	1						S	prist-2-ene		2					Lp
hexadecadiene			1				Lp	anthracene							un
hexadec-1-ene							Lp	10-methyl-C14 fatty acid methyl ester							Lp
n-hexadecane		1					Lp	iso-C15 fatty acid methyl ester				3			Lp
C8H9NO3 (chitin pyrolysis product)	1						S	anti-iso-C15 fatty acid methyl ester				3			Lp
n-C33 fatty acid methyl ester							Lp	octadec-1-ene		2	1				Lp
methyldecane-1,10-dioate				1			Lp	methyl ferulate							L
syringaldehyde				1			L	n-octadecane		1					Lp
n-C13 fatty acid							Lp	iso-C15 fatty acid		1					Lp
iso-C14 fatty acid methyl ester							Lp	anti-iso-C15 fatty acid		1					Lp
4-trans-propenyl-2,6-dimethoxyphenol		1	1		1	1	L	n-C15 fatty acid methyl ester				2			Lp
biphenol	1	1	2		1	1	L	2,6-dimethoxyphenyl-4-propionic acid				2			L
C9-alkylphenol						1	un	n-C15 Fatty acid		1			1	1	Lp
acetosyringone							L	10-methyl-C15 fatty acid methyl ester							Lp
C9-alkylphenol				1			un	iso-C16 fatty acid methyl ester				3			Lp
heptadecadiene				1		1	Lp	phytadiene		2					LP
4-propyl-2,6-dimethoxyphenol			2		1		L	nonadec-1-ene							Lp

*Peak intensities are rated 4, 3, 2, 1 for very high, high, medium, and low respectively. No number is assigned for traces. Origin is S = polysaccharide, L = lignin, P = protein, Lp = lipid, and un = undetermined.

TABLE 14.1.2. *Compounds identified in the pyrolysate of different humic components (continued).*

Compound	Polysaccharide	Humin	Humic acid	Hymatomelan	Fulvic Polyclar	Fulvic acid B	Fulvic acid D	Origin*	Compound	Polysaccharide	Humin	Humic acid	Hymatomelan	Fulvic Polyclar	Fulvic acid B	Fulvic acid D	Origin*
iso-C16:1 fatty acid methyl ester				3				Lp	n-C18 fatty acid methyl ester		2		3	1			Lp
anti-iso-C16:1 fatty acid methyl ester				1				Lp	n-C18 fatty acid	1	1	1		1	1		Lp
n-nonadecane								Lp	10-methyl-C18 fatty acid methyl ester				2				Lp
n-C16 fatty acid methyl ester		1		3				Lp	iso-C19 fatty acid methyl ester								Lp
n-C16 fatty acid	1	3	1	2	1	1		Lp	anti-iso-C19 fatty acid methyl ester								Lp
n-C16 fatty acid ethyl ester		1						Lp	docos-1-ene								Lp
10-methyl-C16 fatty acid methyl ester								Lp	n-docosane						1		Lp
iso-C17 fatty acid methyl ester								Lp	n-C19 fatty acid methyl ester		1		1				Lp
anti-iso-C17 fatty acid methyl ester				2				Lp	methylhexadecane-1,16-dioate				2				Lp
eicos-1-ene		1						Lp	terpenoid		2						un
n-eicosane		1	1			1		Lp	terpenoid		3						un
n-C17 fatty acid methyl ester				1				Lp	terpenoid		3						un
n-C17 fatty acid			1		1			Lp	n-C19 fatty acid		1	1	1	1			Lp
10-methyl-C17 fatty acid methyl ester								Lp	tricos-1-ene								Lp
iso-C18 fatty acid methyl ester								Lp	n-tricosane		2						Lp
C18:2 fatty acid methyl ester				3				Lp	n-C20 fatty acid methyl ester				3				Lp
C18:1 fatty acid methyl ester				3				Lp	n-C20 fatty acid				1				Lp
C18:1 fatty acid methyl ester								Lp	n-C21 fatty acid								Lp
n-heneicosane		1	1					Lp	n-C22 fatty acid								Lp

*Peak intensities are rated 4, 3, 2, 1 for very high, high, medium, and low respectively. No number is assigned for traces. Origin is S = polysaccharide, L = lignin, P = protein, Lp = lipid, and un = undetermined.

14.2. Coal.

Coal is a rock commonly found in nature. Due to its economical value, a significant number of studies are dedicated to this subject [14]. A variety of coals are known and they are made from a combination of fine laminae and thicker bands of different kinds of organic matter, which vary in their proportion in different coals. Therefore, coal is not a uniform macromolecular material but its composition is fairly well understood. Coal main

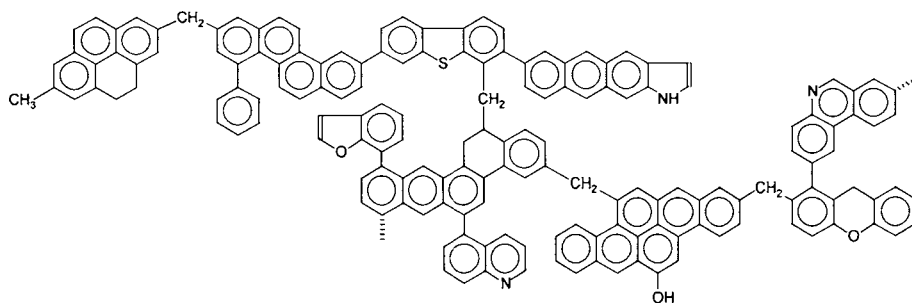
ingredients are vitrain (glassy coal), clarain (striated), durain (dull), and fusain (mineral charcoal). Regarded as minerals, coal components are named *macerals*. Based on maceral components, vitrain is made of vitrinite, fusain from fusinite, clarain from a mixture of vitrinite, xylinite and exinite, durain from a mixture of exinite, cutinite, micronite, etc. Coals are classified by a variety of criteria such as type or rank [14]. The rank refers to the stage of coalification, and the series is anthracite, bituminous coal, subbituminous coal, lignite, and peat. The rank index can be taken as the ratio between fixed carbon % and volatile matter %, although other ranking indexes are utilized [14]. The content of volatiles varies from over 32% for lignite, to 20–30 % for bituminous coal and below 8% for anthracite.

Organic matter of coals consists of macromolecules that contain aromatic and cyclic aliphatic rings linked by aliphatic bridges. Heteroatoms are also present in the structure in a series of heterocycles such as furan, quinone, pyridine, pyrrole, thiophene, etc. In coals with less advanced coalification such as lignites, the lignin structures from the initial woody material that generated the coal can be seen as methoxy groups attached to the aromatic rings.

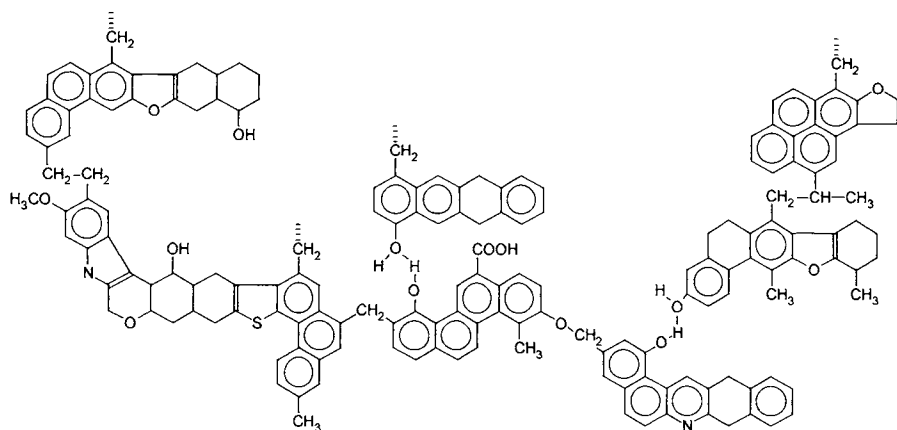
Coal swelling in several organic solvents shows that coal macromolecules are cross-linked. These cross-links are believed to occur by covalent bonds between aromatic molecular clusters with larger fragments connected by donor-acceptor (coordinative) bonds. In the pores of the macromolecular network, coals also contain small organic molecules with MW up to 700 Dalton.

A variety of parameters are commonly measured on coals, such as elemental composition (C, H, O, N, S), content of ash, moisture, as well as physical properties such as calorific power, hardness, and reflectance. These parameters have a wide range of values, and only some ranges can be indicated. For example, the elemental composition (in ash free coals) is 85–92 % C, 2–3% H, and 7–8% O for anthracite, 70–75% C, 5–6% H, and 15–20% O for bituminous coals, and 55–70% C, 6–7% H, and 25–30% O for lignites. Coal may also contain 1–2% N, and up to 4–5% or even higher of S. The content of ash can also vary from a few percent to 20% or higher.

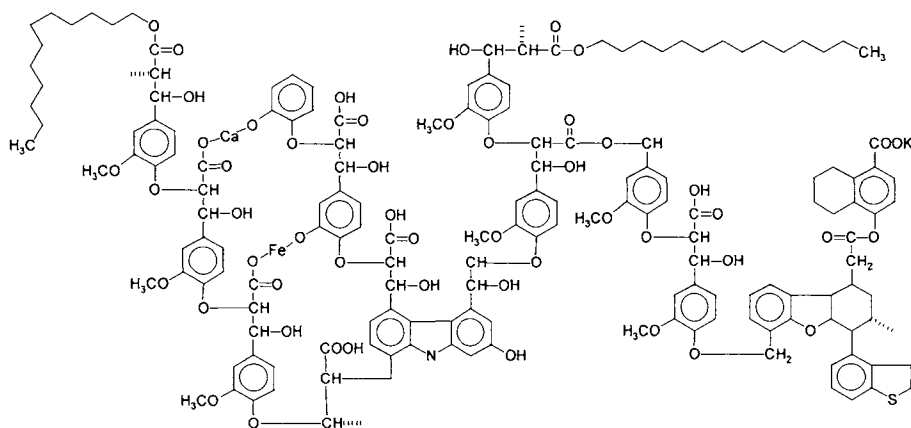
The chemical structure of coals being so complex, only models of different coals can be proposed. As an example, a proposed structure for an anthracitic coal can be the following [15]:



The proposed structure for a bituminous coal is the following [16]:



The model structure for a lignite is the following [15].



Pyrolysis results are very important for coal characterization, as all conversion processes of coal such as combustion, liquefaction, and gasification start with a pyrolytic step. For this reason, pyrolysis was frequently used for the analysis of coals [17, 18]. Pyrolysis data were correlated with coal composition, coal characterization and ranking [18a], prediction of coal reactivity as well as of other properties related to coal utilization. Techniques such as Py-MS, Py-GC/MS with different ionization modes, Py-FTIR, or evolved gas analysis (EGA) [19] were described for coal analysis. Programmed temperature pyrolysis is another technique that has been proposed [17] for a complete evaluation of the two types of molecules present in coal.

Both the small molecules and the macromolecular structures can be evaluated using pyrolysis. The small molecules in coal are usually extractable with solvents and have molecular weights up to 700 Dalton, most commonly in the range 200–400 Dalton. These compounds consist of hydrocarbons (C_nH_{2n-6} to C_nH_{2n-34}), oxygen containing

compounds ($C_nH_{2n-6}O$ to $C_nH_{2n-24}O$ and $C_nH_{2n-6}O_2$ to $C_nH_{2n-30}O_2$), nitrogen containing compounds ($C_nH_{2n-3}N$ to $C_nH_{2n-33}N$ and $C_nH_{2n-6}N_2$ to $C_nH_{2n-26}N_2$), and compounds containing both nitrogen and oxygen ($C_nH_{2n-5}ON$ to $C_nH_{2n-23}ON$ and $C_nH_{2n-10}ON_2$ to $C_nH_{2n-22}ON_2$) [20]. Some of the small molecules are bound to the macromolecular network by electron donor-acceptor interactions.

Pyrolysis of the macromolecular portion of coal can be done after the extraction of the small molecules. Another approach is the evaluation of the pyrolysis products of different macerals [21,22]. A list including compounds generated from the pyrolysis at 610° C of several coal macerals (vitrinite, sporinite, and total inertinite) is given in Table 14.2.1. This list does not include small molecules such as H_2 , H_2O , CO , CO_2 , CH_4 , saturated and unsaturated hydrocarbons with C_2 – C_5 , etc., which are abundantly formed in coal pyrolysis [23]. Also, a significant amount of tar that is usually not analyzed by GC techniques is commonly formed during coal pyrolysis. Although the tar contains a large proportion of carbon, other molecules such as oligomers of the starting components in coal may be present in this tar.

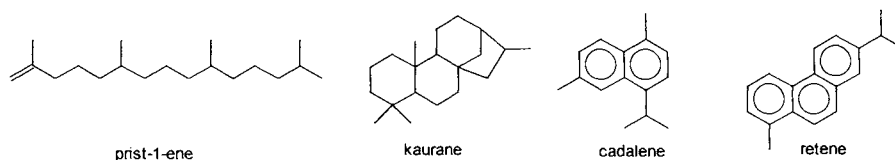
TABLE 14.2.1. *Compounds generated by pyrolysis at 610° C of several coal macerals.*

1	n-hex-1-ene	39	C_3 -benzene
2	n-hexane	40	n-dec-1-ene
3	C_6H_{10}	41	n-decane
4	C_6H_{10}/C_6H_{12}	42	C_3 -benzene
5	C_6H_{10}/C_6H_{12}	43	indane
6	C_6H_{10}	44	indene
7	C_6H_{12}	45	$C_{11}H_{24}$
8	benzene	46	o-cresol
9	thiophene	47	m/p-cresol
10	C_6H_{12}	48	C_4 -benzene
11	C_6H_{10}	49	n-undec-1-ene
12	n-hept-1-ene	50	n-undecane
13	n-heptane	51	C_2 -phenol
14	C_7H_{14}	52	C_5 -benzene
15	C_7H_{14}	53	C_5 -phenol
16	toluene	54	benzothiophene
17	C_1 -thiophene	55	naphthalene
18	C_7H_{12}	56	C_3 -phenol
19	C_8H_{16}	57	n-dodec-1-ene
20	n-oct-1-ene	58	catechol
21	n-octane	59	n-dodecane
22	C_8H_{16}	60	C_3 -phenol
23	ethyl-benzene	61	C_3 -phenol
24	C_2 -thiophene	62	$C_{13}H_{28}$
25	C_2 -thiophene	63	C_3 -phenol
26	m/p-xylene	64	C_3 -phenol
27	C_2 -thiophene	65	C_1 -catechol
28	C_2 -thiophene	66	C_3 -phenol
29	o-xylene	67	C_3 -phenol
30	C_2 -thiophene	68	2-methyl-naphthalene
31	n-non-1-ene	69	$C_{14}H_{30}$
32	n-nonane	70	C_1 -catechol
33	C_9H_{18}	71	1-methyl-naphthalene
34	C_3 -benzene	72	n-tridec-1-ene
35	C_3 -benzene	73	n-tridecane
36	C_3 -benzene	74	C_2 -catechol
37	C_3 -benzene	75	biphenyl
38	phenol	76	C_2 -naphthalene

TABLE 14.2.1. *Compounds generated by pyrolysis at 610° C of several coal macerals (continued).*

77	C ₂ -naphthalene	133	n-eicosane
78	C ₂ -naphthalene	134	C ₂ -phenanthrene/anthracene
79	C ₂ -naphthalene	135	C ₁ -phenyl-naphthalene
80	n-tetradec-1-ene	136	C ₁ -phenyl-naphthalene
81	n-tetradecane	137	n-heneicos-1-ene
82	C ₂ -naphthalene	138	n-heneicosane
83	C ₂ -naphthalene	139	C ₃ -phenanthrene/anthracene
84	C ₁ -biphenyl	140	C ₃ -phenanthrene/anthracene
85	C ₁ -biphenyl	141	C ₂ -phenyl-naphthalene
86	C ₁₆ H ₃₄	142	benzo-fluorene
87	C ₃ -naphthalene	143	C ₂ -phenyl-naphthalene
88	C ₃ -naphthalene	144	n-docos-1-ene
89	C ₃ -naphthalene	145	n-docosane
90	n-pentadec-1-ene	146	C ₁ -benzofluorene
91	C ₃ -naphthalene	147	n-tricos-1-ene
92	C ₃ -naphthalene	148	n-tricosane
93	n-pentadecane	149	C ₃ -phenyl-naphthalene
94	C ₃ -naphthalene	150	C ₃ -phenyl-naphthalene
95	C ₃ -naphthalene	151	C ₃ -phenyl-naphthalene
96	C ₃ -naphthalene	152	n-tetracos-1-ene
97	C ₃ -naphthalene	153	chrysene
98	fluorene	154	n-tetracosane
99	C ₃ -naphthalene	155	C ₂ -benzofluorene
100	C ₁ -naphthol	156	C ₂ -benzofluorene
101	C ₁ -naphthol	157	n-pentacos-1-ene
102	n-hexadec-1-ene	158	n-pentacosane
103	n-hexadecane	159	C ₁ -chrysene
104	nor-pristane	160	C ₁ -chrysene
105	C ₄ -naphthalene	161	C ₃ -benzofluorene
106	C ₁ -fluorene	162	n-hexacos-1-ene
107	C ₁ -fluorene	163	n-hexacosane
108	n-hept-1-ene	164	C ₂ -chrysene
109	n-heptadecane	165	C ₂ -chrysene
110	dibenzothiophene	166	C ₂ -chrysene
111	pristane	167	n-heptacos-1-ene
112	phenanthrene	168	n-heptacosane
113	anthracene	169	benzo-fluoranthene
114	n-octadec-1-ene	170	n-octacos-1-ene
115	n-octadecane	171	n-octacosane
116	C ₁ -dibenzothiophene	172	C ₃ -chrysene
117	phytane	173	C ₁ -benzo-fluoranthene
118	C ₁ -dibenzothiophene	174	C ₁ -benzo-fluoranthene
119	C ₁ -dibenzothiophene	175	n-nonacos-1-ene
120	C ₁ -phenanthrene/anthracene	176	n-nonacosane
121	C ₁ -phenanthrene/anthracene	177	C ₂ -benzofluoranthene
122	C ₁ -phenanthrene/anthracene	178	n-triacont-1-ene
123	C ₁ -phenanthrene/anthracene	179	n-triacontane
124	n-nonadec-1-ene	180	C ₂ -benzo-fluoranthene
125	n-nonadecane	181	n-hentriacont-1-ene
126	C ₂ -dihenzothiophene	182	n-hentriacontane
127	phenyl-naphthalene	183	C ₃ -benzo-fluoranthene
128	C ₂ -dihenzothiophene	184	C ₃ -benzo-fluoranthene
129	C ₂ -dibenzothiophene	185	n-dotriacont-1-ene
130	C ₂ -phenanthrene/anthracene	186	n-dotriacontane
131	C ₂ -phenanthrene/anthracene	187	C ₃ -benzo-fluoranthene
132	n-eicos-1-ene	188	C ₄ -benzo-fluoranthene

Most studies on coal pyrolysis, however, were on whole coal preparates [23,24]. As seen in Table 14.2.1, a variety of pyrolysis products are generated during coal pyrolysis. However, depending on the coal type, rank, place of origin, etc., the number of pyrolysis products can be much larger. In general, the complexity and quality of pyrolysis products increase with decreasing coal rank. Also, with decreasing coal rank the number of functional groups in the coal pyrolysate increases. For example, anthracite pyrolysis generates a variety of polycyclic aromatic hydrocarbons but very few aromatic compounds with functional groups. In bituminous coals the formation of phenols and some heterocyclic compounds is characteristic. Lignite pyrolysis generates methoxyphenols and other compounds more similar to lignin pyrolysis. Coal rank can also be evaluated based on the relative amounts of certain isoprenoid and aromatic markers in the pyrolysates. For example, in a study on brown coals, the most abundant isoprenoid markers were determined to be pristene and kaurane, and the most abundant aromatic markers were cadalene and retene.



A linear dependence was found between the rank of the coal and the ratio of the levels of aromatics and isoprenoid markers, and the higher the aromatic content, the higher the coal rank [24] was found. Several other studies were also focused on characterization of specific types of coal [25, 26] based on Py-MS data or Py-GC/MS data [18a]. For example, in a study done on eight coals of different origins [18a] from South Africa (SA1, SA2 and SA3), two coals from Australia (AU1 and AU2), one from North America (US2), one from Columbia (CO1) and one from Indonesia (ID1), by using conventional coal analyses it was possible to perform a statistical evaluation to generate a dendrogram indicating the hierarchical clustering. This dendrogram is shown in Figure 14.2.1.

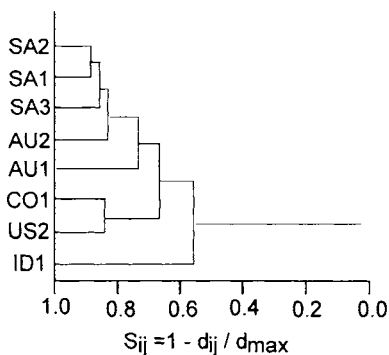


FIGURE 14.2.1. Dendrogram obtained from the Euclidian distance of the first three principal components calculated from results of conventional coal analysis.

The calculation was done by including in a principal component calculation, fourteen conventional coal analysis results as component loadings (% volatiles, % carbon, % hydrogen, % sulfur, % nitrogen, % oxygen, % water, % ash, vitrinite reflectance, % vitrinite, % exinite, % intertinite, % huminite, % liptinite). By calculating the Euclidian distance, for the first three principal components it was possible to generate the dendrogram.

Using Py-GC/MS data and selecting the values of nine parameters for the pyrolysates (the content of long chain aliphatic compounds, content of benzene, toluene relative to total pyrolyzate, toluene relative to aromatic compounds, naphthalene relative to the content of benzene + naphthalene, cresol relative to aromatic compounds, cresols relative to toluene + cresols, and the level of o-cresol relative to total cresols), followed by the use of principal component analysis, it was possible to obtain the dendrogram shown in Figure 14.2.2.

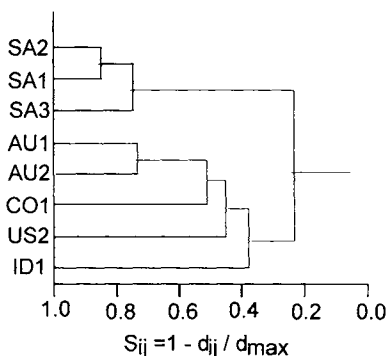


FIGURE 14.2.2. Dendrogram obtained from the Euclidian distance of the first three principal components calculated from results of coal pyrolysis.

Other studies on coal were performed using pyrolysis, such as the measurement of the level of sulfur containing compounds in coal [27,28], or evaluation of polynuclear aromatic hydrocarbons (PAH) in coal [29]. The generation of PAH in coal pyrolysis is an important issue, as some of these compounds are known to have carcinogenic properties. A list of PAHs identified in coal pyrolysates is given in Table 14.2.2. The yield of PAH in coal pyrolyzate depends to some extent on the coal type but mainly on the pyrolysis temperature. The variation of PAH levels as a function of temperature for several bituminous coals is shown in Figure 14.2.3. The yields of other pyrolysis products of coal were also shown to be temperature dependent [30].

Other studies used pyrolysis to determine the influence of different additives on coal thermal degradation [30a,31]. It was found that certain additives such as Na_2CO_3 or K_2CO_3 have significant influence on coal pyrolysis. Pyrolysis of coals of lower rank such as lignites was more influenced by the addition of additives than pyrolysis of higher rank coals.

An important set of studies was done on the kinetics of coal pyrolysis [31a]. However, these types of studies were not immediately related to analytical pyrolysis of coal.

TABLE 14.2.2. *Polynuclear aromatic hydrocarbons generated by pyrolysis of coal.*

MW	Compound name	Formula
128	naphthalene	C ₁₀ H ₈
142	1- and 2-methylnaphthalene	C ₁₁ H ₁₀
152	acenaphthylene	C ₁₂ H ₈
154	biphenyl	C ₁₂ H ₁₀
156	dimethylnaphthalenes	C ₁₂ H ₁₂
166	fluorene	C ₁₃ H ₁₀
178	phenanthrene	C ₁₄ H ₁₀
178	anthracene	C ₁₄ H ₁₀
180	9,10-dihydroanthracene	C ₁₄ H ₁₂
190	methylphenanthrene	C ₁₅ H ₁₂
202	fluoranthene	C ₁₆ H ₁₀
202	pyrene	C ₁₆ H ₁₀
202	acephenanthrene	C ₁₆ H ₁₀
216	methylpyrene	C ₁₆ H ₁₂
228	benzo(a)anthracene	C ₁₈ H ₁₂
228	chrysene	C ₁₈ H ₁₂
228	triphenylene	C ₁₈ H ₁₂
244	cyclopenta(c,d)pyrene	C ₁₉ H ₁₆
252	benzo(b)fluoranthene, benzo(k)fluoranthene, etc.	C ₂₀ H ₁₂
252	benzo(e)pyrene, benzo(a)pyrene	C ₂₀ H ₁₂
256	7,12-dimethylbenzo(a)anthracene	C ₂₀ H ₁₆
276	benzoperylene	C ₂₂ H ₁₂
278	dibenzo(a,h)anthracene, dibenzo(c,d)anthracene	C ₂₂ H ₁₄
300	coronene	C ₂₄ H ₁₂

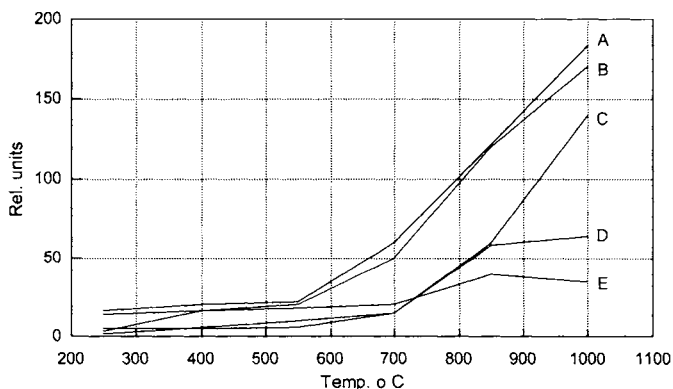


Figure 14.2.3. *The variation of PAH levels as a function of temperature in the pyrolysates of several bituminous coals. (A-USA Mapco, B-South Africa, C-Poland, D-USA McCall, E-Columbia).*

14.3. Peat.

Peat is formed from degradative remains of plant material, mainly of the peat mosses *Sphagnum* and *Hypnum*. Peat types are categorized by botanical composition and degree of coalification. In peat, the coalification process is only beginning, and lignin,

cellulose, and even microorganism proteins can be seen in its structure. While coal still can be treated as a well-defined material, peat looks more like a complex mixture of components. Pyrolysis of peat generates compounds typical for its components, and this allows evaluation of the degree of coalification, identification of information on the peat components, classification the peat by its origin, etc. One particular problem related to peat pyrolysis is sample homogeneity. This explains the need for correlation of sample analysis by pyrolysis with careful sample evaluation by other procedures such as microscopy. In general, peat with a higher degree of degradation (sapric peats) contains a higher proportion of finer particles than less degraded peat (fibric peat). More homogeneous samples can be obtained from peat with finer particles.

Pyrolysis has been used successfully for a variety of purposes related to peat analysis. One application of peat pyrolysis is the evaluation of degree of coalification. In a study of angiosperm and gymnosperm peatified wood [32], sample grouping based on PY-MS data was shown possible. Py-GC/MS data show a clear variation in the dominant compounds in peat pyrolysates, depending on the coalification process. An example of the variation of pyrolysis products in peatified angiosperm wood (*Gordonia* sp.) is given in Table 14.3.1 (small molecules such as H₂, H₂O, CO, CO₂, CH₄, saturated and unsaturated hydrocarbons with C₂-C₅, etc, are not included in the list). The four samples reported [32] are recent wood, peatified wood at the surface, peatified wood buried, and lignitic material.

TABLE 14.3.1. *Pyrolysis products in peatified angiosperm wood (Gordonia sp.). A= recent wood, B=peatified wood at the surface, C=peatified wood buried and D=lignitic material (bold letter indicates dominant component).*

Compound	Origin*	Sample
hydrogen sulfide	?	A, B, C, D
methyl sulfide	?	A, B, C, D
furan	polysaccharide	A, B, C, D
hydroxyacetaldehyde	polysaccharide (hexose)	A, B, C
butan-2,3-dione	polysaccharide	A, B, C
2-methylfuran	polysaccharide	A, B, C
acetic acid	polysaccharide	A, B, C, D
hydroxypropanone	polysaccharide (hexose)	A, B
benzene	modified lignin ?	D
thiophene	?	C
3-hydroxypropanal	polysaccharide	A, B
2-keto-but-3-enal	polysaccharide (hexose)	A, B, C
2-hydroxy-3-ketobutanal	polysaccharide (hexose)	A, B, C
toluene	modified lignin ?	B, C, D
methylthiophene	?	B, C
2,4-pentadienal	polysaccharide	A, B, C
2-furfural	polysaccharide	A, B, C
3,4-furan-2-one	polysaccharide (hexose)	A, B, C
β-angelicalactone	polysaccharide	A, B, C
α-angelicalactone	polysaccharide (hexose)	A, B, C
5-methyl-2-furfural	polysaccharide	A, B, C
2-hydroxy-2-penteno-1,5-lactone	polysaccharide (pentose)	A, B, C
pyran-2,5-dione	polysaccharide (pentose)	A, B, C
phenol	modified lignin	A, B, C, D
2-hydroxy-3-methylcyclopenten-1-one	polysaccharide	A, B, C
o-cresol	modified lignin	C, D
p/m-cresol	modified lignin	C, D
guaiacol	G-lignin	A, B, C, D

TABLE 14.3.1. *Pyrolysis products in peatified angiosperm wood (Gordonia sp.) (continued)*. A= recent wood, B=peatified wood at the surface, C=peatified wood buried and D=lignitic material (**bold letter indicates dominant component**).

Compound	Origin*	Sample
2-methyl-3-hydroxy-pyran-4-one	polysaccharide (hexose)	A, B, C
ethylphenol	modified lignin	B, C, D
methylguaiacol	G-lignin	A, B, C, D
1,2-dihydroxybenzene	modified lignin	A, B, C, D
5-hydroxymethyl-2-furfural	polysaccharide (hexose)	A, B
anhydroxylose	polysaccharide (pentose)	A, B, C
2-methoxy-1,4-dihydroxybenzene	G-lignin	A, B, C, D
methyl 1,2-dihydroxybenzene	modified lignin	B, C, D
guaiacylethane	G-lignin	A, B, C, D
1,4-dideoxy-D-glycero-hex-1-enopyranos-3-ulose	polysaccharide (hexose)	A, B
methyl-1,2-dihydroxybenzene	modified lignin	B, C, D
p-vinyl-guaiacol	G-lignin	A, B, C, D
syringol	S-lignin	A, B, C, D
3-guaiacyl-prop-1-ene	G-lignin	A, B, C, D
guaiacylaldehyde	G-lignin	A, B, C, D
3-guaiacyl-prop-2-ene (cis)	G-lignin	A, B, C, D
anhydrohexose	polysaccharide (hexose)	A, B
methylsyringol	S-lignin	A, B, C, D
guaiacylethanal	G-lignin	A, B, C
3-guaiacyl-prop-2-ene (trans)	G-lignin	A, B , C, D
guaiacylethanone	G-lignin	A, B, C, D
1,6-anhydroglucopyranose (levoglucosan)	polysaccharide (hexose)	A, B, C
guaiacylpropan-2-one	G-lignin	A, B, C, D
syringylethene	S-lignin	A, B, C, D
3-syringyl-prop-1-ene	S-lignin	A, B, C, D
syringaldehyde	S-lignin	A, B , C, D
3-syringyl-prop-2-ene (cis)	S-lignin	A, B, C, D
syringylethanal	S-lignin	A, B, C
3-syringyl-prop-2-ene (trans)	S-lignin	A, B, C, D
syringylethanone	S-lignin	A, B, C, D
3-guaiacyl-prop-2-enal	G-lignin	A, B, C
3-guaiacyl-prop-2-enol (trans)	G-lignin	A
syringylpropanone	S-lignin	A, B, C, D
syringylpropanone	S-lignin	A, B
3-syringylpropan-1-ol	S-lignin	A, B, C
3-syringyl-prop-2-en-1-ol (cis)	S-lignin	A
3-syringyl-prop-2-enal (trans)	S-lignin	A, B, C, D
3-syringyl-prop-2-en-1-ol (trans)	S-lignin	A, B
hexadecanoic acid	Lipid	A, B, C

* S-Lign = syringyl unit in lignin, G-Lign = guaiacyl unit in lignin.

Based on the data from this pyrolysis study, it was concluded that the peatification process begins with the removal of pentosanes (by microbial hydrolysis) that is initiated in the surface litter stage of peatification. This process is followed by cellulose depolymerization and gradual removal of all carbohydrates. Further on, lignin is also modified by macromolecule depolymerization and demethylation. Coalification leads to a predominantly aromatic hydrocarbon network. It is accepted that the first stages in the coalification process are microbially regulated, while later stages are probably geochemically controlled.

Other studies, such as Py-GC/MS characterization of peat components also have been reported. In a study done using Py-GC/MS, subfossil *Sphagnum* leaves and rootlets of heathers (Ericaceae) were analyzed, the Ericaceae having been determined to be the source of aliphatic hydrocarbons in peat [33]. Also, the sources of other peat components were analyzed by pyrolytic techniques. As an example, the fine-grain peat fraction was found to contain monosaccharides mainly from microbial carbohydrates, while coarse-grained peat samples were found to contain monosaccharides from vascular plant carbohydrates [34]. Peat classification has also been done based on its pyrolysis products [35]. A few other applications of peat pyrolysis will be discussed in Part 3 of this book.

14.4. Kerogens.

Kerogens are defined as the organic matter found in sediments that is not soluble in common solvents. Initially, the term referred only to the insoluble organic matter in oil shales, but the insoluble organic fraction of coals should be probably included as a kerogen. Even excluding coal, kerogens are the most abundant form of organic carbon in the earth's crust. Kerogens are made from a complex mixture of components, and a variety of physical and chemical properties are used for their characterization. A simple classification puts kerogens in three classes depending on H/C atomic ratio. Type 1 includes hydrogen rich kerogens with H/C atomic ratio > 1.4 . Type 2 includes kerogens with H/C atomic ratio between 1 and 1.4. Both of these two types are good petroleum source kerogens, and they are commonly derived from algae. Type 3 kerogens have H/C atomic ratio lower than 1, and they are derived predominantly from higher plants. This type is a poor oil source but may be an important source for natural gas. These three kerogen classes are equivalent with coal macerals alginite, exinite, and vitrinite (see Section 14.2) and can be labeled accordingly. A type 4 kerogen was also defined as having H/C atomic ratio below 0.4. This would correspond to the inertinite coal maceral group.

A variety of pyrolytic techniques were applied for the analysis of kerogens [19]. One of these techniques is the sealed vessel pyrolysis where the sample is heated for relatively long periods of time in a sealed vessel and the pyrolytic products analyzed off-line by conventional analytical techniques (GC, GC/MS, FTIR, etc.) [36]. Another technique is bulk flow pyrolysis in which the whole sample is pyrolysed at constant or in gradient temperature in a gas flow with on-line monitoring of the evolving volatiles [37]. This technique is closer to a thermal method of analysis than pyrolysis.

Pyrolysis-trap-GC is another analytical technique applied for kerogen analysis [38]. This type of analysis allows for separate analysis of volatile compounds (free and adsorbed) and large molecule compounds that are pyrolysed. In this type of system the sample is usually heated at programmed temperature, with the volatiles trapped and analyzed on-line by one GC and the pyrolysate analyzed separately by a second on-line GC (see Section 5.2). A schematic diagram of two GC analysis systems is shown in Figure 14.4.1. The need for two GCs results from the fact that at about 200° C a set of volatile compounds (adsorbed molecules) are generated from the shale samples. True pyrolysis is obtained around 600° C when another set of compounds is generated. The production of the two sets of components can be monitored by an on-line detector with no separation (see Figure 14.4.1, Detector 1) in order to decide when the valve will be

switched from the first to the second GC. The use of two GC systems allows the two groups of compounds to be analyzed as they are generated, without the need for the first chromatographic separation to be finished. It also allows more flexibility in the choice of the chromatographic conditions for the separation of the two groups of compounds.

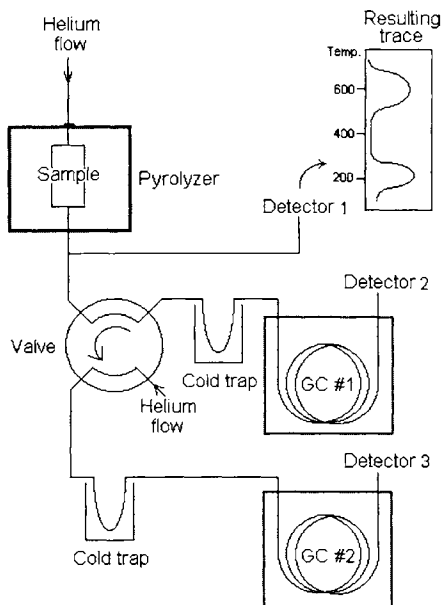


FIGURE 14.4.1. Schematic diagram of a gradient pyrolysis system with two GCs for the analysis of adsorbed volatiles around 200° C and of true pyrolysate around 600° C [38].

The list of several compounds desorbed from a shale sample[38] (Wild Harbor, USA) at 200° C (analyzed in GC #1) is given in Table 14.4.1.

TABLE 14.4.1. List of several compounds desorbed from a shale sample around 200° C.

n-heptane	n-propylbenzene
C ₇ H ₁₄ alkene	dialkylbenzene (2 compounds)
3-hexanone	trialkylbenzene (3 compounds)
cyclohexene	benzaldehyde
C ₅ aldehyde or ketone	benzofuran
phenol	cresol
C ₈ alkane (3 isomers)	C ₆ aldehyde
C ₈ H ₁₆ alkene	naphthalene
xylene (3 isomers)	methylnaphthalene (2 isomers)
styrene	alkyl chloride
chlorobenzene	alkylthiophene
3-heptanal	C ₁₆ H ₃₂ alkene
alkylbenzene (4 compounds)	C ₁₈ H ₃₈ alkane

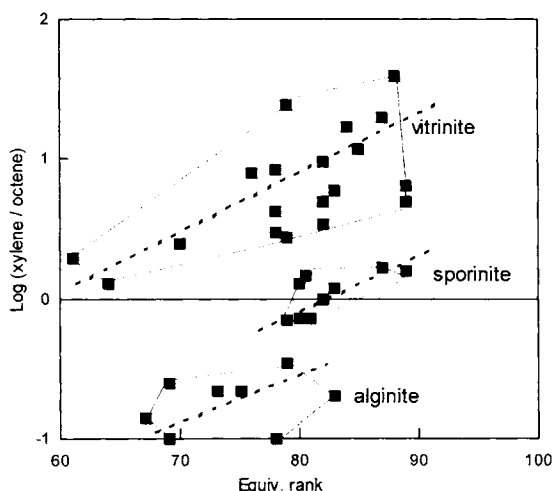
A list of pyrolysate composition of a shale sample at 600° C and analyzed by GC #2 is shown in Table 14.4.2.

TABLE 14.4.2. *List of several compounds in the pyrolysate of a shale sample at 600° C.*

C ₇ H ₁₄ alkene	trialkylbenzenes (3 compounds)
benzene	C ₁₀ hydrocarbons*
C ₈ hydrocarbon	C ₁₁ hydrocarbons
toluene	C ₁₂ hydrocarbons
C ₉ hydrocarbon	C ₁₃ hydrocarbons
dialkylbenzenes (2 compounds)	C ₁₄ hydrocarbons

Hydrocarbons commonly show the pair of 1-ene and normal hydrocarbon with the same number of carbons.

The purpose of many analyses on kerogens is related to their typing, which is very useful for petroleum exploration purposes [39]. As an example, the ratio xylene/octene from the pyrogram of different kerogens can be related to their rank, as shown in Figure 14.4.2 [40]. The presence of aromatic hydrocarbons in the pyrolysate of vitrinites is very high (xylene/octene up to 50), the alginites have low aromaticity, while sporinites have intermediate levels.

FIGURE 14.4.2. *Kerogen typing based on Py-GC/MS data (xylene/octene ratio).*

As seen in Table 14.4.2, pyrolysis of some kerogens generates mainly hydrocarbons. However, the pyrolysate of some other kerogens have a much more complex composition than the Wild Harbor shale sample from Table 14.4.1 and 14.4.2. As an example, a sample from Cariaco Trench (dark olive calcareous clay 1.3 10⁵ years old) [41] generates by pyrolysis at 610° C a variety of compounds that are listed in Table 14.4.3.

Similarly to the study on coal, of significant importance was the evaluation of polycyclic aromatic compounds generated from the pyrolysis of oil shale. This type of study included the evaluation of PAH in shale pyrolysates, and also of sulfur containing polycyclic aromatic compounds, and nitrogen containing polycyclic aromatic compounds [41a].

TABLE 14.4.3. *List of compounds in the pyrolysate of a calcareous clay shale sample obtained at 610° C.*

carbon dioxide	dimethylstyrene
sulfur dioxide	C4-benzene
hydrogen sulfide	dimethylphenol
methanthiol	methylindene
acetone	tetramethylbenzene
butanone	ethylphenol
hydrocarbons C2 to C5	methoxyphenol
3-methylbutanal	methoxymethylphenol
2-methylbutanal	C5-benzene
benzene	naphthalene
thiophene	decan-2-one
hept-1-ene	dodec-1-ene
n-heptane	n-dodecane
pyridine	C2-benzofuran
pyrrole	C13-alkane
toluene	C3-phenol
methylthiophene	hexylbenzene
hexan-2-one	indole
oct-1-ene	ethylmethoxyphenol
n-octane	undecan-2-one
methylpyrrole	methylnaphthalene
C9-alkene	C4-phenol
ethylbenzene	tridec-1-ene
C2-thiophene	isoprenoid C14-alkene
m- and p-xylene	n-tridecane
heptan-2-one	methylnaphthalene
styrene	dihydroxymethoxytoluene
o-xylene	heptylbenzene
non-1-ene	methylindole
n-nonane	2,6,10-trimethyldodecane
benzaldehyde	tetradec-2-ene
n-propylbenzene	n-tetradecane
m- and p-ethyltoluene	C2-naphthalene
mesitylene	C2-dimethoxyphenol
o-ethyltoluene	2-methoxy-4propen-2'-ylphenol
phenol	octylbenzene
C3-thiophene	2,6,10-trimethyltridecane
benzofuran	tridecan-2-one
pseudocumene	pentadec-1-ene
dec-1-ene	n-pentadecane
n-decane	C3-naphthalene
hemimellitene	hexadec-1-ene
indane	n-hexadecane
propylmethylbenzene	2,6,10-trimethylpentadecane
methylstyrene	heptadec-1-ene
indene	n-heptadecane
o-cresol	prist-1-ene
acetophenone	prist-2-ene
n-butylbenzene	octadec-1-ene
m- and p-cresol	n-octadecane
methoxyphenol	nonadec-1-ene
nonan-2-one	n-nonadecane
methylbenzofuran	eicos-1-ene
undec-1-ene	n-eicosane
n-undecane	

Py-GC/MS and Py-MS data also were used for the identification of kerogen origin [41b]. Several chemical characteristics seen in pyrograms may allow the characterization of the kerogen and the identification of an algal origin (leading mainly to type 1 and 2 kerogens) or land plant origin (leading mainly to type 3 or 4 kerogens). The presence of methoxybenzenes or phenols, for example, indicates association with lignin and land plants. The age of the kerogen is also related to its chemical composition. Young kerogens have significantly higher levels of methoxybenzenes while in older materials alkyl phenols become more abundant. Numerous other studies were done for correlation of pyrolysis data with a series of specific kerogen properties [42–45] such as age, depth of extraction, etc. Nevertheless, pyrolysis data were better utilized as fingerprints for differentiation than for the assignment of kerogen origin.

One problem related to the interpretation of pyrolysis data on kerogens is related to the influence of the matrix on pyrolysis products. The clay, diatomaceous materials, and calcareous substrates may have catalytic effects on pyrolysis. For example, it is difficult to determine if some aromatic components in pyrolysates were initially present in the sample or were generated from saturated precursors by dehydrogenation under the influence of heat and the presence of a specific matrix of the kerogen. Terpenoid or steroid related hydrocarbons are better preserved during pyrolysis and may be used as evidence of a certain kerogen origin.

The study of the matrix on pyrolysis result has an additional use besides the understanding of the origin of pyrolysate components. This is related to the influence of the matrix on the generation of specific hydrocarbons from a certain starting organic substrate under the influence of heat and of catalysis [46,47]. However, most of these studies are not directly related to analytical pyrolysis. In these studies, furnace pyrolysers were commonly preferred to small sample and flash pyrolysis [46]. These and other pyrolysis applications for the study of kerogens and also of oil related components such as asphaltenes [47] have been proven extremely useful in practice [19].

References 14.

1. K. Haider, H. R. Schulten, *J. Anal. Appl. Pyrol.*, 8 (1985) 317.
2. C. Saiz-Jimenez, J. W. de Leeuw, *J. Anal. Appl. Pyrol.*, 9 (1986) 99.
3. H. -R. Schulten, P. Leinweber, *J. Anal. Appl. Pyrol.*, 38 (1996) 1.
4. X. Q. Lu, A. M. Vassallo, W. D. Johnson, *J. Anal. Appl. Pyrol.*, 43 (1997) 103.
5. C. Saiz-Jimenez, J. W. de Leeuw, *J. Anal. Appl. Pyrol.*, 11 (1987) 367.
6. F. Martin, J. C. del Rio, F. J. Gonzalez-Vila, T. Verdejo, *J. Anal. Appl. Pyrol.*, 31 (1995) 75.
7. F. Martin, F. J. Gonzalez-Vila, J. C. del Rio, T. Verdejo, *J. Anal. Appl. Pyrol.*, 28 (1994) 71.
8. J. M. Bracewell, G. W. Robertson, *J. Anal. Appl. Pyrol.*, 6 (1984) 19.

- 8a. E. Granada, J. Blasco, L. Comellas, M. Gassiot, *J. Anal. Appl. Pyrol.*, 19 (1991) 193.
9. D. Fabbri, G. Chiavari, G. C. Galletti, *J. Anal. Appl. Pyrol.*, 37 (1996) 161.
10. H. de Haan, G. Halma, T. de Boer, J. Haverkamp, *Hydrobiologia*, 78 (1981) 87.
11. A. Zsolnay, G. R. Harvey, *J. Anal. Appl. Pyrol.*, 8 (1985) 473.
12. C. Saiz-Jimenez, N. Senesi, J. W. de Leeuw, *J. Anal. Appl. Pyrol.*, 15 (1989) 121.
13. C. Saiz-Jimenez, J. W. de Leeuw, *Org. Geochem.*, 6 (1984) 417.
14. H. H. Lowry, (ed.) *Chemistry of Coal Utilization*, Wiley, New York, 1945.
15. P. J. J. Tromp, J. A. Moulijn, J. J. Boon, *J. Anal. Appl. Pyrol.*, 15 (1989) 319.
16. B. D. Blaustein, B. C. Bockrath, S. Friedman (ed.), *New Approaches in Coal Chemistry*, ACS Symp. No 169, Washington, D.C., 1981.
17. A. Marzec, *Anal. Appl. Pyrol.*, 8 (1985) 241.
18. H. L. C. Meuzelaar, A. M. Harper, G. R. Hill, P. H. Given, *Fuel*, 63 (1984) 640.
- 18a. L. Carlsen, J. V. Christiansen, *J. Anal. Appl. Pyrol.*, 35 (1995) 77.
19. K. J. Voorhees, *Analytical Pyrolysis, Techniques and Applications*, Butterworths, London, 1984.
20. D. Bodzek, A. Marzec, *Fuel*, 61 (1982) 670.
21. M. Nip, J. W. de Leeuw, P. A. Schenck, *Geochim. Cosmochim. Acta*, 52 (1988) 637.
22. H. L. C. Meuzelaar, A. M. Harper, R. J. Pugmire, J. Caras, *Int. J. Coal Geol.*, 4 (1984) 143.
23. M. Blazso, T. Szekely, F. Till, G. Varhegyi, E. Jakab, P. Szabo, *J. Anal. Appl. Pyrol.*, 8 (1985) 255.
24. M. Nip, W. Genuit, J. J. Boon, J. W. de Leeuw, P. A. Schenck, M. Blazso, T. Szekely, *J. Anal. Appl. Pyrol.*, 11 (1987) 125.
25. M. Nip, J. W. de Leeuw, P. A. Schenck, H. L. C. Meuzelaar, S. A. Stout, P. H. Given, J. J. Boon, *J. Anal. Appl. Pyrol.*, 8 (1985) 221.
26. A. L. Chaffee, R. B. Johns, M. J. Baerken, J. W. de Leeuw, P. A. Schenck, J. J. Boon, *Org. Geochem.*, 6 (1984) 409.
27. J. P. Boudou, J. Boulegue, L. Malechaux, M. Nip, J. W. de Leeuw, J. J. Boon, *Fuel*, 66 (1987) 1558.

28. T. Zimny, J. V. Weber, G. Krier, M. Schneider, B. Fixari, J. F. Muller, *J. Anal. Appl. Pyrol.*, 8 (1985) 255.
29. L. Bonfanti, L. Comellas, J. L. Lliberia, R. Vallhonrat-Matalonga, M. Pich-Santacana, D. Lopez-Pinol, *J. Anal. Appl. Pyrol.*, 44 (1997) 89.
30. J. V. Christiansen, A. Feldthus, L. Carlsen, *J. Anal. Appl. Pyrol.*, 32 (1995) 51.
- 30a. N. Vanderborgh, C. E. R. Jones, W. J. Verzino, J. Haverkamp, *J. Anal. Appl. Pyrol.*, 5 (1983) 9.
31. P. J. J. Tromp, J. A. Moulijn, J. J. Boon, *Fuel*, 65 (1986) 960.
- 31a. R. M. Morris, *J. Anal. Appl. Pyrol.*, 27 (1993) 97.
32. S. A. Stout, J. J. Boon, W. Spackman, *Geochim. Cosmochim. Acta*, 52 (1988) 405.
33. D. G. van Smeerdijk, J. J. Boon, *J. Anal. Appl. Pyrol.*, 11 (1987) 377.
34. M. E. C. Moers, M. Baas, J. W. de Leeuw, J. J. Boon, P. A. Schenck, *Geochim. Cosmochim. Acta*, 54 (1990) 2463.
35. G. D. Calvert, J. S. Esterle, J. R. Durig, *J. Anal. Appl. Pyrol.*, 16 (1989) 5.
36. M. D. Levan, J. C. Winters, J. H. McDonald, *Science*, 203 (1979) 897.
37. C. Barker, *Fuel*, 53 (1974) 176.
38. J. K. Whelan, J. M. Hunt, A. Y. Huc, *J. Anal. Appl. Pyrol.*, 2 (1980) 79.
39. S. R. Larter, H. Solli, A. G. Douglas, *J. Chromatog.*, 167 (1978) 421.
40. A. G. Douglas, J. R. Maxwell (ed.), *Advances in Organic Geochemistry*, Pergamon, London, 1980.
41. D. van de Meent, S. C. Brown, R. P. Philip, B. R. T. Simoneit, *Geochim. Cosmochim. Acta*, 44 (1980) 999.
- 41a. P. T. Williams, J. M. Nazzari, *J. Anal. Appl. Pyrol.*, 35 (1995) 181.
- 41b. P. F. Greenwood, N. Sherwood, G. D. Willett, *J. Anal. Appl. Pyrol.*, 31 (1995) 177.
42. T. I. Eglinton, S. R. Larter, J. J. Boon, *J. Anal. Appl. Pyrol.*, 20 (1991) 25.
43. J. T. Senftle, S. R. Larter, *Org. Geochem.*, 11 (1987) 407.
44. G. van Graas, J. W. de Leeuw, P. A. Schenck, *Geochim. Cosmochim. Acta*, 45 (1981) 2465.
45. A. W. Stott, G. D. Abbott, *J. Anal. Appl. Pyrol.*, 31 (1995) 227.

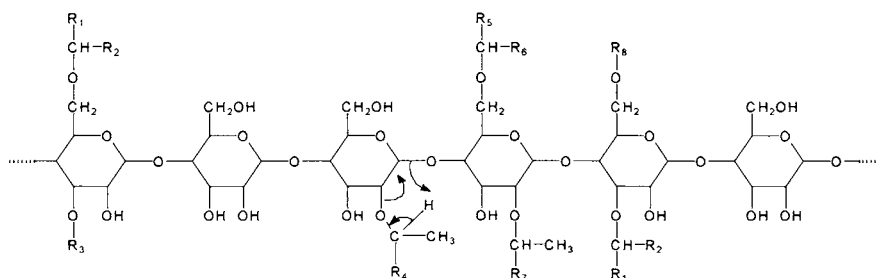
46. B. Horsfield, A. G. Douglas, *Geochim. Cosmochim. Acta*, 44 (1980) 1119.
47. J. Espitalie, M. Madec, B. P. Tissot, *Bull. Amer. Assoc. Petrol. Geol.*, 64 (1980) 59.
48. A. Mascherpa, A. Casalini, *J. High Resol. Chromat.*, 11 (1988) 296.

This Page Intentionally Left Blank

Chapter 15. Analytical Pyrolysis of Other Natural Organic Polymers

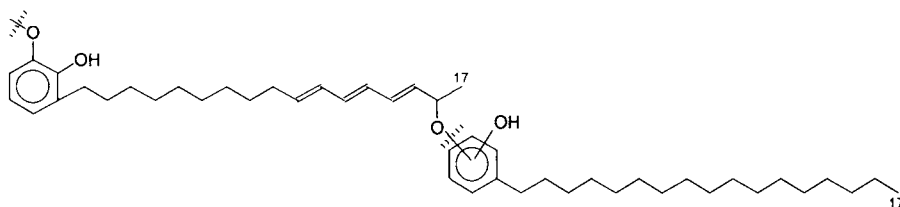
15.1. Uncommon Organic Polymers.

Some organic polymers are rather unique and are not common in nature. An example is the polymer from the leaf cuticle of some plants such as *Agave americana* [1]. This cuticular material contains a macromolecular material that contains polysaccharides and a polymethylene moiety in the estimated ratio 60/40 by weight. Pyrolysis products of an isolated macromolecular fraction of the cuticular material has been proven to have the following structure:



Pyrolysis products show a significant level of long aliphatic chain methyl ketones. These are probably generated by the mechanism suggested in the structure of the polymer. Long chain fatty acids also have been obtained in the pyrolysis of cuticular macromolecular constituents of *Agave americana*.

Pyrolysis also has been utilized for the determination of the structure of unique natural polymers in certain lacquers such as those produced by *Rhus vernicifera* and *Rhus succedanea* [2] and utilized as surface coating for wood, porcelain, etc. in Japan. The pyrolysis products of the two lacquer films at 400° C contain respectively laccol and urushiol, and each also contains alkenes, alkanes, alkenylphenols, and alkylphenols. From these results it was possible to assign the following structure for laccol polymer:



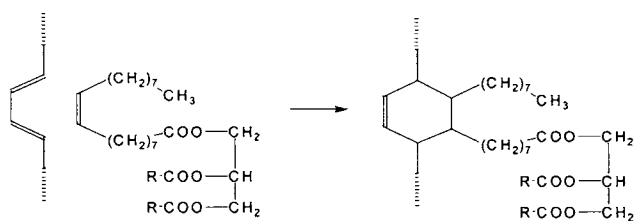
A similar structure (with 15 carbons on the aliphatic chain) was obtained for urushiol polymer.

Different other bioorganic polymers were analyzed using pyrolytic techniques. As an example, sporopollenin, a polymer from the outer wall of pollen particles, was studied using Py-MS [3]. It was found that p-coumaric acid is abundant in the pyrolysate of pollen from several plants, and it was inferred that this molecule is a structural unit of the sporopollenin skeleton.

Other special macromolecules are known, and some were analyzed by pyrolytic techniques. Among these are special gums and lacquers such as mastic, gum elemi, copal, kauri, sandarac, shellac, colophony, amber, etc. [4]. These materials have narrow fields of applications and were not included in this book.

15.2. Diversity of Organic Polymers.

The variety of organic polymers is very broad. Some of them are very uniform materials, such as polyisoprene, cellulose, starch, etc. Others are more complex materials and, although they have a determined structure, are made from a number of units that may be repeated in a variety of manners. Such polymers are the polypeptides, nucleic acids, and proteins. An even more complicated situation is found in the case of lignin or Maillard polymers. These are not repetitive polymers, and their structure may vary depending on the conditions in which they are separated or generated. Finally, an even more complex situation is encountered with several geopolymers. Although there are relatively precise procedures for their isolation as specific fractions such as humic acids or components of coal, they may have a large variability depending on the location where they are collected, the age, etc. These polymers were initially produced by living organisms, but in time they suffered significant transformations. In organic geopolymers for example, small molecules could be incorporated by reactions induced by heat and the presence of catalysis. As an example, the incorporation of a lipid in a larger molecule may take place by the reaction:



These transformations may add new molecular species that are not initially produced by organisms [5].

Finally there are the composite materials that are not uniform but do have identifiable component parts. These component parts can usually be separated and analyzed individually. However, this is not always the chosen procedure for their analysis. Analytical pyrolysis has been applied to composite materials as well as to uniform polymers, depending on the purpose of the analysis. Some examples of the pyrolytic analysis of natural organic composite materials are presented in Part 3 of this book.

References 15.

1. E. W. Tegelaar, J. W. de Leeuw, C. Largeau, S. Derenne, H. -R. Schulten, R. Muller, J. J. Boon, M. Nip, J. C. M. Sprenkels, *J. Anal. Appl. Pyrol.*, 15 (1989) 29.
2. N. Niimura, T. Miyakoshi, J. Onodera, T. Higuchi, *J. Anal. Appl. Pyrol.*, 37 (1996) 199.
3. K. Wehling, Ch. Neister, J. J. Boon, M. T. M. Willemse, R. Wiermann, *Planta*, 179 (1989) 376.
4. A. M. Sherdinsky, T. P. Wampler, N. Indictor, N. S. Baer, *J. Anal. Appl. Pyrol.*, 15 (1989) 393.
5. K. J. Voorhees, *Analytical Pyrolysis, Techniques and Applications*, Butterworths, London, 1984.

This Page Intentionally Left Blank

PART 3.

Applications of Analytical Pyrolysis on Composite Natural Organic Materials.

This Page Intentionally Left Blank

Chapter 16. Analytical Pyrolysis of Plant Materials

16.1. Wood.

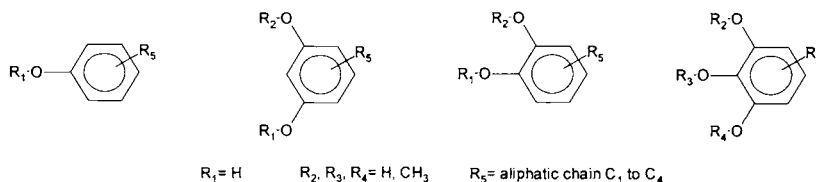
Wood is found mainly in trees and shrubs, although woody tissues are also found in some herbaceous plants. Wood is a complex material and living tree trunks are composed of a variety of tissues (pith, xylem, cambium, phloem, and bark). The wood from most angiosperm trees is known as hardwood, while the wood from gymnosperms is known as softwood.

There are numerous industrial applications of wood pyrolysis with the goal of generation of charcoal, methanol, or acetic acid for practical use. Analytical pyrolysis studies are only a small part of the subject of wood pyrolysis. These pyrolysis studies are performed with a variety of purposes, some for assisting the industrial uses of wood pyrolysis [1].

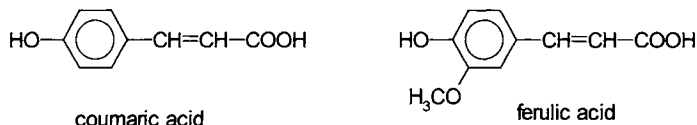
The main components of wood are cellulose, hemicelluloses, lignin, proteins, and small molecules including several inorganic compounds. The pyrolysis products of each individual type of macromolecular component of wood were described in Part 2 of this book. Some differences are seen in the pyrolysis of pure macromolecular components as compared to the pyrolysis results of the same component from the wood matrix. This is seen mainly for cellulose and hemicelluloses. However, the pyrolysis components are well recognizable, and it is common to use wood pyrolysates to trace a certain group of compounds to cellulose, hemicellulose, lignin, small molecules existent in wood, etc. The main applications for analytical pyrolysis studies can be listed as follows:

- fingerprinting for wood characterization [2,2a–5],
- studies of the thermal decomposition of different wood components [6–9],
- studies of kinetics of wood pyrolysis [10–17,17a],
- investigations on thermal decomposition of wood waste (sawdust) for waste utilization purposes [18,19],
- studies on the composition of wood processed by different techniques such as steam explosion, hydrolysis, etc. [20–23],
- studies of pyrolysis and gasification of biomass [24,25], and
- analysis of the smoke composition from different types of wood [26,27].

A special subject related to wood pyrolysis is the study of the composition of wood smoke. Smoke composition studies are important in relation to health issues and particularly to smoking of certain types of food for preservation and for achieving special taste. Smoke is generated both from polymers and from small molecules existent in wood. The main components found in curing smoke are probably phenols. Some of these are indicated below:



These compounds are generated mainly from lignin or from free coumaric and ferulic acids present in wood.



Ferulic acid may undergo decarboxylation followed by the oxidation of the vinyl group to generate an aldehyde. This aldehyde can be further oxidized and decarboxylated to generate phenols. Other compounds with smoke aroma are generated from cellulose and other polysaccharides. The main compounds from this class are dimethylfuran, furancarboxaldehyde, and furanylethanone. Besides phenols and furans, pyrazines play an important role to smoke aroma. Some of these are generated from small molecules from wood, but Maillard polymers and amidated pectin may also play a role in generating these types of compounds. A list of pyrazines generated in smoke of different wood types [26] at 290° C is given in Table 16.1.1.

TABLE 16.1.1. *Pyrazines generated in smoke of different wood types in mg/100g dry wood.*

Wood	pyrazine	3-ethyl-2-methoxy-	2-ethoxy-3-ethyl-	3,6-dimethyl-2-propyl-	2-butyl-3,5-dimethyl-	2-butyl-3,6-dimethyl-	2-acetyl-3-methyl-	2-acetyl-3,5-dimethyl-	Total
white oak	1.67	2.08	5.63	0.88	0.88	2.28	3.63	-	17.05
red oak	2.25	4.09	5.45	1.75	1.74	1.11	6.33	1.12	23.84
walnut	1.32	2.73	4.63	1.09	1.22	2.83	2.97	0.72	17.51
chestnut	1.35	2.41	4.20	0.22	0.55	0.65	1.21	-	10.59
apple	3.24	3.75	6.24	1.80	2.09	1.51	3.17	1.44	23.24
cherry	1.98	3.07	6.13	1.24	1.61	2.30	3.08	1.07	20.48
red alder	5.76	2.81	3.39	1.40	3.40	1.83	4.47	0.97	24.03
redwood	0.92	2.74	2.63	0.37	0.69	1.28	1.49	0.21	10.33
aspen	1.08	4.03	3.52	1.09	1.38	1.24	3.92	0.90	17.16
birch	2.65	3.60	7.79	1.87	1.53	2.71	5.01	1.12	26.28
hard maple	3.26	4.46	6.56	0.86	0.93	0.72	4.36	1.17	22.32
eastern cedar	3.40	4.07	4.43	1.87	1.50	2.24	4.07	0.47	22.05
hickory	1.52	7.68	5.73	3.47	4.16	4.12	10.85	3.50	41.03
Douglas fir (heartwood)	0.85	1.81	3.67	1.46	1.27	3.17	1.60	0.25	14.08
Douglas fir (sapwood)	1.10	3.23	4.31	1.19	1.79	2.05	5.35	1.05	20.07
lodgepole pine (wood)	4.94	4.67	5.35	3.19	2.67	3.44	9.19	2.14	35.59
lodgepole pine (bark)	3.30	4.05	4.51	3.48	1.83	4.71	5.40	2.29	29.57

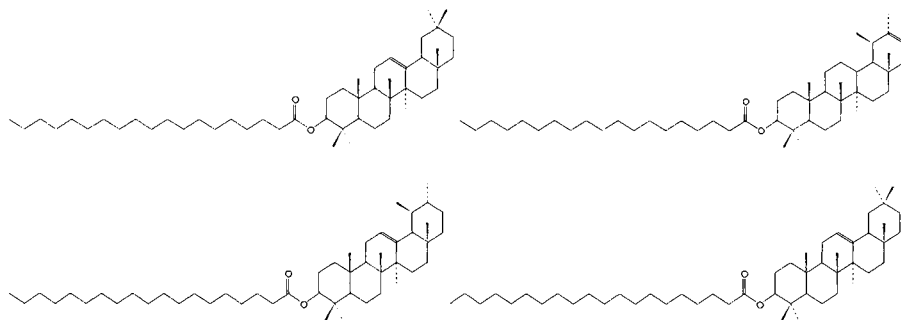
16.2. Leaves and other Plant Parts.

Leaves and other plant parts such as endocarps of certain fruits and straw of herbaceous plants were also studied by pyrolysis. There are various purposes for these studies, but in principle they have the same purpose as the studies done on wood. Some are associated with the analysis of industrial products generated from different

plant materials. Others cover fingerprinting [28,29], the analysis of thermal decomposition products of different plant parts [30,31], studies on fossil and recent materials [32] for comparison purposes (see also Section 16.3), studies on the composition of processed plant parts [33], etc.

As in the case of wood, besides pyrolysate composition, smoke composition of other plant parts such as dry leaves has been the subject of different studies [34]. As plants may contain a variety of biopolymers and small molecules, some of them specific for a certain plant, smoke composition can be very diverse. This explains why certain particular types of smoke are related to specific plants and specific plant parts. As an example, the smoke associated with roasting coffee contains phenols and pyrazines generated from both biopolymers and small molecules. One such small molecule from coffee that generates by pyrolysis a variety of phenols is chlorogenic acid.

Smoke consists mainly of small molecules. However, it may contain relatively large molecules as aerosols that are formed during burning. It is interesting that large molecules are difficult to see in regular pyrolysis, mainly due to condensation effects in pyrolysis instrumentation. However, this problem may be avoided for smoke that can be collected in special traps and then extracted and analyzed for a wide range of molecules. By this procedure it was possible to identify in smoke relatively large molecules such as dipalmitolein ($C_{53}H_{100}O_6$ MW 832), 1-palmitoyl-2-oleyl-3-stearin ($C_{55}H_{104}O_6$ MW 860), and triolein ($C_{57}H_{104}O_6$ MW 860), which were seen in the smoke from certain plant materials [34]. Some other large molecules also can be seen in smoke. For example, in the smoke of burning leaves from the Amazonian forest, triterpenoids esterified with long chain fatty acids with the structure indicated below were identified [34]



- *Pyrolysis of pine needles.*

Special attention was given to the thermal degradation of pine needles. These studies are of special interest for forest fires, providing information on the volatile compounds evolved during the fire. This knowledge is important from an environmental point of view and for fire retardation studies. A list of compounds generated from pyrolysis at 400° C of pine needles from *Pinus halepensis* is shown in Table 16.2.1 [35]. The origin of these compounds can be traced to cellulose, lignin, or volatile oils.

TABLE 16.2.1 *Compounds generated from pine needles pyrolysed at 400° C..*

MW	Compound
44	carbon dioxide
44	acetaldehyde
60	acetic acid
74	1-hydroxy-2-propanone
104	2-propoxyethanol
84	1,2-dimethyl-3-methylenecyclopropane
88	1-hydroxy-2-butanone
96	2-furancarboxaldehyde
98	2-furanmethanol
96	3-methyl-2-cyclopenten-1-one
110	2-furanylethanone
96	2H-pyran-2-one
98	cyclohexanone
110	5-methyl-2-furancarboxaldehyde
112	2-octene
94	phenol
112	bicyclo[2,2,1]heptan-7-ol
112	2 hydroxy-3-methyl-2-cyclopenten-1-one
136	1-methyl-4-(1-methylethenyl)cyclohexene
136	DL-limonene
124	2-methoxyphenol
122	benzeneethanol
144	2,3-dihydro-3,5 dihydroxy-6 methyl-4H-pyran-4-one
138	4-methoxymethylphenol
138	2-methoxy-4-methylphenol
122	benzoic acid
120	2,3-dihydrobenzofuran
110	1,2-benzenediol
152	4-ethyl-2-methoxyphenol
150	2 methoxy-6 vinylphenol
150	2-(propyl-1'-methyl)- phenol
164	2-methoxy-4-(2-propenyl)phenol
164	2-methoxy-4-(1-propenyl)phenol
166	3,4,5,6-tetramethyl-2,5-octadiene

Of particular interest has been the study of forest damage based on the characterization of spruce needles. Pyrolysis field ionization mass spectrometry (Py-FIMS) has been used for the characterization of ozone fumigated spruce needles and of needles treated with acidic fog [36]. The study showed significant differences between normal, ozone degraded, and acidic degraded needles. Ozone fumigation degrades flavones and lignin structures, whereas acidic water changes the polysaccharides. A different study was done on the effect of fire retardants on pine needles pyrolysis. It was shown that $(\text{NH}_4)_2\text{HPO}_4$ and $(\text{NH}_4)_2\text{SO}_4$ lower the pyrolysis temperature and increase the pyrolysis residue [36a]. The process is similar to that noticed also for cellulose (see Section 7.2).

-Pyrolysis products and smoke from the leaf of Nicotiana tabacum.

Pyrolysis studies of the leaf of *Nicotiana tabacum* received significant interest due to its use in cigarette manufacturing. A variety of pyrolysis studies on this subject were reported [37–42]. Some of these were oriented toward tobacco leaf characterization. Other studies were done to understand the origin of certain smoke components. Some

pyrolysis studies were done for plant material identification and classification. These studies focused less on the identification of particular leaf components and mainly for fingerprinting tobacco varieties. For example, the three main tobacco types, flue-cured (Virginia), burley and Oriental, were differentiated using Py-MS [40] and canonical variate data analysis.

Tobacco is a complex plant material containing small organic and inorganic molecules and biopolymers. The biopolymers consist of cellulose, hemicellulose, pectin, lignin, proteins and peptides, nucleic acids, etc. [43]. Tobacco leaf and stem composition for flue-cured and burley tobacco [44] is summarized in Table 16.2.2.

TABLE 16.2.2. Tobacco leaf and stem composition for flue-cured (Virginia) and burley tobaccos [44] expressed as % on a dry weight basis.

Component	Virginia lamina	Virginia stem	Burley lamina	Burley stem
SM ethanol soluble	56.3	41.6	31.5	31.0
SM water soluble lost in dialysis	5.2	13.5	19.5	14.6
SM acid detergent soluble	3.2	4.3	8.8	6.2
cellulose	5.9	11.7	6.4	15.4
starch	3.2	0.4	trace	trace
hemicellulose	3.6	5.0	3.2	4.9
pectin	10.7	12.4	11.5	14.8
lignin	1.7	2.2	2.1	2.4
protein	6.8	3.4	10.4	4.1
ash	3.8	1.5	1.8	1.4
Total accounted for	100.4	96.0	95.2	94.8

Several of the polymeric constituents were characterized by pyrolysis. An example is the characterization of lignin from tobacco using Py-GC/MS [45] (see Section 9.2). Also tobacco pectin was investigated using pyrolysis [46]. The contribution to the generation of volatile compounds of several model carbohydrates and of lignin also has been studied by Py-GC/MS [47]. A comparison of percentage of volatiles detected in several model pyrograms is given in Table 16.2.3.

Tobacco leaf has a complicated chemical composition including a variety of polymers and small molecules. The small molecules from tobacco belong to numerous classes of compounds such as hydrocarbons, terpenes, alcohols, phenols, acids, aldehydes, ketones, quinones, esters, nitriles, sulfur compounds, carbohydrates, amino acids, alkaloids, sterols, isoprenoids [48], Amadori compounds, etc. Some of these compounds were studied by pyrolysis techniques. One example of pyrolytic study is that of cuticular wax of tobacco leaf (green and aged), which was studied by Py-GC/MS [49]. By pyrolysis, some portion of cuticular wax may remain undecomposed. The undecomposed waxes consist of eicosyl tetradecanoate, docosyl octadecanoate, etc. The molecules detected in the wax pyrolysates include hydrocarbons (C_{27} to C_{34} with a maximum of occurrence of iso- C_{31} , normal C_{31} and anti-iso- C_{32}), alcohols (docosanol, eicosanol), acids (hexadecanoic, hexadecenoic, octadecanoic, etc.). The cuticular wax also contains terpenoids such as α - and β -8,13-divatriene-1,3-diols. By pyrolysis, some of these compounds are not decomposed and others generate closely related products such as seco-cembranoids (5-isopropyl-8,12-dimethyl-3E,8E,12E,14-pentadecatrien-2-one, 3,7,13-trimethyl-10-isopropyl-2,6,11,13-tetradecatrien-1al) and manols. By pyrolysis, *cis*-abienol, (12-Z)- λ -12,14-dien-8 α -ol, generates mainly *trans*-neo-abienol.

TABLE 16.2.3. *Percentage of volatiles detected in the pyrograms of three model carbohydrates and of lignin [47].*

No.	Compound	MW	Formula	cellulose	dextrin	sucrose	lignin
1	2-methylfuran	82	C5H6O	0.3			
2	3-methylfuran	82	C5H6O	6.1	19.9	3.0	
3	2-methyl-2-cyclopenten-1-one	96	C6H8O		2.0	0.3	
4	propionic acid methyl ester	88	C4H8O2	1.1	2.5	0.6	
5	2,4-pentanedione	100	C5H8O2		1.8	0.4	
6	2-methyl-2-pentenal	98	C6H10O		1.1		
7	5-methyl-3-hydrofuran-2-one	98	C5H6O2			0.6	
8	2-furaldehyde	96	C5H4O2	20.7	16.7	67.1	
9	2-acetyl-furan	110	C6H6O2	0.8		0.7	
10	5-methyl-2-furaldehyde	110	C6H6O2	2.1	1.7	4.2	
11	3,5,5-trimethyl-2-cyclopenten-1 one	124	C6H12O	0.7	0.6	0.5	
12	dihydro-2(3H)-furanone	86	C4H6O2			0.7	
13	2,3,4-trimethyl-2-cyclopenten-1-one	124	C8H12O		1.1	0.9	
14	2-furanmethanol	98	C5H6O2	2.0	3.8	2.4	0.9
15	5-methyl-2(5H)-furanone	98	C5H6O2	0.9	1.1		
16	3-methyl-2(5H)-furanone	98	C5H6O2	0.7	0.9		
17	3-hydroxybenzaldehyde	122	C7H6O2			0.1	
18	cyclopentanone	84	C5H8O	2.5	2.8	0.5	
19	2-pyrone	96	C5H4O2			0.6	
20	1,3-cyclopentanedione	98	C5H6O2	3.6	6.2	1.6	
21	4H-pyran-4-one	96	C5H4O2		1.5		
22	2-hydroxy-3-methyl-2-cyclopenten-1-one	112	C6H8O2	2.3	2.1	0.5	1.8
23	3-methyl-2,4(3H,5H)-furanidone	114	C5H6O3	5.1			
24	3-hydroxy-2-methylpyran-4-one	126	C6H6O3	10.0	1.1		
25	1,4-dimethoxybenzene	138	C8H10O2				1.3
26	a furancarboxylic acid methyl ester	126	C6H5O3	6.9	1.4	2.0	
27	phenol + o-cresol	94 + 108	C6H6O+ C7H8O	0.9	1.3	0.7	12.3
28	m-cresol + p-cresol	108	C7H8O	0.7	0.5	0.5	16.6
29	4-ethylphenol	122	C8H10O				2.6
30	2-ethyl-5-methylphenol	136	C9H12O				1.3
31	an ethyl dimethyl phenol	150	C10H14O				0.6
32	3,4-dimethoxyphenol	154	C8H10O3				0.7

Other small molecules present in tobacco were also studied by pyrolysis. For example, the pyrolysis products of nicotine at 700° C generate [50] the compounds given in Table 16.2.4.

TABLE 16.2.4. *The list of several pyrolysis products from nicotine generated at 700° C.*

pyridine	quinoline	acridine	phenylacetylene
2-picoline	isoquinoline	azaacridine	benzylacetylene
3-picoline	8-methylquinoline	benzocnitrile	methylphenylacetylene
4-picoline	6-methylquinoline	methylbenzocnitrile	naphthalene
2-vinylpyridine	4-methylquinoline	naphthonitrile	methylnaphthalene
3-vinylpyridine	dimethylquinoline	indole	biphenyl
3-cyanopyridine	cyanoquinoline	azaindole	acenaphthylene
2,2'-bipyridyl	benzo[h]quinoline	benzene	acenaphthene
nicotine	benzo[f]quinoline	toluene	fluorene
		styrene	anthracene

The analysis of tobacco smoke is a subject of numerous studies [51–55]. Both mainstream smoke and sidestream smoke are complex mixtures in which about 4000 compounds have been identified [55a]. As indicated previously (see Section 3.5) smoke is more complex than tobacco pyrolysate, because besides pyrolysis, some other processes such as combustion, distillation, and aerosol formation occur during smoking.

The mainstream smoke is commonly separated into compounds that are not retained by filtration through a special filter pad (Cambridge pad), known as “vapor phase smoke,” and components that are retained on the Cambridge pad known as “particulate phase smoke” components. Pyrolysis at 700° C under nitrogen generates compounds that correlate more closely with component profiles obtained from the particulate phase smoke (mainstream) of a reference cigarette [47]. However, not all compounds in cigarette smoke (and in smoke in general) come from pyrogenesis. A significant portion of the small molecules are distilled, steam distilled or captured in the aerosols formed as smoke.

A chromatogram of vapor phase smoke components from a non-commercial reference cigarette (Kentucky 1R4F) [56] is shown in Figure 16.2.1. The chromatogram does not show the peaks for CO, CO₂, H₂O, CH₄, and C₂H₆ that are present in smoke.

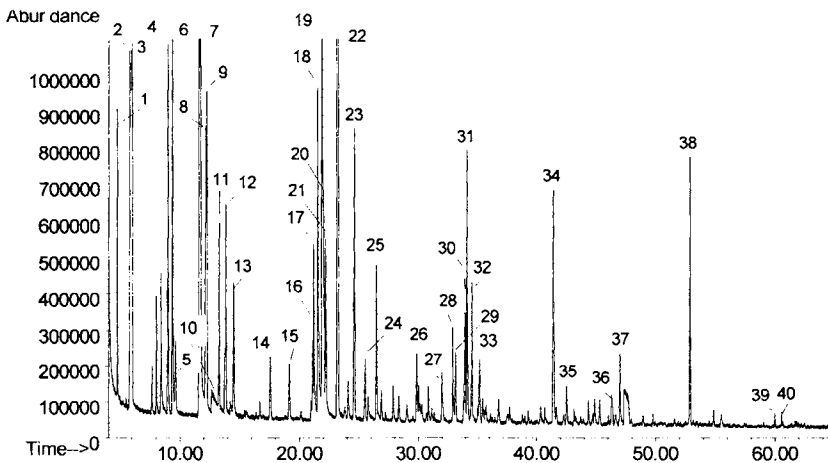


FIGURE 16.2.1. Total ion chromatogram of vapor phase smoke for a 1R4F cigarette [56].

The compounds identified in the chromatogram shown in Figure 16.2.1 are given in Table 16.2.5. This table also shows the normalized area counts obtained using a FID detector for the identified peaks (the normalization was done to 100 total area).

TABLE 16.2.5. *FID area counts (normalized) of selected vapor phase smoke components for a 1R4F cigarette.* The tentative source of each compound is also indicated. (Ps indicates polysaccharides; SM indicates small molecules.)

Peak No.	Compound	Normalized counts	Origin
1	an unknown	0.05	?
2	propene	11.0	sugars, fats, waxes, Ps, SM
3	propane	8.5	sugars, fats, waxes, Ps, SM
4	methylene chloride	2.1	contaminant ?
5	2-methylpropane	0.7	sugars, fats, waxes, Ps, SM
6	acetaldehyde	13.0	sugars, fats, waxes, Ps, SM
7	1-butene	3.3	sugars, fats, waxes, Ps, SM
8	butane	2.3	sugars, fats, waxes, Ps, SM
9	butadiene	2.6	sugars, fats, waxes, Ps, SM
10	methanol	0.7	sugars, esters, Ps, SM
11	2-butene	1.5	sugars, fats, waxes, Ps, SM
12	methanethiol	0.6	amino acids, proteins, SM, ?
13	2-methyl-1-propene	1.3	sugars, fats, waxes, Ps, SM
14	2-methyl-1-butene	0.7	sugars, fats, waxes, Ps, SM
15	2-methylbutane	0.6	sugars, fats, waxes, Ps, SM
16	1-pentene	0.5	sugars, fats, waxes, Ps, SM
17	acrolein	1.8	sugars, fats, waxes, Ps, SM
18	acetonitrile	2.5	amino acids, proteins, SM, ?
19	acetone	7.2	sugars, fats, waxes, Ps, SM
20	furan	1.9	sugars, Ps, SM
21	propanal	1.3	sugars, fats, waxes, Ps, SM
22	isoprene	19.1	SM
23	cyclopentane	2.3	sugars, Ps
24	1,3-pentadiene	0.5	sugars, Ps
25	1,3-cyclopentadiene	1.3	sugars, Ps
26	2-methylpropanal	0.6	sugars, Ps
27	propanenitrile	0.6	amino acids, proteins, SM, ?
28	3-buten-2-one	0.9	sugars, Ps, SM
29	1-hexene	0.7	sugars, fats, waxes, Ps, SM
30	2,3-butanedione	0.7	sugars, fats, waxes, Ps, SM
31	butanone	2.0	sugars, fats, waxes, Ps, SM
32	2-methylfuran	1.1	sugars, Ps
33	2-methyl-2-pentene	0.6	sugars, fats, waxes, Ps
34	benzene	2.4	sugars, fats, waxes, lignin, Ps
35	2-methylbutanal	0.3	sugars, fats, waxes, Ps, SM
36	heptane	0.4	sugars, fats, waxes, Ps, SM
37	2,5-dimethylfuran	0.5	sugars, Ps
38	toluene	1.7	sugars, fats, waxes, lignin, Ps
39	ethylbenzene	0.1	sugars, fats, waxes, lignin, Ps
40	1,2-dimethylbenzene	0.05	sugars, fats, waxes, lignin, Ps

The complexity of the composition of particulate phase smoke can be seen in Figure 16.2.2, which shows the chromatogram (TIC) of this material from a 1R4F Kentucky reference cigarette. The smoke condensate was extracted with *t*-butyl methyl ether and separated on a DB-5 column 60 m long, 0.32 mm i.d., 1 μ film thickness. The GC used a temperature gradient between 50° C and 300° C.

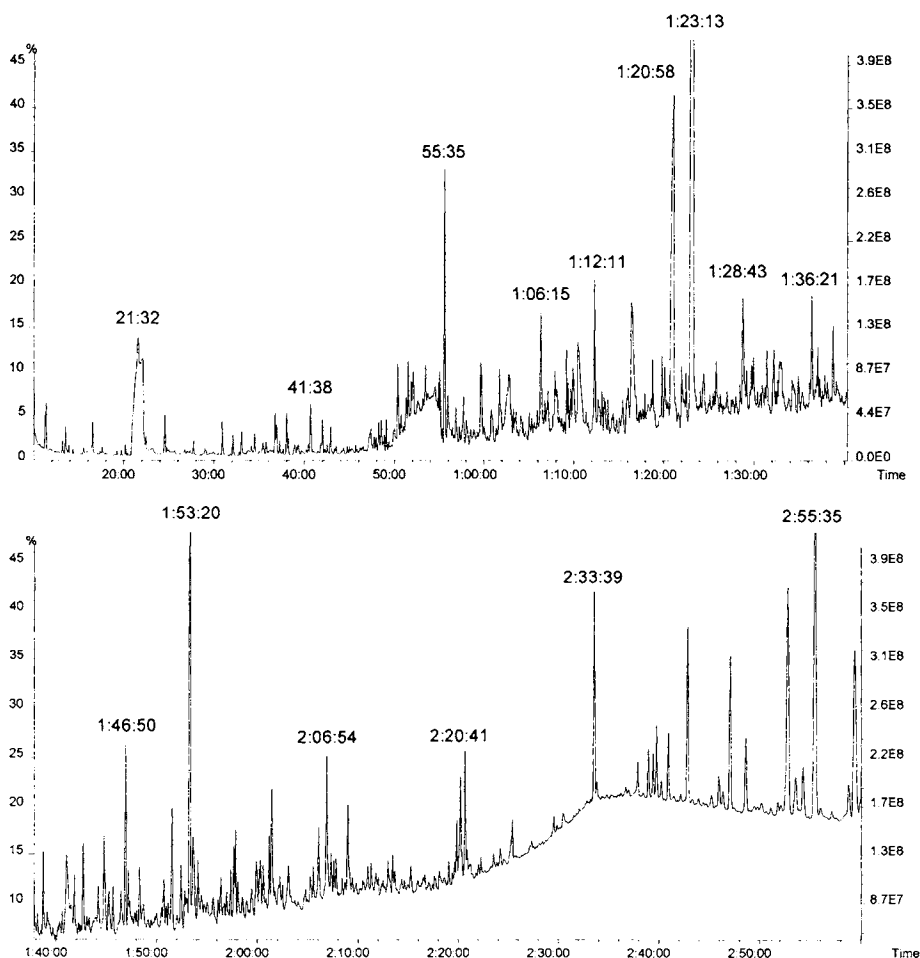


FIGURE 16.2.2. TIC of particulate phase smoke for a 1R4F cigarette.

A series of peak identifications using mass spectra library searches for the chromatogram shown in Figure 16.2.2 are given in Table 16.2.6. The table also shows the tentative source of individual components generated by pyrolysis of biopolymers. Some of the compounds originate from small molecules (SM) and are not generated by pyrolysis but by other processes taking place during smoking (distillation, aerosol formation, etc.).

TABLE 16.2.6. *Compounds generated in cigarette smoke.* (Rel. Int. = intensity relative to nicotine; SM = small molecules; Ps = polysaccharides including cellulose, pectins, hemicellulose etc.; AP = amidated pectin; Pr = protein; Ma = Maillard polymers.)

Ret. time	Compound	Rel. Int.	Possible compound source
0:11:19	solvent impurity (formic acid tert-butyl ester) + methylcyclopentane	3.64	
0:12:51	methylpropanal	>0.02	sugars, Ps, SM
0:13:08	3-methyl butanal	>0.02	sugars, Ps, SM
0:13:26	methyl acetate	0.73	sugars, Ps, SM
0:13:38	2-methyl pentyl acetate	>0.02	sugars, Ps, SM
0:13:50	2-methyl butanal	>0.02	sugars, Ps, SM
0:15:19	3-methyl-4-pentene-2-one	>0.02	sugars, Ps
0:16:00	propanoic acid	>0.02	sugars, Ps, SM
0:16:29	2,3-pentandione	0.91	sugars, Ps, SM
0:16:57	2-propenoic acid	>0.02	sugars, Ps, SM
0:17:27	unknown	>0.02	?
0:17:32	3-hydroxy-2-butanone	>0.02	sugars, Ps, SM
0:19:40	2-oxo-propanoic acid methyl ester	0.21	sugars, Ps, SM
0:20:23	pyrazine	>0.02	SM, amino acids, AP
0:21:32	pyridine	18.18	SM, amino acids, AP
0:22:22	butene nitrile	0.18	SM, amino acids, Pr
0:23:06	unknown	>0.02	?
0:24:23	3-pentanone	0.09	sugars, Ps, SM
0:24:27	toluene	0.09	lignin, SM, amino acids, Pr
0:24:42	acetic acid anhydride ?	>0.02	?
0:27:40	1,1'-oxabis propane	0.27	?
0:27:40	cyclopentanone	>0.02	sugars, Ps, SM
0:28:48	unknown	>0.02	?
0:29:08	unknown	>0.02	?
0:29:49	2-methylheptane	>0.02	esters, waxes, SM
0:30:51	2-methylpyridine	0.73	SM, amino acids, AP
0:32:30	2-methylpyrazine	0.27	SM, amino acids, AP, Ma
0:32:45	unknown	>0.02	?
0:33:00	furfural	1.18	sugars, Ps
0:33:40	2,2-dimethyl-3-butenal	>0.02	sugars, Ps, SM
0:34:08	2-hexen-1-ol	>0.02	sugars, Ps, SM
0:34:28	5-methyl-2-furanone	0.09	sugars, Ps
0:34:58	N-methyl-N-(2-propynyl)-acetamide	>0.02	SM, amino acids, AP
0:35:25	2-heptene	>0.02	sugars, waxes, SM
0:35:42	furanmethanol	0.18	sugars, Ps
0:36:06	2-methyl-butyric acid	>0.02	esters, waxes
0:36:41	3-methyl pyridine	0.82	SM, amino acids, AP
0:37:14	acetyl acetate	>0.02	?
0:37:37	2-ethylfuran	>0.02	sugars, Ps
0:38:10	1,3-dimethylbenzene	>0.02	sugars, Ps, lignin
0:38:52	1-acetoxy-2-propanol	>0.02	?
0:39:07	protoanemonin	>0.02	sugars, Ps, SM
0:39:18	2,6-dimethyl pyridine	>0.02	SM, amino acids, AP
0:39:44	1-octen-3-ol	>0.02	?
0:40:38	styrene	0.39	SM, lignin
0:41:40	2-methylcyclopentanone	>0.02	sugars, Ps
0:41:46	2-ethylpyridine	>0.02	SM, amino acids, AP
0:41:58	2-methyl-2-cyclopenten-1-one	0.91	sugars, Ps
0:42:10	2-furanone	>0.02	sugars, Ps, Ma
0:42:30	2-furanylethanone	>0.02	sugars, Ps
0:42:52	2,6-dimethylpyrazine	>0.02	SM, amino acids, AP, Ma
0:43:30	2,3-dimethylpyrazine	>0.02	SM, amino acids, AP, Ma
0:44:50	2-hydroxycyclopent-2-en-1-one	0.14	sugars, Ps
0:44:43	2,4-dimethylpyridine	>0.02	SM, amino acids, AP, Ma
0:44:58	2,5-dimethylpyridine	>0.02	SM, amino acids, AP, Ma

TABLE 16.2.6. *Compounds generated in cigarette smoke (continued)*. (Rel. Int. = intensity relative to nicotine; SM = small molecules; Ps = polysaccharides including cellulose, pectins, hemicellulose etc.; AP = amidated pectin; Pr = protein; Ma = Maillard polymers.)

Ret. time	Compound	Rel. Int.	Possible compound source
0:45:17	5-methyl-2-furanone	>0.02	sugars, Ps
0:45:17	2-vinylpyridine	>0.02	SM, amino acids, AP, Ma
0:45:38	2,5-dimethyl-2-cyclopenten-1-one	>0.02	sugars, Ps
0:46:07	2-ethylcyclopentanone	>0.02	sugars, Ps
0:47:00	3-methylvaleric acid	>0.02	SM, waxes
0:47:42	propylbenzene	>0.02	lignin
0:47:54	3-ethylpyridine	>0.02	SM, amino acids, AP, Ma
0:48:14	5-methyl-2-furancarboxaldehyde	>0.02	sugars, Ps, Ma
0:48:29	unknown	>0.02	?
0:48:41	benzaldehyde	0.45	lignin, Ps
0:48:50	1-ethyl-2-methylbenzene	0.45	lignin, Ps
0:49:40	3-vinylpyridine	0.73	SM, amino acids, AP, Ma
0:49:22	1,2,3-trimethylbenzene	>0.02	lignin, Ps
0:49:47	phenol like ?	3.18	lignin, Ps
0:50:00	myrcene	0.91	SM
0:50:00	3,5-dimethylpyridine	0.91	SM, amino acids, AP, Ma
0:50:13	phenol	>0.02	lignin, Ps
0:50:28	octanoic acid	>0.02	waxes, lipids
0:50:40	(1-methylvinyl)-benzene	>0.02	lignin, Ps
0:50:58	benzoxonitrile	>0.02	SM, amino acids, AP, Ma
0:51:14	o-CHLOROPHENOL (standard)	0.02	
0:51:27	pentanal ?	>0.02	sugars
0:51:48	2-propylpyridine	>0.02	SM, amino acids, AP, Ma
0:51:59	C3-benzene	>0.02	lignin
0:52:50	2,6-dimethyl-2,6-octadiene	0.73	?
0:52:32	trimethylpyrazine	>0.02	SM, amino acids, AP, Ma
0:52:43	4-pyridincarboxaldehyde	>0.02	AP
0:52:43	α -ionone	>0.02	SM, lignin
0:55:18	glycerin	>0.02	?
0:53:19	unknown	>0.02	?
0:53:28	isoliimonene	>0.02	SM
0:53:40	imidazolic acid ?	0.45	?
0:54:39	C3-benzene	>0.02	lignin, SM
0:54:49	2-hydroxy-3-methyl-2-cyclopenten-1-one	2.73	sugars, Ps
0:55:00	1-methyl-4-(methylethyl)-cyclohexene	>0.02	sugars, Ps
0:55:06	C4-benzene	>0.02	lignin, SM
0:55:17	propenylbenzene	>0.02	lignin, SM
0:55:35	limonene	6.09	SM
0:55:54	2,3-dimethyl-2-cyclopenten-1-one	1.82	sugars, Ps
0:56:22	unknown	>0.02	?
0:56:35	2,4-dihydroxy-3,3-dimethyl- γ -butanolactone	>0.02	sugars, Ps
0:56:50	β -ocimene	1.27	SM
0:57:14	1-H-indene	>0.02	?
0:57:36	2-methylphenol	1.36	lignin, Pr
0:57:55	2,5-dimethyl-4-hydroxy-3-furanone	>0.02	sugars, Ps
0:58:12	2,3,4-trimethyl-2-cyclopenten-1-one	>0.02	sugars, Ps
0:58:27	acetylpyrrole	0.73	SM, amino acids, AP, Ma
0:58:48	5-methyl-tetrahydrofuranmethanol	>0.02	sugars, Ps
0:59:00	C4-benzene	>0.02	lignin
0:59:12	?-methylphenol	>0.02	sugars, lignin, Ps
0:59:32	4-methylphenol	4	SM, sugars, lignin, Ps
0:59:54	C4-phenol ?	>0.02	SM, sugars, lignin, Ps
1:00:20	4-hydroxypyridine	>0.02	AP, Ma
1:00:38	unknown	>0.02	?
1:00:47	2-methoxyphenol	1.55	lignin
1:00:59	undecene	>0.02	waxes, ?

TABLE 16.2.6. *Compounds generated in cigarette smoke (continued)*. (Rel. Int. = intensity relative to nicotine; SM = small molecules; Ps = polysaccharides including cellulose, pectins, hemicellulose etc.; AP = amidated pectin; Pr = protein; Ma = Maillard polymers.)

Ret. Time	Compound	Rel. Int.	Possible compound source
1:01:22	1-methyl-2-(2-propenyl)-benzene	>0.02	lignin
1:01:39	unknown	3.27	?
1:01:52	unknown	>0.02	?
1:02:07	3-hydroxypyridine	0.91	AP, Ma
1:02:30	aminopyrimidine	3.27	AP, Ma
1:02:39	2-BROMOCHLOROBENZENE (standard)	>0.02	
1:03:00	maltol	>0.02	sugars, Ps
1:03:14	3-pyridinol acetate	1.09	SM, AP, Ma
1:03:30	3-ethyl-2-hydroxy-2-cyclopenten-1-one	0.91	sugars, Ps
1:03:42	unknown	>0.02	?
1:04:20	3-aminophenol	>0.02	?
1:04:20	3,4-dimethyl-2,4,6-octatriene	>0.02	sugars, SM
1:04:35	2,3,4-trimethyl-2-cyclopenten-1-one	>0.02	sugars, Ps
1:04:53	2,5-pyrrolidione	>0.02	SM, Pr, AP, Ma
1:05:12	ethylphenol	>0.02	lignin
1:05:34	benzeneacetoneitrile	>0.02	SM, Pr, AP, Ma
1:05:52	6-methyl-2-pyrazinylmethanol	>0.02	SM, Pr, AP, Ma
1:06:15	hydroxymaltol	6.36	sugars, Ps
1:06:27	3,4-dimethylphenol	>0.02	sugars, lignin
1:06:36	2,6-piperidindione	>0.02	SM, Pr, AP, Ma
1:06:57	4-aminophenol	2.73	SM, Pr, AP, Ma
1:07:24	1-methylindene	>0.02	?
1:07:36	3,4-dimethyl-1(H)-pyrrole-2,5-dione	>0.02	Pr, Ma, SM
1:07:47	3-ethylphenol	1.82	lignin
1:08:23	benzoic acid	>0.02	?
1:08:38	a methylphenyl ethanone	>0.02	lignin
1:08:47	2,3-dimethylphenol	>0.02	lignin
1:09:31	2-hepten-1-ol	0.91	?
1:09:40	1-dodecene	>0.02	waxes, SM
1:09:52	1-(methylphenyl)-ethanone (mix)	4.55	lignin
1:10:20	1,2-benzendiol	8.18	sugars, Ps, lignin
1:10:26	naphthalene	>0.02	?
1:10:53	2,3-dihydro-4,7-dimethyl-1H-indene (mix)	>0.02	?
1:10:53	4-methyl-pyridinol acetate	>0.02	AP
1:11:18	triacontane	>0.02	waxes
1:12:11	2,3-dihydrobenzofuran	5.82	sugars, Ps
1:12:37	5-(hydroxymethyl)-2-furancarboxaldehyde	3.64	sugars, Ps
1:12:47	3-(1-methylethyl)-phenol	>0.02	lignin
1:13:30	1,2-benzendiol diacetate	1.18	Ps
1:13:16	3-ethyl-4-methyl-1H-pyrrole-2,5-dione	>0.02	SM, Ma, AP
1:13:42	2-ethyl-5-methylphenol	0.91	lignin
1:14:59	benzeneacetic acid	>0.02	?
1:15:21	α -methyl-benzenmethanol	1.27	lignin
1:15:52	a decane	2.55	waxes
1:16:50	a terpene	>0.02	SM
1:16:22	1,4-benzenediol	14.55	sugar, Ps, lignin
1:16:49	4-ethyl-2-methoxy-phenol	>0.02	sugar, Ps, lignin
1:17:15	2,3-dihydroxy-1-ethanone (mix)	>0.02	sugar, Ps, lignin
1:17:40	1-tridecene	>0.02	waxes
1:17:52	2,3-dihydro-1H-inden-1-one	>0.02	?
1:18:06	4-methylcatechol (mix)	>0.02	sugar, Ps, lignin
1:18:17	tridecane	0.36	waxes
1:18:42	1H-indole	1.82	SM, Ma, AP, Pr
1:19:26	1-methylnaphthalene	>0.02	?
1:19:47	4-vinyl-2-methoxy-phenol	2.36	lignin
1:19:59	hydrocarbon	1.82	waxes

TABLE 16.2.6. *Compounds generated in cigarette smoke (continued)*. (Rel. Int. = intensity relative to nicotine; SM = small molecules; Ps = polysaccharides including cellulose, pectins, hemicellulose etc.; AP = acetyl-pectin; Pr = protein; Ma = Maillard polymers.)

Ret. Time	Compound	Rel. Int.	Possible compound source
1:20:58	triacetin	23.64	Migrated from the cig. filter.
1:21:34	4-aminoindole	>0.02	SM, Ma, AP, Pr
1:21:53	2-methyl-1,4-benzendiol	2.36	sugar, Ps, lignin
1:22:00	4-(2-propenyl)-phenol	>0.02	sugar, Ps, lignin
1:22:24	2,6-dimethoxyphenol	1	sugar, Ps, lignin
1:22:42	2-methylbenzofuran	>0.02	sugar, Ps,
1:23:13	nicotine	100	SM
1:23:31	2,7-naphthalenediol	>0.02	?
1:23:38	1,2-dihydro-1,1,6-trimethylnaphthalene ?	>0.02	?
1:23:58	4-propoxyphenol	0.45	lignin
1:24:22	5-oxoproline methyl ester (mix)	2.18	amino acids, Pr
1:24:22	3-acetyl-2,5-dimethylfuran	>0.02	sugar, Ps,
1:25:07	1-tetradecene	>0.02	waxes
1:25:25	4,7-dimethylbenzofuran	>0.02	sugar, Ps,
1:25:45	7-methyl-1H-indole	2.36	SM, Ma, AP
1:25:57	benzenethanol	>0.02	sugar, Ps,
1:26:21	2-methoxy-3-ethylpyridine	>0.02	SM, Ma, AP
1:26:35	2-methoxy-4-(2-propenyl)-phenol (eugenol)	>0.02	lignin
1:26:56	2,5,8-trimethyl-1,2-dihydronaphthalene	>0.02	?
1:27:13	3-methoxy-3-ethylpyrazine	>0.02	AP, Ma
1:27:35	3-methylbenzothiophene	>0.02	Pr, SM
1:27:26	3-hydroxybenzoic acid methyl ester (mix)	>0.02	lignin
1:27:26	7-methylindanone ?	>0.02	?
1:27:53	4-hydroxybenzenethanol	0.45	lignin
1:28:28	benzothiadiazol ?	1.82	?
1:28:43	3-(3,4-dihydropyrrol-5-yl)-pyridine (myosmine)	4.82	SM
1:28:58	1,5-dimethyl-naphthalene	>0.02	?
1:29:12	3,7,11-trimethyl-(E,E)-2,6,10-dodeca-1-ol (trans farnesol)	0.64	SM
1:29:30	2,3-dimethylhydroquinone	0.82	SM, Ma, AP
1:29:42	2-methoxy-4-(1-propenyl)-phenol	>0.02	lignin
1:29:57	3,7,11,15-tetramethyl-(E,E)-2,6,10-dodeca-1-ol	2.45	?
1:30:17	5-methoxy-2,3-dimethylphenol	>0.02	lignin
1:30:55	1-dodecene	2.45	waxes
1:31:25	norsolanadiene	1.09	SM
1:31:40	3,7,11-trimethyl-1,2,6,10-dodecatetraene (farnesene)	>0.02	?
1:31:58	1,3-dihydro-2H-indol-2-one	>0.02	SM
1:32:90	β -nicotyrine	1.64	?
1:32:24	2,4,6-trimethyl-benzonitrile	>0.02	?
1:32:37	undecane?	>0.02	waxes
1:32:45	nonanoic acid ?	4.09	waxes
1:33:30	2,3-dimethyl-(1H)-indole	>0.02	Ma, Pr, SM
1:33:12	t-butyl-hydroxyanisole	>0.02	?
1:33:48	epoxymegastigmendiol	0.91	SM
1:34:09	2,3,5-trimethyl-1,4-benzendiol	>0.02	sugars, Ps
1:34:26	1-naphthalenol	>0.02	?
1:34:50	2-ethyl-3-methylquinoxaline	1.82	?
1:35:10	2-naphthalenol	>0.02	?
1:36:21	2,2'-bipyridine	3	SM
1:36:42	2-naphthylamine	>0.02	?
1:36:46	1-BROMODODECANE (standard)	>0.02	
1:36:49	4-phenylisothiazole	>0.02	?
1:37:30	3,5-dimethoxyacetophenone	1.45	lignin
1:37:17	benzoic acid 2-propenyl ester	>0.02	?
1:37:32	megastigmatrienone 2	>0.02	SM
1:37:47	5-quinolinamine ?	0.45	?
1:38:00	7-hydroxy-2H-1-benzopyran-2-one	>0.02	sugars, Ps

TABLE 16.2.6. *Compounds generated in cigarette smoke (continued)*. (Rel. Int. = intensity relative to nicotine; SM = small molecules; Ps = polysaccharides including cellulose, pectins, hemicellulose etc.; AP = amidated pectin; Pr = protein; Ma = Maillard polymers.)

Ret. Time	Compound	Rel.int.	Possible compound source
1:38:44	megastigmatrienone	2.09	SM
1:39:10	2,3-dihydroxy-5-methylphenyl-ethanone	>0.02	lignin
1:39:08	4-methylundecane	>0.02	waxes
1:39:16	unknown	>0.02	?
1:40:13	fluorene	>0.02	?
1:40:25	(mix)	>0.02	?
1:40:37	3-hydroxy- β -damascenone	0.91	SM
1:41:10	quinic acid	7.27	sugars, SM
1:41:50	megastigmatrienone 4	1.18	SM
1:42:20	benzodifuran ?	>0.02	sugars, Ps
1:42:14	4,4'-dimethyl-1,1'-biphenyl	>0.02	lignin
1:42:41	4-keto- α -ionol	2.45	SM
1:43:20	3-methyl-1-naphthalenol	>0.02	?
1:43:16	α -nicotyrine	>0.02	SM
1:44:30	1-tetradecanol	0.91	waxes
1:44:10	4-hydroxy- β -ionone	>0.02	SM
1:44:45	bis-(4-pyridyl) methane	1.55	SM
1:44:56	2,4,5-trimethylacetophenone	0.55	?
1:45:14	unknown	0.91	?
1:45:39	2,6-dimethyl-4-(2-propenyl)-phenol (mix)	0.91	lignin
1:46:28	3-oxo-7,8-dihydro- α -ionol	0.55	SM
1:46:50	cotinine	0.45	SM
1:46:58	1,1,2-trimethyl-cycloundecane	4.55	waxes
1:47:13	deacetylphytuberin	>0.02	SM
1:47:20	4-phenoxyphenol	>0.02	lignin
1:47:34	1-(4-hydroxy-3,5-dimethoxyphenyl)-ethanone	>0.02	lignin
1:47:51	hexahydro-4,4-dimethyl-6-(1-methylethylidene)-naphthalen-2-one	>0.02	?
1:48:30	a terpene	>0.02	SM
1:48:16	4-(3-hydroxy-1-propenyl)-3-methoxyphenol	1.27	lignin
1:48:40	1-propenyl-3,4,5-trimethoxybenzene (mix)	>0.02	lignin
1:48:40	6-amino-5-methylnicotinic acid	>0.02	SM
1:49:06	hydrocarbon	>0.02	waxes
1:49:27	1-(2,4,6-trihydroxyphenyl)-2-pentanone	>0.02	sugars, Ps
1:49:57	9H-fluoren-9-one	>0.02	?
1:50:22	3,8-dihydroxy-2-methyl-4H-1-benzopyran-4-one	>0.02	sugars, Ps
1:50:29	6,7-dehydro-7,8-dihydro-3-oxo- α -ionol	>0.02	SM
1:50:43	2,3,6-trimethyl-1,4-naphthalendione	1.09	?
1:50:56	(-) loliolide (mix)	>0.02	?
1:50:56	2,3-dihydro-1-ethyl-(1H)-2-methylcyclopentaquinoxaline	>0.02	?
1:51:11	docosane	0.91	waxes
1:51:31	formylnicotinine	4.09	SM
1:52:25	unknown	1.55	?
1:52:48	anthracene	>0.02	?
1:53:20	neophytadiene	23.64	SM
1:53:39	6,10,14-trimethyl-2-pentadecanone	3.91	waxes
1:54:70	1-methyl-2,3-dihydroxy-7-(2-propenyl)-1,2,3,4,5,6,7,8-octahydronaphthalene	1.18	?
1:54:44	dimethoxyphenol acetate ?	0.91	lignin
1:55:50	1-ethyl-2,3,4,9-tetrahydro-1H-pyrido[3,4-b]indole	>0.02	?
1:55:37	9H-carbazol	>0.02	SM
1:56:07	2-(2-furanyl)-5,6-dimethylpyrazine	>0.02	Ma
1:56:19	theobromine	1.82	SM
1:56:47	nonacosane	>0.02	waxes
1:56:59	2-heptadecanone ?	0.45	?
1:57:21	pentamethyltetracosahexane	1	waxes
1:57:42	farnesylacetone	1.55	SM

TABLE 16.2.6. *Compounds generated in cigarette smoke (continued)*. (Rel. Int. = intensity relative to nicotine; SM = small molecules; Ps = polysaccharides including cellulose, pectins, hemicellulose etc.; AP = amidated pectin; Pr = protein; Ma = Maillard polymers.)

Ret. Time	Compound	Rel. Int.	Possible compound source
1:57:53	decahydrocarotene	2	SM
1:58:07	methyl hexadecanoate	0.82	waxes
1:58:32	unknown	0.45	?
1:59:22	1,4-diaza-2,5-dioxo-3-isobutyl bicyclo[4.3.0]nonane ?	0.45	?
1:59:55	1,4-diaza-2,5-dioxo-3-isobutyl bicyclo[4.3.0]nonane isomer	>0.02	?
2:00:20	farnesol 2	>0.02	SM
2:00:33	5H,10H-dipyrrolo[1,2-A,1',2'-D]pyrazine-5,10-dione	>0.02	?
2:00:54	1-methyl-9H-pyrido[3,4-B]indole-3-carboxylic acid methyl ester	>0.02	?
2:01:00	scopoletin	0.2	SM
2:01:21	7-hydroxy-6-methoxy-2H-1-benzopyran-2-one	4.55	sugars, Ps
2:01:47	5-eicosene	>0.02	waxes
2:02:07	hexatriacontane	1.36	waxes
2:03:30	9H-pyrido[3,4-B]indole	1.18	?
2:03:24	di (2-ethylhexyl) adipate	>0.02	waxes
2:04:10	geranyl linalool isomer B	>0.02	SM
2:04:15	2,6,10,14-tetramethylhexadecane ?	>0.02	waxes, esters
2:04:26	4,4'-DIBROMODIPHENYL (standard)	0.06	
2:04:39	1-(9H-pyrido[3,4-B]indole-1-yl)-ethanone	>0.02	?
2:05:14	duvatriendiol (mix)	>0.02	SM
2:05:14	1-acetyl-4,5-dihydro-2-(1-naphthalenylmethyl)-1H-imidazol	>0.02	?
2:06:07	duvatriendiol	1.45	SM
2:06:43	1-phenyl-3-(2,2,6-trimethyl-7-oxabicyclo[4.1.0]hept-1-yl-2-propen-1-one	>0.02	?
2:06:54	duvatriendiol	2.91	SM
2:07:30	8,11-octadienoic acid methyl ester	>0.02	lipids, waxes
2:07:12	pentadecane ?	1	waxes
2:07:51	phytol	>0.02	SM
2:08:26	octadecanoic acid methyl ester	>0.02	lipids, waxes
2:08:57	unknown	1.82	?
2:10:58	1-acetyl-2-pyridinyl-2,3,4,5-tetrahydropyrrole	>0.02	?
2:11:48	1-docosanol	2.73	waxes
2:19:54	methylsqualene ?	1.82	?
2:20:15	hexamethylpentacosahexaene	1.82	waxes
2:20:24	farnesyl acetone B ?	>0.02	SM
2:20:41	a megastigmatrienone ?	1.82	SM
2:23:32	2,3-dihydro-5,6-di-2-pyridinyl-pyrazine	>0.02	Ma, SM
2:26:42	6,7-dimethoxy-3-phenyl-4H-1-benzopyran-4-one	>0.02	?
2:29:35	hexacosane ?	>0.02	waxes
2:33:39	1-tricosanol ?	5.45	?
2:38:00	heptacosane ?	>0.02	?
2:39:32	solanol	>0.02	SM
2:39:51	lycopersin ?	1.82	?
2:40:20	farnesylacetone ?	>0.02	SM
2:41:20	nonacosane ?	>0.02	waxes
2:42:48	a tricosanol ?	6.36	waxes
2:46:30	(3,β)-cholest-5-en-ol acetate ?	>0.02	SM
2:46:29	dodecatriacontane	>0.02	waxes
2:47:11	dodecene ?	6.36	waxes
2:48:46	tetracontane ?	>0.02	waxes
2:52:55	1-heptadecene	10.91	waxes
2:54:23	(3,β,22Z)-stigmasta-5,22-dien-3-ol acetate	>0.02	SM
2:55:35	1-tetradecene ?	19.09	waxes
2:59:29	vitamin E	9.09	SM

As previously indicated, the GC of an underivatized pyrolysate may not give a complete representation of its constituents. This is also the situation for smoke, and smoke silylation or other derivatization techniques were used in smoke analysis. The chromatographic trace for the silylated smoke from a commercial cigarette [57] is shown in Figure 16.2.3. The chromatogram was obtained from smoke that was silylated with bis-(trimethylsilyl)trifluoroacetamide (BSTFA) and separated on a methyl silicone with 5% phenyl silicone chromatographic column, 60 m long, 0.32 mm i.d., 0.25 μ film thickness. A temperature gradient between 50° C and 300° C was used for the GC.

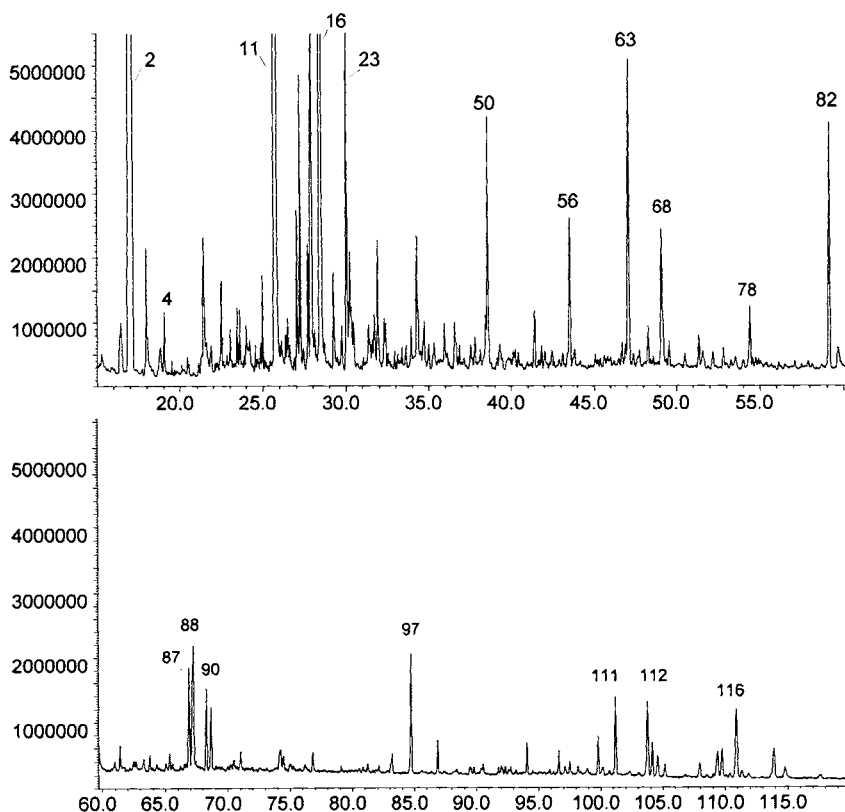


FIGURE 16.2. 3. *Chromatographic trace for silylated smoke from a commercial cigarette.*

A list of peak identifications for the chromatogram shown in Figure 16.2.3 is given in Table 16.2.7. The identifications were done mainly using mass spectral library searches.

TABLE 16.2.7. *Peak identifications for the chromatogram of silylated smoke from a commercial cigarette.* The chromatogram is shown in Figure 16.2.3; the tentative source of individual components obtained by pyrolysis is also shown. (SM = small molecules; Ps = polysaccharides including cellulose, pectins, hemicellulose etc.; AP =amidated pectin; Pr = protein; Ma = Maillard polymers.)

Peak No.	Compound	Possible compound source
1	ethylene glycol	?
2	propylene glycol	commercial cigarette additive
3	phenol	lignin, Ps
4	actic acid	sugars, Ps
5	glycolic acid	sugars, Ps
6	furan carboxylic acid	sugars, Ps
7	3-hydroxypyridine	AP, SM
8	acid 3-hydroxypropanoic	sugars, Ps
9	cresol	lignin, Ps
10	pyrrolidinol	AP, SM
11	reagent	
12	dihydroxyacetone	sugars, Ps
13	xylenol + hydroxyaniline	lignin, Ps, ?
14	xylenol	lignin, Ps
15	benzoic acid	?
16	glycerol	commercial cigarette additive
17	pyridinecarboxylic acid	AP, SM
18	butanedioic acid	?
20	catechol	sugars, lignin, Ps
21	2,3-dihydroxypropanoic acid	?
23	nicotine	SM
24	erythronic acid, 1,4-lactone	sugars, Ps
25	methyl catechol	sugars, lignin, Ps
26	resorcinol	sugars, lignin, Ps
27	methyl catechol	sugars, lignin, Ps
28	dihydroxybutanoic acid	sugars, Ps
29	threonic acid, 1,4-lactone	sugars, Ps
30	methy-dihydroxy-cyclopentenone	sugars, Ps
31	dihydroxy-cyclopentenone	sugars, Ps
32	pyranone	sugars, Ps, Ma
33	methyl dihydroxybenzene	lignin, Ps
34	methyl dihydroxybenzene	lignin, Ps
35	malic acid +	SM
35'	dimethyl dihydroxy cyclopentenone	sugars, Ps
36	threitol	sugars, Ps
37	vinylcatechol	sugars, Ps
38	erythritol	sugars, Ps
39	pyroglutamic acid	SM
40	hydroxyvaleric acid	SM
41	5-methyl-2-hydroxy-4-amino-pyrimidine	?
42	trihydroxybenzene	lignin, sugars, Ps
43	tetronic acid	sugars, Ps
44	dodecanol	waxes
45	hydroxybenzoic acid	?
46	a tetronic acid ?	?
47	phenylethanol	?
48	pentonic acid, 1,4-lactone	sugars, Ps
49	trihydroxybenzene	sugars, Ps, lignin
50	internal standard	
51	1,4-anhydro-2-deoxypentitol, 2-carboxylic acid	sugars, Ps
52	pentonic acid	sugars, Ps
53	dihydroxybenzyl alcohol	lignin
54	methyl dihydroxybenzyl alcohol	lignin
55	1,6-anhydro-mannitol	sugars, Ps
56	levoglucosan	sugars, Ps
57	a pentitol	sugars, Ps
58	a pentitol	sugars, Ps
59	1,6-anhydroglucofuranose	sugars, Ps

TABLE 16.2.7. *Peak identifications for the chromatogram of silylated smoke from a commercial cigarette (continued).* Chromatogram from Figure 16.2.3; tentative source of individual components obtained by pyrolysis is also shown. (SM = small molecules; Ps = polysaccharides including cellulose, pectins, hemicellulose etc.; AP=amidated pectin; Pr = protein; Ma = Maillard polymers.)

Peak No.	Compound	Possible compound source
60	hydroxyhydrocinnamic acid	?
61	deoxyhexonic acid, 1,4-lactone	sugars, Ps
62	deoxyhexonic acid, 1,4-lactone	sugars, Ps
63	quinic acid, 1,4-lactone	sugars, Ps
64	isomer of quinic acid, 1,4-lactone	sugars, Ps
65	fructose	sugars, Ps
66	neophytadiene	SM
67	2,3-dihydroxypropyl hydroxymethyl pyrazine	Ma, AP
68	fructose	sugars, Ps
69	tetradecanoic acid	waxes
70	isomer of quinic acid, 1,4-lactone	sugars, Ps
71	2,3-dihydroxypropyl hydroxyethyl pyrazine	SM, Ma
72	quinic acid	sugars, Ps
73	isomer of inositol	SM, sugars, Ps
74	glucose	sugars, Ps
75	pentitol	sugars, Ps
76	isomer of inositol	sugars, Ps
77	coniferyl alcohol	lignin
78	di-(2,3-dihydroxypropyl) pyrazine or 2,3,4-trihydroxybutyl hydroxymethyl pyrazine	Ma, SM
79	hexitol	SM, sugars, Ps
80	hexitol	SM sugars, Ps
81	glucose	sugars, Ps
82	palmitic acid	waxes
83	sinapyl alcohol	lignin
84	heptadecanoic acid	waxes
85	inositol	SM, sugars, Ps
86	butylpalmitate	waxes
87	linoleic acid	waxes
88	oleic acid	waxes
89	linolenic acid	waxes
90	stearic acid	waxes
91	n-tricosane	waxes
92	butyl stearate	waxes
93	n-tetracosane	waxes
94	eicosanoic acid	waxes
95	n-pentacosane	waxes
96	monopalmitin	lipids
97	internal standard	
98	n-heptacosane	waxes
99	disaccharide	sugars, Ps
100	sucrose	SM, sugars, Ps
101	n-octacosane	waxes
102	tetracosahexaene	waxes
103	tetracosahexaene	waxes
104	tetracosahexaene	waxes
105	tetracosahexaene	waxes
106	n-nonacosane	waxes
107	branched chain hydrocarbon	waxes
108	n-triacontane	waxes
109	5,7-dimethyl tocopherol	SM
110	branched chain hydrocarbon	waxes
111	n-hentriacontane	waxes
112	vitamin E	SM
113	branched chain hydrocarbon	waxes
114	a sterol	SM
115	campesterol	SM
116	stigmasterol	SM
117	sitosterol	SM

As seen in Tables 16.2.5, 16.2.6, and 16.2.7, many compounds in tobacco smoke are generated from the small molecules. However, polymeric material plays an important role in smoke composition. Carbohydrates, including amidated pectins, Maillard polymers, and proteins, all generate smoke components with important roles in smoke sensorial properties.

Of special interest in smoke analysis (both mainstream and sidestream) are a number of compounds that, although present in low levels in cigarette smoke, are considered [58-61] to have adverse effect on human health. A list of the more common such compounds analyzed in cigarette smoke and their likely sources is given in Table 16.2.8. The table also indicates the range of these compounds in the mainstream of a reference cigarette (1R4F).

TABLE 16.2.8. *Compounds in mainstream cigarette smoke considered [58-61] to have adverse effect on human health.* The level (compiled from several reports) is indicated for a 1R4F Kentucky reference cigarette. (SM indicates small molecules; Ps indicates polysaccharides including cellulose, pectins, hemicellulose, etc.; Pr indicates protein; Ma indicates Maillard polymers.)

Compound	Level	Units	Likely source
1,3-butadiene	30	µg/cig.	SM, waxes, Ps
isoprene	180	µg/cig.	SM, waxes, Ps
formaldehyde	20	µg/cig.	SM, waxes, Ps
acetaldehyde	700	µg/cig.	SM, waxes, Ps
propionaldehyde	50	µg/cig.	SM, waxes, Ps
acetone	300	µg/cig.	SM, waxes, Ps
acrolein	60	µg/cig.	SM, waxes, Ps
crotonaldehyde	20	µg/cig.	SM, waxes, Ps
butyraldehyde	40	µg/cig.	SM, waxes, Ps
methylethyl ketone	60	µg/cig.	SM, waxes, Ps
HCN	100	µg/cig.	Pr, SM, Ma
acetonitrile	130	µg/cig.	Pr, SM, Ma
propionitrile	50	µg/cig.	Pr, SM, Ma
acrylonitrile	10	µg/cig.	Pr, SM, Ma
benzene	50	µg/cig.	SM, waxes, Ps, lignin
toluene	80	µg/cig.	SM, waxes, Ps, lignin
styrene	3	µg/cig.	SM, waxes, Ps, lignin
naphthalene	10	µg/cig.	SM, waxes, Ps, lignin
acenaphthalene	present		
acenaphthene	present		
fluorene	2	µg/cig.	SM, waxes, Ps, lignin
phenanthrene	present		
anthracene	present		
fluoranthene	26	ng/cig	SM, PS, Lignin
pyrene	27	ng/cig	SM, PS, Lignin
2,3-benzofluorene	28	ng/cig	SM, PS, Lignin
1,2-benzanthracene	10	ng/cig	SM, PS, Lignin
chrysene	13	ng/cig	SM, PS, Lignin
benzo[b+k]fluoranthene	6	ng/cig	SM, PS, Lignin
benzo[e]pyrene	3	ng/cig	SM, PS, Lignin
benzo[a]pyrene	7	ng/cig	SM, PS, Lignin
perylene	1	ng/cig	SM, PS, Lignin
dibenz[a,h+a,c]anthracene	2	ng/cig	SM, PS, Lignin
dibenzo[a,]pyrene	1	ng/cig	SM, PS, Lignin
benzoperylene	2	ng/cig	SM, PS, Lignin
indeno[1,2,3-cd]pyrene	present		

TABLE 16.2.8. *Compounds in mainstream cigarette smoke considered [58–61] to have adverse effect on human health (continued)*. The level (compiled from several reports) is indicated for a 1R4F Kentucky reference cigarette. (SM indicates small molecules; Ps indicates polysaccharides including cellulose, pectins, hemicellulose, etc.; Pr indicates protein; Ma indicates Maillard polymers.)

Compound	Level	Units	Likely source
5-methylchrysene	present		
phenol	7.2	µg/cig.	SM, PS, Lignin
o-cresol	2.6	µg/cig.	SM, PS, Lignin
m-cresol	2.2	µg/cig.	SM, PS, Lignin
p-cresol	4.8	µg/cig.	SM, PS, Lignin
catechol	45.0	µg/cig.	SM, PS, Lignin
3-methylcatechol	present		
resorcinol	1.1	µg/cig.	SM, PS, Lignin
hydroquinone	39.0	µg/cig.	SM, PS, Lignin
pyrogallol	4.5	µg/cig.	SM, PS, Lignin
1,2,4-trihydroxybenzene	8.4	µg/cig.	SM, PS, Lignin
aniline	225	ng/cig	Pr, SM, Ma
o-toluidine	53	ng/cig	Pr, SM, Ma
m-toluidine	40	ng/cig	Pr, SM, Ma
p-toluidine	20	ng/cig	Pr, SM, Ma
2-ethylaniline	5	ng/cig	Pr, SM, Ma
2,6-dimethylaniline	15	ng/cig	Pr, SM, Ma
2,4-dimethylaniline	20	ng/cig	Pr, SM, Ma
3-ethylaniline	8	ng/cig	Pr, SM, Ma
1-aminonaphthalene	15	ng/cig	Pr, SM, Ma
2-aminonaphthalene	8	ng/cig	Pr, SM, Ma
4-aminobiphenyl	3	ng/cig	Pr, SM, Ma
3-aminobiphenyl	3	ng/cig	Pr, SM, Ma
benzidine	trace	ng/cig	Pr, SM, Ma
tolidine	trace	ng/cig	Pr, SM, Ma
N-nitrosodimethylamine	3	ng/cig	SM
N-nitrosopyrrolidine	10	ng/cig	SM
N-nitrosoornicotine	120	ng/cig	SM
N-nitrosoanatabine	170	ng/cig	SM
N-nitrosoanabasine	35	ng/cig	SM
4-(N-methylnitrosamino)-1-(3-pyridyl)-1-butanone	125	ng/cig	SM
2-amino-9H-pyrido[2,3-b]indole (AaC)	present		SM, Ma
2-amino-3-methyl-9H-pyrido[2,3-b]indole (MeAaC)	present		SM, Ma
2-amino-3-methylimidazo[4,5-b]quinoline (IQ)	present		SM, Ma
3-amino-1,4-dimethyl-5H-pyrido[3,4-b]indole (Trp-P-1)	present		SM, Ma
3-amino-1-methyl-5H-pyrido[3,4-b]indole (Trp-P-2)	present		SM, Ma
2-amino-6-methyl[1,2-a:3',2'-d]imidazole (Glu-P-1)	present		SM, Ma
2-aminodipyrido[1,2-a:3',2'-d]imidazole (Glu-P-2)	present		SM, Ma
2-amino-1-methyl-6-phenylimidazo[4,5-1]pyridine (PhIP)	present		SM, Ma

Detailed analysis of smoke also indicated the presence of polychlorodibenzodioxines and of polychlorodibenzofuranes. However, the level of these compounds in mainstream smoke expressed as tetrachlorodibenzodioxin (TCDD) is very low, in the range of 0.05 to 0.17 pg/cig [61a], which is even lower than the level reported in food [61a].

The origin of most compounds with effects on human health in cigarette smoke and in other types of smoke is not well understood. Studies on pyrolysis of pure substances were performed to find the origin of some of these undesirable compounds [39]. For example for the generation of polynuclear aromatic hydrocarbons (PAH), selected

compounds were pyrolysed at 700° C and the yield was compared with PAH in particulate phase cigarette smoke or in tobacco pyrolysates [39,62]. The results of pyrolysis products of several compounds are shown in Table 16.2.9. The yields of PAHs are expressed in mg/g of pyrolysed material.

TABLE 16.2.9. *The yields of PAHs in the pyrolysates of several compounds, expressed in mg/g of pyrolysed material.* (A = solanesol, B = sterols, C = cholesterol palmitate, D = β -carotene, E = squalene, F = chlorophyll, G = fatty acids, H = cellulose.)

Compound	A	B	C	D	E	F	G	H
naphthalene	5.54	5.88	2.51	1.50	0.83	0.83	0.37	n.a.
2-methylnaphthalene	4.53	1.60	0.848	4.25	0.90	0.23	0.088	n.a.
1-methylnaphthalene	3.08	3.05	2.18	2.84	0.62	0.24	0.120	n.a.
acenaphthylene	1.64	2.42	0.75	0.91	0.21	0.14	0.092	n.a.
1-methylacenaphthylene	0.14	0.81	0.26	0.22	0.056	0.027	0.020	n.a.
fluorene	1.29	1.27	0.34	0.43	0.17	0.057	0.079	n.a.
phenanthrene	3.44	7.32	2.58	0.59	0.17	0.11	0.14	n.a.
anthracene	1.04	0.94	0.39	0.32	0.059	0.032	0.040	n.a.
methylphenanthrenes/anthracenes	4.16	11.9	4.01	2.52	0.42	0.16	0.13	n.a.
fluoranthene	0.69	0.64	0.22	0.19	0.037	0.017	0.030	1.31
acephenanthrylene	0.42	0.58	0.25	0.17	0.030	0.013	0.018	
pyrene	1.19	1.74	0.61	0.44	0.076	0.055	0.053	1.07
methylpyrenes/cyclopentenophen anthrenes	1.21	4.57	8.36	1.04	0.14	0.11	0.059	n.a.
1,2-benzanthracene	0.55	0.84	0.24	0.16	0.023	0.013	0.011	0.48
chrysene	0.66	3.07	0.79	0.13	0.025	0.019	0.012	0.57
methylchryenes and 1,2- benzanthracenes	1.26	1.98	0.43	0.88	0.046	0.042	0.016	n.a.
benzo[b,j and k]fluoranthene	0.32	0.23	0.037	0.062	0.011	0.0074	0.0040	0.28
benzo(e)pyrene	0.22	0.27	0.047	0.035	0.009	0.0053	0.0037	0.16
benzo(a)pyrene	0.40	0.44	0.074	0.077	0.014	0.0092	0.0053	0.41

n.a. = not analyzed

Numerous other pyrolysis studies were performed on tobacco. Many of them were reported at dedicated meetings such as Tobacco Chemists Research Conferences and are referenced in specialized reports [63]. However, because of the extremely large amount of information in this field, the subject cannot be properly included in this book.

- Pyrolysis of other plant tissues.

Several other plant tissues were analyzed by pyrolytic techniques [63–70]. One example is the analysis of plant tissues from carnations (*Dianthus caryophyllus*). Several studies were done on this subject with the purpose of detecting possible differences between resistant and susceptible cultivars to fungal infections. The studies investigated the xylem from stems of healthy and fungus-infected plants for the lignin/polysaccharide ratio, the lignin composition, and for the accumulation of phytoalexins. For example, it is known [64] that the resistance mechanism of carnation to *Fusarium oxysporum* infection resides in the physiological response of the plant after the fungus has invaded the xylem vessels. In the resistant cultivars the vascular parasite becomes localized within the xylem. This is achieved by the production of barriers that are formed by gummosis of affected vessels and by lignification of the primary walls of surrounding cells. Specific phenolic amides (phytoalexins) are also produced to delay the fungal growth. The gums that are formed in the xylem adjacent to

the infected vessels are composed of various amounts of polysaccharides encrusted with polyphenolic compounds. Histochemical tests indicated the presence of guaiacyl lignin but the absence of syringyl (S) constituents in the gums. The walls of unaffected xylem vessels contain a mixed guaiacyl-syringyl (G-S) lignin.

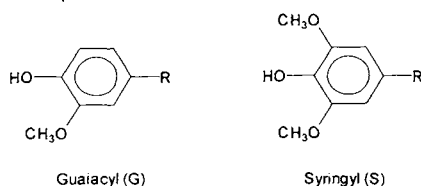
The lignin composition has been studied using Py-MS with pyrolysis of very small pieces of xylem at 510° C followed by MS analysis with low voltage EI ionization (15 eV). Discriminant analysis was performed on Py-MS data using a dedicated computer program [64]. The spectra were considered to be points in a multidimensional space with the mass numbers as coordinate axes. The relative distribution of mass intensities in each spectrum determined the position in the multidimensional space. Similar spectra clustered as one group. From the file of selected spectra an overall average spectrum considered zero point was calculated and served as a reference point for the individual spectra. The difference between the individual spectra was determined by comparison with the zero point spectrum. These data were factor analyzed to produce sets of correlated mass peaks (factors). These mass peaks were linearly combined into new independent variables (discriminant functions), which were represented graphically by reconstructed mass spectra. Dissimilarities were quantitatively expressed in discriminant function scores. The procedure allowed a clear discrimination between resistant and susceptible cultivars. The Py-MS spectra also allowed the identification of dianthramine, methoxydianthramide, and hydroxydianthalexin, which are produced by the affected plants. A similar technique was used for the diagnosis of gangrene in potatoes caused by the fungus *Phoma exigua*.

A variety of other studies using pyrolytic techniques were performed on plant materials, such those following the chemical changes in plants during growth [69,71], modifications during thermal degradation [68], pyrolytic characterization of bromegrass stem cells, coastal Bermuda grass [72] or several forage materials such as alfalfa, characterization of plant tissues during enzymatic or other types of degradation [73,74], etc.

16.3. Decomposing and Subfossil Plant Materials.

The differentiation between subfossil and fossil plant materials is not distinct. While coal or kerogens can be considered indeed as modified fossil plant (or algae) materials, the definition is much more difficult to apply for peat. The degradation of plant materials can be very diverse under the action of different chemical or biological agents. The study of oxidation or of the effects of different fungi or bacteria on plant materials (which are already non-homogeneous) is a complex problem. Pyrolysis studies are particularly appropriate for the analysis of complex plant materials because these substances consist of polymeric molecules that are difficult to analyze by other procedures. This explains the variety of studies performed on decomposing, subfossil, and fossil (peat) plant materials. The purpose of these studies covers subjects such as the evaluation of the stage of the degradation/coalification process [75,76], fingerprinting of the type of fossil material [77–79], identification of the sources contributing to the formation of fossil deposits [80], chemical characterization of different types of fossil plant materials [81], evaluation of the chemical changes during degradation of wood by different fungi [82,74], etc.

Numerous studies of fossil plant materials were performed using Py-MS. This provides a way for rapid assessment of differences or changes in the fingerprint of many materials. In most cases Py-MS results require the use of multivariate mass spectral data processing. Detailed molecular information was also generated in some cases, commonly using Py-GC/MS techniques. For example, it was found that coumaric and ferulic acid esters are present at significantly higher levels in plant materials resistant to degradation. A correlation between the resistance to degradation and the level of several esters of the two acids was proposed [30]. The variation in the composition of different plant parts during aging was also studied using pyrolysis. Fruit endocarps, for example, were studied and again lignin was found to be more resistant to chemical degradation during the coalification process. In fruit endocarps, some carbohydrate polymeric chains also remained unmodified during the lignification process. These findings made possible the use of pyrolysis studies for the determination of the rate of decay of different plant materials in nature. Characterization of recent and buried wood is another example of the use of pyrolytic studies. By calculating the ratios of guaiacyl lignin (G) versus syringyl lignin (S), it was seen that during burial G/S ratio increases [75]. Based on the peak areas in pyrograms, a limited number of compounds resulting in wood pyrolysis were compared. Their structures are indicated below



where the substituents R are H, CH₃, CH=CH₂, CH=CH-CH₃, CHO, CO-CH₃ and CH=CH-CHO. The variation of the ratio G/S for these compounds is shown in Figure 16.3.1 for recent and buried alder (*Alnus rubra*) and recent and buried oak (*Quercus* spp.)

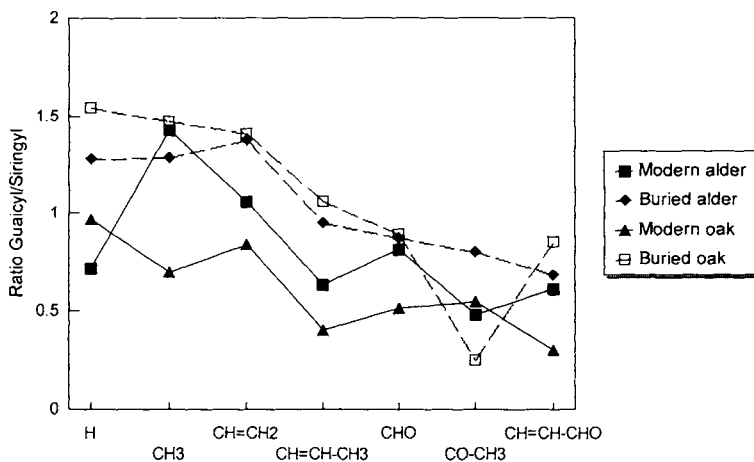


FIGURE 16.3.1. The variation of the ratio G/S for several R-guaiacyl and R-syringyl compounds (R = H, CH₃, CH=CH₂, CH=CH-CH₃, CHO, CO-CH₃) seen in the pyrolysates of wood from recent and buried alder and recent and buried oak [75].

Because they can be recognized in sediments, fossil and subfossil plant materials also were analyzed for the purpose of defining a fossil record that can be applied to geological studies. Several fossil plant parts such as cuticles may contain compounds that are specific for a certain plant. An example is cutin, a specific biomacromolecule separated from fossil ginkgo (*Ginkgo biloba*) or from fossil agave (*Agave americana*). Cutin has a dominantly aliphatic hydrocarbon pyrolysis pattern that can be used for the differentiation from more recent leaf deposits [83]. Other techniques such as the study of carbohydrate derived macromolecules were also used for the study of the "signature" of several geopolymers [84].

16.4. Pulp and Paper.

The impurities in pulp and paper products are of significant practical importance for assuring paper quality or the quality of incoming materials in industries such as those making cellulose acetate. The analysis of small molecules in pulp and paper is done using a variety of standard analytical procedures. The analysis of polymers in pulp and paper, such as residual lignin, chemically modified natural polymers (generated during bleaching, etc.), as well as man made polymers added to paper such as sizing, coating, anti-foaming or adhesive agents, are difficult to analyze without the decomposition of the macromolecules. This explains the extensive use of pyrolytic analytical techniques in this field [85,86]. Some small molecules can also be analyzed at the same time with the polymers. A summary of the common intentional or unintentional polymeric additives found in pulp or paper is given in Table 16.4.1.

TABLE 16.4.1 *Common intentional or unintentional polymeric additives found in pulp or paper.*

Substance	Origin
lignin	wood
resins	wood
rosin	rosin sizing
cross-linked cellulose with AKD, alkenylsuccinic acid anhydride, ethyleneoxide, etc.	sizing
polyamide-epichlorhydrin	sizing
polystyrene	coating agent, sizing
polyacrylates	coating agent, sizing
synthetic polymers	coatings, adhesives
polyisoprene, polyacrylates	adhesives
fatty acids derivatives	anti-foaming

Each of the compounds listed in Table 16.4.1 can be identified by its pyrolysis products and may be used for the characterization of a material (chemical or mechanical pulps), or for the determination of the nature of specks or deposits in pulp or paper, etc. Of particular interest may be the use of pyrolysis for the identification of specific types of inks on paper [87].

One example of the use of pyrolysis for the analysis of pulp is the determination of the amount of sulfur. This can be done by measuring the amount of H₂S, COS, SO₂, CH₃SH, CH₃SCH₃, and CS₂ in the pyrolysates. The study [88] has been done on H, Na and Ca forms of thermomechanical pulp (TMP) and on H, Na and Ca forms of kraft pulp

References 16.

1. V. Arpiainen, M. Lappi, *J. Anal. Appl. Pyrol.*, 16 (1989) 355.
2. J. M. Challinor, *J. Anal. Appl. Pyrol.*, 37 (1996) 1.
- 2a. J. B. Reeves III, G. C. Galletti, *Org. Mass Spectr.*, 28 (1993) 647
3. J. J. Boon, A. D. Powels, G. B. Eijkel, *Biochem. Soc. Trans.*, 15 (1987) 170.
4. W. Windig, H. L. C. Meuzelaar, F. Shafizadeh, R. G. Kelsey, *J. Anal. Appl. Pyrol.*, 6 (1984) 233.
5. M. M. Moulder, J. B. M. Rureveen, J. J. Boon, *J. Anal. Appl. Pyrol.*, 19 (1991) 175.
6. A. D. Pouwels, J. J. Boon, *J. Anal. Appl. Pyrol.*, 17 (1990) 97.
7. A. Seares-Aspax, J. M. Alcaniz-Baldellou, M. Gassiot-Matas, *J. Anal. Appl. Pyrol.*, 8 (1985) 415.
8. W. F. deGroot, W. -P. Pan, M. D. Rahman, G. N. Richards, *J. Anal. Appl. Pyrol.*, 13 (1988) 221.
9. A. D. Pouwels, A. Tom, G. B. Eijkel, J. J. Boon, *J. Anal. Appl. Pyrol.*, 11 (1987) 417.
10. J. Lede, H. Z. Li, J. Villermaux, H. Martin, *J. Anal. Appl. Pyrol.*, 10 (1987) 291.
11. C. A. Zaror, D. L. Pyle, *J. Anal. Appl. Pyrol.*, 10 (1986) 1.
12. G. M. Simmons, M. Sanchez, *J. Anal. Appl. Pyrol.*, 3 (1981) 161.
13. G. M. Simmons, M. Gentry, *J. Anal. Appl. Pyrol.*, 10 (1986) 117.
14. J. R. Richard, J. P. Rouan, *J. Anal. Appl. Pyrol.*, 15 (1989) 307.
15. A. Donnot, P. Magne, X. Deglise, *J. Anal. Appl. Pyrol.*, 21 (1991) 265.
16. A. Donnot, P. Magne, X. Deglise, *J. Anal. Appl. Pyrol.*, 22 (1991) 39.
17. J. M. Blasco, T. Cordero, J. P. Gomez-Martin, J. J. Rodriguez, *J. Anal. Appl. Pyrol.*, 18 (1990) 117.
- 17a. S. S. Alves, J. L. Figueiredo, *J. Anal. Appl. Pyrol.*, 13 (1988) 123.
18. R. Bilbao, J. F. Mastral, M. E. Aldea, J. Ceamanos, *J. Anal. Appl. Pyrol.*, 42 (1997) 189.
19. G. N. Richards, G. Zheng, *J. Anal. Appl. Pyrol.*, 21 (1991) 133.

20. R. H. Marchessault, S. Coulombe, T. Hanai, H. Morikawa, *Trans. (Can. Pulp Paper Assoc.)*, June 1980.
21. A. Rolin, C. Richard, D. Masson, X. Deglise, *J. Anal. Appl. Pyrol.*, 5 (1983) 151.
22. T. A. Milne, M. N. Soltys, *J. Anal. Appl. Pyrol.*, 5 (1983) 111.
23. J. Kelly, M. Mackey, R. J. Helleur, *J. Anal. Appl. Pyrol.*, 19 (1991) 105.
24. J. L. Figueiredo, C. Valenzuela, A. Bernalte, J. M. Encinar, *Biol. Wastes*, 28 (1989) 217.
25. G. C. Galletti, J. B. Reeves III, *J. Anal. Appl. Pyrol.*, 19 (1991) 203.
26. J. A. Maga, Z. Chen, *Flav. Fragr. J.*, 1 (1985) 37.
27. W. Baltes *J. Anal. Appl. Pyrol.*, 8 (1985) 533.
28. P. Pomogyi, E. P. H. Best, J. H. A. Dassen, J. J. Boon, *Aquatic Botany*, 19 (1984) 243.
29. D. G. van Smeerdijk, J. J. Boon, *J. Anal. Appl. Pyrol.*, 11 (1987) 377.
30. J. J. Boon, R. G. Wetzel, G. L. Godshalk, *Limnol. Oceanogr.*, 27 (1982) 839.
31. R. D. Hartley, J. Haverkamp, *J. Sci. Food. Agric.*, 35 (1984) 14.
32. J. J. Boon, S. A. Stout, W. Genuit, W. Spackman, *Acta Bot. Neerl.*, 38 (1989) 391.
33. M. M. Mulder, P. M. Hotten, E. Cowie, J. A. Lomax, A. Chesson, *Animal Feed Sci. Technol.*, 32 (1991) 185.
34. V. O. Elias, B. R. T. Simoneit, A. S. Pereira, J. N. Cardoso, *J. High Res. Chromatog.*, 21 (1998) 87.
35. M. K. Statheropoulos, S. E. Liodakis, N. E. Tzamtzis, A. Pappa, S. Kyriakou, *J. Anal. Appl. Pyrol.*, 43 (1997) 115.
36. H. -R. Schulten, N. Simmleit, H. H. Rump, *Intern. J. Environ. Anal. Chem.*, 27 (1986) 241.
- 36a. A. A. Pappa, N. E. Tzamtzis, M. K. Statheropoulos, S. E. Liodakis, G. K. Parissakis, *J. Anal. Appl. Pyrol.*, 31 (1995) 85.
37. J. M. Halket, H. -R. Schulten, *J. Anal. Appl. Pyrol.*, 8 (1985) 547.
38. B. -H. Muller, *J. Anal. Appl. Pyrol.*, 8 (1985) 577.
39. W. S. Schlotzhauer, O. T. Chortyk, *J. Anal. Appl. Pyrol.*, 12 (1987) 193.

40. M. A. Scheijen, J. J. Boon, *J. Anal. Appl. Pyrol.*, 19 (1991) 153.
41. W. S. Schlotzhauer, M. E. Snook, O. T. Chortyk, R. L. Wilson, *J. Anal. Appl. Pyrol.*, 22 (1992) 231.
42. O. Faix, J. Bremer, D. Meier, I. Fortmann, M. A. Scheijen, J. J. Boon, *J. Anal. Appl. Pyrol.*, 22 (1992) 239.
43. G. H. Bokelman, W. S. Ryan Jr., E. T. Oakley, *J. Agric. Food. Chem.*, 31 (1983) 897.
44. G. H. Bokelman, W. S. Ryan, 37th. TCRC conf. 1983.
45. M. A. Scheijen, J. J. Boon, W. Hass, V. Heemann, *J. Anal. Appl. Pyrol.*, 15 (1989) 97.
46. J. H. Lauterbach, S. C. Moldoveanu, 45th. TCRC conf. 1991.
47. W. S. Schlotzhauer, R. F. Arrendale, O. T. Chortyk, *Beitr. Tabakforsch. Int.*, 13 (1985) 74.
48. C. R. Enzel, *Rec. Adv. Tob. Sci.*, 2 (1976) 32.
49. W. S. Schlotzhauer, R. F. Arrendale, R. F. Severson, O. T. Chortyk, *J. Anal. Appl. Pyrol.*, 17 (1989) 25.
50. W. R. Johnson, R. W. Hale, S. C. Clough, P. H. Chen, *Nature (London)*, 243 (1973) 223.
51. R. A. W. Johnstone, J. R. Plimmer, *Chem. Rev.*, 59 (1959) 885.
52. R. E. Fresenius, *J. Anal. Appl. Pyrol.*, 8 (1985) 561.
53. R. L. Stedman, *Chem. Rev.*, 68 (1968) 153.
54. I. Schmeltz, D. Hoffmann, *Chem. Rev.*, 77 (1977) 295.
55. M. W. Ogden, *J. High Res. Chromatog.*, 11 (1988) 428.
- 55a. M. F. Dube, C. R. Green, *Rec. Adv. Tob. Sci.*, 8 (1982) 48.
56. J. Z. Dong, J. N. Glass, S. C. Moldoveanu, 51 TCRC, Winston-Salem, 1997.
57. J. B. Forehand, unpublished results.
58. R. R. Houlgate, K. S. Dhingra, K. S. Nash, W. H. Evans, *Analyst*, 114 (1989) 355.
59. J. Dumont, F. Larocque-Lazure, C. Iorio, *J. Chromatog. Sci.*, 31 (1993) 371.
60. O. T. Chortyk, W. S. Schlotzhauer, *Beitr. Tabakforsch.*, 7 (1973) 165.

61. D. Hoffmann, I. Hoffmann, *Beitr. Tabakforsch., Int.* 18 (1998) 49.
- 61a. M. Ball, O. Papke, A. Lis, *Beitr. Tabakforsch., Int.* 14 (1990) 393.
62. R. F. Severson, W. S. Schlotzhauer, R. F. Arrendale, M. E. Snook, H. C. Higman, *Beitr. Tabakforsch.,* 9 (1977) 23.
63. *An Indexed Guide to the Tobacco Chemists' Research Conferences, PM USA, Richmond, VA, 1989.*
64. G. J. Niemann, R. P. Baayen, J. J. Boon, *Neth. J. Pl. Path.,* 96 (1990) 133.
65. G. J. Niemann, A. van der Bij, B. Btandt-de Boer, J. J. Boon, R. P. Baayen, *Phys. Mol. Pl. Path.,* 38 (1991) 117.
66. G. J. Niemann, J. J. Boon, J. B. M. Pureveen, G. B. Eijkel, E. van der Heijden, *J. Anal. Appl. Pyrol.,* 19 (1991) 213.
67. G. J. Niemann, R. P. Baayen, J. J. Boon, *Ann. Botany,* 65 (1990) 461.
68. K. Bilba, A. Ouensanga, *J. Anal. Appl. Pyrol.,* 38 (1996) 61.
69. G. C. Galletti, J. B. Reeves III, P. Bocchini, *J. Anal. Appl. Pyrol.,* 39 (1997) 105.
70. A. C. M. Weijman, G. W. van Eijk, H. J. Roeijmans, W. Windig, J. Haverkamp, L. J. Turkensteen, *Neth. J. Pl. Path.,* 90 (1984) 107.
71. P. Pomogyi, E. P. H. Best, J. H. A. Dassen, J. J. Boon, *Aquatic Botany,* 19 (19984) 243.
72. W. H. Morrison III, M. A. Scheijen, J. J. Boon, , *Animal Feed Sci. Tech.,* 32 (1991) 17.
73. J. Ralph, R. D. Hatfield, *J. Agric. Food Chem.,* 39 (1991) 1426.
74. M. M. Mulder, J. B. M. Purveen, J. J. Boon, A. T. Martinez, *J. Anal. Appl. Pyrol.,* 19 (1991) 175
75. C. Saiz-Jimenez, J. J. Boon, J. I. Hedges, J. K. C. Hessels, J. W. de Leeuw, *J. Anal. Appl. Pyrol.,* 11 (1987) 437.
76. S. A. Stout, W. Spackman, J. J. Boon, P. G. Kisemaker, D. F. Bensley, *Int. J. Coal Geol.,* 13 (1989) 41.
77. R. P. Philp, N. J. Russell, T. D. Gilbert, J. M. Friedrich, *J. Anal. Appl. Pyrol.,* 4 (1982) 143.
78. G. Halma, D. van Dam, J. Haverkamp, W. Windig, H. L. C. Meuzelaar, *J. Anal. Appl. Pyrol.,* 7 (1984) 167.

79. C. H. Fuchsman, *Peat and Water*, Elsevier, Amsterdam, 1986.
80. N. J. Ryan, P. H. Given, J. J. Boon, J. W. De Leeuw, *Int. J. Coal Geol.*, 8 (1987) 85
81. M. E. C. Moers, M. Baas, J. J. Boon, J. W. De Leeuw, *Biogeochem.*, 11 (1990) 251
82. O. Faix, J. Bremer, O. Schmidt, T. Stevanovic, *J. Anal. Appl. Pyrol.*, 21 (1991) 147.
83. B. Mosie, P. Finch, M. E. Collinson, A. C. Scott, *J. Anal. Appl. Pyrol.*, 40–41 (1997) 585.
84. G. Almendros, J. Dorado, F. J. Gonzalez-Vila, F. Martin, *J. Anal. Appl. Pyrol.*, 40–41 (1997) 599
85. M. Kleen, G. Gellerstedt, *J. Anal. Appl. Pyrol.*, 19 (1991) 139.
86. H.-L. Hardell, *J. Anal. Appl. Pyrol.*, 27 (1993) 73.
87. T. P. Wampler, E. J. Levy, *LC-GC*, 4 (1988) 1112.
88. P. Selsbo, I. Ericsson, M. Kleen, *J. Anal. Appl. Pyrol.*, 43 (1997) 1.
89. T. Yano, H. Ohtani, S. Tsuge, *Tappi J.*, Feb. (1991) 197.

Chapter 17. Analytical Pyrolysis of Microorganisms

17.1. Characterization of Microorganisms by Pyrolytic Techniques.

The identification of microorganisms uses a range of conventional procedures such as morphological, serological, or other biochemical tests. Conventional diagnostic microbiology involves a significant amount of work and usually requires time for incubation and growth of the microorganisms. Other techniques such as immunological ones are widely applied; however, these also have certain disadvantages such as an extremely high specificity that requires an array of tests for proper identification of the unknowns. Typical analytical techniques such as HPLC, GC, and electrophoresis (classic or capillary) were also used for microorganism identification, commonly after incubation and growth.

Among analytical techniques, the pyrolytic procedures can be applied for microorganism identification due to their sensitivity, need for a minute amount of sample, applicability to a wide range of microorganisms, and the relatively short time required for analysis [1]. Several problems are related to the use of pyrolytic techniques for microorganism characterization. Some are related to sample preparation and are not specific to pyrolytic procedures, while others are related to the pyrolytic technique itself.

The sample preparation for taxonomic applications is an extremely important step for the analysis. It was shown that the growth medium may alter the biochemical profile of the microorganism. Media depleted of a certain component (glucose, mineral ions) may generate microorganisms with different characteristics. Also the incubation time, temperature, pH, oxygen concentration, and traces of additives must be considered when preparing cultures for analysis. The culture medium is also important regarding the type of matrix/contaminants that may be present together with the microorganism when analyzed. Samples may be collected in some applications directly from the culture plate, and then the pyrolysis products of the growth medium may dominate the pyrogram. Elimination of such background requires its perfect reproducibility. The problem can also be addressed by separation of the microorganisms from the growth medium and washing the cells before analysis. However, the washing may modify the chemistry of the microorganisms and can be a significant source of errors. Other separation techniques such as sedimentation, centrifugation, etc. may be applied for microorganism harvesting and may affect the reproducibility of the results. Samples may be lyophilized before analysis, this step being preferable to uncontrolled sample drying on the pyrolyser heating wire or ribbon. One positive element for pyrolytic procedures is that sterilization (heat at 121° C for 15 min.) [2] seems not to affect significantly the analysis.

Besides whole microorganisms that were analyzed by pyrolytic techniques, a variety of preparates were also subject to this type of analysis. Cell walls, capsular extracts or other specific extracts were the subject of pyrolytic analyses. Significant differences can be seen between different preparates, and this imposes another requirement for pyrolytic analysis with taxonomic purposes. The reproducibility of the technique for obtaining the preparates must be very good in order to avoid sample contamination with unwanted cell components.

The pyrolytic process is commonly used for microorganism analysis coupled with GC, GC/MS, or direct MS. The variability and sources of errors in Py-GC, Py-MS, or Py-GC/MS in general were previously discussed (see Sections 5.2, 5.3, and 5.4). Several problems regarding sample loading, pyrolysis temperature control, analytical instrument sensitivity, etc. should be considered regarding this part of the analysis. Among these three techniques, Py-MS is probably the most utilized as it provides rapid results and requires a minute amount of sample even compared to the other pyrolytic techniques. As indicated previously, the structural information from Py-MS studies is not straightforward, but for fingerprinting the samples it is adequate.

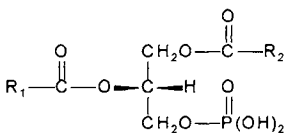
One technique successfully utilized for microorganism fingerprinting has been Py-MS/MS using CAD for more precise differentiation of the source of a given ion. As an example, the ion with $m/z = 59$ was investigated in the pyrolysates of several bacteria including *Mycobacterium tuberculosis* [2a]. Pyrolysis products such as acetamide (CH_3CONH_2), acetaldoxime ($\text{CH}_3\text{CH}=\text{NOH}$), N-methylformamide (HCONHCH_3), C₃-amines ($\text{C}_3\text{H}_7\text{NH}_2$), and guanidine ($\text{H}_2\text{NC}(\text{=NH})\text{NH}_2$), all with MW = 59 have different CAD spectra. The presence of these compounds in different proportions in the pyrolysate of cell wall preparations from different mycobacteria allowed their differentiation.

Data handling in comparing samples and controls is also a very important element in studies done for taxonomic purposes. Automatic data processing procedures, including computer packages that can perform typical statistical multivariate data evaluations, were frequently utilized [3]. A variety of techniques such as discriminant analysis, factor analysis (principal component), cluster analysis, etc. were used to provide pertinent information needed for comparing samples mainly in connection with Py-MS data [3,4]. However, when using Py-MS analysis, it is very difficult to assign a certain mass spectral peak (ion) to a specific component. For this reason, the most common use of the results from Py-MS has been as a fingerprint of a certain microorganism.

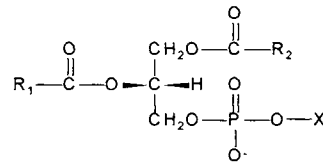
Bacteria species are very diverse and they are grouped into archaea or archaebacteria and eubacteria (pathogens are all eubacteria). Other cellular forms of life are eukaryotes. The chemical constituents of bacteria include proteins, nucleic acids, lipids, and carbohydrates, as well as certain small molecules. The pyrolysis products of these classes of compounds (discussed in detail in Part 2 of this book) consist of a variety of small molecules. Some of these molecules generated by pyrolysis are diagnostic for a certain component, but in most cases a significant level of overlapping exists. A large number of studies were directed to identify the compounds that may differentiate microorganisms and also be seen in their pyrolysate. Specific sets of biomolecules were developed by each microorganism for survival in specific conditions. Such biomolecules include the lipids needed for membrane function and integrity, the respiratory quinones needed for metabolism, and the polysaccharides needed for protection from the environment. The particular collection of these molecules for each microbial species is rather unique. The microbial polar lipids are particularly important for taxonomic purposes. Proteins and nucleic acids on the other hand, although sometimes typical for a certain species, do not have a specific content of amino acids or respectively nucleotides to make them good markers for fingerprinting. As a general rule the structure of these biomolecules differs only by the arrangement of their building blocks.

Phospholipids, which are responsible for the structure of the cell membrane, are easily accessed through simple extraction procedures providing a useful biomarker for microbial detection and identification. However, they are influenced by the growth conditions, nutritional status, and history of a microorganism. These factors cause changes in the phospholipid (phosphoglyceride) profile as the microbe changes its membrane composition in response to its environmental requirements.

The structure of phosphoglycerides offers significant variability and possibilities for identification. Phosphoglycerides (see Section 8.1) consist of four primary functional groups: a glycerol-3-phosphate core on which two fatty acyls (R_1 , R_2) are esterified to the two free hydroxyl groups and a complex alcohol (X) that is esterified to the phosphate group (phosphatidic acids do not contain this alcohol). The alcohol X is the group that defines the specific class to which the phospholipid belongs such as phosphatidylserine, phosphatidylglycerol, phosphatidylethanolamine, phosphatidylinositol, or phosphatidylcholine. The fatty acyls distinguish the individual phospholipid molecular species within each class.



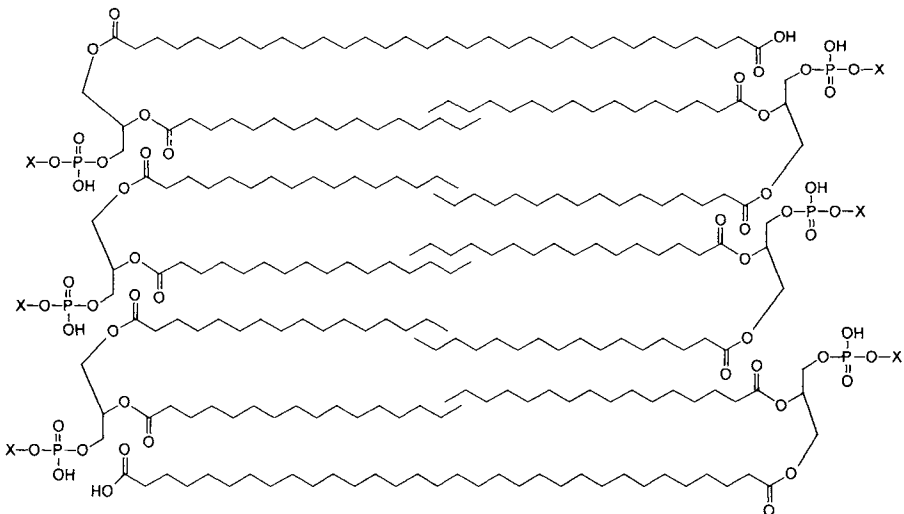
Phosphatidic acid



Glycerophospholipid

R_1, R_2 = long aliphatic chain X = ethanolamine, glycerol, choline, serine, inositol.

Although phospholipids are not usually macromolecules, they can be associated with larger molecules or can form adducts because of van der Waals interactions reaching considerable masses. Such adducts are, for example, typical for the lipids in the membranes of thermophilic bacteria [4a], which contain structures of the type:



Crude lipid extracts are usually obtained from microorganisms by standard procedures applied in microbiology and further analyzed using pyrolytic techniques. Some special lipids such as ether lipids (plasmalogens) that are characteristic for archaea, in contrast to ester-linked membrane lipids that are characteristic for eukaryotes, are, however, more difficult to analyze using pyrolysis because during thermal decomposition the differentiation of the type of bond is lost. Respiratory quinones, being thermally labile, have the same problem for a potential identification using pyrolytic techniques. Triglycerides on the other hand can be utilized well as markers for taxonomy purposes. Their pyrolysis using a methylating agent (TMAH) has been proven very advantageous.

Bacterial polysaccharides can also serve as markers to identify specific bacterial species or genera. Typical microbial polysaccharides include peptidoglycans, lipopolysaccharides, and teichoic/teichuronic acids. Some markers such as muramic acid, D-alanine, and β -hydroxy myristic acid are present in the polysaccharides from eubacteria but are uncommon in higher life forms such as plants and animals. Pyrolysis results on bacterial polysaccharides were discussed in Sections 7.9 and 7.10. Specific pyrolysis products such as propionamide or peaks characteristic for KDO have been used for Py-MS or Py-GC/MS characterization of microorganisms.

Protein analysis also has been utilized for the identification of microorganisms. However, pyrolytic techniques were not the choice for this type of analysis. On the other hand, several studies were done on DNA pyrolysis for microbial identification [4b]. The base identification in ribonucleic acids using pyrolytic techniques is more promising for taxonomic purposes, as more than 80 modified nucleosides can be present mainly in tRNA. However, direct pyrolysis of DNA is not in general informative enough for the detection of minute changes in the DNA composition (see also Section 13.2). In Py-MS studies of whole microorganisms, this detection is even more difficult. As an example, the mass spectrum of an individual nucleoside, thymidine, shown in Figure 17.1.1 displays the ion with $m/z = 117$ that is also typical for protein pyrolysis when phenylacetonitrile is generated from Phe or when indole is generated from Tyr.

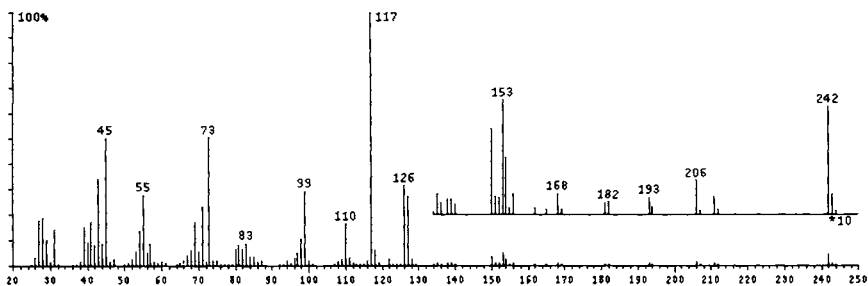


FIGURE 17.1.1. *The mass spectrum of thymidine (70 eV).*

A list of microorganisms analyzed for taxonomic purposes using pyrolytic procedures is given in Table 17.1.1 (compiled from several references including [2,5]).

TABLE 17.1.1. *Microorganisms analyzed for taxonomic purposes using pyrolytic procedures.* (A= algae, BGn = bacteria Gram-negative, BGp = bacteria Gram-positive, F = fungi, O= other).

Organism	Type	Pathogenicity	References
<i>Chlorophycean</i>	A		6
<i>Rhodophycean</i>	A		6
<i>Chlorella</i>	A	protein, carbohydrate source	7
<i>Navicula</i>	A		7
<i>Leptosira</i>	A		8
<i>Oedogonium</i>	A		8
<i>Pleurastrum</i>	A		8
plankton	A		7
<i>Acinetobacter</i>	BGn		9,3
<i>Arthrobacter</i>	BGn		70
<i>Aeromonas</i>	BGn	septicemia, wounds	10
<i>Azotobacter</i>	BGn	soil nitrogen fixation	11
<i>Bacteroides</i>	BGn	appendicitis, blood poisoning	12,13
<i>B. gingivalis</i>	BGn	periodontal disease	66, 68
<i>Citrobacter</i>	BGn	urinary, respiratory tract infection	14,15,16,3
<i>Dyepsiacoli</i>	BGn	dysentery	16
<i>Enterobacter aerogenes</i>	BGn	opportunistic infections	15,17
<i>E. aureescens</i>	BGn	opportunistic infections	17
<i>E. cloacae</i>	BGn	coliform	18,19,16
<i>E. coli</i>	BGn	gastrointestinal, coliform	20,21,22,18,19,27,10,7, 15,16,17,23,24
<i>E. hafniae</i>	BGn	opportunistic infections	21,25,3
<i>Klebsiella</i>	BGn	coliform, opportunistic infections	18,19,15,16,26,23,3
<i>K. pneumoniae</i>	BGn	nosocomial outbreaks	26
<i>Legionella</i>	BGn	legionnaire's disease	19
<i>Moraxella</i>	BGn		29
<i>Neisseria</i>	BGn	meningitis, gonorrhoea	61
<i>Proteus</i>	BGn	eye, ear infections, pneumonia	21,18,19,10,15,25,17,3
<i>P. stuartii</i>	BGn	burn infections	21
<i>Shigella</i>	BGn	dysentery	20,21,27,10,17
<i>Yersinia enterocolitica</i>	BGn	food borne	25,28
<i>Pseudomonas</i>	BGn	water borne, pneumonia	11,22,19,10,15,36,29, 17,9,23,3
<i>Serratia</i>	BGn	pneumonia, septicemia, urinary	11,3
<i>Salmonella</i>	BGn	food poisoning, typhoid	30,31,32,33,10,25,17
<i>Vibrio</i>	BGn	cholera	10
<i>Actinomyces</i>	BGp	actinomycosis, abscess	27
<i>Bacillus</i>	BGp	anthrax	11,34,15,36,38,44,19, 14,35
<i>Cellulomonas</i>	BGp	attacks cellulose	11
<i>Clostridium</i>	BGp	tetanus, botulism, gangrene	11,37,27,15,39
<i>Lactobacillus</i>	BGp	mouth, vagina infections	29,24
<i>Microbacterium</i>	BGp		29, 64
<i>Micrococcus</i>	BGp	occurs in milk	38,44,14,29
<i>Nocardia</i>	BGp	nocardiosis, lungs, abscess	24
<i>Propionibacterium</i>	BGp	skin, gastrointestinal	18,19
<i>Staphylococcus</i>	BGp	urinary and skin infections	22,18,19,27,16,23
<i>Streptococcus</i>	BGp	pneumonia infections, rheumatic fever, meningitis	20,40,41,18,19,27,42, 43,15,16,17,23,24, 69
<i>Streptomyces</i>	BGp		44
<i>Arthroderma</i>	F	dermatophytosis	45,46
<i>Aspergillus</i>	F	bread mold, aspergillosis	44,47,48,49,50
<i>Candida</i>	F	yeast, candidiasis	11,18,19
<i>Ceratocystis</i>	F	phytopathogen	11

TABLE 17.1.1. *Microorganisms analyzed for taxonomic purposes using pyrolytic procedures (continued)*. (A= algae, BGn = bacteria Gram-negative, BGp = bacteria Gram-positive, F = fungi, O= other).

Organism	Type	Pathogenicity	References
<i>Chrysosporium</i>	F		71
<i>Cryptococcus</i>	F	cryptococcosis	19
<i>Endomyces</i>	F		15
<i>Epicoccum</i>	F		50
<i>Eurotium</i>	F	mold	50
<i>Gliocladium</i>	F		15
<i>Hendersonula</i>	F		50
<i>Histoplasma</i>	F	histoplasmosis	27
<i>Microsporium</i>	F	ringworm	45,46
<i>Mycorrhizas</i>	F		134
<i>Nannizzia</i>	F	dermatophytosis	45,46,51
<i>Neurospora</i>	F		48
<i>Penicillium</i>	F	bread mold	52,48,53,54
<i>Petriella</i>	F		15
<i>Rhizopus</i>	F	mold, meats, bread	11,14
<i>Rhodospordium</i>	F		59
<i>Rhodotorula</i>	F		11
<i>Saccharomyces</i>	F	baker's yeast, wine ferment	11,18,19,14
<i>Sporidiobolus</i>	F		65
<i>Trychophyton</i>	F	dermatomycosis, ringworm	46
<i>Torulopsis</i>	F	yeast	18,19
<i>Leptospira</i>	O	helical cells, leptospirosis	55
<i>Mycobacter</i>	O		20,56,57,27,58,60
<i>M. tuberculosis</i>	O	tuberculosis complex	63
<i>M. leprae</i>	O	leprosy	62,67
<i>Mycoplasma</i>	O	pneumonia	14
<i>Trepanasoma</i>	O	African sleeping sickness	27

An interesting application of Py-GC/MS is its possible usefulness in the detection of microorganisms that are used as biological warfare agents [4a]. Py-GC/MS with a short column and capability for complete automation has been shown successful in the detection and discrimination between bacteria such as *Bacillus anthracis*, *B. cereus*, *B. thuringiensis*, *Escherichia coli*, *Legionella pneumophila*, etc. Biological warfare agents were also analysed using a MIMS system coupled with a pyrolyser. The pyrolysis for this analysis can be done in air and the markers for the biological agent transferred to the mass spectrometer through a special semipermeable membrane. As an example [71a], the mass spectrum obtained for *Bacillus anthracis* with the addition of TMAH during the pyrolysis step is shown in Figure 17.1.2. The pyrolysis was done in air at 450° C. TMAH has the effect of methylating the acidic hydrogens (mainly acids).

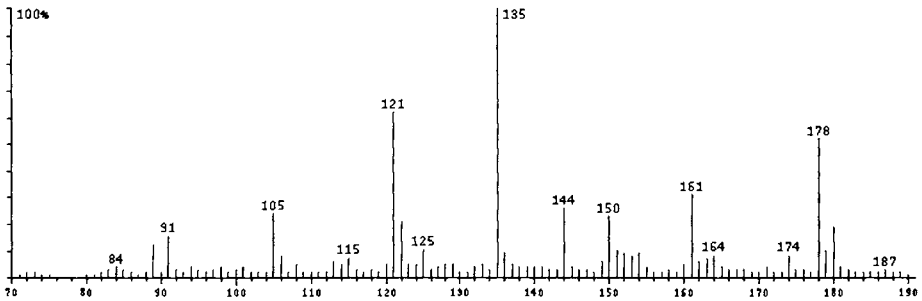


FIGURE 17.1.2. Py-MS results using MIMS on *Bacillus anthracis* using TMAH during pyrolysis in air at 450° C.

There are some other studies done on the determination of types of bacteria, on the evaluation of the differences between bacteria grown in different media, or on bacteria from different body fluids such as urine [71b].

Besides the study of intact microorganisms or microorganism parts, Py-MS has been used for other related purposes such as the characterization of semi-synthetic vaccines. An example is the characterization using Py-MS of a polysaccharide-tetanus toxoid conjugate [71c]. The Py-MS results were used in conjunction with the immunologic results.

17.2. Utilization of Pyrolytic Techniques to Detect Biomass.

Detection of biomass is an important application of analytical pyrolysis and it includes several topics. One such topic is the measurement of microbial biomass in attempts to substitute for traditional microbiological methods. Another topic is the detection of specific biomarkers for geochemical logging purposes. Pyrolytic studies were also useful in organic marine geochemistry [72]. An interesting application of biomass detection is the search for life in extraterrestrial samples.

Bacterial enumeration by most probable number, plate counts, and direct counts are rather tedious techniques. The techniques that require culturing of the organisms underestimate the biomass due to the inability of any media to support all organisms and to the presence of bacteria that are metabolically active but not culturable. Direct count of microbes by microscopy is very difficult or impossible on sample matrices with high solids content and generally suffers high variability. An alternative technique to measure microbial biomass is the measurement of the lipid content of a sample. This can be done using pyrolytic techniques with methylation using for example TMAH as a methylation agent. The fatty acid profile of the polar lipids can be used as a measure of bacterial and eukaryotic viable biomass of a sample, sterols as a measure of eukaryotes, and isoprenoid ether lipids as a measure for archaea. Lipids are components of every cell membrane, are easy to separate from other natural or anthropogenic compounds, and are rapidly degraded upon cell death. Bacterial and eukaryotic polar lipids contain ester-linked fatty acids, while the archaea have ether-linked lipids in their membranes and this can be differentiated. A comparison of polar

lipid fatty acids (PLFA) with adenosine triphosphate as biomarkers for viable microbial biomass measurement in an uncontaminated subsurface aquifer sediment [72a] gave about the same value for cell numbers as direct counts but the better precision has been obtained for the PLFA technique.

Regarding the detection of specific biomarkers for geochemical purposes, bacterial contribution to different sediments was associated with specific compounds found in shale pyrolysates such as certain triterpenoids [73]. A few applications of analytical pyrolysis to kerogen characterization were discussed in Section 14.4.

Applications of pyrolytic techniques were also successful in the characterization of suspended matter in the ocean [73a] and in several rivers [73b].

A very interesting subject is the application of analytical pyrolysis for the study of biomarkers in extraterrestrial samples [2]. Several meteorites and lunar samples were studied using this technique. Also, Viking Lander used a Py-GC/MS system to explore the Martian atmosphere and surface [74]. Commonly, a stepped pyrolysis technique has been used in these studies to determine organic components in an inorganic matrix [75]. The procedure involves a set of four or five temperatures that allow the analysis of trapped gases, analysis of small volatile molecules, and the performance of true pyrolysis on macromolecules.

The pyrolytic studies on meteorites are commonly done at different temperatures. A preheating step is utilized to insure that any possible adsorbed gases on the surface of the meteorite from the terrestrial environment are eliminated. Several organic compounds are monitored in pyrolysates such as polycyclic aromatic compounds. As an example, the results on naphthalene production upon pyrolysis from several carbonaceous chondrites, normalized by the total carbon content before pyrolysis, are shown in Figure 17.2.1 [76].

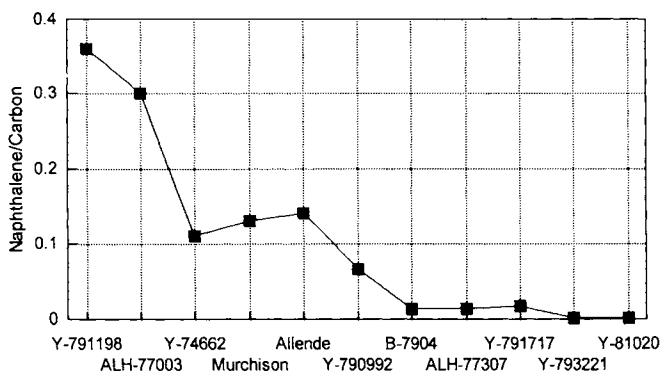


FIGURE 17.2.1. *Naphthalene production upon pyrolysis from several carbonaceous chondrites [76] reported to total carbon.*

The bioorganic nature of the organic compounds generated from several meteorites (chondrites) such as Murchison [77], Allende [78], Orgueil [79] Allen Hills [80], Holbrook [81] is improbable.

References 17.

1. C. S. Gutteridge, in *Methods in Microbiology*, vol. 19, Academic Press, New York, 1987.
2. W. J. Irwin, *Analytical Pyrolysis*, M. Dekker Inc., New York, 1982.
- 2a. K. J. Voorhees, *Analytical Pyrolysis, Techniques and Applications*, Butterworths, London, 1984.
3. H. J. H. MacFie, C. S. Gutteridge, *J. Anal. Appl. Pyrol.*, 4 (1982) 175,
4. M. Goodfellow, D. Jones, F. G. Priest (ed.), *Computer Assisted Bacterial Systematics*, Academic Press, New York (1985) p. 369.
- 4a. C. Fenselau (ed.), *Mass Spectrometry for the Characterization of Microorganisms*, ACS Symp. Ser. 541, Washington, 1994.
- 4b. L. W. Eudy, M. D. Walla, J. R. Hudson, S. L. Morgan, *J. Anal. Appl. Pyrol.*, 7 (1985) 231.
5. S. A. Liebman, E. J. Levy, *Pyrolysis and GC in Polymer Analysis*, M. Dekker Inc., New York (1985), p. 311.
6. H. W. Nichols, D. J. Anderson, J. I. Shaw, M. R. Sommerfeld, *J. Phycol.*, 4 (1968) 362.
7. J. B. Derenbach, M. Ehrhardt, *J. Chromatog.*, 105 (1975) 399.
8. D. C. Sprung, D. E. Wujek, *Phycologia*, 10 (1971) 251.
9. G. L. French, C. S. Gutteridge, I. Phillips, *J. Appl. Bact.*, 49 (1980) 505.
10. J. M. Hadadin, R. M. Stirland, N. W. Preston, P. Collard, *Appl. Microbiol.*, 25 (1973) 40.
11. V. I. Oyama, G. C. Carle, *J. Gas. Chromatog.*, 5 (1967) 151.
12. G. Dahlen, I. Ericsson, *J. Gen. Microbiol.*, 129 (1983) 557.
13. I. Ericsson, L. Larsson, P. Mardh, *Acta Path. Microbiol. Scand. Sect. B Suppl.*, 259 (1977) 43.
14. P. A. Quinn, *J. Chromatog. Sci.*, 12 (1974) 796.
15. C. E. R. Jones, C. A. Cramers (ed.), *Analytical Pyrolysis*, Elsevier, Amsterdam, 1977.
16. K. Wasserfallen, F. Rindreknecht, *Chromatographia*, 11 (1978) 128.

17. R. A. Symuleski, D. M. Wetzel, *Environ. Sci. Technol.*, 13 (1979) 1124.
18. J. R. Hudson, S. L. Morgan, A. Fox, *Anal. Biochem.*, 120 (1982) 59.
19. L. W. Eudy, M. D. Walla, J. R. Hudson, S. L. Morgan, A. Fox, *J. Anal. Appl. Pyrol.*, 7 (1985) 231.
20. E. Reiner, *Nature*, 206 (1965) 1272.
21. E. Reiner, W. H. Ewing, *Nature*, 217 (1968) 191.
22. C. S. Gutteridge, J. R. Norris, *Appl. Envir. Microbiol.*, 40 (1980) 462.
23. G. L. French, I. Phillips, S. Chin, *J. Gen. Microbiol.*, 125 (1981) 347.
24. M. V. Stack, H. D. Donahue, J. E. Tyler, *J. Anal. Appl. Pyrol.*, 3 (1981/1982) 221.
25. N. J. Stern, A. W. Kotula, M. D. Pierson, *Appl. Envir. Microbiol.*, 38 (1979) 1098.
26. L. E. Abbey, A. K. Highsmith, T. F. Moran, E. J. Reiner, *J. Clin. Microbiol.*, 13 (1981) 313.
27. E. Reiner, *J. Gas Chromatog.*, 5 (1967) 65.
28. N. J. Stern, A. W. Kotula, M. D. Pierson, *Appl. Envir. Microbiol.*, 40 (1980) 646.
29. H. J. H. MacFie, C. S. Gutteridge, J. R. Norris, *J. Gen. Microbiol.*, 104 (1978) 67.
30. E. Reiner, J. J. Hicks, M. M. Ball, W. J. Martin, *Anal. Chem.*, 44 (1972) 1058.
31. N. G. Lambert, S. Petrow, S. S. Kasatiya, M. Bouliarne, *Ann. Microbiol.*, 127B (1976) 309.
32. B. S. Emswiler, A. Kotula, *Appl. Environ. Microbiol.*, 35 (1978) 97.
33. F. M. Manger, G. A. Epstein, D. A. Goldberg, E. Reiner, *Anal. Chem.*, 44 (1972) 423.
34. G. S. Oxborrow, N. D. Fields, J. R. Puleo, *Appl. Environ. Microbiol.*, 32 (1976) 306.
35. A. G. O'Donnell, H. J. H. MacFie, J. R. Norris, *J. Gen. Microbiol.*, 119 (1980) 189.
36. G. S. Oxborrow, N. D. Fields, J. R. Puleo, *Appl. Envir. Microbiol.*, 33, (1977) 865.
37. R. D. Cone, R. V. Lechowich, *Appl. Microbiol.*, 19 (1970) 138.
38. P. G. Simmonds, *Appl. Microbiol.*, 20 (1970) 567.
39. C. Blomquist, E. Johansson, B. Soderstrom, S. Wold, *J. Chromatogr.*, 173 (1979) 19.

40. M. V. Stack, H. D. Donoghue, J. E. Tyler, *Appl. Environ. Microbiol.*, 35 (1978) 45.
41. J. H. J. Huis in't Veld, H. L. C. Meuzelaar, A. Tom. *Appl. Microbiol.*, 26 (1973) 92.
42. H. L. C. Meuzelaar, H. G. Ficke, H. C. den Harink, *J. Chromatog. Sci.*, 13 (1975) 12.
43. G.-G. Heden, T. Illeni, (ed.) *New Approaches to the Identification of Microorganisms*, John Wiley & Sons, Inc., New York, 1975, p. 165.
44. E. E. Medley, P. G. Simmonds, S. L. Manatt, *Biomed. Mass Spectrom.*, 2 (1975) 261.
45. A. S. Sekhon, J. W. Carmichael, *Can. J. Microbiol.*, 18 (1972) 1593.
46. J. W. Carmichael, A. S. Sekhon, L. Sigler, *Can. J. Microbiol.*, 19 (1973) 403.
47. P. G. Vincent, M. M. Kulik, *Appl. Microbiol.*, 20 (1970) 957.
48. D. T. Burns, R. J. Stretton, S. D. A. K. Jayatilake, *J. Chromatog.*, 116 (1976) 107.
49. R. J. Stretton, M. Campbell, D. T. Burns, *J. Chromatog.*, 129 (1976) 321.
50. C. Saiz-Jimenez, F. Martin, A. Cert, *Soil Biol. Biochem.*, 11 (1979) 305.
51. A. S. Sekhon, J. W. Carmichael, *Can. J. Microbiol.*, 19 (1973) 409.
52. M. M. Kulik, P. G. Vincent, *Mycopathol. Mycol. Appl.*, 25 (1973) 40.
53. G. Blomquist, E. Johansson, B. Soderstrom, S. Wold, *J. Chromatog.* 173 (1979) 7.
54. G. Blomquist, E. Johansson, B. Soderstrom, S. Wold, *J. Anal. Appl. Pyrol.*, 1 (1979) 53.
55. E. Reiner, J. J. Hicks, C. R. Sulzer, *Can. J. Microbiol.*, 19 (1973) 1203.
56. E. Reiner, G. P. Kubica, *Amer. Rev. Resp. Dis.*, 99 (1969) 42.
57. E. Reiner, R. E. Beam, G. P. Kubica, *Amer. Rev. Resp. Dis.*, 99 (1969) 750.
58. E. Reiner, J. Hicks, R. E. Beam, H. L. David, *Amer. Rev. Resp. Dis.*, 104 (1969) 656.
59. W. Windig, J. Haverkamp, *Studies in Mycol.*, 22 (1982) 56.
60. K. Wickman, *Acta Path. Microbiol. Scand. Sect. B, Suppl.*, 259 (1977) 49.
61. H. L. C. Meuzelaar, R. A. in't Veld, *J. Chromatog. Sci.*, 10 (1972) 213.
62. G. Wieten, J. Haverkamp, L. G. Berwald, D. G. Groothuis, P. Draper, *Ann. Microbiol.*, 133 B (1982) 15.

63. G. Wieten, J. Haverkamp, H. L. C. Meuzelaar, H. W. B. Engel, L. G. Berwald, J. Gen. Microbiol., 122 (1981) 109.
64. J. Haverkamp, G. Weiten, D. G. Groothuis, Int. J. Mass Spectr. Ion Phys., 47 (1983) 67.
65. W. Windig, G. S. De Hoog, Studies Mycol., 22 (1982) 60.
66. F. J. W. Notten, G. B. Eijker, J. J. Boon, M. A. C. van Oosten, F. H. M. Mikx, Antonie van Leeuwenhoek, 51 (1985) 518.
67. G. Wieten, J. J. Boon, D. G. Groothuis, F. Portaels, D. E. Minnikin, FEMS Microbiol. Lett., 25 (1984) 289.
68. J. J. Boon, A. Tom, B. Brandt, G. B. Eijkel, P. G. Kistemaker, Anal. Chim. Acta., 163 (1984) 193.
69. C. S. Smith, S. L. Morgan, C. D. Parks, A. Fox, D. G. Pritchard, Anal. Chem., 59 (1987) 1410.
70. T. H. Risby, A. L. Yergey, J. Phys. Chem., 80 (1976) 2839.
71. A. S. Sekhon, J. W. Carmichael, Sabouraudia, 13 (1975) 83.
- 71a. A. D. Hendricker, F. Basile, K. J. Voorhees, J. Anal. Appl. Pyrol., 46 (1998) 65.
- 71b. S. M. Huff, J. M. Matsen, W. Windig, H. L. C. Meuzelaar, Biomed. Environ. Mass Spec., 13 (1986) 277.
- 71c. E. C. Beuvery, A. v.d. Kaaden, V. Kanhai, A. B. Leussink, Vaccine, 1 (1983) 31.
72. M. L. Sohn, *Organic Marine Geochemistry*, ACS Symp. Ser. 305, Washington, 1986.
- 72a. D. L. Balkwill, F. R. Leach, J. T. Wilson, J. F. McNabb, D. C. White, Microb. Ecol., 16 (1988) 73.
73. G. Ourisson, P. Albrecht, M. Rohmer, Pure Appl. Chem., 52 (1979) 709.
- 73a. A. Saliot, A. Ulloa-Guevara, T. C. Viets, J. W. de Leeuw, P. A. Schenck, J. J. Boon, Org. Geochem., 6 (1984) 295.
- 73b. D. Van de Meent, A. Los, J. W. Leeuw, P. A. Schenk, J. Haverkamp, *Adv. Org. Geochem.*, John Wiley, New York, 1981.
74. D. R. Rushneck, A. V. Diaz, D. W. Howarth, J. Rampacek, K. W. Olsen, W. D. Dencker, P. Smith, L. McDavid, A. Tomassian, M. Harris, K. Bulota, K. Biemann, A. L. Lafleur, J. E. Biller, T. Owen, Rev. Sci. Instrum., 49 (1978) 817.
75. R. L. Levy, C. J. Wolf, J. Oro, J. Chromatog. Sci., 8 (1970) 524.

76. T. Murae, *J. Anal. Appl. Pyrol.*, 32 (1995) 65.
77. G. Holzer, *J. Oro, Org. Geochem.*, 1 (1977) 37.
78. M. H. Studier, R. Hayatsu, E. Anders, *Geochim. Cosmochim. Acta*, 36 (1972) 189.
79. E. L. Bandurski, B. Nagy, *Geochim. Cosmochim. Acta*, 40 (1976) 1397.
80. G. Holzer, *J. Oro, J. Mol. Evol.*, 13 (1979) 265.
81. J. M. Hayes, K. Biemann, *Geochim. Cosmochim. Acta*, 32 (1968) 239.

This Page Intentionally Left Blank

Chapter 18. Other Applications of Analytical Pyrolysis

18.1. Pyrolytic Techniques Used in Pathology.

Pathological conditions may be associated with biochemical modifications that can be detected using chemical analysis. A significant amount of research has been dedicated to this subject in clinical chemistry and other fields. Analytical pyrolysis has a modest place in the array of techniques used to identify chemical changes associated with disease. However, a number of studies have been performed showing the capability of pyrolytic techniques to differentiate normal and abnormal tissues, to detect plant infections, or to characterize specially prepared biological materials. For example, Py-MS has been proven to be able to differentiate leukemic and normal white blood cells [1]. Figures 18.1.1a, 18.1.1b, and 18.1.1c show the Py-MS spectra generated at 358° C using a filament heated pyrolyser from normal white blood cells, polycythemia vera affected, and leukemic white blood cells. The ionization energy in the mass spectrometer was 12 eV [1]. The differences in the spectra are attributed to modifications in nucleic acids (ions with m/z 114, 116, 98, 81, and 70) and modifications in phospholipids (ions with m/z 89, 58, and 50).

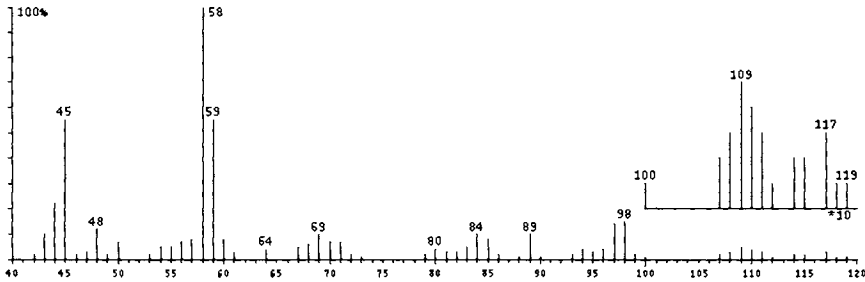


FIGURE 18.1.1a. *Py-MS spectrum of normal white blood cell.* Pyrolysis done at 358° C and MS ionization energy at 12 eV [1].

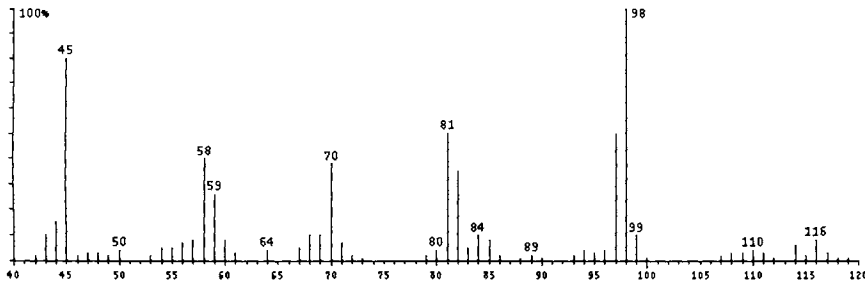


FIGURE 18.1.1b. *Py-MS spectrum of polycythemia vera affected white blood cell.* Pyrolysis done at 358° C and MS ionization energy at 12 eV [1].

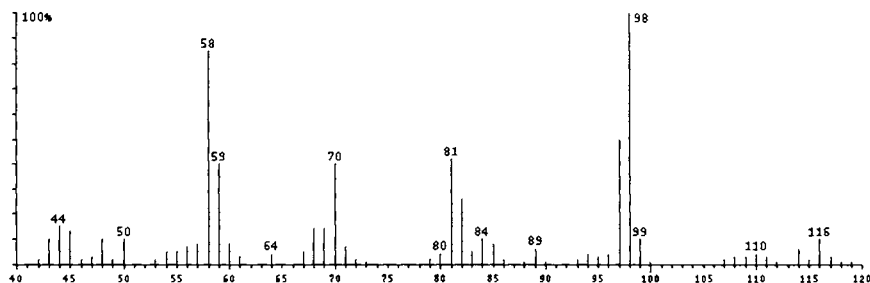


FIGURE 18.1.1b. *Py-MS spectrum of leukemic white blood cell.* Pyrolysis done at 358° C and MS ionization energy at 12 eV [1].

Successful use of Py-MS/MS has been demonstrated in the analysis of different peaks from the Py-MS results of blood cell samples to differentiate the contributions from different bases in the nucleic acids of the pyrolysed sample.

Other applications were done showing the capability to differentiate adult hemoglobin from fetal hemoglobin [2,3], to differentiate adult human normal and nuclear-cataractous lenses [4], to characterize different human cells and amniotic fluid [4a], etc.

18.2. Pyrolytic Techniques Used in Food Characterization.

Pyrolysis studies on components of food such as carbohydrates, lipids, proteins, and Maillard polymers are numerous. Also, there are studies on yeast (*Saccharomyces*) strains and on lactic acid bacteria (*Lactobacillus* sp.). However, the number of pyrolysis studies on whole food is not very large. Some studies were done on tea extracts [5], on orange juice [6], on Scotch whisky [7,8], on food gums [9,10], roasted coffee [9], meat [9a], etc. The studies were mainly done with the purpose of fingerprinting. Statistical data processing was proven very useful for the interpretation of the results. Another aspect of food characterization is related to generation of aromas during heating. This subject is very important in practice and is covered by numerous publications (e.g. [10a]) but although the thermal decomposition of polymers (such as Maillard polymers) play an important role in food flavor, the topic is beyond the purpose of this book.

18.3. Pyrolytic Techniques Used in Forensic Science, Archeology, and Art.

Among other tools applied in forensic science, pyrolytic techniques are very useful as they require a very small amount of sample and are appropriate for comparisons. Being done for a specific purpose, pyrolysis of forensic specimens is done for both small and polymeric molecules. Also, no differentiation between natural or synthetic materials is of interest. However, organic biomolecules play an important role as samples in forensic analyses. Stains of blood [3], traces of saliva [11], hair [12], chewing gums, etc. were subjects of analyses using pyrolytic methods for forensic purposes.

Fibers are another important source of forensic material. Both synthetic and natural fibers were analyzed by pyrolysis, the pyrograms or Py-MS data generating a fingerprint that can be diagnostic for each type of fiber [13].

In archeology, pyrolytic techniques were used in a similar manner as in forensic science. As an example, analytical pyrolysis has been applied for the chemical characterization of charred organic residue obtained from prehistoric pottery. In a study of different types of pottery from a native Roman settlement at Uitgeest-Groot Dorregeest in the Netherlands, numerous bio-organic moieties were detected, including fatty acids, markers for proteins, and polysaccharides. Smoke condensates from open cooking fires were also analyzed from the outside of the pottery. The data were useful variables in the discussion about form, function, and production technology of prehistoric pottery [14]. Another study was focused on the similarity between experimental polysaccharide chars and charred archeological food residues [15].

Analytical pyrolysis has been proven a very useful tool in the identification of resins used for artistic objects [16,17]. The pyrograms of Manila copal, colophony, Venice turpentine, elemi, shellac, dammar, sandarac, and mastic were obtained and used as fingerprints for these materials. Manila copal, colophony, and Venice turpentine were characterized by the presence of a degradation compound from abietic acid (as the source of these resins is from species of Coniferae), probably methyl-isopropyl-naphthalene. Elemi has a characteristic peak for elemicine, shellac showed a series of fatty acids, dammar showed the presence of sesquiterpenes (see Section 6.3), sandarac was characterized by a phenolic compound, totarol, and mastic was also identified by specific sesquiterpenes [17].

Pyrolytic techniques were also very useful in the characterization of amber and its differentiation from forgeries [18,19]

18.4. Pyrolysis Used for Waste Characterization.

Waste materials cover a diversity of products such as wood waste, used tires, waste from agricultural products such as rice husks, and municipal solid waste. Some of these waste materials are very heterogeneous while others are more uniform. Different types of waste are commonly processed using incinerators or reactors that process waste material by heat. The processed materials are commonly classified in char, liquid, and gasses. The municipal solid waste (refuse derived fuel), which is probably the most heterogeneous, is initially processed by the removal of metals, is shredded, dried, and pelletized, and only after that is it processed in heated reactors.

The more homogeneous types of waste are adequate for analysis by pyrolysis. This offers a guide for the results of the processing by heat. For example, used tires were analyzed using pyrolytic techniques in order to obtain information on the possible composition of the pyrolytic oils (see Section 6.3). Other materials are more difficult to analyze using pyrolytic procedures due to the problems of obtaining a small representative sample from heterogeneous materials. Also, the heating in industrial reactors is not well simulated by flash pyrolysis. A comparison between the pyrolysis products from a fluidized bed reactor and a filament heated flash pyrolysis instrument

(Pyroprobe 1000 from CDS) [20] is shown in Figures 18.4.1 and 18.4.2. Figure 18.4.1 shows the yield in several pyrolysis products obtained from almond shells at 850° C, and Figure 18.4.2 shows the same results for municipal solid waste.

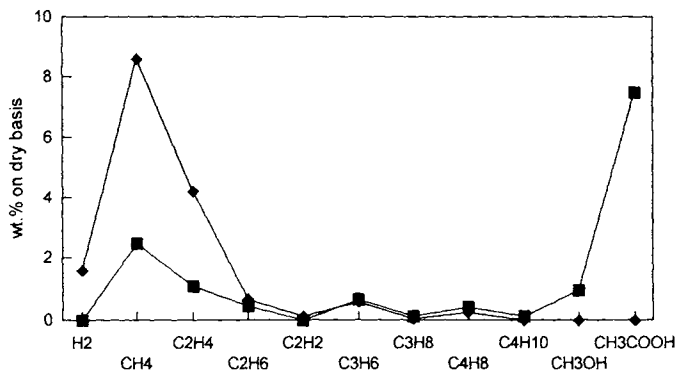


FIGURE 18.4.1. Comparison between the pyrolysis products yields from a fluidized bed reactor (diamonds) and a filament heated flash pyrolysis (squares) [20] performed at 850° C for almond shells.

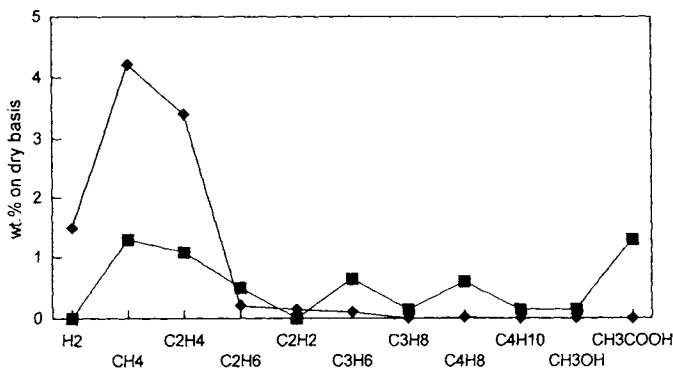


FIGURE 18.4.2. Comparison between the pyrolysis products yields from a fluidized bed reactor (diamonds) and a filament heated flash pyrolysis (squares) [20] performed at 850° C for municipal solid waste.

It appears the flash pyrolysis simulates well the first step occurring in large scale pyrolysis, but a secondary step of pyrolysis may occur in large reactors. A procedure to correct this problem has been the use of a second heating reactor placed between the flash pyrolysis device and the analytical instrument (GC) [20]. Several samples were analyzed by this procedure [20]. Besides analytical pyrolysis, a variety of other analytical techniques were applied for the analysis of the products of heat processed waste [21].

References 18.

1. H. L. C. Meuzelaar, S. M. Huff, *J. Anal. Appl. Pyrol.*, 3 (1981) 111.
2. C. E. R. Jones, C. A. Cramers (ed.), *Analytical Pyrolysis*, Elsevier, Amsterdam, 1977.
3. P. K. Clausen, W. F. Rowe, *J. Forensic Sci.*, 25 (1980) 765.
4. P. M. M. van Haard, H. J. Hoenders, J. Wollensak, J. Haverkamp, *Biochim. Biophys. Acta*, 631 (1980) 177.
- 4a. E. Reiner, L. E. Abbey, T. F. Moran, *J. Anal. Appl. Pyrol.*, 1, (1979) 123.
5. G. G. Birch, K. J. Parker (ed.), *Control of Food Quality and Food Analysis*, Elsevier, London, 1984.
6. R. E. Aries, C. S. Gutteridge, R. Evans, *J. Food Sci.*, 51 (1986) 1183.
7. J. Gilbert (ed.), *Applications of Mass Spectrometry in Food Science*, Elsevier, London, 1987.
8. K. J. G. Reid, J. S. Swan, C. S. Gutteridge, *J. Anal. Appl. Pyrol.*, 25 (1993) 49.
9. W. Baltes, *J. Anal. Appl. Pyrol.*, 8 (1985) 533.
- 9a. D. J. Puckey, S. J. Jones, *J. Anal. Appl. Pyrol.*, 6 (1984) 157.
10. A. -M. Sjoberg, H. Pyysalo, *J. Chromatog.*, 319 (1985) 90.
- 10a. T. H. Parliment, R. J. McGorrin, C. -T. Ho (ed.), *Thermal Generation of Aromas*, ACS, Symp. Ser. 409, Washington, 1989.
11. T. R. Elliot, A. H. Rogers, J. R. Haverkamp, D. Grothuis, *Forensic Sci. Int.*, 26 (1984) 131.
12. T. O. Munson, D. D. Fetterolf, *J. Anal. Appl. Pyrol.*, 11 (1987) 15.
13. W. J. Irwin, *Analytical Pyrolysis*, M. Dekker Inc., New York, 1982.
14. T. F. M. Oudemans, J. J. Boon, *J. Anal. Appl. Pyrol.*, 20 (1991) 197.
15. I. Pastorova, T. F. M. Oudemans, J. J. Boon, *J. Anal. Appl. Pyrol.*, 25 (1993) 63.
16. A. M. Sherdinsky, T. P. Wampler, N. Indictor, N. S. Baer, *J. Anal. Appl. Pyrol.*, 15 (1989) 393.
17. G. Chiavari, D. Fabbri, R. Mazzeo, P. Boccini, G. C. Galletti, *Chromatographia*, 41 (1995) 273.
18. A. M. Shedrinsky, D. A. Grimaldi, J. J. Boon, N. S. Baer, *J. Anal. Appl. Pyrol.*, 25 (1993) 77.

19. L. Carlsen, A. Feldthus, T. Klarskov, A. M. Shedrinsky, *J. Anal. Appl. Pyrol.*, 43 (1997) 71.
20. R. Font, A. Marcilla, A. N. Garcia, J. A. Caballero, J. A. Conesa, *J. Anal. Appl. Pyrol.*, 32 (1995) 41.
21. P. T. Williams, S. Besler, *J. Anal. Appl. Pyrol.*, 30 (1994) 17.

- A**
- ab initio MO 67
- absolute retention time t_R 102
- absorption (or transmission) spectrum 187
- acetylation 280
- actinomycins 380, 385
- activated complex 37, 38, 44
- activation energy 37, 75
- additions 16, 18
- adenine 399–401, 404–406
- adenosine-5'-phosphate 401
- aerosol formation 53, 54
- agar 230, 297
- albumin 386, 389, 390, 395
- aldohexoses 222, 225
- aldoses 217, 218
- alginic acid 230, 298–300
- alkali cellulose 257, 262, 263
- alkali procedure 328
- alkenylsuccinic anhydride 262
- alkylketene dimers 262
- allose 226–228
- AM1 67
- Amadori 363
- Amadori/Heyns 363
- aminosugars 219, 304
- amylopectin 230–233, 273, 274, 279, 305
- amylose 230, 273, 274, 278, 279
- analytical pyrolysis 3
- 1,6-anhydro-D-glucopyranose 296
- 1,6-anhydroglucopyranose 27
- anhydrosugars 235, 236, 245, 252, 291
- anthracitic coal 417
- apparent volume 125
- archaea 472, 220, 223
- archaeobacteria 472
- aromatic hydrocarbons 250
- array detectors 137
- Arrhenius reaction rate equation 37
- artificial neural networks 185
- autosampling 82, 83, 86
- average degree of polymerization 50, 52
- B**
- bamboo 336, 337
- bark 441, 442
- beech 336, 337
- bidimensional Py-GC 119
- biomarkers 477
- bituminous coal 417, 418
- bivariate normal density function 171
- blood 485, 486
- bond dissociation energies 68
- boosted heated filament 84
- bovine serum albumin 386–388, 394
- brown lignin 327
- brown pigments 355
- BSTFA 220, 222–224, 242, 260, 265, 267, 270, 276, 285
- burning 53, 54
- C**
- cadalene 421
- calcium lignosulfonate 328
- calf thymus 403
- californium plasma desorption 161
- cambium 441
- Cannizzaro disproportionation 30
- canonical correlation 179
- canonical variates 179, 184
- capacity factor 103
- capillary columns 102, 105, 108, 110, 115
- caramel colors 355
- carbohydrate(s) 220, 233, 292, 296, 300, 304, 308, 309, 445, 459
- carbonization 25
- carbonyl compounds 245, 279
- Carbowax column 117, 121
- carotenoids 461
- carrageenan 230, 297
- catalytic hydrogenation 29, 99
- catalytic interferences 83
- catalytic pyrolysis 3
- ceiling temperature 34
- cellobiosan 251, 252
- cellulobiose 237
- cellulose 230, 232, 235–265, 267, 268, 271–273, 291, 292, 300, 306, 307
- cellulose acetate 258–261
- cellulose ethers 263
- cellulose nitrate 257
- cellulose xanthate 263
- cellulosic fibers 256
- cellulosic materials 342
- cerebrosides 317, 319
- ceruloplasmin 395, 396
- chain length 51
- chain scissions 239
- α -chain scission 21
- β -chain scission 21, 22
- char 238, 239, 241, 255, 258
- charge site initiation mechanism 56, 60
- charred archeological food 487
- chemical degradation 3
- chemical ionization (CI) 132–134, 143, 154, 297
- chemical shift 192
- chemically modified lignins 345
- chewing gums 486
- chitin 230, 306, 307, 308
- chlorolignins 345–349
- cholesterol 317, 318
- cholesterol esters 317, 318
- chondroitin 6-sulfate 309–311
- chromoproteins 394
- cisplatin 404, 406
- clarain 416
- α cleavage 56
- coal 416–423, 425, 431, 462
- coal macerals 419, 426
- collision activated dissociation-CAD (CID) 138
- colophony 487
- column length L 103, 106

combined reactions 25
 combustion 53, 69
 concentration techniques 124
 conductivity constant 77
 coniferyl alcohol 328, 332, 334, 335, 338, 340
 1,4 conjugate eliminations 14
 continuous wave lasers 88
 correlation coefficient 173
 correlation-type parameters 172
 creatinine 370, 379
 cross-linked starch 281, 282
 cryo-focusing 121
 cryo-trap 121, 125
 cumulative frequency 165, 166, 167, 171
 cumulative frequency distribution 165
 cumulative spectra 143, 144
 cuproxam lignin 327
 Curie point pyrolyser 80, 146, 150
 cutinite 416
 cytosine 399, 400, 405, 406

D

d plots 178
 dammar 214, 487
 data matrix 161
 data pretreatment 162
 data processing in Py-GC 126
 daughter ions 138
 decarboxylation 17, 25
 degree of coalification 422, 423
 degree of freedom 166
 delignification with bisulfites 328
 2'-deoxyadenosine-5'-phosphate 401
 deoxyhexoses 219
 deoxysugars 219, 220, 302, 304
 depolymerization 51, 52, 66
 derivatization 99, 140
 dextran(s) 230, 300
 Diels-Alder reaction 18
 diffusion coefficient 105
 diketopiperazine(s) 64, 65, 376-378, 380, 382,
 383, 385, 391, 392
 dimensionality of the data 185
 dimethoxyacetophenone 339
 dimethylpolysiloxane 116
 dipalmitoylphosphatidylethanolamine 322
 dipeptides 373, 379, 380, 382
 diphenylpolysiloxane 116
 direct insertion probe (DIP) 149
 direct phases 190
 direct probe filament Py-MS techniques 149
 discriminant analysis 179
 disproportionation 23, 24
 distance-type parameters 172
 distearylphosphatidylcholine 322
 distillation 53
 distribution constant 102
 DNA 399, 400, 403, 404-406, 474
 durain 416

E

eddy currents 80
 eddy diffusion 105, 107
 effective plate number 106
 egg albumin 386, 388
 electric sector MS 134
 electrocyclic reactions 58
 electrocyclic rearrangements 15
 electron ionization 132
 electrophilic aromatic substitution 17
 elemi 487
 elimination involving free radicals 13
 elimination reactions 9
 β elimination 9
 endocaps 442, 463
 energy 33, 35, 37-40, 43, 44, 46, 55, 58, 66, 67, 68
 entropy 33, 34
 equilibrium temperature T_{eq} 72
 erythrocytes 395
 ethanolamine 317, 318, 322-324
 ethers 257, 262, 263, 268, 271, 273
 eubacteria 472, 474
 eukaryotes 472, 477
 exinite 416, 425
 expansion chamber 150-152
 extraterrestrial samples 477
 extrusion reactions 13

F

FAB 161, 191
 factor analysis 180
 factor rotation 183
 factor scaling 182
 factor spectrum 179, 184
 fast atom bombardment 161, 191
 feedback controlled temperature filament 84
 felypressin 380, 385
 ferromagnetic alloys 80
 ferulic acid 334, 336
 fiber 486
 field desorption (FD) 147, 154, 155
 field ionization (FI) 154
 final pyrolysis temperature 72
 first order kinetics 36, 40, 43
 fit factor 128
 flash pyrolysis 5, 71, 73, 84, 86
 flight tube 137
 food 376, 379, 395
 food gums 486
 fractionated pyrolysis 5
 fragment ions 133, 142, 153, 154
 fragmentations 12
 fragments generation 55
 Frank-Condon process 55
 free enthalpy 33, 34, 44
 free radical mechanism 10, 16, 20, 21
 free radical substitutions 17
 frequency factor 37, 75
 fructose 219-224
 FTIR 97, 188
 fucoidan 230, 298, 299

- fulvic acids409, 410
 fungal polysaccharides 230, 304, 305
 furcellaran 230
 fusain416
 fusinite416
- G**
- galactose 220, 226, 227, 228, 283, 289, 290,
 292, 296, 299, 302, 304
 ganglioside 317, 319, 320, 323
 gas chromatography 97, 99–102, 109, 110,
 113–115, 120, 132
 gas chromatography-mass spectrometry 97
 gas constant 37
 gases238, 239, 255, 256, 258
 Gaussian 9467, 69
 GC detectors 114, 115, 126
 globulins386
 β -D-glucan236
 glucose218, 220–223, 226, 227, 258, 264, 270,
 273, 289, 291, 296, 301, 302, 304–306, 310
 β -glucosidic structure232
 α -D-glucopyranose 218, 221, 222
 α -L-gulopyranosyluronic acid297
 glucuronic acid291, 300, 302, 310
 glutelins386
 gluten389–391
 glyceraldehyde 217, 293, 305
 glycerol esters317
 glycerol phosphate301
 glycogen 230, 305, 306
 glycolipids317, 320
 glycoproteins 386, 394, 395
 glycosaminoglycans309, 310, 311
 glycosylceramides319
 guaiacol 332–335, 338, 340, 348, 349
 guaiacyl lignin 328, 462, 463
 guaiacyl-syringyl lignins 328
 guanine399, 400, 405, 406
 guar gum230, 289, 290
 gum arabic230, 289
 gum ghatti230, 289
 gum karaya230, 289
 gum tragacanth230, 289
 gums 230, 289, 290
- H**
- hardwood441
 heart-cut 121, 123, 124
 heat transfer rate 77
 height equivalent to a theoretical plate106
 hemicellulose 230, 256, 291, 292, 296, 297
 heparan310
 heterocyclic amines379
 hexoses218, 220, 230, 296
 hexuronic acid 219, 289, 297, 310
 hierarchical algorithms 177
 high-vacuum pyrolysis151
 histones386
 Hofmann's rule 10
- holocellulose292–296
 homolytic dissociation35, 66
 housing heating73, 86
 housing temperature 97
 HPLC97, 100, 157, 188–190, 199
 human hair392
 humic acids409–411
 humin409–411
 hyaluronic acid309, 310
 hydrocarbons317, 321
 hydrogen elimination16, 18
 hydroxyethyl celluloses268
 hydroxyethylation280
 hydroxypropyl methyl cellulose269–271
- I**
- inorganic esters257
 insulin393, 394
 interface (of pyrolyzers)71, 72
 intermolecular chain transfer48
 intramolecular chain transfer23
 intramolecular rearrangement20, 23
 ion fragmentation55
 ion trap mass spectrometer136
 ionization energy57
 ionization process132, 133, 144, 152, 153
 isoprene203–206, 209
 isotherm102
 isothermal and programmed temperature gas
 chromatography111
 isothermal conditions33, 36, 38, 41, 42
 isothermal pyrolysis5
 ITMS136
- K**
- kaurane421
 Kentucky reference cigarette (1R4F)449
 kerogen typing428
 kerogens425, 428, 430, 462
 ketohexoses219, 222, 225
 kinetic factors36
 kinetics in homogeneous systems41
 kinetics of heterogeneous reactions44
 Klason lignin327, 342, 345
 kraft lignin328, 330, 331, 333, 334, 341, 345
 Kraton79, 87
- L**
- laccol polymer435
 lacquers435, 436
Lactobacillus486
 lactones245, 279
 lactyl-peptide bridge301
 laminaran230, 233, 234, 236, 237, 297, 299
 LAMMA152
 larch arabinogalactan230, 296
 laser159, 160
 laser microprobe mass analysis152
 laser micropyrolysis89, 90, 93
 laser Py-MS151

laser pyrolysers 87, 90
 latex 203
 LC/MS 190, 191
 leaf cuticle 435
 leukemic white blood cells 485
 level of sulfur in the pulp 465
 lightpipe 188
 lignin 291–296, 327, 328, 330, 335, 340, 346,
 350, 441–446, 448, 450–454, 457–459,
 461, 463, 464
 lignite 417, 418
 lignosulfonates 328, 345–349
 DL-limonene 203–205, 207, 211
 lipopolysaccharides 230, 302–304
 lipoproteins 394
 liquid matrix 161
 local non-equilibrium 105
 locust bean gum 289, 290
 low-voltage (14 eV) EI mass spectrum 158
 LSIMS 161

M

MAB 159
 macerals 416
 magnetic sector 134, 135, 137, 138
 Maillard condensation 356, 363, 364
 Maillard polymers 442, 450–455, 457–460
 MALDI 91, 159
 maltosan 236
 Manila copal 487
 mannose 226, 227, 234, 235, 290
 mass spectral libraries 138,
 mass spectrometers 132
 McLafferty rearrangement 57
 mean centered (or corrected) value 176
 mean corrected value 176, 179
 meat 486
 metastable ion 159
 methyl scission 21
 microfumace pyrolysers 98
 micro-needles 154, 155
 micronite 417
 microorganism(s) 471–473
 microorganism parts 476
 migration of a group 15
 milled-wood lignin MWL 327, 333–335
 MIMS 156
 MNDO 67
 model for the kinetics 42
 modulated molecular beam 152
 molecular collision 38
 molecular fragmentation 55
 monodisperse system 52
 monosaccharides 217–220, 224, 229, 245, 289
 MOPAC 66–69
 mRNA 399
 MS/MS systems 138
 mucilages 230, 289, 290
 muramic acid 301
 mutagenic compounds 369

N

N-acetylated aminosugars 219
 N-acetylneuraminic acid 319
 NADPH 404
 natural rubber 203, 209
 negative radical ions 133
 neural networks 185
 neuraminic acid 219
Nicotiana tabacum 444
 NMR 97
 nondialyzable melanoidin 361, 364, 365
 nonequilibrium 102
 non-hierarchical algorithms 178
 non-oxidative atmosphere 54
 non-repetitive polymers 47
 nonulosaminic acid(s) 219
 normal distribution 165
 nuclear magnetic resonance (NMR) 191
 nucleic acids 485, 486
 nucleoproteins 394
 nucleosides 399
 nucleotides 399
 number of monomeric units 50, 51

O

odd-electron fragments OE 133
 off-line pyrolysis 71
 on-line pyrolyser 101, 125
 open-tubular columns 102, 115
 organic esters 257
 oxidations and reductions 16
 oxidative pyrolysis 5

P

packed columns 102, 105, 115
 PAE in paper 465
 partition coefficient 102
 PBM 139
 peak broadening 103, 104, 105
 peak capacity 119
 peak width 104
 peat 417, 422, 424, 426
 peat mosses 423
 pectin 230, 231, 282, 283, 285, 287, 288, 442, 445,
 450–455, 457, 458
 pentoses 217, 218, 220, 223, 230
 peptidoglycans 301, 302, 309
 peptidoglycolipids 317
 peptidolipids 317
 phase ratio β 104
 phenols 245
 phloem 441
 phosphate diesters with choline 317
 phosphate triesters 317
 phosphatidic acids 317
 phosphoglycerides 317–319, 473
 phospholipids 473
 phosphoproteins 394
 photoionization (PI) spectra 157, 158
 phytosterols 318
 pine 336, 337

pine needles	443, 444
pith	441
plant exudates	230, 289
PLFA technique	477
PLOT	116
plume	160
PM3	67
point ion detectors	137
pollen	436
polycytemia vera	485
polyethylene glycol	115, 116
polygalacturonic acid	283-288
polymeric chain scission	20, 47, 49
polymerization degrees	50, 51
polypeptides	373, 374, 376, 380, 386
polysulfide bridges	210
pre-column	98, 119
principal component analysis	181
probability based matching	139
prolamines	386
protamines	386
protein analysis	474
proteinaceous material	342, 345
proteoglycans	230, 308-310
PTV	87
pulse mode	71
purge-and-trap	124-126
Py-DCI MS	150
Py-FD MS	155
Py-FI MS	155
Py-GC	97, 100, 101, 443, 112, 113, 117, 124, 126, 127, 132, 138, 143, 144, 148, 154
pyrolysate	4
pyrolyser	71-73, 76, 78, 79, 82-87, 91, 92, 94
pyrolysis	3
pyrolysis in the presence of hydrogen	29
pyrolysis in the presence of oxygen	28
pyrolysis in the presence of quaternary ammonium hydroxides	30
pyrolysis in the presence of water	29
pyrolysis of amino acids	63
pyrolysis of lignin	61
pyrolysis of nucleic acids	66
pyrolysis of polyisoprene	58
pyrolysis of sugars	60
pyrolysis-gas chromatography	5
pyrolysis-gas chromatography/infrared spectroscopy	5
pyrolysis-gas chromatography/mass spectrometry	5
pyrolysis-infrared spectroscopy	5
pyrolysis-mass spectrometry	5
pyrolytic cleavage	13
pyrolytic elimination with E _i mechanism	9
pyrolytic reactions in solid state	45, 46
pyrolyzate	4
Q	
Q-switched lasers	88
quadrupole mass spectrometers	135

R

radiative heating (laser) pyrolysers	87
radical formation	35, 48
radical site initiation	56, 60
random chain scission	20, 21
reactivity indices	66
reagent gas	133, 134, 154
rearrangement	14, 56, 57
recombination	24
red algae	299
reductive pyrolysis	5
relative frequency of occurrence of	
random errors	165
repetitive polymers	47
reproducibility	92
resistively heated filament(s)	82
resolution (chromatographic)	109, 110, 112
retene	421
retention gap	119
retention index	127
retention time t _R	102, 103, 105, 106
retroaldolization	19, 59, 239, 255
retro-Diels-Alder	18, 58
retro-ene reaction	18, 19, 66, 337, 338
reverse aldolization	239, 240, 271
reverse phases	190
reverse (retrograde) addition	18
RF coil	82
ribbon type filament	85
RNA	399, 400, 403-405
rRNA	399
rubber band correction	130

S

saliva	486
sample capacity	110
sample layer thickness	78
sample load	76
sample preparation in Py-MS	148
sandarac	487
scatter plot	163
scleroproteins	386
sealed vessel pyrolysis	87
second order disproportionation	49
second order kinetics	36
second order recombination	49
secondary ionization techniques	160
semiempirical molecular orbital (MO)	66
separation factor α	109
separation of ions (in MS)	134
shale	426-429
β -sheet	376
shellac	487
sialic acids	219
side group E _i elimination	239
side group reactions	25
sigma electron ionization mechanism	56, 57
sigmatropic rearrangements	15
SIM	135
similarity index	127, 128, 172
simple lipids	317, 318, 321

- SIMS 161
 single ion monitoring 135
 single linkage 177
 sitosterol 318
 slow gradient pyrolysis 71, 87
 small molecules 337, 342, 345, 346
 smoke 53, 441–444, 447–460
 smoke aroma 442
 sodium carboxymethyl cellulose 264
 softwood 441
 solid samples 39, 41, 46, 53
 sphingolipids 317, 319
 sphingomyelins 317, 319
 sphingosine 319
 sporopollenin 436
 standard deviation 164
 starch 230, 273, 274, 276, 277–282, 287, 297,
 300, 305, 306
 starting temperature T_0 76
 steam distillation 53, 54
 step pyrolysis 71
 stepwise pyrolysis 5
 Stevenson's rule 57
 stigmasterol 318
 Strecker degradation 376
 Student distribution 166–168
 substitutions 16
 sulfated galactan 298
 sulfatides 317, 319
 sulfation 298, 309, 311
 supercritical fluid chromatography 191
 syringyl lignin 463
- T**
- tamarind kernel powder 230, 289
 tannins 352
 tar 238, 239
 taxonomic applications 471
 teichoic acids 301, 302
 temperature rise time TRT 73
 temperature-programmed pyrolysis 5
 Teq (equilibrium temperature) 72
 theoretical plate number 106
 thermal conductivity 78, 88
 thermal degradations 3
 thermal diffusivity 78, 88
 thermodynamic factors 33
 thermolytic reactions 35
 thin layer chromatography 191
 three-dimensional polymer 241
 thymidine 474
 thymine 399, 400, 405, 406
 time-of-flight spectrometers (TOF) 137
 time-resolved filament pyrolysis 149
- tire pyrolysis 212–214
 TMAH 30, 31, 321, 323, 324, 336, 337
 total heating time (THT) 73
 total ion chromatogram (TIC) 142
 total ion trace (TIT) 149, 150
 total pyrolysis time 73
 transglycosidation 20, 29, 59, 239, 271, 280
 trimeric lignin 61
 trimethyl anilinium hydroxide 30
 tripalmitin 321
 tripeptides 373, 380
 tRNA 399
 TRT 73, 149–151
 Ts 76
 two-temperature zone furnace 87
- U**
- unimolecular reaction 38, 39
 unit variance component scores 182
 univariate data analysis 161, 164
 urushiol 435
- V**
- van Deemter equation 107
 Venice turpentine 487
 vibrational energy 186
 vitamins 317
 vitrain 416
 vitrinite 416, 419, 426
 volatilization 39, 53
 vulcanite 211
 vulcanization 210, 211
 vulcanization accelerators 211
 vulcanized rubber 210
- W**
- waxes 317, 318, 321
 weighing factor 173
 white blood cells 485
 Willstätter lignin 327
- X**
- xanthan 230, 300
 xanthates 257
 xylan 291–296, 298
 xylem 441, 461
 xylinite 416
 xylopyranosyl chain 291
 xylose 283, 289, 292
- Z**
- Zaitsev's rule 10
 zip length 51, 52
 zone spreading 105, 106